UNIVERSITAT POLITÈCNICA DE VALÈNCIA

Research Institute of Water and Environmental Engineering
Department of Hydraulic Engineering and Environment

Ph.D. Thesis

ASSESSMENT OF THE FLAT-PANEL MEMBRANE PHOTOBIOREACTOR TECHNOLOGY FOR WASTEWATER TREATMENT: OUTDOOR APPLICATION TO TREAT THE EFFLUENT OF AN ANAEROBIC MEMBRANE BIOREACTOR

Josué González Camejo
September 2019

Supervisors:

Dr. José Ferrer Polo
Dr. Ramón Barat Baviera

ABSTRACT

Combination of anaerobic membrane reactors (AnMBRs) and microalgae membrane photobioreactor (MPBR) appears as an ideal option within the framework of sustainable technologies for wastewater treatment. This combination enables to produce biogas from the organic matter present in wastewater, while the nutrient content of the AnMBR effluent can be recovered from microalgae biomass. In addition, membrane technology allows obtaining a water effluent which can be suitable for reclamation.

Previous studies have proved the capability of a microalgae culture to recover the nutrients present in AnMBR effluent at lab scale. However, up-scaling from controlled lab conditions to varying outdoor conditions could limit the industrial applications of this technology.

This study consists of the assessment of a microalgae culture in an MPBR pilot plant fed by effluent of an AnMBR system. For this, optimal operating conditions of the MPBR plant were evaluated, considering both the microalgae biological process and the membrane fouling rate. The effect of other parameters that have an influence on the process such as light intensity applied to the photobioreactors (PBRs), temperature, organic matter concentration, presence of other organisms, etc., was also studied; as well as the specific weight of each parameter on the process. Another goal consisted of finding new controlling parameters that ease the continuous operation of the system.

The MPBR system used in this study showed appeared to be capable of treating AnMBR effluent, successfully accomplishing legal discharge limits. However, this was only achieved when the following conditions were reached:

i) PBR light path was as narrow as 10 cm.
ii) Operating conditions (BRT and HRT) were in the appropriate range.
iii) Temperature was under the máximum limit of around 30 ºC.
iv) Nitrite was not accumulated.
v) Ammonium was the main nitrogen source.
vi) Organic matter concentration in the culture was not high.

RESUMEN

La combinación de reactores anaerobios de membranas (AnMBRs) con el cultivo de microalgas en un fotobiorreactor de membranas (MPBR) aparece como una opción ideal dentro del marco de tecnologías sostenibles para la depuración de aguas residuales. Con esta combinación de tecnologías, se puede obtener biogás a partir de la materia orgánica presente en el agua residual, mientras que los nutrientes del efluente de AnMBR se recuperan con la biomasa algal. Además, la tecnología de membranas permite obtener un efluente limpio y apto para su reutilización.

Estudios previos han demostrado la capacidad de un cultivo de microalgas para recuperar los nutrientes presentes en el efluente de un sistema AnMBR a escala laboratorio. Sin embargo, el traslado de esta tecnología a condiciones controladas de laboratorio a condiciones ambientales variables puede suponer una limitación en su aplicación industrial.

Este trabajo consiste en la evaluación del proceso de cultivo de microalgas en una planta piloto MPBR alimentada con el efluente de un sistema AnMBR. Para ello se han evaluado las condiciones óptimas de operación de la planta, teniendo en cuenta tanto el proceso biológico de microalgas como la velocidad de ensuciamiento de las membranas. También se ha estudiado el efecto de otros parámetros que influyen en el proceso, como la intensidad de luz aplicada a los fotobiorreactores (PBRs), temperatura, concentración de materia orgánica, presencia de otros organismos, etc.; así como el peso específico de cada parámetro dentro del proceso. Otro objetivo consiste en la búsqueda de nuevos parámetros de control del proceso que faciliten la operación en continuo del sistema.

El sistema MPBR utilizado en este estudio se mostró capaz de tratar un efluente de AnMBR, cumpliendo con los límites legales de vertido. Sin embargo, esta operación se consiguió únicamente cuando se cumplían una serie de condiciones:

i) El espesor de los fotobiorreactores era estrecho (10 cm).
ii) Las condiciones de operación (BRT y HRT) se mantenían dentro del rango adecuado.
iii) Temperatura se mantenía habitualmente debajo del límite máximo de 30 ºC.
iv) No existía acumulación de nitrito.
v) La fuente principal de nitrógeno era amonio.
vi) La materia orgánica presente en el cultivo no era excesiva.

RESUM

La combinació de reactors anaerobis de membranes (AnMBRs) amb el cultiu de microalgues en un fotobioreactor de membranes (MPBR) apareix com una opció ideal dins el marc de tecnologies sostenibles per a la depuració d'aigües residuals. Amb aquesta combinació de tecnologies, es pot obtenir biogàs a partir de la matèria orgànica present en l'aigua residual, mentre que els nutrients de l'efluent de AnMBR es recuperen amb la biomassa algal. A més, la tecnologia de membranes permet obtenir un efluent net i apte per a la seua reutilització.

Estudis previs han demostrat la capacitat d'un cultiu de microalgues per recuperar els nutrients presents en l'efluent d'un sistema AnMBR a escala laboratori. No obstant això, el trasllat d'aquesta tecnologia de condicions controlades de laboratori a condicions ambientals variables pot suposar una limitació en la seua aplicació industrial.

Aquest treball consisteix en l'avaluació del procés de cultiu de microalgues en una planta pilot MPBR alimentada amb l'efluent d'un sistema AnMBR. Per a això s'han avaluat les condicions òptimes d'operació de la planta, tenint en compte tant el procés biològic de microalgues com la velocitat d'embrutiment de les membranes. També s'ha estudiat l'efecte d'altres paràmetres que influeixen en el procés, com la intensitat de llum aplicada als fotobioreactors (PBRs), temperatura, concentració de matèria orgànica, presència d'altres organismes, etc .; així com el pes específic de cada paràmetre dins del procés. Un altre objectiu consisteix en la recerca de nous paràmetres de control del procés que facilitin l'operació en continu del sistema.

El sistema MPBR utilitzat en aquest estudi es va mostrar capaç de tractar un efluent de AnMBR, complint amb els límits legals d'abocament. No obstant això, aquesta operació es va aconseguir únicament quan es complien una sèrie de condicions:

i) El gruix dels fotobioreactors era estret (10 cm).

ii) Les condicions d'operació (BRT i HRT) es mantenien dins del rang adequat.

iii) La temperatura es mantenia habitualment baix del límit màxim de 30 ºC.

iv) No existia acumulació de nitrit.

v) La font principal de nitrogen era amoni.

vi) La matèria orgànica present en el cultiu no era excessiva.

AGRADECIMIENTOS

El presente trabajo no hubiera podido realizarse sin la ayuda de mucha gente a la que me gustaría dar las gracias a través de las siguientes líneas.

En primer lugar a mis directores José y Ramón, así como a Aurora por depositar en mí su confianza para trabajar con ellos y por darme la oportunidad y la responsabilidad de operar la planta piloto de fotobioreactores de membranas.

También me gustaría dar las gracias a Mónica y Alex, mis mentores en esto de las algas, por ensañarme todos los truquitos del laboratorio y de la planta. A todos los que me ayudaron en algún momento en los experimentos: Patri, Rebecca, Stephanie, Juan Mora, Alex, Freddy, Héctor, Rubén (espero no dejarme a nadie); ya fuera limpiando piscinas, intentando descifrar el código de control de la planta, aguantando las obras de Industrias Marín o limpiando las múltiples telarañas de la planta. A los AnMBRs (Núria, Silvia, Ruth, Óscar, Pau), que tenían siempre preparado dulce alimento para las algas. A María, por hacer esa cobertura en los experimentos que a veces es difícil de ver. A Berta y Eladio, por su apoyo en laboratorio. A Vicky, Ángel, Ramón, Luis, Antonio, Dani por su inestimable ayuda en los experimentos y en la redacción de artículos. A Dagarcas por de vez en cuando levantar el culo de la silla para ir a reparar el ordenador de planta o de laboratorio. Y no me olvido de Álvaro y Paula, por su ayuda en los experimentos de laboratorio.

I would also like to thank Elena Ficara and Simone Rossi for letting me work with them and helped me to improve this work.

Gracias también a todo el personal de la depuradora de la Cuenca del Carraixet, que nos han ofrecido su ayuda desinteresada en numerosas ocasiones.

También quisiera hacer otro tipo de agradecimientos desde el punto de vista personal. A María por hacer siempre de hermana mayor y por "*trigger*" muchas risas. A Patri y Núria por los buenos momentos, entre ellos los juernes en Beni. A las new generations (Miguel, Jesús y Stephanie) por coger el relevo. A Alex y Tao por dejarme hablar de los Simpsons con ellos libremente. A Alberto y Nuria por seguirme el rollo en las cenas. A Guille por enseñarnos que se puede sonreír mientras se hace una tesis. A Antonio por poder utilizar jerga canaria con él. Y a todos en general por haber sido buenos conmigo y haberme hecho sentir que trabajaba entre amigos.

Por último, agradecer a mi familia y amigos, que siempre apoyaron mi decisión de venir a Valencia; en especial a mis hermanos, que quisieron vivir parte de esta etapa a mi

lado. A Clara que me ha acompañado en este camino, a veces excitante y a veces duro. A mis compañeros del Nou Básquet Alboraia y del CB Aldaia, que a menudo pagaban mis frustraciones de la tesis en la cancha de basket. Y en general a toda la gente que se ha interesado por mí durante este tiempo y que alguna vez me preguntó: "¿Qué tal va la tesis?". Gracias a todos.

CONTENTS

CHAPTER I:

INTRODUCTION

CHAPTER I:

INTRODUCTION

1. WASTEWATER TREATMENT

The increasing human population has demanded rising water resources and consequently, large volumes of wastewater are produced (Almomani et al., 2019). Natural water ecosystems have the capacity of degrading some of the pollutants present in wastewaters. Nevertheless, the degradation rate is usually surpassed by the high pollutant loads produced by anthropogenic activities (Ruiz-Martínez, 2015). Hence, the direct wastewater discharge to natural ecosystems without treating them appropriately can imply serious pollution problems (Gonçalves et al., 2017). High organic-pollutant loads can reduce the oxygen of water ecosystems, which involves biodiversity reduction. In addition, emission of nutrients such as nitrogen and phosphorus to water bodies can cause the eutrophication phenomenon (Song et al., 2018a). Eutrophication is often responsible for algal blooms, which can produce water quality losses and health risks (Guldhe et al., 2017; Razzak et al., 2017). For this, wastewater treatment has had a significant role in human activities development during last century (Sikder et al., 2019). In this respect, in ancient wastewater treatment plants (WWTPs), a primary treatment is used to physically remove particles from wastewater, followed by an aerobic biological treatment (the so-called secondary treatment) to degrade the organic matter from water. A tertiary treatment is often used to disinfect water. Some WWTPs also incorporate biological processes to remove nutrients from wastewater through combining anaerobic, anoxic and aerobic reaction zones (Guldhe et al., 2017).

Nowadays, urban WWTPs are extremely efficient in terms of human health and pollutant removal (Almomani et al., 2019). However, classical wastewater treatment implies huge energy demands (Udaiyappan et al., 2017) and nutrient losses (Acién et al., 2016). Wastewater treatment therefore appears as a key sector in which the circular economy concept can be applied to cope with the urge for more sustainable technologies (Puyol et al., 2017).

1.1. Circular economy in wastewater treatment

Within the circular economy concept, wastewater is no longer treated as waste that has to be treated, but as source of energy, nutrients and reclaimed water (Batstone et al., 2015; Robles et al., 2018).

On the one hand, classical aerobic wastewater treatments spend approximately 50% of their energy demand in aeration (Foley et al., 2010). Moreover, nitrogen is usually released to the atmosphere, while phosphorus is often lost within the sludge as a metal salt, preventing their possible reuse (AlMomani and Örmeci, 2016; Gao et al., 2018). This is highly inconvenient since nitrogen and phosphorus contained in sewage can approximately account for 20% of the manufactured nutrients (Puyol et al., 2017).

Alternatively, emerging water resource recovery facilities (WRRFs) not only focus on wastewater treatment itself, but also on the recovery of nutrients, energy and water from sewage (Seco et al., 2018; Song et al., 2018a). In this respect, anaerobic wastewater treatments have been receiving increasing interest from the scientific community since they are able to produce biogas that can even offset the energy demand of the treatment process (Smith et al., 2012). In addition, anaerobic treatments reduce environmental impacts due to their lower energy consumption, sludge production and space requirements in comparison with classical aerobic processes (Smith et al., 2014; Song et al., 2018a; Pretel et al., 2016). By way of example, McCarty et al. (2011) have configured a low energy mainline (LEM) treatment based on the anaerobic treatment of the effluent of the primary settler.

1.2. Anaerobic membrane bioreactors

Anaerobic processes also present some drawbacks. For instance, they need to operate at long biomass retention time (BRT) and/or high temperatures because of the slow growth rate of anaerobic organisms, which implies using high reaction volumes (Giménez, 2014). In addition, the settling rate of these anaerobic microorganisms is low.

To solve these issues, anaerobic membrane bioreactor (AnMBR) technology has been recently expanding (Robles et al., 2018). AnMBRs consist of the combination of anaerobic processes and membrane filtration, which allows decoupling the BRT from the hydraulic retention time (HRT). This decoupling compensates the slow growth grate of anaerobic organisms (Stazi and Tomei, 2018), thus reducing the reacting volume

without washing out the anaerobic microorganisms. Consequently, the economic feasibility of this technology is improved (Smith et al., 2014).

It is remarkable that high sulphate concentrations in wastewater can limit the anaerobic process because of the competition between methanogenic microbes and sulphate reducing organisms (SRO) (Chen et al, 2016). Moreover, the sulphate reduction by SRO produces sulphide, a corrosive and toxic gas for anaerobic microorganisms (Siles et al., 2010). The chemical oxygen demand-sulphate ratio (COD:SO_4) has been reported as the main parameter affecting this competition (Giménez et al., 2012). In this respect, influent COD:SO_4 ratios higher than 10 $gCOD \cdot gSO_4^{-1}$ have been reported not to limit the anaerobic process due to SRO activity (Song et al., 2018b). AnMBR systems have been previously assessed at pilot scale, obtaining high quality effluents regarding organic matter and suspended solids (Giménez, 2014). However, anaerobic organisms are only able to remove up to 10% of the total nitrogen of the influent (Dai et al., 2015). Consequently, AnMBR effluents usually present large nutrient contents (Stuckey, 2012). When emitting to sensitive areas, a post-treatment step is therefore needed.

Different techniques have been applied for nutrient removal/recovery from AnMBR effluents, such as struvite precipitation, anammox processes, osmosis membranes, fertirrigation, microbial fuel cells and microalgae cultivation (Batstone et al., 2015; Robles et al., 2018). Within these nutrient recovery technologies, microalgae cultivation has emerged as an ideal option for nutrient recovery from wastewater because of their low energy consumption and their environmental benefits (Acién et al., 2016; Guldhe et al., 2017; Xu et al., 2019). In addition, AnMBR effluents have been reported to contain all the macro and micronutrients needed for microalgae growth (Ruiz-Martínez et al., 2012).

2. MICROALGAE

Microalgae refer to a wide group of microscopic organisms which include eukaryotic microalgae and prokaryotic cyanobacteria (Garrido-Cárdenas et al., 2018; Straka and Rittman, 2018). The main taxonomic orders of eukaryotic microalgae include *Chlorophyta* (also known green algae), *Rhodophyta* (red algae), *Chrysophyta* (or golden algae) and *Bacillariophyta* (diatoms) (Udaiyappan et al., 2017). Generally, microalgae are photoautrotophic organisms, i.e. they use an inorganic carbon source and light as energy source; although some microalgae are photoheterotropic (they use organic carbon and light) or heterotrophic; i.e. they obtain energy and nutrients from organic

compounds (Behera et al., 2018; Razzak et al., 2017). Some microalgae are also mixotrophic; i.e. they can use both autotrophic and heterotrophic metabolisms, depending on the substrate availability and lighting conditions (Ferreira et al., 2019), although they tend to use the photoautotrophic metabolism since it is faster than heterotrophic (Babaei et al., 2016).

Scientific interest in microalgae biotechnology has remarkably increased in the last decade (Judd et al., 2015), showing a 20-fold increase in the number of publications since 2005 (Garrido-Cárdenas et al., 2018).

2.1. Microalgae metabolism. Photosynthesis

Photosynthesis comprises some reactions that include the absorption of light photons, the reduction of water molecules with the subsequent release of oxygen, the capture of the free electrons and nutrient assimilation for the synthesis of organic compounds (Reynolds, 2006). Some of these reactions require light energy (light reactions) but other can be produced in darkness (dark reactions).

Light reactions are carried out in the thylakoid membranes and are catalysed by the photosynthetic reaction centres (Ruiz-Martínez, 2015). In the photosystem II (PSII) reaction centres, electrons are stripped from water and transported to a reductant pool, releasing oxygen. In photosystem I (PSI) reaction centres, light energy is used to reduce the nicotinamide adenine dinuceotide phosphate from NADP to NADPH and to form adenosine triphosphate (ATP) (Baker, 2008; Binnal and Babu, 2017; Reynolds, 2006).

In the dark reactions (also known as Calvin cycle), the inorganic carbon is reduced to carbohydrates through the carboxylation reaction, which is catalysed by the enzyme ribulose 1,5-biphosphate carboxylase (RuBisCo) using ATP as energy source (Yadav and Sen, 2017). This process can be summarised by [Eq. I.1] (Manhaeghe et al., 2019; Reynolds, 2006; Ruiz-Martínez, 2015) and is schematised in Figure I.1.

$$n\ CO_2 + n\ H_2O + photons \rightarrow (CH_2O)_n + n\ O_2 \qquad [Eq.\ I.1]$$

In case the enzyme Rubisco reduces O_2 instead of CO_2, photorespiration occurs. This is not convenient since energy and fixed carbon are wasted during photorespiration, reducing microalgae growth (Reynolds, 2006).

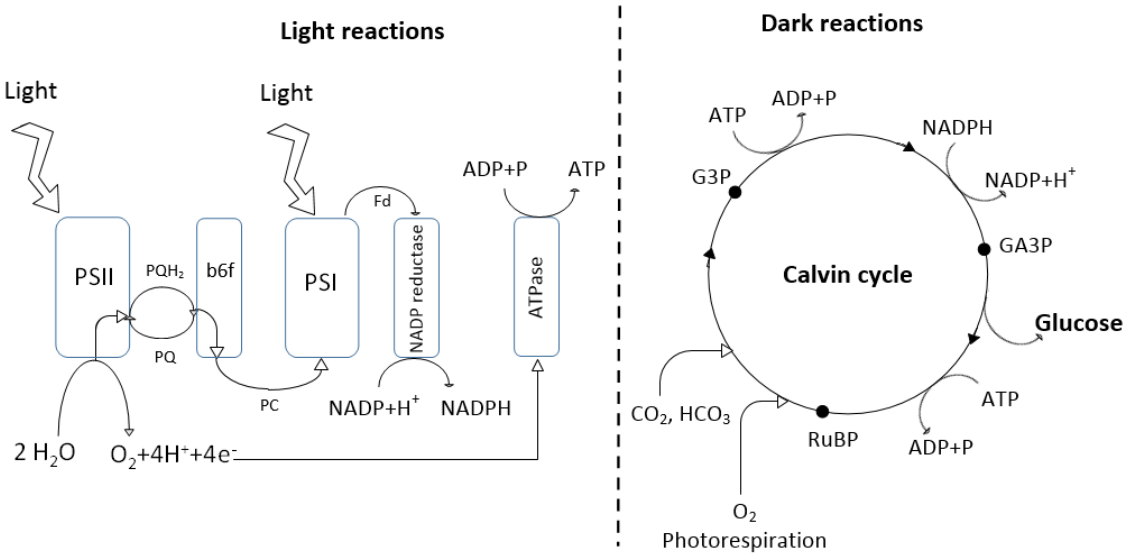

Figure I.1. Light and dark reaction of photosynthesis (based on Baker (2008) and Reynolds (2006)). ADP: adenosine diphosphate; ATP: adenosine triphosphate; b6f: cytochrome b6f complex; Fd: ferredoxin; G3P: glycerate 3-phosphate; GA3P: glyceraldehyde 3-phosphate; PC: plastocyanin; NADP/NADPH: nicotinamide adenine dinuceotide phosphate; PQ: plastoquinone; PQH2: plastoquinol; PSI: photosystem I; PSII: photosystem II; RuBP: ribulose 1,5-biphosphate.

In spite of the fact that microalgae are around 10-50 fold more efficient using light energy than terrestrial plants (Chisti, 2007; Yadav and Sen, 2017), maximum theoretical photosynthetic efficiencies can only reach up to 12% (Raeisossadatti et al., 2019).

There are several reasons for this low photosynthetic efficiency (Behera et al., 2018): i) photosynthetic organisms can only use the photosynthetically active radiation (PAR), i.e., the light fraction in the wavelength range of 400-700 nm (Nwoba et al., 2019; Pires et al., 2017), which accounts for around 43% of the total solar radiation (Ringsmuth et al., 2016); ii) PSI and PSII reaction centres can capture PAR with nearly 100%, but they cannot use all the photons for photosynthetic purposes (Kirst et al., 2017). Dissipation of energy in the form of heat or fluorescence therefore occurs (Baker, 2008; Huang et al., 2017); iii) algae respiration, which can account for 20-30% of the maximum growth rate (Béchet et al., 2013); and iv) photorespiration processes which decrease the energy available for microalgae growth (Ippoliti et al., 2016; Manhaeghe et al., 2019). Net rate of microalgae photosynthesis is therefore vital regarding microalgae growth rate and nutrient absorption (Behera et al., 2018).

2.2. Factors that influence microalgae growth

Microalgae cultivation depends on many factors (Huang et al., 2019). Some of them are related to weather conditions (Jebali et al., 2018; Marazzi et al., 2019; Viruela et al., 2016), while others are associated with operational parameters and the reactor configuration (Chisti, 2007; Pires et al., 2017; Viruela et al., 2018). Some of these factors are explained below:

2.2.1. Light

Light is a key parameter related to the microalgae photoautotrophic metabolism (Ferreira et al., 2019; Shoener et al., 2019) since it influences the amount of ATP and NADPH that will be produced (Yadav and Sen, 2017). Light must thus be applied at the proper intensity, duration and wavelength to obtain optimum microalgae growth (Abu-Ghosh et al., 2016; Xu et al., 2019).

Microalgae growth is directly proportional to light intensity until it reaches an optimum value (Raeisossadati et al., 2019; Reynolds, 2006). If light intensity is below an optimum value, microalgae growth will be limited. On the other hand, if it surpasses the optimum, microalgae will be damaged and suffer from photoinhibition, which decreases microalgae growth and photosynthetic efficiency (Raeisossadati et al., 2019; Straka and Rittman, 2018).

The light intensity effect on the treatment of AnMBR effluent has been previously evaluated in lab-conditions (González-Camejo et al. 2018), showing an enhancement on microalgae performance with increasing light intensity, with a maximum irradiance of 125 $\mu mol \cdot m^{-2} \cdot s^{-1}$. However, in outdoor conditions, microalgae are exposed to continuous changes in light intensity because of diurnal and seasonal variations in solar irradiance (Galès et al., 2019). Changing outdoor conditions can lead to phenomena such as photoacclimation and photodamage (García-Camacho et al., 2012). Due to photoacclimation, microalgae are able to reduce the non-photochemical quenching (Baker, 2008) or increase light absorption under low light irradiances (Straka and Rittman, 2018). However, a sudden rise from low to high light irradiances can lead to photodamage of PSI and PSII (Pires et al., 2017). Photodamage can be repaired by a complex process which involves disassembling the damaged components and reassembling the photosystem units (Straka and Rittman, 2018). Maximum quantum efficiency (F_v/F_m), which is the maximum efficiency at which light absorbed by PSII is used for reducing the primary quinone electron acceptor (Q_A) (Baker, 2008), can be

used as in indirect measure of the PSII efficiency. In this respect, a reduction of F_v/F_m to lower values than around 0.65 is an indicator of photochemical stress of the eukaryotic algae (Moraes et al., 2019).

Outdoor microalgae cultivation is also influenced by the light availability of the culture. Light path depth, microalgae biomass and microalgae's pigments increase the light attenuation within the culture (Abu-Ghosh et al., 2016; Huang et al., 2017; Wagner et al., 2018). Light attenuation implies that microalgae close to the illuminated surface are exposed to high light intensities and are likely to suffer from photoinhibition (Pires et al., 2017), while algae in the deepest places of the reactor remain in darkness (Raeisossadati et al., 2019). Only restricted parts of the reactor will receive light at their saturation point. In these zones, maximum photosynthetic rate would be attained. If the microalgae reactor is well-mixed, the culture will rapidly move from lighting to dark zones (Kubelka et al., 2018), being therefore exposed to an average light irradiance, i.e. total light integration (Barceló-Villalobos et al., 2019). On the other hand, when mixing is poor, microalgae will adapt to intermittent light; i.e. to light:dark (L:D) cycles (Fernández-Sevilla et al., 2018), which is known as local adaptation. It must be noted that light integration enables to obtain higher biomass productivities than local adaptation (Barceló-Villalobos et al., 2019).

To overcome light attenuation in outdoor conditions, additional artificial light can be applied to the microalgae culture in order to achieve higher microalgae performance (Ruiz-Martínez, 2015; Su et al., 2012). Artificial illumination provides better regulation of the light photons and photoperiods; which can enhance photosynthesis performance (Abu-Ghosh et al., 2016). However, artificial illumination is highly energy-demanding.

2.2.2. Temperature

Temperature is another key factor in microalgae growth (Ras et al., 2013). Similar to light intensity, temperatures under the optimum reduce microalgae growth since they lower the rate of enzymatic processes (Reynolds, 2006; Serra-Maia et al., 2016). On the other hand, temperatures above the optimum decrease microalgae performance because the protein degradation is triggered, which can lead to cell death (Koç et al., 2013; Ras et al., 2013).

Most of microalgae can grow in a wide temperature range : around 20-35 °C (Bitog et al., 2011; Chisti, 2007); although the optimum temperature value is species-specific (Enamala et al., 2018). By way of example, Binnal and Babu (2017) reported optimum

temperature for green algae *Chlorella protothecoides* of 25 ºC, while Cabello et al. (2015) obtained optimum temperature of 35 ºC for green microalgae *Scenedesmus obtusiusculus*.

Temperature not only influences microalgae directly, but also affects other parameters related tomicroalgae growth, such as the solubility of CO_2 in the medium, the equilibrium of chemical species and the pH-value (Solimeno et al., 2015), as will be explained below.

2.2.3. pH

Apart from light and temperature, pH is another relevant parameter related to microalgae growth (Pawlowski et al., 2016). Each microalgae strain presents an optimum pH range (Moheimani, 2013). Out of this range, microalgae productivity is hampered (Yadav and Sen, 2017). By way of example, optimal pH range for green microalgae is around 7-8 (Eze et al., 2018; Qiu et al., 2017), while cyanobacteria are favoured at pH values higher than 9.0 (González-López et al., 2012).

It must be considered that microalgae activity raises pH because of CO_2 assimilation (Izadpanah et al., 2018). This is especially relevant under solar illumination, where pH can increase over values of 9 at midday (Acién et al., 2016). The reason is the distribution of carbon species in the equilibrium, which is linked to pH. CO_2 is the major carbon species when pH is under 6, while carbonate (CO_3^{2-}) dominates the equilibrium under pH over 10. At pH 7-9, the predominant form is bicarbonate (HCO_3^-), which is the preferable carbon species for microalgae growth (Huang et al., 2017). On the other hand, microalgae only tolerate a certain amount of free CO_2 concentration, above which it is detrimental (Kumar et al., 2011). Regarding carbonate, most microalgae are not able to absorb it (Bhakta et al., 2015).

Raising pH also affects nitrogen and phosphorus availability in the culture (Ruiz-Martínez, 2015). In this respect, pH over 9 favours ammonia in the ammonium-ammonia (NH_4^+/NH_3) equilibrium (Acién et al., 2016). This is not convenient since ammonia can inhibit the photosynthetic process (Sutherland et al., 2015). Furthermore, nitrogen can be lost from the medium by ammonia stripping (Muñoz and Guieysse, 2006).

With respect to phosphorus, pH over 9 causes the chemical precipitation of phosphorus, which reduces the bioavailability of this nutrient and diminishes the light dispersion in the microalgae culture (Muñoz and Guieysse, 2006). For this, even if wastewater is not

carbon-limited (see section I.2.2.4), CO_2 injection is beneficial to control the culture pH (Acién et al., 2016). In this respect, pH lower than 7.5 has reported negligible ammonia volatilisation and phosphorus precipitation (Tan et al., 2016).

2.2.4. Nutrients

Nutrients are essential elements for microalgae growth and are classified in macronutrients (carbon, nitrogen and phosphorus) and micronutrients such as sulfur, silica, calcium, magnesium, cobalt, potassium, zinc, iron, manganese, copper and trace minerals (Enamala et al., 2018; Romero-Villegas et al., 2018a; Yadav and Sen, 2017).

Nitrogen (N) is a basic element for the synthesis of proteins, photosynthetic pigments and nucleic acids (Baroni et al., 2019) and can account for 3-12% of the microalgae dry weight (Reynolds, 2006). It can be assimilated in the form of ammonium (NH_4), nitrate (NO_3), nitrite (NO_2) and others (Razzak et al., 2017; Ruiz-Martínez, 2015). Within these nitrogen species, NH_4 is the preferred nitrogen source (Barbera et al., 2018; Gao et al., 2018). Nitrogen has to be present in the medium in the proper concentration range, which has been reported to be around 10-100 mg $N \cdot L^{-1}$ (Ling et al., 2019). Values under 10-13 mg $N \cdot L^{-1}$ can limit microalgae growth (Ruiz-Martínez et al., 2014), while NH_4 concentrations over 200 mg $N \cdot L^{-1}$ can be toxic for microalgae because of ammonia formation (Park et al., 2010).

Phosphorus (P) is another macronutrient and is present in essential molecules such as nucleic acids, phospholipids and ATP (Razzak et al., 2017). It is mainly assimilated in the form of orthophosphates (PO_4) (Barbera et al., 2018) and it often accounts for 1-1.2% of microalgae dry weight (Reynolds, 2006). However, microalgae show the capacity of absorbing more phosphorus than needed in the form of polyphosphates (Ruiz-Martínez, 2015), achieving values over 3% of algae dry weight (Powell et al., 2008; Whitton et al., 2016). This is known as luxury uptake (Powell et al., 2009) and depends not only on the phosphate concentration in the medium, but also on ambient conditions such as light and temperature (Powell et al., 2008).

Polyphosphates can be used when phosphorus concentration in the medium is low (Powell et al., 2009). Under these conditions, the intracellular phosphorus content can drop up to 0.2-0.4% of microalgae dry weight (Reynolds, 2006). In fact, microalgae cells can vary their internal nitrogen and phosphorus concentrations, as well as the internal nitrogen:phosphorus (N:P) ratio, according to the N:P ratio of the medium

(Beuckels et al., 2015; Whitton et al., 2016), presenting a wide range of these ratios; i.e. between 7-42 (Beuckels et al., 2015; Ruiz et al., 2013).

Carbon (C) is the main nutrient for microalgae, which can account up to 50% of their biomass (Behera et al., 2018; Yadav and Sen, 2017). It must be considered that wastewater is usually carbon-limited. Hence, an additional inorganic carbon source such as carbon dioxide or bicarbonate is often needed for maximising nitrogen and phosphorus assimilation (Acién et al., 2016; Park et al., 2010). In this respect, Uggetti et al. (2018) reported an increase of 66-100% of biomass concentration when CO_2 was added to the culture.

Sulphur (S) also plays an important role in microalgae metabolism since it is found in membrane sulpholipids, vitamins and various metabolites (Mera et al., 2014; González-Sánchez and Posten, 2017). Furthermore, limiting sulphur conditions have been reported to reduce microalgae activity as it implies the decline of chlorophyll and Rubisco enzyme content (Giordano et al., 2000). However, sulphur excess can limit microalgae growth (Mera et al., 2014); especially in its reduced form (H_2S). By way of example, Küster *et al.* (2005) obtained 50% inhibition of green microalgae *Scenedesmus* at sulphide concentrations of around 2 mg $S \cdot L^{-1}$, while González-Sánchez and Posten (2017) found that green algae *Chlorella* sp. were inhibited at sulphide concentrations higher than 16 mg $S \cdot L^{-1}$.

Other micronutrients (i.e., calcium, magnesium, potassium, etc.) are usually present in the wastewaters in sufficient concentrations to support microalgae growth (Daneshvar et al., 2018).

2.2.5. Abiotic factors

Apart from the aforementioned abiotic factors; i.e. light, temperatures, nutrients and pH, there are others that can significantly affect microalgae growth.

Cultivation mode influences microalgae growth rate and productivity (Behera et al., 2018; Huang et al., 2019). In fact, continuous operation tends to obtain higher biomass productivities in comparison to batch mode (Ruiz et al. 2013). During continuous cultivation, nutrients are added to the culture continuously and microalgae are thus maintained in the exponential growth phase (McGinn et al., 2012). In addition, under continuous operation, parameters such as biomass retention time (BRT) and hydraulic retention time (HRT) can play a significant role in microalgae performance (Valigore et

al., 2012; Xu et al., 2015), since they can affect microalgae biomass productivity and nutrient recovery/removal (Luo et al., 2017).

Another important operating parameter is mixing as it enables to maintain culture homogenisation, improves the CO_2-mass transfer and prevents microalgae sedimentation and cell attachment to the reactor walls (Huang et al., 2017; Yadav and Sen, 2017). Mixing also helps to avoid photorespiration due to excessive O_2 accumulation (Almomani et al., 2019). In addition, mixing involves the microalgae movement from the highly illuminated areas of the reactor to dark zones, as explained in section I.2.2.1. However, excessive mixing increase the operating costs and can damage microalgae cells because of shear stress (Pires et al., 2017; Vo et al., 2019).

2.2.6. Biotic factors

Pure cultures can only be cultivated in highly-controlled conditions in sterilised medium. In other cases, a mix of microalgae and other microorganisms such as bacteria is expected (Acién et al., 2016; Luo et al., 2018). These microorganisms can compete with microalgae for nutrient assimilation (Galès et al., 2019). In this respect, the competition between microalgae and ammonium oxidising bacteria (AOB) for ammonium uptake plays a significant role in culture performance, especially when treating wastewater streams with low organic loads such as AnMBR effluents (González-Camejo et al., 2018). Appropriate lighting and nutrient-replete conditions have been reported to favour microalgae growth (Choi et al., 2010). However, high temperature, poor lighting conditions, low microalgae concentrations or inappropriate dilution rates (i.e. inverse of HRT) can be favourable for nitrifying bacteria growth (Galès et al., 2019; González-Camejo et al., 2018; Marcilhac et al., 2014). The competition between microalgae and nitrifying bacteria for ammonium uptake thus has to be further studied under outdoor conditions since it can seriously affect the operation of this microalgae cultivation system.

On the other hand, under low nutrient concentrations, cyanobacteria proliferation can occur (Arias et al., 2017). It must be also considered that microalgae activity implies the release of algal organic matter (AOM), which can boost heterotrophic bacteria and grazer growth (Luo et al., 2018). Bacteria and cyanobacteria proliferation produces microalgae allelopathic substances and toxins that may damage microalgae cells (Lam et al., 2018; Rajneesh et al., 2017). In addition, t grazers such as protozoans and metazoans are able to predate microalgae, reducing microalgae concentration in the

culture (Day et al., 2017; Galès et al., 2019). Hence, operating conditions of microalgae cultivation systems must be controlled in order to reduce the activity of competing organisms.

3. MICROALGAE APPLICATIONS

The increasing interest in microalgae cultivation relies basically on their capacity to absorb carbon dioxide (Enamala et al., 2018) and remove inorganic nutrients from wastewater (Acién et al., 2016). Microalgae cultivation also implies the production of microalgae biomass that can be used to obtain biofuels and other valuable products (Guldhe et al., 2017; Xu et al., 2019).

It must be considered that the final application of the microalgae biomass depends on the biomass production process (Garrido-Cárdenas et al., 2018). For instance, biomass produced using wastewater as culture medium cannot be used for feeding purposes.

3.1. Wastewater treatment

Algae-based wastewater treatment has appeared as a sustainable option due to the microalgae capacity of recovering nitrogen and phosphorus (Acién et al., 2016; Nayak et al., 2018). In addition, microalgae cultivation has been reported to consume up to 24% less energy than conventional wastewater systems (Romero-Villegas et al., 2018a). Microalgae can also remove other pollutants such as heavy metals, organic pollutants, pathogens and contaminants of emerging concern (López-Serna et al., 2019; Vo et al., 2019).

Hence, algae-based wastewater treatment processes are able to produce a reclaimed water stream with low amounts of nutrients and some valuable microalgae biomass simultaneously (Batstone et al., 2015; Seco et al., 2018).

3.2. Biofuels

Microalgae can be used as renewable energy source . Depending on the transformation process, microalgae biomass can be converted in biogas, biodiesel, bioethanol, biohydrogen, etc. (Guldhe et al., 2017; Ruiz-Martínez, 2015).

Microalgae biomass contains considerable amounts of carbohydrates, lipids and proteins that can be anaerobically digested to produce biogas (Díez-Montero et al., 2018). However, since the microalgae carbon:nitrogen ratio (C:N) is usually too low for optimal anaerobic digestion (Behera et al., 2018), co-digestion of algae with carbon

substrates such as primary sludge appears as a suitable option for improving biogas production (Seco et al., 2018).

Biodiesel can be produced via transesterification of the lipid fraction of microalgae biomass. Biomass with high lipid content is therefore required (Chisti, 2007). It is widely known that algae can accumulate higher amount of lipids under nutrient deplete conditions (Ferreira et al., 2019). However, biodiesel production from algae is still challenging because of the high cultivation costs and the inefficiency of the lipid conversion processes (Guldhe et al., 2019).

Microalgae can also accumulate significant amount of carbohydrates that can be utilised to produce bioethanol. In addition, microalgae biomass can be used for biohydrogen production by two ways: water photolysis or dark fermentation (Guldhe et al., 2017). Nevertheless, these production technologies present high production costs that constrain their feasibility (Behera et al., 2018).

For all the different options related to biofuel production, the harvesting and dewatering step plays a key role since it is a very energy-demanding step of the process (Alkarawi et al., 2018; Molina-Grima et al., 2003) that accounts for around 3-15% of the total production costs of microalgae biomass (Fasaei et al., 2018).

3.3. Valuable products

Microalgae biomass can also be used in the food, cosmetic and pharmacy industries (Guldhe et al., 2017; Leu and Boussiba, 2014) since valuable compounds such as pigments (chlorophylls, carotenoids and phycobilins), omega fatty acids, proteins, vitamins, etc. can be synthesised from it (Garrido-Cárdenas et al., 2018).

Microalgae biomass can also be used as fertilisers for the agricultural industry (Marazzi et al., 2019; Seco et al., 2018). In addition, cyanobacteria can also produce poly-b-hydroxybutyrate (PHB). These molecules have thermoplastic properties and can therefore be utilised to produce bioplastics (Balaji et al., 2013).

4. MICROALGAE-BASED WASTEWATER TREATMENT

4.1. Wastewater streams

Microalgae have been demonstrated to assimilate nutrients from different wastewater streams, such as raw urban wastewater, primary and secondary effluents, centrates, agricultural and industrial wastewater, etc. Each wastewater stream presents different

characteristics such as variable nutrient concentrations, presence of toxic substances, inhibitors, bacteria, etc. (Cai et al., 2013; Ji et al., 2014).

Urban wastewater (or sewage) is composed of a mixed of domestic wastewater (around 80-95%) and industrial wastewater (around 5-20%) (Guldhe et al., 2017). Raw urban wastewater can present high variations on their characteristics depending on the wastewater source (Komolafe et al., 2014), including substances that can be toxic for microalgae such as metals and pathogens (Cai et al., 2013). High suspended solid (TSS) concentrations of raw wastewater can also have a negative effect on autotrophic microalgae because of the reduction of light availability on the culture (Guldhe et al., 2017).

Some research has been developed using raw urban wastewater (Ling et al., 2019). By way of example, Mennaa et al. (2015) assessed the cultivation of 7 microalgae species using pre-treated sewage as culture medium. However, most of the published research using raw wastewater has been evaluated in lab conditions and the behaviour at higher scales (pilot or full scale) might present significant differences (Guldhe et al., 2017).

Primary-treated effluents are expected to be more suitable microalgae media due to their lower TSS concentrations (Valigore et al., 2012). Nevertheless, primary effluents still present a relatively high organic matter load which can induce bacteria proliferation (Guldhe et al., 2017). On the other hand, secondary effluents contain low amounts of solids and organic matter and thus are more appropriate media for microalgae cultivation than primary effluents (Gao et al., 2019). Extensive research has been assessed microalgae cultivation in secondary effluents (AlMomani and Örmeci, 2016; Ruiz et al., 2013; Wu et al., 2017; Xu et al., 2015). However, they often present low nutrient concentrations which can limit microalgae growth (Gao et al., 2019). By way of example, Arbib et al. (2017) treated the secondary effluent of an urban WWTP, having nitrogen in the range of 17.77-20.93 mg $N \cdot L^{-1}$ and phosphorus in the range of 1.58-2.35 mg $P \cdot L^{-1}$. In consequence, biomass concentrations in these systems are usually below 500 mg $VSS \cdot L^{-1}$ (Barbera et al., 2018). On the contrary, AnMBR effluents from urban wastewater, apart from yielding high solids and organic matter removals, usually contain higher nutrient concentrations than secondary effluents because of the mineralisation of the organic matter (Giménez et al., 2011). In fact, nitrogen concentration can vary between 40-100 mg $N \cdot L^{-1}$, while phosphorus concentration can be around 4-10 mg $P \cdot L^{-1}$ (González-Camejo et al., 2018; Viruela et al., 2016). In addition, the main nitrogen source of these effluents is ammonium, which is the

preferable nitrogen species for microalgae (Gao et al., 2018; Eze et al., 2018). Hence, AnMBR effluents appear as ideal media for microalgae cultivation. In this respect, Ruiz-Martínez et al. (2012) reported the suitability of AnMBR effluent to cultivate microalgae in lab-conditions, obtaining nitrogen and phosphorus removal rates of 19.5 mg $N \cdot L^{-1} \cdot d^{-1}$ and 3.7 mg $P \cdot L^{-1} \cdot d^{-1}$, respectively, while biomass productivity reached 234 mg $TSS \cdot L^{-1} \cdot d^{-1}$. It was thus assumed that all the micronutrients needed for microalgae growth (Barbera et al., 2018) were contained in the AnMBR effluent.

Another approach relies on using the centrate of the anaerobically digested activated sludge (ADAS) to cultivate microalgae (Ma et al., 2014; Sepúlveda et al., 2015). This enables to reduce the high nutrient concentrations of the centrate (Marazzi et al., 2019), which can reach up to 1000 mg $N \cdot L^{-1}$ and 30 mg $P \cdot L^{-1}$ (Acién et al., 2016). If this centrate is recycled to the influent WWTP stream, nitrogen load can be increased by 10-20% (Tan et al., 2016). Consequently, if centrate is treated by microalgae, the footprint of the overall wastewater treatment process will be reduced (Guldhe et al., 2017). However, since too high ammonium concentrations are toxic for microalgae (Collos and Harrison, 2014) and centrate can contain inhibitory compounds such as urea, organic acids and pesticides (Djelal et al., 2014), the dilution of the centrate is often required prior to be fed to the microalgae culture (Acién et al., 2016; Tan et al., 2016). This dilution must be optimised; i.e. the optimal centrate concentration of the culture medium has to be evaluated (Guldhe et al., 2017; Sepúlveda et al., 2015). In this respect, nutrient removal rates of 36.9 mg $N \cdot L^{-1} \cdot d^{-1}$ and 5.38 mg $P \cdot L^{-1} \cdot d^{-1}$ have been obtained for the outdoor cultivation of marine microalgae *Nannochloropsis gaditana* in a medium composed of 20% of centrate (Romero-Villegas et al., 2017).

Microalgae can be also cultivated in other wastewater streams such as agro-industrial or industrial. However, cultivation in this media present several drawbacks, such as high variability in nutrient concentrations (Chiu et al., 2017), carbon limitation, high turbidity that reduces light penetration (Udaiyappan et al., 2017) and high amount of pesticides, antibiotics, heavy metals, nanoparticles or other toxic substances (Guldhe et al., 2017).

4.2. Microalgae strains

Many authors have recently evaluated pure microalgae cultures (Gao et al., 2016; Gupta et al., 2016; Ledda et al., 2015; Ma et al., 2014; Mata et al., 2012) with the goals of: i) looking for fast-growth strains, ii) studying the metabolism of the strains and iii)

improving the microalgae efficiency and nutrient removal capacity (Garrido-Cárdenas et al., 2018). In this regard, green microalgae genera *Chlorella, Monoraphidium* and *Scenedesmus* (Figure I.2) have been extensively reported as ideal for wastewater treatment due to their adaptability to such medium (Arias et al., 2018; Babaei et al., 2016; Pachés et al., 2018; Vo et al., 2019).

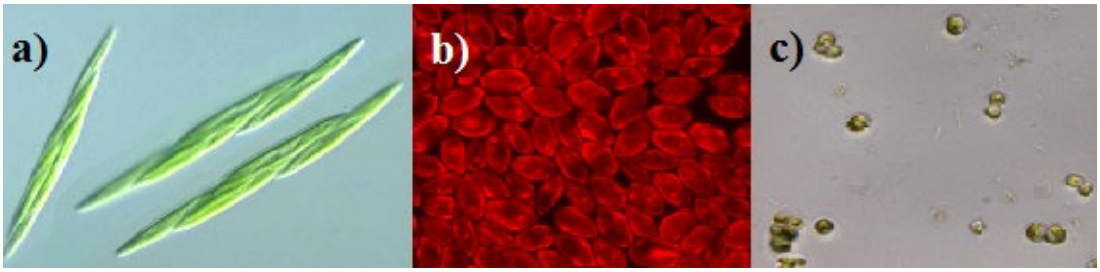

Figure I.2. Common green microalgae for wastewater treatment: a) Monoraphidium; b) Scenedesmus; c) Chlorella.

However, at large scales, cultures consisted of only single genus are difficult to maintain due to the contamination by other microorganisms (Acién et al., 2016; Day et al., 2017). In addition, polycultures can increase microalgae productivity because they are more robust and can use resources more efficiently (Behera et al., 2018; Thomas et al., 2019). In fact, some authors have reported higher biomass productivities and nutrient removal efficiencies in mixed microalgae cultures than in pure cultures (AlMomani and Örmeci, 2016; Gouveia et al. 2016; Wu et al. 2017).

Other authors have used cyanobacteria instead of green algae because of their capacity to produce certain metabolites such as phicobiliproteins and polyhydroxybutyrates; and also due to their soft cell wall, which make them easy to digest (Arias et al., 2017). However, the nitrogen removal (NRE) and the phosphorus removal efficiency (PRE) are usually lower than those obtained for green microalgae (Table I.1). The use of green microalgae thus seems to be preferable for wastewater treatment than cyanobacteria.

Green algae usually outcompete cyanobacteria in wastewater-borne cultures (Arias et al., 2017). However, cyanobacteria are strong competitors under low light conditions and temperatures above 21 ºC (Lam et al., 2018). Cyanobacteria are also favoured in low phosphorus-loaded waters (Arias et al., 2018; Passarge et al., 2006). As a case in point, Garcia et al. (2018) treated a mix of agricultural and urban wastewater in a pilot-scale horizontal tubular PBR. In their study, cyanobacteria outcompeted green algae in

summer and autumn, while in winter and spring, green microalgae dominated the culture.

Another approach regarding algae-based wastewater treatment is using microalgae-bacteria consortia (Delgadillo-Mirquez et al., 2016; Marcilhac et al. 2014; Rada-Ariza et al., 2019). This mixed culture enables the simultaneous removal of organic matter and nutrients due to symbiotic interactions (Lam et al., 2018). During photosynthesis, microalgae produce oxygen which is used by bacteria to oxidise the organic matter. Microalgae also release some organic compounds that can be used by bacteria as carbon source (Luo et al., 2018). As a consequence of the organic matter degradation, carbon dioxide, which can be used by algae as inorganic carbon source, is produced (Gonçalves et al., 2017).

On the contrary, microalgae-bacteria consortia also present some competitive interactions. Firstly, these microorganisms can compete for nutrients. In addition, both microalgae and bacteria can release some toxic compounds that can negatively affect one another. Furthermore, microalgae photosynthetic activity produces an increase in pH that can have detrimental effects on bacteria (Gonçalves et al. 2017; Lam et al., 2018). Using a microalgae-bacteria consortium also prevents the possibility of recovering energy from the organic load of the influent wastewater in the form of biogas. Moreover, the bacteria biomass present in the consortia increases the shadow effect of the culture, therefore decreasing the light availability of algae (Wagner et al., 2018).

To sum up, Table I.1 shows a summary of trials with different microalgae strains and wastewater streams.

Table I.1. Biomass productivities and nutrient removal efficiencies of different microalgae strains and wastewater streams.

Species	Type of wastewater	Productivity (mg VSS·L^{-1}·d^{-1})	NRE (%)	PRE (%)	Reference
Chlorella vulgaris	Secondary effluent	-	55.9	11.5	AlMomani and Örmeci (2016)
Neochloris oleoabundans	Secondary effluent	-	56.8	5.7	AlMomani and Örmeci (2016)
Mix indigenous microalgae	Secondary effluent	-	67.3	30.8	AlMomani and Örmeci (2016)
Cyanobacteria + green algae	ADAS + secondary effluent	120	57.5	83.3	Arias et al. (2018)
Microalgae consortium	Primary effluent	-	83	100	Delgadillo-Mirquez et al. (2016)
Scenedesmus obliquus	Aquaculture	6.2	86.1	82.7	Gao et al. (2016)
Mixed microalgae and bacteria culture	AnMBR effluent	94	> 99	> 99	González-Camejo et al. (2018)
Chlorella sorokiniana	Raw sewage	-	86.9	68.2	Gupta et el. (2016)
Scenedesmus obliquus	Raw sewage	-	98.5	98.0	Gupta et el. (2016)
Chlorella sp.	Centrate	100	95	85	Ledda et al. (2015)
Chlorella + Filamentous microalgae	Horticultural	53.7-57.1	69	79	Liu et al. (2016)
Chlorella vulgaris	Centrate	-	59.2	69.6	Ma et al. (2014)
Scenedesmus obliquus	Synthetic brewery effluent	900	20.8	56.9	Mata et al. 2012
Scendesmus obliquus	Secondary effluent	380	86.8	97.8	Ruiz et al. (2013)
Scenedesmus LX1	Secondary effluent	450	72.6	~100	Wu et al. (2017)
Haematococcus pluvialis	Secondary effluent	350	73.7	~100	Wu et al. (2017)
Scenedesmus LX1 + Haematococcus pluvialis	Secondary effluent	530	85.0	~100	Wu et al. (2017)

4.3. Outdoor microalgae cultivation

All the studies showed in Table I.1 (and many others) were developed under controlled lab conditions. Although these results are generally promising in terms of biomass productivity and nutrient removal efficiency, up-scaling of microalgae cultivation technologies to outdoor conditions are often uncertain (Vo et al., 2019), mainly because of variable ambient conditions (such as light irradiance, temperature and nutrient load), outer contamination, poor mass transfer within the culture and light attenuation (Huang et al., 2017; Ippoliti et al., 2016; Jebali et al., 2018). By way of example, Viruela et al. (2016) attained much lower performance in the treatment of AnMBR effluent under outdoor conditions than Ruiz-Martínez et al. (2012) using similar microalgae strain and substrate. Indeed, nitrogen recovery rate (NRR), phosphorus recovery rate (PRR) and biomass productivity (BP) were reduced by 75%, 83% and 82%, respectively, under outdoor conditions.

When treating real sewage under outdoor conditions, indigenous naturally occurring microalgae polycultures have been reported to achieve higher adaptability than commercial microalgae monocultures (Galès et al., 2019; Thomas et al., 2019). Hence, this is often the preferable choice for outdoor microalgae-based wastewater treatment processes.

Microalgae can be cultivated in open ponds or closed photobioreactors (PBRs) (Ferreira et al., 2019; Nwoba et al., 2019).

4.3.1. Open ponds

Open systems such as raceway ponds (Figure I.3) are generally more cost-efficient and easier to operate than closed PBRs (Razzak et al., 2017; Xu et al., 2019). However, in open systems, the process control is controversial since they are significantly more affected by ambient factors than closed systems (Behera et al., 2018). Moreover, the contamination by other organisms such as heterotrophic bacteria, grazers, viruses and undesirable photosynthetic organisms are difficult to avoid (Day et al., 2017; Lam et al., 2018; Vo et al., 2019). These aspects negatively affect microalgae biomass production (García-Galán et al., 2018; Wang et al., 2012). In addition, open systems present the risk of nitrogen losses due to ammonia stripping, which can account up to 73% (Romero-Villegas et al., 2018a). In case of adding CO_2 for pH control, carbon dioxide would also be lost to the atmosphere in these reactors (Acién et al., 2016).

Figure I.3. Open raceway pond.

Open reactors are usually operated at wastewater depths of 15-40 cm and HRTs of 5-10 days (Arbib et al., 2017; Acién et al., 2016). Hence, another issue of this technology is the large surface areas that are needed to successfully cultivate microalgae (García-Galán et al., 2018; Xu et al., 2019).

4.3.2. Closed photobioreactors

Microalgae cultivation in closed PBRs presents higher process control (Kumar et al., 2011; Moraes et al., 2019). They are usually designed with the goal of attaining high photosynthetic efficiencies in order to increase the biomass productivity and nutrient removal of the microalgae culture (Huang et al., 2017; Razzak et al., 2017). These reactors also enable perfect mixing, allowing nutrient and light homogenisation within the culture (Barceló-Villalobos et al., 2019).

In addition, since PBRs remain close, CO_2 and ammonia losses by stripping are significantly reduced, as well as the risk of contamination by other microorganisms (Behera et al., 2018; Ferreira et al., 2019). However, these reactors present higher operational costs than open reactors (Moraes et al., 2019; Vo et al., 2019), especially when temperature control is needed to avoid overheating. Another controversial aspect is biofouling (Chisti, 2007; García-Galán et al., 2018). It occurs when microalgae get stick to the reactor walls, which reduces the light availability of the culture and hinders nutrient assimilation (Razzak et al., 2017).

Different PBR configurations have been widely reported: tubular, vertical columns and flat-panel PBRs (Huang et al., 2017; Verma and Srivastava, 2018): Figure I.4.

Figure I.4. Closed PBRs: a) Tubular PBRs (de Andrade et al., 2016); b) vertical columns (www.oilalgae.com); c) Flat-panel PBR.

Tubular PBRs consists of a set of cylindrical pipes which can be arranged horizontally, vertically or even in spiral shapes (Ruiz-Martínez et al., 2015). Diameter is generally shorter than 10 cm. Hence, they present high surface to volume (S:V) ratio (Huang et al., 2017). The culture can circulate through the pipes using pumps or airlift systems, which increases the power consumption (Vo et al., 2019). A degassing unit is often needed because the accumulation of oxygen concentrations over 400% of saturation concentration can inhibit microalgae growth (Chisti, 2007).

Column PBRs are arranged vertically and the culture is aerated through its bottom to achieve appropriate culture mixing. This PBR configuration is quite simple and enables good gas-liquid mass transfer (Huang et al., 2019; Vo et al., 2019). However, their costs are high and present scalability problems (Verma and Srivastava, 2018).

Flat-panel PBRs consist of rectangular PBRs with a narrow light path, which enables them to present high S:V ratios (Vo et al., 2019). They also have lower operating costs than other PBR configurations (Huang et al., 2017). However, the aeration is carried out by perforated tubes at the PBR base resulting in dead pockets and sometimes in shear stress that can reduce microalgae performance (Verma and Srivastava, 2018). In addition, flat-panel PBRs are usually more light-limited than other configurations such as tubular PBRs (Romero-Villegas et al., 2018b).

As a case in point, de Vree et al. (2015) compared these different technologies in outdoor conditions and obtained higher photosynthetic efficiencies in the vertical PBRs; i.e. 4.2% for a vertical tubular PBR and 3.8% for a flat-panel PBR; while the horizontal tubular PBR only attained 1.8%. The most likely reason was that vertical configurations

suffered less photoinhibition because solar radiation does not directly illuminate vertical surfaces (Mirón et al., 1999).

Table I.2 displays a summary of studies related to microalgae-based wastewater treatment under outdoor conditions (Table I.2). Results, although promising, must still be improved to increase the process feasibility . Extensive research is therefore needed in order to implement this microalgae-based technology for wastewater treatment at industrial scale.

Table I.2. Average biomass productivities and nutrient removal efficiencies for different outdoor PBR configurations.

Species	Type of wastewater	Type of PBR	HRT (d)	Productivity ($mgVSS \cdot L^{-1} \cdot d^{-1}$)	NRE (%)	PRE (%)	Reference
Scenedesmus obliquus	Secondary effluent	HRAP	10	30	77.0	63.2	Arbib et al. 2013
Scenedesmus obliquus	Secondary effluent	Tubular airlift	5	547	94.9	94.0	Arbib et al. 2013
Green algae + cyanobacteria	Agricultural + urban	Horizontal tubular	5	20	65	> 95	García et al. (2018)
Green algae + cyanobacteria	Agricultural	Horizontal tubular	16	4(1)	95	100	García-Galán et al. (2018)
Mixed green microalgae	Primary effluent	Vertical bubble column	~35	900(2)	98(2)	100(2)	Gouveia et al. (2016)
Desmodesmus apoliensis	Anaerobic pond effluent	HRAP	8	-	76	68	Sutherland et al. (2017)
Chlorella pyrenoidosa	ADAS + secondary effluent	Vertical	14(3)	633	77.5	61.7	Tan et al. (2016)
Microalgal bacterial flocs	Aquaculture	SBR(4)	4-8	8	3.6	0.29	Van den Hende et al. (2014)
Scenedesmus sp.	AnMBR effluent	Flat-panel PBR	8	23.4	41.6	36.1	Viruela et al. (2016)

(1) mg $TSS \cdot L^{-1} \cdot d^{-1}$; (2) maximum values; (3) batch operation. BRT/HRT indicates the duration of the study; (4) SBR: Sequencing batch reactor.

Other PBR´s designs have been reported with the aim at creating a more effective flashing light effect (FLE) in the microalgae culture than the FLE randomly created by mixing (Abu-Ghosh et al., 2016; Xue et al., 2013). Other authors have tried to reduce the dark volume by introducing LED lamps in the cultures (Castrillo et al., 2018).

However, the transition from prototypes to outdoor microalgae cultivation has not been successfully achieved.

4.3.3. Separation of algae biomass

Whichever the microalgae cultivation system is selected (section I.4.3), harvesting of microalgae biomass to separate it from water appears as a key factor of the process (Alkarawi et al., 2018). In fact, a harvesting step is needed because: i) effluents can contain some microalgae that have to be removed if water wants to be reused; ii) the microalgae biomass concentration in the culture is too diluted to produce biofuels or other compounds (section I.3).

Generally, harvesting of microalgae biomass is challenging due to the low recovery efficiencies of some harvesting technologies and their high capital and operational costs (Alkarawi et al., 2018). Separation of algae from water could be attained by gravity sedimentation, flocculation, flotation, centrifugation and filtration (Table I.3).

Gravity sedimentation of microalgae usually presents some difficulties such as biomass losses in the effluent because of the poor settling rate of microalgae biomass (Japar et al., 2017). This also implies obtaining low-quality effluents with regard to suspended solids. For this, some authors have developed microalgae technologies different from those based in algal suspensions such as sequencing batch reactors (Arias et al., 2018) or biofilm systems (Zhang et al., 2018). In these reactors, microalgae tend to form flocs together with bacteria, cyanobacteria or filamentous algae, promoting the harvesting capacity of the culture but reducing light availability.

Flocculation can be used to aggregate microalgae cells in order to create bigger flocs that settle faster, easing the sedimentation process (Mata et al., 2010). However, flocculation implies the use chemical reagents (flocculants) with the subsequent cost increase (Brennan and Owende, 2010; Daverey et al., 2019). Some of the most common flocculants are metal salts that can damage microalgae, disabling them for some purposes (Molina-Grima, 2003).

On the other hand, as microalgae have low density, flotation seems to be a suitable approach to separate them from water (Alkarawi et al., 2018). In flotation, microalgae particles will float upwards more quickly with the help of air bubbles (Japar et al., 2017). However, as it occurs with flocculation, a surfactant or a coagulant such as cetyl-trimethyl-ammonium bromide (CTAB), chitosan is usually needed to make the cells hydrophobic and to expand the mass transfer between the air and microalgae cells for

the enhancement of particles separation. CTAB has been reported to disrupt algae cell walls, enhancing cell lysis (Alkarawi et al., 2018). This fact prevents the recirculation of microalgae biomass to the culture in case BRT would want to be decoupled from HRT.

Centrifugation consists of applying a centrifugal force that is higher than the gravitational force to separate the components with different density; i.e., algae and water (Razzak et al., 2017). Although this process is rapid and has shown its capability of harvesting most microalgae cell types (Japar et al., 2017), it is also very energetically costly (Molina-Grima, 2003) and can damage microalgae because of the shear stress applied (Harun et al., 2010). In addition, the removal of the extracellular organic matter (EOM) released by algae from the water media is not usually very efficient (Yu et al., 2018).

On the other hand, membrane filtration appears as one of the most competitive separation methods (Harun et al., 2010; Judd et al., 2015). Membrane technology enables to retain the majority of microalgae biomass in one side of the membrane, therefore achieving higher biomass concentrations in the culture and a high-quality permeate (Razzak et al., 2017; Udaiyappan et al., 2017). However, a major concern of membrane-based systems is fouling (section I.5.4).

Table I.3. Advantages and disadvantages of microalgae biomass separation technologies.

	Advantages	Disadvantages	References
Sedimentation	- Simple - Low capital and operation costs	- Poor settling rate of microalgae - Low quality of effluent - Biomass losses - Time consuming - Diluted biomass concentration	Alkarawi et al., (2018) Baroni et al., (2019) Japar *et al.* (2017) Razzak et al. (2017)
Flocculation	- Faster settling rate than sedimentation - Better quality of effluent	- Use of chemical reagents (metal salts mainly) - Extra cost - Metal can disable microalgae	Baroni et al. (2019) Brennan and Owende (2010) Daverey et al. (2019) Molina-Grima et al. (2003)
Flotation	- Low capital costs - Faster than sedimentation - High efficiencies	- Use of reagents - Extra cost - Possible disruption of microalgae	Alkarawi et al. (2018) Japar et al. (2017)
Centrifugation	- Rapid - Capable of harvesting most algal cell types	- Very energetically costly -Shear stress - Low EPS removal	Molina-Grima et al. (2003) Harun et al. (2010) Japar et al. (2017) Razzak et al. (2017) Yu et al. (2018)
Filtration	- High-quality permeate in terms of TSS - Higher biomass concentration in the culture - Low space requirement - Operational simplicity	- Air-sparging costs - Membrane fouling.	Molina-Grima et al. (2003) Harun et al. (2010) Judd et al., 2015 Qasim et al. (2018)

5. FLAT-PANEL MEMBRANE PHOTOBIOREACTORS (MPBR)

Flat-panel membrane photobioreactor technology consists of the combination of microalgae cultivation in flat-panel PBRs and membrane technology to separate the algae biomass from the water. This allows decoupling BRT from HRT. Hence, more concentrated microalgae biomass and higher quality effluents can be achieved.

Some MPBR approaches have been evaluated in lab conditions, attaining promising results (Table I.4). However, the up-scaling to outdoor conditions has been scarcely reported. Further research must thus be developed in outdoor flat-panel MPBR plants in order to improve the feasibility of this technology. Special efforts have to be made regarding the operating conditions of MPBR systems (such as BRT and HRT), light availability of the culture, control and automation of the process, membrane operation, etc. In addition, the effect of ambient conditions in MPBR performance must be deeper studied to get some information of both the simple effect of one parameter (for instance, light and temperature), as well as the combined effects of all the factors related to microalgae growth. The effect of possible inhibitions by abiotic (section I.2.2.5) and biotic factors (section I.2.2.6) can also be relevant in MPBR performance and has to be therefore evaluated.

Table I.4. Average biomass productivities and nutrient removal efficiencies for lab-scale MPBR systems.

Species	Type of wastewater	BRT (d)	HRT (d)	Productivity ($mgVSS \cdot L^{-1} \cdot d^{-1}$)	NRE (%)	PRE (%)	Reference
Chlorella vulgaris	Aquaculture	16(1)	1	7.3	86.1	82.7	Gao et al. (2016)
Chlorella vulgaris	Synthetic secondary effluent	21.1	2	48.8	76.9	88	Gao et al. (2018)
Chlorella vulgaris	Synthetic secondary effluent	9	1	52	31	30	Luo et al. (2018)
Chlorella vulgaris	MBR effluent	12	1	30.7	70	97	Marbelia et al. (2014)
Euglena sp.	Secondary effluent	60	4	11.2	96	70	Sheng et al. (2017)(2)
Chlorella vulgaris	Secondary effluent	10	1	98	95.3	94.9	Xu et al. (2015)

(1) Duration of the study; (2) Sequencing batch MPBR.

5.1. Decoupling of BRT and HRT

Microalgae have been reported to have relatively low growth rates (μ). By way of example, for green algae *Chlorella,* growth rates in the range of 0.186-0.87 d^{-1} have been found (Ledda et al., 2015; Ruiz-Marín et al., 2010; Xu et al., 2015), while for green algae *Scenedesmus,* growth rates of 0.285-0.94 d^{-1} have been reported (Nayak et al., 2018; Ruiz et al., 2013; Ruiz-Marín et al., 2010). According to Ruiz et al. (2013), maximum biomass productivity is obtained when BRT is equivalent to double of the inverse of the maximum specific growth rate of microalgae ($2 \cdot \mu^{-1}$). This would imply that, in the case of *Chlorella*, optimum BRT would be in the range of 2.3-10.8 d, while for *Scenedesmus* it would be in the range of 2.1-7 d. In fact, these values are similar than those reported in the literature for outdoor microalgae cultivation (Table I.2).

On the other hand, to achieve maximum nutrient recovery of microalgae, high nutrient loading rates are needed (Gao et al., 2016). In fact, Ruiz et al. (2013) reported that maximum nutrient recovery rates are attained when HRT values are similar than the inverse of the maximum specific growth rate (μ^{-1}). This would mean an HRT in the

range of 1.1-5.4 d for *Chlorella* , and in the range of 1.0-3.5 d for *Scenedesmus*. Hence, to obtain maximum biomass productivity and nutrient recovery from microalgae cultivation it seems necessary to decouple HRT from BRT, which implies a separation of microalgae culture from the water.

Optimum BRT and HRT are species-specific. In this respect, Arias et al. (2018) reported that, in a green algae-cyanobacteria culture, BRTs over 9 days tended to favour cyanobacteria, while shorter BRTs favoured green algae growth. This can be explained by the fact that organisms with higher specific growth rates would be favoured at lower HRT and BRT (Winkler et al., 2017). This means that too low HRT can also favour the proliferation of heterotrophic bacteria (Arias et al., 2018). Hence, BRT and HRT not only can play a significant role in achieving optimal microalgae performance in terms of nutrient recovery and biomass productivity, but also in the evolution of the competition between green algae and other microorganisms (Arias et al., 2018). Hence, further research must be developed regarding optimal BRT and HRT of continuous microalgae cultivation systems in order to better control the biological process.

5.2. Light path

Light path appears as a key parameter in the PBR´s design o. If light path is too wide, an important amount of the culture will remain in darkness because cells close to the surface absorb most of the applied light radiation (Abu-Ghosh et al., 2016). This is known as shadow effect, also called self-shading (Park and Lee, 2001) and causes a reduction in the light efficiency of microalgae (Gris et al., 2014). On the contrary, if light path is too short, microalgae can suffer from photoinhibition (Straka and Rittman, 2018) due to the high light intensity received. In this respect, Arbib et al. (2017) reported higher biomass volumetric productivity in 0.15 m-deep HRAP than in HRAP with a depth of 0.30 m.

Narrow light paths would also imply an increase in the surface area needed for the application of microalgae in wastewater treatment plants, which is one of their major drawbacks (García-Galán et al., 2018).

5.3. Performance indicators

A constraining factor in the application of microalgae cultivation technology is the inefficiency of large-scale cultivation techniques (Barbosa et al., 2003). Monitoring,

automation and control of microalgae cultivation process therefore is essential to implement microalgae-based technology for wastewater treatment.

As already mentioned, parameters such as light, pH and temperature have a direct influence on microalgae growth (section I.2.2). These parameters can be effectively measured by low-cost online sensors, which are reliable and involve low investment, maintenance and operational costs (Ruano et al., 2009).

Nonetheless, the data obtained by these low-cost sensors cannot be not directly used to monitor the performance of microalgae cultivation process. Other off-line measurements such as suspended solids and nutrient concentrations are usually employed instead, although these parameters often imply chemical analyses that are expensive, time-consuming and require certain delay (Foladori et al., 2018).

Hence, finding new indicators of microalgae performance have to be found to optimally monitor and control the process.

5.4. Membrane operation

Membrane filtration allows the separation of microalgae biomass (which is retained in one side of the membrane) from the water stream, which can be taken off the system as permeate (Bilad et al., 2018).

When microalgae cells and their secretions accumulate in the surface of the membranes (and inside their pores) a cake layer that hinders the permeate flux is formed and membrane permeability is therefore reduced (Bilad et al., 2014). This process is known as fouling and increases membrane maintenance and replacement costs (Qasim et al., 2018; Udaiyappan et al., 2017). Fouling can be reversible, which is mainly due to cake layer formation, or irreversible (for instance, cell debris retention in the pores). In the case of reversible fouling, biomass is not firmly attached to the membrane surface, so it can be removed by physical means, such as backwashing and/or gas-assisted membrane scouring (Qasim et al., 2018; Song et al., 2018a). On the other hand, irreversible fouling can only be removed by chemical reagents such as sodium hydroxide, sodium hypochlorite, acids, chelates or surfactants that weaken the cohesion forces between the membrane and the foulants (Porcelli and Judd, 2010; Song et al., 2018a). The use of these reagents increases membrane operation costs, generate wastes and determines the membrane life (Drews, 2010; Qasim et al., 2018). Thus, membrane filtration has to be adequately operated in order to present fouling rates as low as possible. In fact, membrane fouling has been reported to depend on membrane operating conditions such

as membrane flux, duration and frequency of the operating stages; i.e. filtration, relaxation and back-flushing (Robles et al., 2018). Membrane fouling has also been reported to depend on other factors such as BRT, HRT, temperature, wastewater characteristics, microalgae strains, membrane properties and the presence of EOM in the culture (Babaei and Mehrnia, 2018; Song et al., 2018a).

If microalgae is filtered in a separate tank, the tank volume is also a key factor to be considered as microalgae will remain in darkness inside it. In this respect, Viruela et al. (2018) raised the NRR, PRR and BP of an outdoor flat-panel MPBR by 15%, 67% and 41%, respectively, when reduced the non-photic volume (i.e., the percentage of the membrane tank volume with respect with the total volume) from 27.2% to 13.6%.

6. PERSPECTIVES OF MICROALGAE CULTIVATION SYSTEMS

In spite of the plenty advantages of microalgae-based wastewater treatment processes (Garrido-Cárdenas et al., 2018), they still present several challenges such as high capital and operating costs, which include CO_2 addition , temperature control, maintenance and periodic cleaning of the PBRs (Acién et al., 2016; Huang et al., 2017), etc. One possibility to reduce the capital costs is increasing the production capacity by optimising the cultivation process (Salama et al., 2017). However, actual PBRs are not able to reach high-dense cultures, mainly due to the variability of ambient conditions, moderate microalgae growth rates, contamination by other microorganisms and suboptimal operating and design conditions (Lam et al., 2018; Viruela et al., 2018). In consequence, the light efficiency of outdoor microalgae cultures are usually lower than expected. For industrial applications, microalgae rarely achieve photosynthetic efficiencies higher than 1.5-2% (Nwoba et al., 2019). This value is far from maximum photosynthetic efficiency, which is theoretically around 10% (Romero-Villegas et al., 2017).

Hence, new research on microalgae cultivation technology must focus on:

i) increasing light efficiency by reducing photoinhibition and photolimitation effects, for instance, by inducing appropriate light-dark (L/D) cycles;

ii) evaluating the optimal operating conditions;

iii) increasing the robustness of the microalgae-based process to avoid culture crashes;

iv) avoiding the proliferation of competing organisms without damaging microalgae;

v) decreasing the commonly operated HRT of around 5-10 days to reduce land requirements;

vi) reducing the power consumption of the process;

vii) looking for the most appropriate microalgae strains that support the ambient stress conditions;

vii) looking for the most efficient harvesting system in terms of costs and quality of the permeate;

viii) improving the downstream production processes to obtain biofuels or other products.

ix) using flue gas as carbon source to reduce operating costs.

Some of these research lines are further discussed in this PhD thesis.

REFERENCES

1. Abu-Ghosh, S., Fixler, D., Dubinsky, Z., Iluz, D., 2016. Flashing light in microalgae biotechnology. Bioresour. Technol. 203, 357-363. http://dx.doi.org/10.1016/j.biortech.2015.12.057
2. Acién, F.G., Gómez-Serrano, C., Morales-Amaral, M.M., Fernández-Sevilla, J.M., Molina-Grima E., 2016. Wastewater treatment using microalgae: how realistic a contribution might it be to significant urban wastewater treatment? Appl. Microbiol. Biotechnol. 100, 9013–9022. http://dx.doi.org/10.1007/s00253-016-7835-7
3. Alkarawi, M.A.S., Caldwell, G.S., Lee, J.G.M., 2018. Continuous harvesting of microalgae biomass using foam flotation. Algal Res.36, 125-138.https://doi.org/10.1016/j.algal.2018.10.018
4. AlMomani, F.A., Judd, S., Bhosale, R.R., Shurair, M., Al-Jaml, K., Khraisheh, M., 2019. Intergraded wastewater treatment and Carbon bio-fixation from flue gases using *Spirulina platensis* and mixed algal culture. Process Safety and Environmental 124, 240-250. https://doi.org/10.1016/j.psep.2019.02.009
5. AlMomani, F.A., Örmeci, B., 2016. Performance Of *Chlorella Vulgaris*, *Neochloris Oleoabundans*, and mixed indigenous microalgae for treatment of primary effluent, secondary effluent and centrate, Ecol. Eng. 95, 280-289. http://dx.doi.org/10.1016/j.ecoleng.2016.06.038
6. Arbib, Z., de Godos, I., Ruiz, J., Perales, J.A., 2017. Optimization of pilot high rate algal ponds for simultaneous nutrient removal and lipids production. Sci. Total Environ. 589, 66–72. http://dx.doi.org/10.1016/j.scitotenv.2017.02.206
7. Arbib, Z., Ruiz, J., Álvarez-Díaz, P., Garrido-Pérez, C., Barragan, J., Perales, J.A., 2013. Long term outdoor operation of a tubular airlift pilot photobioreactor and a high rate algal pond as tertiary treatment of urban wastewater. *Ecol. Eng.*, 52, 143-153. http://dx.doi.org/10.1016/j.ecoleng.2012.12.089

8. Arias, D.M., Rueda, E., García-Galán, M.J., Uggetti, E., García, J., 2018. Selection of cyanobacteria over green algae in a photo-sequencing batch bioreactor fed with wastewater. Sci. Total Environ. 653, 485-495. https://doi.org/10.1016/j.scitotenv.2018.10.342
9. Arias, D.M., Uggetti, E., García-Galán, M.J., García, J., 2017. Cultivation and selection of cyanobacteria in a closed photobioreactor used for secondary effluent and digestate treatment. Sci. Total Environ. 587-588, 157-167. https://doi.org/10.1016/j.scitotenv.2017.02.097
10. Babaei, A., Mehrnia, M.R., 2018. Fouling in microalgal membrane bioreactor containing nitrate-enriched wastewater under different trophic conditions, Algal Res. 36, 167–174. https://doi.org/10.1016/j.algal.2018.10.017
11. Babaei, A., Mehrnia, M.R., Shayegan, J., Sarrafzadeh, M.H., Comparison of different trophic cultivations in microalgal membrane bioreactor containing N-riched wastewater for simultaneous nutrient removal and biomass production. Process Biochemistry 51(10), 1568-1575. http://dx.doi.org/doi:10.1016/j.procbio.2016.06.011
12. Baker, N.R., 2008. Chlorophyll Fluorescence: A Probe of Photosynthesis in Vivo. Annu. Rev. Plant Biol. 59, 89-113. https://doi.org/10.1146/annurev.arplant.59.032607.092759
13. Balaji, S., Gopi, K., Muthuvelan, B., 2013. A review on production of poly ß hydroxybutyrates from cyanobacteria for the production of bio plastics. Algal Res. 2, 278-285. https://doi.org/10.1016/j.algal.2013.03.002
14. Barbera, E., Bertucco, A., Kumar, S., 2018. Nutrients recovery and recycling in algae processing for biofuels production. Renew. Sust. Energy Rev. 90, 28–42. https://doi.org/10.1016/j.rser.2018.03.004
15. Barbosa, M.J., Janssen, M., Ham, N., Tramper, J., Wijffels, R.H., 2003. Microalgae Cultivation in Air-Lift Reactors: Modeling Biomass Yield and Growth Rate as a Function of Mixing Frequency. Biotechnol. Bioeng. 82(2), 170-179. https://doi.org/10.1002/bit.10563
16. Barceló-Villalobos, M., Fernández-del Olmo, P., Guzmán, J.L., Fernández-Sevilla, J.M., Acién Fernández, F.G., 2019. Evaluation of photosynthetic light integration by microalgae in a pilot-scale raceway reactor. Bioresour. Technol. 280, 404-411. https://doi.org/10.1016/j.biortech.2019.02.032
17. Baroni, E.G., Yap, K.Y., Webley, P.A., Scales, P.J., Martin, G.J.O., 2019. The effect of nitrogen depletion on the cell size, shape, density and gravitational settling of *Nannochloropsis salina*, *Chlorella* sp. (marine) and *Haematococcus pluvialis*. Algal Res. 39, 101454. https://doi.org/10.1016/j.algal.2019.101454

18. Batstone, D.J., Hülsen, T., Mehta, C.M., Keller, J., 2015. Platforms for energy and nutrient recovery from domestic wastewater: A review. Chemosphere 140, 2–11. http://dx.doi.org/10.1016/j.chemosphere.2014.10.021
19. Béchet, Q., Shilton, A., Guieysse, B., 2013. Modeling the effects of light and temperature on algae growth: State of the art and critical assessment for productivity prediction during outdoor cultivation. Biotechnol. Adv. 31, 1648–1663. https://doi.org/10.1016/j.biotechadv.2013.08.014
20. Behera, B., Acharya, A., Gargey, I.A., Aly, N., Balasubramanian, P., 2018. Bioprocess engineering principles of microalgal cultivation for sustainable biofuel production. Bioresour. Technol. Reports 5, 297-316. https://doi.org/10.1016/j.biteb.2018.08.001
21. Beuckels, A., Smolders, E. Muylaert, K., 2015. Nitrogen availability influences phosphorus removal in microalgae-based wastewater Treatment. Water Res. 77, 98-106. http://dx.doi.org/10.1016/j.watres.2015.03.018
22. Bhakta, J.N., Lahiri, S., Pittman, J.K., Jana, B.B., 2015. Carbon dioxide sequestration in wastewater by a consortium of elevated carbon dioxide-tolerant microalgae. J. CO_2 Util. 10, 105–112. https://doi.org/10.1016/j.jcou.2015.02.001
23. Bilad, M.R., Azizo, A.S., Wirzal, M.D.H., Jia, L.J., Putra, Z.A., Nordin, NA.H.M., Mavukkandy, M.O., Jasni, M.J.F., Yusoff, A.R.M., 2018. Tackling membrane fouling in microalgae filtration using nylon 6,6 nanofiber membrane. J. Environ. Manag. 223, 23–28. https://doi.org/10.1016/j.jenvman.2018.06.007
24. Bilad, M.R., Arafat, H.A., Vankelecom, I.F.J., 2014. Membrane technology in microalgae cultivation and harvesting: A review. Biotechnol. Adv. 32, 1283–1300. http://dx.doi.org/10.1016/j.biotechadv.2014.07.008
25. Binnal, P., Babu, P.N., 2017. Optimization of environmental factors affecting tertiary treatment of municipal wastewater by *Chlorella protothecoides* in a lab scale photobioreactor. Journal of Water Process Engineering 17, 290-298. http://dx.doi.org/10.1016/j.jwpe.2017.05.003
26. Bitog, J.P., Lee, I.B., Lee, C.G., Kim, K.S., Hwang, H.S., Hong, S.W., Seo, I.H., Kwon, K.S., Mostafa, E., 2011. Application of computational fluid dynamics for modeling and designing photobioreactors for microalgae production: A review. Comput. Electron. Agric. 76(2), 131–47. https://doi.org/10.1016/j.compag.2011.01.015
27. Brennan, L., Owende, P., 2010. Biofuels from microalgae—a review of technologies for production, processing, and extractions of biofuels and co-products. Renew. Sust. Energ. Rev. 14(2), 557–577. https://doi.org/10.1016/j.rser.2009.10.009
28. Cabello, J., Toledo-Cervantes, A., Sánchez, L., Revah, S., Morales, M., 2015. Effect of the temperature, pH and irradiance on the photosynthetic activity by *Scenedesmus*

obtusiusculus under nitrogen replete and deplete conditions. Bioresour. Technol. 181, 128–135. http://dx.doi.org/10.1016/j.biortech.2015.01.034

29. Cai, T., Park, S.Y., Li, Y., 2013. Nutrient recovery from wastewater streams by microalgae: status and prospects. Renew. Sust. Energy Rev. 19, 360–369. https://doi.org/10.1016/j.rser.2012.11.030
30. Castrillo, M., Díez-Montero, R., Tejero, I., 2018. Model-based feasibility assessment of a deep solar photobioreactor for microalgae culturing. Algal Res. 29, 304–318. https://doi.org/10.1016/j.algal.2017.12.004
31. Chen, C., Guo, W., Ngo, H.H., Lee, D.-J., Tung, K.-L., Jin, P., Wang, J., Wu, Y., 2016. Challenges in biogas production from anaerobic membrane bioreactors. Renew. Energy 98, 120-134. https://doi.org/10.1016/j.renene.2016.03.095
32. Chisti, Y., 2007. Biodiesel from microalgae, Biotechnol. Adv. 25, 294-306. https://doi.org/10.1016/j.biotechadv.2007.02.001
33. Choi, O., Das, A., Yu, C.P., Hu, Z., 2010. Nitrifying Bacterial Growth Inhibition in the Presence of Algae and Cyanobacteria. Biotechnol. Bioeng. 107(6), 1004-1011. https://doi.org/10.1002/bit.22860
34. Collos,Y., Harrison, P.J., 2014 Acclimation and toxicity of high ammonium concentrations to unicellular algae. Mar. Pollut. Bull. 80, 8–23. https://doi.org/10.1016/j.marpolbul.2014.01.006
35. Daneshvar, E., Antikainen, L., Koutra, E., Kornaros, M., Bhatnagar, A., 2018. Investigation on the feasibility of *Chlorella vulgaris* cultivation in a mixture of pulp and aquaculture effluents: Treatment of wastewater and lipid extraction. Bioresour. Technol. 255, 104–110. https://doi.org/10.1016/j.biortech.2018.01.101
36. Dai, W., Xu, X., Liu, B., Yang, F. 2015. Toward energy-neutral wastewater treatment: A membrane combined process of anaerobic digestion and nitritation–anammox for biogas recovery and nitrogen removal. Chem. Eng. J. 279, 725-734. https://doi.org/10.1016/j.cej.2015.05.036
37. Daverey, A., Pandey, D., Verma, P., Verma, S., Shah, V., Dutta, K., Arunachalam, K., Recent advances in energy efficient biological treatment of municipal wastewater. Bioresour. Technol. Rep. 7, 100252. https://doi.org/10.1016/j.biteb.2019.100252
38. Day, J.G., Gong, Y., Hu, Q., 2017. Microzooplanktonic grazers – A potentially devastating threat to the commercial success of microalgal mass culture. Algal Res. 27, 356-365. http://dx.doi.org/10.1016/j.algal.2017.08.024
39. de Andrade, G.A., Berenguel, M., Guzmán, J.L., Pagano, D.J., Acién, F.G., 2016. Optimization of biomass production in outdoor tubular photobioreactors. Journal of Process Control 37, 58–69. http://dx.doi.org/10.1016/j.jprocont.2015.10.001

40. De Vree, J.H., Bosma, R., Janssen, M., Barbosa, M.J., Wijffels, R.H., 2015. Comparison of four outdoor pilot-scale photobioreactors. Biotechnol. Biofuels, 8:215. https://doi.org/10.1186/s13068-015-0400-2
41. Delgadillo-Mirquez, L., Lopes, F., Taidi, B., Pareau, D., Nitrogen and phosphate removal from wastewater with a mixed microalgae and bacteria culture, Biotechnology Reports 11, 18-26. https://doi.org/10.1016/j.btre.2016.04.003
42. Diez-Montero, R., Solimeno, A., Uggetti, E., García-Galán, M.J., García, J., 2018. Feasibility assessment of energy-neutral microalgae-based wastewater treatment plants under Spanish climatic conditions. Process Safety and Environmental Protection. 119, 242-252. https://doi.org/10.1016/j.psep.2018.08.008
43. Djelal, H., Tahrani, L., Fathallah, S., Cabrol, A., Mansour, H., 2014. Treatment process and toxicities assessment of wastewater issued from anaerobic digestion of household wastes. Environ. Sci. Pollut. Res. 21(4), 2437-2447. https://doi.org/10.1007/s11356-013-2158-z
44. Drews, A., 2010. Membrane fouling in membrane bioreactors—characterisation, contradictions, cause and cures. J. Membr. Sci. 363(1–2), 1–28. https://doi.org/10.1016/j.memsci.2010.06.046
45. Enamala, M.K., Enamala, S., Chavali, M., Donepudi, J., R. Yadavall, B. Kolapalli, T.V. Aradhyula, J. Velpuri, C. Kuppam, 2018. Production of biofuels from microalgae - A review on cultivation, harvesting, lipid extraction, and numerous applications of microalgae. Renew. Sust. Energy Rev. 94, 49–68. https://doi.org/10.1016/j.rser.2018.05.012
46. Eze, V.C, Velasquez-Orta, S.B., Hernández-García, A., Monje-Ramírez, I., Orta-Ledesma, M.T., 2018. Kinetic modelling of microalgae cultivation for wastewater treatment and carbon dioxide sequestration. Algal Res. 32, 131–141. https://doi.org/10.1016/j.algal.2018.03.015
47. Fasaei, F., Bitter, J.H., Slegers, P.M., Van Boxtel, A.J.B., 2018. Techno-economic evaluation of microalgae harvesting and dewatering systems. Algal Res. 31, 347-362. https://doi.org/10.1016/j.algal.2017.11.038
48. Fernández-Sevilla, J.M., Brindley, C., Jiménez-Ruíz, N., Acién, F.G., 2018. A simple equation to quantify the effect of frequency of light/dark cycles on the photosynthetic response of microalgae under intermittent light. Algal Res. 35, 479–487. https://doi.org/10.1016/j.algal.2018.09.026
49. Ferreira, G.F., Ríos Pinto, L.F., Maciel Filho, R., Fregolente, L.V., 2019. A review on lipid production from microalgae: Association between cultivation using waste streams and fatty acid profiles. Renew. Sust. Energy Rev. 109, 448–466. https://doi.org/10.1016/j.rser.2019.04.052

50. Foladori, P., Petrini, S., Andreottola, G., 2018. Evolution of real municipal wastewater treatment in photobioreactors and microalgae-bacteria consortia using real-time parameters, Chem. Eng. J. 345, 507–516. https://doi.org/10.1016/j.cej.2018.03.178
51. Foley, J., de Haas, D., Hartley, K., Lant, P., 2010. Comprehensive life cycle inventories of alternative wastewater treatment systems. Water Res. 44, 1654–1666. https://doi.org/10.1016/j.watres.2009.11.031
52. Galès, A., Bonnafous, A., Carré, C., Jauzein, V. Lanouguère, E., Le Floc'ha, E., Pinoit, J., Poullain, C., Roques, C., Sialve, B., Simier, M., Steyer, J.P., Fouilland, E., 2019. Importance of ecological interactions during wastewater treatment using High Rate Algal Ponds under different temperate climates, Algal Res. 40, 101508. https://doi.org/10.1016/j.algal.2019.101508
53. Gao, F., Cui, W., Xu, J.P., Li, C., Jin, W.H., Yang H.L., 2019. Lipid accumulation properties of *Chlorella vulgaris* and *Scenedesmus obliquus* in membrane photobioreactor (MPBR) fed with secondary effluent from municipal wastewater treatment plant. Renew. Energy 136, 671-676. https://doi.org/10.1016/j.renene.2019.01.038
54. Gao, F., Penga, Y.Y., Lia, C., Cuia, W., Yang, Z.H., Zeng, G.M., 2018. Coupled nutrient removal from secondary effluent and algal biomass production in membrane photobioreactor (MPBR): Effect of HRT and long-term operation. Chem. Eng. J. 335, 169-175. http://dx.doi.org/10.1016/j.cej.2017.10.151
55. Gao, F., Li, C., Yang, Z., Zeng, G., Feng, L., Liu, J., Liu, M., Cai, H., 2016. Continuous microalgae cultivation in aquaculture wastewater by a membrane photobioreactor for biomass production and nutrients removal, Ecol. Eng. 92, 55-61. http://dx.doi.org/10.1016/j.ecoleng.2016.03.046
56. García, J., Ortiz, A., Álvarez, E., Belohlav, V., García-Galán, M.J., Díez-Montero, R., Álvarez, J.A., Uggetti, E., 2018. Nutrient removal from agricultural run-off in demonstrative full scale tubular photobioreactors for microalgae growth. Ecological Eng. 120, 513–521. https://doi.org/10.1016/j.ecoleng.2018.07.002
57. García-Camacho, F., Sánchez-Mirón, A., Molina-Grima, E., Camacho-Rubio, F., Merchuck, J.C., 2012. A mechanistic model of photosynthesis in microalgae including photoacclimation dynamics. J. Theor. Biol. 304, 1–15. http://dx.doi.org/10.1016/j.jtbi.2012.03.021.
58. García-Galán, M.J., Gutiérrez, R., Uggetti, E., Matamoros, V., García, J., Ferrer, I., 2018. Use of full-scale hybrid horizontal tubular photobioreactors to process agricultural runoff. Biosyst. Eng. 166, 138-149. https://doi.org/10.1016/j.biosystemseng.2017.11.016

59. Garrido-Cárdenas, J., Manzano-Agugliaro, F., Acién-Fernández, F.G., Molina-Grima, E., 2018. Microalgae research worldwide. Algal Res. 35, 50-60. https://doi.org/10.1016/j.algal.2018.08.005
60. Giménez, J.B., 2014. Study of the anaerobic treatment of urban wastewater in membrane bioreactors (Estudio del tratamiento anaerobio de aguas residuales urbanas en biorreactores de membranas). PhD Thesis, University of valencia, Spain.
61. Giménez, J. B., Martí, N., Ferrer, J., Seco, A., 2012 Methane recovery efficiency in a submerged anaerobic membrane bioreactor (SAnMBR) treating sulphate-rich urban wastewater: evaluation of methane losses with the effluent. Bioresour. Technol. 118, 67–72. https://doi.org/10.1016/j.biortech.2012.05.019
62. Giménez, J.B., Robles, A., Carretero, L., Durán, F., Ruano, M.V., Gatti, M.N., Ribes, J., Ferrer, J., Seco, A., 2011. Experimental study of the anaerobic urban wastewater treatment in a submerged hollow-fibre membrane bioreactor at pilot scale. Bioresour. Technol. 102, 8799–8806. https://doi.org/10.1016/j.biortech.2011.07.014
63. Giordano, M., Pezzoni, V., Hell, R., 2000. Strategies for the allocation of resources under sulfur limitation in the green alga *Dunaliella salina*, Plant Physiol. 124, 857–864. https://doi.org/10.1104/pp.124.2.857
64. Gonçalves, A.L., Pires, J.C.M., Simões, M., 2017. A review on the use of microalgal consortia for wastewater treatment, Algal Res. 24, 403–415. http://dx.doi.org/10.1016/j.algal.2016.11.008
65. González-Camejo, J., Barat, R., Pachés, M., Murgui, M., Ferrer, J., Seco, A., 2018. Wastewater Nutrient Removal in a Mixed Microalgae-bacteria Culture: Effect of Light and Temperature on the Microalgae-bacteria Competition. Environ. Technol. 39 (4), 503–515. https://doi.org/10.1080/09593330.2017.1305001
66. González-López, C.V., Acién Fernández, F.G., Fernández-Sevilla, J.M., Sánchez Fernández, J.F., Molina Grima, E., 2012. Development of a process for efficient use of CO2 from flue gases in the production of photosynthetic microorganisms. Biotechnol. Bioeng. 109(7), 1637-1650. https://doi.org/10.1002/bit.24446
67. González-Sánchez, A., Posten, C., 2017. Fate of H_2S during the cultivation of *Chlorella* sp. deployed for biogas upgrading. J. Environ. Manag. 191, 252-257. http://dx.doi.org/10.1016/j.jenvman.2017.01.023
68. Gouveia, L., Graça, S., Sousa, C., Ambrosano, L., Ribeiro, B., Botrel, E.P., Neto, P.C., Ferreira, A.F., Silva, C.M., 2016. Microalgae biomass production using wastewater: Treatment and costs Scale-up considerations. *Algal Res.* 16, 167-176. http://dx.doi.org/10.1016/j.algal.2016.03.010
69. Gris, B., Morosinotto, T., Giacometti, G.M., Bertucco, A., Sforza, E., 2014. Cultivation of Scenedesmus obliquus in Photobioreactors: Effects of Light Intensities and Light–

Dark Cycles on Growth, Productivity, and Biochemical Composition, Appl. Biochem. Biotechnol. 172, 2377–2389. http://dx.doi.org/10.1007/s12010-013-0679-z

70. Guldhe, A., Singh, P., Renuka, N., Bux, F., 2019. Biodiesel synthesis from wastewater grown microalgal feedstock using enzymatic conversion: A greener approach. Fuel 237, 1112–1118. https://doi.org/10.1016/j.fuel.2018.10.033
71. Guldhe, A., Kumari, S., Ramanna, L., Ramsundar, P., Singh, P., Rawat, I., Bux, F., 2017. Prospects, recent advancements and challenges of different wastewater streams for microalgal cultivation. J. Environ. Manag. 203, 299-315. http://dx.doi.org/10.1016/j.jenvman.2017.08.012
72. Gupta, S.K., Ansari, F.A., Shriwastav, A., Sahoo, N.K., Rawat, I., Bux, F., Dual role of *Chlorella sorokiniana* and *Scenedesmus obliquus* for comprehensive wastewater treatment and biomass production for bio-fuels, J. Clean. Prod. 115, 255-264. http://dx.doi.org/10.1016/j.jclepro.2015.12.040
73. Harun, R., Singh, M., Forde, G.M., Danquah, M.K., 2010. Bioprocess engineering of microalgae to produce a variety of consumer products. Renew. Sust. Energy Rev. 14, 1037–1047. https://doi.org/10.1016/j.rser.2009.11.004
74. Huang, J., Hankame, B., Yarnold, J., 2019. Design scenarios of outdoor arrayed cylindrical photobioreactors for microalgae cultivation considering solar radiation and temperature. Algal Res. 41, 101515. https://doi.org/10.1016/j.algal.2019.101515
75. Huang, Q., Jiang, F., Wang, L., Yang, C., 2017. Design of Photobioreactors for Mass Cultivation of Photosynthetic Organisms. Engineering 3, 318-329. http://dx.doi.org/10.1016/J.ENG.2017.03.020
76. Ippoliti, D., Gómez, C., Morales-Amaral, M.M., Pistocchi, R., Fernández-Sevilla, J.M., Acién, F.G., 2016. Modeling of photosynthesis and respiration rate for *Isochrysis galbana* (T-Iso) and its influence on the production of this strain. Bioresour. Technol. 203, 71–79. http://dx.doi.org/10.1016/j.biortech.2015.12.050
77. Izadpanah, M., Gheshlaghi, R., Mahdavi, M.A., Elkamel, A., 2018. Effect of light spectrum on isolation of microalgae from urban wastewater and growth characteristics of subsequent cultivation of the isolated species. Algal Res. 29 (2018) 154–158. https://doi.org/10.1016/j.algal.2017.11.029
78. Japar, A.S., Takriff, M.S., Yasin, N.H.M., 2017. Harvesting microalgal biomass and lipid extraction for potential biofuel production: A review. Journal of Environmental Chemical Engineering 5, 555–563. http://dx.doi.org/10.1016/j.jece.2016.12.016
79. Jebali, A., Acién, F.G., Rodriguez Barradas, E., Olguín, E.J., Sayadi, S., Molina Grima, E., 2018. Pilot-scale outdoor production of *Scenedesmus* sp. in raceways using flue gases and centrate from anaerobic digestion as the sole culture medium. Bioresour. Technol. 262, 1-8. https://doi.org/10.1016/j.biortech.2018.04.057

80. Ji, M.K., Kabra, A.N., Salama, el S., Roh, H.S., Kim, J.R., Lee, D.S., Jeon, B.H., 2014. Effect of mine wastewater on nutrient removal and lipid production by a green microalga *Micratinium reisseri* from concentrated municipal wastewater. Bioresour. Technol. 157, 84-90. https://doi.org/10.1016/j.biortech.2014.01.087
81. Judd, S., van den Broeke, L.J.P., Shurair, M., Kuti, Y., Znad, H., 2015. Algal remediation of CO_2 and nutrient discharges: a review. Water Res. 87, 356-366. http://dx.doi.org/10.1016/j.watres.2015.08.021
82. Kirst, H., Gabilly, S. T., Niyogi, K. K., Lemaux, P. G., Melis, A., 2017. Photosynthetic antenna engineering to improve crop yields. *Planta*, *245*(5), 1009-1020. https://doi.org/10.1007/s00425-017-2659-y
83. Koç, C., Anderson, G.A., Kommareddy, A., 2013. Use of Red and Blue Light-Emitting Diodes (LED) and Fluorescent Lamps to Grow Microalgae in a Photobioreactor. The Israeli Journal of Aquaculture 65, 1-8. http://hdl.handle.net/10524/32474
84. Komolafe, O., Velasquez Orta, S.B., Monje-Ramirez, I., Yanez Noguez, I., Harvey, A.P., Orta Ledesma, M.T., 2014. Biodiesel production from indigenous microalgae grown in wastewater. Bioresour. Technol. 154, 297-304. https://doi.org/10.1016/j.biortech.2013.12.048
85. Kubelka, B.G., Roselet, F., Pinto, W.T., Abreu, P.C., The action of small bubbles in increasing light exposure and production of the marine microalga *Nannochloropsis oceanica* in massive culture systems, Algal Res. 35, 69-76. https://doi.org/10.1016/j.algal.2018.09.030
86. Kumar, K., Dasgupta, C.N., Nayak, B., Lindblad, P., Das, D., 2011. Development of suitable photobioreactors for CO2 sequestration addressing global warming using green algae and cyanobacteria, Bioresour. Technol. 102, 4945–4953. https://doi.org/10.1016/j.biortech.2011.01.054
87. Küster E., Dorusch, F., Altenburguer, R., 2005. Effects of hydrogen sulfide to *Vibrio fischeri, Scenedesmus vacuolatus,* and *Daphnia magna*. Environmental Toxicology and Chemistry 24(10), 2621-2629.
88. Lam, T.P., Lee, T.M., Chen, C.Y., Chang, J.S., 2018. Strategies to control biological contaminants during microalgal cultivation in open ponds. Bioresour. Technol. 252, 180-187. https://doi.org/10.1016/j.biortech.2017.12.088
89. Ledda, C., Idà, A., Allemand, D., Mariani, P., Adani, F., 2015. Production of wild *Chlorella* sp. cultivated in digested and membrane-pretreated swine manure derived from a full-scale operation plant. Algal Res. 12, 68-73. http://dx.doi.org/10.1016/j.algal.2015.08.010
90. Leu, S., Boussiba, S., 2014. Advances in the production of high-value products by microalgae. Ind. Biotechnol. 10, 169–183. https://doi.org/10.1089/ind.2013.0039

91. Ling, Y., Sun, L.P., Wang, S.Y., Lin, C.S.K., Sun, Z., Zhou, Z.G., 2019. Cultivation of oleaginous microalga *Scenedesmus obliquus* coupled with wastewater treatment for enhanced biomass and lipid production. Biochem. Eng. J. 148, 162–169. https://doi.org/10.1016/j.bej.2019.05.012
92. Liu, J., Danneels, B., Vanormelingen, P., Vyverman, W., 2016. Nutrient removal from horticultural wastewater by benthic filamentous algae *Klebsormidium* sp., *Stigeoclonium* spp. and their communities: From laboratory flask to outdoor Algal Turf Scrubber (ATS). Water Res. 92, 61-68. http://dx.doi.org/10.1016/j.watres.2016.01.049
93. Luo, Y., Le-Clech, P., Henderson, R.K., 2018. Assessment of membrane photobioreactor (MPBR) performance parameters and operating conditions. Water Res. 138, 169-180. https://doi.org/10.1016/j.watres.2018.03.050
94. Luo, Y., Le-Clech, P., Henderson, R.K., 2017. Simultaneous microalgae cultivation and wastewater treatment in submerged membrane photobioreactors: A review. Algal Res. 24B, 425-437. http://dx.doi.org/10.1016/j.algal.2016.10.026
95. Manhaeghe, D., Michels, S., Rousseau, D.P.L., Van Hulle, S.W.H., 2019. A semi-mechanistic model describing the influence of light and temperature on the respiration and photosynthetic growth of *Chlorella vulgaris.* Bioresour. Technol. 274, 361-370. https://doi.org/10.1016/j.biortech.2018.11.097
96. Marazzi, F., Bellucci, M., Rossi, S., Fornaroli, R., Ficara, E., Mezzanotte, V., 2019. Outdoor pilot trial integrating a sidestream microalgae process for the treatment of centrate under non optimal climate conditions. Algal Res. 39, 101430. https://doi.org/10.1016/j.algal.2019.101430
97. Marbelia, L., Bilad, M.R., Passaris, I., Discart, V., Vandamme, D., Beuckels, A., Muylaert, K., Vankelecom, I.F.J., 2014. Membrane photobioreactors for integrated microalgae cultivation and nutrient remediation of membrane bioreactors effluent. Bioresour.Technol. 163, 228–235. https://doi.org/10.1016/j.biortech.2014.04.012
98. Marcilhac, C., Sialve B., Pourcher A.M., Ziebal C., Bernet N., Béline F., 2014. Digestate color and light intensity affect nutrient removal and competition phenomena in a microalgal-bacterial ecosystem, Water Res. 64, 278-287. http://dx.doi.org/10.1016/j.watres.2014.07.012
99. Mata, T.M., Melo, A.C., Simões, M., Caetano, N.S., Parametric study of a brewery effluent treatment by microalgae *Scenedesmus obliquus*. Bioresour. Technol. 107, 151-158. http://dx.doi.org/10.1016/j.biortech.2011.12.109
100. Mata, T.M., Martins, A.A., Caetano, N.S., Microalgae for biodiesel production and other applications: A review. Renew. Sust. Energy Rev. 14, 217–232. https://doi.org/10.1016/j.rser.2009.07.020

101. McCarty, P.L., Bae, J., Kim, J., 2011. Domestic wastewater treatment as a net energy producer – can this be achieved? Environ. Sci. Technol. 45, 7100–7106. https://doi.org/10.1021/es2014264

102. McGinn, P.J., Dickinson, K.E., Park, K.C., Whitney, C.G., MacQuarrie, S.P., Black, F.J., Frigon, J.C., Guiot, S.R., O'Leary, S.J.B., 2012. Assessment of the bioenergy and bioremediation potentials of the microalga *Scenedesmus* sp. AMDD cultivated in municipal wastewater effluent in batch and continuous mode. Algal Res., 1(2) 155-165. https://doi.org/10.1016/j.algal.2012.05.001

103. Mennaa, F.Z., Arbib, Z., Perales, J.A., 2015. Urban wastewater treatment by seven species of microalgae and an algal bloom: Biomass production, N and P removal kinetics and harvestability. Water Res. 83, 42-51. http://dx.doi.org/10.1016/j.watres.2015.06.007

104. Mera, R., Torres, E., Abalde, J., 2014. Sulphate, more than a nutrient, protects the microalga *Chlamydomonas moewusii* from cadmium toxicity. Aquatic Toxicology 148. 92–103.

105. Mirón, A.S., Gómez, A.C., Camacho, F.G., Grima, E.M., and Chisti, Y., 1999. Comparative evaluation of compact photobioreactors for large-scale monoculture of microalgae, in Prog. Ind. Microbiol., Osinga, R., Tramper, J., Burgess, J.G., and Wijffels, R.H., Editors. 1999, Elsevier. p. 249-270.

106. Moheimani, N.R., 2013. Inorganic carbon and pH effect on growth and lipid productivity if *Tetraselmis suecica* and *Chlorella* sp. (Chlorophyta) grown outdoors in bag photobioreactors. J. Appl. Phycol. 25, 387-398. https://doi.org/10.1007/s10811-012-9873-6

107. Molina Grima, E., Belarbi, E.H., Acién Fernández, F.G., Robles Medina, A., Chisti, Y., Recovery of microalgal biomass and metabolites: process options and economics. Biotechnol. Adv. 20, 491–515.

108. Moraes, L., Martins, G., Morillas, A., Oliveira, L., Greque, M., Molina-Grima, E., Vieira, J.A., Acién, F.G., 2019. Engineering strategies for the enhancement of *Nannochloropsis gaditana* outdoor production: influence of the CO_2 flow rate on the culture performance in tubular photobioreactors. Process Biochem. 76, 171-177. https://doi.org/10.1016/j.procbio.2018.10.010

109. Muñoz, R., Guieysse, B., 2006. Algal–bacterial processes for the treatment of hazardous contaminants: A review. Water Res. 40(15), 2799-2815. https://doi.org/10.1016/j.watres.2006.06.011

110. Nayak, M., Dhanarajan, G., Dineshkumar, R., Sen, R., 2018. Artificial intelligence driven process optimization for cleaner production of biomass with co-

valorization of wastewater and flue gas in an algal biorefinery. J. Clean. Prod. 201, 1092-1100. https://doi.org/10.1016/j.jclepro.2018.08.048

111. Nwoba, E.G., Parlevliet, D.A., Laird, D.W., Alameh, K., Moheimani, N.R., 2019. Light management technologies for increasing algal photobioreactor efficiency. Algal Res. 39, 101433. https://doi.org/10.1016/j.algal.2019.101433

112. Pachés, M., Martínez-Guijarro, R., González-Camejo, J., Seco, A., Barat, R., 2018. Selecting the most suitable microalgae species to treat the effluent from an anaerobic membrane bioreactor. Environ. Technol. (in press). https://doi.org/10.1080/09593330.2018.1496148

113. Park, J., Jin, H., Lim, B. R., Park, K. Y., Lee, K., 2010. Ammonia removal from anaerobic digestion effluent of livestock waste using green alga *Scenedesmus* sp. Bioresour. Technol. 101, 8649-8657. https://doi.org/10.1016/j.biortech.2010.06.142.

114. Park, K.H., Lee, C.G., 2001. Effectiveness of flashing light for increasing photosynthetic efficiency of microalgal cultures over a critical cell density, Biotechnology and Bioprocess Engineering 6, 189-193.

115. Passarge, J., Hol, S., Escher, M., Huisman, J., 2006. Competition for nutrients and light: stable coexistence, alternative stable states, or competitive exclusion? Ecological Monographs*,* 76(1), 57–72.

116. Pawlowski, A., Frenández, I., Guzmán, J.L., Berenguel, M., Acién, F.G., Dormido, S., 2016. Event-based selective control strategy for raceway reactor: A simulation study. IFAC-Papers OnLine 49(7), 478–483. https://doi.org/10.1016/j.ifacol.2016.07.388

117. Pires, J.C.M., Alvim-Ferraz, M.C.M., Martins, F.G., 2017. Photobioreactor design for microalgae production through computational fluid dynamics: A review. Renew. Sust. Energy Rev. 79, 248–254. https://doi.org/10.1016/j.rser.2017.05.064

118. Porcelli N., Judd S., 2010. Chemical cleaning of potable water membranes: a review, Sep. Purif. Technol. 71, 137–143. https://doi.org/10.1016/j.seppur.2009.12.007

119. Powell, N., Shilton, A., Chisti, Y., Pratt, S., 2009. Towards a luxury uptake process via microalgae – Defining the polyphosphate dynamics. Water Res. 43, 4207-4213. https://doi:10.1016/j.watres.2009.06.011

120. Powell, N., Shilton, A.N., Pratt, S., Chisti, Y., 2008. Factors influencing luxury uptake of phosphorus by microalgae in waste stabilization ponds. Environ. Sci. Technol. 42, 5958–5962. https://doi.org/10.1021/es703118s

121. Pretel, R., Robles, A., Ruano, M.V., Seco, A., Ferrer, J., 2016. Economic and environmental sustainability of submerged anaerobic MBR-based (AnMBR-based) technology as compared to aerobic-based technologies for moderate-/high-loaded urban

wastewater treatment. J. Environ. Manag. 166, 45-54. http://dx.doi.org/10.1016/j.jenvman.2015.10.004

122. Puyol, D., Batstone, D.J., Hülsen, T., Astals, S., Peces, M., Krömer, J.O., 2017. Resource recovery from wastewater by biological technologies: opportunities, challenges, and prospects, Frontiers in Microbiology 7(2106), 1–23. http://dx.doi.org/10.3389/fmicb.2016.02106

123. Qasim, M., Darwish, N.N., Mhiyo, S., Darwish, N.A., Hilal, N., 2018. The use of ultrasound to mitigate membrane fouling in desalination and water treatment, Desalination 443, 143-164. https://doi.org/10.1016/j.desal.2018.04.007

124. Qiu, R., Gao, S., Lopez, P.A., Ogden, K.L., 2017. Effects of pH on cell growth, lipid production and CO_2 addition of microalgae *Chlorella sorokiniana*, Algal Res. 28, 192-199. http://dx.doi.org/10.1016/j.algal.2017.11.004

125. Rada-Ariza, A.M., Fredy, D., Lopez-Vazquez, C.M., Van der Steen, N.P., Lens, P.N.L., 2019. Ammonium removal mechanisms in a microalgal-bacterial sequencingbatch photobioreactor at different solids retention times. Algal Res. 39, 101468. https://doi.org/10.1016/j.algal.2019.101468

126. Raeisossadati, M., Moheimani, N.R., Parlevliet, D., 2019. Luminescent solar concentrator panels for increasing the efficiency of mass microalgal production. Renew. Sust. Energy Rev. 101, 47–59. https://doi.org/10.1016/j.rser.2018.10.029

127. Rajneesh, Singh, S. P., Pathak, J., Sinha, R.P., 2017. Cyanobacterial factories for the production of green energy and value-added products: An integrated approach for economic viability. Renew. Sust. Energy Rev. 69, 578–595. https://doi.org/10.1016/j.rser.2016.11.110

128. Ras, M., Steyer, J.P., Bernard, O., 2013. Temperature effect on microalgae: a crucial factor for outdoor production, Rev. Environ. Sci. Biotechnol. 12, 153-164. https://doi.org/10.1007/s11157-013-9310-6

129. Razzak, S.A., Ali, S.A.M., Hossain, M.M., deLasa, H., 2017. Biological CO_2 fixation with production of microalgae in wastewater – A review. Renew. Sust. Energy Rev. 76, 379–390.http://dx.doi.org/10.1016/j.rser.2017.02.038

130. Reynolds, C.S., 2006. The ecology of phytoplankton (ecology, biodiversity and conservation). Cambridge: Cambridge University Press; United Kingdom.

131. Ringsmuth, A.K., Landsberg, M.J., Hankamer, B., 2016. Can photosynthesis enable a global transition from fossil fuels to solar fuels, to mitigate climate change and fuel supply limitations? Renew. Sust. Energy Rev. 62, 134–63. https://doi.org/10.1016/j.rser.2016.04.016

132. Robles, A., Ruano, M.V., Charfi, A., Lesage, G., Heran, M., Harmand, J., Seco, A., Steyer, J.P., Batstone, D.J., Kim, J., Ferrer, J., 2018. A review on anaerobic

membrane bioreactors (AnMBRs) focused on modeling and control aspects, Bioresour. Technol. 270, 612-626. https://doi.org/10.1016/j.biortech.2018.09.049

133. Romero-Villegas, G.I., Fiamengo, M., Acién-Fernández, F.G., Molina-Grima, E., 2018a. Utilization of centrate for the outdoor production of marine microalgae at the pilot-scale in raceway photobioreactors, J. Environ. Manag. 228, 506–516. https://doi.org/10.1016/j.jenvman.2018.08.020

134. Romero-Villegas, G.I., Fiamengo, M., Acién Fernández, F.G., Molina Grima, E., 2018b. Utilization of centrate for the outdoor production of marine microalgae at pilot-scale in flat-panel photobioreactors. J. Biotechnol. 284, 102-114. https://doi.org/10.1016/j.jbiotec.2018.08.006

135. Romero-Villegas, G.I., Fiamengo, M., Acién-Fernández, F.G., Molina-Grima, E., 2017. Outdoor production of microalgae biomass at pilot-scale in seawater using centrate as the nutrient source. Algal Res. 25, 538–548. http://dx.doi.org/10.1016/j.algal.2017.06.016

136. Ruano, M.V., Ribes, J., Seco, A., Ferrer, J., 2009. Low cost-sensors as a real alternative to on-line nitrogen analysers in continuous systems. Wat. Sci. Tech., 60(12), 3261-3268. http://dx.doi.org/10.2166/wst.2009.607

137. Ruiz, J., Álvarez-Díaz, P.D., Arbib, Z., Garrido-Pérez, C., Barragán, J., Perales, J.A., 2013. Performance of a flat panel reactor in the continuous culture of microalgae in urban wastewater: Prediction from a batch experiment. Bioresour. Technol. 127, 456-463. http://dx.doi.org/10.1016/j.biortech.2012.09.103

138. Ruiz-Martinez, A., 2015. Nutrient removal from an anaerobic membrane bioreactor effluent using microalgae. Study and modeling of the process. PhD Thesis, Polytechnic University of Valencia, Spain.

139. Ruiz-Martinez, A., Serralta, J., Pachés, M., Seco, A., Ferrer, J., 2014. Mixed microalgae culture for ammonium removal in the absence of phosphorus: Effect of phosphorus supplementation and process modeling. Process Biochem. 49, 2249-2257. http://dx.doi.org/10.1016/j.procbio.2014.09.002

140. Ruiz-Martínez, A., Martín García, N., Romero, I., Seco, A., Ferrer, J., 2012. Microalgae cultivation in wastewater: nutrient removal from anaerobic membrane bioreactor effluent. Bioresour. Technol. 126, 247–253. http://dx.doi.org/10.1016/j.biortech.2012.09.022

141. Ruiz-Marin, A., Mendoza-Espinosa, L.G., Stephenson, T., 2010. Growth and nutrient removal in free and immobilized green algae in batch and semi-continuous cultures treating real wastewater. Bioresour. Technol. 101, 58–64. http://doi:10.1016/j.biortech.2009.02.076

142. Salama, E.S., Jeon, B.H., Chang, S.W., Lee, S.h., Roh, H.-S., Yang, I.S., Kurade, M.B., El-Dalatony, M.M., Kim, D.-H., Kim, K.H., Kim, S., 2017. Interactive effect of indole-3-acetic acid and diethyl aminoethyl hexanoate on the growth and fatty acid content of some microalgae for biodiesel production. J. Clean. Prod. 168, 1017-1024. https://doi.org/10.1016/j.rser.2017.05.091

143. Seco, A., Aparicio, S., González-Camejo, J., Jiménez-Benítez, A., Mateo, O., Mora, J.F., Noriega-Hevia, G., Sanchis-Perucho, P., Serna-García, R., Zamorano-López, N., Giménez, J.B., Ruiz-Martinez, A., Aguado, D., Barat, R., Borrás, L., Bouzas, A., Martí, N., Pachés, M., Ribes, J., Robles, A., Ruano, M.V., Serralta, J. and Ferrer, J., 2018. Resource recovery from sulphate-rich sewage through an innovative anaerobic-based water resource recovery facility (WRRF). Water Science and Technology 78 (9), 1925-1936. https://doi.org/10.2166/wst.2018.492

144. Sepúlveda, C., Acién, F.G., Gómez, C., Jiménez-Ruíz, N., Riquelme, C., Molina-Grima, E., 2015. Utilization of centrate for the production of the marine microalgae *Nannochloropsis gaditana*, Algal Res. 9, 107-116. http://dx.doi.org/10.1016/j.algal.2015.03.004

145. Serra-Maia, R., Bernard, O., Gonçalves, A., Bensalem, S., Lopes, F., 2016. Influence of temperature on *Chlorella vulgaris* growth and mortality rates in a photobioreactor, Algal Res. 18, 352–359. http://dx.doi.org/10.1016/j.algal.2016.06.016

146. Sheng, A.L.K., Bilad, M.R., Osman, N.B., Arahman, N., 2017. Sequencing batch membrane photobioreactor for real secondary effluent polishing using native microalgae: process performance and full-scale projection. J. Clean. Prod. 168, 708-715. http://dx.doi.org/10.1016/j.jclepro.2017.09.083

147. Shoener, B.D., Schramm, S.M., Béline, F., Bernard, O., Martínez, C., Plósz, B.G., Snowling, S., Steyer, J.P., Valverde-Pérez, B., Wágner, D., Guest, J.S., 2019. Microalgae and cyanobacteria modeling in water resource recovery facilities: A critical review. Water Res. X 2, 100024. https://doi.org/10.1016/j.wroa.2018.100024

148. Sikder, M.T., Rahman, M.M., Jakariya, M., Hosokawa, T., Kurasaki, M., Saito, T., 2019. Remediation of water pollution with native cyclodextrins and modified cyclodextrins: a comparative overview and perspectives. Chem. Eng. J. 355, 920–941. https://doi.org/10.1016/j.cej.2018.08.218

149. Siles, J.A., Brekelmans, J., Martin, M.A., Chica, A.F., Martin, A. 2010. Impact of ammonia and sulphate concentration on thermophilic anaerobic digestion. Bioresour. Technol., 101(23), 9040-9048. https://doi.org/10.1016/j.biortech.2010.06.163

150. Smith, A.L., Stadler, L.B., Cao, L., Love, N.G., Raskin, L., Skerlos, S.J., 2014. Navigating wastewater energy recovery strategies: a life cycle comparison of anaerobic

membrane bioreactor and conventional treatment systems with anaerobic digestion. Environ.Sci.Technol. 48, 5972–5981. https://doi.org/10.1021/es5006169

151. Smith, A.L., Stadler, L.B., Love, N.G., Skerlos, S.J., Raskin, L. 2012. Perspectives on anaerobic membrane bioreactor treatment of domestic wastewater: a critical review. Bioresour. Technol., 122, 149-159. https://doi.org/10.1016/j.biortech.2012.04.055

152. Solimeno, A., Samso, R., Uggetti, E., Sialve, B., Steyer, J.P., Gabarro, A., García, J., 2015. New mechanistic model to simulate microalgae growth. Algal Res.12, 350–358. https://doi.org/10.1016/j.algal.2015.09.008

153. Song, X., Luo, W., Hai, F.I., Price, W. E., Guo, W., Ngo, H.H., Nghiem, L.D., 2018a. Resource recovery from wastewater by anaerobic membrane bioreactors: Opportunities and challenges. Bioresour. Technol. 270, 669-677. https://doi.org/10.1016/j.biortech.2018.09.001

154. Song, X., Luo, W., McDonald, J., Khan, S.J., Hai, F.I., Guo, W., Ngo, H.H., Nghiem, L.D., 2018b. Effects of sulphur on the performance of an anaerobic membrane bioreactor: Biological stability, trace organic contaminant removal, and membrane fouling. Bioresour. Technol., 250, 171-177. https://doi.org/10.1016/j.biortech.2017.11.021

155. Stazi, V., Tomei, M.C., 2018. Enhancing anaerobic treatment of domestic wastewater: State of the art, innovative technologies and future perspectives. Sci. Total Environ. 635, 78–91. https://doi.org/10.1016/j.scitotenv.2018.04.071

156. Straka, L., Rittmann, B.E., 2018. Light-dependent kinetic model for microalgae experiencing photoacclimation, photodamage, and photodamage repair. Algal Res. 31, 232–238. https://doi.org/10.1016/j.algal.2018.02.022

157. Stuckey, D.C., 2012. Recent developments in anaerobic membrane reactors. Bioresour. Technol. 122, 137-148. https://doi.org/10.1016/j.biortech.2012.05.138

158. Su, Y., Mennerich, A., Urban, B., 2012. Coupled nutrient removal and biomass production with mixed algal culture: Impact of biotic and abiotic factors. Bioresour. Technol. 118, 469-476. http://dx.doi.org/10.1016/j.biortech.2012.05.093

159. Sutherland, D.L., Turnbull, M.H., Craggs, R.J., 2017. Environmental drivers that influence microalgal species in fullscale wastewater treatment high rate algal ponds. Water Res. 124, 504-512. http://dx.doi.org/10.1016/j.watres.2017.08.012

160. Sutherland, D.L., Howard-Williams, C., Turnbull, M.H., Broady, P.A., Craggs, R.J., 2015. Enhancing microalgal photosynthesis and productivity in wastewater treatment high rate algal ponds for biofuel production. Bioresour. Technol. 184, 222-229. https://doi.org/10.1016/j.biortech.2014.10.074

161. Tan, X.B., Zhang, Y.L., Yang, L.B., Chu, H.Q., Guo, J., 2016. Outdoor cultures of *Chlorella pyrenoidosa* in the effluent of anaerobically digested activated sludge: The effects of pH and free ammonia. Bioresour. Technol. 200, 606-615. http://dx.doi.org/10.1016/j.biortech.2015.10.095

162. Thomas, P.K., Dunn, G.P., Good, A.R., Callahan, M.P., Coats, E.R., Newby, D.T., Feris, K.P., 2019. A natural algal polyculture outperforms an assembled polyculture in wastewater-based open pond biofuel production. Algal Res. 40, 101488. https://doi.org/10.1016/j.algal.2019.101488

163. Udaiyappan, A.F.M., Hasan, H.A., Takriff, M.S., Abdullah, S.R.S, 2017. A review of the potentials, challenges and current status of microalgae biomass applications in industrial wastewater treatment. Journal of Water Process Engineering 20, 8–21. http://dx.doi.org/10.1016/j.jwpe.2017.09.006

164. Uggetti, E., Sialve, B., Hamelin, J., Bonnafous, A., Steyer, J.P., 2018. CO2 addition to increase biomass production and control microalgae species in high rate algal ponds treating wastewater. J. CO_2 Util. 28, 292–298. https://doi.org/10.1016/j.jcou.2018.10.009

165. Valigore, J.M., Gostomski, P.A., Wareham, D.G., O'Sullivan, A.D., 2012. Effects of hydraulic and solids retention times on productivity and settleability of microbial (microalgal-bacterial) biomass grown on primary treated wastewater as a biofuel feedstock. Water Res. 46(9), 2957-2964. https://doi.org/10.1016/j.watres.2012.03.023

166. Van Den Hende, S., Beelen V., Bore G., Boon N., Vervaeren H., 2014. Up-scaling aquaculture wastewater treatment by microalgal bacterial flocs: From lab reactors to an outdoor raceway pond. Bioresour. Technol. 159, 342–354. http://dx.doi.org/10.1016/j.biortech.2014.02.113

167. Verma, R., Srivastava, A., 2018. Carbon dioxide sequestration and its enhanced utilization by photoautotroph microalgae, Environ. Dev. 27, 95–106. https://doi.org/10.1016/j.envdev.2018.07.004

168. Viruela, A., Robles, A., Durán, F., Ruano, M.V., Barat, R., Ferrer, J., Seco, A., 2018. Performance of an outdoor membrane photobioreactor for resource recovery from anaerobically treated sewage. J. Clean. Prod. 178, 665-674. https://doi.org/10.1016/j.jclepro.2017.12.223

169. Viruela, A., Murgui, M., Gómez-Gil, T., Durán, F., Robles, Á, Ruano, M.V., Ferrer, J., Seco, A., 2016. Water resource recovery by means of microalgae cultivation in outdoor photobioreactors using the effluent from an anaerobic membrane bioreactor fed with pre-treated sewage. Bioresour. Technol. 218, 447-454. http://dx.doi.org/10.1016/j.biortech.2016.06.116

170. Vo, H.N.P., Ngo, H.H., Guo, W., Minh, T., Nguyen, H., Liu, Y., Liu, Y., Nguyen, D.D., Chang, S.W., 2019. A critical review on designs and applications of microalgae-based photobioreactors for pollutants treatment. Sci. Total Environ. 651(1), 1549-1568. http://dx.doi.org/10.1016/j.scitotenv.2018.09.282

171. Wagner, D.S., Valverde-Perez, B., Plosz, B.G., 2018. Light attenuation in photobioreactors and algal pigmentation under different growth conditions – Model identification and complexity assessment, Algal Res. 35, 488-499. https://doi.org/10.1016/j.algal.2018.08.019

172. Wang, B., Lan, C.Q., Horsman, M., 2012. Closed photobioreactors for production of microalgal biomasses. Biotechnol. Adv. 30(4), 904-912. https://doi.org/10.1016/j.biotechadv.2012.01.019.

173. Whitton, R., Le Mével, A., Pidou, M., Ometto, F., Villa, R., Jefferson, B., 2016. Influence of microalgal N and P composition on wastewater nutrient remediation. Water Res. 91, 371-378. https://doi.org/10.1016/j.watres.2015.12.054

174. Winkler, M.K.H., Boets, P., Hahne, B., Goethals, P., Volcke, E.I.P., 2017**.** Effect of the dilution rate on microbial competition: r-strategist can win over k-strategist at low substrate concentration. PLoS ONE 12(3): e0172785. https://doi.org/10.1371/journal.pone.0172785

175. Wu, Y.H., Zhu, S.F., Yu, Y., Shi, X.J., Wu, G.X., Hu, H.Y., 2017. Mixed cultivation as an effective approach to enhance microalgal biomass and triacylglycerol production in domestic secondary effluent. Chem. Eng. J. 328, 665-672. http://dx.doi.org/10.1016/j.cej.2017.07.088

176. http://www.oilgae.com/blog/2015/09/cultivation-of-chlorella-vulgaris-in-column photobioreactor-for-biomass-production-and-lipid-accumulation.html (01-06-2019)

177. Xu, X., Gu, X., Wang, Z., Shatner, W., Wang, Z., 2019. Progress, challenges and solutions of research on photosynthetic carbon sequestration efficiency of microalgae. Renew. Sust. Energy Rev. 110, 65–82. https://doi.org/10.1016/j.rser.2019.04.050

178. Xu, M., Li, P., Tang, T., Hu, Z., 2015. Roles of SRT and HRT of an algal membrane bioreactor system with a tanks-in-series configuration for secondary wastewater effluent polishing. Ecol. Eng. 85, 257-264. http://dx.doi.org/10.1016/j.ecoleng.2015.09.064

179. Xue, S., Zhang, Q., Wu, X., Yan, C., Cong, W., 2013. A novel photobioreactor structure using optical fibers as inner light source to fulfill flashing light effects of microalgae. Bioresour. Technol. 138, 141-147. http://dx.doi.org/10.1016/j.biortech.2013.03.156

180. Yadav, G., Sen, R., 2017. Microalgal green refinery concept for biosequestration of carbon-dioxide vis-à-vis wastewater remediation and bioenergy production: Recent technological advances in climate research. J. CO_2 Util. 17, 188–206. http://dx.doi.org/10.1016/j.jcou.2016.12.006

181. Zhang, Y., Wu, H., Sun, M., Peng, Q., Li, A., 2018. Photosynthetic physiological performance and proteomic profiling of the oleaginous algae *Scenedesmus acuminatus* reveal the mechanism of lipid accumulation under low and high nitrogen supplies. Photosynthesis Res. 138, 73–102. https://doi.org/10.1007/s11120-018-0549-1

CHAPTER II:

OBJECTIVES

CHAPTER II:

OBJECTIVES

The global aim of this PhD thesis is to assess the performance of an outdoor flat-panel MPBR system fed by the effluent of an AnMBR system. Furthermore, this work aims at obtaining the best configuration and operating conditions of the MPBR plant at variable ambient conditions:

To reach this aim, the partial objectives described below were accomplished:

i) to assess the inhibition of microalgae by the sulphide present in the substrate. This objective is explained in Chapter IV and corresponds to a manuscript published in Bioresource Technology (2017).

ii) to corroborate the benefits of decoupling the HRT and BRT in terms of nutrient recovery and biomass productivity. This goal was achieved in Chapter V and was published in Water Science and Technology (2018).

iii) to optimise the outdoor microalgae cultivation process, obtaining the optimal operating conditions, which was reached in Chapter VI. This study has been published in Journal of Environmental Management (2019).

iv) to evaluate the effect of different light intensity, duration and photoperiods on the microalgae activity. This goal is commented in Chapter VII, which was published in Algal Research (2019).

v) to assess the effect of temperature variations in a mixed microalgae culture and in the microalgae-nitrifying bacteria competition, which is stated in Chapter VIII.

vi) to evaluate the effect of the light path of the flat-panel PBR. This goal is developed in Chapter IX.

vii) to re-evaluate the outdoor microalgae cultivation for the best configuration of the MPBR plant, obtaining some key performance indicators. This aim is also achieved in Chapter IX.

viii) to obtain a parameter based on pH data that can assess the photosynthetic activity in microalgae cultivation systems in an easy and rapid way. The evaluation of this goal is explained in Chapter X.

ix) to study the stress conditions that make microalgae produce a higher amount of organic matter. This topic is discussed in Chapter XI.

x) to assess the inhibition of microalgae by the nitrite produced by AOB. This point is commented in Chapter XII.

xi) to evaluate the competition for nutrients between microalgae and ammonium oxidising bacteria. Information related to this goal can be found in Chapters V and XII.

x) to find the most relevant factors related to microalgae performance and nitrifying bacteria activity, considering all data obtained during the continuous outdoor cultivation of microalgae to treat the effluent of an AnMBR system. This goal is achieved in Chapter XIII.

CHAPTER III:

MATERIAL AND METHODS

CHAPTER III:

MATERIAL AND METHODS

1. MPBR PILOT PLANT

The MPBR plant (Figure III.1) was operated located in the Carraixet WWTP (39º30'04.0''N 0º20'00.1''W, Valencia, Spain). It mainly consisted of two flat-plate methacrylate PBRs (i.e., PBR-1 and PBR-2) connected to a membrane tank (MT). In addition, there were other two PBRs (PBR-A and PBR-B) that were not connected to the membrane tank (Figure III.1). PBR-1 and PBR-2 had a working volume of 230 L, and dimensions of 1.15-m height, 2-m width and 0.10-m depth; while PBR-A and PBR-B had the same surface (i.e., 1.15-m height, 2-m width) but they were 0.25 m deep. Hence, they have a working volume of 550 L. All four PBRs were east-west orientated, which allowed microalgae to receive higher solar intensity and better distributed along the day (Romero-Villegas et al., 2018).

PBRs were continuously stirred by CO_2-enriched air (maximum CO_2 concentration of 4%) to prevent wall fouling, ensure the culture homogenisation and maintain pH values at 7.5 ± 0.3. At this pH values, ammonia volatilisation and phosphorous precipitation were considered negligible (Whitton et al., 2016).

Both PBRs had an additional artificial white light source consisted of twelve LED lamps (Unique Led IP65 WS-TP4S-40W-ME) that were installed at the back of each PBR offering a continuous light irradiance of 300 $\mu E \cdot m^{-2} \cdot s^{-1}$ (measured at the PBRs surface).

A water heating and cooling device with a thermostat (Daikin Inverter R410A) was installed in the plant to control the temperature of the PBRs. To distribute the water (heated or cooled) to the PBRs, a pump and 20-m long coil pipe rolled in circles was equipped in each PBR. The chosen temperature set-point for heating was 30ºC and 16ºC for cooling. The cooling/heating fluid was pumped to each PBR by opening an electrovalve whenever the temperature exceeded a temperature range of 21-25 ºC.

The membrane tank consisted of a hollow-fibre ultrafiltration membrane bundle extracted from an industrial-scale membrane unit (PURON® Koch Membrane Systems (PUR-PSH31), 0.03 µm pores). It had a total working volume of 14 L and a filtration area of 3.4 m^2. For membrane scouring, air was introduced to the MT through its bottom.

1.1. MPBR plant operation

In order to control the biomass retention time (BRT), the corresponding amount of microalgae biomass was purged from the system and the anaerobic membrane bioreactor (AnMBR) effluent (see Section III.3) was fed into the system during daylight hours. To control the hydraulic retention time (HRT), the corresponding amount of permeate was extracted from the system as effluent during daylight hours. The same amount of substrate was introduced into the system to replace the volume taken out of the system. According to de Andrade et al. (2016), this is the optimum way to continuously feed a microalgae reactor.

The filtration unit was also run during night-time for the correct assessment of the filtration process. The amount of permeate that was not produced to control the HRT was recycled into the system.

A fraction of the microalgae culture was continuously fed into the MT at a flowrate of 300 $L \cdot h^{-1}$. The permeate flowrate was set to around 85-102 $L \cdot h^{-1}$. The rejection of the membrane unit was recycled to the PBR as shown in Figure III.1b.

Membrane operation consisted of a combination of the classical stages of filtration–relaxation (F–R) and back-flushing. Ventilation and degasification stages were also considered (Robles et al., 2013). The membrane operating mode followed a sequence of 300-s basic F-R cycle (250 s filtration and 50 s relaxation), 40 s of back-flush every 10 F–R cycles, 60 s of ventilation every 20 F–R cycles and 60 s of degasification every 50 F–R cycles. The gross 20ºC-standardised transmembrane flux (J_{20}) was kept around 22-30 LMH. The average specific gas demand per unit of membrane area (SGD_m) was kept around 0.3-0.4 $Nm^3 \cdot h^{-1} \cdot m^{-2}$. This gave an average specific gas demand per volume of produced permeate (SGD_P) of around 8-12 Nm^3 of gas per m^3 of permeate.

1.2 MPBR instrumentation, automation, and control

The on-line sensors equipped in the MPBR plant to automate and control the microalgae cultivation process were four pH-temperature transmitters (pHD sc DPD1R1, Hach Lange) and four dissolved oxygen sensors (LDO sc LXV416.99.20001, Hach Lange); i.e., one in each PBR. In addition, an irradiation sensor (Apogee Quantum SQ-200) was set on the PBR-1 surface to measure the photosynthetically active radiation (PAR).

Moreover, four liquid flowrate transmitters (for pumps P1A, P1B, P2 and P3); three level transmitters (for MT, CIP and DC2); one liquid pressure transmitter to monitor the

transmembrane pressure of the MT; one gas pressure transmitter in the blower outlet; and five gas flowrate transmitters (one in the air inlet of each PBR, one in the inlet of the MT and one to measure the CO_2 injection).

The MPBR pilot plant also included five frequency converters to regulate the rotational speed of the blower and pumps (P1A, P1B, P2 and P3); five regulating valves to control the air flowrate through the PBRs, and the membrane tanks; and on-off valves to control biomass wastage, CO_2 dosage and the membrane operation stage; i.e., filtration, back-flush, ventilation, standby, relaxation and degasification (Robles et al., 2013).

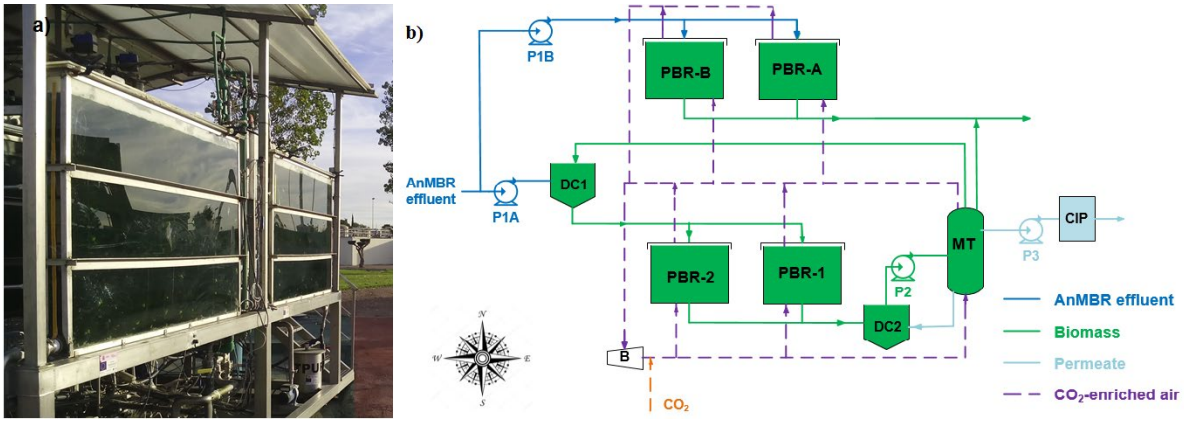

Figure III.1. a) Outdoor MPBR pilot plant. b) Flow diagram of the process. PBR: photobioreactor; MT: membrane tank; P: pump; DC: distribution chamber; B: blower; CIP: clean-in-place-tank.

2. MICROALGAE

Microalgae were originally isolated from the walls of the secondary clarifier in the Carraixet WWTP (Valencia, Spain), which consisted of a complex ecosystem which contained microalgae (including cyanobacteria), algae and bacteria (both heterotrophic and autotrophic). Prior to the inoculation in the MPBR plant, the sample from the secondary clarifier was filtered to remove most of filamentous bacteria and zooplankton from the inoculum. The culture was adapted to the growth medium (see Section III.3) under lab conditions of continuous illumination (85 $\mu E \cdot m^{-2} \cdot s^{-1}$), temperature of 22 ± 1 ºC and pH of 7.4 ± 0.3 (González-Camejo et al., 2018). *Scenedesmus* and *Chlorella* were the main microalgae genus present in the culture.

3. WASTEWATER

The effluent of an AnMBR pilot plant was used as microalgae PBR influent. This AnMBR plant was fed by the primary effluent of the Carraixet WWTP. Further details of the AnMBR plant can be found in Seco et al. (2018).

The main characteristics of the AnMBR effluent during the whole experimental period are displayed in Table III.1:

Table III.1: AnMBR effluent characteristics

Parameter	Unit	Mean ± SD
NH_4	mg $N \cdot L^{-1}$	48.5 ± 6.6
NO_2	mg $N \cdot L^{-1}$	0.4 ± 0.2
NO_3	mg $N \cdot L^{-1}$	3.5 ± 1.8
P	mg $P \cdot L^{-1}$	5.7 ± 1.5
N:P	molar ratio	20.7 ± 4.1
COD	mg $COD \cdot L^{-1}$	67 ± 7
BOD	mg $O_2 \cdot L^{-1}$	27 ± 2
Alk	mg $CaCO_3 \cdot L^{-1}$	729 ± 98
VFA	mg $COD \cdot L^{-1}$	1.7 ± 0.2
SO_4	mg $SO_4 \cdot L^{-1}$	35.9 ± 4.2
H_2S	mg $S \cdot L^{-1}$	93.6 ± 16.3
Turbidity	NTU	< L.D.

NH_4: ammonium; NO_2: nitrite; NO_3: nitrate; P: phosphorus; N:P: nitrogen:phosphorus ratio; COD: chemical oxygen demand; BOD: biochemical oxygen demand; Alk: alkalinity; VFA: volatile fatty acids; SO_4: sulphate; H_2S: Sulphur; L.D.: limit of detection.

It is relevant that the N:P molar ratio in the effluent was a bit higher than that reported by Reynolds (2006) for green microalgae; i.e., 16. Hence, the system was expected to be phosphorus-limited.

Regarding organic matter loading, most of the COD of this AnMBR effluent was inert since BOD only accounted for 27 ± 2 mg $O_2 \cdot L^{-1}$. Photoautotrophic metabolism typical of microalgae was thus enhanced, while heterotrophic activity was limited.

Volatile fatty acids (VFA) concentrations, which can affect microalgae growth (Huo et al., 2018), were very low (Table III.1).

4. LAB-SCALE ASSAYS

4.1. Lab-scale PBRs

The lab-scale PBR consisted of a cylindrical transparent tank with a working volume of 8L (20 cm internal diameter). The culture was air-stirred at a flowrate of 0.2-0.3 vvm through four fine bubble diffusers placed crosswise at the bottom in order to achieve the culture homogenisation and avoid biofilm formation on the walls. To fix the pH value in the PBR at 7.5, pure CO_2 (99.9%) was injected from a pressurised cylinder into the stream when the pH rose above the aforementioned ph set-point (Figure III.2). Controlling pH in the reactor helped to prevent undesirable phenomena such as phosphate precipitation and the ammonia stripping losses (Whitton et al., 2016).

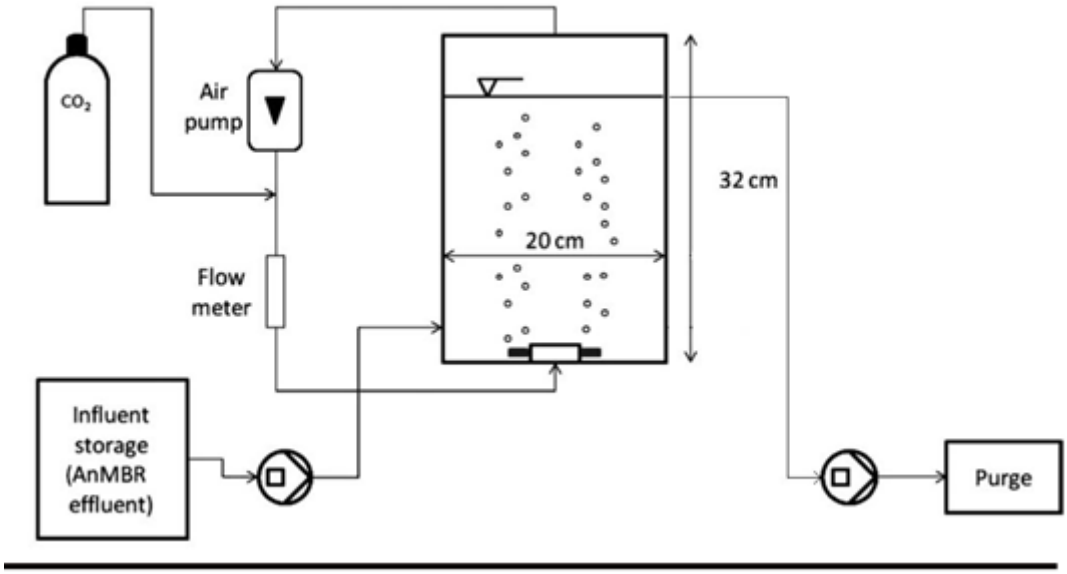

Figure III.2. Lab-scale photobioreactor (González-Camejo et al., 2018).

The lab-scale PBR was lit by four cool-white LED lamps (T8 LED-Tube 9 w) to supply a light intensity of 100 $\mu mol \cdot m^{-2} \cdot s^{-1}$ measured at the PBR surface.

Temperature, pH and dissolved oxygen of the microalgae culture were monitored and logged in a PC using data acquisition software. For pH, the signal from the corresponding electrodes was processed by a multiparametric analyser (CONSORT C832, Belgium), while temperature and dissolved oxygen were measured by a 4-Star multiparametric analyser (Thermo Scientific) connected to a 087003RDO probe.

The PBR was operated in a semi-continuous mode (BRT ≡ HRT). The feed was the AnMBR effluent described in Section III.3.

4.2. Respirometric tests

A 400-mL cylindrical closed PBR was lit by four cool-white LED lamps (T8 LED-Tube 9 w) to supply a light intensity of 100 $\mu mol \cdot m^{-2} \cdot s^{-1}$ on the PBR surface and placed inside climate chamber to carry out the respirometric tests at constant temperature of around 21-23 ºC. For these respirometric tests, a mix of microalgae culture from the MPBR plant (section III.1) and AnMBR effluent (section III.3) was used, maintaining similar biomass concentration during each set of tests. Hence, differences regarding shadow effect (Abu-Ghosh et al., 2016) between tests were negligible.

20 mg $C \cdot L^{-1}$ in the form of bicarbonate were added to the microalgae samples before each respirometric tests to avoid carbon limitation. Diluted sulphuric (0.1 M) was added to maintain the pH at around 7.5. The PBR was stirred by a magnetic mixing (200 rpm) which enabled oxygen homogenisation and avoided microalgae sedimentation.

An oxygen probe (WTW CellOx 325) monitored the dissolved oxygen (DO) concentration and temperature of the culture during the time that each test lasted (i.e. around 30 minutes). This data was retrieved and used to obtain the oxygen production rate (OPR) by fitting the experimental DO data to a model considering the coexistence of oxygen mass transfer, due to mixing, and the biological DO production rates (section 6.6).This OPR can be used as an indirect measurement of the photosynthetic activity (Rossi et al., 2018).

It must be considered that the OPR obtained during these respirometric tests is a net value composed by several factors: i) microalgae photosynthesis; ii) activity of nitrifying bacteria, both ammonium oxidising bacteria (AOB) and nitrite oxidising bacteria (NOB) iii) microalgae respiration; and iv) respiration of heterotrophic bacteria (Rossi et al., 2018).

However, nitrifying bacteria activity was expected to be low because allylthiourea (ATU) was added to the culture in these tests to inhibit AOB growth (Krustok et al., 2016). Moreover, microalgae respiration was expected to affect all the tests in a similar way because each set of respirometric tests was developed with the same culture sample from the MPBR plant (Section III.1). Furthermore, the activity of heterotrophic bacteria was expected to be low because of the low organic loads of the AnMBR effluent (Section III.3). In conclusion, the net OPR obtained in the tests was considered as a valid indirect measurement of the microalgae activity.

5. SAMPLING AND ANALYTICAL METHODS

Grab samples from the AnMBR effluent (i.e., the influent of the MPBR plant), the microalgae culture and from the MPBR effluent were collected in duplicate three times a week. Ammonium (NH_4), nitrite (NO_2), nitrate (NO_3) and phosphate (PO_4) were analysed according to methods 4500-NH3-G, 4500-NO2-B, 4500-NO3-H and 4500-P-F, respectively, of Standard Methods (APHA *et al.*, 2005), using an automatic analyser (Smartchem 200, WestcoScientific Instruments, Westco). The total suspended solids (TSS) and volatile suspended solids (VSS) concentration was also measured three times a week in duplicate, according to methods 2540 D and 2540 E of Standard Methods (APHA et al., 2005).

Once a week, the total chemical oxygen demand (COD), soluble (sCOD), total nitrogen (N) and total phosphorus (P) were also measured. Total and soluble COD were performed according to Standard Methods (APHA et al., 2005), 5220-COD-C and 522-COD-D, respectively.

Total nitrogen concentration was measured in the medium by colorimetric analysis using the nitrogen total cell test kit (Merckoquant 1.14537.001, Merck, Germany). Total phosphorus concentration was measured in the same culture medium after a total digestion at 150 ºC for two hours, followed by orthophosphate determination according to Standard Methods, 4500-P-F, (APHA *et al.*, 2005), using the aforementioned automatic analyser (Smartchem 200, WestcoScientific Instruments, Westco).

Optical density at 680 nm (OD680) and maximum quantum yield of photosystem II (F_v/F_m) were measured in-situ with a portable fluorometer AquaPen-C AP-C 100 (Photon Systems Instruments). To measure the quantum yield, samples had to remain in dark conditions for ten minutes to get dark-adapted (Ferro et al., 2018). The turbidity of the influent was measured by a portable turbidimeter (Lovibond T3 210IR).

The measurement of the wavelength spectrum (400-700 nm) was measured by a spectrophotometer (Spectroquant® Pharo 100, Merck, Germany) and was used to obtain the extinction coefficient of the microalgae culture (Franco et al., 2019).

Total eukaryotic cells (TEC) concentration was measured in duplicate twice a week. 50 µL of sample were filtered with 0.2 µm membranes (Millipore GTTP). The filters were washed with distilled water to eliminate the retained salt and then dehydrated with ethanol washes. Cell counts were performed by epifluorescence microscopy on a Leica DM2500, using the 100x-oil immersion lens. A minimum of 300 cells were counted and

at least 100 cells of the most abundant genera were counted with an error of less than 20% (Pachés et al., 2012).

The presence of *Escherichia coli* and other coliform pathogens in permeate was quantitatively determined through positive β-glucorinidase assay using membrane filters, following the UNE-EN ISO 9308-1:2014 standard method.

SYTOX Green DNA staining dye (Invitrogen S7020) was used to monitor cell viability (Sato et al., 2004). 0.1µL of SYTOX Green 5mM was added to 50µL microalgae sample. Samples were incubated in dark conditions for 5 minutes. After that, the samples were excited using a fluorescence microscope (DM2500, Leica, Germany) set at 450 – 490 nm for excitation and 515 nm for emission. More than 400 cells were counted in duplicate for viability calculation in a Neubauer counting chamber.

6. CALCULATIONS

6.1. MPBR performance

6.1.1. Nutrient recovery

The nutrient recovery capacity of the system was assessed by nutrient recovery rates; i.e., nitrogen recovery rate (NRR) (mg $N \cdot L^{-1} \cdot d^{-1}$) (Eq. III.1) and phosphorus recovery rate (PRR) (mg $P \cdot L^{-1} \cdot d^{-1}$) (Eq. III.2); and nutrient recovery efficiencies, both nitrogen recovery efficiency (NRE) (Eq. III.3) and phosphorus recovery efficiency (PRE) (Eq. III.4).

$$NRR = \frac{F \cdot (N_{inf} - N_{ef})}{V_{MPBR}} \quad \text{[Eq. III.1]}$$

$$PRR = \frac{F \cdot (P_{inf} - P_{ef})}{V_{MPBR}} \quad \text{[Eq. III.2]}$$

$$NRE\ (\%) = \frac{N_{inf} - N_{ef}}{N_{inf}} \cdot 100 \quad \text{[Eq. III.3]}$$

$$PRE\ (\%) = \frac{P_{inf} - P_{ef}}{P_{inf}} \cdot 100 \quad \text{[Eq. III.4]}$$

where F is the treatment flow rate ($m^3 \cdot d^{-1}$); N_{inf} is the influent nitrogen concentration (mg $N \cdot L^{-1}$); N_{ef} is the nitrogen concentration of the effluent (mg $N \cdot L^{-1}$); V_{MPBR} is the volume of the culture in the MPBR plant (m^3); P_{inf} is the phosphorus concentration of the influent (mg $P \cdot L^{-1}$); P_{ef} is the phosphorus concentration of the effluent (mg $P \cdot L^{-1}$).

NRR and PRR were considered more adequate parameters to compare different experimental periods since nutrient recovery efficiencies are a function of the influent nutrient concentrations (Sepúlveda et al., 2015).

However, since nutrient recovery of microalgae is highly influenced by the variability of the light irradiance under outdoor conditions (Viruela et al., 2016), NRR and PRR were normalised by the total photosynthetic active radiation (PAR) supplied to the PBRs in order to compare the nutrient recovery rates of different experimental periods. Nitrogen recovery rate:light irradiance ratio (NRR:I) (mg $N \cdot mol^{-1}$) and phosphorus recovery rate:light irradiance ratio (PRR:I) (mg $P \cdot mol^{-1}$) were thus obtained according to Eq. III.5 and Eq. III.6.

$$NRR{:}I = \frac{NRR \cdot V_{MPBR} \cdot 10^9}{tPAR \cdot S \cdot 24 \cdot 3600} \quad \text{[Eq. III.5]}$$

$$PRR{:}I = \frac{PRR \cdot V_{MPBR} \cdot 10^9}{tPAR \cdot S \cdot 24 \cdot 3600} \quad \text{[Eq. III.6]}$$

where tPAR is the total PAR supplied to the PBR surface (i.e. the 24-hour average PAR plus the PAR from the LED lamps) (μmol photons$\cdot m^{-2} \cdot s^{-1}$); and S is the illuminated PBR surface (m^2).

On the other hand, the activity of nitrifying bacteria can be assessed by the production of nitrite and nitrate in the culture (Bilanovic et al., 2016). Hence, the nitrification rate (NOxR) (mg $N \cdot L^{-1} \cdot d^{-1}$), which was calculed by Eq. III.7 was used to evaluate the activity of nitrifying bacteria.

$$\text{NOxR} = \frac{F \cdot (NOx_{ef} - NOx_{inf})}{V_{MPBR}} \quad \text{[Eq. III.7]}$$

where NOx_{ef} is the concentration of nitrite plus nitrate of the effluent (mg $N \cdot L^{-1}$) and NOx_{inf} is the concentration of nitrite plus nitrate of the influent (mg $N \cdot L^{-1}$).

6.1.2. Biomass productivity and efficiency

The biomass productivity (BP) (mg $VSS \cdot L^{-1} \cdot d^{-1}$); i.e., the biomass produced and taken out of the PBRs (de Andrade et al., 2016) was calculated by Eq. III.8:

$$BP = \frac{F_w \cdot VSS}{V_{MPBR}} \quad \text{[Eq. III.8]}$$

where F_w ($L \cdot d^{-1}$) is the flow of the biomass wasted with the purge; VSS (mg $VSS \cdot L^{-1}$) is the volume of the culture in the MPBR plant (m^3).

Similarly to nutrient recovery, the biomass productivity was also normalised y the light radiation to compare between different experimental periods. The biomass productivity:light irradiance ratio (BP:I, g $VSS \cdot mol^{-1}$) was thus obtained by Eq. III.9. The photosynthetic efficiency (PE) (%) was also used as comparable parameter for different periods (Eq. III.10):

$$BP{:}\,I = \frac{BP \cdot V_{MPBR} \cdot 1000}{tPAR \cdot S \cdot 24 \cdot 3600} \quad \text{[Eq. III.9]}$$

$$PE\ (\%) = \frac{BP_m \cdot H}{tIr \cdot S \cdot 24 \cdot 3600} \cdot 100 \quad \text{[Eq. III.10]}$$

where tPAR is the total PAR supplied to the PBR surface (i.e. the 24-hour average PAR plus the PAR from the LED lamps) (μmol photons·m^{-2}·s^{-1}); S is the illuminated PBR surface (m^2); BP_m is the microalgae productivity measured as g VSS·d^{-1}; H is the enthalpy of dry biomass (22.9 KJ·g VSS^{-1}); tIr is the total irradiance of light measured as energetic flux density (KJ·m^{-2}·s^{-1}).

To transform the photosynthetic photon flux density (PPFD) which corresponds to tPAR to tIr, Eq. III.11 was used:

$$tIr = \frac{tPAR \cdot c \cdot h \cdot n}{\lambda \cdot 10^9} \quad \text{[Eq. III.11]}$$

where c is the speed of light ($3 \cdot 10^8$ m·s^{-1}), h is the Planck constant ($6.63 \cdot 10^{-34}$ J·s), n is the Avogadro number ($6.022 \cdot 10^{23}$ mol^{-1}) and λ is the light wavelength; i.e., $550 \cdot 10^{-9}$ m for white light.

The carbon fixed by microalgae (CO_2-BF) (kg CO_2·$m^3_{influent}$) was calculated by Eq. III.12:

$$CO_2 - BF = \frac{BP_m}{Y_{CO2} \cdot F \cdot 10^3} \quad \text{[Eq. III.12]}$$

where BP_M is the microalgae productivity measured as kg VSS·d^{-1}; F is influent flow (m^3·d^{-1}); and Y_{CO2} is the stoichiometric CO_2 capture for microalgae growth (0.52 kg VSS·kg CO_2^{-1}). It must be noted that for the stoichiometric calculations of the microalgae biomass, the chemical formula used was $C_{106}H_{181}O_{45}N_{16}P$ (Viruela et al., 2018).

The total carbon biofixation (C-BF) will be composed by both the theoretical carbon that will be absorbed for microalgae growth (i.e., CO_2-BF) and the CO_2 emissions that would be saved if microalgae biomass is digested for biogas production, with a conversion factor of 0.30 kg CO_2·kWh^{-1} (Viruela et al., 2018). The energy recovery from the digestion of microalgae biomass (ER-BM) (kWh·$m^{-3}_{influent}$) was obtained by Eq. III.13:

$$ER - BM = \frac{BP_{COD} \cdot Y_{CH4} \cdot LHV \cdot \eta}{F} \quad \text{[Eq. III.13]}$$

where BP_{COD} is the microalgae biomass productivity measured as kg COD·d^{-1}; Y_{CH4} is the theoretical methane yield (0.35 m^3 CH_4· kg COD^{-1}); LHV is the lower heating value

for methane (9.94 kWh·m^{-3}); and η is the power generation efficiency of a methane-powered turbine electrical generator (set to 35%).

6.2. Intracellular nutrient content

The intracellular nutrient contents (i.e., N_i and P_i) (%) of microalgae were approximately calculated considering that all the VSS corresponded to microalgae biomass:

$$N_i = \frac{N_{PBR}}{VSS} \cdot 100 \qquad \text{[Eq. III.14]}$$

$$P_i = \frac{P_{PBR}}{VSS} \cdot 100 \qquad \text{[Eq. III.15]}$$

where N_{PBR} and P_{PBR} are the suspended concentration of nitrogen (mg N·L^{-1}) and phosphorus (mg P·L^{-1}) of the microalgae culture, respectively.

6.3. Optical properties

The average irradiance (I_{av}) (µmol photons·m^{-2}·s^{-1}) inside the PBRs was calculated by the Lambert-Beer law Eq. III.16:

$$I_{av} = \frac{I_0}{(K_a \cdot Lp \cdot VSS)} \cdot (1 - e^{(K_a \cdot LP \cdot VSS)}) \qquad \text{[Eq. III.16]}$$

where I_0 (µmol photons·m^{-2}·s^{-1}) is the irradiance on the PBR surface; Lp is the light path of the flat-panel PBR (m) and K_a (m^2·g^{-1}) is the extinction coefficient (Eq. III.17):

$$K_a = \frac{OD_{400-700}}{VSS \cdot Lp_c} \qquad \text{[Eq. III.17]}$$

where $OD_{400\text{-}700}$ (-) is the average optical density in the range of 400-700 nm; and Lp_c (m) is the light path of the spectrophotometer´s cuvette.

The duty cycle (φ); i.e., the proportion of time at which microalgae are exposed to light (Barceló-Villalobos et al., 2019) was calculated according to Eq. III.18:

$$\varphi = \frac{I_{av}}{I_0} \qquad \text{[Eq. III.18]}$$

6.4. Membrane filtration

To assess membrane filtration, the 20 ºC-standardised transmembrane flux (J_{20}) (LMH), the fouling rate (FR) (mbar·min^{-1}), and the specific gas demand per volume of permeate produced (SGD_p) (m$^3_{air}$·m$^{-3}_{permeate}$) were calculated in based on on-line monitored transmembrane flux (J) (LMH) and transmembrane pressure (TMP_{Jn}) data:

$$J_{20} = J \cdot e^{-0.0239 \cdot (T-20)} \qquad \text{[Eq. III.19]}$$

$$FR = \frac{n \cdot \sum_1^n (TMP_i \cdot t_i) + \sum_1^n TMP_i \cdot \sum_1^n t_i}{n \cdot \sum_1^n TMP_i^2 - (\sum_1^n TMP_i)^2} \quad \text{[Eq. III.20]}$$

$$SGD_P = \frac{F_{air}}{J_{20} \cdot S_{memb}} \quad \text{[Eq. III.21]}$$

where T is the culture temperature (ºC); t_{Jn} is the time of the filtration stage (min); F_{air} is the air flow for membrane scouring ($m^3 \cdot h^{-1}$) and S_{memb} is the membrane surface area (m^2).

6.5. Growth rate

Microalgae growth rate (μ) (d^{-1}) was calculated by applying the Verhulst logistic kinetic model (Verhulst, 1838) to the OD680 evolution during the batch stages of some experiments, as shown in Eq. III.22:

$$\mu = \frac{OD680_m \cdot OD680_0 \cdot e^{\mu \cdot t}}{OD680_m - OD680_0 + OD680_0 \cdot e^{\mu \cdot t}} \quad \text{[Eq. III.22]}$$

where $OD680_m$, $OD680_o$ and OD680 are the optical density at 680 nm at an operation time which corresponded to infinite, zero, and *t*, respectively; and *t* is the time of batch operation (d).

6.6. Respirometric tests

To calculate the net oxygen production rate (OPR) (mg $O_2 \cdot L^{-1} \cdot h^{-1}$), Eq. III.23 was used:

$$\frac{dDO}{dt} = k_L a \cdot (DO_{sat} - DO) + OPR \quad \text{[Eq. III.23]}$$

where dDO/dt is the variation of the oxygen concentration over time (mg $O_2 \cdot L^{-1} \cdot h^{-1}$), k_La is the oxygen mass transfer coefficient (h^{-1}), DO_{SAT} is the oxygen saturation concentration at the culture temperature (mg $O_2 \cdot L^{-1}$), DO is the oxygen concentration in the culture (mg $O_2 \cdot L^{-1}$).

k_La was evaluated by doing respirometric tests with clean water as medium in duplicate. To calculate the OPR, the minimum square error criterion was used to obtain the optimal fit to Eq. III.23 (Rossi et al., 2018).

7. STATISTICAL ANALYSIS

All analytical determinations were performed in duplicate. The results are given as the average with its corresponding standard deviation.

To assess the difference between groups of variables, the Student's t-test was used through Statgraphics Centurion XVII. An analysis of variance (ANOVA) was also

performed by SPSS 16.1. Differences were considered statistically significant when p-value < 0.05.

Principal component analysis (PCA) (Aguado et al., 2008) was conducted to assess the effect of different ambient, operating and design conditions on the performance of the outdoor MPBR plant. In addition, PLSR algorithm (Wold et al., 2001) was carried out to evaluate the effect of predictors (X) on responses (Y) by using the mixOmics library (http://www.mixOmics.org) through the software R version 3.2.3 (http://www.R-project.org).

REFERENCES

1. Abu-Ghosh, S., Fixler, D., Dubinsky, Z., Iluz, D., 2016. Flashing light in microalgae biotechnology. Bioresour. Technol. 203, 357-363. http://dx.doi.org/10.1016/j.biortech.2015.12.057
2. Aguado, D., Montoya, T., Borras, L., Seco, A., Ferrer, J., 2008. Using SOM and PCA for analysing and interpreting data from a P-removal SBR. Engineering Applications of Artificial Intelligence 21, 919–930. https://doi.org/10.1016/j.engappai.2007.08.001
3. APHA-AWWA-WPCF, 2005. Standard methods for the examination of water and wastewater, 21st edition. American Public Health Association, American Water Works Association, Water Pollution Control Federation. Washington DC, USA.
4. Barceló-Villalobos, M., Fernández-del Olmo, P., Guzmán, J.L., Fernández-Sevilla, J.M., Acién Fernández, F.G., 2019, Evaluation of photosynthetic light integration by microalgae in a pilot-scale raceway reactor, Bioresour. Technol. 280, 404-411. https://doi.org/10.1016/j.biortech.2019.02.032
5. Bilanovic, D., Holland, M., Starosvetsky, J., Armon, R., 2016. Co-cultivation of Microalgae and Nitrifiers for Higher Biomass Production and Better Carbon Capture, Bioresour. Technol. 220, 282-288. http://dx.doi.org/10.1016/j.biortech.2016.08.083
6. de Andrade, G.A., Berenguel, M., Guzmán, J.L., Pagano, D.J., Acién, F.G., 2016. Optimization of biomass production in outdoor tubular photobioreactors. Journal of Process Control 37 (2016) 58–69. http://dx.doi.org/10.1016/j.jprocont.2015.10.001
7. Ferro, L, Gorzsás, A., Gentili, F.G., Funk, C., 2018, Subarctic microalgal strains treat wastewater and produce biomass at low temperature and short photoperiod, Algal Res. 35, 160-167. https://doi.org/10.1016/j.algal.2018.08.031
8. Franco, B.M., Navas, L.M., Gómez, C., Sepúlveda, C., Acién, F.G., 2019. Monoalgal and mixed algal cultures discrimination by using an artificial neural network. Algal Res. (in press). https://doi.org/10.1016/j.algal.2019.101419

9. González-Camejo, J., Barat, R., Pachés, M., Murgui, M., Ferrer, J., Seco, A., 2018. Wastewater Nutrient Removal in a Mixed Microalgae-bacteria Culture: Effect of Light and Temperature on the Microalgae-bacteria Competition. Environ. Technol. 39 (4), 503–515. https://doi.org/10.1080/09593330.2017.1305001
10. González-Camejo, J., Serna-García, R., Viruela, A., Pachés, M., Durán, F., Robles, A., Ruano, M.V., Barat R., Seco, A., 2017. Short and long-term experiments on the effect of sulphide on microalgae cultivation in tertiary sewage treatment. Bioresour. Technol. 244, 15-22. http://dx.doi.org/10.1016/j.biortech.2017.07.126
11. Huo, S., Kong, M., Zhu, F., Zou, B., Wang, F., Xu, L., Zhang, C., Huang, D., 2018. Mixotrophic Chlorella sp. UJ-3 cultivation in the typical anaerobic fermentation effluents. Bioresour. Technol. 249, 219-225. https://doi.org/10.1016/j.biortech.2017.10.042
12. Krustok, I., Odlare, M., Truu, J., Nehrenheim, E., 2016. Inhibition of nitrification in municipal wastewater-treating photobioreactors: effect on algal growth and nutrient uptake. Bioresour. Technol. 202, 238–243. http://dx.doi.org/10.1016/j.biortech.2015.12.020
13. Pachés, M., Romero, I., Hermosilla, Z. and Martinez-Guijarro, R. 2012. PHYMED: An ecological classification system for the Water Framework Directive based on phytoplankton community composition. Ecological Indicators 19, 15-23. https://doi.org/10.1016/j.ecolind.2011.07.003
14. Reynolds, C.S., 2006. The ecology of phytoplankton (ecology, biodiversity and conservation). Cambridge: Cambridge University Press; United Kingdom.
15. Robles, A., Ruano, M.V., Ribes, J., Ferrer, J., 2013. Factors that affect the permeability of commercial hollow-fibre membranes in a submerged anaerobic MBR (HF-SAnMBR) system. Water Res. 47, 1277-1288. http://dx.doi.org/10.1016/j.watres.2012.11.055
16. Romero-Villegas, G.I., Fiamengo, M., Acién Fernández, F.G., Molina Grima, E., 2018. Utilization of centrate for the outdoor production of marine microalgae at pilot-scale in flat-panel photobioreactors. Journal of Biotechnology 284, 102-114. https://doi.org/10.1016/j.jbiotec.2018.08.006
17. Rossi, S., Bellucci, M., Marazzi, F., Mezzanotte, V., Ficara, E., 2018. Activity assessment of microalgal-bacterial consortia based on respirometric tests. Water Sci Technol. 78(1-2), 207-215. https://doi.org/10.2166/wst.2018.078.
18. Sato, M., Murata, Y., Mizusawa, M., Iwahashi, H., Oka, S. I., 2004. A simple and rapid dual-fluorescence viability assay for microalgae. Microbiol Cult Coll, 20(2), 53-59.
19. Seco, A., Aparicio, S., González-Camejo, J., Jiménez-Benítez, A., Mateo, O., Mora, J.F., Noriega-Hevia, G., Sanchis-Perucho, P., Serna-García, R., Zamorano-López, N.,

Giménez, J.B., Ruiz-Martinez, A., Aguado, D., Barat, R., Borrás, L., Bouzas, A., Martí, N., Pachés, M., Ribes, J., Robles, A., Ruano, M.V., Serralta, J. and Ferrer, J., 2018. Resource recovery from sulphate-rich sewage through an innovative anaerobic-based water resource recovery facility (WRRF). Water Science and Technology 78 (9), 1925-1936. https://doi.org/10.2166/wst.2018.492

20. Sepúlveda, C., Acién, F.G., Gómez, C., Jiménez-Ruíz, N., Riquelme, C., Molina-Grima, E., 2015. Utilization of centrate for the production of the marine microalgae Nannochloropsis gaditana, Algal Res. 9, 107-116. http://dx.doi.org/10.1016/j.algal.2015.03.004
21. UNE EN ISO 9308-1:2014, AENOR, 2014. Water Quality - Enumeration of Escherichia Coli And Coliform Bacteria - Part 1: Membrane Filtration Method For Waters With Low Bacterial Background Flora (Iso 9308-1:2014/Amd 1:2016), Asociación Española de Normalización (AENOR).
22. Verhulst, P.-F.: Notice sur la loi que la population poursuit dans son accroissement. Corresp. Math. Phys. 10, 113–121 (1838).
23. Viruela, A., Robles, A., Durán, F., Ruano, M.V., Barat, R., Ferrer, J., Seco, A., 2018. Performance of an outdoor membrane photobioreactor for resource recovery from anaerobically treated sewage. J. Clean. Prod. 178, 665-674. https://doi.org/10.1016/j.jclepro.2017.12.223
24. Viruela, A., Murgui, M., Gómez-Gil, T., Durán, F., Robles, Á, Ruano, M.V., Ferrer, J., Seco, A., 2016. Water resource recovery by means of microalgae cultivation in outdoor photobioreactors using the effluent from an anaerobic membrane bioreactor fed with pre-treated sewage. Bioresour. Technol. 218, 447-454. http://dx.doi.org/10.1016/j.biortech.2016.06.116
25. Whitton, R., Le Mével, A., Pidou, M., Ometto, F., Villa, R., Jefferson, B., 2016. Influence of microalgal N and P composition on wastewater nutrient remediation. Water Res. 91, 371-378. https://doi.org/10.1016/j.watres.2015.12.054
26. Wold, S., Sjöström, M., Eriksson, L., 2001. PLS-regression: a basic tool of chemometrics. Chemom. Intell. Lab. Syst. 58, 109–130.

CHAPTER IV:

SHORT AND LONG-TERM EXPERIMENTS ON THE EFFECT OF SULPHIDE ON MICROALGAE CULTIVATION IN TERTIARY SEWAGE TREATMENT

CHAPTER IV:

SHORT AND LONG-TERM EXPERIMENTS ON THE EFFECT OF SULPHIDE ON MICROALGAE CULTIVATION IN TERTIARY SEWAGE TREATMENT

González-Camejo, J., Serna-García, R., Viruela, A., Pachés, M., Durán, F., Robles, A., Ruano, M.V., Barat R., Seco, A., 2017. Short and long-term experiments on the effect of sulphide on microalgae cultivation in tertiary sewage treatment. Bioresour. Technol. 244, 15-22. http://dx.doi.org/10.1016/j.biortech.2017.07.126

ABSTRACT

Microalgae cultivation appears to be a promising technology for treating nutrient-rich effluents from anaerobic membrane bioreactors, as microalgae are able to consume nutrients from sewage without an organic carbon source, although the sulphide formed during the anaerobic treatment does have negative effects on microalgae growth. Short and long-term experiments were carried out on the effects of sulphide on a mixed microalgae culture. The short-term experiments showed that the oxygen production rate (OPR) dropped as sulphide concentration increased: a concentration of 5 mg $S \cdot L^{-1}$ reduced OPR by 43%, while a concentration of 50 mg $S \cdot L^{-1}$ came close to completely inhibiting microalgae growth.

The long-term experiments revealed that the presence of sulphide in the influent had inhibitory effects at sulphide concentrations above 20 mg $S \cdot L^{-1}$ in the culture, but not at concentrations below 5 mg $S \cdot L^{-1}$. These conditions favoured *Chlorella* growth over that of *Scenedesmus*.

1. INTRODUCTION

Anaerobic membrane bioreactors (AnMBRs) have been reported as a more promising technology for wastewater treatment than conventional aerobic treatments for their several advantages: i) higher energy recovery from organic matter as biogas, ii) reduced power consumption, and iii) up to 90% reduction in sludge production (Giménez et al., 2011). However, AnMBRs are not able to remove nutrients from wastewater (Aiyuk, 2006), which means some post-treatment is required before discharging wastewater in

sensitive areas (European Directive 91/271/CEE). In this respect, microalgae cultivation appears to be a sustainable technology for treating AnMBR effluent, allowing not only nutrient removal but also the possibility of moving towards water resource recovery in the sewage treatment field (Ruiz-Martínez et al., 2012; Viruela et al., 2016).

Autotrophic microalgae are photosynthetic microorganisms which use light energy and inorganic carbon (CO_2 and HCO_3^-) to grow. They also require high amounts of inorganic compounds, such as ammonium (NH_4^+) and phosphate (PO_4^{3-}), which can be obtained from a nutrient-rich wastewater stream (Tan et al., 2016). The microalgae biomass generated can be used as an energy source, since it can be converted into biogas, biodiesel, biohydrogen, fertilizers and high-value products (Maroneze et al., 2016). The combination of an AnMBR and a microalgae cultivation system is therefore a win-win strategy, since it would be feasible to recover both nutrients and other resources such as energy and water from the wastewater. However, among other issues, it must be taken into account that sulphate is reduced to sulphide in an AnMBR by means of sulphate reducing bacteria (SBR). In acid sulphate soils, such as those typically found in the Mediterranean Basin, water (and therefore wastewater) contains high concentrations of sulphate. AnMBR effluent is thus expected to have high sulphide concentrations but low sulphate concentrations (Giménez, 2014).

Sulphide has been reported to inhibit the photosynthesis process of microalgae, as it reduces the electron flow between the photosystem II (PSII) and photosystem I (PSI) (Pearson et al., 1987; Miller and Bebout, 2004). By way of example, Küster *et al.* (2005) studied the toxicity of the *Scenedesmus* microalgae through the inhibition of cellular reproduction during a one-generation cycle lasting 24 hours. Their results showed 50% inhibition when the sulphide concentration was around 2 mg $S \cdot L^{-1}$. González-Sánchez and Posten (2017) studied the deployment of a *Chlorella* sp. culture for biogas upgrading and found that these microalgae were inhibited at sulphide concentrations higher than 16 mg $S \cdot L^{-1}$. However, as sulphur acts as macronutrient for microalgae growth, the absence of sulphide or sulphate in the medium can also limit microalgae growth (González-Sánchez and Posten, 2017). This means that before setting up a microalgae culture to treat sewage on an industrial scale, it will be necessary to analyse the effects of introducing sulphide into the system, such us inhibition, nutrient limitation, species distribution in the culture, etc.

The aim of this work was thus to study the effect of sulphide on mixed microalgae culture in tertiary sewage treatment. Short-term experiments were carried out on a bench-scale and long-term pilot-scale experiments in an outdoor membrane photobioreactor (MPBR) using as growth medium the nutrient-loaded effluent from an AnMBR plant at the Carraixet full-scale WWTP (Giménez et al., 2011).

2. MATERIAL AND METHODS

2.1. Microalgae substrate

The microalgae substrate used for both the short and long-term experiments was the nutrient-rich effluent from an AnMBR plant, which is described in detail in Giménez et al. (2011) and Robles et al. (2013). The AnMBR influent was from the pre-treatment of the Carraixet WWTP (Valencia, Spain): screening, degritter and grease removal. The average nutrient concentrations of the microalgae substrate during the experimental period were: ammonium 58.4 ± 4.8 mgN·L^{-1} and phosphate 7.5 ± 0.5 mgP·L^{-1}, with an N:P molar ratio of 17.3 ± 1.3. Nitrite and nitrate concentrations were negligible. The substrate also had a total COD concentration of 57 ± 8 mg COD·L^{-1}, alkalinity of 810 ± 47 mg $CaCO_3$·L^{-1}, VFA of 1.5 ± 0.6 mg HAc·L^{-1}, and sulphide of 112.7 ± 13.8 mg S·L^{-1}. Sulphate was detected in negligible concentrations. This microalgae substrate was expected to favour microalgae growth over other organisms as it contained low amounts of COD and TSS but high concentrations of nutrients.

The variability of the nutrient load during the experimental period was associated with variations in both WWTP and AnMBR performance.

2.2. Microalgae inoculum

The microalgae used in this study were originally collected from the walls of the secondary clarifier in the Carraixet WWTP (Alboraya, Spain). The inoculum consisted of a culture dominated by *Scenedesmus* (>99% eukaryotic cells), but it also contained other genera such as *Chlorella*, *Monoraphidium*, as well as diatoms, bacteria and cyanobacteria in negligible concentrations. This inoculum was used because these microalgae had already been adapted to the outdoor conditions (light, temperature, etc.) of the location.

Prior to the inoculation of the photobioreactors (PBRs) in the MPBR plant, the culture was adapted to the microalgae substrate (see Section IV.2.1) under laboratory

conditions as described in González-Camejo et al. (2017). After this pre-cultivation step, a start-up phase was carried out in the MPBR pilot plant, which consisted of the following: i) inoculation of the PBR with the microalgae culture from the laboratory (pre-cultivation: 10% of the total working volume with a biomass concentration between 300-500 mg $VSS \cdot L^{-1}$ and 90% of the total working volume with microalgae substrate: AnMBR effluent); ii) conditioning stage in batch mode until reaching pseudo-steady state conditions (i.e. reaching stable microalgae biomass concentration); and iii) semi-batch mode maintaining constant biomass retention time (BRT) and hydraulic retention time (HRT) (see Section IV.2.3.2 for a detailed description).

2.3. Experimental set-up and operation

2.3.1. Short-term experiments

The microalgae photosynthetic activity was determined by respirometric tests (Decostere et al., 2013). The oxygen production rate (OPR) was obtained by measuring the dissolved oxygen (DO) slope under well-defined experimental conditions in order to assess the photosynthetic activity of different sulphide concentrations in the microalgae culture.

2.3.1.1. Experimental set-up

The short-term experiments were carried out in a covered 500 mL flask with a magnetic stirrer to homogenise the microalgae culture inside a climatic chamber with air temperature set to 24ºC. 4 LED lamps (Seven ON LED 11 W) continuously illuminated the flask, supplying a light intensity of 300 $\mu E \cdot m^{-2} \cdot s^{-1}$ measured at the flask surface. In order to determine the OPR, an Orion TM-3 Star Plus portable oximeter (Thermo Scientific TM) was connected to a computer with BioCalibra® software installed (Ribes et al., 2012), which continuously registered dissolved oxygen (DO) concentration and temperature for data monitoring and storage. The short-term experimental assembly is shown in Figure IV.1.

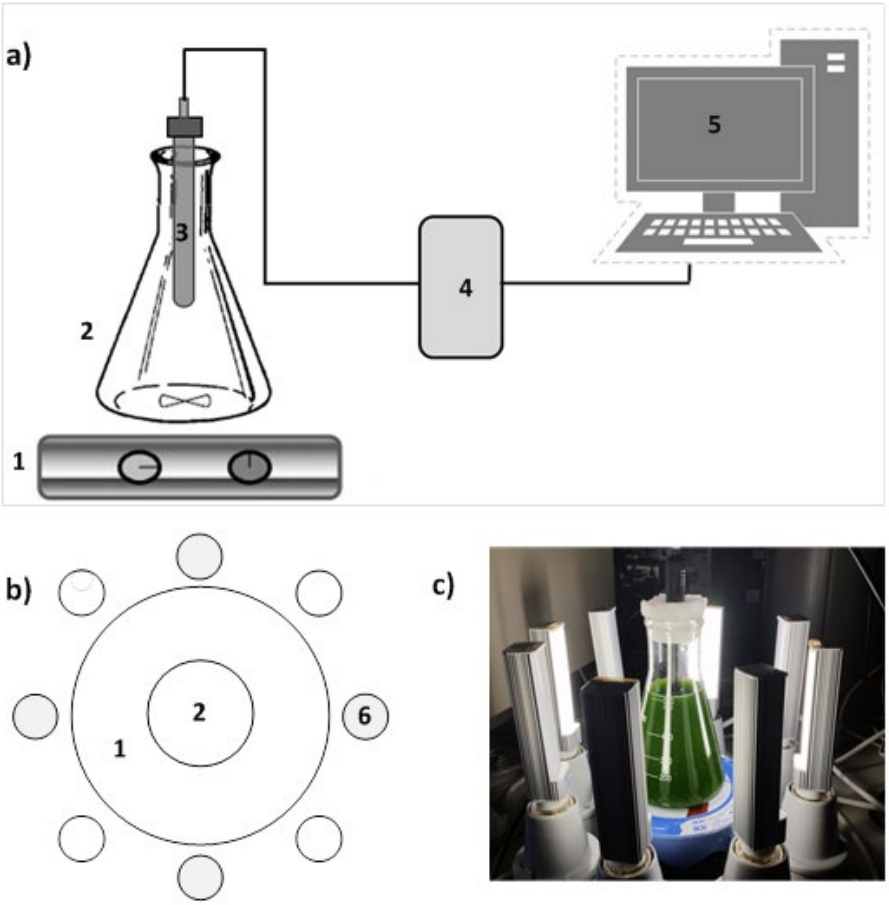

Figure IV.1. General view: a) Front view; b) Top view; c) Experimental set-up. Nomenclature: 1: Magnetic stirrer; 2: Erlenmeyer flask; 3: Oxygen and temperature probe; 4: Oximeter; 5: Biocalibra software; 6: Led lamp on.

2.3.1.2. Experimental procedure

Seven different short-term experiments were performed in duplicate with microalgae culture collected from the MPBR plant (see Section IV.2.3.2) at different sulphide levels. Table IV.1 gives the sulphide concentrations used. To reach these concentrations, the microalgae culture from MPBR plant was diluted with the appropriate amount of AnMBR effluent (Section IV.2.1).

Prior to each assay, the samples were kept in darkness to prevent the photosynthetic process from producing oxygen, and were bubbled with nitrogen for 3 minutes to remove any remaining dissolved oxygen.

Table IV.1. Sulphide concentration in each short-term experiment.

Experiment	Sulphide concentration (mg S L^{-1})
ST1	0
ST2	5
ST3	10
ST4	20
ST5	30
ST6	40
ST7	50

2.3.2. Long-term experiments

The long-term effect of sulphide on microalgae activity was evaluated on an outdoor pilot-scale microalgae cultivation system for tertiary sewage treatment. This system was fed with the nutrient-loaded effluent from an AnMBR plant that treated the effluent from the pre-treatment of the Carraixet full-scale WWTP as growth medium (see Section IV.2.1).

2.3.2.1. Experimental set-up

The pilot plant mainly consisted of an outdoor 1.1 m^3 MPBR system located in the Carraixet WWTP (39º30'04.0''N 0º20'00.1''W, Valencia, Spain). The MPBR consisted of two outdoor flat-plate PBRs made of transparent methacrylate. Each PBR had total and working volumes of 0.625 m^3 and 0.55 m^3, respectively. Both PBRs were south-facing in order to take full advantage of solar irradiance and both had an additional source of artificial light from twelve LED lamps (Unique Led IP65 WS-TP4S-40W-ME) installed at the rear of the PBRs, offering a continuous light irradiance of 300 $\mu E \cdot m^{-2} \cdot s^{-1}$ (measured on the surface of the reactor) in order to favour night-time microalgae growth over ammonium oxidising bacteria.

The membrane tank (MT) contained an industrial-scale hollow-fibre ultrafiltration membrane unit (PURON® Koch Membrane Systems (PUR-PSH31), 0.03-µm pores) with a filtration area of 3.44 m^2. This MT allowed microalgae biomass filtration and therefore the possibility of decoupling BRT and HRT.

The PBRs and the MT were continuously stirred by CO_2 enriched gas sparging by a blower (C) to prevent wall fouling and ensured adequate CO_2 transference within the broth column. pH was kept at 7.5 ± 0.3 by introducing pure pressurised CO_2 (99.9%) into the system, so that abiotic processes such as ammonia volatilisation and phosphorus precipitation were considered negligible (Whitton et al., 2016). Figure IV.2 shows the flow diagram of the MPBR plant used, which is further described in Viruela et al. (2016).

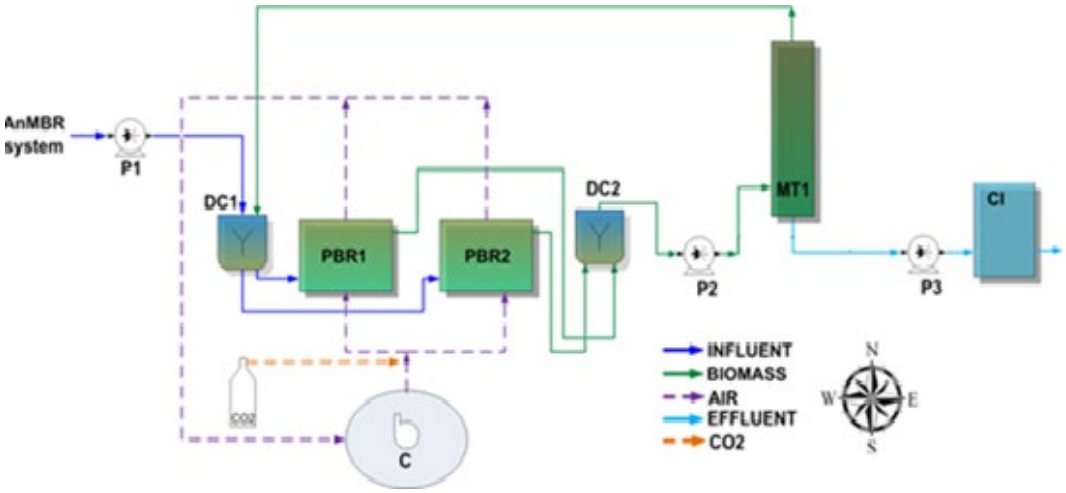

Figure IV.2. Flow diagram of the PBR pilot plant. Nomenclature: P: pumps; DC: distribution chambers; PBR: photobioreactors; MT1: membrane tank; CI: clean-in-place; C: blower.

2.3.2.2. Experimental procedure

During the entire operating period, the MPBR pilot plant was operated under outdoor conditions of variable solar light and temperature. Two different experiments (LT1 and LT2) were carried out in the period of February to May 2015.

Experiment LT1

Experiment 1 lasted 38 days and was carried out without biomass separation, so that HRT was equivalent to BRT. The PBRs were fed in a semi-batch regime, which means that the PBRs were purged with the total amount of culture to maintain a constant BRT of 6 days. The PBRs were then refilled with the AnMBR effluent described in Section IV.2.1. This experiment was divided into two sub-periods: LT1A and LT1B.

During sub-period LT1A, which lasted 15 days, the AnMBR effluent was pre-aerated before being fed to the MPBR plant in order to oxidise the sulphide to sulphate, for which a pre-aeration step in a regulation tank was applied to the AnMBR effluent through a blower before entering the MPBR plant. An on-off controller was used to keep the DO concentration in the tank at around 2 $mg \cdot L^{-1}$. The controller turned the blower on and off when DO was lower than 1 $mg \cdot L^{-1}$ and higher than 3 $mg \cdot L^{-1}$, respectively. These DO set points achieved complete sulphide oxidation and avoided raising the pH, which remained at values around 7.8, avoiding ammonia volatilisation and phosphorus precipitation (Whitton et al., 2016). After this pre-aeration step, a sulphate concentration of 324.1 ± 51.0 mg $SO_4 \cdot L^{-1}$ was measured in the regulation tank, meanwhile no sulphide was detected. The sulphide was therefore considered to have been completely oxidised in sub-period LT1A.

During LT1B, which lasted 23 days, the AnMBR effluent was fed to the MPBR system with a sulphide concentration of 116.5 ± 2.1 mg $S \cdot L^{-1}$, i.e. the AnMBR effluent was not pre-aerated, so that the sulphide concentration in the culture media reached values around 20 mg $S \cdot L^{-1}$. However, due to the air-stirring, sulphide oxidation did occur inside the PBRs, reaching a sulphate concentration of 332.4 ± 27.3 mg $SO_4 \cdot L^{-1}$.

Experiment LT2

In the 44-days experiment LT2 the BRT and HRT were decoupled through microalgae filtration. The influent was fed to the MPBR plant in continuous mode during daylight hours, maintaining a BRT of 9 days and a HRT of 2.5 days. This long-term experiment was divided into three sub-periods: LT2A, LT2B and LT2C.

In LT2A, which lasted 22 days, the AnMBR effluent was pre-aerated before entering the MPBR plant following the above-mentioned procedure. In LT2B, which lasted 8 days, the AnMBR effluent was fed to the MPBR system with a sulphide concentration of 102.7 ± 10.8 mg $S \cdot L^{-1}$, i.e. the AnMBR effluent was not pre-aerated. Consequently, the maximum sulphide concentration in the PBRs in sub-period LT2B was around 5 mg $S \cdot L^{-1}$.

In LT2C, which lasted 14 days, the AnMBR effluent was pre-aerated again to determine whether the microalgae culture would return to its initial state. When the substrate was pre-aerated (sub-periods LT2A and LT2C), the sulphide was completely oxidised to sulphate, so that the sulphate concentration in the regulation tank was 319.4 ± 38.1 mg

$SO_4 \cdot L^{-1}$. When the AnMBR effluent was not pre-aerated, the sulphide in the substrate fed to the PBRs was oxidised to sulphate due to the PBR air sparging, giving a sulphate concentration in the culture media in sub-period LT2B of 313.0 ± 38.1 mg $SO_4 \cdot L^{-1}$.
The outdoor PBR conditions in experiments LT1 and LT2 can be seen in Table IV.2.

Table IV.2. Operation conditions of long-term experiments LT1 and LT2.

Experiment	Sub-period	Days of operation	Daily natural average light intensity ($\mu E \cdot m^{-2} \cdot s^{-1}$)	Temperature (ºC)	Max. [HS] in PBR culture (mg $S \cdot L^{-1}$)	BRT (d)	HRT (d)
Exp. LT1	Sub-period LT1A	15	270 ± 149	20.3 ± 3.0	< LD	6	6
	Sub-period LT1B	23	350 ± 82	23.2 ± 1.1	20	6	6
Exp. LT2	Sub-period LT2A	22	326 ± 94	25.5 ± 1.4	< LD	9	2.5
	Sub-period LT2B	8	288 ± 86	24.9 ± 1.4	5	9	2.5
	Sub-period LT2C	14	252 ± 90	24.2 ± 0.8	< LD	9	2.5

2.4. Sampling and Analytical Methods

2.4.1. Short-term experiments

The sulphide (S^{2-}) and sulphate (SO_4^{2-}) concentrations were measured at the beginning of each short-term experiment just before DO started to rise after the initial lag phase, i.e., at the initial point of the slope (see Figure IV.3a). S^{2-} and SO_4^{2-} were also measured at the end of the experiment. Sulphide and sulphate were evaluated at the soluble fraction (filtrate) obtained by vacuum filtration with 0.45 mm pore size filters (Millipore) according to Standard Methods (APHA *et al.*, 2005): Methods 4500-S^{2-}D and 4500-SO_4^{2-}-F, respectively.
The cell death index was obtained by counting the cells in the counting chamber (Neubauer, LO Laboroptic, Friedrichsdorfs, Germany) and dividing by the number of positive dead cells determined by SYTOX Green nucleic acid stain (Molecular Probes by life technologies TM), (Roth et al., 1997). Algae (50 µL) and SYTOX Green stain (0.1 µL) were mixed and incubated for 5 minutes in darkness. 10 µL of the mixture was then added to the Neubauer counting chamber (in duplicate). The total number of stained cells and algae (excitation 504 nm, emission 523 nm) were determined by

means of a Leica DM2500 epifluorescence microscope equipped with a DFC420c digital camera.

2.4.2. Long-term experiments

Grab samples were collected in duplicate from the influent and effluent streams of the MPBR pilot plant three times a week. The soluble fraction (filtrate) was obtained by vacuum filtration with 0.45 mm pore size filters (Millipore). The following parameters were analysed for the influent and the effluent: ammonium (NH_4-N), nitrite (NO_2-N), nitrate (NO_3-N), phosphate (PO_4-P), sulphide (S^{2-}) and sulphate (SO_4^{2-}) according to Standard Methods (APHA *et al.*, 2005): 4500-NH3-G, 4500-NO2-B, 4500-NO3-H and 4500-P-F, respectively, in a Smartchem 200 automatic analyser (Westco Scientific Instruments). The sulphide and sulphate concentrations were also measured according to Methods 4500-S^{2-}D and 4500-SO_4^{2-}-F, respectively (APHA et al., 2005). VSS was analysed according to Method 2540 E (APHA et al., 2005); Total eukaryotic cell number (TE) was obtained by the epifluorescence methods (Pachés et al., 2012) and cell death was determined as in the short-term experiments (see Section IV.2.4.1).

2.5. Calculations

Biomass productivity (BP) (mg VSS·L^{-1}·d^{-1}), nitrogen removal rate (NRR) (mg N·L^{-1}·d^{-1}) and phosphorus removal rate (PRR) (mg P·L^{-1}·d^{-1}) were calculated as follows:

$$BP = \frac{X_{VSS}}{BRT} \qquad \text{[Eq. IV.1]}$$

where X_{VSS} (mg VSS·L^{-1}) is the volatile suspended solids concentration in the PBRs and BRT is the biomass retention time (d) of the microalgae culture.

$$NRR = \frac{F \cdot (N_i - N_e)}{V_{MPBR}} \qquad \text{[Eq. IV.2]}$$

where F is the treatment flow rate (m^3·d^{-1}); N_i is the nitrogen concentration of the influent (mg N·L^{-1}), N_e is the nitrogen concentration of the effluent (mg N·L^{-1}), t is the period of time considered (d), and V_{MPBR} is the volume of the culture in the MPBR plant (L).

$$PRR = \frac{F \cdot (P_{inf} - P_{ef})}{V_{MPBR}} \qquad \text{[Eq. IV.3]}$$

where P_i is the phosphorus concentration of the influent (mg P·L^{-1}) and P_e is the phosphorus concentration of the effluent (mg P·L^{-1}).

In order to compare different operating periods with variations in solar irradiance, the nitrogen removal rate-light irradiance ratio was calculated according to Eq. [IV.4]:

$$NRR{:}I = \frac{NRR \cdot V_{PBR} \cdot 10^6}{I \cdot S \cdot 24 \cdot 3600} \qquad \text{[Eq. IV.4]}$$

where NRR:I is the nitrogen removal rate-light irradiance ratio (mg N·mol photons^{-1}), I is the total light PAR irradiance on the PBR surface, i.e. the 24-hour average solar irradiance plus the light from the LED lamps (μmol photons·m^{-2}·s^{-1}) and S is the illuminated PBR surface (m^2).

2.6. Statistical analysis

All results are shown as mean ± standard deviation of the duplicates. STATGRAPHICS Centurion XVI.I. was used for conducting ANOVA analysis. P-values < 0.05 were considered statistically significant.

3. RESULTS AND DISCUSSION

3.1. Short-term experiments

By way of example, Figure IV.3a shows the evolution of DO concentration during the short-term experiment conducted at a sulphide concentration of 20 mg S·L^{-1}. As can be seen in Figure IV.3a, a lag phase occurred in all the experiments when the oxygen concentration in the microalgae culture was under the detection limit. It was also noticed that the duration of this lag phase increased as the sulphide concentration rose. This suggests that algae were undergoing photosynthesis, but the oxygen produced was being used to oxidise the sulphide towards sulphate. For example, when the initial sulphide concentration of the culture was 20 mg S·L^{-1}, there was a lag of around 420 minutes (Figure IV.3a).

The analysis of the sulphide concentration in the microalgae culture throughout the experiments confirmed that the sulphide concentration was negligible when the oxygen concentration in the culture started to rise, i.e. at the end of the lag phase, so that OPR could only be measured when all sulphide had been oxidised.

Figure IV.3b shows the oxygen production rates obtained from the short-term experiments (ST1-ST7) at different sulphide concentrations and it can be seen that OPR drops at higher sulphide concentrations. The microalgae could not produce oxygen at the same rate when sulphide content rose because of reduced photosynthetic capacity

(Küster et al., 2005). This indicates that the low sulphide concentration (5 mg $S \cdot L^{-1}$) markedly reduced OPR (43%); while concentrations between 5 and 30 mg $S \cdot L^{-1}$ reduced OPR by 60-72%; those above 40 mg $S \cdot L^{-1}$ were close to completely inhibiting microalgal photosynthetic activity: OPR decreased by 87 and 94% with sulphide concentrations of 40 and 50 mg $S \cdot L^{-1}$, respectively. These results suggest that the microalgae evaluated in these assays, which grew in the effluent of an AnMBR system (Giménez et al., 2011), were sensitive to very low sulphide concentrations, which indicates that the presence of sulphide limited the photosynthetic capacity of a culture in which *Scenedesmus* and *Chlorella* were the predominant genera (80% and 16% of total eukaryotic cells, respectively). Previous studies have also reported algae restricted by sulphide in natural water, e.g. Küster et al. (2005) found strongly inhibited *Scenedesmus* reproduction with hydrogen sulphide concentrations above 2 mg $S \cdot L^{-1}$.

In order to model this inhibition of photosynthetic activity by sulphide, the OPR values were adjusted to an inhibition function, as shows in Eq. (IV.5):

$$\mathrm{OPR} = OPR_{max} \frac{K_I}{K_{I+}[S^{2-}]} \qquad \text{(Eq. IV.5)}$$

Where OPR_{max} (g $O_2 \cdot L^{-1} \cdot d^{-1}$) is the OPR value with no sulphide effect on the culture and K_I is the sulphide inhibition constant.

Figure IV.3b shows that the proposed kinetic function accurately predicts the inhibition effect of sulphide on microalgae during photosynthesis. The K_I obtained from these experimental values was 8.7 mg S L^{-1}, which suggests that a sulphide concentration of 8.7 mg S L^{-1} was enough to reduce the microalgae oxygen production rate by half.

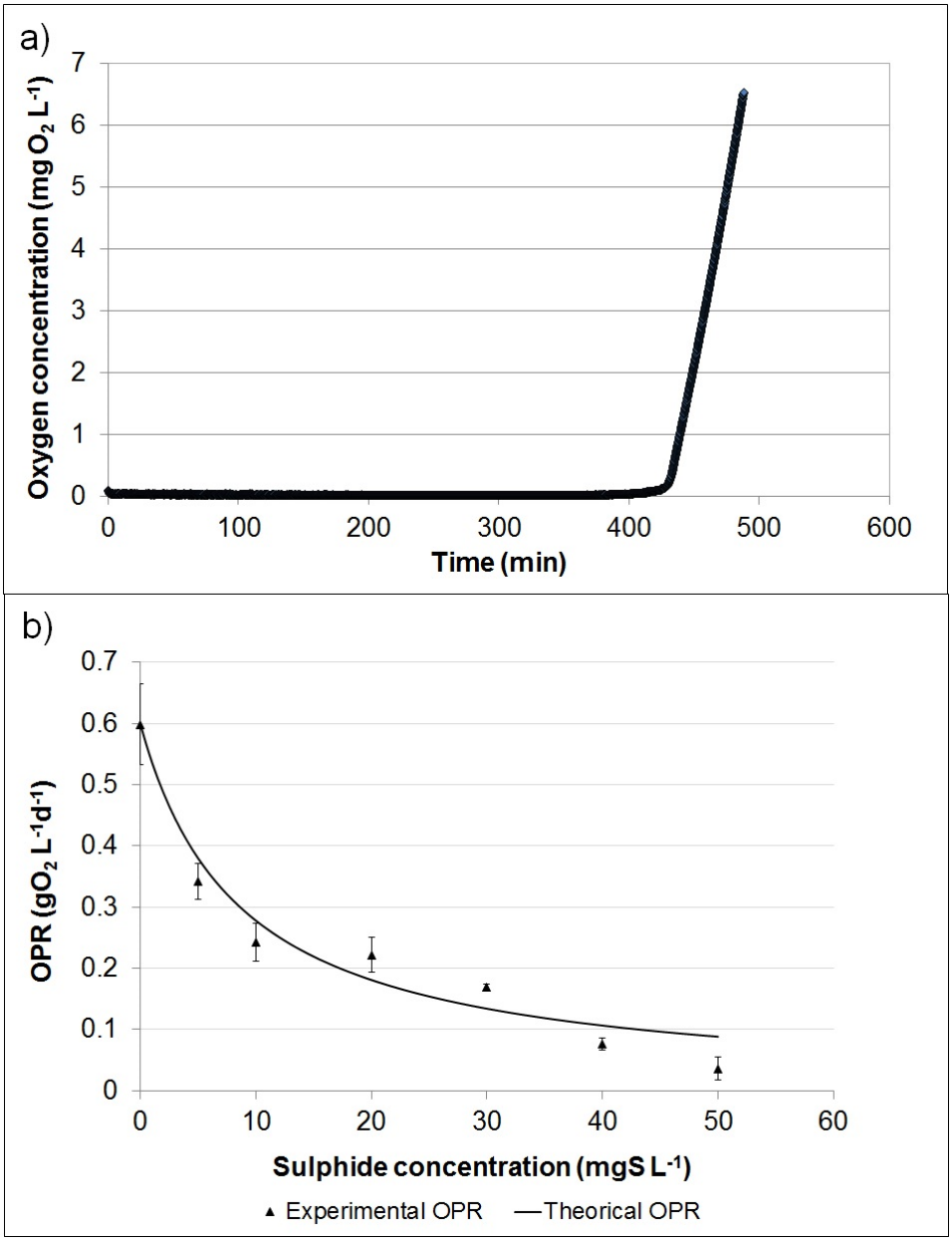

Figure IV.3. a) Time evolution of the oxygen concentration at a sulphide concentration of 20 mg S·L^{-1}. b) Oxygen production rates obtained at different sulphide concentrations in the microalgae culture.

The microalgae viability study showed that cell viability decreased as sulphide concentration increased. Differences of less than 5% were observed in assays at low sulphide concentrations (0, 5, and 10 mg S·L^{-1}). At higher concentrations (20, 30, 40 and 50 mg S·L^{-1}), there were significant differences: microalgae viability dropped by 44, 50, 56 and 58% at concentrations of 20, 30, 40 and 50 mg S·L^{-1}, respectively, at the

end of the experiment. The cell viability study indicated that higher sulphide concentration implies higher mortality.

The results of the short-term experiments suggest that increasing the culture sulphide concentration negatively affects the microalgae´s photosynthetic capacity. These results agree with the findings of Miller and Bebout (2004), who observed that the refill of electrons in the PSII reaction centres during photosynthesis was reduced if sulphide was present. The results also showed that high concentrations of sulphide reduce culture performance. In fact, the maximum sulphide concentration studied (50 mg $S \cdot L^{-1}$) reduced OPR by 94% and mortality by 58%.

3.2. Long-term experiments

3.2.1. Experiment LT1

Figure IV.4.a shows the evolution of nutrients removal values in experiment LT1. This figure shows that in sub-period LT1A (no sulphide in the influent), the NRR reached higher values than in LT1B (116.5 ± 2.1 mg $S \cdot L^{-1}$ influent sulphide). In fact, the mean values of NRR were 7.4 ± 1.5 and 6.0 ± 1.8 mg $N \cdot L^{-1} \cdot d^{-1}$ for LT1A and LT1B, respectively. The NRR values obtained in experiment LT1 were similar to the findings of other studies concerning the application of microalgae cultivation for wastewater treatment. For instance, Park and Jin (2010) attained a nitrogen removal rate of 5-6 mg $N \cdot L^{-1} \cdot d^{-1}$ by *Scenedesmus* sp. when treating the effluent from an anaerobic digester fed with piggery wastewater and applying cycles of artificial light (PAR of 200 $\mu E \cdot m^{-2} \cdot s^{-1}$ for 12 hours per day). Marcilhac et al. (2014) obtained a maximum nitrogen removal rate of 8.5 mg $N \cdot L^{-1} \cdot d^{-1}$ at lab-scale using a green microalgae culture dominated by *Scenedesmus* sp. for treating digestate supernatant (PAR of 244 $\mu E \cdot m^{-2} \cdot s^{-1}$ for 12 hours per day).

With regard to phosphorus, no significant differences (p-value > 0.05) in PRR were found between sub-periods LT1A and LT1B: 1.1 ± 0.2 mg $P \cdot L^{-1} \cdot d^{-1}$ and 1.3 ± 0.3 mg $P \cdot L^{-1} \cdot d^{-1}$, respectively. Rasoul-Amini et al. (2014) reported similar PRR values for *Chlorella* sp. fed by wastewater from a secondary effluent: 1.1-1.4 mg $P \cdot L^{-1} \cdot d^{-1}$.

However, it should be remembered that the performance of an outdoor PBR strongly depends on environmental factors such as solar radiation and temperature. Many authors have reported that the higher the light irradiance is, the higher the nitrogen removal rate, as long as it remains below the light saturation level (Anbalagan et al., 2015; Viruela et

al., 2016; Yan et al., 2016). However, the average solar PAR during LT1A (NRR of 7.4 ± 1.5 mg $N \cdot L^{-1} \cdot d^{-1}$) was lower than LT1B (NRR of 6.0 ± 1.8 mg $N \cdot L^{-1} \cdot d^{-1}$): 270 ± 149 and 350 ± 81 ($\mu mol \cdot m^{-2} \cdot s^{-1}$), which disagrees with the aforementioned findings, probably due to the sulphide effect, which will be discussed below.

The NRR-light irradiance ratio was calculated to compare NRR values in LT1A and LT1B, and gave mean values of NRR:I of 20.7 ± 6.4 and 13.6 ± 4.3 mg $N \cdot mol\ photons^{-1}$ for LT1A and LT1B, respectively. There was thus a significantly higher NRR:I value in LT1A than in LT1B (p-value < 0.05). Temperature remained fairly constant throughout experiment LT1. Other authors have found that temperature can affect biomass productivity more than the nutrient removal rates (Viruela et al., 2016). According to these results, it can be concluded that the presence of sulphide in the influent affected PBR performance when the maximum sulphide concentration in the PBRs was 20 mg $S \cdot L^{-1}$.

The sulphide in the PBRs influent not only had an inhibitory effect, as observed in the short-term experiments, but also changed the culture population. In LT1A, the total eukaryotic cells concentration was fairly stable and *Scenedesmus* (Sc) remained the predominant genus (> 99% of total eukaryotic cells); whereas *Chlorella* (Chl) presented a negligible concentration (see Figure IV.4b). Nevertheless, in LT1B, when aeration stopped in the AnMBR effluent (at a sulphide concentration of 116.5 ± 2.1 mg $S \cdot L^{-1}$ in the influent), *Chlorella* growth increased dramatically and there was a shift in the population of the microalgae culture: *Chlorella* replaced *Scenedesmus* as the predominant genus (see Figure IV.4b), which suggests that *Chlorella* is more resistant to sulphide inhibition than *Scenedesmus*. According to Küster et al. (2005), *Scenedesmus* is strongly inhibited at sulphide concentrations of around 2 mg $S \cdot L^{-1}$. On the other hand, González-Sanchez and Posten (2017) obtained *Chlorella* sp. inhibition at sulphide concentrations higher than 16 mg $S \cdot L^{-1}$, which agrees with the results obtained in the present study. The microalgae viability of both *Scenedesmus* and *Chlorella* in experiment LT1 was always above 87%.

Another consequence of the culture shift was the lack of phosphorus for microalgae growth in sub-period LT1B. In LT1A, the phosphorus concentration in the effluent remained at 0.90 ± 0.62 mg $P \cdot L^{-1}$. However, once the microalgae population changed from *Scenedesmus* to *Chlorella* (from day 20), the effluent phosphorous concentration was negligible (see Figure IV.4c). This agrees with the findings of Sommer (1986), who

reported a competitive advantage of *Chlorella* over *Scenedesmus* at low phosphorus concentrations.

The microalgae population shift was also reflected in the N:P molar ratio consumed in both sub-periodsLT1A and LT1B. In particular, in sub-period LT1A, the average N:P molar ratio was 14.4 ± 3.2, whereas in LT1B it dropped to 12.4 ± 3.4. *Chlorella* thus consumed a proportionally higher amount of phosphorus than *Scenedesmus*, which could have caused the lack of phosphorus in LT1B (see Figure IV.4c). According to Arbib et al. (2013), the optimal molar N:P ratio of *Scenedesmus obliquus* is in the range 9-13; while Kapdan and Aslan (2008) and Silva *et al.* (2015) reported a lower optimal N:P molar ratio of around 8 for *Chlorella* sp.

VSS and TE significantly decreased at the end of LT1B. As can be seen in Figure IV.4c, MPBR effluent phosphorous content reached negligible values from day 20 to the end of LT1B, suggesting that the absence of phosphorus in the culture could have caused the decay of microalgae, as reported by Ruiz-Martinez et al. (2014). The lack of phosphorus could also have been responsible for the cyanobacteria proliferation in the microalgae culture at the end of the long-term experiment LT1 (data not shown). According to Arias *et al.* (2017), cyanobacteria proliferation is favoured at low nutrient concentrations, in contrast to green microalgae. The cyanobacteria could therefore have affected the microalgae culture (see e.g. Kim et al., 2007; Leão et al., 2009; Zak et al., 2011) since there was a significant drop in total eukaryotic cells after day 33 (see Figure IV.4b). Further research is needed to clarify long-term culture behaviour.

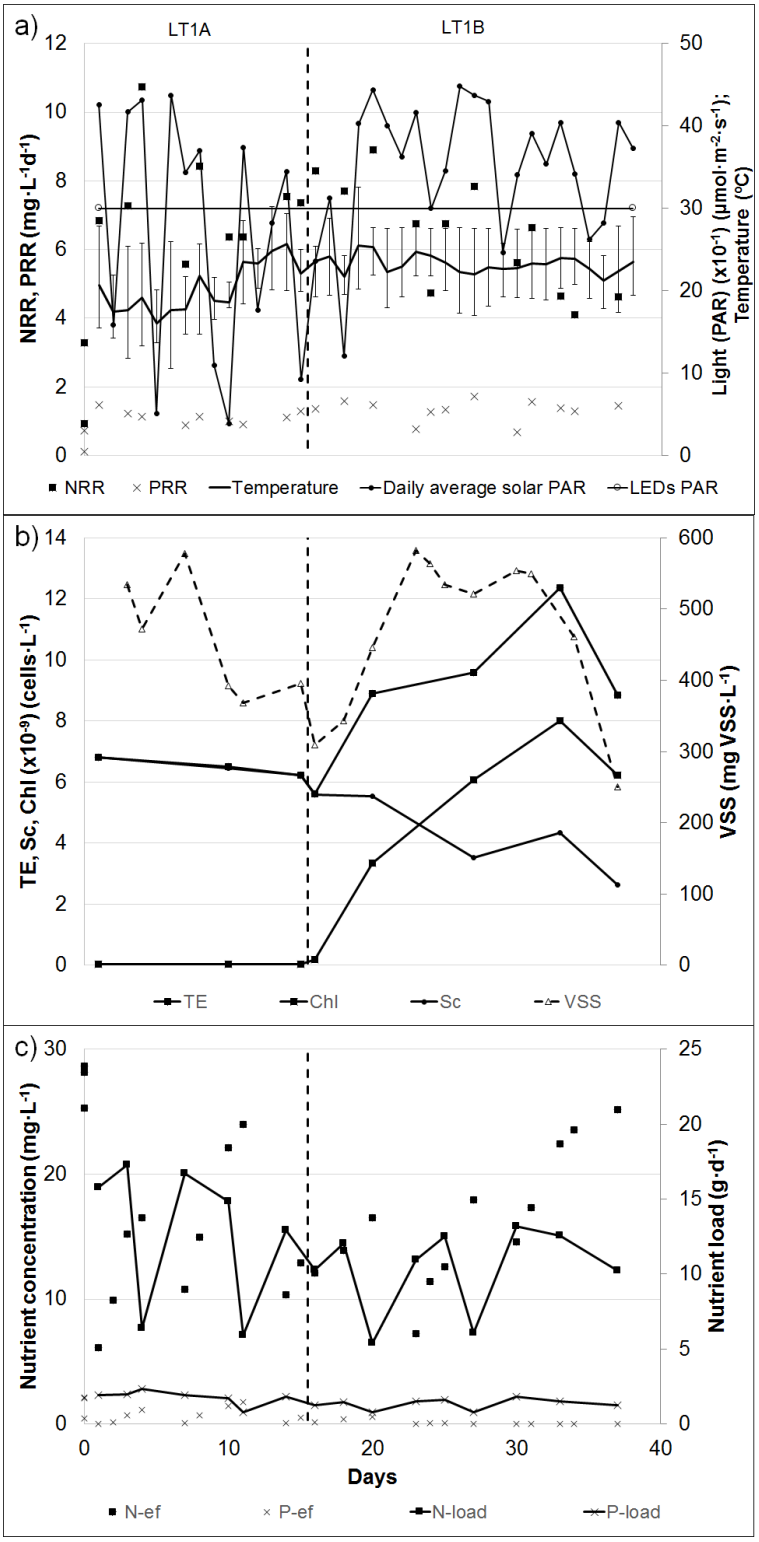

Figure IV.4: Experiment LT1: HRT = BRT = 6 d. Time evolution of: a) Nitrogen removal rate (mg $N \cdot L^{-1} \cdot d^{-1}$), phosphorus removal rate (mg $P \cdot L^{-1} \cdot d^{-1}$), light (PAR) (µmol·$m^{-2} \cdot s^{-1}$) and temperature (ºC); b) cell concentration (cells·L^{-1}) of total eukaryotic cells (TE), Scenedesmus (Sc) and Chlorella (Chl) and volatile suspended solids concentration (mg VSS·L^{-1}); c) nutrient concentration (mg·L^{-1}) and nutrient load (g·d^{-1}).

3.2.2. Experiment LT2

Among the physical factors that affect microalgae cultivation performance (besides sulphide concentration), solar irradiance varied significantly throughout LT2, as can be seen in Figure IV.5a and Table IV.2. NRR in sub-periods LT2A, LT2B and LT2C thus could not be directly compared because of the strong influence of solar irradiance on the nitrogen removal rate. The NRR-light irradiance ratio was found to be 33.3 ± 3.0, 39.2 ± 4.8 and 37.1 ± 3.7 mg N·mol photons^{-1} in LT2A, LT2B and LT2C, respectively. Even though these values apparently differ, the ANOVA analysis found no statistical differences between these mean values (p-value > 0.05). It can thus be concluded that the microalgae culture did not suffer from significant sulphide inhibition in experiment LT2 at an influent sulphide concentration of 102.7 ± 10.8 mg S·L^{-1} and that sulphide inhibition of the microalgae culture in the MPBR studied is not significant at concentrations below 5 mg S·L^{-1}.

In Figure IV.5b it can be seen that Experiment LT2 started with a mixed culture of *Scenedesmus* and *Chlorella*. During sub-period LT2A, *Scenedesmus* became the predominant genus, especially after day 16, when there was a significant increase in TE, probably due to increased solar irradiance after several days with little sunlight (see Figure IV.5a). However, once the AnMBR effluent ceased to be aerated (in LT2B), TE rose due to the proliferation of *Chlorella* (see Figure IV.5b). This behaviour was also observed in LT1B, which would be in agreement with Küster et al. (2005), and González-Sanchez and Posten (2017), who reported that *Chlorella* sp. resist higher sulphide concentrations than *Scenedesmus*. It should be noted that when AnMBR effluent aeration was restored and the sulphide was oxidised to sulphate in the regulation tank, *Scenedesmus* again became the predominant eukaryotic algae genus (see Figure IV.5b). In this experiment, the microalgae viability of both *Scenedesmus* and *Chlorella* remained higher than 85%.

Unlike in experiment LT1, in LT2 no significant cyanobacteria proliferation took place in the microalgae culture, probably because phosphate concentration in the culture media was always above 2.90 mgP·L^{-1} (see Figure IV.5c).

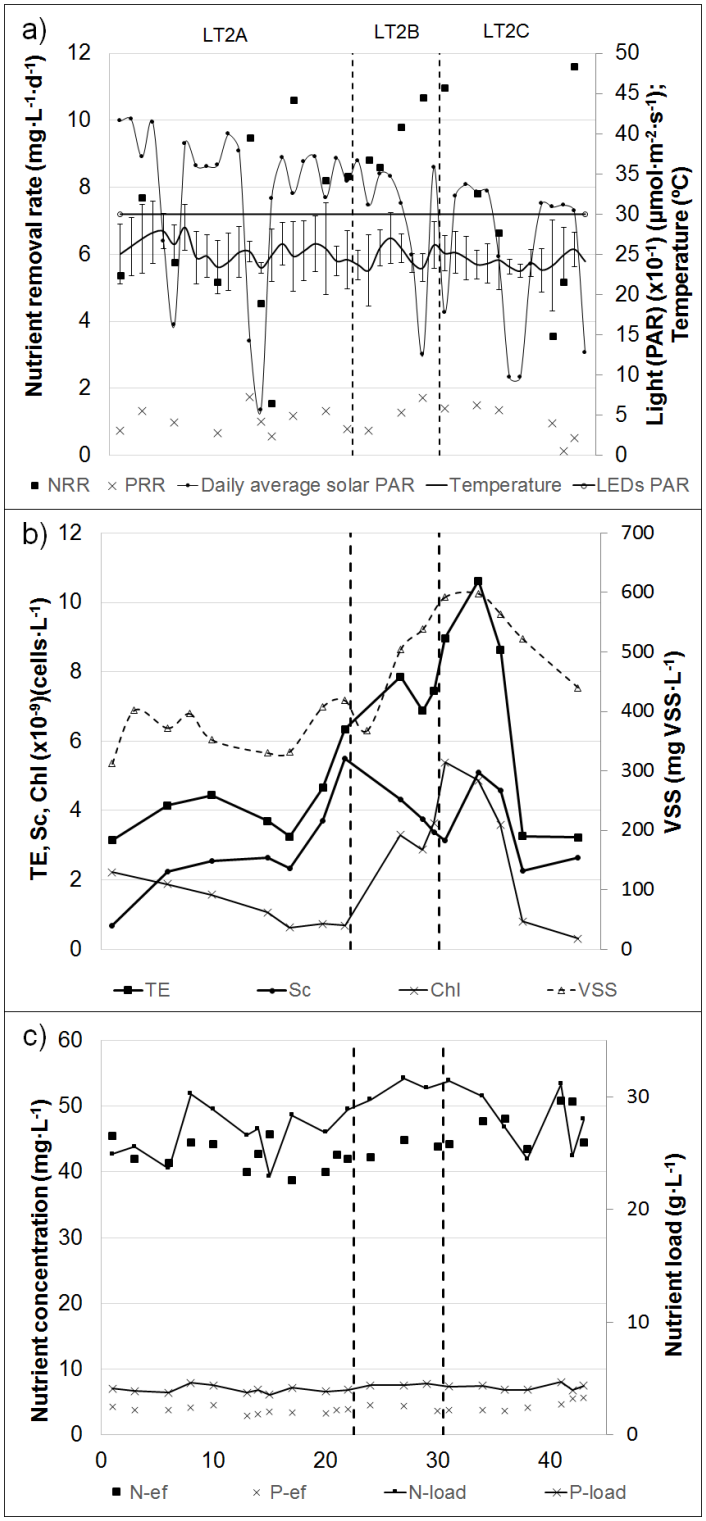

Figure IV.5: Experiment LT2: BRT = 9 d; HRT = 22.5 d. Time evolution of: a) Nitrogen removal rate (mg $N \cdot L^{-1} \cdot d^{-1}$), phosphorus removal rate (mg $P \cdot L^{-1} \cdot d^{-1}$), light (PAR)(µmol $\cdot m^{-2} \cdot s^{-1}$) and temperature (ºC); b) cell concentration (cells $\cdot L^{-1}$) of total eukaryotic cells (TE), Scenedesmus (Sc) and Chlorella (Chl) and volatile suspended solids concentration (mg VSS $\cdot L^{-1}$); c) nutrient concentration (mg $\cdot L^{-1}$) and nutrient load (g $\cdot d^{-1}$).

The results obtained in experiments LT1 and LT2 suggest that *Scenedesmus* was the predominant genus under the given outdoor conditions when the PBRs were fed with AnMBR effluent without sulphide. Viruela et al. (2016) also found *Scenedesmus* to be the main genus of the microalgae culture in similar working conditions. On the other hand, when a sulphide concentration of around 112.7 ± 13.8 mg $S \cdot L^{-1}$ was introduced with the influent, *Chlorella* became the predominant microalgae genus, since they are known to support a higher sulphide concentrations than *Scenedesmus* (Küster et al. 2005; González-Sanchez and Posten, 2017). This situation did not negatively affect microalgae growth when there was no nutrient limitation and the sulphide concentration remained under 5 mg $S \cdot L^{-1}$ in the PBRs (experiment LT2). However, in LT1, with higher sulphide concentrations in the PBRs (20 mg $S \cdot L^{-1}$), the system became phosphorus-limited when *Chlorella* proliferated and led to the appearance of cyanobacteria. This was an unfavourable situation because cyanobacteria compete for nutrients with eukaryotic microalgae and can damage microalgae cells (Rajneesh et al., 2017). It can therefore be concluded that in outdoor conditions, oxidising the AnMBR effluent sulphide to sulphate plays an important role in avoiding microalgae sulphide inhibition and cyanobacteria proliferation, especially at low phosphorus concentrations.

4. CONCLUSIONS

The short-term results showed that sulphide reduces microalgae´s photosynthetic capacity and viability. A low sulphide concentration (5 mg $S \cdot L^{-1}$) reduced OPR by 43% and sulphide concentrations above 40 mg $S \cdot L^{-1}$ almost inhibited microalgae growth, reaching maximum mortality (58%) and minimum OPR at 50 mg $S \cdot L^{-1}$.

The long-term experiments revealed that the presence of sulphide had inhibitory effects when the sulphide concentration reached 20 mg $S \cdot L^{-1}$, but not when less than 5 mg $S \cdot L^{-1}$. The presence of sulphide was responsible for *Chlorella* replacing *Scenedesmus* as the predominant genus due to its higher resistance to sulphide.

ACKNOWLEDGEMENTS

This research work has been supported by the Spanish Ministry of Economy and Competitiveness (MINECO, CTM2011-28595-C02-01 and CTM2011-28595-C02-02) jointly with the European Regional Development Fund (ERDF), both of which are gratefully acknowledged. It was also supported by the Spanish Ministry of Education,

Culture and Sport via a pre doctoral FPU fellowship to author J. González-Camejo (FPU14/05082) and by the Spanish Ministry of Economy and Competitiveness via a pre doctoral FPI fellowship to author R. Serna-García (project CTM2014-54980-C2-1-R).

REFERENCES

1. Aiyuk, S., Forrez, I., Lieven, D.K., van Haandel, A., Verstraete, W., 2006. Anaerobic and complementary treatment of domestic sewage in regions with hot climates: a review. Bioresour. Technol. 97, 2225–2241.

2. Anbalagan, A., Schwede, S., Nehrenheim, E., 2015. Influence of light emitting diodes on indigenous microalgae cultivation in municipal wastewater. Energy Procedia 75, 786-792.

3. APHA-AWWA-WPCF (2005). Standard methods for the examination of water and wastewater, 21st edition. American Public Health Association (APHA), American Water Works Association (AWWA), Water Pollution Control Federation (WPCF).

4. Arbib, Z., Ruiz, J., Álvarez-Díaz, P., Garrido-Pérez, C., Barragan, J., Perales, J. 2013. Photobiotreatment: Influence of Nitrogen and Phosphorus Ratio in Wastewater on Growth Kinetics of Scenedesmus Obliquus. International Journal of Phytoremediation, 15 (8), 774-788.

5. Arias, D. M., Uggetti, E., García-Galán, M.J., García, J., 2017. Cultivation and selection of cyanobacteria in a closed photobioreactor used for secondary effluent and digestate treatment. Sci. Total Environ., in press, doi: 10.1016/j.scitotenv.2017.02.097.

6. Decostere, B., Janssens, N., Alvarado, A., Maere, T., Goethals, P., Van Hulle, S.W.H., Nopens, I., 2013. A combined respirometer-titrimeter for the determination of microalgae kinetics: Experimental data collection and modeling. Chemical Engineering Journal 222, 85-93.

7. European Comission Directive 91/271/EEC of 21 May 1991, concerning urban waste-water treatment. OJ L 135, 30.5.1991, p. 40–52.

8. Giménez, J. B. (2014). Estudio del tratamiento anaerobio de aguas residuales urbanas en biorreactores de membranas. PhD Thesis. University of Valencia, Spain.

9. Giménez, J.B., Robles, A., Carretero, L., Durán, F., Ruano, M.V., Gatti, M.N., Ribes, J., Ferrer, J., Seco, A., 2011. Experimental study of the anaerobic urban wastewater treatment in a submerged hollow-fibre membrane bioreactor at pilot scale. Bioresour. Technol. 102, 8799–8806.

10. González-Camejo, J., Barat, R., Pachés, M., Murgui, M., Ferrer, J., Seco, A., 2017. Wastewater Nutrient Removal in a Mixed Microalgae-bacteria Culture: Effect of Light and Temperature on the Microalgae-bacteria Competition. Environ. Technol. 30(4), 503-515.

11. González-Sánchez, A., Posten, C., 2017. Fate of H_2S during the cultivation of *Chlorella* sp. deployed for biogas upgrading. Journal of Environmental Management 191, 252-257.

12.Kapdan, K., Aslan, S., 2008. Application of the Stover–Kincannon kinetic model to nitrogen removal by Chlorella vulgaris in a continuously operated immobilized photobioreactor system. J. Chem. Technol. Biotechnol. 83, 998–1005.

13.Kim, J.-D., Kim, B., Lee, C.-G., 2007. Alga-lytic activity of *Pseudomonas fluorescens* against the red tide causing marine alga *Heterosigma akashiwo* (Raphidophyceae). Biological Control 41, 296–303.

14.Küster E., Dorusch, F., Altenburguer, R., 2005. Effects of hydrogen sulfide to *Vibrio fischeri, Scenedesmus vacuolatus,* and *Daphnia magna*. Environmental Toxicology and Chemistry 24 (10), 2621-2629.

15.Leão, P.N., Teresa, M., Vasconcelos, S.D., Vasconcelos, V.M., 2009. Allelopathy in freshwater cyanobacteria. Critical Reviews in Microbiology 35, 271–282.

16. Marcilhac, C., Sialve, B., Pourcher, A-.M., Ziebal, C., Bernet, N., Béline, F., 2014. Digestate color and light intensity affect nutrient removal and competition phenomena in a microalgal-bacterial ecosystem. Water Res. 64, 278-287.

17. Maroneze, M.M., Siqueira, S.F., Vendruscolo, R.G., Wagner, R., Menezes, C.R., Zepka, L.Q., Jacob-Lopes, E., 2016. The role of photoperiods on photobiorectors – A potential strategy to reduce costs. Bioresour. Technol. 219, 493-499.

18. Miller, S. R., Bebout, B., M., 2004. Variation in sulfide tolerance of photosystem II in phylogenetically diverse cyanobacteria from sulfidic habitats. Appl. Environ. Microbiol. 70, 736-744.

19. Pachés, M., Romero, I., Hermosilla, Z. and Martinez-Guijarro, R. 2012. PHYMED: An ecological classification system for the Water Framework Directive based on phytoplankton community composition. Ecological Indicators 19, 15-23.

20. Park, J., Jin, H., 2010. Ammonia removal from anaerobic digestion effluent of livestock waste using green alga *Scenedesmus* sp. Bioresour. Technol. 101, 8649–8657.

21. Pearson, H. W., Mara, D. D., Mills, S.W., 1987. Factors determining algal populations in waste stabilization ponds and influence of algae on pond performance. Wat. Sci. Technol. 19, 131-140.

22. Rajneesh, Singhb, S. P., Pathaka, J., Sinha, R.P., 2017. Cyanobacterial factories for the production of green energy and value-added products: An integrated approach for economic viability. Renewable and Sustainable Energy Reviews 69, 578–595.

23. Rasoul-Amini, S., Montazeri-Najafabady, N., Shaker, S., Safari, A., Kazemi, A.,Mousavi, P., Ali Mobasher, M., Ghasemi, Y., 2014. Removal of nitrogen and phosphorus from wastewater using microalgae free cells in bath culture system. Biocatal. Agric. Biotechnol. 3, 126–131

24. Ribes, J., Seco, A., García-Usach, F., Durán, F., Ferrer, J., (2012) BioCalibra: dispositivo para la calibración y seguimiento de procesos de fangos activados en una EDAR. Tecnología del Agua. 337, 64–71.

25. Robles, A., Ruano, M.V., Ribes, J., Ferrer, J., 2013. Factors that affect the permeability of commercial hollow-fibre membranes in a submerged anaerobic MBR (HF-SAnMBR) system. Water Res. 47, 1277-1288.

26. Roth, B. L, Poot, M., Yue, S. T., Millard, P.J., 1997. Bacterial viability and antibiotic susceptibility testing with SYTOX Green nucleic acid stain. Applied and Environmental Microbiology. 63, 2421–2431.

27. Ruiz-Martínez, A., Martín García, N., Romero, I., Seco, A., & Ferrer, J., 2012. Microalgae cultivation in wastewater: nutrient removal from anaerobic membrane bioreactor effluent. Bioresour. Technol. 126, 247–253.

28. Ruiz-Martinez, A., Serralta, J., Pachés, M., Seco, A., Ferrer, J., 2014. Mixed microalgae culture for ammonium removal in the absence of phosphorus: Effect of phosphorus supplementation and process modeling. Process Biochemistry 49, 2249-2257.

29. Silva, N. F. P., Gonçalves, A. L., Moreira, F. C., Silva, T. F. C. V., Martins, F. G., Alvim-Ferraz, M. C. M., Boaventura, R. A. R., Vilar, V. J. P., Pires, J. C. M., 2015. Towards sustainable microalgal biomass production by phycoremediation of a synthetic wastewater: A kinetic study. Algal Res. 11, 350-358.

30. Sommer, U., 1986. Phytoplankton Competition along a Gradient of Dilution Rates. Oecologia, vol. 68, no. 4, 503-506.

31. Tan, X.B., Zhang, Y.L., Yang, L.B., Chu, H.Q., Guo, J., 2016. Outdoor cultures of Chlorella pyrenoidosa in the effluent of anaerobically digested activated sludge: The effects of pH and free ammonia. Bioresour. Tecnol. 200, 606-615.

32. Viruela, A., Murgui, M., Gómez-Gil, T., Durán, F., Robles, A., Ruano, M. V., Ferrer, J., Seco, A., 2016. Water resource recovery by means of microalgae cultivation in outdoor photobioreactors using the effluent from an anaerobic membrane bioreactor fed with pre-treated sewage. Bioresour. Technol. 218, 447-454.

33. Whitton, R., Le Mével, A., Pidou, M., Ometto, F., Villa, R., Jefferson, B., 2016. Influence of microalgal N and P composition on watewater nutrient remediation. Water Res. 91, 371-378.

34. Yan, C., Muñoz, R., Zhu, L., Wang, Y., 2016. The effects of various LED (light emitting diode) lighting strategies on simultaneous biogas upgrading and biogas slurry nutrient reduction by using of microalgae *Chlorella* sp. Energy. 106, 554-561.

35. Zak, A.; Misiewicz, K. & Kosakowska, A. (2011). Allelophatic activity of the Baltic cyanobacteria against microalgae. Estaurine, Coastal and Shelf Science 112, 4-10.

APPENDIX IV.A. SUPPLEMENTARY MATERIAL

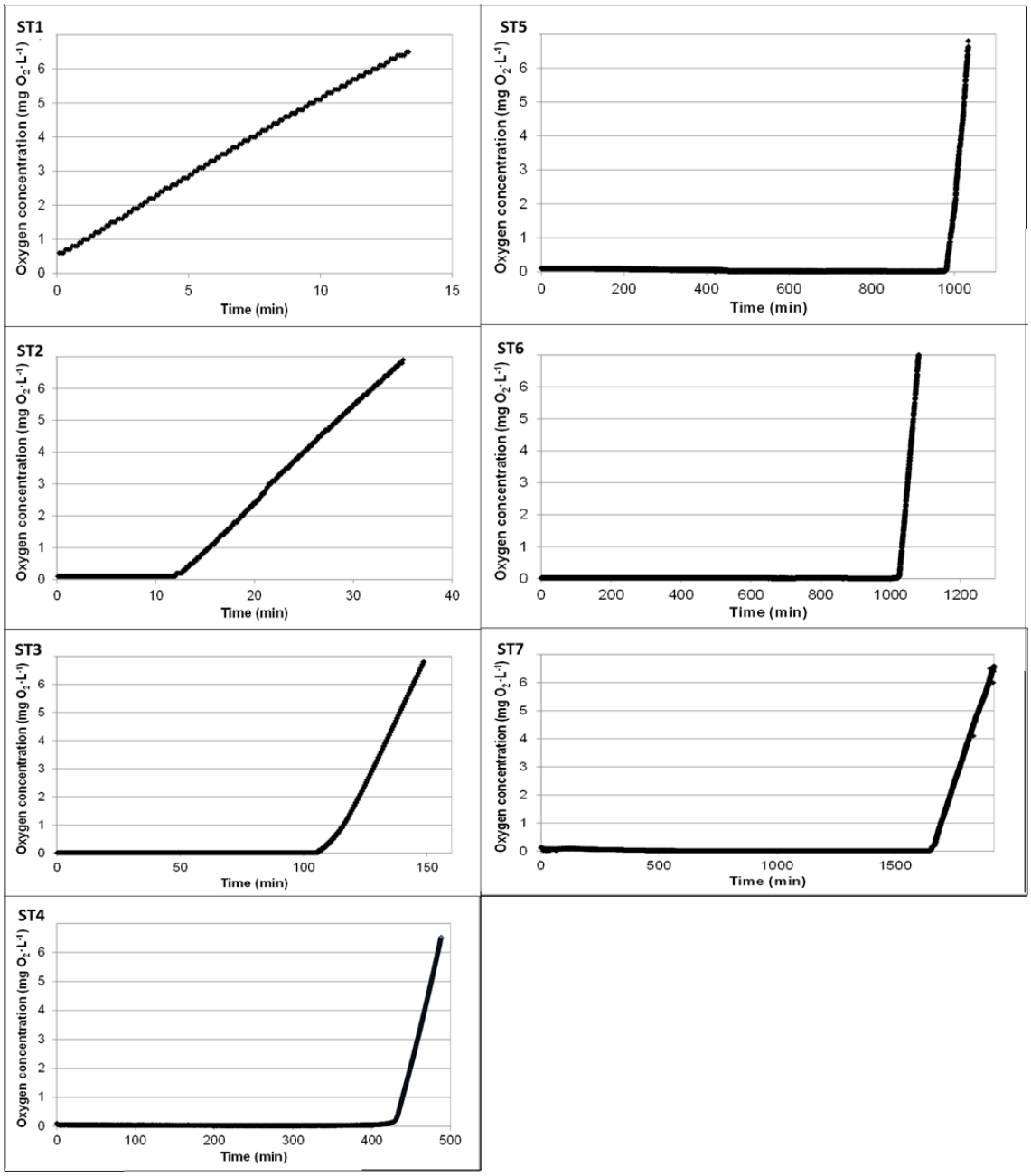

Figure IV.A.1: Time evolution of the oxygen concentration at a sulphide concentration in the culture of: ST1 = 0 mg $S \cdot L^{-1}$; ST2 = 5 mg $S \cdot L^{-1}$; ST3 = 10 mg $S \cdot L^{-1}$; ST4 = 20 mg $S \cdot L^{-1}$; ST5 = 30 mg $S \cdot L^{-1}$; ST6 = 40 mg $S \cdot L^{-1}$; ST5 = 50 mg $S \cdot L^{-1}$.

CHAPTER V:

OUTDOOR FLAT-PANEL MEMBRANE PHOTOBIOREACTOR TO TREAT THE EFFLUENT OF AN ANAEROBIC MEMBRANE BIOREACTOR. INFLUENCE OF OPERATING, DESIGN, AND ENVIRONMENTAL CONDITIONS

CHAPTER V:

OUTDOOR FLAT-PANEL MEMBRANE PHOTOBIOREACTOR TO TREAT THE EFFLUENT OF AN ANAEROBIC MEMBRANE BIOREACTOR. INFLUENCE OF OPERATING, DESIGN, AND ENVIRONMENTAL CONDITIONS

González-Camejo, J., Barat, R., Ruano, M.V., Seco, A., Ferer, J., 2018. Outdoor flat-panel membrane photobioreactor to treat the effluent of an anaerobic membrane bioreactor. Influence of operating, design and environmental conditions. Water Sci. Technol. 78(1) 195-206. http://dx.doi.org/10.2166/wst.2018.259

ABSTRACT

As microalgae have the ability to simultaneously remove nutrients from wastewater streams while producing valuable biomass, microalgae-based wastewater treatment is a win-win strategy. Although recent advances have been made in this field in lab conditions, the transition to outdoor conditions on an industrial scale must be further investigated. In this work, an outdoor pilot-scale membrane photobioreactor plant was operated for tertiary sewage treatment. The effect of different parameters on microalgae performance were studied, including: temperature, light irradiance (solar and artificial irradiance), hydraulic retention time (HRT), biomass retention time (BRT), air sparging system, and influent nutrient concentration. In addition, the competition between microalgae and ammonium oxidising bacteria for ammonium was also evaluated. Maximum nitrogen and phosphorus removal rates of 12.5 ± 4.2 mg $N \cdot L^{-1} \cdot d^{-1}$ and 1.5 ± 0.4 mg $P \cdot L^{-1} \cdot d^{-1}$, respectively, were achieved at a BRT of 4.5 days and HRT of 2.5 days, while a maximum biomass productivity of 78 ± 13 mg $VSS \cdot L^{-1} \cdot d^{-1}$ was reached. While the results obtained so far are promising, they need to be improved to make the transition to industrial scale operations feasible.

1. INTRODUCTION

Microalgae are microorganisms that carry out photosynthesis and thus require inorganic carbon and light (energy source) to grow. They also require nutrients (mainly nitrogen and phosphorus), which can be obtained from wastewater streams (Ledda et al. 2015), avoiding eutrophication of natural water bodies.

Algae based wastewater treatment has some interesting advantages over other classical technologies: i) it produces valuable biomass; ii) reduces chemicals, and iii) reduces sludge production (Gao et al. 2016). Green microalgae seem to be more appropriate for wastewater treatment than other types of microalgae such as cyanobacteria (Arias et al. 2017). In this respect, green algae *Chlorella* and *Scenedesmus* have been extensively reported as ideal for wastewater treatment because of their adaptability to such media (Xu et al. 2015; Wu et al. 2017).

Many authors have studied pure microalgae cultures in highly controlled lab conditions looking for fast-growth strains. However, single-genus cultures are difficult to maintain on a large scale under outdoor conditions. On the other hand, polycultures can increase microalgae performance, since they are more robust before contamination by other microorganisms (Gouveia et al. 2016).

Microalgae can be used to treat different types of wastewater streams: urban (raw wastewater, primary and secondary effluents, centrate), aquaculture, etc. Each type has different characteristics which can affect microalgae growth positively or negatively. In this regard, Ledda et al. (2015) reported that the organic matter was the main factor affecting microalgae growth, as it was directly related with turbidity and that nutrient content did not affect the microalgae process, while Gao et al. (2016) found that high nutrient concentrations are needed to maintain high microalgae growth rates.

There are two main groups of microalgae cultivation systems: open ponds and closed photobioreactors (PBRs). Open ponds allow CO_2 uptake by microalgae directly from the atmosphere, but CO_2 can also be supplied by an aerator. Although they have lower investment and operational costs than PBRs, they also have disadvantages: large surface areas are required; contamination by predators; high CO_2 diffusion to the atmosphere; ineffective light distribution from the surface to the bottom of the reactor and high evaporative losses. PBRs are designed to improve photosynthesis efficiency by increasing the light available to the microalgae culture. While they are perfectly mixed to avoid wall fouling and enable light and nutrient homogenisation, their investment and maintenance costs are high. Moreover, photoinhibition, overheating, biofouling and oxygen accumulation can cause microalgae growth inhibition (Arbib et al. 2013). Table V.1 summarises the results of different microalgae cultivation systems which treated wastewater under outdoor conditions.

Table V.1. Results of algae based wastewater treatment studies under outdoor conditions.

Type of PBR	Type of wastewater	HRT (d)	N-Feed (mg $N \cdot L^{-1}$)	P-Feed (mg $P \cdot L^{-1}$)	Productivity (mg $VSS \cdot L^{-1} \cdot d^{-1}$)	NRE (%)	PRE (%)	Reference
Vertical PBR	Primary effluent	13(1)	133	8.3	100	84	95	Gouveia et al. 2016
HRAP	Secondary effluent	8	25.7	2.2	30	56.3	86.5	Arbib et al. 2013
Rectangular PBR	Municipal wastewater	15(1)	30.5	2.6	-	96	99	Woertz et al. 2009
Rectangular PBR	ADAS(2) + Secondary effluent	21(1)	259.7	42.6	109	73.3	66.5	Tan et al. 2016
Flat-panel PBR	AnMBR effluent	8	44.7	5.2	23.4	41.6	36.1	Viruela et al. 2016
Flat-panel PBR	AnMBR effluent	14	81.5	9.2	13.8	50.9	50.9	Viruela et al. 2016

(1) Batch operation. HRT indicates the length of the study; (2) ADAS: Anaerobically digested activated sludge.

Generally, closed PBRs obtained high nitrogen (NRE) and phosphorus removal efficiencies (PRE) (around 80-100%), while open ponds are less efficient. Moreover, Table V.1 shows that the highest productivities and nutrient removal efficiencies were obtained in batch experiments. However, both batch and high HRT operations would imply considerably high surface areas to treat wastewater at industrial scale. Thus, algae based wastewater treatment technologies must operate at minimum HRT. In this respect, membrane photobioreactors (MPBR), which are the combination of PBRs and membrane technology, appear as an ideal solution for microalgae cultivation to treat wastewater. Membranes separate the microalgae biomass from the water effluent, so that high nutrient loads can be maintained while microalgae biomass wash-out is avoided (Gao et al. 2016).

This paper summarises the results obtained from an outdoor MPBR pilot plant under different environmental, design, and operating conditions. This plant was fed by the effluent of an anaerobic membrane bioreactor (AnMBR) treating sewage. The aim of the MPBR plant was to simultaneously reduce the nutrient load in the AnMBR effluent and to produce microalgae biomass.

2. MATERIAL AND METHODS

2.1. The substrate

The microalgae substrate consisted of the nutrient-rich effluent from an AnMBR plant that treated real sewage (Giménez et al. 2011). Its nutrient concentration varied in the range of 40-80 mg $N \cdot L^{-1}$ and 4-10 mg $P \cdot L^{-1}$ due to variations on wastewater characteristics and AnMBR performance. The substrate also contained large amounts of sulphide (around 100-120 $mgS \cdot L^{-1}$), which inhibit microalgae growth (González-Camejo et al. 2017). The substrate was therefore aerated before feeding the PBRs to oxidise the sulphide to sulphate (González-Camejo et al. 2017). Moreover, the AnMBR effluent presented a COD concentration of 72 ± 37 $mgCOD \cdot L^{-1}$ (mostly non-biodegradable) and an alkalinity of 370 ± 67 $CaCO_3 \cdot L^{-1}$.

2.2. Pilot plant

The MPBR pilot plant was located in the Carraixet WWTP (Valencia, Spain), and consisted of two outdoor flat-panel PBRs connected to a filtration system. Each PBR had a working volume of 550 L: 2.00 m long x 1.10 m high x 0.25 m wide. The aeration system consisted of two perforated pipes (5 mm diameter) placed on the bottom of the PBRs, which continuously introduced air at a flow rate of 0.09 vvm. This way, microalgae settling and wall fouling were minimised. Whenever the pH value of the culture was over 7.5 (set point), pure CO_2 (99.9%) was introduced into the air system, reaching a maximum percentage of CO_2 in the air flow of 4%. This way, phenomena such as ammonia volatilisation and phosphorus precipitation were considered negligible (Whitton *et al.,* 2016).

Both PBRs had twelve white LED lamps (Unique Led IP65 WS-TP4S-40W-ME) installed at the back, offering a continuous light irradiance of 300 $\mu E \cdot m^{-2} \cdot s^{-1}$ (Light:Dark cycle of 24:0 h).

Both PBRs were connected to a filtration system, which mainly consisted of two membrane tanks which included industrial hollow-fibre ultrafiltration membrane units (PURON® Koch Membrane Systems (PUR-PSH31), 0.03 µm pore size), with a working volume of 38 L and filtering area of 6.8 m^2. They were stirred by the same CO_2-enriched air flow as the PBRs to reduce cake formation and avoid undesirable phenomena.

During the experiments with inhibition of nitrification, a concentration of 5 $mg \cdot L^{-1}$ of allylthiourea (ATU) was maintained in the PBRs to inhibit AOB growth (Table V.2).

2.3. Experimental periods

Before each operating period, the MPBR plant went through a start-up phase, consisting of: i) adding 10% of the working volume with microalgae biomass (300-500 mg VSS·L^{-1}; mainly *Scenedesmus* and *Chlorella*; although bacteria and cyanobacteria were also present) and 90% of the working volume with the aforementioned substrate; ii) batch mode until reaching a biomass concentration of around 250-400 mg VSS·L^{-1} (data not shown); and iii) continuous feeding maintaining the desired BRT and HRT.

The experimental set-up consisted of 4 periods in which the MPBR was operated under different environmental (temperature, solar irradiance and influent nutrient concentration), operating (BRT and HRT) and design (bubble size of the air sparging system and operating the MPBR plant without membrane filtration, i.e. as a PBR system) conditions. Moreover, artificial light and ATU addition were also modified (Table V.2).

Period 1 was operated without microalgae biomass filtration so that BRT was equal to HRT (PBR system). No additional artificial light source was used. It was divided into 4 sub-periods: 1) 1A was operated at HRT of 8 days and ATU was continuously added; 2) 1B was operated at the same HRT without ATU; 3) in sub-period 1C, HRT was increased to 14 days without ATU. 4) In 1D, an initial ATU dose of 5 mg·L^{-1} was added. The rest of the sub-period was operated at HRT of 14 days without further ATU addition.

In Period 2, the pilot plant was also operated as a PBR system (without membranes), maintaining HRT (i.e. BRT) at 8 days. A neoprene diffuser with 0.5 mm pore size was installed in PBR-1. In PBR-2, the same air sparging system (5 mm pore size) was maintained. The rest of the operating and outdoor conditions were the same for both PBRs. Thus, only in this period, PBR-1 and PBR-2 were operated separately in order to compare the effect of different bubble size of the air sparging system.

In Period 3, the plant was operated as an MPBR system at BRT of 4.5 days and variable HRT: 2.5, 2 and 3 days, for sub-periods 3A, 3B and 3C, respectively.

Period 4 was operated as an MPBR system at a BRT and HRT of 4.5 days and 2.5 days, respectively, but the period started with a microalgae biomass concentration of 160 mg VSS·L^{-1} (lower than the other periods).

Table V.2. Operation and outdoor conditions of each period.

Sub-period	Days of operation	Daily average solar PAR ($\mu E \cdot m^{-2} \cdot s^{-1}$)	Average artificial PAR ($\mu E \cdot m^{-2} \cdot s^{-1}$)	Temperature (ºC)	BRT (d)	HRT (d)	NLR(1) (g $N \cdot d^{-1}$)	PLR(1) (g $P \cdot d^{-1}$)	ATU (mg $\cdot L^{-1}$)
1A	17	171 ± 55	0	28.0 ± 1.5	8	8	2.5 ± 0.2	0.3 ± 0.0	5
1B	13	164 ± 34	0	25.4 ± 1.9	8	8	3.0 ± 0.2	0.4 ± 0.0	0
1C	21	294 ± 100	0	24.4 ± 2.2	14	14	1.7 ± 0.3	0.2 ± 0.0	0
1D	33	249 ± 111	0	16.8 ± 2.3	14	14	2.2 ± 0.5	0.3 ± 0.1	5(2)
2(3)	24	119 ± 32	300	23.0 ± 1.1	8	8	3.9 ± 0.3	0.4 ± 0.1	5
3A	20	234 ± 19	300	23.5 ± 0.3	4.5	2.5	9.7 ± 2.3	1.3 ± 0.2	5
3B	22	259 ± 43	300	26.9 ± 4.0	4.5	2	14.4 ± 1.8	1.8 ± 0.1	5
3C	47	283 ± 75	300	24.8 ± 1.3	4.5	3	8.4 ± 1.1	1.1 ± 0.2	5
4	40	357 ± 105	300	23.2 ± 2.1	4.5	2.5	13.6 ± 2.0	1.4 ± 0.2	5

(1) Nutrient loading rate to each PBR; (2) single ATU dosage; (3) Smaller pore size diameter in PBR-1 than PBR-2.

2.4. Analytical Methods

Grab samples were collected in duplicate from the influent and effluent streams of the MPBR pilot plant three times a week. Ammonium, nitrite, nitrate, and phosphate were analysed in a Smartchem 200 automatic analyser (Westco Scientific Instruments), according to Standard Methods (APHA et al. 2005).VSS was also analysed following APHA et al. (2005).

50 µL of sample were measured twice a week according to Pachés *et al*. (2012) to count (in duplicate) the total eukaryotic cells (TEC).

2.5. Calculations

Biomass productivity (BP) (mg $VSS \cdot L^{-1} \cdot d^{-1}$), nitrogen removal rate (NRR) (mg $N \cdot L^{-1} \cdot d^{-1}$), phosphorus removal rate (PRR) (mg $P \cdot L^{-1} \cdot d^{-1}$), nitrogen removal efficiency (NRE) (%) and phosphorus removal efficiency (PRE) (%) were calculated by the equations V.1, V.2, V.3, V.4, and V.5, respectively:

$$BP = \frac{X_{VSS}}{BRT} \quad \text{[Eq. V.1]}$$

$$NRR = \frac{F \cdot (N_i - N_e)}{V_{MPBR}} \quad \text{[Eq. V.2]}$$

$$\mathrm{PRR} = \frac{F \cdot (P_i - P_e)}{\mathrm{V}_{MPBR}} \qquad \text{[Eq. V.3]}$$

$$\mathrm{NRE} = \frac{(N_i - N_e)}{N_i} \cdot 100 \qquad \text{[Eq. V.4]}$$

$$\mathrm{PRE} = \frac{(P_i - P_e)}{\mathrm{P}_i} \cdot 100 \qquad \text{[Eq. V.5]}$$

where X_{VSS} (mg VSS·L^{-1}) is the volatile suspended solids concentration in the PBRs, BRT is the biomass retention time (d), F is the wastewater flow rate (L·d^{-1}), N_i is the nitrogen concentration of the influent (mg N·L^{-1}), N_e is the nitrogen concentration of the effluent (mg N·L^{-1}), P_i is the phosphorus concentration of the influent (mg P·L^{-1}), P_e is the phosphorus concentration of the effluent (mg P·L^{-1}) and V_{MPBR} is the total volume of the MPBR plant (L).

In order to compare different operating periods with variations in solar irradiances, the NRR:light irradiance ratio (NRR:I) (mg N·mol photons^{-1}), and PRR:light irradiance ratio (PRR:I) (mg P·mol photons^{-1}) were calculated by equations V.6 and V.7, respectively:

$$NRR{:}I = \frac{NRR \cdot V_{MPBR} \cdot 10^6}{I \cdot S \cdot 24 \cdot 3600} \qquad \text{[Eq. V.6]}$$

$$PRR{:}I = \frac{PRR \cdot V_{MPBR} \cdot 10^6}{I \cdot S \cdot 24 \cdot 3600} \qquad \text{[Eq. V.7]}$$

where I is the total light PAR irradiance on the PBR surface, i.e. the 24-hour average solar irradiance plus the light from the LED lamps (μmol photons·m^{-2}·s^{-1}) and S is the illuminated PBR surface (m^2).

3. RESULTS

3.1. Period 1

In this period, in which *Scenedesmus* remained the main microalgae genus (>99% of TEC), the effect of different BRT (i.e. HRT) under different environmental conditions and the competition of microalgae and ammonium oxidising bacteria (AOB) for ammonium was evaluated.

In sub-period 1A, AOB growth was inhibited by ATU addition, so that nitrite and nitrate concentration remained at negligible values, although ammonium and phosphate stayed at high values during the entire sub-period (Figure V.1a).

In sub-period 1B, ATU was not added, but nitrite and nitrate concentrations remained at negligible concentrations, which suggested that no nitrifying bacteria proliferation occurred. Biomass concentration dropped from 301 ± 15 mg VSS·L^{-1}in sub-period 1A to 213 ± 28 mg VSS·L^{-1} in 1B. Since temperature has been shown to have a direct effect

on biomass productivity (Viruela et al. 2016), the biomass reduction was assumed to be due to the temperature dropping from 28.0 ± 1.5 ºC in sub-period 1A to 25.4 ± 1.9 ºC in 1B. This temperature reduction could have also favoured microalgae over AOB (González-Camejo et al. 2018).

In sub-period 1C, the HRT (i.e. BRT) was raised from 8 to 14 days. In consequence, VSS concentration achieved a maximum concentration of 304 mg $VSS \cdot L^{-1}$ (Figure V.1b). However, this increased biomass concentration could also have been related to a solar PAR increase from 164 ± 34 $\mu mol \cdot m^{-2} \cdot s^{-1}$ in sub-period 1B to 294 ± 100 $\mu mol \cdot m^{-2} \cdot s^{-1}$ in 1C. On the other hand, by the end of sub-period 1C, nitrite concentration reached a maximum value of 18.5 mg $N \cdot L^{-1}$ (Figure V.1a), which indicated that an AOB proliferation occurred.

Lastly, a single ATU dose was added at the beginning of sub-period 1D to inhibit AOB growth. Consequently, nitrite concentration dropped due to the nitrate oxidising bacteria (NOB) proliferation, which oxidised nitrite to nitrate (Figure V.1a). When the nitrite was exhausted, the NOB could no longer grow and nitrate concentration declined due to wash-out.

In terms of microalgae biomass, sub-period 1D started with a concentration of 360 mg $VSS \cdot L^{-1}$, but steadily decreased mainly due to a significant reduction in the culture temperature (Figure V.1b).

It is worth mentioning that HRT was not directly related to nutrient loading rates due to both WWTP intake dynamics and AnMBR plant performance. For instance, sub-period 1A (HRT of 8 days) had a similar NLR and PLR to 1D (HRT of 14 days) (Table V.2). Hence, NLR and PLR must also be considered as controlling parameter.

In this period, the highest biomass productivities were achieved in sub-periods 1A and 1B (Table V.3), probably because the temperature was higher (Table V.2). Similar results were obtained by Viruela et al. (2016). Moreover, the nutrient removal rates in terms of NRR:I and PRR:I were also higher in sub-periods 1A and 1B, although the solar irradiances were considerably lower than in sub-periods 1C and 1D (Table V.2). Since nutrient removal rates have been reported to be directly related to light irradiance (Viruela et al., 2016), these results suggested that the culture could have been nutrient-limited in during sub-periods 1C and 1D. In fact, the ammonium concentration remained under 10 mg $N \cdot L^{-1}$ during days 49-63; i.e., in sub-periods 1C and 1D (Figure V.1a). In this respect, ammonium values below 10 mg $N \cdot L^{-1}$ have been reported to limit ammonium absorption by microalgae (Ruiz-Martinez et al., 2014). This low ammonium

concentration in sub-periods 1C and 1D was mainly due to an AOB proliferation, which competed with microalgae for ammonium (González-Camejo et al., 2018). Hence, the proliferation of AOB did not seem to be desirable, as the system can get nutrient-limited. Further research in this topic must be developed in order to better understand the operating conditions which favour microalgae growth over AOB.

When the system was non-nutrient-limited, the effluent nutrient concentration followed approximately the same trend as the influent (Figure V.1a). This tendency was in agreement with Arbib et al. (2013), who reported higher effluent nutrient concentrations at higher influent nutrient concentrations in outdoor microalgae cultivation.

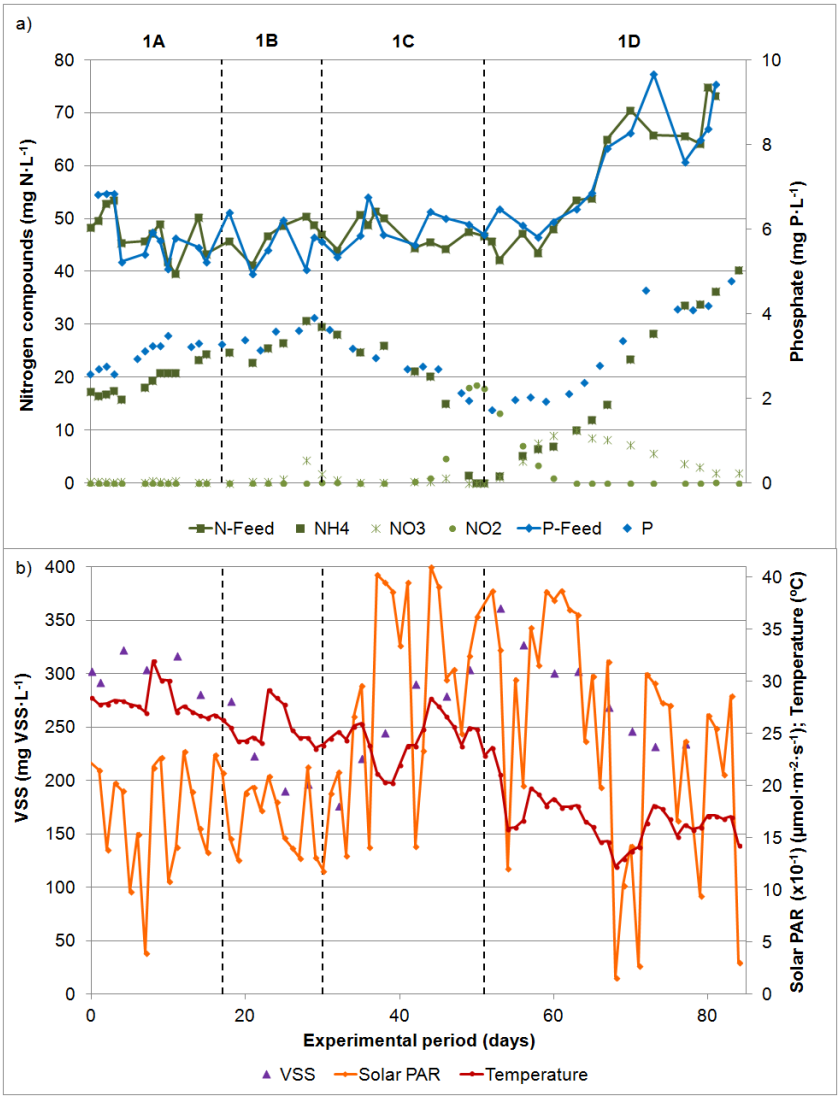

Figure V.1. Evolution during Period 1 (HRT = BRT; with or without ATU addition) of: a) Effluent concentration of: ammonium (NH_4); nitrite (NO_2); nitrate (NO_3) and soluble phosphorus (P); and feed concentration of nitrogen (N-feed) and phosphorus (P-Feed); b) VSS concentration, solar PAR and culture temperature.

3.2. Period 2

The effect of the bubble size of the air sparging system was studied in this period. Pore size diameter in PBR-1 was reduced to 0.5 mm, while it remained at 5 mm in PBR-2. PBR-1 and PBR-2 showed similar behaviour (Figure V.2), reaching no significant differences between nutrient removal rates and biomass productivity (Table V.3).

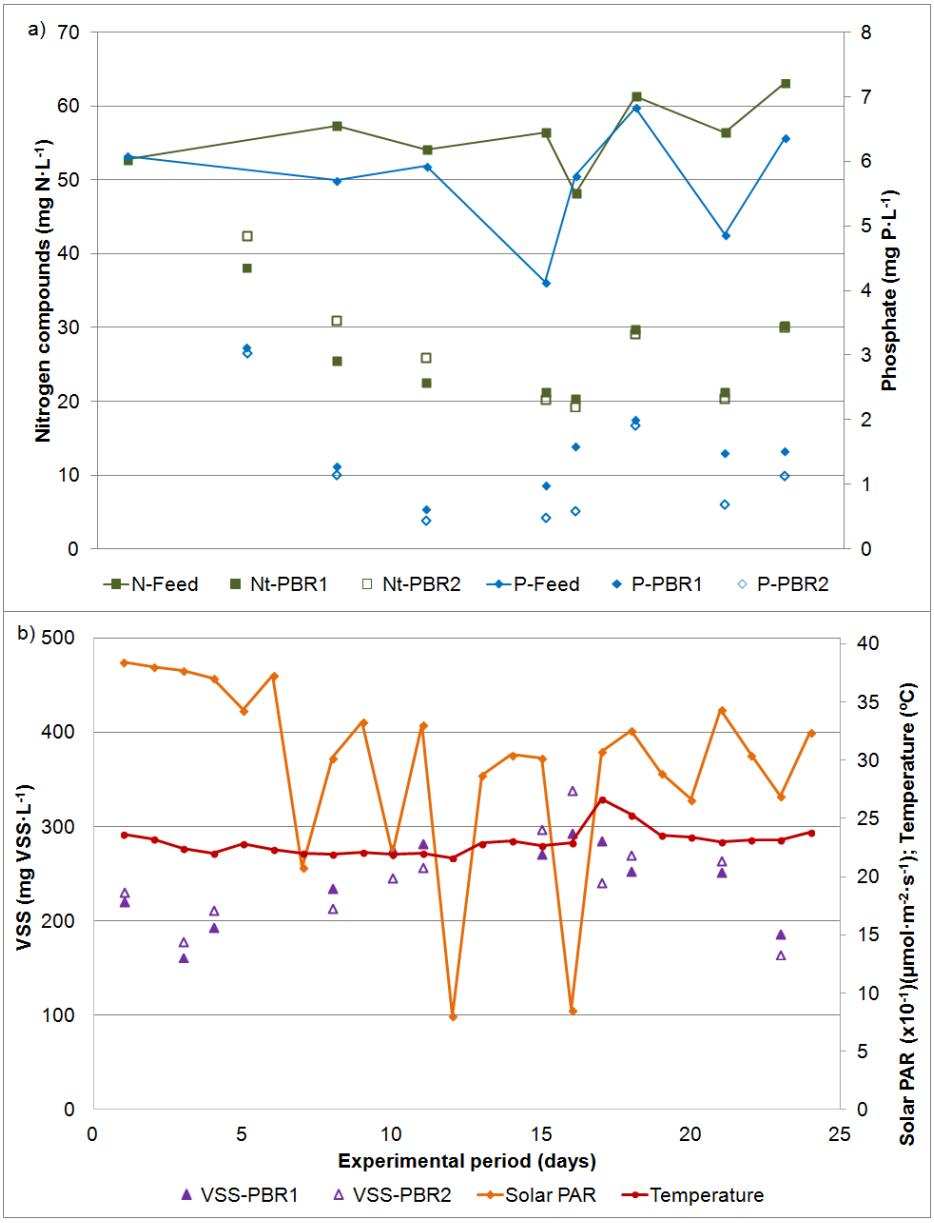

Figure V.2. Evolution during Period 2 in PBR-1 and PBR-2 (smaller pore size diameter in PBR-1 than PBR-2) of: a) Effluent concentration of: soluble nitrogen (Nt) and soluble phosphorus (P); and feed concentration of nitrogen (N-feed) and phosphorus (P-feed); b) solar PAR, culture temperature and VSS concentration.

However, the genera distribution in the cultures was different; PBR-1 had 40 % *Scenedesmus* and 55 % *Chlorella*, while PBR-2 had 85 % *Scenedesmus* and 10% *Chlorella*. Moreover, by the end of period, the phosphorus concentration in PBR-2 was slightly lower than in PBR-1.These differences could have been related to a cyanobacteria proliferation observed in PBR-1 at the end of Period 2 (Figure V.3). This agrees with Kin et al. (2014), who reported that small bubble size favours cyanobacteria growth over green algae. The proliferation of cyanobacteria is not desirable, as they have been reported to excrete some allelopathic substances that can damage green microalgae (Leão et al. 2009).

The results obtained in this period showed that nutrient removal rates and nutrient removal efficiencies were higher in Period 2 than in Period 1 (Table V.3), mainly due to an additional light source that had not been used in Period 1. Increasing the light irradiance on the PBRs was therefore considered beneficial for nutrient removal in outdoor conditions.

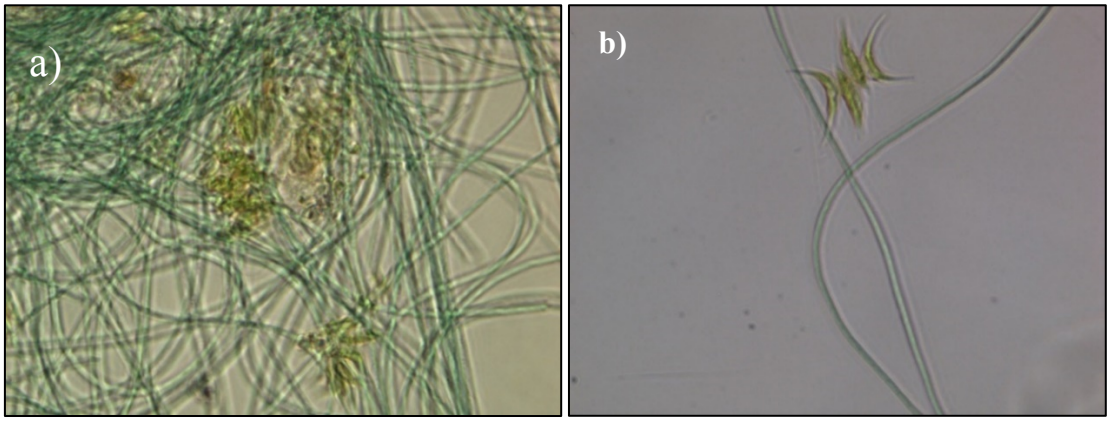

Figure V.3. Samples observed under epifluorescence microscope (Leica DM2500/ DFC420c digital camera, 63x) in Period 2 (day 21). a) PBR-1: Cyanobacteria and green algae (mainly Scenedesmus and Chlorella) floc; b) PBR-2: Scenedesmus in four-cell coenobia and a small amount of cyanobacteria.

3.3. Period 3

The use of the membrane system in this period enhanced the treatment capacity of the MPBR plant: HRT was significantly reduced from 8 (Period 2) to 2.5 days (sub-period 3A). This means that nutrient loading rates were considerably higher during this period (Table V.2), which has been reported to favour microalgae growth (Gao et al. 2016). In consequence, nutrient removal rates and biomass productivity were considerably higher

in Period 3 than in the previous periods (Table V.3), reaching maximum NRR, PPR and biomass productivity in sub-period 3A: 12.5 ± 4.2 mg $N \cdot L^{-1} \cdot d^{-1}$, 1.5 ± 0.4 mg $P \cdot L^{-1} \cdot d^{-1}$ and 78 ± 13 mg $VSS \cdot L^{-1} \cdot d^{-1}$, respectively. The light use efficiency of the microalgae improved in this period (operating as an MPBR system), since NRR:I and PRR:I values were around 2-fold and 3-fold higher than in the previous periods, in which the system operated as a PBR (Table V.3).

In sub-period 3B nutrient removal rates started at values around 15 mg $N \cdot L^{-1} \cdot d^{-1}$ and 1.7 mg $P \cdot L^{-1} \cdot d^{-1}$, but after day 30 they suddenly dropped to 7-10 mg $N \cdot L^{-1} \cdot d^{-1}$ and 1.0 mg $P \cdot L^{-1} \cdot d^{-1}$ and did not recover their high initial values (Figure V.4c). This reduced nutrient removal rates could have been due to a significant increase in the culture temperature from around 25 to 33ºC in days 30-35 (Figure V.4b). These high temperatures could have affected biomass productivity. Indeed, the biomass concentration dropped from around 400 to 300 mg $VSS \cdot L^{-1}$. Consequently, nutrient removal capacity also decreased.

In sub-period 3C, temperature stabilised and NRR was solar PAR-dependent (Figure V.4c), which was in agreement with Viruela et al. (2016). However, NRR and PRR were lower in sub-period 3C than in sub-periods 3A and 3B, which could be explained by: i) after the high temperatures in sub-period 3B, the system took around two weeks to recover the initial microalgae biomass (Figure V.4b), so that its nutrients removal capacity was reduced; ii) sub-period 3C had the lowest nutrient loading rates of Period 3 (Table V.2). Consequently, effluent nitrogen concentration (which was mainly ammonium) was reduced to values of 10-15 mg $N \cdot L^{-1}$ during days 55-68 (Figure V.4a). Ruiz-Martinez et al. (2014) reported that NRR decreased whenever ammonium concentration in the culture was below 10-13 mg $N \cdot L^{-1}$. Hence, in sub-period 3C, the culture was considered to be nutrient-limited; iii) in spite of having received a higher solar PAR in sub-period 3C (Table V.3), this irradiance was more variable than in sub-periods 3A and 3B (Figure V.4c). This means that the alternation of very sunny days, in which photoinhibition could have occurred, with photo-limited days could have negatively affected microalgae growth.Throughout Period 3, *Scenedesmus* remained as dominant genus (80-95% of TEC) and *Chlorella* only reached 5-20 % of TEC.

The best efficiencies of this period (67 ± 11% and 69 ± 9%, for nitrogen and phosphorus, respectively) were obtained at an HRT of 2.5 days, even though solar PAR in sub-period 3A was the lowest of the period (Table V.2). On the other hand, in sub-period 3C, with the lowest nutrient loading rates, the culture could be nutrient-limited

and therefore nutrient removal efficiencies were lower than in 3A (Table V.3). NLR and PLR thus appear to be key parameters in assessing MPBR performance.

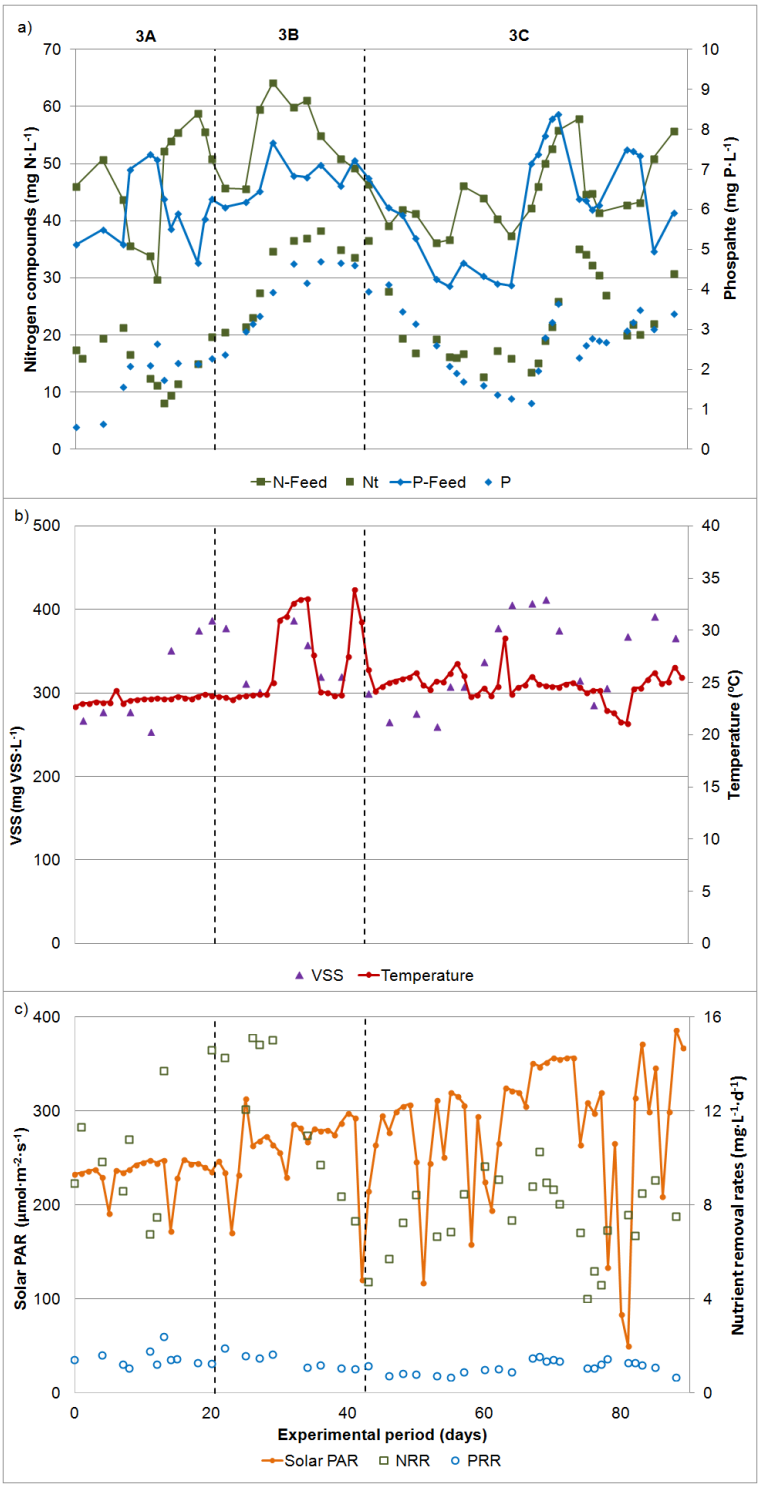

Figure V.4. Evolution during Period 3 (variable HRT) of: a) Effluent concentration of: soluble nitrogen (Nt) and soluble phosphorus (P); and feed concentration of nitrogen (N-feed) and phosphorus (P-feed); and feed concentration of nitrogen and phosphorus; b) culture temperature and VSS concentration; c) solar PAR and nutrient removal rates.

3.4. Period 4

The same HRT and BRT were used in Period 4 as in sub-period 3A, but at higher nutrient loading rates (Table V.2), however the results obtained were significantly different (Table V.3).

As Figure V.5b shows, microalgae biomass concentration was under 250 mg VSS·L^{-1} for the entire period, while in sub-period 3A it always remained over 250 mg VSS·L^{-1} (Figure V.4b), so that the nutrient removal capacity of the system diminished and nutrient removal rates were not as high as in sub-period 3A (Table V.3). This lower biomass concentration could have been influenced by the lower initial microalgae concentration in the start-up period: 160 mg VSS·L^{-1} in Period 4, while sub-period 3A started at 270 mg VSS·L^{-1}. Su et al. (2012) also obtained higher NRR and PRR in the culture with a higher initial biomass concentration. Moreover, Feng et al. (2011) reported that cultures with denser initial biomass concentration achieved higher biomass productivity and adapted quickly to outdoor conditions.

Solar PAR, in spite of being higher than in sub-period 3A (Table V.2), was quite variable in period 4 (Figure V.5c) and, as in Period 3, could have negatively affected microalgae growth.

Nutrient removal rates could also have been influenced by a shift in the microalgae culture. In Period 4 there was a proliferation of *Monoraphidium* (45 % TEC) which co-habited with *Scenedesmus* (50 % TEC). No significant amount of *Chlorella* was present.

Table V.3. Results obtained in each sub-period.

Sub-period	Biomass productivity (mg VSS·L^{-1}·d^{-1})	NRE (%)	PRE (%)	NRR (mg N·L^{-1}·d^{-1})	PRR (mg P·L^{-1}·d^{-1})	NRR:I (mg N·mol^{-1})	PRR:I (mg P·mol^{-1})
1A	38 ± 2	56 ± 9	46 ± 8	2.8 ± 1.0	0.3 ± 0.1	36.4 ± 9.5	4.0 ± 2.1
1B	27 ± 4	40 ± 6	38 ± 6	1.9 ± 1.4	0.2 ± 0.1	31.3 ± 25.8	3.8 ± 2.0
1C	19 ± 3	49 ± 7	52 ± 10	2.3 ± 0.5	0.3 ± 0.1	25.8 ± 12.7	3.5 ± 1.5
1D	20 ± 3	57 ± 8	60 ± 8	1.6 ± 0.7	0.2 ± 0.1	24.6 ± 13.7	3.6 ± 1.8
2-PBR-1(1)	28 ± 6	57 ± 4	76 ± 7	3.3 ± 2.0	0.3 ± 0.2	37.1 ± 32.2	3.7 ± 2.3
2-PBR-2	28 ± 6	56 ± 7	87 ± 10	3.1 ± 1.2	0.4 ± 0.1	31.7 ± 28.1	4.3 ± 3.4
3A	72 ± 8	67 ± 11	69 ± 9	12.5 ± 4.2	1.5 ± 0.4	64.2 ± 22.5	12.7 ± 3.4
3B	69 ± 5	43 ± 11	43 ± 10	11.5 ± 2.9	1.4 ± 0.3	56.4 ± 15.4	11.8 ± 2.9
3C	78 ± 13	50 ± 15	56 ± 12	7.5 ± 1.8	1.1 ± 0.3	36.3 ± 9.5	9.6 ± 2.5
4	53 ± 15	33 ± 7	49 ± 12	7.8 ± 2.5	1.2 ± 0.3	33.5 ± 9.9	9.5 ± 2.4

(1) Pore size diameter: 0.5 mm.

As happened in Period 1, in Period 4 the effluent nutrient concentrations followed the same trend as the influent nutrient concentrations (Figure V.5a), since the system was not nutrient-limited. According to Arbib et al. (2013), in these conditions, microalgae are mainly limited by outdoor conditions.

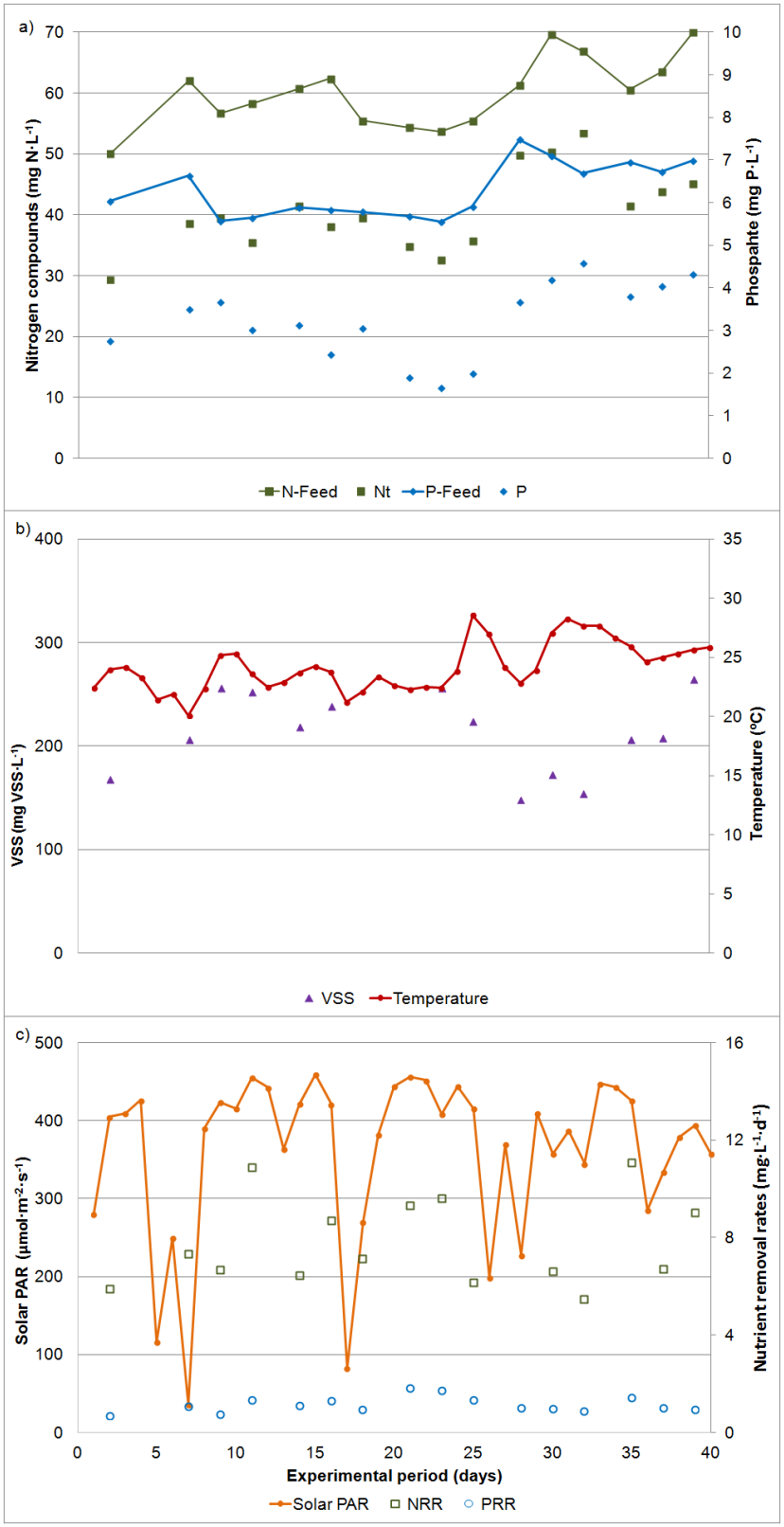

Figure V.5. Evolution during Period 4 (BRT = 4.5 d; HRT = 2.5 d) of: a) Effluent concentration of: soluble nitrogen (Nt) and soluble phosphorus (P); and feed concentration of nitrogen (N-feed) and phosphorus (P-feed); and feed concentration of nitrogen and phosphorus; b) culture temperature and VSS concentration; c) solar PAR and nutrient removal rates.

4. DISCUSSION

The performance of this outdoor MPBR pilot plant treating AnMBR effluent within a wide range of environmental, design, and operating conditions produced some interesting results, which deserve to be commented on.

When the plant was operated as a PBR system without membrane filtration (Periods 1 and 2), the highest values in terms of nutrient removal and biomass productivity were obtained when HRT was 8 days (Table V.3). When the plant was operated as an MPBR system (Periods 3 and 4), the best results were achieved at a BRT and HRT of 4.5 days and 2.5 days, respectively (sub-period 3A, Table V.3). In this respect, optimum BRT and HRT must be assessed to further improve MPBR performance.

Comparing PBR and MPBR performance, nutrient removal rates and biomass productivity were significantly higher in MPBR as the use of membranes to separate microalgae from water enabled to operate at lower HRT (i.e. higher nutrient loading rates), avoiding microalgae wash-out.

Generally, the plant performance was strongly dependent on outdoor conditions; solar irradiance seemed to be one of the main factors affecting nutrient removal, while temperature variations had a major impact on biomass productivity. The plant performance yields were reduced when the culture was nutrient-limited, which meant that high nutrient loading rates were required to reach high nutrient removal rates. In this respect, the proliferation of AOB in the culture can worsen PBR performance since they compete with microalgae for ammonium consumption.

Increasing the light supply to the microalgae seemed to be beneficial for nutrient removal as nutrient removal rates were lower in Period 1 with no artificial lighting (Table V.3).

Small bubble size (0.5 mm diameter) in the air sparging system was not found to be suitable, as it favoured the proliferation of filamentous cyanobacteria, which could hinder green microalgae growth.

The initial biomass concentration appeared to have some influence on the plant performance, since higher biomass concentrations attained better results at quite similar operating conditions.

Overall, as the nutrient removal efficiencies achieved in this continuously-operated MPBR under outdoor conditions and using real anaerobically-treated sewage were not particularly high, some improvements need to be made to comply with legal requirements. Special efforts should be focused on increasing the efficiency of the light

applied to the PBRs, lowering the plant HRT to further increase its treatment capacity, controlling BRT (and HRT when treatment capacity can be variable) to optimise microalgae productivity and nutrient removal, avoiding AOB growth without using chemical inhibitors, and reducing operating costs.

5. CONCLUSIONS

In this study, an MPBR plant was operated outdoors under different conditions: BRT, HRT, temperature, light irradiance, influent nutrient concentration, ATU addition, and bubble size of the air sparging system; reaching maximum biomass productivity and nitrogen and phosphorus removal rates of 78 ± 13 mg $VSS \cdot L^{-1} \cdot d^{-1}$, 12.5 ± 4.2 mg $N \cdot L^{-1} \cdot d^{-1}$ and 1.5 ± 0.4 mg $P \cdot L^{-1} \cdot d^{-1}$, respectively. Although these values are promising, further research needs to be carried out to make this technology feasible on an industrial scale. The main challenges to overcome include: increasing the efficiency of the light supplied to the PBRs, avoiding AOB growth, improving the plant's treatment capacity and reducing its operating costs.

ACKNOWLEDGEMENTS

This research work has been supported by the Spanish Ministry of Economy and Competitiveness (MINECO, CTM2011-28595-C02-01 and CTM2011-28595-C02-02) jointly with the European Regional Development Fund (ERDF), both of which are gratefully acknowledged. It was also supported by the Spanish Ministry of Education, Culture and Sport via a pre doctoral FPU fellowship to author J. González-Camejo (FPU14/05082).

REFERENCES

1. APHA, AWWA &WPCF 2005. Standard methods for the examination of water and wastewater, 21st edition. American Public Health Association (APHA), American Water Works Association (AWWA), Water Pollution Control Federation (WPCF).
2. Arbib Z., Ruiz J., Álvarez-Díaz P., Garrido-Pérez C., Barragan J. & Perales J.A. 2013 Long term outdoor operation of a tubular airlift pilot photobioreactor and a high rate algal pond as tertiary treatment of urban wastewater. *Ecol. Eng.*, 52, 143-153.
3. Arias D.M., Uggetti E., García-Galán M.J. & García, J. 2017 Cultivation and selection of cyanobacteria in a closed photobioreactor used for secondary effluent and digestate treatment. *Science of the Total Environment*, 587-588, 157-167.

4. Feng P., Deng Z., Hu Z. & Fan L. 2011 Lipid accumulation and growth of *Chlorella zofingiensis* in flat plate photobioreactors outdoors. *Bioresour. Technol.*, 102(22), 10577-10584.
5. Gao F., Li C., Yang Z., Zeng G., Feng L., Liu J., Liu M. & Cai, H. 2016 Continuous microalgae cultivation in aquaculture wastewater by a membrane photobioreactor for biomass production and nutrients removal, *Ecol. Eng.,* 92, 55-61.
6. Giménez J.B., Robles A., Carretero L., Durán F., Ruano M.V., Gatti M.N., Ribes J., Ferrer J. & Seco A. 2011 Experimental study of the anaerobic urban wastewater treatment in a submerged hollow-fibre membrane bioreactor at pilot scale. *Bioresour. Technol*. 102, 8799–8806.
7. González-Camejo J., Serna-García R., Viruela A., Pachés M., Durán F., Robles A., Ruano M.V., Barat R. & Seco A. 2017 Short and long-term experiments on the effect of sulphide on microalgae cultivation in tertiary sewage treatment. *Bioresour. Technol*., 244, 15-22.
8. González-Camejo J., Barat R., Pachés M., Murgui M., Ferrer J. & Seco A. 2018 Wastewater Nutrient Removal in a Mixed Microalgae-bacteria Culture: Effect of Light and Temperature on the Microalgae-bacteria Competition. *Environ. Technol.* 39(4), 503-515.
9. Gouveia L., Graça S., Sousa C., Ambrosano L., Ribeiro B., Botrel E.P., Neto P.C., Ferreira A.F. & Silva C.M. 2016 Microalgae biomass production using wastewater: Treatment and costs Scale-up considerations. *Algal Res.,* 16, 167-176.
10. Kin K., Choi J., Ji Y., Park S., Do H., Hwang C. & Lee B. 2014 Impact of bubble size on growth and CO_2 uptake of Artrhospira (Spirulina) platensis KMMCC CY-007. *Bioresour. Tecnol., 170*, 310-315.
11. Leão P.N., Teresa M., Vasconcelos,S.D. & Vasconcelos V.M. 2009 Allelopathy in freshwater cyanobacteria. *Critical Reviews in Microbiology* 35, 271–282.
12. Ledda C., Idà A., Allemand D., Mariani P. & Adani F. 2015 Production of wild *Chlorella* sp. cultivated in digested and membrane-pretreated swine manure derived from a full-scale operation plant. *Algal Res.,* 12, 68-73.
13. Pachés, M., Romero, I., Hermosilla, Z. & Martinez-Guijarro, R. 2012 PHYMED: An ecological classification system for the Water Framework Directive based on phytoplankton community composition. *Ecological Indicators* 19, 15-23.
14. Ruiz-Martinez A., Serralta J., Pachés M., Seco A. & Ferrer J. 2014 Mixed microalgae culture for ammonium removal in the absence of phosphorus: Effect of phosphorus supplementation and process modeling. *Process Biochemistry*, 49, 2249-2257.
15. Su Y., Mennerich A. & Urban B. 2012 Coupled nutrient removal and biomass production with mixed algal culture: Impact of biotic and abiotic factors, *Bioresour. Technol.,* 118, 469-476.

16. Tan X.B., Zhang Y.L., Yang L.B., Chu H.Q. & Guo J. 2016 Outdoor cultures of Chlorella pyrenoidosa in the effluent of anaerobically digested activated sludge: The effects of pH and free ammonia, *Bioresour. Technol*. 200, 606-615.
17. Viruela A., Murgui M., Gómez-Gil T., Durán F., Robles A., Ruano M. V., Ferrer J. & Seco A. 2016 Water resource recovery by means of microalgae cultivation in outdoor photobioreactors using the effluent from an anaerobic membrane bioreactor fed with pre-treated sewage. *Bioresour. Technol.,* 218, 447-454.
18. Whitton R., Le Mével A., Pidou M., Ometto F., Villa R. & Jefferson B. 2016 Influence of microalgal N and P composition on wastewater nutrient remediation. *Water Res.,* 91, 371-378.
19. Woertz I., Feffer A., Lundquist T. & Nelson Y. 2009 Algae grown on dairy and municipal wastewater for simultaneous nutrient removal and lipid production for biofuel feedstock. *J. Environ. Eng.*, 135(11), 1115–1122.
20. Wu Y.H., Zhu S.F., Yu Y., Shi X.J., Wu G.X. & Hu H.Y. 2017 Mixed cultivation as an effective approach to enhance microalgal biomass and triacylglycerol production in domestic secondary effluent. *Chemical Engineering Journal*, 328, 665-672.
21. Xu M., Li P., Tang T. & Hu Z. 2015 Roles of SRT and HRT of an algal membrane bioreactor system with a tanks-in-series configuration for secondary wastewater effluent polishing. *Ecol. Eng*. 85, 257-264.

CHAPTER VI:

OPTIMISING AN OUTDOOR MEMBRANE PHOTOBIOREACTOR FOR TERTIARY SEWAGE TREATMENT

CHAPTER VI:

OPTIMISING AN OUTDOOR MEMBRANE PHOTOBIOREACTOR FOR TERTIARY SEWAGE TREATMENT

González-Camejo, J., Jiménez-Benítez, A., Ruano, M.V., Robles, A., Barat, R., Ferrer, J., 2019. Optimising an outdoor membrane photobioreactor for tertiary sewage treatment. J. Environ. Manag. 245, 76-85.
https://doi.org/10.1016/j.jenvman.2019.05.010

ABSTRACT

The operation of an outdoor membrane photobioreactor plant which treated the effluent of an anaerobic membrane bioreactor was optimised. Biomass retention times of 4.5, 6, and 9 days were tested. At a biomass retention time of 4.5 days, maximum nitrogen recovery rate:light irradiance ratios, photosynthetic efficiencies and carbon biofixations of 51.7 ± 14.3 mg $N \cdot mol^{-1}$, 4.4 ± 1.6% and 0.50 ± 0.05 kg $CO_2 \cdot m^3_{influent}$, respectively, were attained. Minimum membrane fouling rates were achieved when operating at the shortest biomass retention time because of the lower solid concentration and the negligible amount of cyanobacteria and protozoa.

Hydraulic retention times of 3.5, 2, and 1.5 days were tested at the optimum biomass retention times of 4.5 days under non-nutrient limited conditions, showing no significant differences in the nutrient recovery rates, photosynthetic efficiencies and membrane fouling rates. However, nitrogen recovery rate:light irradiance ratios and photosynthetic efficiency significantly decreased when hydraulic retention time was further shortened to 1 day, probably due to a rise in the substrate turbidity which reduced the light availability in the culture. Optimal carbon biofixations and theoretical energy recoveries from the biomass were obtained at hydraulic retention time of 3.5 days, which accounted for 0.55 ± 0.05 kg $CO_2 \cdot m^{-3}_{influent}$ and 0.443 ± 0.103 $kWh \cdot m^{-3}_{influent}$, respectively.

1. INTRODUCTION

Wastewater treatment has played a key role in the development of human activities since the direct discharge of wastewaters to the environment without the appropriate treatment can imply a variety of pollution problems (Gonçalves et al., 2017) such as

eutrophication, which can produce water quality losses and health risks (Guldhe et al., 2017). However, classical wastewater treatment plants (WWTPs) usually implies huge energy demands (Udaiyappan et al., 2017) and nutrient losses (Acién et al., 2016). On the other hand, water resource recovery facilities (WRRFs) use wastewater as a source of energy, nutrients and reclaimed water.

Membrane photobioreactor (MPBR) technology (which is the combination of membrane and microalgae cultivation) emerges as a suitable option within these novel WRRFs (Seco et al., 2018). Microalgae are able to efficiently reduce the nutrient load from wastewater while obtaining valuable microalgae biomass that can be anaerobically digested to produce biogas (Acién et al., 2016; Guldhe et al., 2017). The nutrient content in both the effluent of the anaerobic digestion and the digestate can be recovered for nutrient valorisation. In addition, the membrane filtration of the microalgae culture obtains a high-quality permeate in terms of suspended solids and pathogens, thus being a source of reclaimed water (Seco et al., 2018).

The filtration of microalgae also allows operating at shorter hydraulic retention times (HRTs) and longer biomass retention times (BRTs), enabling to recover large quantities of nutrients without washing out the microalgae culture (Gao et al., 2019). This can improve the microalgae performance while increasing the nutrient load to the system which would reduce the large areas of land that are needed for microalgae cultivation (Acién et al., 2016). By way of example, Bilad et al. (2014) reported in lab conditions 9-fold higher microalgae biomass productivity than a PBR system when HRT and BRT were decoupled by membrane filtration. On the other hand, a previous study in outdoor conditions (González-Camejo et al., 2018a) reported double biomass productivity, 3.8-fold higher nitrogen and phosphorus recovery rates in an MPBR system in comparison with a PBR system. The area of land required for the microalgae cultivation was 3.2-fold lower.

When operating membrane-based systems, fouling is a major concern that must be considered (Robles et al., 2013; Gong et al., 2019) especially in microalgae cultivation systems (Wang et al., 2019). Fouling occurs when microalgae cells, their secretions and the cell debris accumulate on the membrane surface and inside the pores, reducing its permeability because of the cake-layer formation and the partial block of the membrane pores (Zhang and Fu, 2018), which increases the energy consumption of the process (Wang et al., 2019). The cake layer mainly produces reversible fouling and can be removed by physical means such as gas-assisted membrane scouring and/or

backwashing (Gong et al., 2019). On the other hand, cell debris retention in the pores is the major cause of irreversible fouling, which can only be removed by chemical reagents (Porcelli and Judd, 2010), determining the membrane lifetime (Zhang and Fu, 2018). The performance of the filtration process in this type of system therefore has to be adequately assessed in order to achieve the most optimal microalgae cultivation process.

Several authors have studied the optimum operating ranges of BRT and HRT for lab-scale MPBR systems (Gao et al., 2018; Luo et al., 2018; Xu et al., 2015). However, outdoor microalgae cultivation from sewage is affected by environmental conditions in many different ways, such as the variable solar irradiance, ambient temperature and nutrient loads (Foladori et al., 2018; González-Camejo et al., 2018a). In fact, Van den Hende et al. (2014) reported under outdoor conditions a reduction of the nutrient recovery efficiency with a factor of 1-3 and with a factor of 10-13 in the case of biomass productivity. Hence, it is essential to optimise the microalgae cultivation performance to make the process feasible at large scale (Nayak et al., 2018).

The effect of several design factors such as the culture recirculation mode and the non-photic volume of the MPBR plant of this study has been previously evaluated (see Table VI.1). These previous studies (González-Camejo et al., 2018a; Viruela et al., 2018) reported the outdoor microalgae performance not only at different BRT and HRT but also within variable operating/design conditions. Thus, this effect of BRT and HRT on process performance was not isolated. For instance, the decline in the MPBR performance reported by Viruela et al. (2018) when decreasing the BRT from 4.5 to 9 days (Table VI.1) was also highly influenced by a fall in solar irradiance and temperature. In addition, the results obtained by González-Camejo et al. (2018a) at BRT of 4.5 days and different HRTs (Table VI.1) were influenced by periods of nutrient limitation due to a significant reduction in the influent nutrient load and also by periods of temperature peaks. Thus, optimal BRT and HRT must be evaluated under nutrient-replete conditions (González-Camejo et al., 2019) and optimal design and operating conditions. Moreover, membrane fouling has not been previously assessed in this MPBR system, which would finally determine the technical and economic feasibility of the treatment process.

Table VI.1. Summary of the results obtained in previous studies.

Type of reactor	Parameter evaluated	Results			Reference
		NRR	PRR	BP	
PBR	BRT = 8 d	2.8	0.3	38	González-Camejo et al., 2018[a]
	BRT = 14 d	1.6	0.2	20	
MPBR	PS: Cavity pump	6.9[1]	0.6[2]	22[3]	Gómez-Gil et al., 2015
	PS: Airlift	6.9[1]	0.6[2]	21[3]	
MPBR	BRT = 4.5 d[a]	8.1	1.0	51	Viruela et al., 2018
	BRT = 9 d[a]	3.3	0.4	32	
MPBR	NPV = 27.2%	6.6	0.6	22	Viruela et al., 2018
	NPV = 13.6%	7.6	1.0	31	
MPBR	HRT = 2 d[b]	11.5[4]	1.4[5]	69[6]	González-Camejo et al., 2018a
	HRT = 2.5 d[b]	12.5[4]	1.5[5]	72[6]	
	HRT = 3 d[b]	7.5	1.1	78[6]	

NRR: nitrogen recovery rate (mg $N \cdot L^{-1} \cdot d^{-1}$); PRR: phosphorus recovery rate (mg $P \cdot L^{-1} \cdot d^{-1}$); BP: biomass productivity (mg $VSS \cdot L^{-1} \cdot d^{-1}$); PBR: photobioreactor (HRT ≡ BRT); MPBR: membrane photobioreactor; BRT: biomass retention time; PS: pumping system; NPV: non-photic volume; HRT: hydraulic retention time; a: HRT = 2-4 days; b: HRT = 4.5 days; group of numbers (1,2,3,4,5,6): non statistically significant differences.

The present work thus aimed to go one step further of the previous studies (Gómez-Gil et al., 2015; González-Camejo et al., 2018a; Viruela et al., 2018) in the optimisation of the outdoor operational conditions of a MPBR system, evaluating different BRT and HRT combinations to optimise the energy and nutrient recovery, photosynthetic efficiency (PE), carbon biofixation (C-BF) and membrane fouling rates (FR).

2. MATERIALS AND METHODS

2.1. Pilot plant description

Microalgae were cultivated in an outdoor MPBR plant (39º30'04.0''N 0º20'00.1''W, Valencia, Spain), so that the solar light irradiance applied to the PBRs was variable (Table VI.2). It consisted of two flat-plate PBRs connected to a membrane tank (MT) (Figure VI.1). Each PBR had a working volume of 550 L, and dimensions of 1.25-m high by 2-m wide and 0.25-m deep. Both PBRs had an additional artificial light source consisting of twelve white LED lamps (Unique Led IP65 WS-TP4S-40W-ME) installed at their back surface, which emitted a continuous light irradiance of 300 $\mu mol \cdot m^{-2} \cdot s^{-1}$ (measured on the PBRs surface). The PBRs were continuously stirred by air sparging to prevent wall fouling and ensure culture homogenisation. pH was kept at 7.5 ± 0.3 by introducing pure pressurised CO_2 (99.9%) into the air system (Figure VI.1b).

The MT had a total working volume of 14 L, which corresponded to a non-photic culture volume of 1.2%. It was formed by one hollow-fibre ultrafiltration membrane bundle extracted from an industrial-scale membrane unit (PURON® Koch Membrane Systems (PUR-PSH31), 0.03 μm pores). The bundle had a filtration area of 3.4 m^2 and 2-m length. Air was introduced into the bottom of the MT to reduce membrane fouling by membrane scouring (Figure VI.1b).

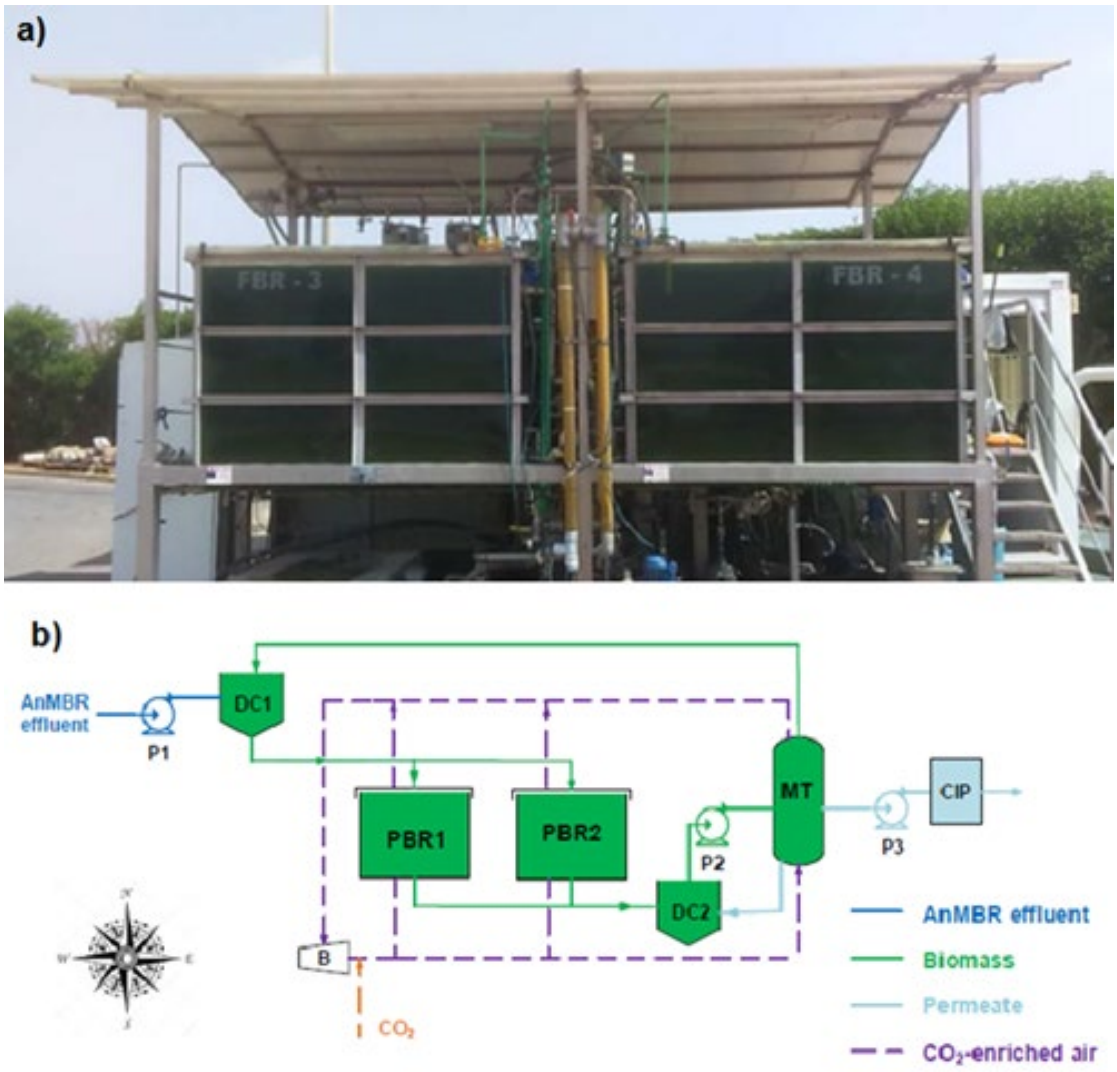

Figure VI.1.a) Outdoor MPBR pilot plant. b) Flow diagram of the process. PBR: photobioreactor; MT: membrane tank; P: pump; DC: distribution chamber; B: blower; CIP: clean-in-place-tank.

2.1.1. MPBR plant operation

To control the BRT, a given amount of microalgae biomass was wasted from the system and the cultivation substrate (anaerobically-treated sewage, see section VI.2.2) was fed into the system during daylight hours to replace it. To control the HRT, the corresponding amount of permeate was produced and extracted from the system as effluent during daylight hours. The filtration unit was also run during night-time for the correct evaluation of the filtration process performance, recycling to the system the amount of permeate that was not taken out of the MPBR plant to control the HRT. A fraction of the microalgae culture was continuously fed into the MT at a flow rate of

300 $L \cdot h^{-1}$. The permeate flow rate was set to around 85-102 $L \cdot h^{-1}$. The rejection of the membrane unit was recycled to the PBRs as shown in Figure VI.1b.

Membrane operation consisted of a combination of the classical stages of filtration–relaxation (F–R) and back-flushing. Ventilation and degasification stages were also considered (Robles et al., 2013). The membrane operating mode followed a sequence of 300-s basic F-R cycle (250 s filtration and 50 s relaxation), 40 s of back-flush every 10 F–R cycles, 60 s of ventilation every 20 F–R cycles and 60 s of degasification every 50 F–R cycles. The gross 20ºC-standardised transmembrane flux (J20) was kept around 22-30 LMH ($L \cdot m^{-2} \cdot s^{-1}$). The average specific gas demand per unit of membrane area (SGDm) was kept around 0.3-0.4 $Nm^3 \cdot h^{-1} \cdot m^{-2}$. This gave an average specific gas demand per volume of produced permeate (SGDP) of around 8-12 Nm^3 of gas per m^3 of permeate.

Further information about the instrumentation, control and automation of the MPBR plant can be found in Viruela et al. (2018).

2.2. Microalgae substrate and inoculum

The microalgae substrate consisted of nutrient-rich effluent from an AnMBR plant that treated real sewage, which is fully described in Giménez et al. (2011). The average characteristics of this substrate were a chemical oxygen demand (COD) concentration of 66 ± 31 mg $COD \cdot L^{-1}$, a nitrogen concentration of 58.5 ± 6.1 mg $N \cdot L^{-1}$ (mainly ammonium; i.e., > 95%), a phosphorus concentration of 6.6 ± 0.9 mg $P \cdot L^{-1}$, a sulphide concentration of 99 ± 23 mg $S \cdot L^{-1}$ and a turbidity below 50 NTU. The AnMBR effluent was aerated in a regulation tank before being fed to the PBRs to completely oxidise the sulphide to sulphate, avoiding the sulphide inhibition of microalgae (González-Camejo et al., 2017).

Microalgae were obtained from the walls of the secondary clarifier in the Carraixet WWTP (Valencia, Spain) and consisted of a mixture of microalgae (including cyanobacteria), algae and bacteria (both heterotrophic and autotrophic). Prior to the inoculation in the MPBR plant, these microalgae were filtered in order to remove most of filamentous bacteria and zooplankton from the inoculum. The culture, which was mainly composed by *Scenedesmus* and *Chlorella,* was adapted to the growth medium (AnMBR effluent) under lab conditions as explained in González-Camejo et al. (2018b).

2.3. Experimental periods

Seven experiments were carried out in order to find the optimal operating conditions of the MPBR plant. Three of them (i.e., BRT4.5, BRT6 and BRT9) were developed at constant HRT of 2.5 days and a BRT of 4.5, 6 and 9 days, respectively. Moreover, four experiments (HRT3.5, HRT2, HRT1.5 and HRT1) were done at constant BRT of 4.5 days and at HRT of 3.5, 2, 1.5 and 1 days, respectively. The duration of each experiment varied according to the days that the culture was maintained in pseudo-steady state (Table VI.2); i.e., when there was similar volatile suspended solids (VSS) concentration in the culture (Figures VI.2 and VI.3) and temperature was in the range of 20-30 ºC (González-Camejo et al., 2019).

Table VI.2. Operating and outdoor conditions during BRT and HRT Experiments (mean ± standard deviation).

Experiment	Days	BRT (d)	HRT (d)	Solar PAR ($\mu mol \cdot m^{-2} \cdot s^{-1}$)*	NLR ($g\ N \cdot d^{-1}$)	PLR ($g\ P \cdot d^{-1}$)
BRT4.5	23	4.5	2.5	268 ± 148	27.0 ± 3.0	2.8 ± 0.5
BRT6	40	6	2.5	319 ± 126	27.2 ± 3.1	2.6 ± 0.7
BRT9	27	9	2.5	226 ± 50	26.8 ± 3.7	4.1 ± 0.4
HRT3.5	20	4.5	3.5	310 ± 57	16.8 ± 1.4	2.0 ± 0.4
HRT2	20	4.5	2	266 ± 46	34.4 ± 4.4	3.8 ± 0.4
HRT1.5	13	4.5	1.5	318 ± 103	42.2 ± 5.5	5.0 ± 0.8
HRT1	22	4.5	1	290 ± 104	53.1 ± 5.7	7.5 ± 2.3

BRT: biomass retention time; HRT: hydraulic retention time; Solar PAR: daily average solar photosynthetic active radiation; NLR: nitrogen loading rate; PLR: phosphorus loading rate.

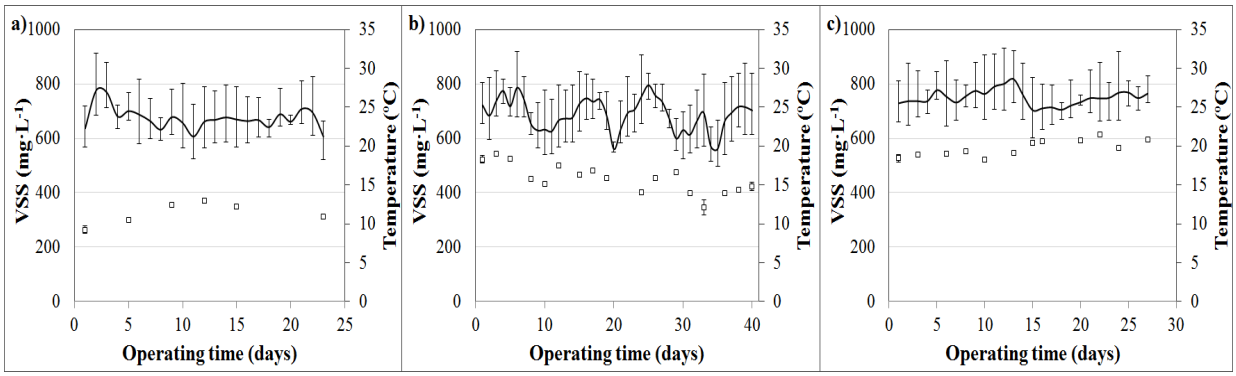

Figure VI.2. Evolution of the volatile suspended solids concentration (□) (mg VSS·L^{-1}) and temperature (—) (ºC) (bars indicate maximum and minimum temperatures) during BRT experiment: a) BRT4.5; b) BRT6; c) BRT9.

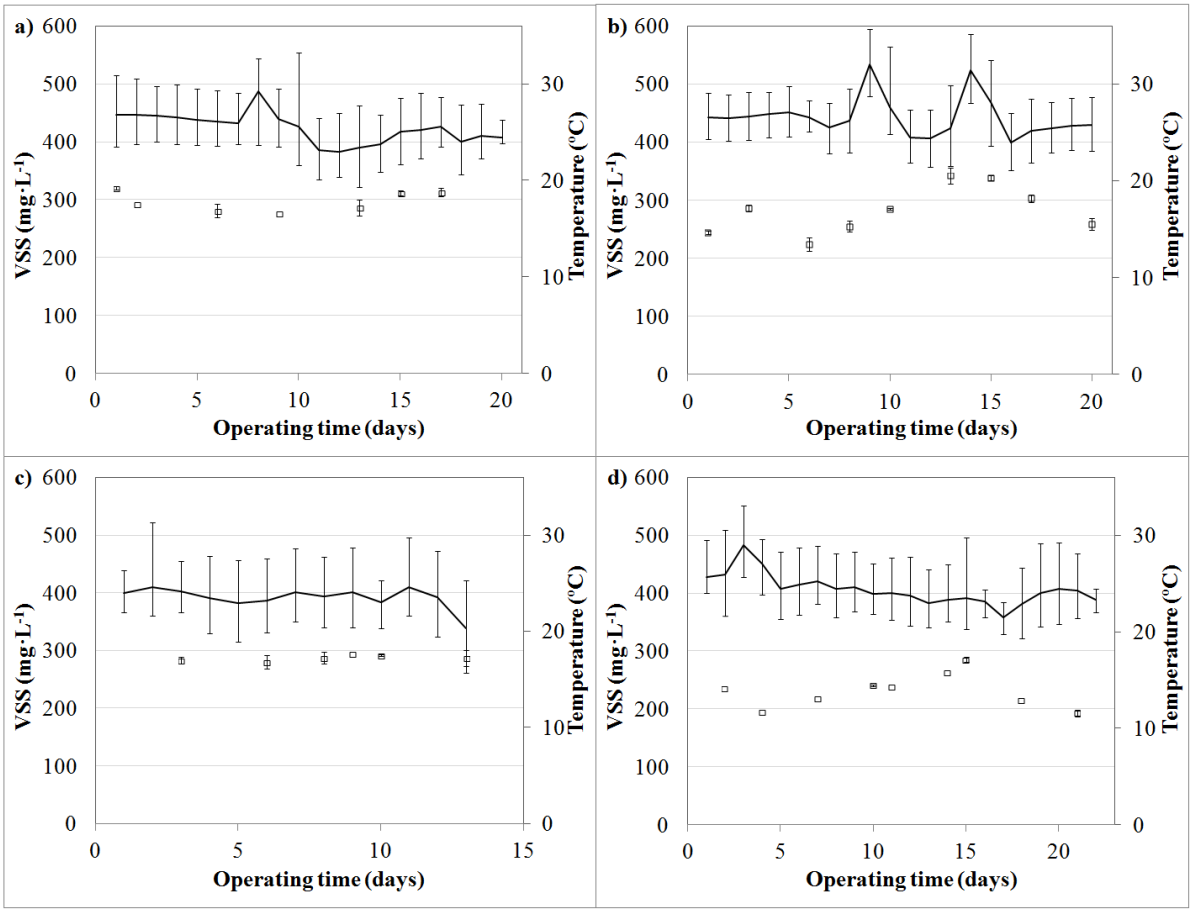

Figure VI.3. Evolution of the volatile suspended solids concentration (□) (mg VSS·L^{-1}) and temperature (—) (ºC) (bars indicate maximum and minimum temperatures) during HRT experiment: a) HRT3.5; b) HRT2; c) HRT1.5; d) HRT1.

MPBR performance was evaluated under nutrient-replete conditions during the pseudo-steady states of all BRT and HRT experiments; i.e., nitrogen concentrations over 10 mg $N \cdot L^{-1}$ (González-Camejo et al., 2019) and phosphorus concentration in non-negligible concentrations (Figures VI.4 and VI.5).

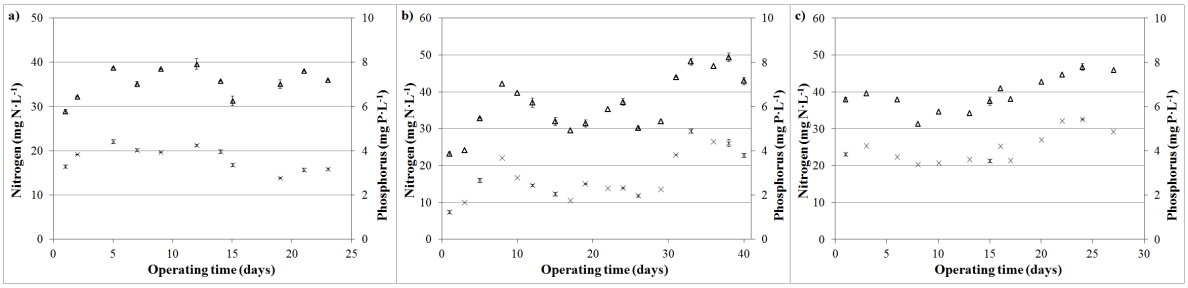

Figure VI.4. Evolution of the effluent nitrogen (Δ) (mg $N \cdot L^{-1}$) and phosphorus (x) (mg $P \cdot L^{-1}$) concentrations in the PBRs during BRT experiments: a) BRT4.5; b) BRT6; c) BRT9

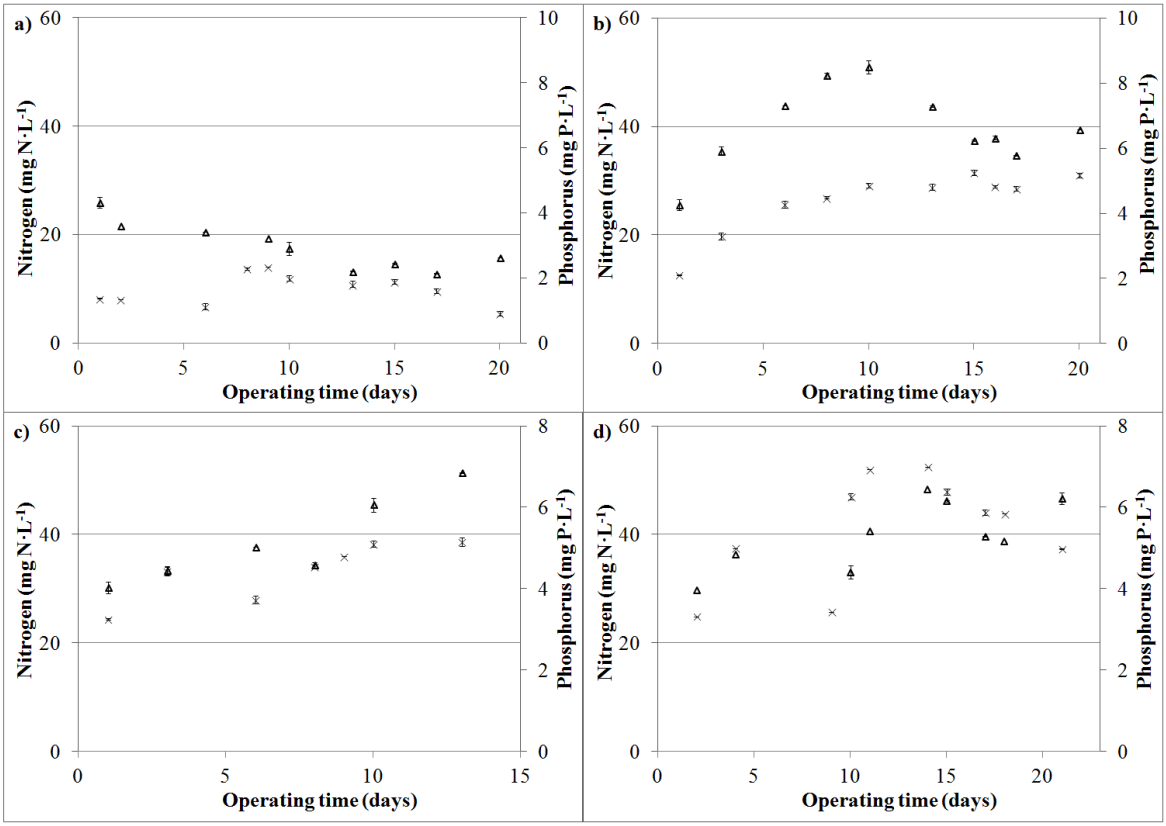

Figure VI.5. Evolution of the effluent nitrogen (Δ) (mg $N \cdot L^{-1}$) and phosphorus (x) (mg $P \cdot L^{-1}$) concentrations in the PBRs during HRT experiment: a) HRT3.5; b) HRT2; c) HRT1.5; d) HRT1.

In order to inhibit nitrification, allylthiourea (ATU) was added to the culture to maintain a concentration of 1-5 $mg \cdot L^{-1}$ in the PBRs (González-Camejo et al., 2018a). In addition, the pH set-point value of the culture (7.5) made ammonia volatilisation and phosphorus precipitation be negligible (Whitton et al., 2016) so that microalgae were considered as the main responsible for nutrient recovery.

Each experiment began with a start-up phase consisting of: i) adding 10% of the working volume with the inoculum from the previous experiment and 90% of the working volume with the substrate described in Section VI.2.2.; ii) batch mode until reaching a biomass concentration of around 400-500 mg $VSS \cdot L^{-1}$; iii) continuous feeding to maintain the corresponding BRT and HRT (as described in section VI.2.1.1); and iv) reaching the pseudo-stationary state. These start-up phases were not considered in the evaluation of the MPBR performance.

Before each experiment, a chemical cleaning of the membranes was done in order to start every experiment with similar filtration conditions. The cleaning was carried out in two steps: 1) basic cleaning (pH of 10.5) by a solution composed of 2,000 $mg \cdot L^{-1}$ of NaClO for 6 hours; and 2) acid cleaning (pH of 2.5) by a solution composed of 2,000 $mg \cdot L^{-1}$ of citric acid for 6 hours.

2.4. Sampling, analytical methods and calculations

Grab samples were collected in duplicate from the influent (AnMBR effluent), the culture and the effluent of the MPBR pilot plant three times a week. Ammonium (NH_4), nitrite (NO_2), nitrate (NO_3) and phosphate (PO_4) concentrations were analysed according to Standard Methods (APHA et al., 2005): Methods 4500-NH3-G, 4500-NO2-B, 4500-NO3-H and 4500-P-F, respectively, in a Smartchem 200 automatic analyser (WestcoScientific Instruments, Westco). Volatile suspended solids (VSS) of the culture were analysed according to method 2540 E of Standard Methods (APHA et al., 2005).

The maximum quantum efficiency (F_v/F_m) was measured in-situ with a portable fluorometer AquaPen-C AP-C 100 (Photon Systems Instruments). Before measuring, the samples were kept in the dark for ten minutes to become dark-adapted (Moraes et al., 2019). The turbidity of the influent was measured by a portable turbidimeter (Lovibond T3 210IR).

50 µL of culture sample were taken in duplicate twice a week to measure the total eukaryotic cells (TEC) concentration. Cells were counted by epifluorescence

microscopy on a Leica DM2500 using the 100x-oil immersion lens. A minimum of 100 cells of the most abundant genus were counted with an error of less than 20% (Pachés et al., 2012).

The presence of *Escherichia coli* and other coliform pathogens in the permeate was quantitatively determined through a positive β-glucorinidase assay using membrane filters, following the UNE-EN ISO 9308-1:2014 standard method.

Calculations are shown in Section III.6 (Chapter III).

2.5. Statistical analysis

The results obtained were statistically analysed by Statgraphics Centurion XVII. ANOVA analysis was carried out to evaluate the significance of the differences in the mean values. When p-values < 0.05, differences were considered statistically significant.

3. RESULTS AND DISCUSSION

3.1. Continuous microalgae cultivation

3.1.1. BRT experiments

A significant reduction of NRR:I (p-value < 0.05) was observed with increasing BRT, from 51.7 ± 14.3 in Experiment BRT4.5 to 40.3 ± 8.6 mg $N \cdot mol^{-1}$ in Experiment BRT9 (Figure VI.6a). The trend of photosynthetic efficiency with respect to BRT was similar to that of NRR:I, obtaining 4.4 ± 1.6 % in Experiment BRT4.5 and 3.5 ± 0.5 % in BRT9 (Figure VI.6c). This suggests that nitrogen recovery was related to the photosynthetic efficiency for biomass production. As for PRR:I, no significant differences were observed (p-value > 0.05) within the evaluated BRT experiments (Figure VI.6b). Since phosphorus can be stored as polyphosphates (Powell et al., 2009), the phosphorus consumption by microalgae not only will depend on the operating and outdoor conditions, but also on their intracellular phosphorus reserves (Shoener et al., 2019). In terms of carbon biofixation, it was also reduced significantly (p-value < 0.05) from 0.50 ± 0.05 kg $CO_2 \cdot m^{-3}_{influent}$ in Experiment BRT4.5 to 0.44 ± 0.02 kg $CO_2 \cdot m^{-3}_{influent}$ in Experiment BRT9.

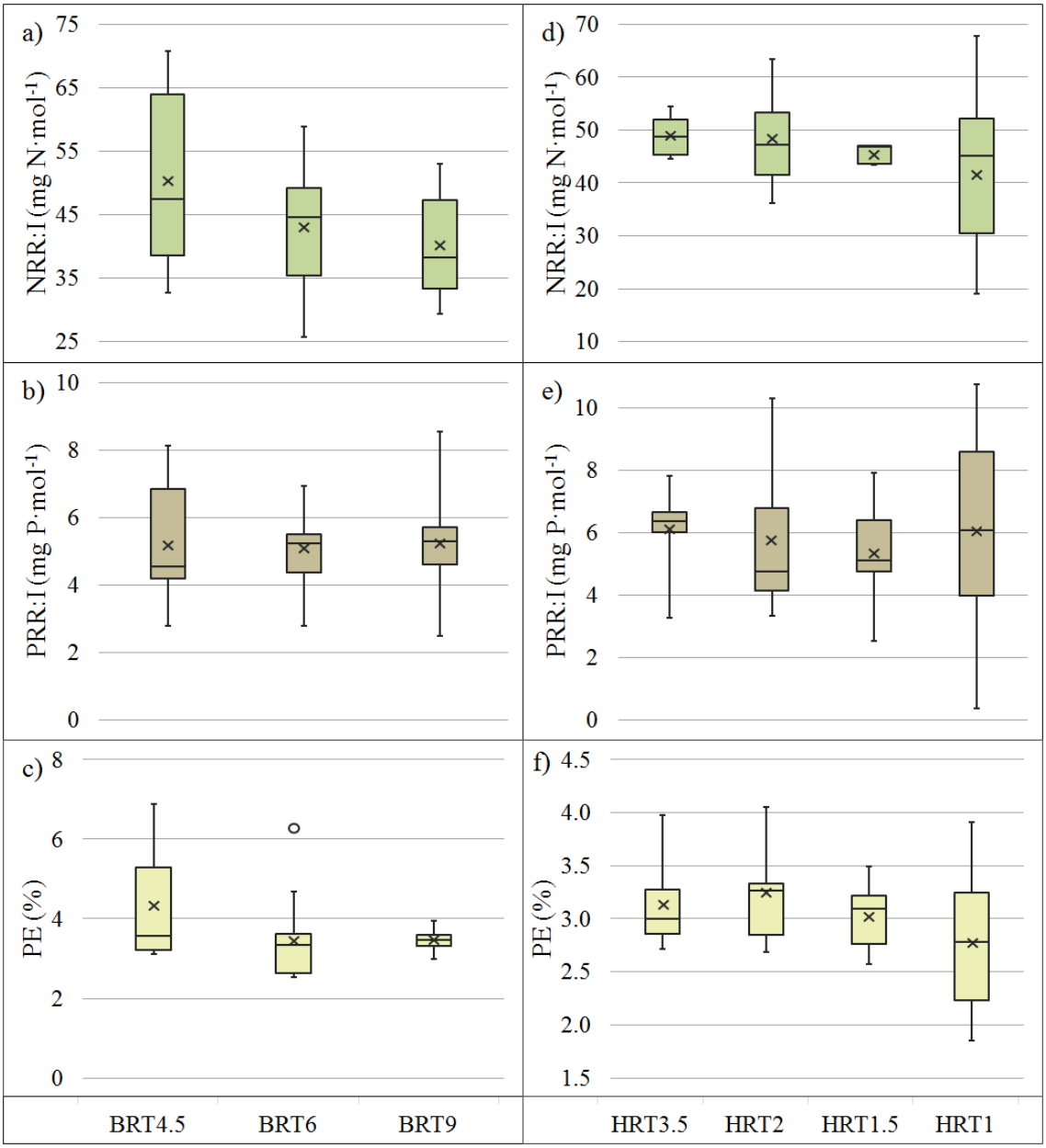

Figure VI.6. Box-plots of BRT experiments: a) nitrogen recovery rate:light irradiance ratio (NRR:I); b) phosphorus recovery rate:light irradiance ratio (PRR:I); and c) photosynthetic efficiency. Box-plots of HRT experiments: d) nitrogen recovery rate:light irradiance ratio (NRR:I); e) phosphorus recovery rate:light irradiance ratio (PRR:I); and f) photosynthetic efficiency.

These results therefore suggest that increasing the BRT involved a reduction in the system's performance yields, reaching the best operating conditions at 4.5 days BRT, which was close to the theoretically optimum BRT determined in batch conditions; i.e., 4.6-5 days of BRT (González-Camejo et al., 2019). This optimum BRT is significantly lower than those reported by other authors (Table VI.3).

Table VI.3. Optimal BRTs obtained under different conditions.

BRT (d)	Species	Type of wastewater	Type of PBR	Reference
4.5	*Scenedesmus* dominance	AnMBR effluent	Outdoor Flat-panel MPBR	This study
5-10	*Scendesmus obliquus*	Secondary effluent	Lab-scale Flat-panel MPBR	Xu et al. (2015)
9-18	*Chlorella vulgaris*	Synthetic secondary effluent	Lab-scale Flat-panel MPBR	Luo et al. (2018)
21	*Chlorella vulgaris*	Synthetic secondary effluent	Lab-scale Flat-panel MPBR	Gao et al. (2018)

A possible explanation for the reduced NRR:I in experiments BRT6 and BRT9 could be the higher amount of biomass concentration reached in these experiments (Figure VI.2). In fact, for experiments BRT4.5, BRT6 and BRT9, the VSS concentration was 326 ± 40, 452 ± 53, and 564 ± 30 mg VSS·L^{-1}, respectively (p-value < 0.05). The higher VSS concentration reduced the light availability of microalgae (Abu-Ghosh et al., 2016), reducing the MPBR performance. However, it is striking that increasing the BRT from 4.5 to 9 days implied a reduction in NRR:I at increasing BRT, but the photosynthetic efficiency and the C-BF remained constant in Experiment BRT4.5 and BRT6. The worst results obtained in Experiment BRT9 were probably due to a proliferation of microorganisms other than green microalgae. In consequence, a significant amount of the biomass considered within the VSS concentration measurements did not correspond to microalgae biomass in Experiment BRT9. In fact, the TEC increased from $5.53 \cdot 10^9$ ± $1.57 \cdot 10^9$ to $7.77 \cdot 10^9$ ± $1.17 \cdot 10^9$ cells·L^{-1} when BRT was raised from 4.5 to 6 days, respectively (p-value < 0.05) but did not increase when the BRT was further extended to 9 days (TEC of $7.04 \cdot 10^9$ ± $1.33 \cdot 10^9$ cells·L^{-1}, p-value > 0.05). In this respect, the microscopic microbiological examination revealed that the quantity of cyanobacteria, protozoans and rotifers significantly increased during Experiment BRT9, as observed under microscope (González-Camejo et al., 2019). These microorganisms are favoured at longer BRTs, when higher amounts of organic carbon are released by more severe

microalgae decay (Luo et al., 2018). It must be noted that this proliferation is not convenient since these organisms can negatively affect microalgae growth. For instance, *Bacillus fusiformis* bacteria have been reported to be lethal to microalgae genera *Chlorella* and *Scenedesmus* (Mu et al., 2007), while the rotifer *Brachionus plicatilis* is able to devour up to 3000 microalgae cells per hour (Montagnes et al., 2001). With respect to cyanobacteria, Rajneesh et al. (2017) found that these microorganisms can inhibit microalgae growth by excreting toxic extracellular substances. This culture affection was indirectly measured by the maximum quantum efficiency, which is an indirect measure of the photosystem II efficiency. F_v/F_m suffered a statistically significant drop from 0.70 ± 0.04 and 0.69 ± 0.03 in experiments BRT4.5 and BRT6, respectively, to 0.62 ± 0.03 in Experiment BRT9. According to Moraes et al. (2019), a reduction in the F_v/F_m from around 0.65 to lower values is an indicator of photochemical stress of the eukaryotic algae.

Regarding microalgae strains, in Experiment BRT4.5 *Scenedesmus* dominated the culture with around 95% of the TEC because the inoculum of this experiment was mainly composed of *Scenedesmus* (90% of TEC). In Experiment BRT6, the culture started off dominated by *Scenedesmus*, but later *Chlorella* became dominant (85% of TEC). Experiment BRT9 was dominated by *Chlorella* at around 90% of TEC (apart from the aforementioned proliferation of cyanobacteria protozoans and rotifers). This shift in the dominance of the culture was attributed to the better acclimatisation to the effective light applied to the PBR of *Chlorella* in comparison with *Scenedesmus*. During experiments BRT6 and BRT9, the biomass concentration was significantly higher than in Experiment BRT4.5 (as already mentioned), reducing the average light intensity received by microalgae (Abu-Ghosh et al., 2016). In this respect, *Chlorella* have been reported to be more competitive than *Scenedesmus* at lower light intensities (Marcilhac et al., 2014; Sanchis-Perucho et al., 2018).

With respect to nutrient accumulation, the highest intracellular nitrogen content was reached in Experiment BRT6 (8.5% ± 1.3), which was operated with the highest N:P influent molar ratio (23.4 ± 1.8). On the other hand, the lowest intracellular nitrogen content (7.4% ± 0.6) was obtained in Experiment BRT9, which was operated with the lowest N:P influent molar ratio; i.e., 19.4 ± 0.9 (Table VI.4). This behaviour was probably due to the capacity of microalgae to modify their intracellular N:P ratio as a consequence of fluctuating nutrient loads (Schoener et al., 2019). Tan et al. (2016) obtained similar intracellular nitrogen contents for *Chlorella pyrenoidosa*: 7.2-10.6%,

while Ruiz et al. (2014) reported 4.9-8.0% for *Scenedesmus obliquus*. Regarding phosphorus, no statistically significant differences were observed (p-value > 0.05): 1.1-1.3%. These results were within the range of those reported by Beuckels et al. (2015) for *Chlorella:* 0.5-1.3%, and by Ruiz et al. (2014) for *S. obliquus*: 0.7-2.3%.

Table VI.4. Intracellular nutrient content obtained during the pseudo-stationary stages of BRT and HRT Experiments (mean ± standard deviation).

Parameter	BRT4.5	BRT6	BRT9	HRT3.5	HRT2	HRT1.5	HRT1
N:P influent*	22.2±2.4	23.4±1.8	19.4±0.9	19.8±5.0	20.6± 4.8	19.1±2.3	14.4±3.2
N (%)	7.8±2.5	8.5±1.3	7.4±0.6	7.6±2.1	10.4±0.6	8.6±0.5	5.9±2.2
P (%)	1.1±0.1	1.3±0.2	1.3±0.4	1.2±0.1	1.1±0.1	1.1±0.2	1.1±0.2
N:P culture*	16.6±5.9	15.0±3.9	14.0±3.9	13.4±0.8	21.2±4.6	17.3±5.5	12.7±3.4

**Molar basis*

3.1.2. HRT experiments

As can be seen in Figure VI.6, the NRR:I and photosynthetic efficiency did not change significantly in experiments HRT3.5, HRT2, HRT1.5 (p-value > 0.05), showing NRR:I values of 49.0 ± 4.0, 48.6 ± 9.5 and 45.6 ± 1.9 mg $N \cdot mol^{-1}$ and photosynthetic efficiencies of 3.1 ± 0.5%, 3.2 ± 0.4% and 3.0 ± 0.4%, respectively, for experiments HRT3.5, HRT2 and HRT1.5. However, in Experiment HRT1, the NRR:I and photosynthetic efficiency fell significantly to 41.7 ± 14.9 mg $N \cdot mol^{-1}$ and 2.8 ± 0.7 %, respectively (p-value < 0.05).

It must be noted that in Experiment HRT1, substrate turbidity increased from less than 50 NTU (experiments HRT3.5, HRT2 and HRT1.5) to around 200-300 NTU (Experiment HRT1). The substrate turbidity increased during Experiment HRT1 because the pre-aeration system was not able to fully oxidise the increasing sulphide load. As a result, some of the sulphides partially oxidised to elemental sulphur and was suspended in the substrate, increasing its turbidity. This turbidity reduced the light available for the microalgae culture, limiting microalgae growth (González-Camejo et al., 2019). Variations in both turbidity and solar PAR were probably the main responsible for the high dynamics of the data measured in Experiment HRT1, as displayed in the box-plots of HRT experiments (Figure VI.6). When the substrate

presented high values of turbidity and low solar PAR, the average irradiance inside the culture was thus low and vice versa, decreasing or increasing the microalgae performance.

Similarly to BRT experiments, PRR:I showed no significant differences in HRT experiments (Figure VI.6e). In conclusion, HRT did not have a direct influence on either nutrient recovery or photosynthetic efficiency under nutrient-replete conditions and quite stable temperatures as in this case (González-Camejo et al., 2019).

According to the results of HRT experiments, the appropriate treatment of the AnMBR effluent for sensitive areas which accounts for 15 mg $N \cdot L^{-1}$ and 2 mg $P \cdot L^{-1}$ for a WWTP between 10,000-100,000 population equivalent (p.e.) (Council Directive 91/271/CEE) was only achieved with the operating conditions of Experiment HRT3.5. On the other hand, effluent nutrient concentrations in the rest of the experiments were far above the legal limits (Figure VI.5). Hence, the optimum HRT of the system will depend on the nutrient loads. HRTs shorter than the optimum would mean that the microalgae would not have enough time to absorb the nutrients from the substrate, reaching an effluent nutrient concentration close to that of the influent, while excessively long HRTs would make the system nutrient-limited. In addition, C-BF was the highest in Experiment HRT3.5, i.e., 0.55 ± 0.05 kg $CO_2 \cdot m^{-3}_{influent}$. For the rest of HRT experiments, the C-BF was 0.32 ± 0.06 kg $CO_2 \cdot m^{-3}_{influent}$ (Experiment HRT2); 0.25 ± 0.03 kg $CO_2 \cdot m^{-3}_{influent}$ (Experiment HRT1.5); and 0.14 ± 0.02 kg $CO_2 \cdot m^{-3}_{influent}$ (Experiment HRT1).

Consequently, the optimum HRT in the operated outdoor conditions was considered to be 3.5 days. If the microalgae obtained in Experiment HRT3.5 were anaerobically digested, energy recovery from microalgae biomass could reach up to 0.443 $kWh \cdot m^{-3}_{influent}$. In comparison with other PBR configurations such as the tubular PBRs operated by García et al. (2018), a reduction of the operating HRT would be achieved in the present study, from 5 to 3.5 days, which would imply a reduction of 30% of the working volume. The results obtained in this study are therefore promising, but the efficiency of the system must be further increased to operate it at lower HRTs. This would imply the reduction of the wastewater treatment footprint, which is one of the major drawbacks of microalgae-based systems (Acién et al., 2016).

Unlike BRT experiments, in HRT experiments, no shift in the dominating microalgae genera of the culture was observed and the culture was mainly composed of *Chlorella* (> 95% of TEC) in all HRT experiments. The dominance of this genus in the inoculum

of Experiment HRT3.5 was hypothesised to have an influence on the high percentage of this strain during the HRT experiments.

As in BRT experiments, the nitrogen content of the biomass generated during HRT experiments increased with the N:P influent molar ratio (Table VI.4), and the intracellular nitrogen content varied in the range of 5.9-10.4%, in agreement with the values obtained by Beuckels et al. (2015) for *Chlorella*: 5.0-10.1%. No significant differences were observed regarding intracellular phosphorus content, resulting in values similar to those obtained in BRT experiments: 1.1-1.2%.

It must be highlighted that the values obtained in this study for the photosynthetic efficiency; i.e. (in the range of 3.0-4.4%, see Figure VI.6) are quite higher than those obtained by Romero-Villegas et al. (2018) in outdoor flat-panel PBRs (2.8%); although they were considerably lower than the 7.4% reported by Alcántara et al. (2013) in lab conditions. Further research is therefore required to improve the microalgae photosynthetic efficiency in this MPBR plant in order to achieve its maximum potential.

3.2. Membrane filtration

To fully assess the feasibility of MPBR technology, it is necessary to evaluate the behaviour of the membrane filtration during the continuous operation of the MPBR plant.

During Experiment BRT4.5, fouling rate remained low (below 5 mbar·min^{-1}) for almost 18 days, but it rose sharply up to 25 mbar·min^{-1} at day 21 (Figure VI.7a). Experiment BRT6 (VSS concentration of 452 ± 53 mg VSS·L^{-1}) started with similar operating filtration conditions (i.e., J_{20} and SGD_p) as BRT4.5 (Figure VI.7b) but at higher VSS concentration: 326 ± 40 mg VSS·L^{-1} (Figure VI.2). However, this increase in microalgae biomass did not seem to significantly affect the membrane performance since the evolution of the fouling rate at the beginning of both experiments BRT4.5 and BRT6 were similar (Figure VI.7).

At day 18 of Experiment BRT6, fouling rate exceeded the value of 5 mbar·min^{-1} and the SGD_p was doubled at day 22 to verify whether fouling rate could be reduced. Figure VI.7b shows that fouling remained stable around 7-10 mbar·min^{-1} for 10 additional days (until day 32 of Experiment BRT6). However, fouling rate surged up to 35 mbar·min^{-1} at day 37 of Experiment BRT6 (Figure VI.7), indicating a significant membrane fouling propensity under the evaluated operating conditions. Experiment BRT9 showed a sharp increase in fouling rate after 7 days of operation, indicating a higher membrane fouling

propensity, even though J_{20} was slightly lower than in experiments BRT4.5 and BRT6 (Figure VI.7c). This higher fouling propensity could be attributed not only to the increased VSS concentration (Figure VI.2) but also to the aforementioned proliferation of filamentous microorganisms such as cyanobacteria (section VI.3.1.1). In fact, membrane filtration has been reported to worsen as contamination by microzooplankton increases (Wang et al., 2019). Hence, operating at a BRT of 9 days was not only detrimental for the MPBR performance in terms of nutrient recovery (section VI.3.1.1), but also for the membrane operation.

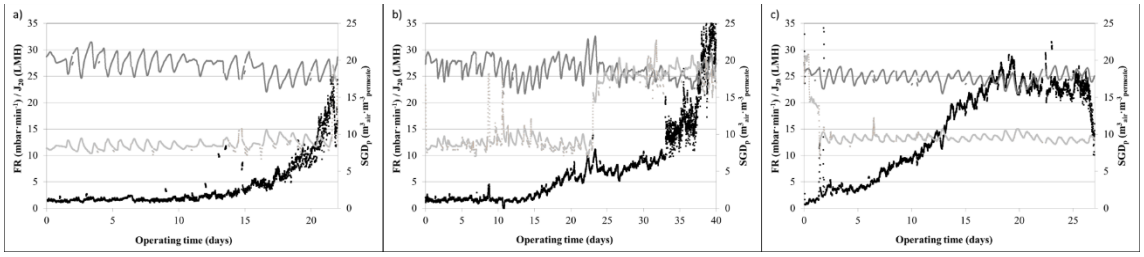

Figure VI.7. Membrane filtration performance at the pilot plant. Fouling rate (▬) (mbar·min^{-1}), J_{20} (▬) (LMH) and SGD_p (▬) ($m^3_{air}·m^{-3}_{permeate}$) for BRT Exteriments: a) BRT4.5; b) BRT6; c) BRT9.

Figure VI.8 shows that there were no significant differences in fouling rates during the performance of the membrane unit in HRT experiments. The operating conditions and VSS concentrations during these experiments remained practically stable (see Figure VI.8 and Figure VI.3).

It should be noted that it was possible to remove most of the fouling from the membrane surface by intensive physical cleaning procedures, mainly based on back-flushing. However, in order to obtain comparable conditions with the next experiment in terms of filtration performance, additional chemical cleaning was carried out to ensure the membranes recovered their filtration capacity before starting a new experiment. It is also important to note that this chemical cleaning frequency is regarded as excessive since it has a negative effect on the membrane lifespan and increases operating and maintenance costs (Zhang and Fu, 2018).

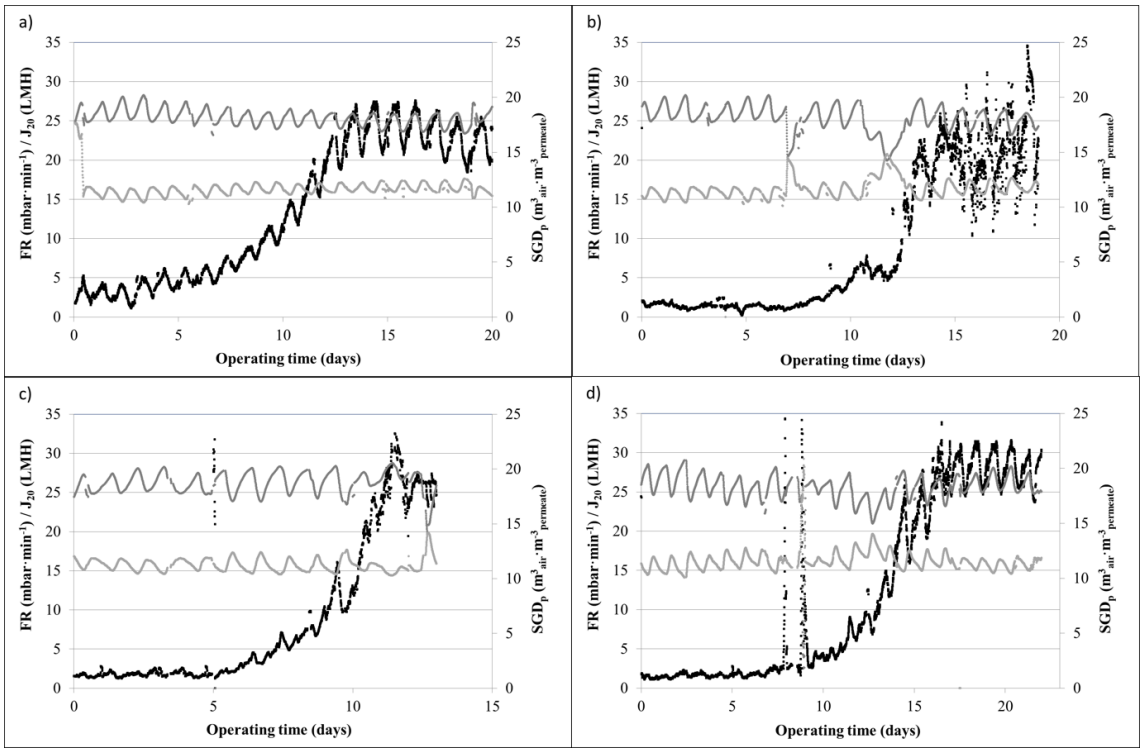

Figure VI.8. Membrane filtration performance at the pilot plant. Fouling rate (▬) (mbar·min^{-1}), J_{20} (▬) (LMH) and SGD_p (▬) ($m^3_{air}·m^{-3}_{permeate}$) for HRT Experiments: a) HRT3.5; b) HRT2; c) HRT1.5; d) HRT1

Overall, the system was operated at high J_{20} (22-30 LMH) during the experiments by applying fairly low SGD_p (8-12 $Nm^3_{air}·m^{-3}_{permeate}$, excluding second half of Experiment BRT6), which highlights the potential of membrane filtration for microalgae cultivation in MPBRs. For example, SGD_p of 15.4 and 16.5 $m^3_{air}·m^{-3}_{permeate}$ have been reported by Judd & Judd (2011) for treating municipal and industrial wastewater, respectively, corresponding to an SGD_m of 0.30 and 0.23 $m^3_{air}·h^{-1}·m^{-2}$ and J_{20} of 19.5 and 15.4 LMH, respectively. The operating costs associated with air sparging in the membrane tank are thus expected to be low when operating at optimised membrane performance.

Neither *E.coli* cfu per 100 mL nor helminthic eggs were detected in the final treated water. A source of reclaimed water can therefore be produced by this MPBR technology for irrigation or different urban and industrial purposes. It is important to note that there is a need to move towards feasible treatment solutions aimed at producing reclaimed water to help to alleviate the water scarcity problems related to hydric stress.

4. CONCLUSIONS

Maximum NRR:I ratios, photosynthetic efficiencies and carbon biofixations were obtained at BRT of 4.5 days, worsening the MPBR performance at longer BRT.

Regarding HRTs, similar results in terms of photosynthetic efficiencies, NRR:I and PRR:I ratios were observed for HRTs of 3.5, 2 and 1.5 days under non-nutrient-limited conditions. However, microalgae performance worsened at HRT of 1 day due to a reduction of light availability of the culture. Maximum values of C-BF (0.55 ± 0.05 kg $CO_2 \cdot m^{-3}_{influent}$) were achieved in Experiment HRT3.5, which was considered the optimum HRT.

Fouling rate increased when operating at the longest BRT (9 days), mainly due to higher biomass concentrations and the proliferation of filamentous organisms in the culture. In contrast, it remained similar when the HRT was ranged from 1 to 3.5 days.

MPBR technology could be considered a source of reclaimed water since no pathogens were found in the permeate. Moreover, the combination of MPBR and anaerobic digestion technology could recover up to 0.443 kWh per $m^3_{influent}$ from microalgae biomass.

ACKNOWLEDGEMENTS

This research work was supported by the Spanish Ministry of Economy and Competitiveness (MINECO, Projects CTM2014-54980-C2-1-R and CTM2014-54980-C2-2-R) jointly with the European Regional Development Fund (ERDF), which are gratefully acknowledged. It also received support from the Spanish Ministry of Education, Culture and Sport via a pre-doctoral FPU fellowship to the first author (FPU14/05082).

REFERENCES

1. Abu-Ghosh, S., Fixler, D., Dubinsky, Z., Iluz, D., 2016. Flashing light in microalgae biotechnology. Bioresour. Technol. 203, 357-363. http://dx.doi.org/10.1016/j.biortech.2015.12.057
2. Acién, F.G., Gómez-Serrano, C., Morales-Amaral, M.M., Fernández-Sevilla, J.M., Molina-Grima E., 2016. Wastewater treatment using microalgae: how realistic a contribution might it be to significant urban wastewater treatment? Appl. Microbiol. Biotechnol. 100, 9013–9022. http://dx.doi.org/10.1007/s00253-016-7835-7

3. Alcántara, C., García-Encina, P.A., Muñoz, R., 2013. Evaluation of mass and energy balances in the integrated microalgae growth-anaerobic digestion process. Chem. Eng. J. 221, 238-246. http://dx.doi.org/10.1016/j.cej.2013.01.100
4. APHA-AWWA-WPCF, 2005. Standard methods for the examination of water and wastewater, 21st edition. American Public Health Association, American Water Works Association, Water Pollution Control Federation. Washington DC, USA.
5. Bilad, M.R., Discart, V., Vandamme, D., Foubert, I., Muylaert, K., Vankelecom, I.F.J., 2014. Coupled cultivation and pre-harvesting of microalgae in a membrane photobioreactor (MPBR). Bioresour Technol. 155, 410–417. http://dx.doi.org/10.1016/j.biortech.2013.05.026
6. Beuckels, A., Smolders, E. Muylaert, K., 2015. Nitrogen availability influences phosphorus removal in microalgae-based wastewater Treatment. Water Res. 77, 98-106. http://dx.doi.org/10.1016/j.watres.2015.03.018
7. Council Directive 91/271/EEC of 21 May 1991 concerning urban waste-water treatment, OJ L 135, 30.5.1991, p. 40-52.
8. Foladori, P., Petrini, S., Andreottola, G., 2018. Evolution of real municipal wastewater treatment in photobioreactors and microalgae-bacteria consortia using real-time parameters, Chem. Eng. J. 345, 507–516. https://doi.org/10.1016/j.cej.2018.03.178
9. Gao, F., Cui, W., Xu, J.P., Li, C., Jin, W.H., Yang H.L., 2019. Lipid accumulation properties of *Chlorella vulgaris* and *Scenedesmus obliquus* in membrane photobioreactor (MPBR) fed with secondary effluent from municipal wastewater treatment plant. Renewable Energy 136, 671-676. https://doi.org/10.1016/j.renene.2019.01.038
10. Gao, F., Penga, Y.Y., Lia, C., Cuia, W., Yang, Z.H., Zeng, G.M., 2018. Coupled nutrient removal from secondary effluent and algal biomass production in membrane photobioreactor (MPBR): Effect of HRT and long-term operation. Chem. Eng. J. 335, 169-175. http://dx.doi.org/10.1016/j.cej.2017.10.151
11. García, J., Ortiz, A., Álvarez, E., Belohlav, V., García-Galán, M.J., Díez-Montero, R., Álvarez, J.A., Uggetti, E., 2018. Nutrient removal from agricultural run-off in demonstrative full scale tubular photobioreactors for microalgae growth. Ecological Eng. 120, 513–521. https://doi.org/10.1016/j.ecoleng.2018.07.002
12. Giménez, J.B., Robles, A., Carretero, L., Durán, F., Ruano, M.V., Gatti, M.N., Ribes, J., Ferrer, J., Seco, A., 2011. Experimental study of the anaerobic urban wastewater treatment in a submerged hollow-fibre membrane bioreactor at pilot scale. Bioresour. Technol. 102, 8799–8806. https://doi.org/10.1016/j.biortech.2011.07.014
13. Gómez-Gil, T., Viruela, A., Murgui, M., Durán, F., Robles, A., Ruano, M.V., Barat, R., Seco, A., Ferrer, J., 2015. Design/operating Factors Affecting The Performane Of An Outdoor MPBR for Tertiary Sewage Treatment. IWA Specialist Conference on Nutrient Removal and Recovery 2015. 18-21 May 2015. Gdansk, Poland.

14. Gonçalves, A.L., Pires, J.C.M., Simões, M., 2017. A review on the use of microalgal consortia for wastewater treatment, Algal Res. 24, 403–415. http://dx.doi.org/10.1016/j.algal.2016.11.008
15. Gong, H., Jin Z., Xu H., Yuan Q., Zuo J., Wu J., Wang K., 2019. Enhanced membrane-based pre-concentration improves wastewater organic matter recovery: Pilot-scale performance and membrane fouling. J. Clean. Prod. 206, 307-314. https://doi.org/10.1016/j.jclepro.2018.09.209
16. Gonzalez-Camejo, J., Jiménez-Benítez, A., Ruano, M.V., Robles, A., Barat, R., Ferrer, J., 2019. Preliminary tests to optimise the performance of an outdoor membrane photobioreactor. J. Environ. Manag. Data in brief (submitted).
17. Gonzalez-Camejo, J., Barat, R., Ruano, M.V., Seco, A., Ferrer, J., 2018a. Outdoor flat-panel membrane photobioreactor to treat the effluent of an anaerobic membrane bioreactor. Influence of operating, design and environmental conditions. Water Sci. Technol. 78(1) 195-206. http://dx.doi.org/10.2166/wst.2018.259
18. González-Camejo, J., Barat, R., Pachés, M., Murgui, M., Ferrer, J., Seco, A., 2018b. Wastewater Nutrient Removal in a Mixed Microalgae-bacteria Culture: Effect of Light and Temperature on the Microalgae-bacteria Competition. Environ. Technol. 39(4), 503-515. http://dx.doi.org/10.1080/09593330.2017.1305001.
19. González-Camejo, J., Serna-García, R., Viruela, A., Pachés, M., Durán, F., Robles, A., Ruano, M.V., Barat R., Seco, A., 2017. Short and long-term experiments on the effect of sulphide on microalgae cultivation in tertiary sewage treatment. Bioresour. Technol. 244, 15-22. http://dx.doi.org/10.1016/j.biortech.2017.07.126
20. Guldhe, A., Kumari, S., Ramanna, L., Ramsundar, P., Singh, P., Rawat, I., Bux, F., 2017. Prospects, recent advancements and challenges of different wastewater streams for microalgal cultivation. J. Environ. Manag. 203, 299-315. http://dx.doi.org/10.1016/j.jenvman.2017.08.012
21. Judd, S., Judd, C., 2011. The MBR Book: Principles and Applications of Membrane Bioreactors in Water and Wastewater Treatment, 2nd Edition. Elsevier. ISBN: 978-0-08-096682-3.
22. Luo, Y., Le-Clech, P., Henderson, R.K., 2018. Assessment of membrane photobioreactor (MPBR) performance parameters and operating conditions. Water Res. 138, 169-180. https://doi.org/10.1016/j.watres.2018.03.050
23. Marcilhac, C., Sialve B., Pourcher A.M., Ziebal C., Bernet N., Béline F., 2014. Digestate color and light intensity affect nutrient removal and competition phenomena in a microalgal-bacterial ecosystem, Water Res. 64, 278-287. http://dx.doi.org/10.1016/j.watres.2014.07.012

24. Montagnes, D.J.S., Kimmance, S.A., Tsounis, G., Gumbs, J.C., 2001. Combined effect of temperature and food concentration on the grazing rate of the rotifer *Brachionus plicatilis*. Mar. Biol. 139, 975–979. https://doi.org/10.1007/s002270100632
25. Moraes, L., Martins, G., Morillas, A., Oliveira, L., Greque, M., Molina-Grima, E., Vieira, J.A., Acién, F.G., 2019. Engineering strategies for the enhancement of *Nannochloropsis gaditana* outdoor production: influence of the CO2 flow rate on the culture performance in tubular photobioreactors. Process Biochemistry 76, 171-177. https://doi.org/10.1016/j.procbio.2018.10.010
26. Mu, R.M., Fan, Z.Q., Pei, H.Y., Yuan, X.L., Liu, S.X., Wang, X.R., 2007. Isolation and algae lysing characteristics of the algicidal bacterium B5. J. Environ. Sci. 19, 1336–1340. https://doi.org/10.1016/S1001-0742(07)60218-6
27. Nayak, M., Dhanarajan, G., Dineshkumar, R., Sen, R., 2018. Artificial intelligence driven process optimization for cleaner production of biomass with co-valorization of wastewater and flue gas in an algal biorefinery. J. Clean. Prod. 201, 1092-1100. https://doi.org/10.1016/j.jclepro.2018.08.048
28. Pachés, M., Romero, I., Hermosilla, Z. and Martinez-Guijarro, R. 2012. PHYMED: An ecological classification system for the Water Framework Directive based on phytoplankton community composition. Ecological Indicators 19, 15-23. https://doi.org/10.1016/j.ecolind.2011.07.003
29. Powell, N., Shilton, A., Chisti, Y., Pratt, S., 2009. Towards a luxury uptake process via microalgae – Defining the polyphosphate dynamics. Water Res. 43, 4207-4213. https://doi:10.1016/j.watres.2009.06.011
30. Porcelli N., Judd S., 2010. Chemical cleaning of potable water membranes: a review, Sep. Purif. Technol. 71, 137–143. https://doi.org/10.1016/j.seppur.2009.12.007
31. Rajneesh, Singh, S. P., Pathak, J., Sinha, R.P., 2017. Cyanobacterial factories for the production of green energy and value-added products: An integrated approach for economic viability. Renewable and Sustainable Energy Reviews 69, 578–595. https://doi.org/10.1016/j.rser.2016.11.110
32. Robles, A., Ruano, M.V., Ribes, J., Ferrer, J., 2013. Factors that affect the permeability of commercial hollow-fibre membranes in a submerged anaerobic MBR (HF-SAnMBR) system. Water Res. 47, 1277-1288. http://dx.doi.org/10.1016/j.watres.2012.11.055
33. Romero-Villegas, G.I., Fiamengo, M., Acién-Fernández, F.G., Molina-Grima, E., 2018. Utilization of centrate for the outdoor production of marine microalgae at the pilot-scale in raceway photobioreactors, J. Environ. Manag. 228, 506–516. https://doi.org/10.1016/j.jenvman.2018.08.020
34. Ruiz, J., Arbib, Z., Álvarez-Díaz, P.D., Garrido-Pérez, C., Barragán, J., Perales, J.A., 2014. Influence of light presence and biomass concentration on nutrient kinetic removal from

urban wastewater by *Scenedesmus obliquus*. J. Biotechnol., 178, 32-37. http://dx.doi.org/10.1016/j.jbiotec.2014.03.001

35. Sanchis-Perucho, P., Duran, F., Barat, R., Pachés, M., Aguado, D., 2018. Microalgae population dynamics growth with AnMBR effluent: effect of light and phosphorous concentration, Water Sci. Technol. 77(11-12) (2018) 2566-2577. http://dx.doi.org/10.2166/wst.2018.207
36. Seco, A., Aparicio, S., González-Camejo, J., Jiménez-Benítez, A., Mateo, O., Mora, J.F., Noriega-Hevia, G., Sanchis-Perucho, P., Serna-García, R., Zamorano-López, N., Giménez, J.B., Ruiz-Martinez, A., Aguado, D., Barat, R., Borrás, L., Bouzas, A., Martí, N., Pachés, M., Ribes, J., Robles, A., Ruano, M.V., Serralta, J. and Ferrer, J., 2018. Resource recovery from sulphate-rich sewage through an innovative anaerobic-based water resource recovery facility (WRRF). Water Science and Technology 78 (9), 1925-1936. https://doi.org/10.2166/wst.2018.492
37. Shoener, B.D., Schramm, S.M., Béline, F., Bernard, O., Martínez, C., Plósz, B.G., Snowling, S., Steyer, J.P., Valverde-Pérez, B., Wágner, D., Guest, J.S., 2019. Microalgae and cyanobacteria modeling in water resource recovery facilities: A critical review. Water Research X 2, 100024. https://doi.org/10.1016/j.wroa.2018.100024
38. Tan, X.B., Zhang, Y.L., Yang, L.B., Chu, H.Q., Guo, J., 2016. Outdoor cultures of *Chlorella pyrenoidosa* in the effluent of anaerobically digested activated sludge: The effects of pH and free ammonia. Bioresour. Technol. 200, 606-615. http://dx.doi.org/10.1016/j.biortech.2015.10.095
39. Udaiyappan, A.F.M., Hasan, H.A., Takriff, M.S., Abdullah, S.R.S, 2017. A review of the potentials, challenges and current status of microalgae biomass applications in industrial wastewater treatment. Journal of Water Process Engineering 20, 8–21. http://dx.doi.org/10.1016/j.jwpe.2017.09.006
40. UNE EN ISO 9308-1:2014, AENOR, 2014. Water Quality - Enumeration of Escherichia Coli And Coliform Bacteria - Part 1: Membrane Filtration Method For Waters With Low Bacterial Background Flora (Iso 9308-1:2014/Amd 1:2016), Asociación Española de Normalización (AENOR).
41. Van Den Hende, S., Beelen V., Bore G., Boon N., Vervaeren H., 2014. Up-scaling aquaculture wastewater treatment by microalgal bacterial flocs: From lab reactors to an outdoor raceway pond. Bioresour. Technol. 159 (2014) 342–354. http://dx.doi.org/10.1016/j.biortech.2014.02.113
42. Viruela A., Robles A., Durán F., Ruano M.V., Barat R., Ferrer J., Seco A., 2018. Performance of an outdoor membrane photobioreactor for resource recovery from

anaerobically treated sewage. J. Clean. Prod. 178, 665-674. https://doi.org/10.1016/j.jclepro.2017.12.223

43. Wang, L., Pan, B., Gao, Y., Li, C., Ye, J., Yang, L., Chen, Y., Hu, Q., Zhang, X., 2019. Efficient Membrane Microalgal Harvesting: Pilot-scale Performance and Technoeconomic Analysis. J. Clean. Prod. 218, 83-95. https://doi.org/10.1016/j.jclepro.2019.01.321
44. Whitton, R., Le Mével, A., Pidou, M., Ometto, F., Villa, R., Jefferson, B., 2016. Influence of microalgal N and P composition on wastewater nutrient remediation. Water Res. 91, 371-378. https://doi.org/10.1016/j.watres.2015.12.054
45. Xu, M., Li, P., Tang, T., Hu, Z., 2015. Roles of SRT and HRT of an algal membrane bioreactor system with a tanks-in-series configuration for secondary wastewater effluent polishing. Ecol. Eng. 85, 257-264. http://dx.doi.org/10.1016/j.ecoleng.2015.09.064
46. Zhang, Y., Fu, Q., 2018. Algal fouling of microfiltration and ultrafiltration membranes and control strategies: A review. Separation and Purification Technology 203, 193-208. https://doi.org/10.1016/j.seppur.2018.04.040

PRELIMINARY DATA SET TO ASSESS THE PERFORMANCE OF AN OUTDOOR MEMBRANE PHOTOBIOREACTOR (DATA IN BRIEF)

J. González-Camejo, A. Jiménez-Benítez, M.V. Ruano, A. Robles, R. Barat, J. Ferrer. Preliminary data set to assess the performance of an outdoor membrane photobioreactor. Data in Brief (under review). August 2019.

ABSTRACT

This data in brief (DIB) article is related to a Research article entitled ´Optimising an outdoor membrane photobioreactor for tertiary sewage treatment´ (González-Camejo et al., 2019).

Data related to the effect of substrate turbidity, the ammonium concentration at which the culture reaches nitrogen-deplete conditions and the microalgae growth rate under outdoor conditions is provided.

Microalgae growth rates under different substrate turbidity were obtained to assess the reduction of the culture´s light availability. Lab-scale experiments showed growth rates reductions of 22-44%.

Respirometric tests were carried to know the limiting ammonium concentration in this microalgae-based wastewater treatment system.

Growth rates (μ) of green microalgae *Scenedesmus* and *Chlorella* obtained under outdoor conditions; i.e. 0.40 d^{-1} (R^2 = 0.993) and 0.43 d^{-1} (R^2 = 0.995), respectively, can be useful to obtain optimum operating conditions of membrane photobioreator (MPBR).

VALUE OF THE DATA

- The effect of high and low turbidity in the substrate, which is related to the culture´s light availability, can be evaluated.
- The data enables to assess the ammonium concentration which limits microalgae activity.
- Growth rates could be used to compare different microalgae species and cultivation systems.
- Growth rates can be used to obtain the theoretically optimal biomass retention time (BRT) and hydraulic retention time (HRT) (Ruiz et al., 2013).
- This data highlights some relevant aspects that influence the operation of a microalgae cultivation system.

- Data of this DiB article can be applied to outdoor microalgae cultivation systems.

1. DATA

Several tests were elaborated: i) substrate turbidity; ii) the ammonium concentration at which the culture reaches nitrogen-deplete conditions; and iii) the microalgae growth rate under outdoor conditions.

To see the substrate turbidity effect on microalgae, culture growth rate was measured at different turbidity values (Figure VI.A.1). Raw data regarding the evolution of optical density which was used to calculate microalgae growth can be found in Supplementary material.

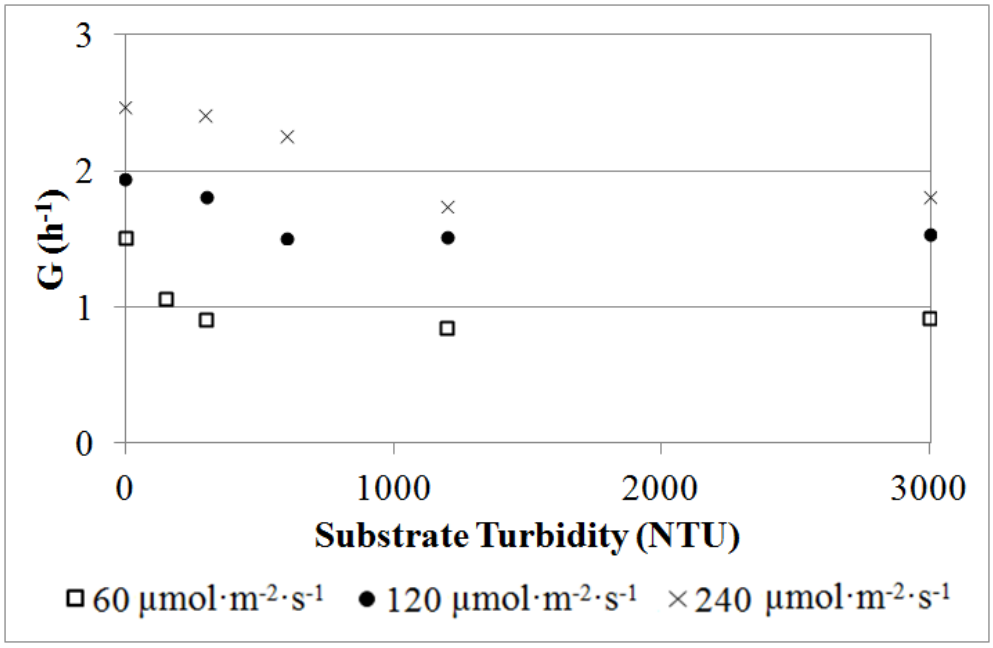

Figure VI.A.1. Microalgae growth under different light intensities.

Respirometric tests were carried out under different nitrogen concentrations to obtain the oxygen production rates (OPR) (Figure VI.A.2). Raw data regarding the evolution of oxygen which was used to calculate OPRs can be found in Supplementary material.

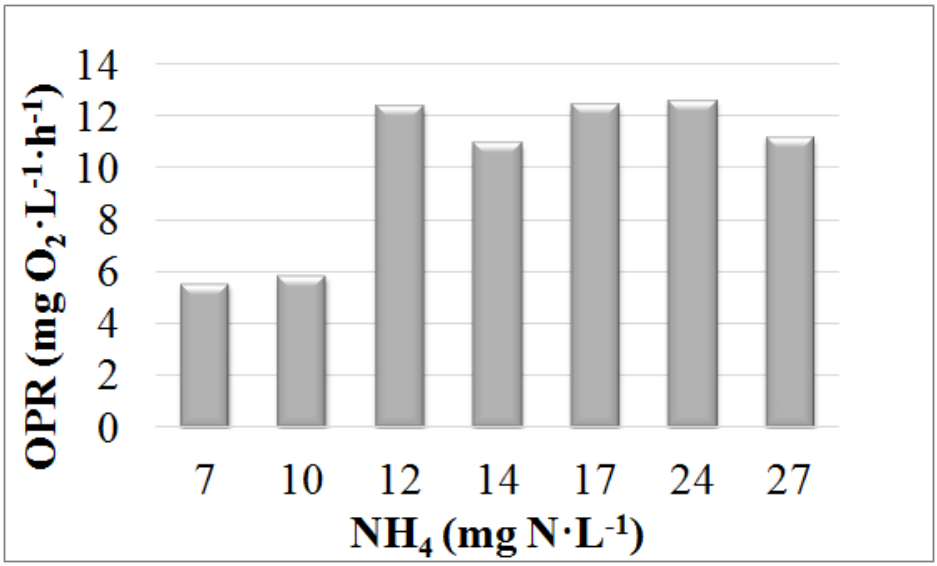

Figure VI.A.2. Oxygen production rates (OPRs) obtained during the respirometric tests under different ammonium (NH_4) concentrations.

The growth rate of microalgae cultures can be very helpful to operate microalgae cultivation systems, since maximum biomass productivity is reached when biomass retention time (BRT) equals $2 \cdot \mu^{-1}$ (Ruiz et al., 2013). Growth rates can be obtained by the time-evolution of the culture´s optical density (see Supplementary Material). Growth rates of 0.40 d^{-1} ($R^2 = 0.993$) and 0.43 d^{-1} ($R^2 = 0.995$), were observed for Assay (Figure VI.A.3a) and b (Figure VI.A.3b).

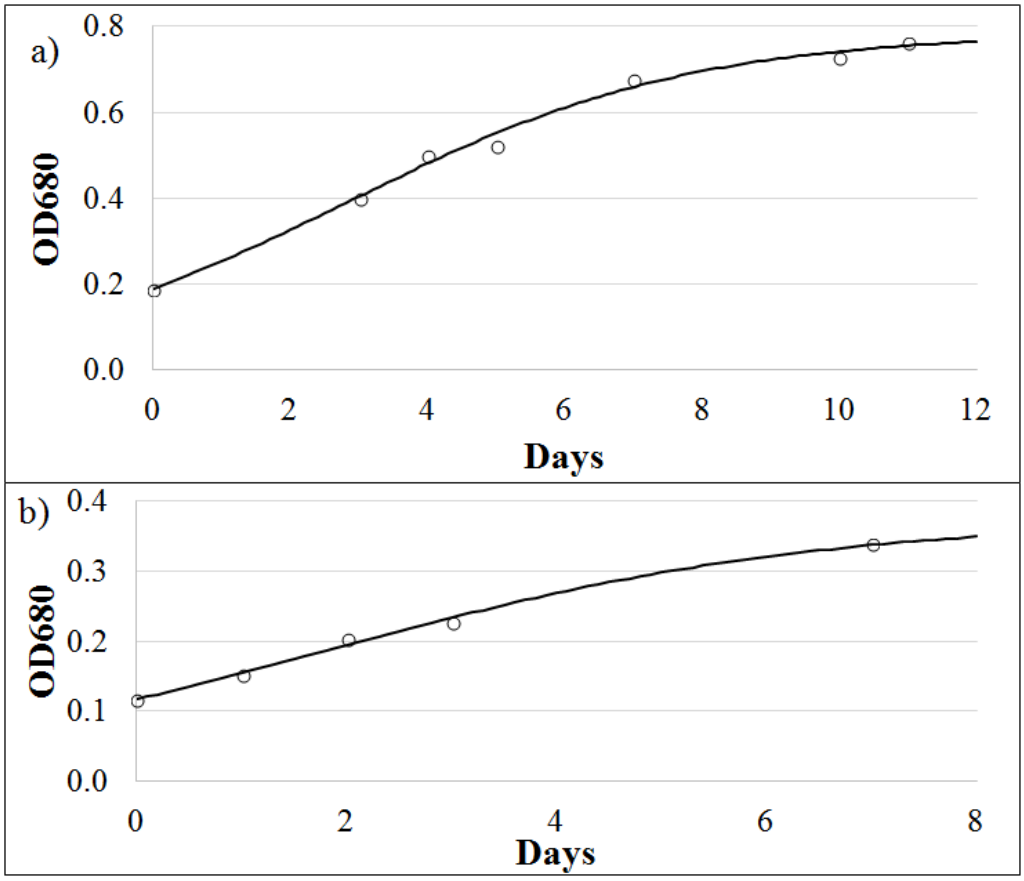

Figure VI.A.3. Evolution of optical density at 680 nm (OD680) during batch stage of: a) Experiment BRT4.5 (Scenedesmus-dominated) and b) Experiment HRT3.5 (Chlorella-dominated).

It must be also considered that operating the MPBR at BRTs out of their optimal range can imply the proliferation of competing organisms (Figure VI.A.4).

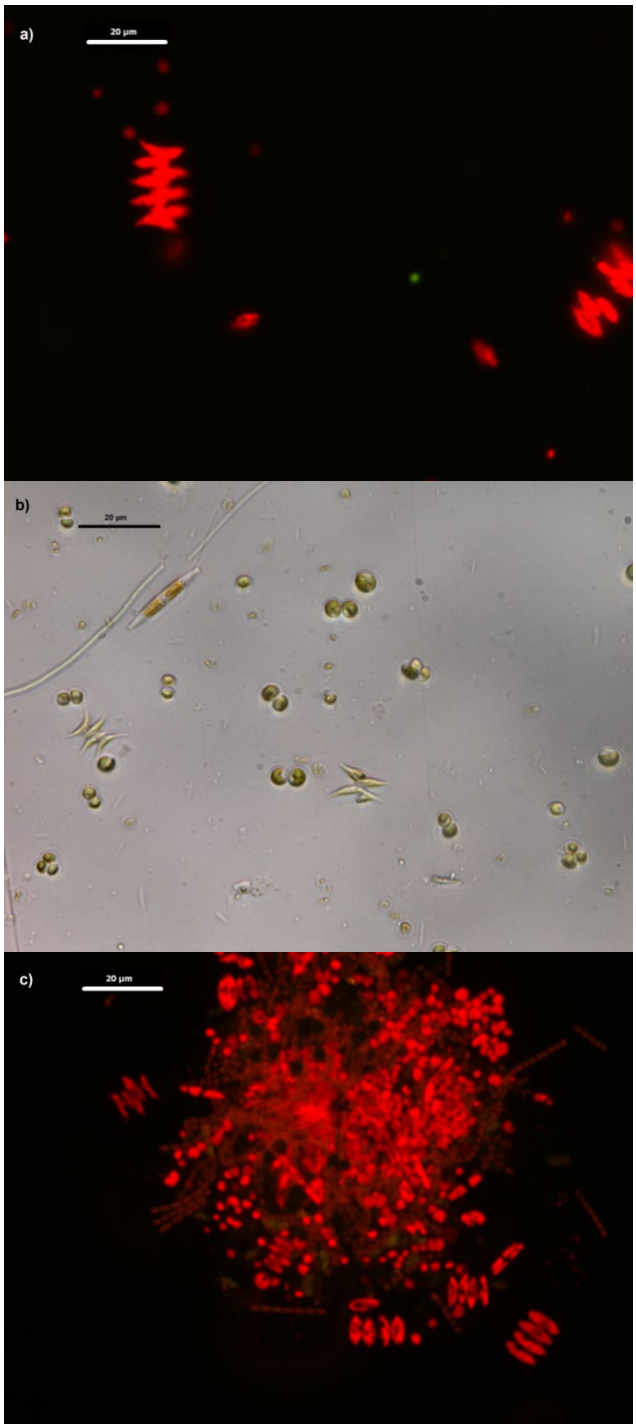

Figure VI.A.4. Samples observed under epifluorescence microscope (Leica DM2500/ DFC420c digital camera) using a 63x objective. Scale bar=20 µm. BRT Experiments in (González-Camejo et al., 2019); a) Experiment BRT4.5: *Scenedesmus* and scarce density of *Chlorella;* b) Experiment BRT6, bright-field image showing *Scendesmus, Chlorella* and scarce cyanobacteria and diatoms; c) Experiment BRT9, a mixture of *Scenedesmus* and *Chlorella* and high concentration of cyanobacteria.

2. EXPERIMENTAL DESIGN, MATERIALS AND METHODS

2.1. Substrate turbidity

To evaluate the effect of substrate turbidity, lab-scale assays were performed in 500-mL Erlenmeyer flasks, each one of which was lighted at different intensities: 60, 120 and 240 $\mu mol \cdot m^{-2} \cdot s^{-1}$ (measured on the flask surface). These intensities were achieved by varying the number of LED lamps (SevenOn 11w): 1, 2 and 4 lamps, respectively.

The culture for the experiments was composed of 100 mL of microalgae taken from the MPBR plant during the continuous operation of Experiment HRT1, and 100 mL of AnMBR effluent, i.e. microalgae substrate (González-Camejo et al., 2019). The initial microalgae biomass concentration was measured by means of optical density at 680 nm (OD680) by a MERC Spectroquant Pharo 300 spectrophotometer, obtaining values of around 1.74-1.8, so that the shadow effect due to microalgae was not considered.

Each assay consisted of several tests in which the turbidity value of AnMBR effluent varied by adding different quantities of kaolin (Table VI.A.1). In each test the microalgae growth was monitored by measuring the OD680 evolution for two hours. Microalgae growth (G) for each test was calculated as the slope of the line obtained in the OD680 evolution with time.

Table VI.A.1. Turbidity of the substrate and initial biomass concentration of each test.

	Turbidity (NTU)				
	Test 1	*Test 2*	*Test 3*	*Test 4*	*Test 5*
240 $\mu mol \cdot m^{-2} \cdot s^{-1}$	0	300	600	1200	3000
120 $\mu mol \cdot m^{-2} \cdot s^{-1}$	0	300	600	1200	3000
60 $\mu mol \cdot m^{-2} \cdot s^{-1}$	0	150	300	1200	3000

2.2. Respirometric tests

A 400-mL cylindrical closed PBR was placed inside a climate chamber to carry out the respirometric tests at constant temperature; i.e. 21-23 ºC. It was lit by four cool-white LED lamps (T8 LED-Tube 9 w) to supply a light intensity of 100 $\mu mol \cdot m^{-2} \cdot s^{-1}$. An oxygen probe (WTW CellOx 325) monitored the dissolved oxygen (DO) concentration and temperature of the culture during the 30 minutes that each test lasted. Before each respirometric test, bicarbonate (20 mg $C \cdot L^{-1}$) was added to the microalgae sample to avoid carbon limitation. In addition, diluted sulphuric (0.1 M) was injected whenever the pH rose over a set-point of 7.5.

Seven respirometric tests were done at ammonium concentrations of 7, 10, 12, 14, 17, 24 and 27 mg $N \cdot L^{-1}$. Microalgae were obtained from a sample from the MPBR plant during the continuous operation of Experiment BRT4.5 (González-Camejo et al., 2019). This sample was diluted with tap water in order to reduce the ammonium concentration up to 7 mg $N \cdot L^{-1}$. To obtain the rest of the ammonium concentrations, the corresponding amount of a standard dilution of 1000 mg $NH_4 \cdot L^{-1}$ was added to microalgae. Similar biomass concentrations; i.e., OD680 in the range of 0.30-0.33 were maintained for all the tests.

OPR was selected as reliable parameter since it has been reported to be proportional to biomass production rate (Ippoliti et al., 2016).

To calculate the net oxygen production rate (OPR) (mg $O_2 \cdot L^{-1} \cdot h^{-1}$), Eq. VI.A.1 was used:

$$\frac{dDO}{dt} = k_L a \cdot (DO_{sat} - DO) + OPR \qquad \text{[Eq. VI.A.1]}$$

where dDO/dt is the variation of the oxygen concentration over time (mg $O_2 \cdot L^{-1} \cdot h^{-1}$), k_La is the oxygen mass transfer coefficient (h^{-1}), DO_{SAT} is the oxygen saturation concentration at the culture temperature (mg $O_2 \cdot L^{-1}$), DO is the oxygen concentration in the culture (mg $O_2 \cdot L^{-1}$).

k_La was evaluated by doing respirometric tests with clean water as medium in duplicate. An average value of 0.432 h^{-1} was obtained. To calculate the OPR, the minimum square error criterion was used to obtain the optimal fit to Eq. VI.A.1 (Rossi et al., 2018).

It must be considered that the OPR obtained by Eq. VI.A.1 in a mixed culture like the one used in this study is actually a net value which is composed by several factors: i) microalgae photosynthesis; ii) microalgae respiration; iii) respiration of heterotrophic

bacteria; and iv) activity of nitrifying bacteria, both ammonium oxidising bacteria (AOB) and nitrite oxidising bacteria (NOB) (Rossi et al., 2018).

However, activity of heterotrophic bacteria was expected to be low because of the low organic loads of the substrate (González-Camejo et al., 2019). Nitrifying bacteria activity was also expected to be low because allylthiourea (ATU) was added to inhibit AOB growth (González-Camejo et al., 2018). On the other hand, microalgae respiration was expected to affect all the tests at a similar way because the sample used was the same in all the tests. In conclusion, the net OPR obtained by Eq. VI.A.1 was considered as a valid indirect measurement of the microalgae activity.

Ammonium concentrations were analysed according to Standard Method 4500-NH3-G (APHA, 2005) in a Smartchem 200 automatic analyser (WestcoScientific Instruments, Westco).

2.3. Growth rate under outdoor conditions

Microalgae growth rate (μ) was calculated by applying the Verhulst logistic kinetic model (Verhulst, 1838) to the OD680 evolution (Eq. VI.A.2):

$$\mu = \frac{OD680_m \cdot OD680_0 \cdot e^{\mu \cdot t}}{OD680_m - OD680_0 + OD680_0 \cdot e^{\mu \cdot t}} \qquad \text{[Eq. VI.A.2]}$$

where μ is the specific growth rate (d^{-1}), $OD680_m$, $OD680_o$ and OD680 are the optical density at 680 nm at an operation time which corresponded to infinite, zero, and *t*, respectively; and *t* is the time of batch operation (d).

Growth rates were evaluated during the start-up stages of Experiments BRT4.5 and HRT3.5 (González-Camejo et al., 2019). In Experiment BRT4.5, the culture was dominated by the green microalgae *Scenedesmus* (90% of TEC) with low *Chlorella* presence (around 10% of TEC). On the other hand, in Experiment HRT3.5 *Chlorella* was the dominant genus with 90% of TEC, while *Scenedesmus* reached only 10% of TEC. Other microorganisms such as bacteria and cyanobacteria were also present in the inoculums to a lesser extent but were not quantified.

ACKNOWLEDGEMENTS

This research work was supported by the Spanish Ministry of Economy and Competitiveness (MINECO, Projects CTM2014-54980-C2-1-R and CTM2014-54980-C2-2-R) jointly with the European Regional Development Fund (ERDF), which are gratefully acknowledged. It also received support from the Spanish Ministry of

Education, Culture and Sport via a pre-doctoral FPU fellowship to the first author (FPU14/05082).

REFERENCES

1. APHA-AWWA-WPCF, 2005. Standard methods for the examination of water and wastewater, 21st edition. American Public Health Association, American Water Works Association, Water Pollution Control Federation. Washington DC, USA.
2. González-Camejo, J., Jiménez-Benítez, A., Ruano, M.V., Robles, A., Barat, R., Ferrer, F., 2019. Optimising an outdoor membrane photobioreactor for tertiary sewage treatment. J. Environ. Manag. 245, 76-85. https://doi.org/10.1016/j.jenvman.2019.05.010
3. González-Camejo, J., Barat, R., Ruano, M.V., Seco, A., Ferer, J., 2018. Outdoor flat-panel membrane photobioreactor to treat the effluent of an anaerobic membrane bioreactor. Influence of operating, design and environmental conditions. Water Sci. Technol. 78(1) 195-206. http://dx.doi.org/10.2166/wst.2018.259
4. Ippoliti, D., Gómez, C., Morales-Amaral, M.M., Pistocchi, R., Fernández-Sevilla, J.M., Acién, F.G., 2016. Modeling of photosynthesis and respiration rate for *Isochrysis galbana* (T-Iso) and its influence on the production of this strain. Bioresour. Technol. 203, 71–79. http://dx.doi.org/10.1016/j.biortech.2015.12.050
5. Rossi, S., Bellucci, M., Marazzi, F., Mezzanotte, V., Ficara, E., 2018. Activity assessment of microalgal-bacterial consortia based on respirometric tests. Water Sci Technol. 78(1-2), 207-215. https://doi.org/10.2166/wst.2018.078
6. Ruiz, J., Álvarez-Díaz, P.D., Arbib, Z., Garrido-Pérez, C., Barragán, J., Perales, J.A., 2013. Performance of a flat panel reactor in the continuous culture of microalgae in urban wastewater: Prediction from a batch experiment. Bioresour. Technol. 127, 456-463. http://dx.doi.org/10.1016/j.biortech.2012.09.103
7. Verhulst, P.F. (1838). Notice sur la loi que la population poursuit dans son accroissement. Corresp. Math. Phys. 10, 113–121.

CHAPTER VII:

EFFECT OF LIGHT INTENSITY, LIGHT DURATION AND PHOTOPERIODS IN THE PERFORMANCE OF AN OUTDOOR PHOTOBIOREACTOR FOR URBAN WASTEWATER TREATMENT

CHAPTER VII:

EFFECT OF LIGHT INTENSITY, LIGHT DURATION AND PHOTOPERIODS IN THE PERFORMANCE OF AN OUTDOOR PHOTOBIOREACTOR FOR URBAN WASTEWATER TREATMENT

González-Camejo, J., Viruela, A., Ruano, M.V., Barat, R., Seco, A., Ferrer, J., 2019. Effect of light intensity, light duration and photoperiods in the performance of an outdoor photobioreactor for urban wastewater treatment. Algal Res. 40, 101511. https://doi.org/10.1016/j.algal.2019.101511

ABSTRACT

A series of eight experiments were carried out to analyse the effects of light intensity, light duration and photoperiods on a microalgae culture for treating AnMBR effluent at an outdoor photobioreactor (PBR) plant.

Improved performance was achieved in terms of nutrient recovery rates, biomass productivity and effluent nutrient concentrations at a higher net photon flux. However, the higher irradiance was also responsible for lower biomass productivity:light irradiance ratios.

None of the experiments with different lighting regimes and the same net photon flux showed any significant differences. The data obtained suggest that microalgae performance in this system did not depend on the time of day when light was applied or the length of the photoperiods, but on the net photon flux. No photoinhibiton was observed in any of the experiments, probably because of the significant shadow effect on the microalgae in the PBRs.

1. INTRODUCTION

Discharging nutrients such as nitrogen and phosphorus into sensitive water bodies can cause the eutrophication and deterioration of water ecosystems (Su et al., 2012). In this respect, microalgae-based processes have recently been receiving increasing attention (Garrido-Cárdenas et al., 2018) due to their high capacity to recover nitrogen and phosphorus from wastewater streams (Rinna et al., 2017) while producing valuable microalgae biomass (Gonçalves et al., 2016).

Anaerobic membrane bioreactor (AnMBR) effluents emerge as an ideal source of nutrients for microalgae growth, since they contain fairly high amounts of nutrients (Giménez et al., 2011). Nutrient recovery by microalgae from AnMBR effluents has several advantages over other conventional treatments (Romero-Villegas et al., 2018): i) nitrogen and phosphorus can be removed from the AnMBR effluent without adding either extra chemical reagents or an additional source of organic carbon (Tan et al., 2016); ii) the discharged effluent is oxygenated; and iii) the microalgae biomass cultivated in the process can be digested for biogas production (Guldhe et al., 2017). In this case, the digested sludge would be nutrient-enriched and have enhanced fertiliser properties (Cabanelas et al., 2013; Seco et al., 2018). Combining microalgae cultivation with AnMBR effluents therefore makes it possible to recover both nutrients and energy from sewage, thus reducing the process's carbon footprint (Seco et al., 2018).

Microalgae can be cultivated in open ponds or closed photobioreactors (PBRs) (Behera et al., 2018; Nwoba et al., 2019; Viruela et al., 2016). Open ponds generally present less operating costs than closed systems (Razzak et al., 2017; Vo et al., 2019). However, the biological process is more difficult to control in open reactors since they are remarkably more affected by ambient factors than closed PBRs (Behera et al., 2018). Furthermore, part of the nitrogen (up to 73% according to Romero-Villegas et al. (2018)) is lost in open systems due to ammonia stripping (Acién et al., 2016). Similarly, carbon dioxide would also be stripped in case of adding CO_2 for pH control (Acién et al., 2016). On the other hand, closed PBRs are designed to enhance the photosynthetic efficiency of microalgae, which allows to increasing the biomass productivity and nutrient recovery (Huang et al., 2017; Razzak et al., 2017; Vo et al., 2019). In this respect, De Vree et al. (2015) reported a photosynthetic efficiency of 2.7-3.8% in flat-panel PBRs, while for open ponds it only accounted for 0.5-1.5%.

Light is a key parameter in microalgae cultivation (Carvalho et al., 2011; Ferro et al., 2018; Iasimone et al., 2018; Lehmuskero et al., 2018; Liao et al., 2017; Mehan et al., 2018). In fact, light intensity, light frequency and photoperiods have been reported to influence microalgae productivity and nutrient removal efficiency (Abu-Ghosh et al., 2016; Binnal and Babu, 2017). Microalgae growth is proportional to light intensity until reaching a saturation point at which the photosynthetic activity of microalgae achieves their maximum value (Raeisossadati et al., 2019). When it falls below this optimal value, microalgae growth will be limited (Lehmuskero et al., 2018; Martínez et al., 2018). On the other hand, if the light intensity values exceed the optimum, photosystem

I (PSI) and photosystem II (PSII) will be damaged, causing microalgae photoinhibition (Binnal and Babu, 2017; Ramanna et al., 2017). Photoinhibition can be reduced by combining periods of high light irradiance with periods of darkness (Raeisossadati et al., 2019). Since algae have been reported to respond to light intensity almost instantaneously (Martínez et al., 2018), the temporary lack of light is considered to allow the dark reactions of photosynthesis, which are slower than the light reactions (Barceló-Villalobos et al., 2019), to use the stored energy from light reactions (Abu-Ghosh et al., 2016) without the addition of extra photons that cannot be used for photosynthesis. In fact, the excess of photons absorbed by microalgae is emitted as heat or fluorescence and reduce photosynthetic efficiency (Baker, 2008; Behera et al., 2018; Lehmuskero et al., 2018). In this context, the use of appropriate light-dark (L:D) photoperiods has been reported to reduce the light energy demand with similar or even higher productivity (Jacob-lopes et al., 2009; Park and Lee, 2001). Nevertheless, longer than optimum dark periods could result in lower mass productivity (Ferro et al., 2018).

Photoperiods can be divided into three main groups: i) long-term photoperiods, which refer to L:D cycles in hours (Jacob-lopes et al., 2009); ii) frequency photoperiods, which go through several L:D cycles per day (Zhou et al., 2015); and iii) short photoperiods, also known as the flashing light effect (FLE), which involve L:D cycles of seconds or even milliseconds (Abu-Ghosh et al., 2016; Park and Lee, 2001). Although different L:D cycles can lead to variations in photosynthetic performance (Verma and Srivastava, 2018), the studies available in the literature provide conflicting reports (Table VII.1).

Table VII.1. Biomass productivities and growth rates obtained at different L:D cycles in lab-scale experiments.

Microalgae	Intensity ($\mu mol \cdot m^{-2} \cdot s^{-1}$)	L:D cycle (h:h)	Productivity ($mg \cdot L^{-1} \cdot d^{-1}$)	Growth rate (d^{-1})	Ref.
Aphanothece microscopica Nägeli	150	24:0 16:8 12:12	770 240 301	-	Jacob-Lopes et al. (2009)
Chlorella kessleri	45	24:0 12:12	-	~ 0.1 ~ 0.1	Lee and Lee (2001)
Chlorella pyrenoidosa	128* 90* 69*	24:0* 16:8* 12:12*	~ 85 ~ 77 ~ 60	-	Li et al. (2016)
Chlorella vulgaris	200	24:0 16:8 12:12	-	1.18 1.20 1.15	Atta et al. (2013)

**Constant energy consumption of 0.8 Kwh·d^{-1}.*

Solar light is the most economical option for outdoor microalgae cultivation (Mehan et al., 2018; Otondo et al., 2018), but variations in the weather, day:night cycles and seasonal changes affect light intensity and its spectrum (Castrillo et al., 2018), which can negatively affect microalgae (Jebali et al., 2018; Ramanna et al., 2017). In addition, in high-dense microalgae cultures, the light is not uniformly distributed (Raeisossadati et al., 2019). The cells close to the PBR surface receive high light intensities that can reach up to 1800 $\mu mol \cdot m^{-2} \cdot s^{-1}$ at midday (Viruela et al., 2016) and hence are likely to suffer from photoinhibition (Deng et al., 2019; Raeisossadati et al., 2019). Also, the cells near the surface absorb most of the applied light irradiance, causing a dark zone where photosynthesis is limited (Barceló-Villalobos et al., 2019; Gris et al., 2014), known as the shadow effect or self-shading (Jebali et al., 2018; Martínez et al., 2018; Park and lee, 2001). The volume of the dark zone depends on the microalgae biomass concentration, microalgae pigments, light intensity, light path, culture turbidity and PBR opacity (Abu-Ghosh et al., 2016; Lehmuskero et al., 2018; Martínez et al., 2018; Wagner et al., 2018). The shadow effect also affects the amount of pigments (such as chlorophyll) in microalgae. Chlorophyll is not synthesised in complete darkness, but when the microalgae is illuminated inside a PBR, the pigment concentration increases at

low light intensities to take advantage of the photons available to reach the cells (Chen et al., 2011; Lehmuskero et al., 2018).

Mixing of the microalgae culture can help to mitigate this shadow effect since it involves the movement of algae from the highly illuminated areas of the reactor to dark zones (Barceló-Villalobos et al., 2019), therefore reducing photoinhibition (Wang et al., 2012) and applying a random FLE to the culture (Iluz and Abu-Ghosh, 2016). In contrast, mixing is usually poor within open systems (Barceló-Villalobos et al., 2019).

Light attenuation caused by the shadow effect can also be overcome by applying additional artificial lighting to the microalgae culture. This way, higher nutrient recovery efficiencies and biomass productivities can be achieved in shorter retention times (Abu-Ghosh et al., 2015; Su et al., 2012). Although artificial illumination can better regulate the light photons and photoperiods which can enhance photosynthesis performance (Abu-Ghosh et al., 2016), it also requires large amounts of energy. The illumination regime should therefore be used efficiently, with the appropriate L:D cycles.

The criteria used for selecting the artificial light source include electric energy efficiency, low heat dissipation, high reliability, long durability, low cost and emissions within the microalgae spectrum (Carvalho et al., 2011). Table VII.A.1 in (González-Camejo et al., 2019) briefly summarises the main advantages and disadvantages of different artificial light sources, in which LED lamps seem to be the most beneficial artificial light source for microalgae growth.

The effects of light intensity, photoperiods and light wavelength have been extensively reported under lab conditions (Castrillo et al., 2018; Chen et al., 2011; Yan et al., 2013). Other studies describe design proposals for new PBR prototypes to simulate an FLE in the microalgae culture (Abu-Ghosh et al., 2016; Iluz and Abu-Ghosh, 2016) or to increase the light available to the culture (Raeisossadati et al., 2019). However, the transition from prototypes (or lab scale PBRs) to outdoor microalgae cultivation has not been successfully studied (Iasimone et al., 2018) because of the complexity produced by the variations in natural light (Abu-Ghosh et al., 2016) and the difficulty of decoupling the light effect from the other parameters which influence outdoor microalgae growth, such as ambient temperature (Viruela et al., 2016).

In this context, the goal of the present study was to examine the effects of light intensity, light duration and photoperiods on an outdoor microalgae culture which

treated AnMBR effluent. PBR performance was evaluated by considering nutrient recovery rates, effluent nutrient concentrations and microalgae biomass productivity.

2. MATERIAL AND METHODS

2.1. Microalgae culture and substrate

The microalgae used in this study consisted of an indigenous mixed culture, originally collected from the walls of the secondary clarifier of the Carraixet WWTP (39º30'04.0''N 0º20'00.1''W, Valencia, Spain).

The microalgae were mainly composed of green algae *Scenedesmus* and *Chlorella*; although diatoms, cyanobacteria, heterotrophic and autotrophic bacteria were also present in lower concentrations.

The microalgae substrate consisted of the nutrient-rich effluent from an AnMBR plant that treated real sewage (Giménez et al., 2011) with high nutrient concentrations; i.e., 56.6 ± 9.7 mg $N \cdot L^{-1}$ (n = 99) for nitrogen (mainly in the form of ammonium) and 6.5 ± 1.3 mg $P \cdot L^{-1}$ (n = 99) for phosphorus.

The AnMBR effluent also had low COD values (92 ± 32 mg $COD \cdot L^{-1}$, n = 34), mainly non-biodegradable, and a negligible suspended solids concentration. The substrate was previously aerated to oxidise the large amounts of sulphide (around 112.7 ± 13.8 mg $S \cdot L^{-1}$, n = 34) to sulphate, as described in González-Camejo et al. (González-Camejo et al., 2017).

2.2. Photobioreactors

Microalgae were cultivated in two outdoor flat-panel 1.25-m high x 2-m wide x 0.25-m deep methacrylate PBRs (PBR-A and PBR-B) with a working volume of 550 L each, continuously stirred by an airflow of 0.10 vvm and sparged by two perforated pipes on the PBR floor. This setup provided nutrient and light homogenisation, lowered thermal stratification (Behera et al., 2018) and reduced wall fouling. Pure CO_2 (99.9%) was added to the airflow through an automatic valve whenever the pH value went over 7.5 to avoid undesirable phenomena such as ammonia volatilisation and phosphorus precipitation (Muñoz and Guieysse, 2006).

An irradiation sensor (Apogee Quantum SQ-200) on the surface of PBR-A continuously measured photosynthetically active radiation (PAR). In addition to natural light, an artificial light source was used consisting of twelve LED lamps (Unique Led IP65 WS-

TP4S-40W-ME). Six of them were cold white (6500K) and the other six were neutral white (4500K). They were installed at the back of the tanks to illuminate the PBR surface that did not receive any sunlight. When all the lamps were on, an average light irradiance of 300 $\mu E \cdot m^{-2} \cdot s^{-1}$ was measured on the surface but this dropped to 150 $\mu E \cdot m^{-2} \cdot s^{-1}$ when only half the lamps were in action.

2.3. Operating conditions

Eight different experiments were carried out (Table VII.2) in which both PBRs were inoculated with the same inoculum and substrate concentration. The PBR start-up phase (not included in the data analysis) was as described in González-Camejo et al. (2018) and was designed to obtain a consistent initial microalgae biomass concentration. Both PBRs were then fed in semi-continuous operation with the same nutrient load, maintaining a hydraulic retention time (HRT) of 8 days. Temperature was in the range of 18-27ºC, which is within the optimum range for green algae *Scenedesmus* and *Chlorella*: 15-25ºC (García-Cubero et al., 2018; Xin et al., 2011).

As the PBR pilot plant was operated outdoors, which meant that solar light intensity was variable, the different experiments could not be compared with one another, although the two PBRs used in each experiment were oriented in the same direction, so that they only differed in the artificial lighting regime, which varied the total net photon flux as shown in Table VII.2. Three different effects were studied: i) light intensity; ii) light duration (and the time of day when artificial light was applied, i.e. day or night); and iii) light photoperiods.

Light intensity was studied in Experiments 1 and 2, which were designed to determine whether the addition of artificial light would improve the PBR performance. Three different artificial light intensities were evaluated: 0, 150 and 300 $\mu mol \cdot m^{-2} \cdot s^{-1}$.

Light duration and the time of day when light was applied were assessed in Experiments 3, 4 and 5. Experiment 3 included different L:D cycles of 12:12 h and 24:0 h at the same light intensity. In Experiment 4, the same L:D cycles (12:12 h) and same light intensity were applied, but PBR-A was illuminated at night and PBR-B was lit during the day. Different L:D cycles and different light intensities were chosen in Experiment 5 (Table VII.2).

The light photoperiods were studied in Experiments 6, 7 and 8. Three different on:off photoperiod cycles (which represented the total time that the artificial lamps were continuously on and off) were tested: 1.5:1.5 h, 0.75:0.75 h and 1:2 h, in Experiments 6,

7 and 8, respectively. These photoperiods were compared to continuous illumination with the same quantity of photons per day, which were L:D cycles of 12:12, 12:12 and 8:16 h, respectively (Table VII.2).

Table VII.2. Outdoor and artificial lighting conditions of PBR-A and PBR-B in each experiment.

Exp	Days	Solar PAR ($\mu mol \cdot m^{-2} \cdot s^{-1}$)	Artificial light							
			Intensity ($\mu mol \cdot m^{-2} \cdot s^{-1}$)		L:D cycle (h:h)[1]		on:off cycle (h:h)[2]		Time[3]	
			PBR-A	*PBR-B*	*PBR-A*	*PBR-B*	*PBR-A*	*PBR-B*	*PBR-A*	*PBR-B*
1	25	277 ± 146	300	0	24:0	0:24	24:0	0:24	D-N	-
2A	14	99 ± 12	300	150	24:0	24:0	24:0	24:0	D-N	D-N
2B	28	107 ± 20	150	150	24:0	24:0	24:0	24:0	D-N	D-N
3	30	89 ± 15	300	300	24:0	12:12	24:0	12:12	D-N	N
4	26	124 ± 23	300	300	12:12	12:12	12:12	12:12	N	D
5	32	109 ± 53	300	150	12:12	24:0	12:12	24:0	N	D-N
6	15	120 ± 54	300	300	12:12	12:12	1.5:1.5	12:12	D-N	N
7	20	132 ± 56	300	300	12:12	12:12	0.75:0.75	12:12	D-N	N
8	27	124 ± 44	300	300	8:16	8:16	1:2	8:16	D-N	N

[1]*L:D cycles represent the number of total hours a day that artificial lights are either in light or dark.*

[2]*On:off cycles represent the maximum consecutive time that lights are either on or off.*

[3]*D: Artificial lights on during daylight hours; N: Artificial lights on during night hours; D-N: Artificial lights on during day and night.*

2.4. Sampling and Analytical Methods

Grab samples were collected from the PBR influent and effluent streams as well as from the microalgae culture three times a week. The soluble fraction of the sample was obtained by vacuum filtration with 0.45 mm pore size filters (Millipore). Ammonium (NH_4), nitrite (NO_2), nitrate (NO_3), and phosphate (PO_4) were analysed according to Standard Methods (APHA, 2005): 4500-NH3-G, 4500-NO2-B, 4500-NO3-H and 4500-P-F, respectively, in a Smartchem 200 automatic analyser (Westco Scientific Instruments, Westco). The sum of NH_4, NO_2 and NO_3 concentrations was considered to

be equivalent to total soluble nitrogen (Ns). Volatile suspended solids (VSS) were determined according to Standard Method 2540-E (APHA, 2005).

COD and sulphide concentrations of the influent, as well as total eukaryotic cell (TEC) and chlorophyll concentrations of the culture were measured once a week. COD and sulphide were performed according to Standard Methods (APHA, 2005) 522-COD-D and 4500-S^{2-}D, respectively. TEC was counted by epifluorescence (Pachés et al., 2012) and chlorophyll content was determined by the tricromatic method based on visible spectroscopy (APHA, 2005). Jeffrey and Humphrey equations (Jeffrey and Humphrey, 1975) were used to obtain chlorophyll concentration. Pigment was extracted with acetone 90%.

Maximum quantum efficiency (F_v/F_m) was measured in-situ three times a week with a portable fluorometer AquaPen-C AP-C 100 (Photon Systems Instruments, Czech Republic) after the samples had remained in the dark for ten minutes (Baker, 2008).

All measurements were done in duplicate.

2.5. Calculations

It was assumed that all the nutrient reduction from wastewater was recovered by the microalgae biomass. Nitrogen recovery rate (NRR) (mg $N \cdot L^{-1} \cdot d^{-1}$), phosphorus recovery rate (PRR) (mg $P \cdot L^{-1} \cdot d^{-1}$) and biomass productivity (BP) (mg $VSS \cdot L^{-1} \cdot d^{-1}$) were calculated according to Eqs. VII.1, VII.2 and VII.3, respectively:

$$NRR = \frac{(N_i - N_e) \cdot F}{V_{PBR}} \qquad \text{[Eq. VII.1]}$$

where N_i is the nitrogen concentration of the influent (mg $N \cdot L^{-1}$), N_e is the nitrogen concentration of the effluent of PBR-A or PBR-B (mg $N \cdot L^{-1}$), F is the flow rate of the substrate ($L \cdot d^{-1}$), and V_{PBR} is the culture volume in the PBRs (L).

$$PRR = \frac{(P_i - P_e) \cdot F}{V_{PBR}} \qquad \text{[Eq. VII.2]}$$

where P_i is the phosphorus concentration of the influent (mg $P \cdot L^{-1}$) and P_e is the phosphorus concentration of the effluent of PBR-A or PBR-B (mg $P \cdot L^{-1}$).

$$BP = \frac{VSS \cdot V_p}{V_{PBR}} \qquad \text{[Eq. VII.3]}$$

where VSS (mg $VSS \cdot L^{-1}$) is the volatile suspended solids concentration in the PBRs and Vp is the volume of the microalgae culture purged ($L \cdot d^{-1}$).

The biomass productivity:light irradiance ratio (BP:I, g $VSS \cdot mol^{-1}$) was calculated according to Eq. VII.4 (modified from Cuaresma et al. (2011)).

$$\text{BP:I} = \frac{\text{BP}\cdot V_{PBR}\cdot 1000}{\text{TP}\cdot t\cdot S\cdot 24\cdot 3600} \qquad \text{[Eq. VII.4]}$$

where TP is the total photon flux applied to the PBR surface (i.e. the sum of solar irradiance plus artificial lighting, μmol·m^{-2}·s^{-1}); t is the period of time considered (d) and S is the PBR surface (m^2).

Similarly, the nitrogen and phosphorus recovery rate:light irradiance ratios (NRR:I and PRR:I) were calculated with Eq. VII.5 and Eq. VII.6, respectively:

$$NRR{:}I = \frac{NRR\cdot V_{PBR}\cdot 10^6}{TP\cdot S\cdot 24\cdot 3600} \qquad \text{[Eq. VII.5]}$$

$$PRR{:}I = \frac{PRR\cdot V_{PBR}\cdot 10^6}{TP\cdot S\cdot 24\cdot 3600} \qquad \text{[Eq. VII.6]}$$

2.6. Statistical analysis

All the values were expressed as the mean ± standard deviation. The data were analysed on Statgraphics Centurion XVII statistical software. Statistically significant differences were considered with p-values < 0.05.

3. RESULTS

3.1. Effect of light intensity

In Experiment 1, PBR-B was lit by natural light only. In PBR-A, one surface received sunlight (277 ± 146 μmol·m^{-2}·s^{-1}, n = 25), while the other was lit artificially at an intensity of 300 μmol·m^{-2}·s^{-1}. This artificial light source was not considered to cause some photochemical stress to microalgae since F_v/F_m remained at high values in both PBRs (Lazar, 1999); i.e., 0.76 ± 0.03 in PBR-A and 0.75 ± 0.01 in PBR-B (p-value = 0.20; n = 12). As can be seen in Table VII.3, in Experiment 1 PBR-A achieved 37.5% higher NRR and 58.4% higher PRR than PBR-B, which indicated lower effluent nutrient concentrations in PBR-A than in PBR-B (Figure VII.1a). PBR-A also reached higher biomass productivity (Table VII.3) due to the significantly higher biomass concentration: 538 ± 101 mg VSS·L^{-1} and 333 ± 86 mg VSS·L^{-1} for PBR-A and PBR-B, respectively (p-value = 0.01; n = 12), indicating 63.9% more microalgae biomass in the artificially lit PBR. However, the efficiency in the use of light was higher in PBR-B since PBR-A presented lower BP:I than PBR-B; i.e., 0.48 ± 0.15 g VSS·mol^{-1} and 0.61 ± 0.20 g VSS·mol^{-1}, respectively (p-value = 0.02; n = 12). These values are in the range of those reported by Morales-Amaral et al. (2015), who obtained values of BP:I in the range of 0.2-0.6 g VSS·mol^{-1} for a *Scenedesmus* sp. culture.

Table VII.3. Nutrient recovery rates and biomass productivities obtained in each experiment.

	NRR (mg N·L^{-1}·d^{-1})			**PRR (mg P·L^{-1}·d^{-1})**			**BP (mg VSS·L^{-1}·d^{-1})**		
Exp	**PBR-A**	**PBR-B**	**p-value**	**PBR-A**	**PBR-B**	**p-value**	**PBR-A**	**PBR-B**	**p-value**
1	7.7±1.6	5.6±2.2	0.00*	1.03±0.21	0.65±0.24	0.00*	100±32	61±20	0.01*
2A	5.0±1.2	3.1±1.5	0.09*	0.71±0.14	0.47±0.13	0.05*	55±6	42±5	0.00*
2B	2.3±1.0	2.2±0.5	0.70	0.31±0.21	0.29±0.18	0.82	27±7	25±7	0.59
3	3.5±1.8	2.2±1.1	0.03*	0.50±0.19	0.35±0.23	0.09*	34±6	26±5	0.00*
4	2.7±0.7	3.0±0.9	0.47	0.31±0.14	0.33±0.11	0.68	30±2	29±2	0.19
5	3.2±1.8	3.2±1.7	0.99	0.46±0.18	0.49±0.24	0.73	31±9	34±9	0.44
6	2.7±1.0	3.3±1.2	0.31	0.29±0.11	0.31±0.13	0.81	27±6	23±6	0.26
7	3.7±1.5	3.5±1.1	0.80	0.53±0.17	0.50±0.15	0.76	46±7	46±8	0.93
8	1.7±1.1	1.5±0.7	0.55	0.32±0.18	0.26±0.13	0.46	27±4	25±2	0.20

**Showed statistically significant differences.*

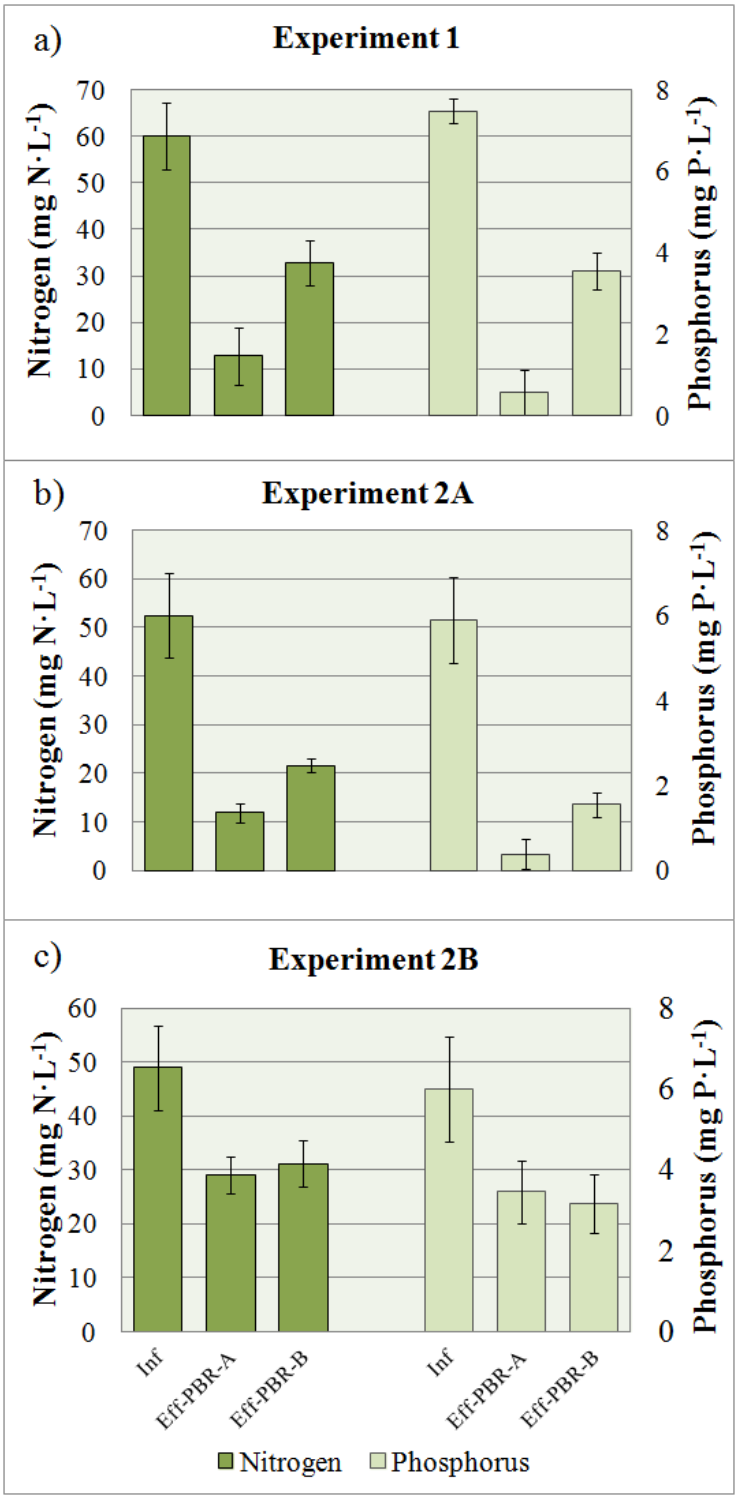

Figure VII.1. Effect of light intensity. Average measures (and standard deviation) of nitrogen and phosphorus concentration in the influent (Inf) and effluent of PBR-A (Eff-PBR-A) and PBR-B (Eff-PBR-B) in: a) Experiment 1; b) Experiment 2A; and c) Experiment 2B.

It should be also noted that, despite the different VSS concentration in the PBRs during Experiment 1, TEC concentration in PBR-A was not significantly higher than in PBR-

B: $7.33 \cdot 10^9 \pm 1.21 \cdot 10^9$ cells·L^{-1} and $6.27 \cdot 10^9 \pm 1.63 \cdot 10^9$ cells·L^{-1}, respectively (p-value = 0.27; n = 5), both having a similar strain distribution; i.e. around 90% of the TEC was *Scenedesmus* and around 10% was *Chlorella*.

Regarding nutrient recovery:light irradiance rates, PBR-A attained lower NRR:I than PBR-B (37.3 ± 7.7 mg N·mol^{-1} and 55.9 ± 22.0 mg N·mol^{-1}, respectively; p-value = 0.00; n = 7). PRR:I was also lower in PBR-A than in PBR-B (5.3 ± 1.0 mg P·$mol^{-1}$and 6.5 ± 2.4 mg P·mol^{-1}, respectively; p-value = 0.00; n = 7).

With respect to photosynthetic pigments, PBR-A achieved higher intracellular chlorophyll content than PBR-B (6.35 ± 2.35 mg chl·g VSS^{-1} and 5.72 ± 1.83 mg chl·g VSS^{-1}, respectively). Although this difference was not statistically significant (p-value = 0.83; n = 5), the chlorophyll content per microalgae cell was significantly higher for PBR-A ($5.34 \pm 1.43 \cdot 10^{-10}$ mg chl·$cell^{-1}$) than for PBR-B; i.e., $2.43 \pm 0.74 \cdot 10^{-10}$ mg chl·$cell^{-1}$ (p-value = 0.00; n = 5).

Experiment 2 was divided into two: 2A and 2B. In Experiment 2A, PBR-A remained at an artificial light intensity of 300 µmol·m^{-2}·s^{-1}; while PBR-B was continuously lit artificially at an intensity of 150 µmol·m^{-2}·s^{-1}; i.e. half of the net photon flux emitted by LED lamps. The aim of this period was therefore to assess whether the continuous artificial light intensity of 300 µmol·m^{-2}·s^{-1} was excessive for optimum microalgae growth since the photoinhibition point has been reported to be at light irradiances of around 200 µmol·m^{-2}·s^{-1} (Raeisossadati et al., 2019).

According to the results shown in Table VII.3, in Experiment 2 PBR-A showed significantly higher NRR, PRR and biomass productivity than PBR-B. Consequently, PBR-A presented significantly lower effluent nutrient concentrations than PBR-B (Figure VII.1b).

As in Experiment 1, the TEC concentration was not significantly different in Experiment 2A in both PBRs: $8.75 \cdot 10^9 \pm 1.86 \cdot 10^9$ cells·L^{-1} and $7.54 \cdot 10^9 \pm 2.17 \cdot 10^9$ cells·L^{-1}, for PBR-A and PBR-B, respectively (p-value = 0.48; n = 4), even though the VSS concentrations were statistically different: 410 ± 58 mg VSS·L^{-1} and 320 ± 28 mg VSS·L^{-1}, respectively (p-value = 0.01; n = 5). Since genera distribution was similar in both PBRs (around 30% of TEC was *Scenedesmus* and around 70% *Chlorella*), cell size might have been different in both PBRs (Gris et al., 2014).

Similarly to Experiment 1, PBR-B in Experiment 2A was more efficient as regards biomass production:light irradiance ratios than PBR-A: 0.46 ± 0.04 g VSS·mol^{-1} and 0.38 ± 0.03 g VSS·mol^{-1}, respectively (p-value = 0.02; n = 5). On the other hand, both

PBRs showed similar nutrient recovery rates:light irradiance ratios (i.e. NRR:I 30.8 ± 6.0 mg $N \cdot mol^{-1}$ and 32.4 ± 11.7 mg $N \cdot mol^{-1}$ for PBR-A and PBR-B, respectively (p-value = 0.99; n = 5), while PRR:I 6.3 ± 0.7 mg $P \cdot mol^{-1}$ and 5.4 ± 1.2 mg $P \cdot mol^{-1}$ were measured in PBR-A and PBR-B, respectively (p-value = 0.39; n = 5).

In Experiment 2B the light intensity in PBR-A was reduced to 150 $\mu mol \cdot m^{-2} \cdot s^{-1}$. As can be seen, even though PBR-A started at lower effluent nutrient concentrations, its performance tended to be similar to PBR-B, meeting stable operations with similar effluent nutrient concentrations (Figure VII.2b). In the case of microalgae biomass, PBR-A started Experiment 2B at a concentration of 400 mg $VSS \cdot L^{-1}$, while PBR-B started with a biomass concentration of 285 mg $VSS \cdot L^{-1}$. However, from day 19 until the end of Experiment 2B, the microalgae biomass concentration was similar in both PBRs, so that both reached significantly similar NRR, PRR and biomass productivity (Table VII.3).

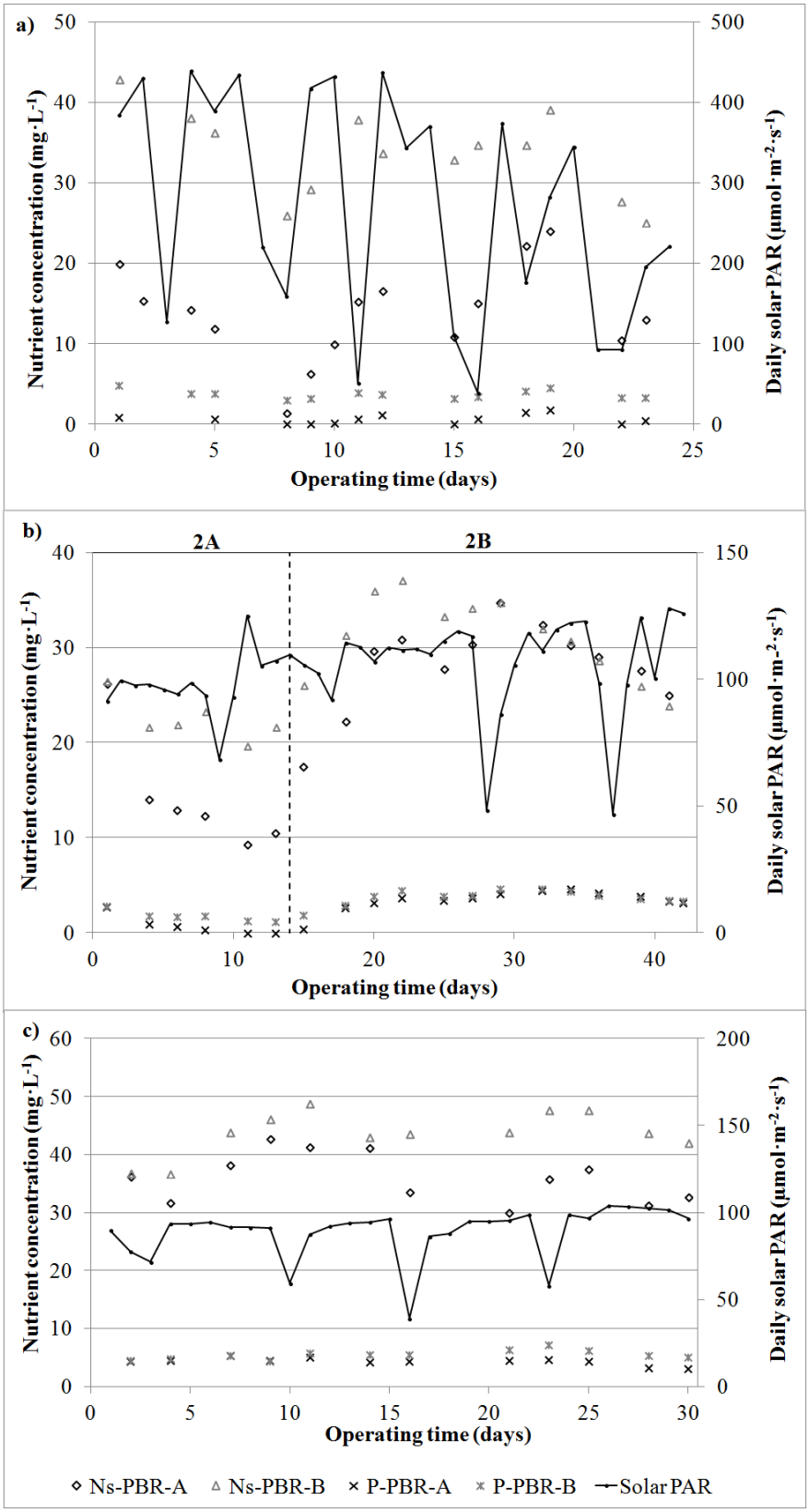

Figure VII.2. Evolution of nitrogen (Ns) and phosphorus (P) effluent concentrations and daily average solar PAR in the experiments related to light intensity: a) Experiment 1; b) Experiment 2; c) Experiment 3.

3.2. Effect of light duration

Different L:D cycles of artificial light were tested in Experiment 3. PBR-A was operated with continuous artificial lighting and PBR-B was only lit during the hours of darkness (L:D cycle of 12:12 h), so that PBR-A received twice as much artificial photon flux than PBR-B. As a result, PBR-A performance was significantly higher than PBR-B in terms of NRR, PRR and biomass productivity (Table VII.3). The PBR-A effluent nutrient concentrations were therefore lower than in PBR-B (Figure VII.3a).

With respect to light efficiency, BP:I of PBR-B in Experiment 3 was higher than in PBR-A: 0.59 ± 0.06 g VSS·mol^{-1} and 0.24 ± 0.03 g VSS·mol^{-1}, respectively (p-value = 0.00; n = 13), but the nutrient recovery rate:light irradiance ratios were similar for both PBRs. PBR-A showed NRR:I and PRR:I of 25.0 ± 10.0 mg N·mol^{-1} and 3.5 ± 0.6 mg P·mol^{-1}, respectively; while PBR-B obtained 25.0 ± 10.1 mg N·mol^{-1} and 3.3 ± 1.5 mg P·mol^{-1}, respectively (p-values = 0.99 and 0.76, respectively; n = 13).

Unlike Experiments 1 and 2A, the higher biomass concentration obtained in PBR-A (277 ± 39 mg VSS·L^{-1}) than in PBR-B; i.e., 208 ± 41 mg VSS·L^{-1} (p-value = 0.00; n = 13), was related to a higher TEC concentration in PBR-A in comparison to PBR-B: $9.96 \cdot 10^{9} \pm 6.10 \cdot 10^{8}$ cells·L^{-1} and $4.50 \cdot 10^{9} \pm 2.38 \cdot 10^{9}$ cells·L^{-1}, respectively (p-value = 0.01; n = 6); although the strain distribution was similar, i.e. 85% of TEC consisted of *Chlorella* and 15% was *Scenedesmus* in PBR-A, while 80% of the TEC consisted of *Chlorella* and 20% was *Scenedesmus* in PBR-B. On the other hand, the chlorophyll content in PBR-A (which received a higher photon flux) was noticeably lower than PBR-B: 4.48 ± 1.12 mg chl·g VSS^{-1} and 6.7 ± 2.04 mg chl·g VSS^{-1}, respectively (p-value = 0.04; n = 6). This also occurred with the chlorophyll content per cell; i.e. $1.01 \pm 0.25 \cdot 10^{-10}$ mg chl·cell^{-1} for PBR-A and $1.74 \pm 0.32 \cdot 10^{-10}$ mg chl·cell^{-1} for PBR-B (p-value = 0.01; n = 6).

Experiment 4 evaluated the effect of artificially illumination during day or night. PBR-A (which was illuminated at night with a 12:12 h L:D cycle) obtained similar nutrient effluent concentrations than PBR-B (which was lit during daylight with the same L:D cycle and was therefore in complete darkness at night) (Figure VII.3b). Neither did the NRR, PRR and biomass productivity (Table VII.3) nor chlorophyll content show any significant differences: 11.97 ± 0.37 mg chl·g VSS^{-1} and 11.28 ± 0.30 mg chl·g VSS^{-1}, respectively (p-value = 0.18; n = 4).

The goal of Experiment 5 was to assess the most efficient artificial light regime for the culture; i.e. with a high-intensity 12:12 h L:D cycle during the night (300 μmol·m^{-2}·s^{-1}):

PBR-A, or with continuous low-intensity illumination (150 µmol·m^{-2}·s^{-1}): PBR-B, both with the same net photon flux. The results of this experiment did not show any statistically significant differences between both PBRs (Table VII.3 and Figure VII.3c).

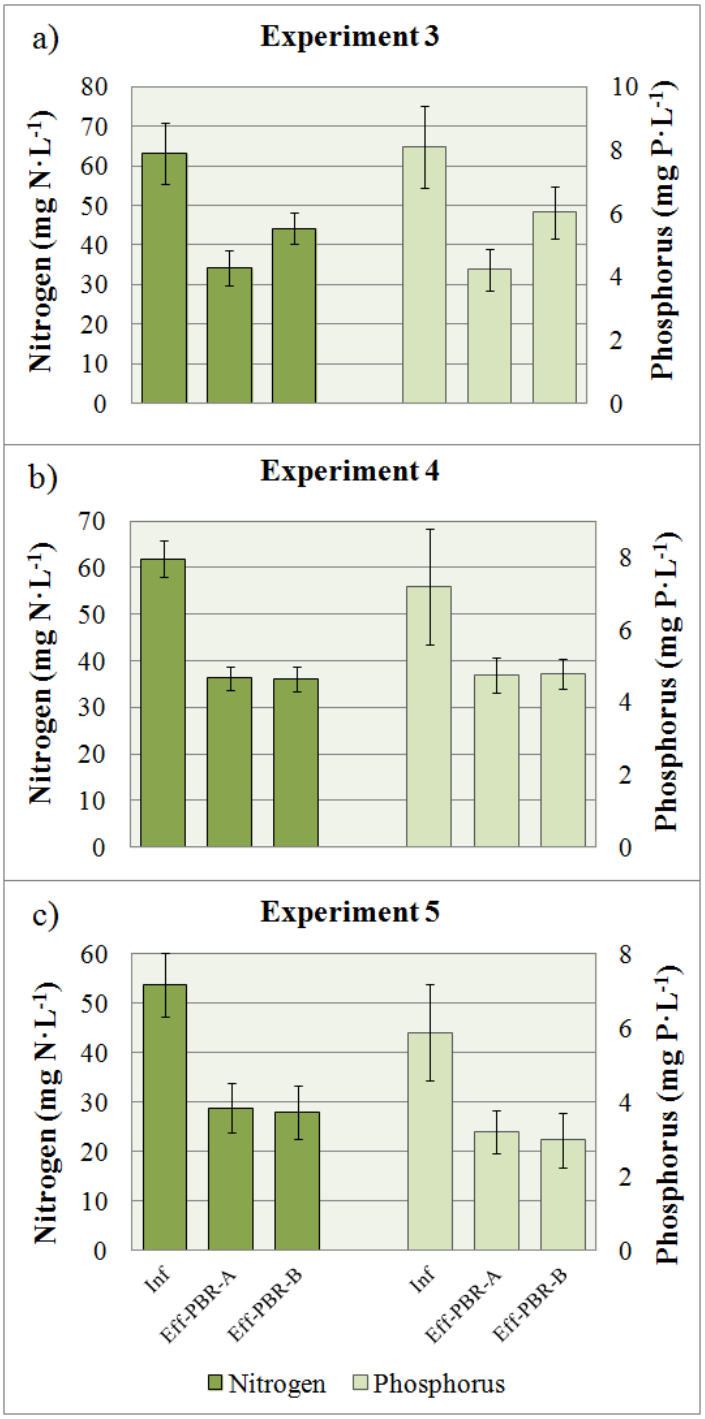

Figure VII.3. Effect of light duration. Average measures (and standard deviation) of nitrogen and phosphorus concentration in the influent (Inf) and effluent of PBR-A (Eff-PBR-A) and PBR-B (Eff-PBR-B) in: a) Experiment 3; b) Experiment 4; and c) Experiment 5.

3.3. Effect of photoperiods

The long-term photoperiods and frequency photoperiods (Jacob-Lopes et al., 2009; Zhou et al., 2015) were compared in Experiments 6, 7 and 8. In all three experiments, PBR-B was continuously illuminated at night, i.e. the on:off cycles (which is the maximum period of time when artificial lights were on and off) were equal to the L:D cycles. In Experiments 6 and 7, PBR-B was operated with 12:12 h L:D cycles, while in Experiment 8 the L:D cycle was reduced to 8:16 h. PBR-A was operated under the same L:D cycles as PBR-B, but with different on:off cycles: in Experiment 6, this cycle was 1.5:1.5 h and in Experiment 7 this frequency was reduced to 0.75:0.75 h. In Experiment 8 the lights were left on for 1 h and switched off for 2 h.

The effluent nutrient concentrations in both PBRs showed no significant differences throughout Experiments 6, 7 and 8 (Figure VII.4). Neither were the differences in terms of nutrient recovery rates and biomass productivity statistically significant (Table VII.3). Similar behaviour was observed in the chlorophyll content of microalgae, obtaining: i) in Experiment 6, 8.29 ± 1.06 mg chl·g VSS^{-1} and 9.38 ± 2.23 mg chl·g VSS^{-1}, for PBR-A and PBR-B, respectively (p-value = 0.41; n = 4); ii) in Experiment 7, 6.64 ± 1.08 mg chl·g VSS^{-1} and 7.08 ± 0.55 mg chl·g VSS^{-1}, for PBR-A and PBR-B, respectively (p-value = 0.49; n = 5); and, iii) in Experiment 8, 7.59 ± 2.01 mg chl·g VSS^{-1} and 8.29 ± 2.52 mg chl·g VSS^{-1}, for PBR-A and PBR-B, respectively (p-value = 0.61; n = 6).

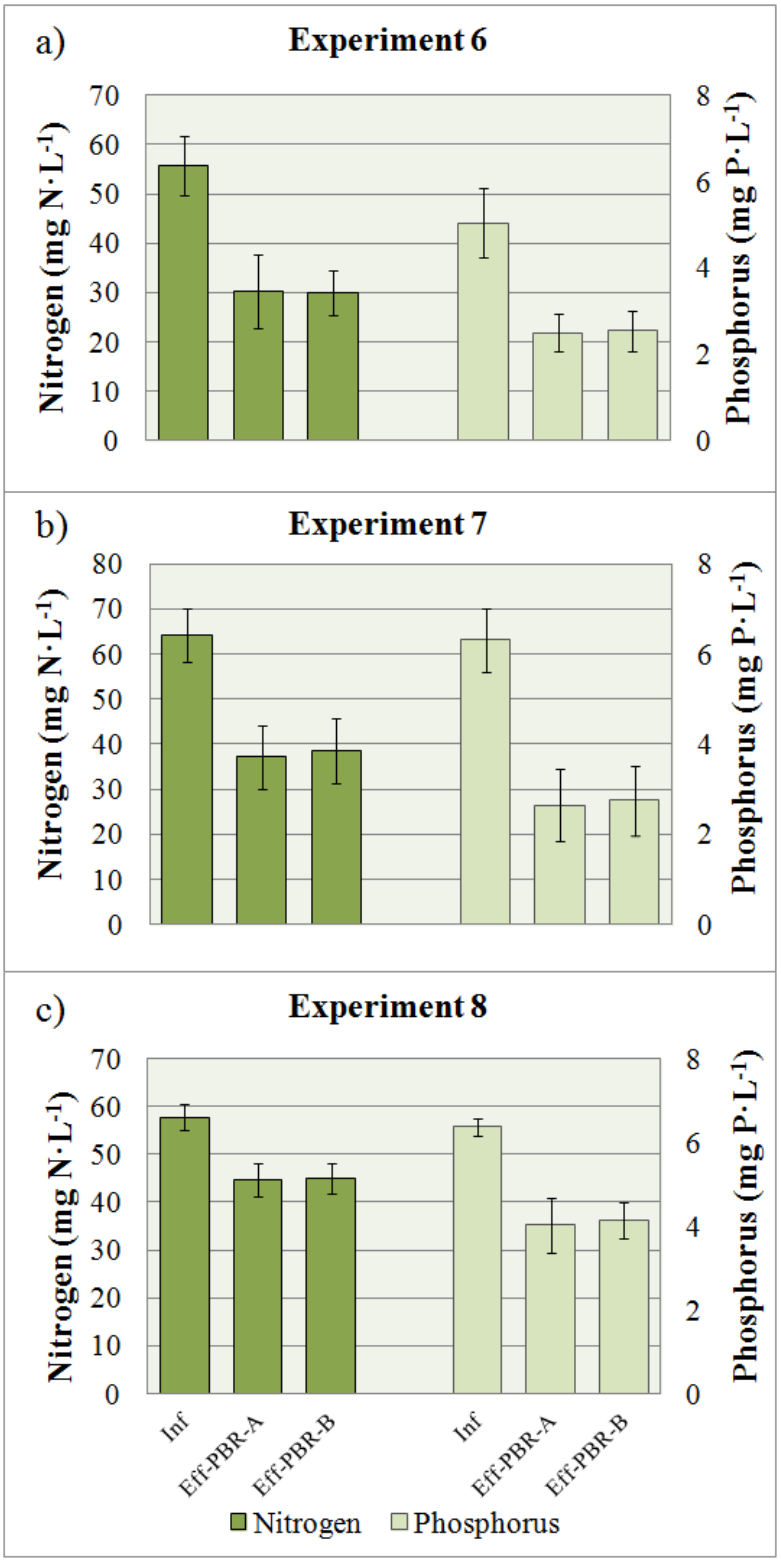

Figure VII.4. Effect of photoperiods. Average measures (and standard deviation) of nitrogen and phosphorus concentration in the influent and effluent of PBR-A and PBR-B, in: a) Experiment 6; b) Experiment 7; and c) Experiment 8.

4. DISCUSSION

The results have been discussed according to the two different situations in the Experiments evaluated: i) the net photon flux was higher in PBR-A than in PBR-B (Experiments 1, 2A and 3); and ii) the net photon flux was the same for both PBR-A and PBR-B (Experiments 2B, 4, 5, 6, 7 and 8).

It must be highlighted that factors which influence microalgae growth such as solar irradiance (Mehan et al., 2018; Otondo et al., 2018), temperature (García-Cubero et al., 2018, Xin et al., 2011), nutrient loading rates (González-Camejo et al., 2018; Guldhe et al., 2017) and culture mixing (Barceló-Villalobos et al., 2019; Huang et al., 2017) were the same for PBR-A and PBR-B in each experiment, only differing in the artificial lighting regime. In addition, nutrients were maintained in replete conditions (i.e., nitrogen higher than 10 mg $N \cdot L^{-1}$ and phosphorus above negligible concentration as explained in Pachés et al. (2018)) during all the Experiments except for 1 and 2A (Figure VII.2a). Hence, microalgae were only considered to be nutrient-limited in PBR-A during Experiments 1 and 2A.

4.1. *Different net photon flux*

When PBR-A was lit by a higher photon flux than PBR-B (i.e., in Experiments 1, 2A and 3), it achieved higher performance in terms of nutrient effluent concentrations, nutrient recovery rates and biomass productivities. It can thus be concluded that the highest artificial lighting (300 $\mu mol \cdot m^{-2} \cdot s^{-1}$) increased the nutrient recovery capacity and biomass production of the PBRs, which suggested that the system was light-limited.

Other lab-scale experiment showed different results. For instance, Gris et al. (2014) did not observe any enhancement in the growth rate of *Scenedesmus obliquus* at light intensities over 150 $\mu mol \cdot m^{-2} \cdot s^{-1}$, while Deng et al. (2019) obtained optimal daily average irradiances of 90 $\mu mol \cdot m^{-2} \cdot s^{-1}$ for *Chlorella kessleri*. In these lab-scale photobioreactors, microalgae were expected to suffer from photoinhibition since it usually occurs at light irradiances of around 200 $\mu mol \cdot m^{-2} \cdot s^{-1}$ (Raeisossadati et al., 2019). However, the light path of those lab-scale photobioreactors was short (lower than 10 cm). On the contrary, PBRs of this study presented a considerably wide light path (i.e., 25 cm). Consequently, the shadow effect in this PBR (González-Camejo et al., 2019) might be more significant than those of lab-scale studies in spite of receiving higher light irradiance, leaving a significant volume of the PBR in darkness (Barceló-Villalobos et al., 2019; González-Camejo et al., 2019), hence reducing the light

availability in the pilot-scale PBRs. The PBR light path therefore plays a significant role in making light available to the culture (Abu-Ghosh et al., 2016; Wagner et al., 2018). Indeed, there is a current tendency to reduce PBR depth in order to increase the algae's photosynthetic efficiency, although this requires a larger area (Castrillo et al., 2018). Further research needs to be done to find the best PBR width without excessively increasing the surface area required for microalgae cultivation.

It must be also noted that in Experiments 1, 2A and 3, the efficiency in the use of light for biomass production (i.e., BP:I) was always higher in PBR-B, where less artificial photon flux was supplied than in PBR-A (artificial light intensity of 300 $\mu mol \cdot m^{-2} \cdot s^{-1}$). This indicated a lower photosynthetic efficiency at higher photon fluxes (Markou et al., 2017; Sepúlveda et al., 2015). One hypothesis for this behaviour is that most of the algae in the culture were acclimatised to poor lighting because of the large dark volume of the PBRs (González-Camejo et al., 2019). In these light-limited conditions, microalgae tend to assemble a larger photosynthetic antenna which forces the poorly light-adapted cells to absorb excessive photons when lit (Pires et al., 2017; Raeisossadati et al., 2019; Straka and Rittman, 2018), reducing their efficiency (Nwoba et al., 2019). This effect could be expected to be greater in PBR-A.

With respect to the efficiency of light use for nutrient recovery (i.e., NRR:I and PRR:I), PBR-B also showed higher values than PBR-A, but only during Experiment 1, when none artificial light source was applied to PBR-B. This could have been related to the fact that microalgae can assimilate nutrients in dark conditions until reaching maximum biomass nutrient content, although they cannot synthesise new algae biomass (Ferro et al., 2018; Ruiz et al., 2014). Nutrient consumption in Experiment 1 could also have been influenced by the limited nitrogen and phosphorus in PBR-A, since this has been reported to reduce nitrogen recovery rates (Pachés et al., 2018; Ruiz-Martínez et al., 2014). On the contrary, when PBR-B was lit by artificial light intensity of 150 $\mu mol \cdot m^{-2} \cdot s^{-1}$, both PBRs showed similar results in NRR:I and PRR:I, possibly due to PBR-B not being in complete darkness at any time. Since the algae were continuously lit artificially in both PBRs during Experiments 2A and 3 (although at different net photon fluxes), they were always able to grow, preventing the extra accumulation of intracellular nutrients (Ruiz et al., 2014).

Regarding cell concentration, there were no significant differences between PBR-A and PBR-B in Experiments 1 and 2A, which suggests that the higher biomass productivity achieved in PBR-A during these Experiments was probably due to the larger cell size of

its microalgae. In fact, microalgae can vary their size by up to 100% (Lehmuskero et al., 2018). In this respect, Wu et al. (2015) found that the inhibition of microalgae cell division was not directly related to light intensity, but to the availability of phosphorus in the culture, which is the main element in the synthesis of DNA and RNA (Powell et al., 2009). In addition, Baroni et al. (2019) reported a cell size increase when nitrogen was scarce since it prevented protein synthesis. Under nutrient starvation (as in the case of PBR-A in Experiments 1 and 2A, see Figure VII.2), there was probably limited synthesis of proteins and genetic materials in the microalgae cells, which could have led to less cell division. Nonetheless, the synthesis of other materials such as carbohydrates and lipids is not so seriously affected by a short-term scarcity of nutrients (Baroni et al., 2019; Shoener et al., 2019; Wu et al., 2015), so that they were able to increase in size in Experiments 1 and 2A. On the contrary, in Experiment 3 the microalgae culture was not nutrient-limited (Figure VII.2c) and algae were therefore able to synthesise new genetic material and proteins (Baroni et al., 2019; Wu et al., 2015). PBR-A therefore probably used the higher amount of light photons to produce new cells instead of increasing their cell size, showing a higher cell concentration in PBR-A in comparison to PBR-B during Experiment 3 (section VII.3.2).

In the case of Experiment 1, the extra photons supplied by the artificial lighting could have triggered the chlorophyll synthesis in PBR-A, since chlorophyll was not synthesised in darkness. Consequently, higher chlorophyll concentration was obtained in PBR-A than in PBR-B. On the other hand, in Experiment 3, both PBRs were continuously lit, but at different photon flux; i.e., PBR-A had an artificial light L:D cycle of 24:0, while PBR-B alternated the natural radiation during daytime and artificial lighting at night time. In this situation, higher chlorophyll content was obtained in PBR-B, which agrees with Chen et al. (2011). These authors found that microalgae synthesise more chlorophyll under lower net photon flux in order to absorb as many photons as possible.

4.2. Same net photon flux

Experiments 4, 5, 6, 7 and 8 were carried out using different light duration or photoperiods, but maintaining the same net photon flux in both PBRs during each experiment. As a result, no significant differences between PBR-A and PBR-B were observed in the effluent nutrient concentrations (Figures VII.3 and VII.4), nutrient recovery rates, biomass productivities (Table VII.3) and chlorophyll content (section

VII.3). This disagrees with the results of other authors obtained under lab conditions. For instance, Li et al. (2016), under constant light energy consumption, observed higher microalgae productivity under continuous illumination than with 12:12 h L:D cycles. In addition, Abu-Ghosh et al. (2016) and Park and Lee (2001) reported an enhancement of the microalgae photosynthetic activity when dark periods were shortened.

A possible reason for the similar results obtained in this study could lie in the culture mixing. In mixed PBRs, microalgae cells rapidly move between the illuminated areas near the surface and the deeper dark zones (Barceló-Villalobos et al., 2019), creating a random flashing light effect which can enhance photosynthetic efficiency (Iluz and Abu-Ghosh, 2016; Raeisossadati et al., 2019). According to Barceló-Villalobos et al. (2019), the effect of this random flashing light effect on the photosynthetic rate of microalgae can be more significant than light intensity on the PBR surface. Hence, the theoretical benefits on microalgae performance caused by L:D cycles applied to the PBRs (Lee and Lee, 2001; Park and Lee, 2001) seemed to be vanished by this random flashing light effect produced due to mixing.

On the other hand, nutrient recovery rates were significantly lower in Experiment 8 than in the rest of experiments, probably due to the lower light exposure (L:D cycles of 8:16 h) (Binnal and Babu, 2017). These results therefore suggest that microalgae performance depends on the net photon flux received, and not on the lighting regime or the time of day that this energy is received. In fact, in Experiment 2A and 3, in which PBR-B received the same photon flux with different lighting regime, an analogous behaviour with respect to PBR-A was observed (section VII.4.1).

Further studies will be required to assess the long-term feasibility of adding an artificial light source to treat AnMBR effluents and/or designing PBRs with enhanced light availability. Raising the net photon flux by an artificial light source would increase nutrient recovery rates and biomass productivity. Higher nutrient recoveries would enable shorter operating HRT, thus reducing total PBR volume, while high biomass productivities would increase biofuel production from the microalgae biomass (Guldhe et al., 2017), although this would involve higher operating costs.

Results from Experiment 2B suggest the initial state of the microalgae culture did not have a significant influence on the performance of microalgae in this system. Similar behaviour was found in lab conditions by Su et al. (2012); when they cultivated microalgae with initial concentrations of 200, 500 and 800 mg VSS·L^{-1}, NRR increased with higher initial concentration, from 5.4 to 10.8 mg N·L^{-1}·d^{-1} in batch experiments

which lasted a maximum of 9 days. When the batch experiments were lengthened to 14 days, NRR were similar: 4.4-4.8 mg $N \cdot L^{-1} \cdot d^{-1}$. On the other hand, in a previous study in an outdoor membrane photobioreactor (MPBR) plant (González-Camejo et al., 2018), 60.3% higher NRR was obtained with higher initial biomass (270 mg $VSS \cdot L^{-1}$ in comparison to 160 mg $VSS \cdot L^{-1}$). The initial concentration of 160 mg $VSS \cdot L^{-1}$ obtained in this previous study was unlikely to be consistent enough to obtain optimum performance. However, in the present work, PBR-B started Period 2B with a consistent concentration of 300 mg $VSS \cdot L^{-1}$.

5. CONCLUSIONS

The PBR in an outdoor operation of a mixed microalgae culture treating AnMBR effluent supplied with higher net photon flux (either higher light intensity or duration) obtained better results in terms of nutrient recovery and biomass productivity. Maximum NRR, PRR and biomass productivity of 7.7 ± 1.6 mg $N \cdot L^{-1} \cdot d^{-1}$, 1.03 ± 0.21 mg $P \cdot L^{-1} \cdot d^{-1}$ and 100 ± 32 mg $VSS \cdot L^{-1} \cdot d^{-1}$, respectively, were obtained under continuous artificial illumination with an average light intensity of 300 $\mu mol \cdot m^{-2} \cdot s^{-1}$. No photoinhibiton was observed at the highest net photon flux, probably because of the significant shadow effect on the microalgae inside the PBRs. The system thus appeared to be light-limited. However, the biomass productivity:light irradiance ratios were higher with reduced net photon flux, indicating that the higher net photon flux entailed lower light-use efficiency.

When the system was phosphorus-limited, the increase in microalgae biomass was seen to be due to larger cell size and not to higher cell numbers.

None of the experiments with the same net photon flux showed any significant differences, showing that the microalgae performance in this outdoor PBR in the operating conditions evaluated did not depend on the time of day when light was supplied or the length of the photoperiods, but on the net photon flux.

The mixing rate of the PBR and the significant PBR light path (25 cm) were probably responsible for creating a random flashing light effect, which could have outweighed the effects of the frequency photoperiods.

Further studies on PBR width and on the light supply inside the culture will be required to improve photosynthetic efficiency. This would provide higher nutrient recovery and biomass productivity in outdoor microalgae cultivation treating AnMBR effluent.

ACKNOWLEDGEMENTS

This research work was supported by the Spanish Ministry of Economy and Competitiveness (MINECO, Projects CTM2014-54980-C2-1-R, CTM2014-54980-C2-2-R, CTM2011-28595-C02-01 and CTM2011-28595-C02-02) jointly with the European Regional Development Fund (ERDF), both of which are gratefully acknowledged. It was also supported by the Spanish Ministry of Education, Culture and Sport via a pre doctoral FPU fellowship to author J. González-Camejo (FPU14/05082).

AUTHORS' CONTRIBUTION

J. González-Camejo, M.V. Ruano and R. Barat designed the experiments. J. González-Camejo and A. Viruela carried out the maintenance of the pilot plant and the analysis of the samples. J. González-Camejo interpreted the data and elaborated the numerical information (i.e., graphics, tables, statistical information, etc). J. González-Camejo, M.V. Ruano and R. Barat were in charge of writing the manuscript. A. Seco and J. Ferrer supervised the work and were involved in the deep discussion and revision of the manuscript.

CONFLICT OF INTEREST STATEMENT

The authors declare that there are no financial and personal relationships with other people or organizations that could influence their work.

STATEMENT OF INFORMED CONSENT, HUMAN/ANIMAL RIGHTS

No conflicts, informed consent, human or animal rights applicable.

DECLARATION OF AUTHORS' AGREEMENT

The authors agree to submit this research manuscript for publication in Algal Research. No other people have been involved in this study.

REFERENCES

1. Abu-Ghosh, S., Fixler, D., Dubinsky, Z., Iluz, D., 2016. Flashing light in microalgae biotechnology. Bioresour. Technol. 203, 357-363. http://dx.doi.org/10.1016/j.biortech.2015.12.057
2. Abu-Ghosh, S. Fixler, D., Dubinsky, Z., Iluz, D., 2015. Continuous background light significantly increases flashing-light enhancement of photosynthesis and growth of

microalgae. Bioresour. Technol. 187, 144–148. https://doi.org/10.1016/j.biortech.2015.03.119

3. Acién, F.G., Gómez-Serrano, C., Morales-Amaral, M.M., Fernández-Sevilla, J.M., Molina-Grima E., 2016. Wastewater treatment using microalgae: how realistic a contribution might it be to significant urban wastewater treatment? Appl. Microbiol. Biotechnol. 100, 9013–9022. http://dx.doi.org/10.1007/s00253-016-7835-7
4. A.P.H.A., A.W.W.A., W.P.C.F., 2005. Standard methods for the examination of water and wastewater, 21st edition, American Public Health Association, American Water Works Association, Water Pollution Control Federation, Washington DC, USA.
5. Atta, M., Idris, A., Bukhari, A., Wahidin, S., 2013. Intensity of blue LED light: A potential stimulus for biomass and lipid content in fresh water microalgae *Chlorella vulgaris*. Bioresour. Technol. 148, 373‑378. http://dx.doi.org/10.1016/j.biortech.2013.08.162
6. Baker, N.R., 2008. Chlorophyll Fluorescence: A Probe of Photosynthesis in Vivo. Annu. Rev. Plant Biol. 59, 89-113. https://doi.org/10.1146/annurev.arplant.59.032607.092759
7. Barceló-Villalobos, M., Fernández-del Olmo, P., Guzmán, J.L., Fernández-Sevilla, J.M., Acién Fernández, F.G., 2019. Evaluation of photosynthetic light integration by microalgae in a pilot-scale raceway reactor. Bioresour. Technol. 280, 404-411. https://doi.org/10.1016/j.biortech.2019.02.032
8. Baroni, E.G., Yap, K.Y., Webley, P.A., Scales, P.J., Martin, G.J.O., 2019. The effect of nitrogen depletion on the cell size, shape, density and gravitational settling of *Nannochloropsis salina*, *Chlorella* sp. (marine) and *Haematococcus pluvialis*. Algal Res. 39, 101454. https://doi.org/10.1016/j.algal.2019.101454
9. Behera, B., Acharya, A., Gargey, I.A., Aly, N., Balasubramanian, P., 2018. Bioprocess engineering principles of microalgal cultivation for sustainable biofuel production. Bioresour. Technol. Reports 5, 297-316. https://doi.org/10.1016/j.biteb.2018.08.001
10. Binnal, P., Babu, P.N., 2017. Optimization of environmental factors affecting tertiary treatment of municipal wastewater by *Chlorella protothecoides* in a lab scale photobioreactor. J. Water Process Eng. 17, 290-298. http://dx.doi.org/10.1016/j.jwpe.2017.05.003
11. Cabanelas, I.T.D., Ruiz, J., Arbib, Z., Chinalia, F.A., Garrido-Pérez, C., Rogalla, F., Nascimento, I.A., Perales, J.A., 2013. Comparing the use of different domestic wastewaters for coupling microalgal production and nutrient removal. Bioresour. Technol. 131, 429–436. https://doi.org/10.1016/j.biortech.2012.12.152

12. Carvalho, A.P., Silva, S.O., Baptista, J.M., Malcata, F.X., 2011. Light requirements in microalgal photobioreactors: an overview of biophotonic aspects. Appl. Microbiol. Biotechnol. 89, 1275-1288. https://doi.org/10.1007/s00253-010-3047-8
13. Castrillo, M., Díez-Montero, R., Tejero, I., 2018. Model-based feasibility assessment of a deep solar photobioreactor for microalgae culturing. Algal Res. 29, 304–318. https://doi.org/10.1016/j.algal.2017.12.004
14. Chen, X., Goh, Q.Y., Tan, W., Hossain, I., Chen, W.N., Lau, R., 2011. Lumostatic strategy for microalgae cultivation utilizing image analysis and chlorophyll a content as design parameters. Bioresour. Technol. 102, 6005-6012. https://doi.org/10.1016/j.biortech.2011.02.061
15. Cuaresma, M., Janssen, M., van den End, E.J., Vílchez, C., Wijffels, R.H., 2011. Luminostat operation: A tool to maximize microalgae photosynthetic efficiency in photobioreactors during the daily light cycle? Bioresour. Technol. 102, 7871-7878. https://doi.org/10.1016/j.biortech.2011.05.076
16. Deng, X., Chen, B., Xue, C., Li, D., Hu, X., Gao, K., 2019. Biomass production and biochemical profiles of a freshwater microalga *Chlorella kessleri* in mixotrophic culture: effects of light intensity and photoperiodicity. Bioresour. Technol. 273, 358-367. https://doi.org/10.1016/j.biortech.2018.11.032
17. De Vree, J.H., Bosma, R., Janssen, M., Barbosa, M.J., Wijffels, R.H., 2015. Comparison of four outdoor pilot-scale photobioreactors. Biotechnol. Biofuels, 8:215. https://doi.org/10.1186/s13068-015-0400-2
18. Ferro, L., Gorzsás, A., Gentili, F.G., Funk, C., 2018. Subarctic microalgal strains treat wastewater and produce biomass at low temperature and short photoperiod. Algal Res. 35, 160-167. https://doi.org/10.1016/j.algal.2018.08.031
19. García-Cubero, R., Moreno-Fernández, J., Acién-Fernández, F.G., García-González, M., 2018. How to combine CO_2 abatement and starch production in *Chlorella vulgaris*. Algal Res. 32, 270-279. https://doi.org/10.1016/j.algal.2018.04.006
20. Garrido-Cárdenas, J., Manzano-Agugliaro, F., Acién-Fernández, F.G., Molina-Grima, E., 2018. Microalgae research worldwide. Algal Res. 35, 50-60. https://doi.org/10.1016/j.algal.2018.08.005
21. Giménez, J.B., Robles, A., Carretero, L., Durán, F., Ruano, M.V., Gatti, M.N., Ribes, J., Ferrer, J., Seco, A., 2011. Experimental study of the anaerobic urban wastewater treatment in a submerged hollow-fibre membrane bioreactor at pilot scale. Bioresour. Technol. 102, 8799–8806.
22. Gonçalves, A.L., Pires, J.C.M., Simões, M., 2016. Biotechnological potential of *Synechocystis salina* co-cultures with selected microalgae and cyanobacteria: Nutrients

removal, biomass and lipid production. Bioresour. Technol. 200, 279-286. https://doi.org/10.1016/j.biortech.2015.10.023

23. González-Camejo, J., Viruela, A., Ruano, M.V., Barat, R., Seco, A., Ferrer, J., 2019. Dataset to assess the shadow effect of an outdoor microalgae culture. Data in Brief 25, 104143. https://doi.org/10.1016/j.dib.2019.104143
24. Gonzalez-Camejo, J., Barat, R., Ruano, M.V., Seco, A., Ferrer, J., 2018. Outdoor flat-panel membrane photobioreactor to treat the effluent of an anaerobic membrane bioreactor. Influence of operating, design and environmental conditions. Water Sci. Technol. 78(1) 195-206. http://dx.doi.org/10.2166/wst.2018.259
25. González-Camejo, J., Serna-García, R., Viruela, A., Pachés, M., Durán, F., Robles, A., Ruano, M.V., Barat R., Seco, A., 2017. Short and long-term experiments on the effect of sulphide on microalgae cultivation in tertiary sewage treatment. Bioresour. Technol. 244, 15-22. http://dx.doi.org/10.1016/j.biortech.2017.07.126
26. Gris, B., Morosinotto, T., Giacometti, G.M., Bertucco, A., Sforza, E., 2014. Cultivation of Scenedesmus obliquus in Photobioreactors: Effects of Light Intensities and Light–Dark Cycles on Growth, Productivity, and Biochemical Composition, Appl. Biochem. Biotechnol. 172, 2377–2389. http://dx.doi.org/10.1007/s12010-013-0679-z
27. Guldhe, A., Kumari, S., Ramanna, L., Ramsundar, P., Singh, P., Rawat, I., Bux, F., 2017. Prospects, recent advancements and challenges of different wastewater streams for microalgal cultivation. J. Environ. Manag. 203, 299-315. http://dx.doi.org/10.1016/j.jenvman.2017.08.012
28. Huang, Q., Jiang, F., Wang, L., Yang, C., 2017. Design of Photobioreactors for Mass Cultivation of Photosynthetic Organisms. Engineering 3, 318-329. http://dx.doi.org/10.1016/J.ENG.2017.03.020
29. Iasimone, F., Panico, A., De Felice, V., Fantasma, F., Iorizzi, M., Pirozzi, F., 2018. Effect of light intensity and nutrients supply on microalgae cultivated in urban wastewater: Biomass production, lipids accumulation and settleability characteristics. Journal of Environ. Manag. 223, 1078–1085. https://doi.org/10.1016/j.jenvman.2018.07.024
30. Iluz, D., Abu-Ghosh, S. 2016. A novel photobioreactor creating fluctuating light from solar energy for a higher light-to-biomass conversion efficiency. Energy Conversion and Management 126. 767–773. https://doi.org/10.1016/j.enconman.2016.08.045
31. Jacob-Lopes, E., Scoparo, C.H.G., Lacerda, L.M.C.F., Franco, T.T., 2009. Effect of light cycles (night/day) on CO_2 fixation and biomass production by microalgae in photobioreactors. Chem. Eng. Process. 48, 306-310. http://dx.doi.org/10.1016/j.cep.2008.04.007

32. Jebali, A., Acién, F.G., Rodriguez Barradas, E., Olguín, E.J., Sayadi, S., Molina Grima, E., 2018. Pilot-scale outdoor production of *Scenedesmus* sp. in raceways using flue gases and centrate from anaerobic digestion as the sole culture medium. Bioresour. Technol. 262, 1-8. https://doi.org/10.1016/j.biortech.2018.04.057
33. Jeffrey, S.W., Humphrey, G.F., 1975. New spectrophotometric equations for determining chlorophylls *a, b, c1* and *c2* in higher plants, algae and natural phytoplankton. Biochem. Physiol. Pflanzen (BPP), Bd. 167, 191-194.
34. Lazar, D., 1999. Chlorophyll a fluorescence induction. Biochimica et Biophysica Acta 1412, 1-28.
35. Lee, K., Lee, C.G., 2001. Effect of light/dark cycles on wastewater treatments by microalgae. Biotechnology Bioprocess Engineering 6(3), 194-199.
36. Lehmuskero, A., Chauton, M.S., Boström, T., 2018. Light and photosynthetic microalgae: A review of cellular- and molecular-scale optical processes. Progress in Oceanography 168, 43-56. https://doi.org/10.1016/j.pocean.2018.09.002
37. Li, J., Bin, H., Lin, J., Chen, F., Miao, X., 2016. Effects of light-emitting diodes under capped daily energy consumption with combinations of electric power and photoperiod on cultivation of *Chlorella pyrenoidosa.* Bioresour. Technol. 205, 126-132. http://dx.doi.org/10.1016/j.biortech.2016.01.041
38. Liao, Q., Sun, Y., Huang, Y., Xia, A., Fu, Q., Zhu, X., 2017. Simultaneous enhancement of *Chlorella vulgaris* growth and lipid accumulation through the synergy effect between light and nitrate in a planar waveguide flat-plate photobioreactor. Bioresour. Technol. 243, 528-538. http://dx.doi.org/10.1016/j.biortech.2017.06.091
39. Markou, G., Dao, L.H.T., Muylaert, K., Beardall, J., 2017. Influence of different degrees of N limitation on photosystem II performance and heterogeneity of *Chlorella vulgaris*. Algal Res. 26, 84-92. h ttp://dx.doi.org/10.1016/j.algal.2017.07.005
40. Martínez, C., Mairet, F., Bernard, O., 2018. Theory of turbid microalgae cultures. Journal of Theoretical Biology 456, 190-200. http://dx.doi.org/10.1016/j.jtbi.2018.07.016
41. Mehan, L., Verma, R., Kumar, R., Srivastava, A., 2018. Illumination wavelengths effect on *Arthrospira platensis* production and its process applications in River Yamuna water treatment, J. Water Process Eng. 23, 91-96. https://doi.org/10.1016/j.jwpe.2018.03.010
42. Morales-Amaral, M., Gómez-Serrano, C., Acién, F.G., Fernández-Sevilla, J.M., Molina-Grima, E., 2015. Outdoor production of *Scenedesmus* sp. in thin-layer and raceway reactors using centrate from anaerobic digestion as the sole nutrient source. Algal Res. 12, 99-108. http://dx.doi.org/10.1016/j.algal.2015.08.020

43. Muñoz, R., Guieysse, B., 2006. Algal–bacterial processes for the treatment of hazardous contaminants: A review. Water Res. 40(15), 2799-2815. https://doi.org/10.1016/j.watres.2006.06.011
44. Nwoba, E.G., Parlevliet, D.A., Laird, D.W., Alameh, K., Moheimani, N.R., 2019. Light management technologies for increasing algal photobioreactor efficiency. Algal Res. 39, 101433. https://doi.org/10.1016/j.algal.2019.101433
45. Otondo, A., Kokabian, B., Stuart-Dahl, S., Gude, V.G., 2018. Energetic evaluation of wastewater treatment using microalgae *Chlorella vulgaris*. J. Environ. Chem. Eng. 6(2) (2018) 3213-3222. https://doi.org/10.1016/j.jece.2018.04.064M
46. Pachés, M., Martínez-Guijarro, R., González-Camejo, J., Seco, A., Barat, R., 2018. Selecting the most suitable microalgae species to treat the effluent from an anaerobic membrane bioreactor. Environ. Technol. (in press). https://doi.org/10.1080/09593330.2018.1496148
47. Pachés, M., Romero, I., Hermosilla, Z., Martinez-Guijarro, R., 2012. HYMED: An ecological classification system for the Water Framework Directive based on phytoplankton community composition. Ecological Indicators 19, 15-23. https://doi.org/10.1016/j.ecolind.2011.07.003
48. Park, K.H., Lee, C.G., 2001. Effectiveness of flashing light for increasing photosynthetic efficiency of microalgal cultures over a critical cell density, Biotechnology and Bioprocess Engineering 6, 189-193.
49. Pires, J.C.M., Alvim-Ferraz, M.C.M., Martins, F.G., 2017. Photobioreactor design for microalgae production through computational fluid dynamics: A review. Renew. Sust. Energy Rev. 79, 248–254. https://doi.org/10.1016/j.rser.2017.05.064
50. Powell, N., Shilton, A., Chisti, Y., Pratt, S., 2009. Towards a luxury uptake process via microalgae – Defining the polyphosphate dynamics. Water Res. 43, 4207-4213. https://doi:10.1016/j.watres.2009.06.011
51. Raeisossadati, M., Moheimani, N.R., Parlevliet, D., 2019. Luminescent solar concentrator panels for increasing the efficiency of mass microalgal production. Renew. Sust. Energy Rev. 101, 47–59. https://doi.org/10.1016/j.rser.2018.10.029
52. Ramanna, L., Rawat, I., Bux, F., 2017. Light enhancement strategies improve microalgal biomass productivity. Renew. Sust. Energy Rev. 80, 765–773. http://dx.doi.org/10.1016/j.rser.2017.05.202
53. Razzak, S.A., Ali, S.A.M., Hossain, M.M., deLasa, H., 2017. Biological CO_2 fixation with production of microalgae in wastewater – A review. Renew. Sust. Energy Rev. 76, 379–390.http://dx.doi.org/10.1016/j.rser.2017.02.038
54. Rinna, F., Buono, S., Cabanelas, I.T.D., Nascimento, I.A., Sansone, G., Barone, C.M.A., 2017. Wastewater treatment by microalgae can generate high quality biodiesel

feedstock. J. Water Process Eng. 18, 144-149. http://dx.doi.org/10.1016/j.jwpe.2017.06.006

55. Romero-Villegas, G.I., Fiamengo, M., Acién-Fernández, F.G., Molina-Grima, E., 2018. Utilization of centrate for the outdoor production of marine microalgae at the pilot-scale in raceway photobioreactors, J. Environ. Manag. 228, 506–516. https://doi.org/10.1016/j.jenvman.2018.08.020
56. Ruiz, J., Arbib, Z., Álvarez-Díaz, P.D., Garrido-Pérez, C., Barragán, J., Perales, J.A., 2014. Influence of light presence and biomass concentration on nutrient kinetic removal from urban wastewater by *Scenedesmus obliquus*. J. Biotechnol. 178, 32-37. http://dx.doi.org/10.1016/j.jbiotec.2014.03.001
57. Ruiz-Martinez, A., Serralta, J., Pachés, M., Seco, A., Ferrer, J., 2014. Mixed microalgae culture for ammonium removal in the absence of phosphorus: Effect of phosphorus supplementation and process modeling. Process Biochem. 49, 2249-2257. http://dx.doi.org/10.1016/j.procbio.2014.09.002
58. Seco, A., Aparicio, S., González-Camejo, J., Jiménez-Benítez, A., Mateo, O., Mora, J.F., Noriega-Hevia, G., Sanchis-Perucho, P., Serna-García, R., Zamorano-López, N., Giménez, J.B., Ruiz-Martinez, A., Aguado, D., Barat, R., Borrás, L., Bouzas, A., Martí, N., Pachés, M., Ribes, J., Robles, A., Ruano, M.V., Serralta, J. and Ferrer, J., 2018. Resource recovery from sulphate-rich sewage through an innovative anaerobic-based water resource recovery facility (WRRF). Water Science and Technology 78 (9), 1925-1936. https://doi.org/10.2166/wst.2018.492
59. Sepúlveda, C., Acién, F.G., Gómez, C., Jiménez-Ruíz, N., Riquelme, C., Molina-Grima, E., 2015. Utilization of centrate for the production of the marine microalgae *Nannochloropsis gaditana*, Algal Res. 9, 107-116. http://dx.doi.org/10.1016/j.algal.2015.03.004
60. Shoener, B.D., Schramm, S.M., Béline, F., Bernard, O., Martínez, C., Plósz, B.G., Snowling, S., Steyer, J.P., Valverde-Pérez, B., Wágner, D., Guest, J.S., 2019. Microalgae and cyanobacteria modeling in water resource recovery facilities: A critical review. Water Res. X 2, 100024. https://doi.org/10.1016/j.wroa.2018.100024
61. Straka, L., Rittmann, B.E., 2018. Light-dependent kinetic model for microalgae experiencing photoacclimation, photodamage, and photodamage repair. Algal Res. 31, 232–238. https://doi.org/10.1016/j.algal.2018.02.022
62. Su, Y., Mennerich, A., Urban, B., 2012. Coupled nutrient removal and biomass production with mixed algal culture: Impact of biotic and abiotic factors. Bioresour. Technol. 118, 469-476. http://dx.doi.org/10.1016/j.biortech.2012.05.093
63. Tan, X.B., Zhang, Y.L., Yang, L.B., Chu, H.Q., Guo, J., 2016. Outdoor cultures of *Chlorella pyrenoidosa* in the effluent of anaerobically digested activated sludge: The

effects of pH and free ammonia. Bioresour. Technol. 200, 606-615. http://dx.doi.org/10.1016/j.biortech.2015.10.095

64. Verma, R., Srivastava, A., 2018. Carbon dioxide sequestration and its enhanced utilization by photoautotroph microalgae, Environ. Dev. 27, 95–106. https://doi.org/10.1016/j.envdev.2018.07.004
65. Viruela, A., Murgui, M., Gómez-Gil, T., Durán, F., Robles, Á, Ruano, M.V., Ferrer, J., Seco, A., 2016. Water resource recovery by means of microalgae cultivation in outdoor photobioreactors using the effluent from an anaerobic membrane bioreactor fed with pre-treated sewage. Bioresour. Technol. 218, 447-454. http://dx.doi.org/10.1016/j.biortech.2016.06.116
66. Vo, H.N.P., Ngo, H.H., Guo, W., Minh, T., Nguyen, H., Liu, Y., Liu, Y., Nguyen, D.D., Chang, S.W., 2019. A critical review on designs and applications of microalgae-based photobioreactors for pollutants treatment. Sci. Total Environ. 651(1), 1549-1568. http://dx.doi.org/10.1016/j.scitotenv.2018.09.282
67. Wagner, D.S., Valverde-Perez, B., Plosz, B.G., 2018. Light attenuation in photobioreactors and algal pigmentation under different growth conditions – Model identification and complexity assessment, Algal Res. 35, 488-499. https://doi.org/10.1016/j.algal.2018.08.019
68. Wang, B., Lan, C.Q., Horsman, M., 2012. Closed photobioreactors for production of microalgal biomasses. Biotechnol. Adv. 30(4), 904-912. https://doi.org/10.1016/j.biotechadv.2012.01.019.
69. Wu, Y.H., Yu, Y., Hu, H.Y., 2015. Microalgal growth with intracellular phosphorus for achieving high biomass growth rate and high lipid/triacylglycerol content simultaneously. Bioresour. Technol. 192, 374-381. http://dx.doi.org/10.1016/j.biortech.2015.05.057
70. Xin, L., HU, H.Y., Yu-Ping, Z., 2011. Growth and lipid accumulation properties of a freshwater microalga *Scenedesmus* sp. under different cultivation temperature. Bioresour. Technol. 102, 3098-3102. doi:10.1016/j.biortech.2010.10.055
71. Yan, C., Zhang, L., Luo, X., Zheng, Z., 2013. Effects of various LED light wavelengths and intensities on the performance of purifying synthetic domestic sewage by microalgae at different influent C/N ratios. Ecol. Eng. 51, 24-32. http://dx.doi.org/10.1016/j.ecoleng.2012.12.051
72. Zhou, Q., Zhang, P., Zhan, G., Peng, M., 2015. Biomass and pigments production in photosynthetic bacteria wastewater treatment: Effects of photoperiod. Bioresour. Technol. 190, 196-200. http://dx.doi.org/110.1016/j.biortech

DATASET TO ASSESS THE SHADOW EFFECT OF AN OUTDOOR MICROALGAE CULTURE (DATA IN BRIEF)

González-Camejo, J., Viruela, A., Ruano, M.V., Barat, R., Seco, A., Ferrer, J., 2019. Dataset to assess the shadow effect of an outdoor microalgae culture. Data in Brief 25, 104143. https://doi.org/10.1016/j.dib.2019.104143

ABSTRACT

This data in brief (DIB) article is related to a Research article (González-Camejo et al., 2019).

Microalgae biomass absorb the light photons that are supplied to the culture, reducing the light availability in the inner parts of the photobioreactors. This is known as self-shading or shadow effect. This effect has been widely studied in lab conditions, but information about self-shading in outdoor photobioreactors is scarce.

How this shadow effect affects the light availability in an outdoor photobioreactor was evaluated. In addition, advantages and disadvantages of different artificial light sources which can overcome light limitation are described.

VALUE OF THE DATA

- This data can be used to select the most appropriate artificial light source to cultivate microalgae.
- The shadow effect of a microalgae culture is evaluated under natural conditions.
- A comparison between shadow effect at high and low biomass concentration is presented.
- This data can be useful to reduce the light limitation in outdoor microalgae cultivation systems.

1. DATA

This data includes information related to the reduction of light intensity within a microalgae culture and how this reduction varies with the microalgae biomass concentration (Figure VII.A.1). The microalgae close to the surface in a photobioreactor (PBR) absorb most of the photons, restricting the light received in the inner part of the PBR (Barceló-Villalobos et al., 2019). This is known as shadow effect or self-shading

(Liao et al., 2017; Nwoba et al., 2019). According to Figure VII.A.1, the difference in the solar radiation between PAR-2 (outside of the PBR) and PAR-1 (2 cm away from the front wall) varied with respect to the volatile suspended solids (VSS) concentration, which was used as measurement of microalgae biomass. It started with a biomass concentration of 160 mg VSS·L^{-1} (solar irradiance decreased by 15%) and finished with a biomass concentration of 420 mg VSS·L^{-1}, causing a 71% reduction in solar irradiance (Figure VII.A.1).

PAR-1 was also placed 5 cm from the front wall, at which point light intensity was noticed.

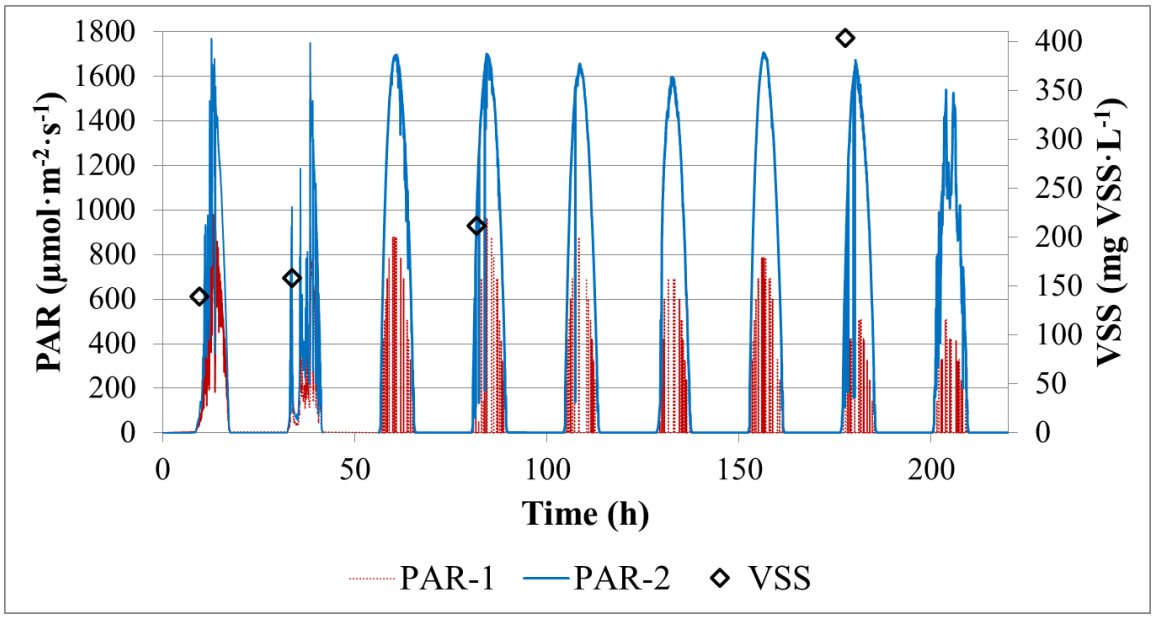

Figure VII.A.1. Evolution of light irradiance inside the culture (PAR-1) and outside the PBR (PAR-2) with increasing volatile suspended solids (VSS) concentration.

The shadow effect have been previously evaluated in lab conditions, showing significant reductions of light availability in the culture. By way of example, Huesemann et al. (2016) reported that light penetration in open ponds becomes critical when microalgae biomass is around 500 mg·L^{-1}, while Anbalagan et al. (2016) obtained a light reduction from 150 to 7-10 µmol·m^{-2}·s^{-1} at a depth of 10 cm in a lab-scale PBRs with biomass concentrations of around 250 mg·L^{-1}. To overcome this shadow effect, additional artificial lighting can be applied to the microalgae culture (Abu-Ghosh et al., 2015). Table VII.A.1 briefly summarises some advantages and disadvantages of different artificial light sources.

Table VII.A.1. Advantages and disadvantages of different artificial light sources.

	Advantages	Disadvantages	References
Incandescent light bulbs	- Low cost	- Light emitted in infrared region. - Light radiated in all directions.	Carvalho et al. (2011) Matthijs et al. (1996)
Halogen lamps	- Better energetic efficiency than light bulbs.	- Similar spectrum than light bulbs.	Carvalho et al. (2011) Matthijs et al. (1996)
Fluorescent lamps	- Similar spectrum to daily light.	- More expensive than light bulbs and halogen lamps.	Carvalho et al. (2011)
LED lamps	- Narrow wavelength. - High efficiency. - Long lifespan. - Reduce light stress. - Dissipate less energy.	- High cost.	Carvalho et al. (2011) Nwoba et al. (2019) Singh et al. (2015) Yan et al. (2013)

2. EXPERIMENTAL DESIGN, MATERIALS AND METHODS

In order to assess the shadow effect in the outdoor photobioreactor (PBR) plant (González-Camejo et al., 2019), an irradiation sensor (Apogee Quantum SQ-200) was placed inside the PBR-A, 2 cm away from the front wall during the start-up phase of Experiment 1 (PAR-1), and another sensor was placed outside the PBR-A (PAR-2) (González-Camejo et al., 2019).

VSS concentration was measured according to Standard Method 2540-E (APHA, 2005).

REFERENCES

1. Abu-Ghosh, S. Fixler, D., Dubinsky, Z., Iluz, D., 2015. Continuous background light significantly increases flashing-light enhancement of photosynthesis and growth of microalgae. Bioresour. Technol. 187, 144–148. https://doi.org/10.1016/j.biortech.2015.03.119
2. Anbalagan, A., Schwede, S., Lindberg, C.F., Nehrenheim, E., 2016. Influence of hydraulic retention time on indigenous microalgae and activated sludge process. Water Res. 91, 277-284. https://doi.org/10.1016/j.watres.2016.01.027
3. A.P.H.A., A.W.W.A., W.P.C.F., 2005. Standard methods for the examination of water and wastewater, 21st edition, American Public Health Association, American Water Works Association, Water Pollution Control Federation, Washington DC, USA.
4. Barceló-Villalobos, M., Fernández-del Olmo, P., Guzmán, J.L., Fernández-Sevilla, J.M., Acién Fernández, F.G., 2019. Evaluation of photosynthetic light integration by microalgae in a pilot-scale raceway reactor. Bioresour. Technol. 280, 404-411. https://doi.org/10.1016/j.biortech.2019.02.032
5. Carvalho, A.P., Silva, S.O., Baptista, J.M., Malcata, F.X., 2011. Light requirements in microalgal photobioreactors: an overview of biophotonic aspects. Appl. Microbiol. Biotechnol. 89, 1275-1288. https://doi.org/10.1007/s00253-010-3047-8
6. González-Camejo, J., Viruela, A., Ruano, M.V., Barat, R., Seco, A., Ferrer, J., 2019. Effect of light intensity, light duration and photoperiods in the performance of an outdoor photobioreactor for urban wastewater treatment. Algal Res. 40, 101511. https://doi.org/10.1016/j.algal.2019.101511
7. Huesemann, M., Crowe, B., Waller, P., Chavis, A., Hobbs, S. Edmundson, S., Wigmosta, M., 2016. A validated model to predict microalgae growth in outdoor pond cultures subjected to fluctuating light intensities and water temperatures. Algal Res. 13, 195–206. https://doi.org/10.1016/j.algal.2015.11.008
8. Liao, Q., Sun, Y., Huang, Y., Xia, A., Fu, Q., Zhu, X., 2017. Simultaneous enhancement of *Chlorella vulgaris* growth and lipid accumulation through the synergy effect between light and nitrate in a planar waveguide flat-plate photobioreactor. Bioresour. Technol. 243, 528-538. http://dx.doi.org/10.1016/j.biortech.2017.06.091
9. Matthijs, H.C.P., Balke, H., van Hes, U.M., Kroon, B.M.A., Mur, L.R., Binot, A., 1996. Application of light-emitting diodes in bioreactors: flashing light effects and energy economy in algal culture (*Chlorella pyrenoidosa*). Biotechnol. Bioeng. 50, 98-107.

10. Nwoba, E.G., Parlevliet, D.A., Laird, D.W., Alameh, K., Moheimani, N.R., 2019. Light management technologies for increasing algal photobioreactor efficiency. Algal Res. 39, 101433. https://doi.org/10.1016/j.algal.2019.101433
11. Singh, D., Basu, C., Meinhardt-Wollweber, M., Roth, B., 2015. LEDs for energy efficient greenhouse lighting, Renew. Sust. Energy Rev. 49, 139-147. http://dx.doi.org/10.1016/j.rser.2015.04.117
12. Yan, C., Zhang, L., Luo, X., Zheng, Z., 2013. Effects of various LED light wavelengths and intensities on the performance of purifying synthetic domestic sewage by microalgae at different influent C/N ratios. Ecol. Eng. 51, 24-32. http://dx.doi.org/10.1016/j.ecoleng.2012.12.051

CHAPTER VIII:

EFFECT OF AMBIENT TEMPERATURE VARIATIONS ON AN INDIGENOUS MICROALGAE-NITRIFYING BACTERIA CULTURE DOMINATED BY *CHLORELLA*

CHAPTER VIII:

EFFECT OF AMBIENT TEMPERATURE VARIATIONS ON AN INDIGENOUS MICROALGAE-NITRIFYING BACTERIA CULTURE DOMINATED BY *CHLORELLA*

González-Camejo, J., Aparicio, A., Ruano, M.V., Borrás, L., Barat, R., Ferrer, J., 2019. Effect of ambient temperature variations on an indigenous microalgae-nitrifying bacteria culture dominated by Chlorella. Bioresour. Technol. 290, 121788. https://doi.org/10.1016/j.biortech.2019.121788

ABSTRACT

Two outdoor photobioreactors were operated to evaluate the effect of variable ambient temperature on an indigenous microalgae-nitrifying bacteria culture dominated by *Chlorella*. Four experiments were carried out in different seasons, maintaining the temperature-controlled PBR at around 25 ºC (by either heating or cooling), while the temperature in the non-temperature-controlled PBR was allowed to vary with the ambient conditions. Temperatures in the range of 15-30 ºC had no significant effect on the microalgae cultivation performance. However, when the temperature rose to 30-35 ºC microalgae viability was significantly reduced. Sudden temperature rises triggered AOB growth in the indigenous microalgae culture, which worsened microalgae performance, especially when AOB activity made the system ammonium-limited. Microalgae activity could be recovered after a short temperature peak over 30 ºC once the temperature dropped, but stopped when the temperature was maintained around 28-30 ºC for several days.

1. INTRODUCTION

Since wastewater contains large amounts of nitrogen and phosphorus, these nutrients have traditionally been removed from water to avoid eutrophication issues (Song et al., 2018). However, classical nitrification-denitrification and phosphorus precipitation processes release nitrogen into the atmosphere and lose phosphorus with the sludge (Acién et al., 2016). On the other hand, microalgae are able to recover the nutrients present in wastewater (AlMomani et al., 2019; Ledda et al., 2015), while producing

valuable microalgae biomass (Acién et al., 2016). Microalgae-based wastewater treatment thus presents as a win-win solution to recover nutrients from water.

Due to their adaptability to wastewater and their striking resistance against protozoa, the green microalgae *Chlorella* is one of the most frequently used to recover nutrients from wastewater (Gupta et al., 2019; Sforza et al., 2014; Yang and Kong, 2011). To achieve maximum growth, microalgae must be maintained at optimum temperature (Huang et al., 2019; Ippoliti et al., 2016). Lower than optimal temperatures limit their growth rate by affecting the kinetics of the cell enzymatic processes (Binnal and Babu, 2017; Huang et al., 2017; Manhaeghe et al., 2019; Serra-Maia et al., 2016). On the other hand, temperatures over the limit deactivate some of the proteins involved in photosynthesis, which reduces the performance of microalgae and can even lead to cell death (Nwoba et al., 2019; Ras et al., 2013; Serra-Maia et al., 2016). In addition, temperature also affects some other parameters related to microalgae growth, e.g. the level of CO_2 solubility in the medium and the pH-value (Binnal and Babu, 2017; Xu et al., 2019). It also affects the light intensity above which microalgae get photoinhibited (Huang et al, 2017), e.g. microalgae tolerate higher light irradiance at temperatures near the optimum (Nwoba et al., 2019). Optimal temperatures of *Chlorella* species have been widely reported in the literature. However, these optimal temperatures are species-specific and results are often controversial. For instance, Sforza et al. (2014) found the optimal temperature of *C. protothecoides* for the treatment of primary effluent to be 30 ºC; while Binnal and Babu (2017) obtained 25 ºC as optimum for the growth of *C. protothecoides* in secondary effluent and Huang et al. (2019) reported 38.7 ºC as the optimum for *C. pyrenoidosa* grown in synthetic water. It should also be borne in mind that all of these studies were carried out in controlled lab conditions However, these lab-scale assays do not reflect the fluctuation of ambient temperatures when microalgae are cultivated outdoors (Gupta et al., 2019; Ling et al., 2019). Temperature variations under outdoor conditions can be especially critical for microalgae growth in closed photobioreactors (PBRs) since there are no evaporation losses that can regulate temperature (Yeo et al., 2018); especially during the summer time in temperate regions (Huang et al., 2017; Nwoba et al., 2019) such as those of the Mediterranean coast. Indeed, Wang et al. (2012) reported that the temperature inside a closed PBR can be around 10-30 ºC higher than the ambient temperature. Hence, the outdoor evaluation of the appropriate temperature range of indigenous microalgae cultivated in photobioreactors appears to be essential for the application of this technology at industrial scale. However, scarce studies have focused

on evaluating the single effect of temperature on the performance of outdoor microalgae PBRs.

It must be also considered that under outdoor conditions, indigenous microalgae tend to dominate the culture since they are better adapted to such conditions, obtaining higher performance than pure cultures (Thomas et al., 2019). Indigenous microalgae coexist with other microorganisms present in wastewater, such as heterotrophic and nitrifying bacteria, protozoa, rotifers, etc. (Sforza et al., 2014), which compete with microalgae for nutrients. In this respect, the competition between microalgae and ammonium-oxidising bacteria (AOB) for ammonium uptake should be controlled, since AOB can reduce microalgae growth by depleting the ammonium concentration in the media (González-Camejo et al., 2018a), hence limiting the performance of the process. Within this microalgae-AOB competition, temperature plays a key role since AOB growth increases sharply at higher temperatures (Jiménez, 2010). This effect has been previously observed under lab conditions of constant temperature (González-Camejo et al., 2018b). However, to the best of our knowledge the effect of variable ambient temperature on microalgae-AOB competition has not been evaluated before. Further research is therefore needed to fully understand the behaviour of an indigenous microalgae culture in outdoor wastewater treatment.

In this context, the aim of this study was to analyse the effect of ambient temperature variations on an indigenous microalgae-nitrifying bacteria culture (dominated by *Chlorella*) which continuously treated the effluent from a sewage-fed AnMBR system. The optimal temperature range of indigenous *Chlorella* growth was first evaluated by operating two flat-panel PBRs during different seasons of the year (without nitrification). Later, the microalgae-AOB competition for ammonium was assessed during the continuous operation of the PBRs under variable ambient temperatures.

2. MATERIAL AND METHODS

2.1. Microalgae substrate and inoculum

The substrate used in this study was the effluent of an AnMBR plant that treated effluent from the primary settler of the Carraixet wastewater treatment plant (WWTP) (39º30’04.0’’N 0º20’00.1’’W, Valencia, Spain). This plant is described in Seco et al. (2018).

Nitrogen concentration varied in the 35-58 mg $N \cdot L^{-1}$ range, while phosphorus concentration was between 3.5-6.0 mg $P \cdot L^{-1}$. As the AnMBR effluent was aerated in a

regulation tank to fully oxidise sulphide into sulphate before being fed to the PBRs, negligible concentrations of sulphide were detected in the PBR influent, thus avoiding microalgae limitation by sulphide (González-Camejo et al., 2017).

Indigenous microalgae were obtained from a mixed culture dominated by green microalgae *Chlorella* (> 99% total eukaryotic cells (TEC)). *Scenedesmus* (< 1% TEC), cyanobacteria, nitrifying and heterotrophic bacteria were also present in lower concentrations.

2.2. PBR pilot plant

Microalgae were cultivated in two outdoor, flat-plate, 1.10-m high x 2-m wide x 0.25-m deep, methacrylate PBRs (PBR-A and PBR-B) with working volumes of 550 L.

The PBRs were continuously sparged by air at a flow rate of 0.10 vvm through two perforated pipes (on the bottom of the PBRs) to homogenise the culture and reduce wall fouling. Oxygen concentrations in the PBRs were in the range of 10-15 mg $O_2 \cdot L^{-1}$, thus avoiding oxygen inhibition of microalgae (Pawlowski et al., 2016). Pure CO_2 (99.9%) was injected into the air system whenever pH was over a set-point of 7.5.

The PBRs were illuminated by twelve LED lamps (Unique Led IP65 WS-TP4S-40W-ME) installed on the rear wall, offering an average light irradiance of 300 $\mu E \cdot m^{-2} \cdot s^{-1}$.

Each PBR incorporated one pH-temperature transmitter (pHD sc Hach Lange), one dissolved oxygen sensor (LDO Hach Lange) and one irradiation sensor (Apogee Quantum) attached to the PBR surface to measure only photosynthetically active radiation (PAR). These on-line sensors allowed continuous data acquisition as explained in Viruela et al. (2018).

PBR temperature was controlled by a water heating and cooling device with a thermostat (Daikin Inverter R410A). Heated or cooled water was supplied to the PBRs by a pump and 20-m long coiled pipe (set inside each PBR). The chosen temperature set-point for heating was 30 ºC and 16 ºC for cooling. The cooling/heating fluid was automatically pumped into the PBRs by opening an electrovalve whenever the temperature went outside the set-point range of 21-25 ºC.

Further information about the PBR plant can be found in González-Camejo et al. (2019).

2.3. Experimental set-up

The effect of temperature on the mixed microalgae culture was assessed in terms of: i) biomass productivity and nutrient recovery, and ii) microalgae-AOB competition. Before each experiment, a start-up phase (described in González-Camejo et al., 2018a) was initiated to reach a consistent culture with a biomass concentration of around 300-400 mg VSS·L^{-1}.

2.3.1. Effect of temperature in nutrient recovery and biomass productivity

The effect on nutrient recovery and biomass productivity was analysed through 4 experiments carried out in different periods of the year: autumn, winter, spring and summer. During this first set of experiments, the PBRs were in semi-continuous operation under the same nutrient loading rate, air sparging flow rate and hydraulic retention time (HRT) of 6 days (i.e. 6-day BRT). They also received the same average solar PAR (Table VIII.1). A concentration of 5 mg·L^{-1} of allylthiourea (ATU) was maintained in both reactors to inhibit AOB growth (González-Camejo et al., 2018a; Krustok et al., 2016). The only parameter that varied was the culture temperature. PBR-A was the temperature-controlled PBR, which was heated up in autumn and winter and cooled down in spring and summer to maintain a culture temperature of around 25 ºC (Table VIII.1). PBR-B was the non-temperature-controlled PBR and thus varied freely with natural temperature variations throughout the year (Gupta et al., 2019).

Table VIII.1. Operating conditions in the evaluation of the effect of temperature in nutrient recovery and biomass productivity.

Exp.	Days of operation	Light intensity (µmol·m^{-2}·s^{-1})	Temperature (ºC)		Temperature control	
			PBR-A	PBR-B	PBR-A	PBR-B
1.1	29	254 ± 147	24.0 ± 1.4	20.6 ± 1.6	H	NC
1.2	14	184 ± 130	22.8 ± 2.4	16.4 ± 2.7	H	NC
1.3	16	225 ± 40	25.0 ± 1.5	28.8 ± 1.5	C	NC
1.4	25	262 ± 85	25.6 ± 1.4	31.5 ± 1.8	C	NC

H: heating; NC: no control of temperature; C: cooling.

2.3.2. Effect of temperature in microalgae-AOB bacteria competition

In a second set of experiments (2.1 and 2.2) PBR-A and PBR-B were operated in the same conditions (BRT = HRT = 6 days) in which temperature was allowed to vary but was the same in both PBRs. However, ATU concentration was kept at 5 $mg \cdot L^{-1}$ in PBR-A to inhibit AOB growth (González-Camejo et al., 2018a), thus being the nitrification-inhibited PBR. On the other hand, no AOB inhibitor was added to PBR-B. PBR-B was hence the non-nitrification-inhibited PBR.

2.4. Sampling and calculations

Duplicate grab samples were collected from the microalgae substrate (influent) and PBR effluent three times a week. Ammonium (NH_4), nitrite (NO_2), nitrate (NO_3) and phosphate (PO_4) were analysed according to Standard Methods (APHA, 2005): 4500-NH3-G, 4500-NO2-B, 4500-NO3-H and 4500-P-F, respectively, on an automatic analyser (Smartchem 200, WestcoScientific Instruments, Westco). Volatile suspended solids (VSS) concentration was also measured three times a week in duplicate according to method 2540 E of the Standard Methods (APHA, 2005).

Nitrogen recovery efficiency (NRE), phosphorus recovery efficiency (PRE) and biomass productivity (BP) were calculated according to Eq.VIII.1, Eq. VIII.2 and Eq. VIII.3, respectively:

$$\text{NRE}\ (\%) = \frac{N_i - N_e}{\text{N}_\text{i}} \cdot 100 \qquad \text{[Eq. VIII.1]}$$

where N_i is the nitrogen concentration of the influent (mg $N \cdot L^{-1}$) and N_e is the nitrogen concentration of the effluent (mg $N \cdot L^{-1}$).

$$\text{PRE}\ (\%) = \frac{\text{P}_i - \text{P}_e}{\text{P}_\text{i}} \cdot 100 \qquad \text{[Eq. VIII.2]}$$

where P_i is the phosphorus concentration of the influent (mg $P \cdot L^{-1}$) and P_e is the phosphorus concentration of the effluent (mg $P \cdot L^{-1}$).

$$\text{BP} = \frac{\text{VSS}}{\text{HRT}} \qquad \text{[Eq. VIII.3]}$$

where BP (mg $VSS \cdot L^{-1} \cdot d^{-1}$) is biomass productivity, VSS (mg $VSS \cdot L^{-1}$) is the PBR volatile suspended solids concentration and HRT is the microalgae culture hydraulic retention time (d).

To compare between experiments operating under different solar PAR, the biomass productivity:light irradiance ratio (BP:I, g $VSS \cdot mol^{-1}$) was calculated according to Eq. 4.

$$\text{BP:I} = \frac{\text{BP}\cdot V_{PBR}\cdot 1000}{\text{TP}\cdot t\cdot S\cdot 24\cdot 3600} \qquad \text{[Eq. VIII.4]}$$

where TP is the total photon flux applied to the PBR surface (i.e. solar irradiance plus artificial lighting, $\mu mol\cdot m^{-2}\cdot s^{-1}$); t is the period of time considered (d) and S is the PBR surface (m^2).

In order to assess the growth of nitrifying bacteria, the nitrification rate (NOxR) (mg $N\cdot L^{-1}\cdot d^{-1}$) was obtained by Eq. VIII.5:

$$\text{NOxR} = \frac{F\cdot(NOx_e - NOx_i)}{V_{PBR}} \qquad \text{[Eq. VIII.5]}$$

where F is the treatment flow rate ($m^3\cdot d^{-1}$); NOx_e is the concentration of nitrite plus nitrate of the effluent (mg $N\cdot L^{-1}$); N_i is the concentration of nitrite plus nitrate of the influent (mg $N\cdot L^{-1}$); and V_{PBR} is the volume of the culture in the PBRs (m^3).

SYTOX Green DNA staining dye (Invitrogen S7020) was used to monitor cell viability (Sato et al., 2004). 0.1µL of SYTOX Green 5mM was added to 50µL of 250-400 $mg\cdot L^{-1}$ suspended solids concentration of microalgae culture. As SYTOX Green is light-sensitive, the samples were incubated in darkness for 5 minutes. After the given reaction time had elapsed, the samples were excited by fluorescence microscope (DM2500, Leica, Germany) equipped with a filter set at 450 – 490 nm for excitation and 515 nm for emission. More than 400 cells were counted in duplicate for viability calculation in a Neubauer counting chamber in each experiment.

2.5. Statistical analysis

All results are shown as mean ± standard deviation of the duplicates. To determine the effect of temperature on microalgae performance, productivity, nitrogen and phosphorus removal efficiencies of R-A (temperature control) and R-B (non-temperature control) were compared. A t-test was carried out between the means values obtained for each reactor. In the case of comparing different seasons, an analysis of variance (ANOVA) was performed to evaluate statistical significant differences. Statistical analysis was assessed by STATGRAPHICS Centurion XVI.I. p-values < 0.05 were considered statistically significant with a level of significance of 95%.

3. RESULTS AND DISCUSSION

3.1. Effect of temperature on biomass productivity and nutrient recovery

In the first set of experiments, the temperature-controlled PBR was kept at a mean value of around 25 ºC (Table VIII.1).

Average NRE, PRE and biomass productivity values are shown in Figure VIII.1.

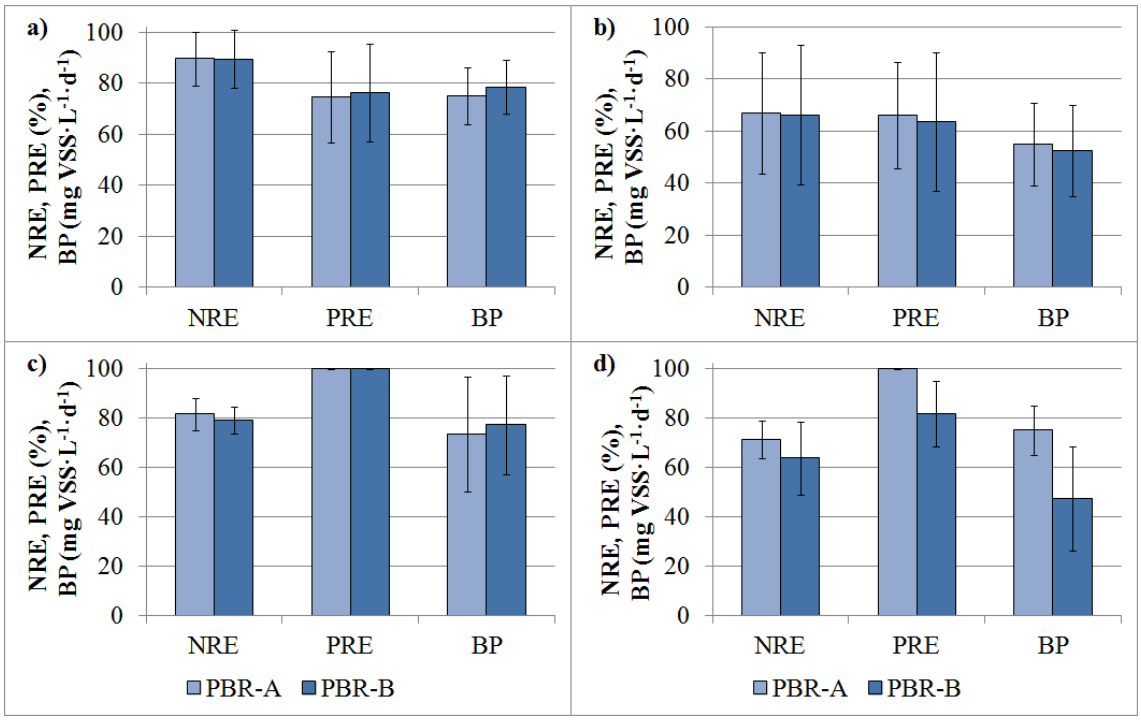

Figure VIII.1. Effect of temperature in biomass productivity and nutrient recovery. Mean values of NRE, PRE and productivity. PBR-A: temperature controlled at around 25 ºC; PBR-B: free temperature. a) Experiment 1.1 (autumn); b) Experiment 1.2 (winter); c) Experiment 1.3 (spring); d) Experiment 1.4 (summer).

Experiments in autumn, winter and spring did not show any significant differences in terms of NRE, PRE and biomass productivity between the temperature-controlled and the non-temperature-controlled PBR; i.e., p-values were higher than 0.05. Microalgae cell viability was also similar in both PBRs, being in the range of 95-99% of viable cells. The results obtained in autumn and spring were as expected, since the temperatures remained within moderate ranges between 20-30 ºC (Figure VIII.2). In fact, Suthar and Verma (2018) reported this temperature range of 20-30 ºC as optimum for the growth *C. vulgaris*.

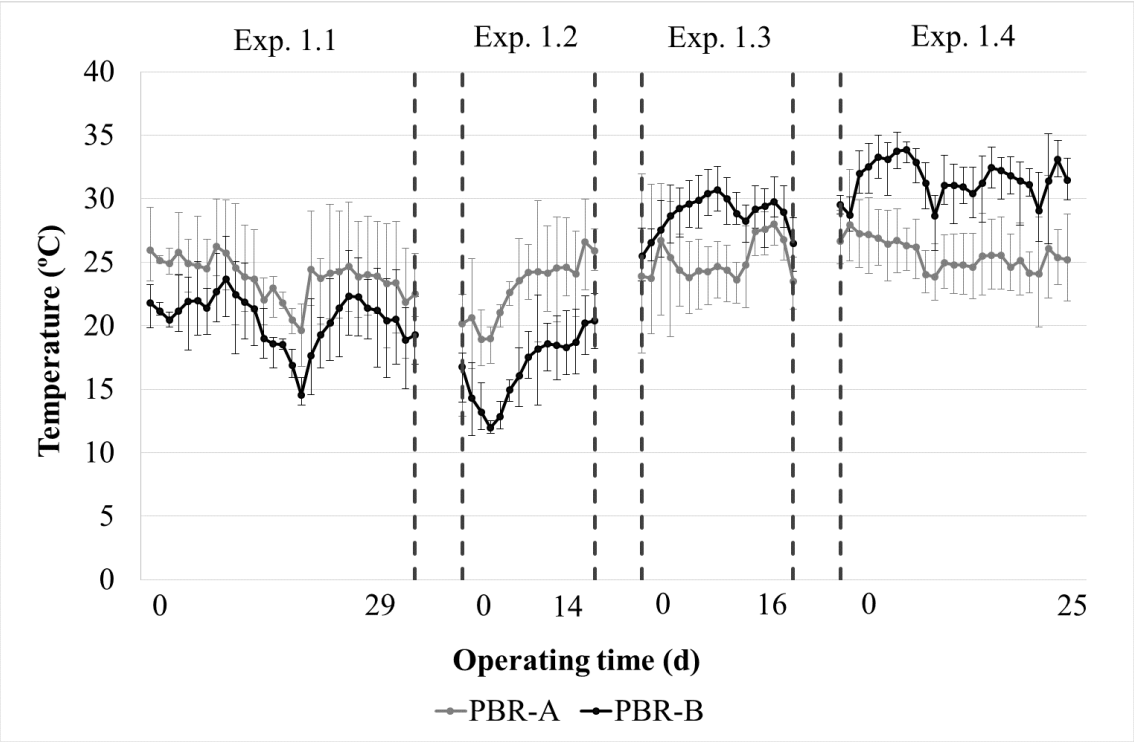

Figure VIII.2. Evolution of average temperatures (with minimum and maximum intervals) during the first set of experiments.

On the other hand, in winter experiment, when temperatures in the non-temperature-controlled PBR varied between 12-20 ºC (Figure VIII.2), surprisingly, there were non-significant differences between both PBRs (p-value > 0.05, see Figure VIII.1b). These results disagree with other authors who reported lower microalgae performance when temperature falls to moderate values; i.e., under 15 ºC (Gupta et al., 2019; Sforza et al., 2014; Xu et al., 2019). According to Bussotti (2004), reducing the temperature slows down the electron transfer in photosynthesis. Several factors could have been responsible for this unexpected behaviour: i) the minimum temperature of around 12 ºC in the non-temperature-controlled PBR (Figure VIII.2) may not have been low enough to significantly affect this indigenous culture. In this respect, Posadas et al. (2015) reported efficient nutrient removal of *Scenedesmus* sp. in raceways at average temperatures of 10-11 ºC; ii) the temperature reached values below 15 ºC only during 50% of the winter experiment. In this respect, Serra-Maia et al. (2016) reported that microalgae productivity could recover when temperature rises again after a significant reduction; iii) other factors such as daily light variations, PBR orientation, light gradients, etc. (Slegers et al., 2011) could have had a stronger influence on microalgae performance, lessening the temperature effect. In fact, Ferro et al. (2018) reported that

adapted microalgae strains could grow at 5 ºC as long as they had enough light irradiance, but did not proliferate when light intensity was low.

On the contrary, experiment in summer did show significant differences (p-value < 0.05) between the temperature-controlled and the non-temperature-controlled PBR, although both reactors started at similar nutrient and VSS concentrations. In addition, when comparing the light-normalised biomass productivity (BP:I) between different experiments no significant differences (p-value > 0.05) were observed in all cases, with the exception of the BP:I of the non-temperature-controlled PBR during summer, which was the lowest (Table VIII.2).

Table VIII.2. Biomass productivity:light irradiance ratio (BP:I) for the first set of experiments.

Exp.	BP:I	
	PBR-A	**PBR-B**
1.1	0.39 ± 0.10	0.41 ± 0.11
1.2	0.35 ± 0.10	0.33 ± 0.08
1.3	0.44 ± 0.12	0.42 ± 0.09
1.4	0.36 ± 0.04	0.22 ± 0.10[(1)]

[(1)] Showed significant differences (p-value < 0.05).

During summer, the non-temperature-controlled PBR remained at the highest mean temperatures of 31.5 ± 1.8 ºC, reaching peak values over 35 ºC for several days. As a consequence, cell viability dropped to 69 ± 1% in this PBR but remained at 96 ± 2% in the temperature-controlled PBR, which suggests that a culture deterioration occurred in the non-temperature-controlled PBR due to heat stress (Manhaeghe et al., 2019; Nwoba et al., 2019). Dead microalgae cells can release their nutrient content into the medium, as reported by Serra-Maia et al. (2016). In fact, from day 16 onwards nutrients started to accumulate in the non-temperature-controlled PBR, especially phosphorus, which remained at negligible values in the temperature-controlled PBR, but reached over 2 mg $P \cdot L^{-1}$ in the non-temperature-controlled PBR at the end of summer experiment (Figure VIII.3a).

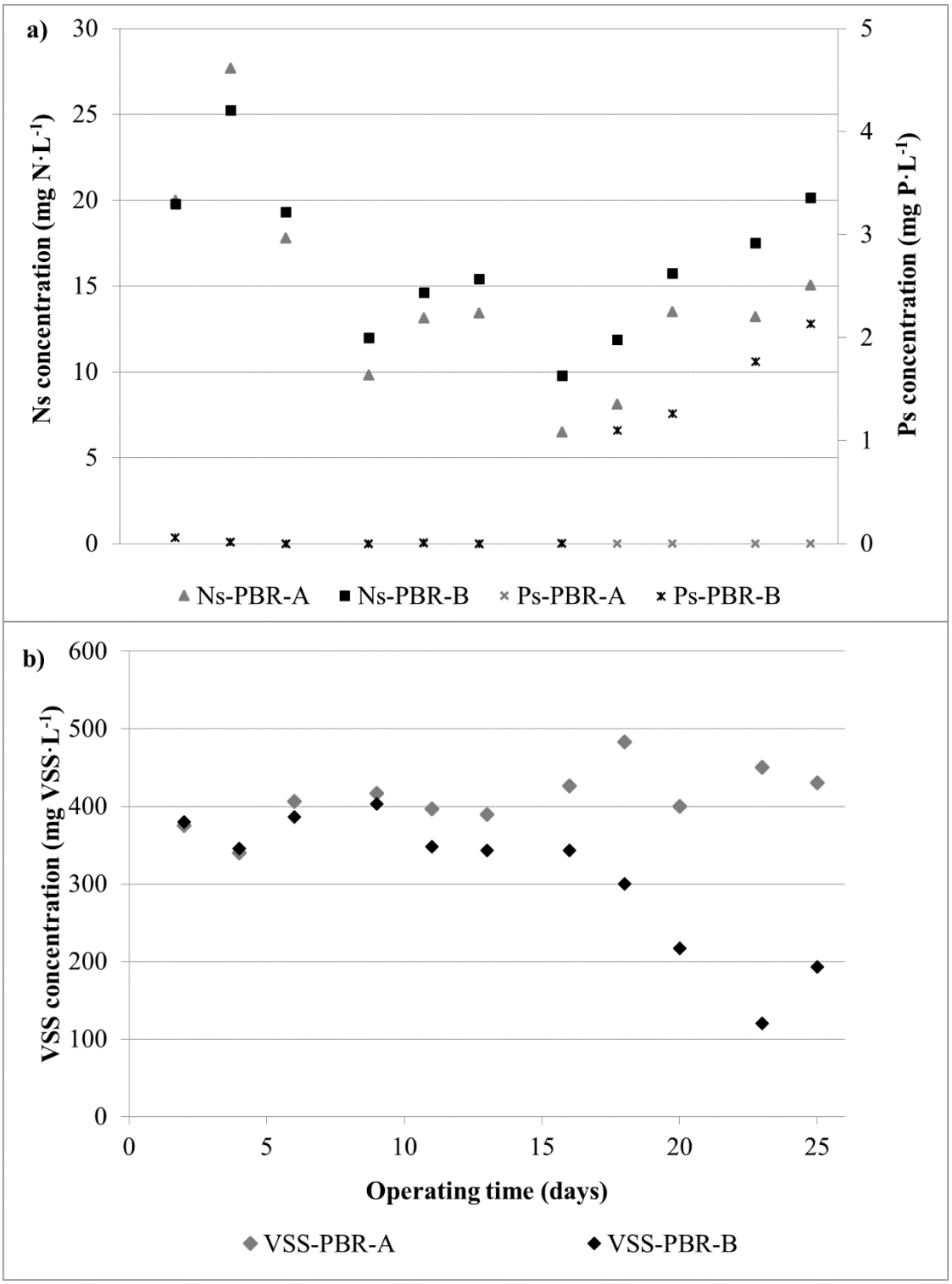

Figure VIII.3. Evolution during Experiment 1.4 (summer) in PBR-A and PBR-B of: a) nitrogen (Ns) and phosphorus (Ps) concentrations; b) volatile suspended solids (VSS) concentration.

Other authors have also reported the unequal effects of high and low temperatures on the microalgae culture (Almomani et al., 2019; Ras et al., 2013; Serra-Maia et al., 2016). Microalgae growth drops much more abruptly at high than low temperatures. In

fact, most microalgae strains can tolerate temperatures around 15 ºC below the optimum, but exceeding the optimum temperature by only 2-4 ºC can be detrimental for algae growth (Venkata Subhash et al., 2014). Hence, it is essential to find out the maximum tolerable temperature of the microalgae culture in order to obtain an optimal performance in the microalgae cultivation process. In this respect, Binnal and Babu (2017) observed a noticeable decrease in the performance of *Chlorella protothecoides* when temperature attained 30 ºC. Similarly, García-Cubero et al. (2018) obtained lower biomass productivity of *Chlorella vulgaris* at 30 ºC but no microalgae growth was observed at 35 ºC.

It can thus be concluded that the indigenous microalgae used in this study (mainly composed of *Chlorella*) can be processed without temperature limits or inhibition in the range of around 15-30 ºC. Further research is needed to determine the lowest temperature at which microalgae restrictions begin. This optimum temperature range of the indigenous microalgae culture is wider than those reported for pure cultures grown in synthetic media. For instance, Suthar and Verma (2018) reported maximum growth of *Chlorella vulgaris* in the range of 20-30 ºC, while Babel et al. (2002) obtained 28-35 ºC as the optimal for *Chlorella* sp. growth. In the study of García-Cubero et al. (2018), *C. vulgaris* obtained the highest biomass productivity in the temperature range of 15-25 ºC.

At higher temperatures peaks of around 35 ºC, microalgae could be cultivated but its performance was significantly reduced. Hence, in this microalgae-based system, temperature has to be kept under 35 ºC to reduce microalgae mortality and avoid culture collapse. Cooling microalgae in summer can be challenging (Huang et al., 2019) since, apart from the ambient temperature, the culture can be heated by the excess of light energy received by algae, emitted as fluorescence or heat through non-photochemical pathways (Huang et al., 2017; Nwoba et al., 2019). Efforts will thus have to be made to look for efficient ways of cooling microalgae on hot days to make the transition of this technology feasible on a large scale. By way of example, Almomani et al. (2019) reported a net energy benefit from cooling the culture in summer by using flue gas as the carbon source for microalgae growth.

3.2. Effect of temperature in microalgae-AOB bacteria competition

Temperature affects not only microalgae metabolism but also other organisms present in the culture, such as nitrifying bacteria (Jiménez, 2010). AOB proliferation is not

desirable, since they compete with microalgae for ammonium uptake and can worsen microalgae performance (González-Camejo et al., 2018a). Another set of experiments (2.1 and 2.2) was thus carried out to assess the effect of temperature on microalgae-AOB competition.

In these experiments, the same ambient and operating conditions were maintained in both PBRs, except for ATU concentration, which was added only to the nitrification-inhibited PBR. The main difference between Experiments 2.1 and 2.2 was the mean temperature of both PBRs, which was 18.5 ± 2.5 and 26.7 ± 1.1 ºC, respectively.

The NOxR, i.e. the production of nitrite and nitrate in the mixed microalgae-nitrifying bacteria culture, was used to assess nitrifying bacteria activity (Rossi et al, 2018). It should be noted that NOxR is an approximate value since it does not include the nitrate and nitrite consumed by algae. These nitrite and nitrate absorbed by microalgae were expected to be low, since the ammonium uptake is far higher than that of nitrate (Eze et al., 2018). However, if the nitrate uptake rate were to be higher than the nitrification rate, negative NOxR values would be obtained.

3.2.1. Experiment 2.1

This experiment lasted 81 days and was carried out in autumn-winter, so that temperature presented a mean value of 18.5 ± 2.5 ºC. It was divided into two periods: Period 2.1.I (41 days) and Period 2.1.II (40 days). Figure VIII.4 shows the evolution of the nutrient concentrations and the nitrification rate during this experiment. The high variability of nutrient concentrations can be seen in Figure VIII.4a. This was due not only to PBR performance, but also to the large variations in the nutrient load (data not shown).

In Period 2.1.I mean temperatures remained under 25 ºC and no significant differences were observed between the nitrification-inhibited and the non-nitrification-inhibited PBR in terms of nutrient concentrations (Figure VIII.4a) and nitrification rates, which were in the range of -1/+1 mg $N \cdot L^{-1} \cdot d^{-1}$ (Figure VIII.4b). Microalgae cell viability was also similar; i.e. 94 ± 7% in the nitrification-inhibited PBR and 92 ± 4% in the non-nitrification-inhibited PBR. This suggests that AOB activity was not significant in Period 2.1.I in either reactor.

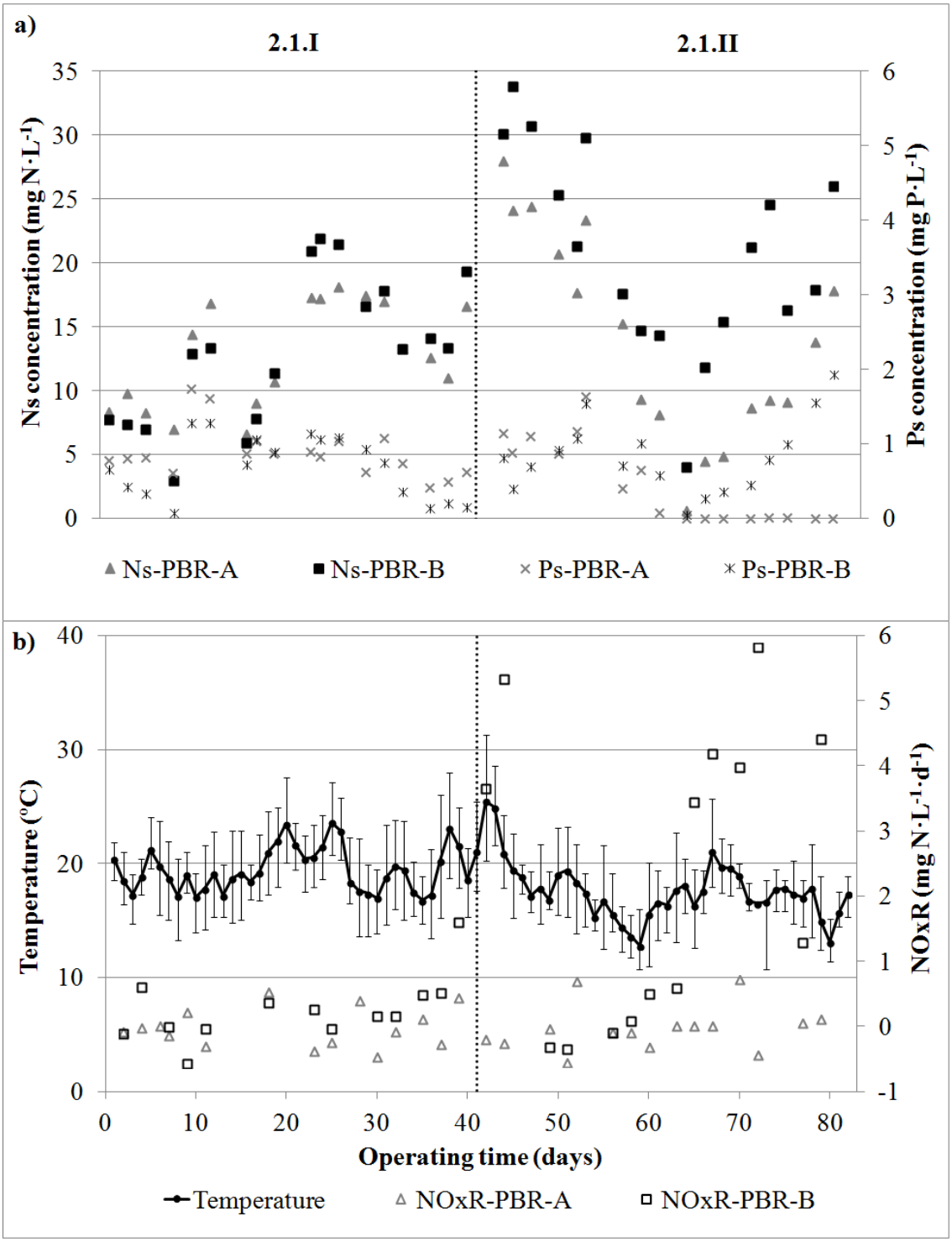

Figure VIII.4. Evolution during experiment 2.1 in PBR-A (inhibited nitrification) and PBR-B (free nitrification) of: a) nitrogen (Ns), and phosphorus (Ps) concentrations; b) temperature and nitrification rate (NOxR).

However, on days 42 and 43 (beginning of Period 2.1.II) it presented average values over 25 ºC with peaks over 30 ºC (Figure VIII.4b), which sharply increased nitrifying bacteria activity, reaching NOxR values in the range of 3-6 mg $N \cdot L^{-1} \cdot d^{-1}$. On the other

hand, when the temperature dropped steadily on days 44-60, the nitrification rates returned to negligible values (Figure VIII.4b). It is well known that AOB growth is strongly favoured at high temperatures and is around 0.77 d^{-1} at 18 ºC, which is similar to that of *Chlorella*; i.e. 0.65-0.87 d^{-1} (Ledda et al., 2015; Xu et al., 2015). However, at 25 ºC it can reach up to 1.61 d^{-1} (Jiménez, 2010), while *Chlorella* remain in the former range.

After day 60, nitrifying bacteria activity again started to rise, with a sharp peak on day 64. This time the temperature stayed at mean values in the range of 15-18 ºC (Figure VIII.4b), so that AOB activity had to be theoretically low (Jiménez, 2010), as previously mentioned. However, at this time, the non-nitrification-inhibited PBR had nitrogen concentrations under 10 mg $N \cdot L^{-1}$ (Figure VIII.4a). It has previously been reported that microalgae activity is significantly reduced at nitrogen concentrations below 10 mg $N \cdot L^{-1}$ (Pachés et al., 2018). Under these conditions, the microalgae growth rate in the non-nitrification-inhibited PBR was therefore reduced because of limiting nitrogen, and AOB activity was favoured when the ammonium load increased after day 65, reaching an NOxR of 3.9 ± 2.1 mg $N \cdot L^{-1} \cdot d^{-1}$.

The higher nitrifying bacteria activity worsened microalgae performance in the non-nitrification-inhibited PBR after day 65. In fact, both nitrogen and phosphorus concentrations accumulated in this PBR, which meant lower nutrient recovery rates than the nitrification-inhibited PBR. In addition, microalgae cell viability fell slightly, reaching values of 84 ± 3% in the non-nitrification-inhibited PBR, while it remained at 93 ± 2% in the nitrification-inhibited PBR during Period 2.1.II.

Another factor that could have favoured nitrifying activity in Period 2.1.II was light intensity, since it was significantly higher in Period 2.1.I (308 ± 110 $\mu mol \cdot m^{-2} \cdot s^{-1}$) than in Period 2.1.II; i.e., 256 ± 152 $\mu mol \cdot m^{-2} \cdot s^{-1}$. Light irradiance has been reported to inhibit nitrifying bacteria growth (Guerrero and Jones, 1996), especially under conditions of high oxygen concentrations (Prosser, 1990), as in this case. A previous lab study (González-Camejo et al., 2018b) has also shown that the threshold temperature at which AOB growth is favoured increases with higher light intensity; i.e. AOB rose at 22 ± 1ºC and 40 $\mu mol \cdot m^{-2} \cdot s^{-1}$, but at 85 $\mu mol \cdot m^{-2} \cdot s^{-1}$, AOB activity did not significantly notice until 27-28 ºC was reached. Lastly, at a light irradiance of 125 $\mu mol \cdot m^{-2} \cdot s^{-1}$, negligible AOB activity was seen below 32 ºC. These results suggest that AOB activity is significant only when their growth rate is considerably higher than that of microalgae.

3.2.2. Experiment 2.2

As Experiment 2.2 was carried out in spring and summer, culture temperatures were considerably higher than in Experiment 2.1 (i.e., mean value of 26.7 ± 1.1 ºC), and remained fairly stable (Figure VIII.5b).

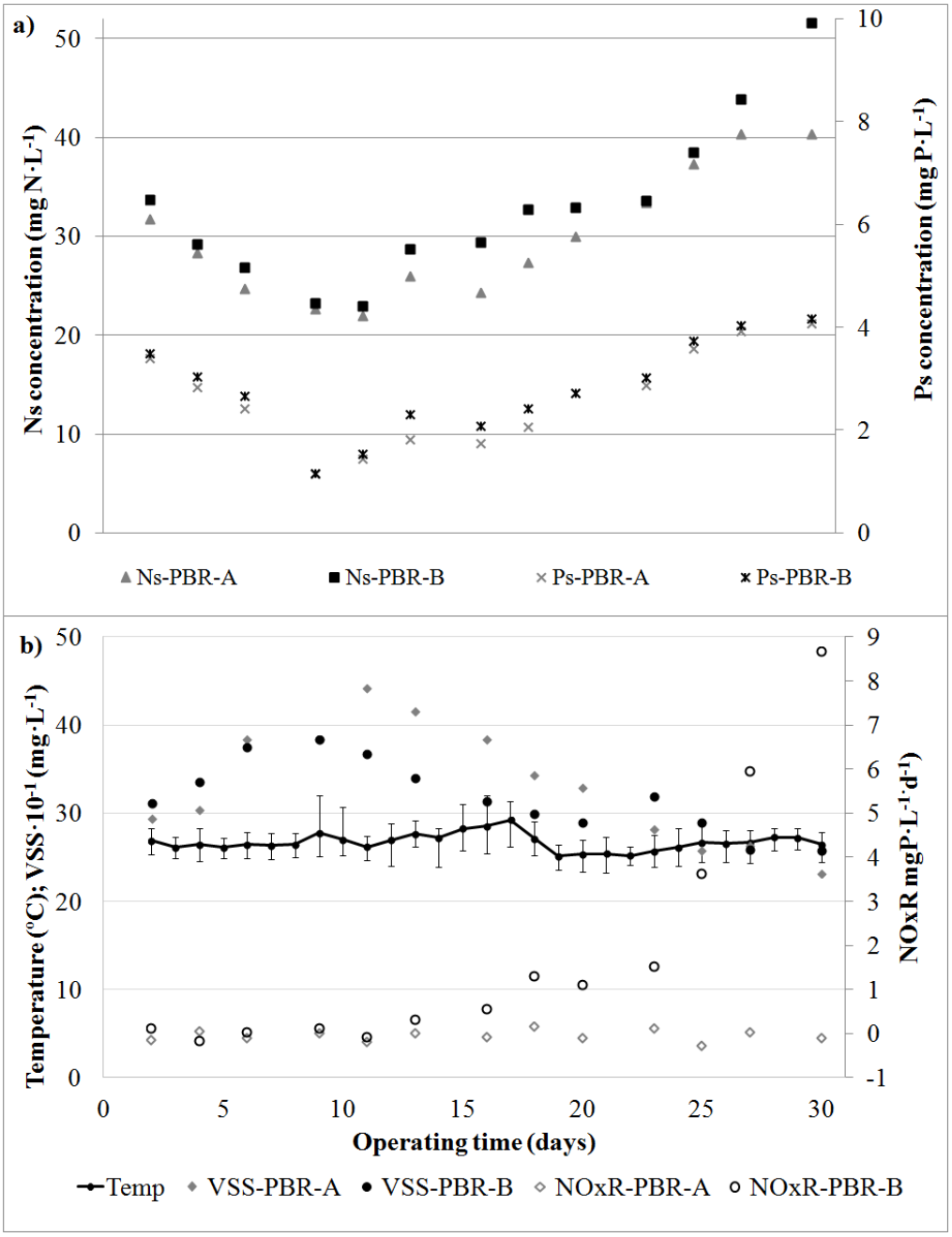

Figure VIII.5. Evolution during experiment 2.2 in PBR-A (inhibited nitrification) and PBR-B (free nitrification) of: a) nitrogen (Ns), and phosphorus (Ps) concentrations; b) temperature, volatile suspended solids (VSS) concentration and nitrification rate (NOxR).

At these high temperatures, AOB growth was expected to rapidly surpass that of the microalgae, due to their theoretically higher growth rate than *Chlorella,* as mentioned in Section VIII.3.2.1. However, there were negligible differences in the nitrification rates of both PBRs at the beginning of the experiment, even after maximum temperatures over 30 ºC on days 9-10 (Figure VIII.5b). As reported by other authors (Lau et al., 2019; Ras et al., 2013; Yadav and Sen, 2017), it is possible that this indigenous microalgae could have been adapted to high temperatures since the start-up phase of Experiment 2.2 was performed at similar temperatures to those of its continuous operation (data not shown), thus being more competitive than AOB and reaching a consistent microalgae biomass of 384 mg $VSS \cdot L^{-1}$ at day 10 (in Period 2.1.I, the VSS concentration prior to nitrification only achieved 299 ± 22 mg $VSS \cdot L^{-1}$). However, after 3 days of temperatures over 30 ºC (days 16-18), NOxR rose steadily in the non-nitrification-inhibited PBR (Figure VIII.5b), probably because of two simultaneous effects: i) the increasing AOB activity at higher temperatures (Jiménez, 2010) as explained in section VIII.3.2.1; ii) the reduction of the microalgae performance under temperatures of 30-35 ºC, as already stated in section VIII.3.1. Consequently, nitrifying bacteria outcompeted the microalgae from day 25 on, which implied that nitrogen concentration in the non-nitrification-inhibited PBR was higher than in the nitrification-inhibited PBR at the end of Experiment 2.2 (Figure VIII.5b) and viability in the non-nitrification-inhibited PBR fell to 80 ± 17%.

It is possible that sudden temperature rises also had an influence on microalgae-AOB competition. It seems that under normal light and mild temperature situations, microalgae growth is higher than AOB (Marcilhac et al., 2014; Risgaard-Petersen et al., 2004), therefore increasing their biomass concentration and outcompeting nitrifying bacteria. However, sudden temperature rises can prompt accelerate AOB growth, making them able to compete with microalgae for ammonium uptake. After this sharp increase in AOB, if the ambient conditions such as high temperatures are maintained favourable for nitrifying bacteria growth (as in Experiment 2.2), nitrification will rise steadily and the nitrifiers will outcompete the microalgae, as occurred at the end of Experiment 2.2 (Figure VIII.5). This suggests that the competition between microalgae and nitrifying bacteria leads to competitive exclusion (Passarge et al., 2006). On the other hand, if the temperature is re-established after its peak, the nitrification rate will drop and microalgae performance can recover, as was seen in Experiment 2.1 (Section VIII.3.2.1).

To sum up, variability of temperature plays an important role in the competition between microalgae and AOB. Temperature peaks over 30 ºC and the maintenance of the culture high temperatures can make nitrifying bacteria outcompete microalgae, which can imply the culture collapse.

4. CONCLUSIONS

The optimal temperature range for the growth of indigenous microalgae was around 15-30 ºC. Within this range, no significant differences were found in microalgae cultivation performance. However, microalgae viability was significantly reduced at temperatures over 30-35 ºC.

Sudden temperature rises favoured AOB activity within the indigenous microalgae culture, after which the microalgae could recover when the ambient temperature fell as the nitrification rate was reduced. However, when ambient temperatures stayed high, the nitrifying bacteria could outcompete the microalgae, collapsing the culture.

Since nitrifiers can exhaust the ammonium in the culture, it seems essential to keep nitrifying bacteria activity low.

ACKNOWLEDGMENTS

This research work was supported by the Spanish Ministry of Economy and Competitiveness (MINECO, Projects CTM2014-54980-C2-1-R and CTM2014-54980-C2-2-R) jointly with the European Regional Development Fund (ERDF), both of which are gratefully acknowledged. It also received support from the Spanish Ministry of Education, Culture and Sport via a pre-doctoral FPU fellowship to authors J. González-Camejo (FPU14/05082) and S. Aparicio (FPU/15/02595).

REFERENCES

1. Acién, F.G., Gómez-Serrano, C., Morales-Amaral, M.M., Fernández-Sevilla, J.M., Molina-Grima E., 2016. Wastewater treatment using microalgae: how realistic a contribution might it be to significant urban wastewater treatment? Appl. Microbiol. Biotechnol. 100, 9013–9022. http://dx.doi.org/10.1007/s00253-016-7835-7
2. Almomani, F., Al Ketife, A.M.D., Judd, S., Shurair, M., Bhosale, R., Znad, H., Tawalbeh, M., 2019. Impact of CO_2 concentration and ambient conditions on microalgal growth and nutrient removal from wastewater by a photobioreactor. Sci. Total Environ. 662, 662-671. https://doi.org/10.1016/j.scitotenv.2019.01.144

3. A.P.H.A., A.W.W.A., W.P.C.F., Standard methods for the examination of water and wastewater, 21st edition, American Public Health Association, American Water Works Association, Water Pollution Control Federation, Washington DC, 2005.
4. Babel, S., Takizawa, S., Ozaki, H., 2002. Factors affecting seasonal variation of membrane filtration resistance caused by *Chlorella* algae. Water Res. 36(5), 1193-1202
5. Binnal, P., Babu, P.N., 2017. Optimization of environmental factors affecting tertiary treatment of municipal wastewater by *Chlorella protothecoides* in a lab scale photobioreactor. J. Water Process Eng. 17, 290-298. http://dx.doi.org/10.1016/j.jwpe.2017.05.003
6. Bussotti, F., 2004. Assessment of stress conditions in *Quercus ilex* L. leaves by O-J-I-P chlorophyll *a* fluorescence analysis, Plant Biosystems 138, 101-109.
7. Eze, V.C, Velasquez-Orta, S.B., Hernández-García, A., Monje-Ramírez, I., Orta-Ledesma, M.T., 2018. Kinetic modelling of microalgae cultivation for wastewater treatment and carbon dioxide sequestration. Algal Res. 32, 131–141. https://doi.org/10.1016/j.algal.2018.03.015
8. Ferro, L., Gorzsás, A., Gentili, F.G., Funk, C., 2018. Subarctic microalgal strains treat wastewater and produce biomass at low temperature and short photoperiod. Algal Res. 35, 160-167. https://doi.org/10.1016/j.algal.2018.08.031
9. García-Cubero, R., Moreno-Fernández, J., Acién-Fernández, F.G., García-González, M., 2018. How to combine CO_2 abatement and starch production in *Chlorella vulgaris*. Algal Res. 32, 270-279. https://doi.org/10.1016/j.algal.2018.04.006
10. González-Camejo, J., Viruela, A., Ruano, M.V., Barat, R., Seco, A., Ferrer, J., 2019. Effect of light intensity, light duration and photoperiods in the performance of an outdoor photobioreactor for urban wastewater treatment. Algal Res. 40, 101511. https://doi.org/10.1016/j.algal.2019.101511
11. Gonzalez-Camejo, J., Barat, R., Ruano, M.V., Seco, A., Ferrer, J., 2018a. Outdoor flat-panel membrane photobioreactor to treat the effluent of an anaerobic membrane bioreactor. Influence of operating, design and environmental conditions. Water Sci. Technol. 78(1) 195-206. http://dx.doi.org/10.2166/wst.2018.259
12. González-Camejo, J., Barat, R., Pachés, M., Murgui, M., Ferrer, J., Seco, A., 2018b. Wastewater Nutrient Removal in a Mixed Microalgae-bacteria Culture: Effect of Light and Temperature on the Microalgae-bacteria Competition. Environ. Technol. 39(4), 503-515. http://dx.doi.org/10.1080/09593330.2017.1305001
13. González-Camejo, J., Serna-García, R., Viruela, A., Pachés, M., Durán, F., Robles, A., Ruano, M.V., Barat R., Seco, A., 2017. Short and long-term experiments on the effect of sulphide on microalgae cultivation in tertiary sewage treatment. Bioresour. Technol. 244, 15-22. http://dx.doi.org/10.1016/j.biortech.2017.07.126

14. Guerrero, M.A., Jones, R.D., Photoinhibition of marine nitrifying bacteria. I. Wavelength-dependent response. Mar. Ecol. Prog. Ser. 141 (1996) 183-192.
15. Gupta S., Pawar, S.B., Pandey, R.A., 2019. Current practices and challenges in using microalgae for treatment of nutrient rich wastewater from agro-based industries. Sci. Total Environ. 687, 1107–1126. https://doi.org/10.1016/j.scitotenv.2019.06.115
16. Huang, J., Hankame, B., Yarnold, J., 2019. Design scenarios of outdoor arrayed cylindrical photobioreactors for microalgae cultivation considering solar radiation and temperature. Algal Res. 41, 101515. https://doi.org/10.1016/j.algal.2019.101515
17. Huang, Q., Jiang, F., Wang, L., Yang, C., 2017. Design of Photobioreactors for Mass Cultivation of Photosynthetic Organisms. Engineering 3, 318-329. http://dx.doi.org/10.1016/J.ENG.2017.03.020
18. Ippoliti, D., Gómez, C., Morales-Amaral, M.M., Pistocchi, R., Fernández-Sevilla, J.M., Acién, F.G., 2016. Modeling of photosynthesis and respiration rate for *Isochrysis galbana* (T-Iso) and its influence on the production of this strain. Bioresour. Technol. 203, 71–79. http://dx.doi.org/10.1016/j.biortech.2015.12.050
19. Jiménez, E., 2010. Mathematical modelling of the two-stage nitrification process. Developement of modelling calibration methodologies for a SHARON reactor and activated sludge process (Modelación matemática del proceso nitrificación en dos etapas. Desarrollo de metodologías de calibración del modelo para un reactor SHARON y un proceso de fangos activados). PhD Thesis, Polytechnic University of Valencia, Spain.
20. Krustok, I., Odlare, M., Truu, J., Nehrenheim, E., 2016. Inhibition of nitrification in municipal wastewater-treating photobioreactors: Effect on algal growth and nutrient uptake. Bioresour Technol. 202, 238-243. http://dx.doi.org/10.1016/j.biortech.2015.12.020
21. Lau, A.K.S., Bilad, M.R., Osman, N.B., Marbelia, L., Putra, Z.A., Nordin, N.A.H.M., Wirzal, M.D.H., Jaafar, J., Khan, A.L., 2019. Sequencing batch membrane photobioreactor for simultaneous cultivation of aquaculture feed and polishing of real secondary effluent, Journal of Water Process Engineering 29, 100779. https://doi.org/10.1016/j.jwpe.2019.100779
22. Ledda, C., Idà, A., Allemand, D., Mariani, P., Adani, F., 2015. Production of wild *Chlorella* sp. cultivated in digested and membrane-pretreated swine manure derived from a full-scale operation plant. Algal Res. 12, 68-73. http://dx.doi.org/10.1016/j.algal.2015.08.010
23. Ling, Y., Sun, L.P., Wang, S.Y., Lin, C.S.K., Sun, Z., Zhou, Z.G., 2019. Cultivation of oleaginous microalga *Scenedesmus obliquus* coupled with wastewater treatment for

enhanced biomass and lipid production. Biochem. Eng. J. 148, 162–169. https://doi.org/10.1016/j.bej.2019.05.012

24. Manhaeghe, D., Michels, S., Rousseau, D.P.L., Van Hulle, S.W.H., 2019. A semi-mechanistic model describing the influence of light and temperature on the respiration and photosynthetic growth of *Chlorella vulgaris.* Bioresour. Technol. 274, 361-370. https://doi.org/10.1016/j.biortech.2018.11.097
25. Marcilhac, C., Sialve B., Pourcher A.M., Ziebal C., Bernet N., Béline F., 2014. Digestate color and light intensity affect nutrient removal and competition phenomena in a microalgal-bacterial ecosystem, Water Res. 64, 278-287. http://dx.doi.org/10.1016/j.watres.2014.07.012
26. Nwoba, E.G., Parlevliet, D.A., Laird, D.W., Alameh, K., Moheimani, N.R., 2019. Light management technologies for increasing algal photobioreactor efficiency. Algal Res. 39, 101433. https://doi.org/10.1016/j.algal.2019.101433
27. Pachés, M., Martínez-Guijarro, R., González-Camejo, J., Seco, A., Barat, R., 2018. Selecting the most suitable microalgae species to treat the effluent from an anaerobic membrane bioreactor. Environ. Technol. (in press). https://doi.org/10.1080/09593330.2018.1496148
28. Passarge, J., Hol, S., Escher, M., Huisman, J., 2006. Competition for nutrients and light: stable coexistence, alternative stable states, or competitive exclusion? Ecological Monographs*,* 76(1), 57–72.
29. Pawlowski, A., Frenández, I., Guzmán, J.L., Berenguel, M., Acién, F.G., Dormido, S., 2016. Event-based selective control strategy for raceway reactor: A simulation study. IFAC-Papers OnLine 49(7), 478–483. https://doi.org/10.1016/j.ifacol.2016.07.388
30. Posadas, E., Morales, M.M., Gomez, C., Acién, F.G., Muñoz, R., 2015. Influence of pH and CO_2 source on the performance of microalgae-based secondary domestic wastewater treatment in outdoors pilot raceways. Chem. Eng. J. 265, 239–248. http://dx.doi.org/10.1016/j.cej.2014.12.059
31. Prosser, J.I., 1990. Autotrophic nitrification in bacteria. In *Advances in microbial physiology* (Vol. 30, pp. 125-181). Academic Press.
32. Ras, M., Steyer, J.P., Bernard, O., 2013. Temperature effect on microalgae: a crucial factor for outdoor production, Rev. Environ. Sci. Biotechnol. 12, 153-164. https://doi.org/10.1007/s11157-013-9310-6
33. Risgaard-Petersen, N., Nicolaisen, M.H., Revsbech, N.P., Lomstein, B.A., 2004. Competition between ammonia oxidizing bacteria and benthic microalgae. Appl. Environ. Microb. 70(9), 5528-5537. https://doi.org/10.1128/AEM.70.9.5528-5537.2004

34. Rossi, S., Bellucci, M., Marazzi, F., Mezzanotte, V., Ficara, E., 2018. Activity assessment of microalgal-bacterial consortia based on respirometric tests. Water Sci Technol. 78(1-2), 207-215. https://doi.org/10.2166/wst.2018.078
35. Sato, M., Murata, Y., Mizusawa, M., Iwahashi, H., Oka, S.I., 2004. A simple and rapid dual-fluorescence viability assay for microalgae. Microbiol. Cult. Coll. 20(2), 53-59.
36. Seco, A., Aparicio, S., González-Camejo, J., Jiménez-Benítez, A., Mateo, O., Mora, J.F., Noriega-Hevia, G., Sanchis-Perucho, P., Serna-García, R., Zamorano-López, N., Giménez, J.B., Ruiz-Martinez, A., Aguado, D., Barat, R., Borrás, L., Bouzas, A., Martí, N., Pachés, M., Ribes, J., Robles, A., Ruano, M.V., Serralta, J. and Ferrer, J., 2018. Resource recovery from sulphate-rich sewage through an innovative anaerobic-based water resource recovery facility (WRRF). Water Science and Technology 78 (9), 1925-1936. https://doi.org/10.2166/wst.2018.492
37. Serra-Maia, R., Bernard, O., Gonçalves, A., Bensalem, S., Lopes, F., 2016. Influence of temperature on *Chlorella vulgaris* growth and mortality rates in a photobioreactor. Algal Res. 18, 352–359. http://dx.doi.org/10.1016/j.algal.2016.06.016
38. Sforza, E., Ramos-Tercero, E.A., Gris, B., Bettin, F., Milani, A., Bertucco, A., 2014. Integration of *Chlorella protothecoides* production in wastewater treatment plant: From lab measurements to process design. Algal Res. 6, 223–233. http://dx.doi.org/10.1016/j.algal.2014.06.002
39. Slegers, P.M., Wijffels, R.H., van Straten, G., van Boxtel, A.J.B., 2011. Design scenarios for flat panel photobioreactors. Appl. Energy 88, 3342–3353. https://doi.org/10.1016/j.apenergy.2010.12.037
40. Song, X., Luo, W., Hai, F.I., Price, W. E., Guo, W., Ngo, H.H., Nghiem, L.D., 2018. Resource recovery from wastewater by anaerobic membrane bioreactors: Opportunities and challenges. Bioresour. Technol. 270, 669-677. https://doi.org/10.1016/j.biortech.2018.09.001
41. Suthar, S., Verma, R., 2018. Production of *Chlorella vulgaris* under varying nutrient and abiotic conditions: A potential microalga for bioenergy feedstock. Process Safety and Environmental Protection 113, 141–148. https://doi.org/10.1016/j.psep.2017.09.018
42. Thomas, P.K., Dunn, G.P., Good, A.R., Callahan, M.P., Coats, E.R., Newby, D.T., Feris, K.P., 2019. A natural algal polyculture outperforms an assembled polyculture in wastewater-based open pond biofuel production. Algal Res. 40, 101488. https://doi.org/10.1016/j.algal.2019.101488
43. Venkata Subhash, G., Rohit, M.V., Prathima Devi, M., Swamy, Y.V., Venkata Mohan, S., 2014. Temperature induced stress influence on biodiesel productivity during mixotrophic microalgae cultivation with wastewater. Bioresour Technol. 169, 789–93. http://dx.doi.org/10.1016/j.biortech.2014.07.019

44. Viruela A., Robles A., Durán F., Ruano M.V., Barat R., Ferrer J., Seco A., 2018. Performance of an outdoor membrane photobioreactor for resource recovery from anaerobically treated sewage. J. Clean. Prod. 178, 665-674. https://doi.org/10.1016/j.jclepro.2017.12.223
45. Wang, B., Lan, C.Q., Horsman, M., 2012. Closed photobioreactors for production of microalgal biomasses. Biotechnol. Adv. 30(4), 904-912. https://doi.org/10.1016/j.biotechadv.2012.01.019.
46. Xu, X., Gu, X., Wang, Z., Shatner, W., Wang, Z., 2019. Progress, challenges and solutions of research on photosynthetic carbon sequestration efficiency of microalgae. Renew. Sust. Energy Rev. 110, 65–82. https://doi.org/10.1016/j.rser.2019.04.050
47. Xu, M., Li, P., Tang, T., Hu, Z., 2015. Roles of SRT and HRT of an algal membrane bioreactor system with a tanks-in-series configuration for secondary wastewater effluent polishing. Ecol. Eng. 85, 257-264. http://dx.doi.org/10.1016/j.ecoleng.2015.09.064
48. Yadav, G., Sen, R., 2017. Microalgal green refinery concept for biosequestration of carbon-dioxide vis-à-vis wastewater remediation and bioenergy production: Recent technological advances in climate research. J. CO_2 Util. 17, 188–206. http://dx.doi.org/10.1016/j.jcou.2016.12.006
49. Yang, Z., Kong, F., 2011. Enhanced growth and esterase activity of *Chlorella pyrenoidosa* (Chlorophyta) in response to short-term direct grazing and grazing-associated infochemicals from *Daphnia carinata*. J. Freshw. Ecol. 26, 553–561. https://doi.org/10.1080/02705060.2011.577973
50. Yeo, U.H., Lee, I.B., Seo, I.H., Kim, R.W., 2018. Identification of the key structural parameters for the design of a large-scale PBR. Biosist. Eng. 171, 165-178. https://doi.org/10.1016/j.biosystemseng.2018.04.012

APPENDIX VIII.A. ASSESSMENT OF THE MICROALGAE-NITRIFYING BACTERIA COMPETITION FOR AMMONIUM UPTAKE IN LAB-CONDITIONS

When microalgae cultivation systems are used to treat the effluent of anaerobic membrane bioreactors (AnMBRs) (Robles et al., 2018), the ammonium competition between microalgae and ammonium oxidising bacteria (AOB) is likely to occur (González-Camejo et al., 2018a; Molinuevo-Salces et al., 2010). AOB are autotrophic bacteria which oxidises ammonium to nitrite (i.e., first step of the nitrification process). Nitrite oxidising bacteria (NOB) can in turn oxidise this nitrite to nitrate, carrying out the second step of nitrification (Risgaard-Petersen et al., 2004; Winkler and Straka, 2019). Hence, the nitrifying bacteria (both AOB and NOB) activity is not usually desirable in microalgae cultivation systems since they reduce the amount of ammonium (González-Camejo et al., 2018), which is the main nitrogen source for microalgae (Eze et al., 2018; Najm et al., 2017), therefore decreasing its recovery in the microalgae biomass.

Since AOB activity is highly influenced by temperature (Jiménez, 2010; Weon et al., 2004), AOB are likely to grow significantly in closed PBRs operated in warm regions (for instance, Valencia, Spain). Hence, evaluating the affection of AOB on a mixed microalgae culture would help to understand the role of these microorganisms in the application of this technology for industrial purposes.

EXPERIMENTAL DESIGN, MATERIALS AND METHODS

3 lab-scale assays (i.e., A1, A2 and A3) were elaborated. Each of them was carried out by using microalgae samples taken from PBR-B of the PBR plant (see section VIII.2.2). For each assay, two 8-L vertical reactors (i.e., R-A and R-B) were used. Both of them were placed in a climatic chamber which maintained the culture in temperatures around 25-27 ºC. They were air-stirred in order to homogenise the culture and avoid biofilm formation. CO_2 was added to maintain the culture pH at a maximum set-point value of 7.5. Five LED lamps (Trilux 9w) were placed vertically around each reactor to supply a light PAR of 125 $\mu mol \cdot m^{-2}s^{-1}$ (measured at the reactor´s surface).

Both reactors were filled with 50% of substrate (i.e., AnMBR effluent, see section VIII.2.1) and 50% of the microalgae culture from the aforementioned PBR plant. The

characteristics of each media; i.e., ammonium (NH_4), soluble nitrogen (N_s) and volatile suspended solids (VSS) concentration, are shown in Table VIII.A.1.

Table VIII.A.1. Characteristics of the microalgae culture and substrate of the lab assays.

Assay	Substrate			Culture		
	NH_4 (mg $N \cdot L^{-1}$)	N_s (mg $N \cdot L^{-1}$)	VSS (mg $VSS \cdot L^{-1}$)	NH_4 (mg $N \cdot L^{-1}$)	N_s (mg $N \cdot L^{-1}$)	VSS (mg $VSS \cdot L^{-1}$)
A1	46.6	56.1	< LOD*	16.9	38.5	214
A2	42.3	57.8	< LOD*	22.6	27.9	390
A3	45.7	46.9	< LOD*	0.5	21.3	413

*LOD: Limit of detection

The difference between the reactors was their allylthiourea (ATU) content. In R-A the nitrification process was free to occur because ATU was not injected (similar to the operation in the MPBR plant). On the contrary, ATU was added in R-B until reaching 10 $mg \cdot L^{-1}$. Consequently, AOB activity in R-B was inhibited (González-Camejo et al., 2018a).

Ammonium (NH_4), nitrite (NO_2) and nitrate (NO_3) were analysed according to Standard Methods (APHA, 2005): 4500-NH3-G, 4500-NO2-B and 4500-NO3-H, respectively, using an automatic analyser (Smartchem 200, WestcoScientific Instruments, Westco). Soluble nitrogen (N_s) was calculated as the sum of all the nitrogen species measured; i.e., NH_4 NO_2 and NO_3. The volatile suspended solids (VSS) concentration was measured according to Standard Methods (APHA, 2005): method 2540 E.

The performance of both reactors was compared in terms of nitrogen removal rate and biomass productivity along one-day batch operation.

DATA

From the evolution of the concentration of nutrients and VSS during Assays A1, A2 and A3 (Figures VIII.A.1., VIII.A.2 and VIII.A.3, respectively), ammonium, nitrate and nitrogen recovery rates, nitrification rate (measured as the production of nitrite and nitrate as an approximation) and biomass productivity of both reactors were obtained (Tables VIII.A.2, VIII.A.3 and VIII.A.4). It must be noted that negative values of slope

represent consumption of nutrients, while positive values mean production of nutrients or biomass.

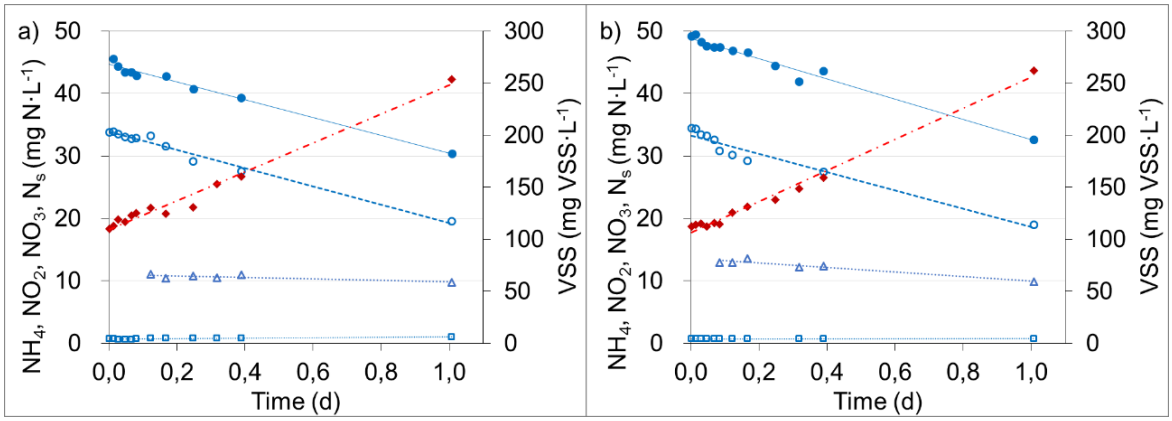

Figure VIII.A.1. Evolution of NH_4 (○), NO_2 (□), NO_3 (Δ), N_s (●) and VSS (♦) concentration during Assay A1: a) R-A; b) R-B.

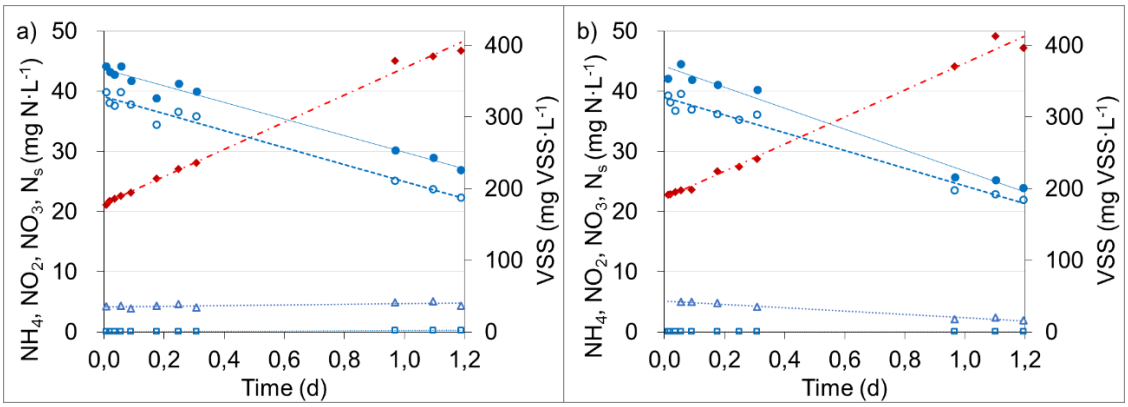

Figure VIII.A.2. Evolution of NH_4 (○), NO_2 (□), NO_3 (Δ), N_s (●) and VSS (♦) concentration during Assay A2: a) R-A; b) R-B.

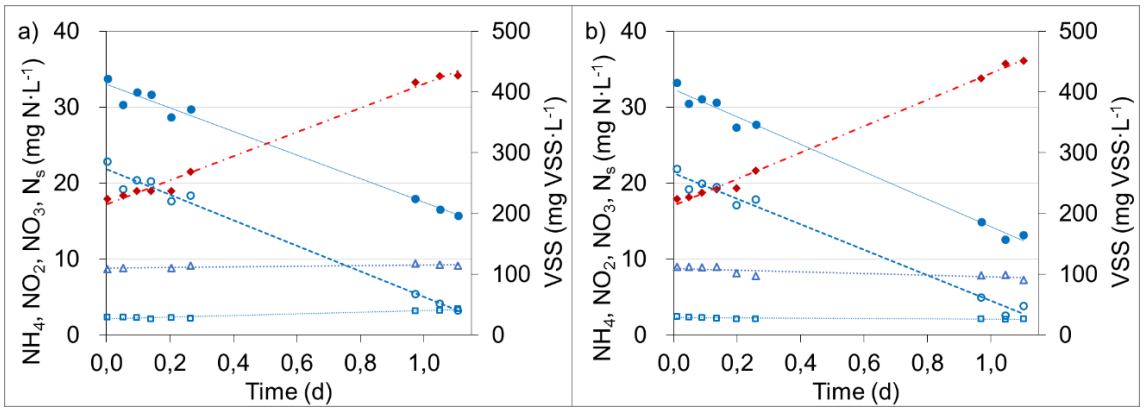

Figure VIII.A.3. Evolution of NH_4 (○), NO_2 (□), NO_3 (Δ), N_s (●) and VSS (♦) concentration during Assay A3: a) R-A; b) R-B.

Table VIII.A.2. Nitrogen recovery rates, biomass production and nitrification rates obtained in both reactors during Assay A1.

	R-A		R-B	
	Slope ($mg \cdot L^{-1} \cdot d^{-1}$)	R^2	Slope ($mg \cdot L^{-1} \cdot d^{-1}$)	R^2
NH_4	-14.6	0.982	-14.7	0.989
NO_2	0.3	0.895	0.0	0.137
NO_3	-1.2	0.645	-3.6	0.927
N_s	-14.2	0.986	-16.3	0.975
VSS	139	0.979	150	0.989

Table VIII.A.3. Nitrogen recovery rates, biomass production and nitrification rates obtained in both reactors during Assay A2.

	R-A		R-B	
	Slope ($mg \cdot L^{-1} \cdot d^{-1}$)	R^2	Slope ($mg \cdot L^{-1} \cdot d^{-1}$)	R^2
NH_4	-14.2	0.974	-14.7	0.979
NO_2	0.2	0.926	0.0	0.258
NO_3	0.5	0.433	-2.8	0.977
N_s	-13.7	0.976	-17.4	0.981
VSS	189	0.995	189	0.992

Table VIII.A.4. Nitrogen recovery rates, biomass production and nitrification rates obtained in both reactors during Assay A3.

	R-A		R-B	
	Slope ($mg \cdot L^{-1} \cdot d^{-1}$)	R^2	Slope ($mg \cdot L^{-1} \cdot d^{-1}$)	R^2
NH_4	-16.9	0.987	-16.8	0.987
NO_2	1.1	0.929	-0.2	0.574
NO_3	0.4	0.659	-1.1	0.643
N_s	-15.5	0.983	-18.1	0.989
VSS	198	0.991	218	0.996

As expected, the nitrifying bacteria activity in the three assays in reactor R-B was negligible since AOB were inhibited by the ATU addition. On the other hand, the AOB activity in reactor R-A (no nitrification inhibition) accounted for 0.3, 0.7 and 1.5 mg $N \cdot L^{-1} \cdot d^{-1}$ in Assays A1, A2 and A3, respectively. The soluble nitrogen recovery rates of R-B in Assays A1, A2 and A3 were 14.8%, 27.0% and 16.8% higher than those of R-A. Regarding biomass production, it was also higher in R-B than in R-A for Assays A1 and A3 (7.9% and 9.9%, respectively), but similar in Assay A2 (Table VIII.A3). This data therefore confirms that the nitrification process worsen the microalgae performance as was suggested in previous studies at lab-scale (González-Camejo et al., 2018b) and pilot-scale (González-Camejo et al., 2018a). However, in these previous studies, microalgae affection was also influenced by nutrient limitation, but in these lab Assays, nutrient did not get depleted. These results contradicts those of Rada-Ariza et al. (2017), who did not observe any negatively affection of microalgae due to nitrification in flat-panel sequencing batch photo-bioreactors.

It must be noted that the differences in the ammonium consumption were not significant between R-A and R-B, even during Assay A3, where nitrification rate was the highest (Table VIII.A.4). Hence, the lower microalgae activity in R-A had to be compensated with the AOB activity so that both R-A and R-B had similar ammonium recovery rates.

As aforementioned, ammonium is the main nitrogen source of microalgae (Eze et al., 2018; Najm et al., 2017). In fact, some authors have stated that other nitrogen compounds such as nitrate and nitrite are not consumed by microalgae until ammonium is completely depleted (Jebali et al., 2018; Ramanna et al., 2014) since microalgae need to reduce these compounds to ammonium prior to use them (Gupta et al., 2019; Reynolds, 2006; Shoener et al., 2019). However, R-B showed nitrate recovery rates in all the assays in spite of not being nitrogen-limited (Figures VIII.A.1, VIII.A.2, and VIII.A.3); although they were 4.1-15.3-fold lower than their corresponding ammonium recovery rates, which corroborated that ammonium is the preferred nitrogen source of this culture. On the contrary, R-A displayed nitrate production in Assays A2 and A3 because of their nitrifying bacteria activity (Tables VIII.A.3 and VIII.A.4), only obtaining a nitrate consumption in Assay A1, where the activity of nitrifiers was the lowest (Table VIII.A.2). It was therefore considered that the activity of AOB limits microalgae, reducing not only the microalgae biomass production and ammonium uptake, but also the nitrate consumption.

REFERENCES

1. A.P.H.A., A.W.W.A., W.P.C.F., 2005. Standard methods for the examination of water and wastewater, 21st edition, American Public Health Association, American Water Works Association, Water Pollution Control Federation, Washington DC, USA.
2. Eze, V.C, Velasquez-Orta, S.B., Hernández-García, A., Monje-Ramírez, I., Orta-Ledesma, M.T., 2018. Kinetic modelling of microalgae cultivation for wastewater treatment and carbon dioxide sequestration. Algal Res. 32, 131–141. https://doi.org/10.1016/j.algal.2018.03.015
3. González-Camejo, J., Barat, R., Ruano, M.V., Seco, A., Ferrer, J., 2018a. Outdoor flat-panel membrane photobioreactor to treat the effluent of an anaerobic membrane bioreactor. Influence of operating, design and environmental conditions, Water Sci. Technol. 78(1) 195-206. http://dx.doi.org/10.2166/wst.2018.259
4. González-Camejo, J., Barat, R., Pachés, M., Murgui, M., Ferrer, J., Seco, A., 2018b. Wastewater Nutrient Removal in a Mixed Microalgae-bacteria Culture: Effect of Light and Temperature on the Microalgae-bacteria Competition. Environ. Technol. 39 (4), 503–515. https://doi.org/10.1080/09593330.2017.1305001
5. Gupta S., Pawar, S.B., Pandey, R.A., 2019. Current practices and challenges in using microalgae for treatment of nutrient rich wastewater from agro-based industries. Sci. Total Environ. 687, 1107–1126. https://doi.org/10.1016/j.scitotenv.2019.06.115
6. Jebali, A., Acién, F.G., Rodriguez Barradas, E., Olguín, E.J., Sayadi, S., Molina Grima, E., 2018. Pilot-scale outdoor production of *Scenedesmus* sp. in raceways using flue gases and centrate from anaerobic digestion as the sole culture medium. Bioresour. Technol. 262, 1-8. https://doi.org/10.1016/j.biortech.2018.04.057
7. Jiménez, E., 2010. Mathematical modelling of the two-stage nitrification process. Developement of modelling calibration methodologies for a SHARON reactor and activated sludge process (Modelación matemática del proceso nitrificación en dos etapas. Desarrollo de metodologías de calibración del modelo para un reactor SHARON y un proceso de fangos activados). PhD Thesis, Polytechnic University of Valencia, Spain.
8. Molinuevo-Salces, B., García-González, M.C., González-Fernández, C., 2010. Performance comparison of two photobioreactors configurations (open and closed to the atmosphere) treating anaerobically degraded swine slurry. Bioresour. Technol. 101, 5144–5149. https://doi.org/10.1016/j.biortech.2010.02.006
9. Najm, Y., Jeong, S., Leiknes, T., 2017. Nutrient utilization and oxygen production by *Chlorella vulgaris* in a hybrid membrane bioreactor and algal membrane

photobioreactor system. Bioresour. Technol. 237, 64-71. http://dx.doi.org/10.1016/j.biortech.2017.02.057

10. Rada-Ariza, A.M., Lopez-Vazquez, C.M., van der Steen, N.P., Lens, P.N.L., 2017. Nitrification by microalgal-bacterial consortia for ammonium removal in flat panel sequencing batch photo-bioreactors. Bioresour. Technol. 245, 81–89. http://dx.doi.org/10.1016/j.biortech.2017.08.019
11. Ramanna, L., Guldhe, A., Rawat, I., Bux, F., 2014. The optimization of biomass and lipid yields of *Chlorella sorokiniana* when using wastewater supplemented with different nitrogen sources. Bioresour. Technol. 168, 127–135. https://doi.org/10.1016/j.biortech.2014.03.064.
12. Reynolds, C.S., 2006. The Ecology of Phytoplankton (Ecology, Biodiversity and Conservation). Cambridge: Cambridge University Press, UK.
13. Risgaard-Petersen, N., Nicolaisen, M.H., Revsbech, N.P., Lomstein, B.A., 2004. Competition between ammonia oxidizing bacteria and benthic microalgae, Appl. Environ. Microb. 70(9), 5528-5537. https://doi.org/10.1128/AEM.70.9.5528-5537.2004
14. Robles, A., Ruano, M.V., Charfi, A., Lesage, G., Heran, M., Harmand, J., Seco, A., Steyer, J.P., Batstone, D.J., Kim, J., Ferrer, J., 2018. A review on anaerobic membrane bioreactors (AnMBRs) focused on modeling and control aspects, Bioresour. Technol. 270, 612-626. https://doi.org/10.1016/j.biortech.2018.09.049
15. Shoener, B.D., Schramm, S.M., Béline, F., Bernard, O., Martínez, C., Plósz, B.G., Snowling, S., Steyer, J.P., Valverde-Pérez, B., Wágner, D., Guest, J.S., 2019. Microalgae and cyanobacteria modeling in water resource recovery facilities: A critical review. Water Res. X 2, 100024. https://doi.org/10.1016/j.wroa.2018.100024
16. Weon, S.Y., Lee, S.I., Koopman, B., 2004. Effect of Temperature and Dissolved Oxygen on Biological Nitrification at High Ammonia Concentrations. Environ. Technol. 25(11), 1211-1219. https://doi.org/10.1080/09593332508618369
17. Winkler, M.K.H., Straka, L., 2019. New directions in biological nitrogen removal and recovery from wastewater, Current Opinion in Biotechnology 57C, 50–55. https://doi.org/10.1016/j.copbio.2018.12.007

CHAPTER IX:

IMPROVING MEMBRANE PHOTOBIOREACTOR PERFORMANCE BY REDUCING LIGHT PATH: OPERATING CONDITIONS AND KEY PERFORMANCE INDICATORS

IMPROVING MEMBRANE PHOTOBIOREACTOR PERFORMANCE BY REDUCING LIGHT PATH: OPERATING CONDITIONS AND KEY PERFORMANCE INDICATORS

González-Camejo, J., Aparicio, S., Jiménez-Benítez, A., Pachés, M., Ruano, M.V., Borrás, L., Barat, R., Seco, A. Improving membrane photobioreactor performance by reducing light path: operating conditions and key performance indicators. Water Res. (under review) September 2019.

ABSTRACT

Reducing the light path from 25 to 10 cm increased the nitrogen and phosphorus recovery rates, biomass productivity and photosynthetic efficiency by 150, 103, 194 and 67%, respectively. In addition, the areal biomass productivity (aBP) also increased when the light path was reduced, reflecting the better use of light in the 10-cm MPBR plant. The treatment capacity of the 10-cm MPBR plant also increased by 20%.

Discharge limits were met when the 10-cm MPBR plant was operated at biomass retention (BRTs) of 3-4.5 d and hydraulic retention times (HRTs) of 1.25-1.5 d. At these BRT/HRT ranges, the process could be operated without a high fouling propensity with gross permeate flux (J_{20}) of 15 LMH and specific gas demand (SGD_p) between 16 and 20 $Nm^3_{air} \cdot m^{-3}_{permeate}$, which highlights the potential of membrane filtration in MPBRs.

When the continuous operation of the MPBR plant was evaluated, an optical density of 680 nm (OD680) and soluble chemical oxygen demand (sCOD) were found to be good indicators of microalgae cell and algal organic matter (AOM) concentrations, while dissolved oxygen appeared to be directly related to MPBR performance. Nitrite and nitrate (NO_x) concentration and the soluble chemical oxygen demand:volatile suspended solids ratio (sCOD:VSS) were used as indicators of nitrifying bacteria activity and the stress on the culture, respectively. These parameters were inversely related to nitrogen recovery rates and biomass productivity and could thus help to prevent possible culture deterioration.

1. INTRODUCTION

Within the multiple applications of microalgae, algae-based wastewater treatment fits in with the concept of circular economy, since they can recover nitrogen and phosphorus from wastewater, obtaining water streams with low amounts of nutrients and microalgae biomass that can be used to produce biofuels and bio-stimulants (Vo et al., 2019).

However, outdoor microalgae cultivation is challenging due to the lower microalgae growth rates than other microorganisms such as heterotrophic bacteria. This means outdoor photobioreactors (PBRs) must be operated at long hydraulic retention times (HRTs) of around 3.5-10 d (Arbib et al., 2017; Romero-Villegas et al., 2018), which implies high surface needs (Acién et al., 2016).

As a solution, membrane separation of microalgae from permeate allows operations at different biomass retention (BRT) and hydraulic retention times (HRT). BRT is directly related to biomass production (González-Camejo et al., 2019), while HRT controls the nutrient loading rate (González-Camejo et al., 2018). Decoupling the BRT and HRT can therefore increase the nutrient load while biomass washout is avoided (Gao et al., 2019; Rada-Ariza et al., 2019), enhancing microalgae performance. On the other hand, operating at too low HRT values can be detrimental for nutrient recovery efficiency, since the microalgae may not be able to absorb all the nutrient content in the wastewater, therefore losing significant amounts of nitrogen and phosphorus with the effluent (Judd et al., 2015) and not meeting the legal requirements. This means that the optimum HRT and BRT of each microalgae cultivation system must be assessed.

MPBRs can also obtain high quality effluents in terms of suspended solids and pathogens, since they efficiently separate the microalgae and pollutants present in the culture from water (Gao et al., 2019) providing a source of reclaimed water (González-Camejo et al., 2019). Nevertheless, membrane operation aims at reducing membrane fouling, as it considerably affects the OPEX of membrane technology, i.e. the economic sustainability of MPBR technology (Seco et al., 2018). Fouling has been reported to be affected by operating conditions such as temperature, pH and BRT and can be intensified by the presence of AOM (Liu et al., 2017). AOM is commonly released by microalgae activity (Henderson et al., 2008), but its production is intensified under conditions of microalgae stress (Lee et al., 2018), showing the need for operating conditions that produce lower amounts of AOM.

Another controversial aspect of microalgae technology is the light available to the PBRs, which is the main factor limiting microalgae growth (Barceló-Villalobos et al.,

2019). Dense microalgae cultures absorb the light irradiance along the PBR light path (Huang et al., 2019), which means low photosynthetic efficiencies of 1.5-2% are usually found in large-scale PBRs (Nwoba et al., 2019). In this respect, the PBR light path plays an important role in photosynthetic efficiency, since light is attenuated as it passes through the culture (Fernández-Sevilla et al., 2018). Several studies have assessed the effect of light path on microalgae-based wastewater reactors, although the results are controversial (Table IX.1). The optimum light path therefore needs to be evaluated separately in each microalgae cultivation system.

Table IX.1. Optimal light path for outdoor microalgae cultivation systems.

Lp (cm)	Type of reactor	Reference
30	Raceway pond	Arbib et al. (2017)
< 10	PBR	Acién et al. (2016)
10-15	Cylindrical PBR	Huang et al. (2019)
2-5	Flat-panel PBR	Slegers et al. (2011)

Lp: Light path

In order to improve the implementation of microalgae cultivation systems, they have to be optimally operated to obtain maximum yields. A previous study on optimising an MPBR plant with 25-cm-wide PBRs obtained the best performance with a BRT and HRT of 4.5 and 3.5 d (González-Camejo et al., 2019). However, as these 25-cm PBRs were found to be highly light-limited, their light path was reduced to 10 cm. The goal of this study was thus to assess the effect of the PBR light path on microalgae performance in an outdoor 10-cm MPBR plant that treats effluent from an AnMBR system. The following key performance indicators (KPI) were evaluated during the continuous operation of an outdoor membrane photobioreactor: nutrient recovery rates, biomass productivity, OD680, sCOD:VSS, total eukaryotic cells (TEC), dissolved oxygen (DO) and NO_x concentrations.

2. MATERIALS AND METHODS

2.1. Microalgae and substrate

Indigenous microalgae were obtained from a mixed culture used in previous work (González-Camejo et al., 2019), mainly consisting of eukaryotic microalgae dominated by *Chlorella* (> 95% of TEC). Green microalgae *Scenedesmus,* cyanobacteria, nitrifying and heterotrophic bacteria were also present in low concentrations.

The substrate consisted of the nutrient-rich effluent from an AnMBR plant that treated real effluent from a primary settler (described in Seco et al. (2018)). The average characteristics of this substrate were a chemical oxygen demand (COD) concentration of 71 ± 35 mg $COD \cdot L^{-1}$, a nitrogen concentration of 45.0 ± 9.1 mg $N \cdot L^{-1}$ and a phosphorus concentration of 4.7 ± 1.3 mg $P \cdot L^{-1}$, which meant an N:P molar ratio of 22.7 ± 6.8.

2.2. MPBR pilot plant

The outdoor MPBR plant was operated in the Carraixet WWTP (39º30'04.0''N 0º20'00.1''W, Valencia, Spain). It mainly consisted of two flat-panel PBRs connected to a membrane tank (MT) (see González-Camejo et al. (2019)). The PBRs had a surface area of 2.3 m^2 (1.15 x 2 m). In a previous study, these PBRs had a light path of 25 cm, but this was reduced to 10 cm for the present study.

The PBRs were continuously air-stirred at 0.22 vvm, so that the culture could be as well-mixed (Huang et al., 2019). The PBR inner surfaces were brushed three times a week to avoid biofouling inside the reactors, which can block the light flux.

CO_2 was injected into the air system to maintain pH values at 7.5 ± 0.3. In this way, ammonia volatilisation and phosphorous precipitation were considered negligible (Whitton et al., 2016) and carbon-replete conditions were ensured.

Both PBRs had an additional artificial white light source consisting of twelve LED lamps (Unique Led IP65 WS-TP4S-40W-ME) installed at the back of the PBRs offering a continuous light irradiance of 300 $\mu E \cdot m^{-2} \cdot s^{-1}$ measured on the PBR surface.

The MT had a total working volume of 14 L and a filtration area of 3.4 m^2. It consisted of one hollow-fibre ultrafiltration membrane bundle extracted from an industrial-scale membrane unit (PURON® Koch Membrane Systems (PUR-PSH31), 0.03 μm pores). Air was introduced at the base of the MT to reduce membrane fouling by membrane scouring.

The membrane operating mode followed a sequence of 300-s basic F-R cycle (250 s filtration and 50 s relaxation), 40 s of back-flush every 10 F–R cycles, 60 s of ventilation every 20 F–R cycles and 60 s of degasification every 50 F–R cycles. The gross 20 ºC-standardised transmembrane flux (J_{20}) was kept at 15-26 LMH. The average specific gas demand per volume of produced permeate (SGD_P) was around 16-20 Nm^3 of gas per m^3 of permeate for two operating specific gas demands per m^2 of membrane (SGD_m), i.e. 0.3 and 0.4 $Nm^3 \cdot m^{-2} \cdot h^{-1}$, respectively.

Further details of the automation of the MPBR plant can be found in González-Camejo et al. (2019).

2.2.1. MPBR plant operation

The present study was divided in two sets of experiments: the first consisted of evaluating the light path effect on microalgae performance by comparing the results obtained for two different MPBR light paths: a 25-cm-wide MPBR plant (an extensive description of the operating conditions in this plant can be found in González-Camejo et al. (2019) and a 10-cm-wide MPBR plant. Both plants were operated at a BRT of 4.5 d and an HRT of 1.5 d. Allylthiourea (ATU) was added to maintain a concentration of 5 $mg \cdot L^{-1}$, so that nitrification was inhibited in both cases and the competition between microalgae and the growth of ammonium oxidising bacteria (AOB) for ammonium uptake was avoided (González-Camejo et al., 2018). The microalgae culture was dominated by *Chlorella* in both MPBR plants.

The second set of experiments consisted of the continuous operation of the 10-cm MPBR plant without nitrification inhibition. The aim was to determine the optimal operating conditions of this 10-cm MPBR plant and to assess the process KPI. Based on previous studies (González-Camejo et al., 2019) and the growth rates obtained during the batch stages of the cultivation process (Appendix A), BRT and HRT were modified in the range of 2-4.5 and 1-1.5 d, respectively, in 3 different experimental periods (Table IX.2). In Periods 1, 2 and 3 the pseudo-steady state was reached with a temperature in the range of 20-30 ºC and similar VSS concentrations.

Table IX.2. Operation and outdoor conditions of each operation period.

Period	Days of operation	Solar PAR ($\mu mol \cdot m^{-2} \cdot s^{-1}$)	Temperature (ºC)	BRT (d)	HRT (d)	NLR ($g\ N \cdot d^{-1}$)	PLR ($g\ P \cdot d^{-1}$)
1	35	281 ± 119	23.9 ± 1.7	4.5	1.5	12.6 ± 3.0	1.2 ± 0.5
2	25	344 ± 46	24.2 ± 1.7	3	1.5	16.9 ± 3.5	1.8 ± 0.4
3	25	266 ± 72	25.5 ± 1.2	3	1.25	15.1 ± 1.9	1.5 ± 0.3

All periods were preceded by chemical cleaning of the membranes and a start-up phase (as explained in detail in González-Camejo et al. (2019)).

2.3. Sampling and analytical methods

Grab samples of MPBR and AnMBR effluents, as well as of the microalgae culture, were collected in duplicate three times a week. Ammonium (NH_4), nitrite (NO_2), nitrate (NO_3) and phosphate (PO_4) were analysed according to Standard Methods (APHA, 2005): 4500-NH3-G, 4500-NO2-B, 4500-NO3-H and 4500-P-F, respectively, using an automatic analyser (Smartchem 200, WestcoScientific Instruments, Westco). Volatile suspended solids (VSS) concentration was also measured in duplicate, according to method 2540 E of the Standard Methods (APHA, 2005).

Total and soluble chemical oxygen demand (COD and sCOD) were tested once a week in duplicate according to Standard Methods (APHA, 2005) 5220-COD-C and 522-COD-D, respectively.

Total nitrogen (tN) concentration of the culture was measured by colorimetric analysis using the nitrogen total cell test kit (Merckoquant 1.14537.001, Merck, Germany) according to the manufacturer's instructions. Total phosphorus (tP) concentration was also measured in culture after total digestion at 150 ºC for two hours, followed by orthophosphate determination according to Standard Methods, 4500-P-F, (APHA, 2005), using an automatic analyser (Smartchem 200, WestcoScientific Instruments, Westco).

The OD680 and maximum quantum yield of photosystem II (F_v/F_m) were measured in-situ with a portable fluorometer AquaPen-C AP-C 100 (Photon Systems Instruments). Before measuring the F_v/F_m, the samples remained in the dark for ten minutes to become dark-adapted.

The wavelength spectrum (400-700 nm) was recorded by a spectrophotometer (Spectroquant® Pharo 100, Merck, Germany).

Total eukaryotic cells (TEC) were counted in duplicate twice a week. 50 µL of the sample were filtered through 0.2 µm membranes (Millipore GTTP). Cell counts were performed by epifluorescence microscopy on a Leica DM2500, using the 100x-oil immersion lens. A minimum of 300 cells were counted, with an error of less than 20%.

2.4. Calculations

Biomass productivity (BP) (mg $VSS \cdot L^{-1} \cdot d^{-1}$), nitrogen recovery rate (NRR) (mg $N \cdot L^{-1} \cdot d^{-1}$), phosphorus recovery rate (PRR) (mg $P \cdot L^{-1} \cdot d^{-1}$), and the nitrogen recovery rate:light irradiance (NRR:I) and phosphorus recovery rate-light irradiance (PRR:I) ratios were calculated as described in González-Camejo et al. (2018).

The culture extinction coefficient (K_a) and the average irradiance inside the PBRs (I_{av}) were calculated as proposed in Romero-Villegas et al. (2017).

The remaining parameters, i.e. intracellular nitrogen content (Ni), intracellular phosphorus content (Pi), photosynthetic efficiency (PE), energy recovery from the microalgae biomass (ER-BM), the 20 ºC-standardised transmembrane flux (J_{20}), fouling rate (FR), specific gas demand per volume of permeate produced (SGD_p) and per unit of membrane area (SGD_m) were obtained by the equations shown in Section III.6.

2.5. Statistical analysis

An analysis of variance (ANOVA) was carried out on SPSS 16.0, considering the following parameters: solar photosynthetic active radiation (PAR), temperature, VSS, OD680, TEC, DO concentration, F_v/F_m, nutrient (nitrogen and phosphorus) concentrations, chemical oxygen demand, NRR, PRR and biomass productivity. The correlation between the variables was considered significant at p-value < 0.05.

3. RESULTS AND DISCUSSION

3.1. Effect of MPBR light path

Under the same operating conditions, the 25-cm and 10-cm MPBR plants obtained significantly different results (see Table IX.3).

Table IX.3. Results obtained (mean ± standard deviation) for 25-cm MPBR plant (González-Camejo et al., 2019); and 10-cm MPBR plant (present study).

Parameter	Unit	Light path	
		25 cm	10 cm
Solar PAR	$\mu mol \cdot m^{-2} \cdot s^{-1}$	318 ± 103	271 ± 142
Temperature	ºC	23.5 ± 1.1*	23.3 ± 1.6*
VSS	$mg\ VSS \cdot L^{-1}$	288 ± 30	920 ± 110
sCOD	$mg\ COD \cdot L^{-1}$	76 ± 39	197 ± 114
BP	$mg\ VSS \cdot L^{-1} \cdot d^{-1}$	66 ± 6	194 ± 24
BP:I	$g\ VSS \cdot mol^{-1}$	0.29 ± 0.02	0.42 ± 0.05
aBP	$g\ VSS \cdot m^{-2} \cdot d^{-1}$	15.7 ± 1.4	20.0 ± 2.4
NRR	$mg\ N \cdot L^{-1} \cdot d^{-1}$	9.1 ± 1.5	22.8 ± 4.8
PRR	$mg\ P \cdot L^{-1} \cdot d^{-1}$	1.07 ± 0.54	2.18 ± 0.54
NRR:I	$mg\ N \cdot mol^{-1}$	45.6 ± 1.9*	48.9 ± 4.7*
PRR:I	$mg\ P \cdot mol^{-1}$	5.34 ± 1.42*	4.59 ± 0.85*
aNRR	$g\ N \cdot m^{-2} \cdot d^{-1}$	2.18 ± 0.36*	2.37 ± 0.54*
aPRR	$g\ P \cdot m^{-2} \cdot d^{-1}$	0.29 ± 0.13*	0.22 ± 0.06*
NRE	%	33.8 ± 6.5	73.5 ± 14.6
PRE	%	36.0 ± 9.1	53.0 ± 15.3
PE	%	3.02 ± 0.36	5.04 ± 1.63
N:VSS	$mg\ N \cdot g\ VSS^{-1}$	139 ± 23	111 ± 27
K_a	$m^2 \cdot g^{-1}$	0.41 ± 0.03	0.34 ± 0.02
P:VSS	$mg\ P \cdot g\ VSS^{-1}$	18 ± 8	11 ± 3
FR	$mbar \cdot min^{-1}$	~5	22-30

**Showed non-statistically significant differences (p-value < 0.05).*

A considerably higher biomass concentration was achieved in the 10-cm light path MPBR, which obtained higher biomass productivity than the 25-cm MPBR (Table IX.3). This was because the photon flux density is exponentially reduced along the light path (Fernández-Sevilla et al., 2018), with a greater volume of the culture in darkness in the 25-cm than in the 10-cm PBRs.

Similarly Huang et al. (2019) obtained higher biomass productivity at lower light path. However, areal productivity (aBP) was lower in the narrowest PBR. According to Huang et al. (2019), wider light paths reach lower biomass concentrations, the shadow effect was thus expected to be less significant in the 25-cm MPBR plant. On the other

hand, in the present study the narrowest PBRs achieved higher aBP, as well as a higher biomass productivity:light irradiance ratio (BP:I) and photosynthetic efficiency (see Table IX.2). This clearly demonstrated the more efficient use of light in the 10-cm MPBR plant than in the 25-cm MPBR plant. In fact, the extinction coefficient (K_a), which represents light scattering in the culture due to the light path, culture biomass and the optical properties of microalgae cells (Romero-Villegas et al., 2017), was significantly lower in the 10-cm MPBR plant than in the 25-cm MPBR plant: 0.34 ± 0.02 $m^{-2} \cdot g^{-1}$ and 0.41 ± 0.03 $m^2 \cdot g^{-1}$, respectively.

Regarding nutrients, the 10-cm PBRs showed significantly higher nutrient recovery rates; i.e. NRR was 150% and PRR was 103% higher than the 25-cm PBRs, so that the nutrient recovery efficiencies obtained in the 10-cm PBRs were considerably higher than in the widest PBRs (see Table IX.3). On the other hand, areal nutrient recovery rates and nutrient recovery rates:light irradiance ratios did not present any statistically significant differences (Table IX.3). This can be explained by the capability of microalgae to assimilate nutrients in darkness until they reach their maximum intracellular nutrient content, although they are not able to synthesise new biomass in the dark (Ruiz et al., 2014). In the 25-cm PBRs, which had higher volumes in darkness, the microalgae therefore presented higher nutrient content per unit of biomass, as shown in Table IX.3. Overall, reducing the MPBR light path from 25 to 10 cm provided better microalgae performance in AnMBR effluent treatment. This suggests that the light path should be optimised to obtain maximum MPBR performance. However, it also has to be remembered that too narrow light paths can significantly increase biofouling, which sharply reduces the light available to the culture.

Apart from the better results obtained from the 10-cm PBRs (Table IX.3), the higher biomass concentration in these PBRs has been reported to strengthen microalgae culture and protect it against grazers (Day et al., 2017), making it more consistent. It can also reduce the possible harvesting costs of post-treatment of the microalgae biomass for resource recovery (Huang et al., 2019). However, increasing biomass concentration in the 10-cm MPBR plant involved a rise in sCOD concentration from 76 ± 39 mg $COD \cdot L^{-1}$ in the 25-cm MPBR plant to 197± 114 mg $COD \cdot L^{-1}$ in the 10-cm MPBR plant. sCOD concentration was used as an indicator of the culture's AOM concentration, which has been reported to negatively affect the filtration process (Liu et al., 2017; Henderson et al., 2008). The fouling rate (FR) obtained in the 10-cm MPBR plant was thus significantly higher than that in the 25-cm MPBR plant under similar J_{20}

of around 26 LMH (Table IX.3). It must be highlighted that as *Chlorella* was the dominant species in both MPBR plants, the differences related to the rheology of the culture were not considered.

It should also be considered that the BP:I value of 0.42 ± 0.05 g VSS·mol^{-1} obtained in the 10-cm PBRs was significantly lower than that reported by Jebali et al. (2018), i.e. 1.0 g VSS·mol^{-1}. In addition, the photosynthetic efficiency of 5.04 ± 1.63% attained in the narrowest PBRs, in spite of being higher than the common values in large scale plants, which are usually in the range of 1.5-2% (Nwoba et al., 2019), is still far from the theoretical optimum of microalgae: around 10% (Romero-Villegas et al., 2017). The high biomass concentration of 920 ± 110 mg VSS·L^{-1} was thought to be mainly responsible for this light limitation, since the microalgae close to the surface absorb most of the light photons, scattering the deeper PBR zones (Barceló-Villalobos et al., 2019; Nwoba et al., 2019). In this respect, BRT has been reported as a key parameter in adjusting biomass concentration and improving light availability (Huang et al., 2019; Rada-Ariza et al., 2019). As this optimum BRT varies with the type of reactor, in spite of having defined the optimal operating conditions for the 25-cm PBRs in a previous study (González-Camejo et al., 2019), the optimum range of operating conditions must be defined for the more efficient 10-cm MPBR plant, with the goal of obtaining a robust culture that can also take full advantage of the solar light received.

3.2. Optimisation of operating conditions

During the entire operating period of the 10-cm MPBR plant, the culture was dominated by the indigenous *Chlorella* genus (> 99% of TEC). *Chlorella* has been reported to have a strong resistance to protozoa, especially when they are adapted to the region in which they are cultivated (Thomas et al., 2019). *Scenedesmus* was also present in the original inoculum (see Section IX.2.1). However, their presence during the operation of the MPBR plant was negligible, probably because the operating conditions favoured the growth of *Chlorella*, which are strong competitors for light and nutrients (Galès et al., 2019).

During Period 1 (BRT = 4.5 d; HRT = 1.5 d); Period 2 (BRT = 3 d; HRT = 1.5 d); and Period 3 (BRT = 3 d; HRT = 1.25 d), the MPBR plant effluent was able to meet the legal requirements of Directive 91/271/CEE for a 10,000-100,000-p.e WWTP, i.e. effluent nutrient concentrations under 15 mg N·L^{-1} and 2 mg P·L^{-1} (except for several days in Period 2, when nitrogen effluent concentration reached 20 mg N·L^{-1} due to the

sudden increase in nitrogen load (see Figure IX.1)). Nitrogen recovery efficiency (NRE) and phosphorus recovery efficiency (PRE) attained the high values of 80-85% and 90-99%, respectively, which also accomplished the legal requirements of Directive 91/271/CEE, i.e. 70-80% and 70% for nitrogen and phosphorus, respectively.

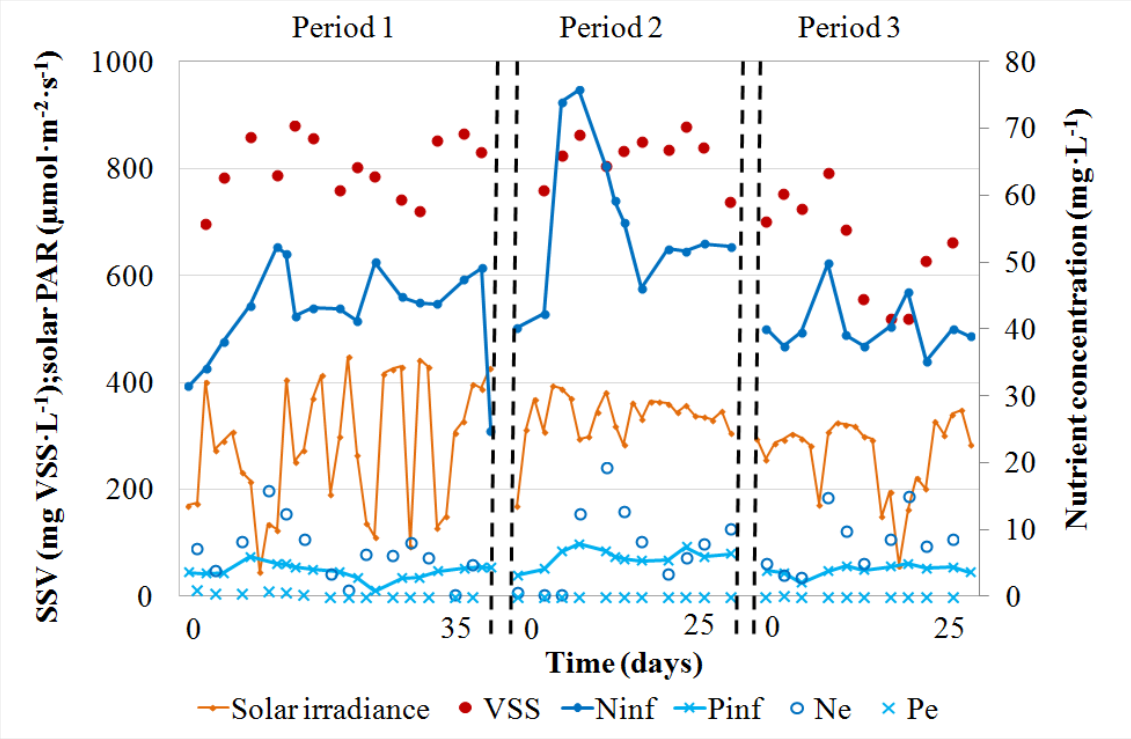

Figure IX.1: Pseudo-steady state conditions. Evolution of the concentration of the volatile suspended solids (VSS) (mgVSS·L^{-1}), daily average solar photosynthetic active radiation (PAR) (µmol·m^{-2}·s^{-1}), nitrogen concentration of the influent (Ninf) and effluent (Ne) (mg N·L^{-1}) and phosphorus concentration of the influent (Pinf) and effluent (Pe) (mg P·L^{-1})

On the other hand, when the 10-cm MPBR plant was operated at a HRT of 1 d and BRT of 2 d, heterotrophic and nitrifying bacteria activity was favoured, which negatively affected microalgae performance. The legal requirements were thus not complied with these operating conditions (Appendix B). It can thus be concluded that the MPBR plant was able to properly treat AnMBR effluent at BRT and HRT in the range of 3-4.5 d and 1.25-1.5 d, respectively.

It is surprising that the lowest HRT that accomplished legal requirements (i.e. 1.25 d) in the 10-cm MPBR plant was significantly lower than that which managed to satisfy the legal limits in the 25-cm MPBR plant; i.e. 3.5 d (González-Camejo et al., 2019). This means an increase of 20% in the plant's treatment capacity. It should also be noted that

this improvement was obtained without nitrification inhibition, unlike the previous study (González-Camejo et al., 2019). However, significant nitrification was not considered to occur during the operation of the 10-cm MPBR plant, since NO_x concentrations, which served as an indicator of nitrifying bacteria activity (see Section IX.3.3) always remained at low values (< 7.5 mg $N \cdot L^{-1}$).

The I_{av} values obtained for Periods 1, 2 and 3 (i.e., 21 ± 5 $\mu mol \cdot m^{-2} \cdot s^{-1}$, 21 ± 2 $\mu mol \cdot m^{-2} \cdot s^{-1}$ and 24 ± 2 $\mu mol \cdot m^{-2} \cdot s^{-1}$, respectively) were significantly lower than the ones obtained by Jebali et al. (2018) for green microalgae *Scenedesmus* sp. (125-263 $\mu mol \cdot m^{-2} \cdot s^{-1}$). According to Barceló-Villegas et al. (2019), the minimum light irradiance for photosynthesis is around 40 $\mu mol \cdot m^{-2} \cdot s^{-1}$, so that the system was likely to be photolimited. The high values of the extinction coefficient obtained in the 10-cm MPR plant (in spite of being lower than in the 25-cm MPBR plant) were considered the main reason of the low light availability. For Periods 1, 2 and 3, the plant's K_a value accounted for 0.35 ± 0.01 $m^2 \cdot g^{-1}$, 0.37 ± 0.01 $m^{-2} \cdot g^{-1}$ and 0.34 ± 0.03 $m^2 \cdot g^{-1}$, respectively; while Jebali et al. (2018) achieved extinction coefficients in the range of 0.06-0.13 $m^2 \cdot g^{-1}$. The shadow effect in the MPBR plant was thus highly relevant.

Period 2 (BRT of 3 d and HRT of 1.5 d) presented the highest NRR and PRR values of all three periods analysed: 29.7 ± 4.6 mg $N \cdot L^{-1} \cdot d^{-1}$ and 3.8 ± 0.6 mg $P \cdot L^{-1} \cdot d^{-1}$, respectively. These values are notably higher than most of the results reported so far for similar microalgae-based pilot plants (Table IX.4). In fact, only the authors who treated centrate (Romero-Villegas et al., 2017; 2018) obtained higher values than those obtained in the present study, due to the fact that centrate contains higher nutrient concentrations than wastewater from both secondary and AnMBR effluents (Gao et al., 2019). Period 2 also attained the highest biomass productivity: 258 ± 20 mg $VSS \cdot L^{-1} \cdot d^{-1}$. If this microalgae biomass would be anaerobically digested, the biogas produced could obtain a source of energy of 0.940 ± 0.073 $Kwh \cdot m^{-3}_{influent}$.

Table IX.4. Nutrient removal rates of algae based wastewater treatment studies under outdoor conditions.

Type of reactor	Type of wastewater	HRT (d)	BRT (d)	NRR (mg $N \cdot L^{-1} \cdot d^{-1}$)	PRR (mg $P \cdot L^{-1} \cdot d^{-1}$)	Reference
Flat-panel MPBR	AnMBR effluent	1.5	3	29.7	3.8	This study
HRAP(1)	Secondary effluent	10	10	3.99	0.36	Arbib et al., 2017
Flat-panel MPBR	AnMBR effluent	3.5	4.5	11.1	1.42	González-Camejo et al., 2019
HRAP(1)	Raw urban wastewater	10	10	1.9	0.32	Iasimone et al., 2017
Tubular PBR	Seawater + centrate	3.3	3.3	36.9	5.38	Romero-Villegas et al., 2017
Raceway	Seawater + centrate	3.3	3.3	28.7	3.99	Romero-Villegas et al., 2018
Flat-panel PBR	AnMBR effluent	3-4	4.5	8.1	1.0	Viruela et al., 2018
Flat-panel PBR	AnMBR effluent	3-4	9	3.3	0.4	Viruela et al., 2018

(1) HRAP: High rate algal pond

Nevertheless, as Periods 1, 2 and 3 received different levels of solar irradiance (Table IX.2), the periods were compared by normalising the parameters related to MPBR performance (NRR, PRR and BP) by light irradiance, i.e., NRR:I, PRR:I and photosynthetic efficiency, respectively (González-Camejo et al., 2019). The results (see Figure IX.2) show similar values for Periods 2 and 3 (p-value > 0.05). Hence, similar results were obtained by operating the system within an HRT range of 1.25-1.5 d. On the other hand, in Period 1 (BRT 4.5 d and HRT 1.5 d), the legal requirements were accomplished (Figure IX.1), although NRR:I, PRR:I and photosynthetic efficiency were significantly lower than in Periods 2 and 3 (Figure IX.2), so that operating at a BRT of 4.5 d was not considered appropriate to optimise this system. Under these operating conditions, microalgae were probably not at their exponential growth rate, since 4.5-d BRT was longer than the theoretical optimum BRT of 2.3-3 d (see Appendix IX.A). These results highlight the importance of operating an MPBR plant at the optimum BRT/HRT range of around 3/1.25-1.5 d to achieve the best MPBR performance.

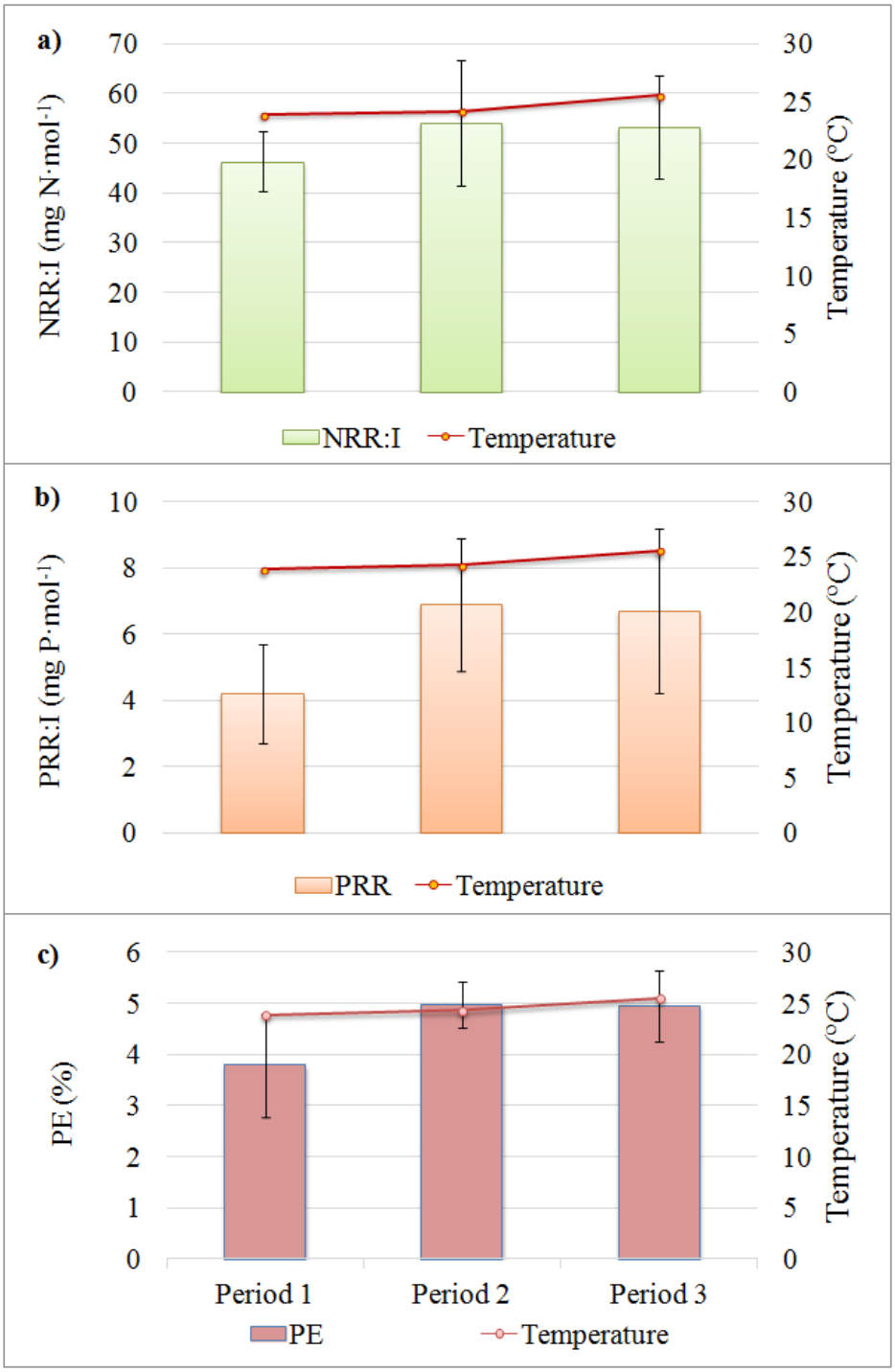

Figure IX.2. Average values of the control parameters during pseudo-steady state conditions of Period 1 (BRT = 4.5 d, HRT = 1.5 d); Period 2 (BRT = 3 d, HRT = 1.5 d) and Period 3 (BRT = 3 d, HRT = 1.25 d). a) Nitrogen recovery rate (NRR) (mg $N \cdot L^{-1} \cdot d^{-1}$); b) phosphorus recovery rate (PRR) (mg $P \cdot L^{-1} \cdot d^{-1}$); and c) photosynthetic efficiency (PE) (%).

With respect to the filtration process, the MPBR plant started operations with a J_{20} of around 26 LMH and SGD_p of 16-20 $Nm^3_{air} \cdot m^{-3}_{permeate}$ during Period 1 (Figure IX.3). However, the maximum TMP of 0.5 bar was rapidly reached after 14 days (data not shown). At this point the membrane needed chemical cleaning, which reduced FR to 10 $mbar \cdot min^{-1}$. Similarly, after 11 days of operation at similar J_{20} and SGD_p, FR rapidly increased, reaching maximum TMP on day 25. The membranes were therefore chemically cleaned again on day 26, which reduced FR to 13 $mbar \cdot min^{-1}$ (Figure IX.3). Hence, working at a J_{20} of 26 LMH was confirmed not to be appropriate for this MPBR system, as frequent chemical cleaning was required and this increased the operating costs (Seco et al., 2018) and reduced membrane life. For this reason, J_{20} was reduced significantly from 26 to 15 LMH after day 26, so that FR remained at low values (7-13 $mbar \cdot min^{-1}$) until the end of Period 1. At the same time, SGD_p was kept approximately constant (16-20 $Nm^3_{air} \cdot m^{-3}_{permeate}$), which meant that SGD_m fell from 0.4 to 0.3 $Nm^3 \cdot m^{-2} \cdot h^{-1}$ on average. This entailed reducing the OPEX associated with air pumping and lowered energy consumption (Seco et al., 2018).

The membrane performance in Period 2 showed no significant differences with Period 1 (from day 26 until day 35) as regards the fouling rate since it remained at 5-15 $mbar \cdot min^{-1}$ (Figure IX.3); probably because the average VSS and sCOD concentrations were similar (Lee et al., 2018); i.e., 801 ± 60 mg $VSS \cdot L^{-1}$ and 228 ± 44 mg $COD \cdot L^{-1}$ for Period 1; and 823 ± 44 mg $VSS \cdot L^{-1}$ and 239 ± 43 mg $COD \cdot L^{-1}$ for Period 2 (p-value > 0.05). On the other hand, Period 3 started with a similar FR to Period 2 (around 5-15 $mbar \cdot min^{-1}$); however, due to reduced solar irradiance (Figure IX.1), microalgae activity fell, which entailed VSS concentration dropping from 731 ± 42 mg $VSS \cdot L^{-1}$ to 531 ± 21 mg $VSS \cdot L^{-1}$ and sCOD concentration decreased from 248 ± 2 mg $COD \cdot L^{-1}$ to 75 ± 7 mg $COD \cdot L^{-1}$. The lower VSS and sCOD concentrations were thus considered to be related to the FR falling from 10 to 3 $mbar \cdot min^{-1}$ during days 15-20 of Period 3 (Figure IX.3).

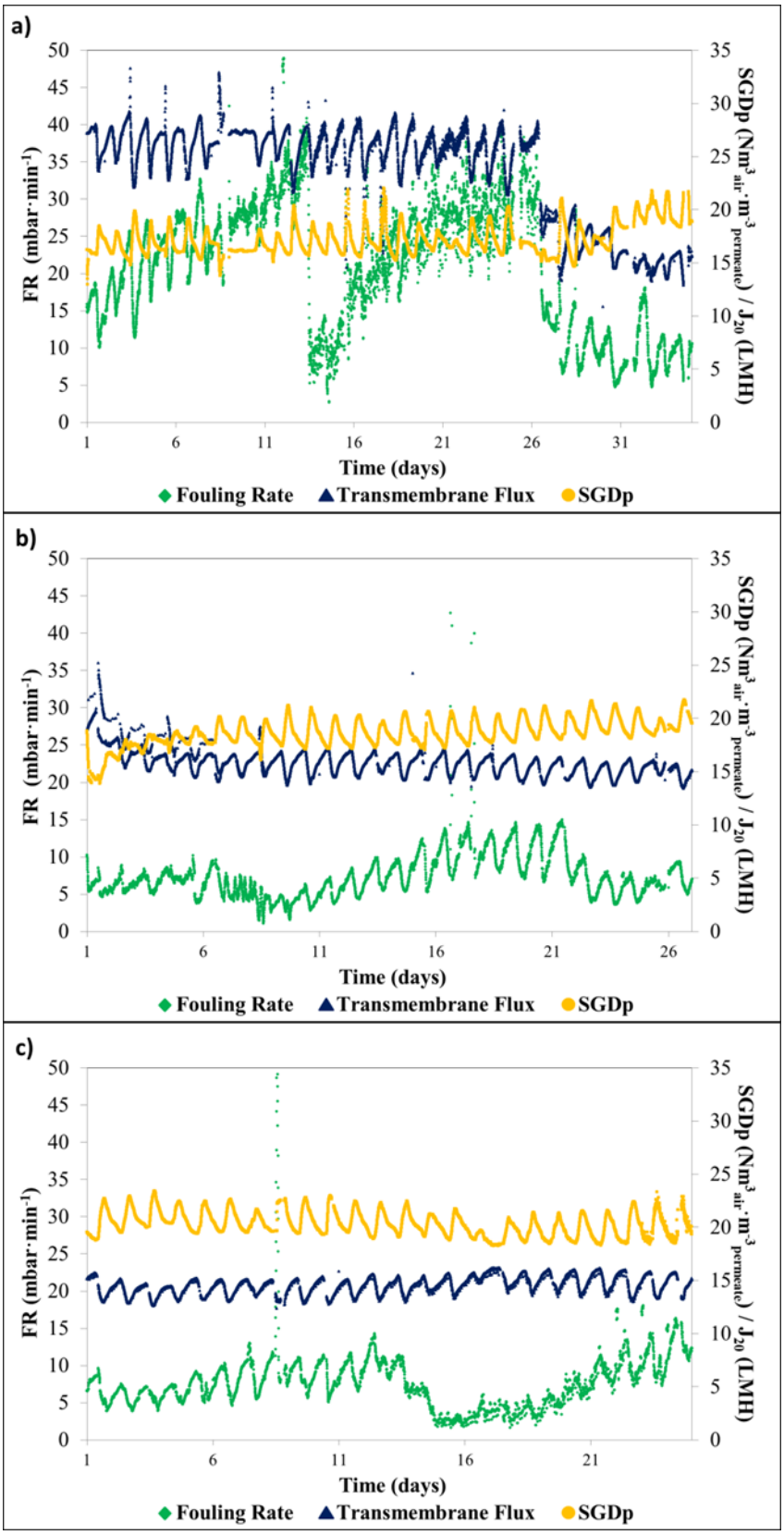

Figure IX.3. Membrane filtration performance at the MPBR plant during pseudo-steady state conditions: a) Period 1 (BRT = 4.5 d, HRT = 1.5 d); b) Period 2 (BRT = 3 d, HRT = 1.5 d); c) Period 3 (BRT = 3 d, HRT = 1.25 d).

Overall, non-significant differences in the membrane performance were observed under the operating BRTs and HRTs. The filtration process could be operated with a low fouling propensity when J_{20} of 15 LMH and SGD_p between 16 and 20 $Nm^3_{air} \cdot m^{-3}_{permeate}$ were applied, which highlights the potential of membrane filtration for microalgae cultivation in MPBRs.

3.3. Key performance indicators

An ANOVA analysis was carried out on data collected during the entire study period (around 8 months, excluding cleaning and start-up stages), considering only the parameters mentioned in Section IX.2.5. The results are shown in Table IX.5.

Table IX.5. Results of the ANOVA analysis for the long-term MPBR plant operation (only shows the paired parameters with a significant correlation: p-value < 0.05; in bold, p-value < 0.01).

		PAR	T	DO	VSS	NO_x	F_v/F_m	COD	sCOD	NRR	PRR	BP
PAR	R^2	1.000	N/A	N/A	N/A	N/A	N/A	N/A	N/A	**0.456**	**0.276**	N/A
	N	122								118	118	
T	R^2	N/A	1.000	N/A	N/A	N/A	N/A	N/A	N/A	0.220	0.226	N/A
	N		122							118	118	
DO	R^2	N/A	N/A	1.000	0.310	N/A	N/A	N/A	N/A	**0.246**	N/A	**0.337**
	N			122	114					115		109
VSS	R^2	N/A	N/A	**0.310**	1.000	**-0.500**	**-0.380**	**0.905**	**0.581**	0.215	N/A	**0.417**
	N			114	114	114	107	24	30	113		111
NO_x	R^2	N/A	N/A	N/A	**-0.500**	1.000	N/A	-0.490	**-0.485**	**-0.239**	N/A	-0.232
	N				114	122		26	30	118		112
F_v/F_m	R^2	N/A	N/A	N/A	**-0.380**	N/A	1.000	N/A	N/A	N/A	N/A	-0.214
	N				107		114					105
COD	R^2	N/A	N/A	N/A	**0.905**	-0.490	N/A	1.000	**0.591**	N/A	-0.462	-0.232
	N				24	26		26	24		26	112
sCOD	R^2	N/A	N/A	N/A	**0.581**	**-0.485**	N/A	**0.591**	1.000	N/A	N/A	N/A
	N				30	30		24	30			
NRR	R^2	**0.456**	0.220	**0.246**	0.215	**-0.239**	N/A	N/A	N/A	1.000	**0.548**	0.495
	N	118	118	115	113	118				118	118	109
PRR	R^2	**0.276**	0.226	N/A	N/A	N/A	N/A	-0.462	N/A	**0.548**	1.000	**0.364**
	N	118	118					26		118	118	109
BP	R^2	N/A	N/A	**0.337**	**0.417**	-0.232	-0.214	N/A	N/A	**0.495**	**0.364**	1.000
	N			109	111	112	105			109	109	112

PAR: photosynthetically active par; T: temperature; DO: dissolved oxygen; OD680: optical density at 680 nm; NOx: nitrite + nitrate concentration in the effluent; F_v/F_m: maximum quantum efficiency; COD: chemical oxygen demand; sCOD: soluble chemical oxygen demand; NRR: nitrogen recovery rate; PRR: phosphorus recovery rate; BP: biomass productivity; R^2: correlation coefficient; N: number of samples.

A high correlation was found between VSS concentration and OD680 (p-value < 0.01; R^2 = 0.908). VSS concentration was also highly correlated with TEC (p-value < 0.01; R^2 = 0.753), which suggests that the culture biomass was mainly composed of eukaryotic microalgae, even when there was noticeable growth of heterotrophic and nitrifying bacteria (Periods 3b and 4 in Appendix IX.B). OD680 therefore seems to be a good indicator of microalgae cell concentration in this culture.

The results also showed a correlation between ambient conditions (i.e. light and temperature) and nutrient recovery rates (NRR and PRR), as previously reported

(Viruela et al., 2018). However, the data was disperse (i.e. low R^2 values), probably because of the high variability of these ambient conditions throughout the day (Galès et al., 2019; Rada-Ariza et al., 2019) and seasonal variations. Sunlight and temperatures are thus key parameters and should be continuously monitored to correctly assess MPBR performance.

It should be noted that the correlation of PRR with ambient conditions was lower than that of NRR (lower R^2; see Table IX.5), probably because the MPBR plant was operated in P-deplete conditions for many days, as can be seen in Figure IX.1. However, P-depletion was not considered to limit microalgae growth since they have been reported to successfully grow under P-starvation (Marcilhac et al., 2014) using intracellular phosphorus. In fact, a significant correlation was found between PRR and biomass productivity (Table IX.5).

DO concentration was related to NRR and biomass productivity (Table IX.5) in spite of being influenced not only by microalgae photosynthetic activity (Fernández-Sevilla et al., 2018; Rada-Ariza et al., 2019) but also by other factors such as temperature and bacterial activity (Rossi et al., 2018), and thus could be used as an MPBR performance indicator during the continuous MPBR operations.

NO_x concentration can be used as an indirect measure of nitrifying bacteria activity (Galès et al., 2019; González-Camejo et al., 2018). It was inversely correlated to VSS, COD, NRR and biomass productivity (Table IX.5), which confirmed that the proliferation of nitrifying bacteria worsened MPBR performance due to microalgae-AOB competition for ammonium uptake.

sCOD in the feed (which was analogous to total COD as it was preceded by a filtration process (see Section IX.2.1.)) only accounted for 71 ± 35 mg $COD \cdot L^{-1}$, while sCOD inside the PBRs rose to 153 ± 73 mg $COD \cdot L^{-1}$, probably because of microalgae activity (Lee et al., 2018) as explained in Appendix IX.A. . In fact, a significant correlation was found between VSS concentration (which was in turn related to microalgae cells) and sCOD (Table IX.5). However, most of the organic matter in the culture was retained by the ultrafiltration membranes (Liu et al., 2017), with an effluent COD concentration of only 44 ± 22 mg $COD \cdot L^{-1}$, which accomplished the legal requirements (Directive 91/271/CEE)

It should also be considered that AOM concentration in microalgae cultures tends to increase under stress (Lee et al., 2018), which can reduce microalgae activity. The culture age can also boost AOM in the culture (Henderson et al., 2008). In this respect,

the normalisation of the sCOD with the microalgae biomass (sCOD:VSS) could be used as an indicator of the level of stress on the culture, since it would not include changes in sCOD due to microalgae growth (Appendix A). Significant increases of sCOD:VSS could favour heterotrophic bacteria growth (Galès et al., 2019) and, in turn, the growth of other superior organisms such as protozoa or rotifers, which can collapse the microalgae culture (Appendix B). As a result, significant inverse correlations were found between the sCOD:VSS ratio and NRR (p-value < 0.05; R^2 = 0.364; N = 16) and biomass productivity (p-value < 0.05; R^2 = 0.578; N = 20), which confirms that the culture was negatively affected by stress. The NOx concentration and sCOD:VSS ratio can therefore be used to prevent microalgae culture deterioration.

On the other hand, F_v/F_m, which has been reported to be related to the efficiency of PSII (Jebali et al., 2018), did not show any significant relationship with NRR and biomass productivity during the operating period, which indicates that F_v/F_m does not seem an appropriate parameter to assess the microalgae performance of this outdoor MPBR plant.

4. CONCLUSIONS

Light path appears to be a key design factor, since reducing it from 25 to 10 cm enhanced the MPBR performance significantly. In fact, maximum NRR, PRR, biomass productivity and photosynthetic efficiency were obtained of 26.3 ± 4.6 mg $N \cdot L^{-1} \cdot d^{-1}$, 3.77 ± 0.60 mg $P \cdot L^{-1} \cdot d^{-1}$, 258 ± 20 mg $VSS \cdot L^{-1} \cdot d^{-1}$ and 4.97 ± 0.45%, respectively. Moreover, the narrower MPBR light path raised light availability and treatment capacity.

Discharge limits were met when the 10-cm MPBR plant was operated at BRTs of 3-4.5 d and HRTs of 1.25-1.5 d, although nutrient recovery and photosynthetic efficiency were reduced when operated at 4.5-d BRT, in comparison to 3-d BRT. When BRT was shortened to 2 d and HRT to 1 day, MPBR performance decreased due to nitrifying and heterotrophic bacteria competing with microalgae.

The high VSS and sCOD concentrations obtained in the 10-cm MPBR plant forced it to operate at a transmembrane flux of around 15 LMH, which lowered the membrane's specific gas demand and allowed process OPEX to be reduced.

The ANOVA analysis showed that OD680 was an appropriate indicator of eukaryotic cell concentration, while sCOD concentration appeared as an indirect measurement of AOM concentration. Moreover, dissolved oxygen could be directly used as an indicator

of MPBR performance, while NO_x concentration and sCOD:VSS ratio could help prevent possible culture deteriorations since they were found to be inversely related to nitrogen recovery rates and biomass productivity.

ACKNOWLEDGMENTS

This research work was supported by the Spanish Ministry of Economy and Competitiveness (MINECO, Projects CTM2014-54980-C2-1-R and CTM2014-54980-C2-2-R) jointly with the European Regional Development Fund (ERDF), both of which are gratefully acknowledged. It was also supported by the Spanish Ministry of Education, Culture and Sport via a pre-doctoral FPU fellowship to authors J. González-Camejo (FPU14/05082) and S. Aparicio (FPU/15/02595).

REFERENCES

1. Acién, F.G., Gómez-Serrano, C., Morales-Amaral, M.M., Fernández-Sevilla, J.M., Molina-Grima E., 2016. Wastewater treatment using microalgae: how realistic a contribution might it be to significant urban wastewater treatment? Appl. Microbiol. Biotechnol. 100, 9013–9022. http://dx.doi.org/10.1007/s00253-016-7835-7
2. APHA-AWWA-WPCF (2005). Standard methods for the examination of water and wastewater, 21st edition. American Public Health Association (APHA), American Water Works Association (AWWA), Water Pollution Control Federation (WPCF).
3. Arbib, Z., de Godos, I., Ruiz, J., Perales, J.A., 2017. Optimization of pilot high rate algal ponds for simultaneous nutrient removal and lipids production. Sci. Total Environ. 589, 66–72. http://dx.doi.org/10.1016/j.scitotenv.2017.02.206
4. Barceló-Villalobos, M., Fernández-del Olmo, P., Guzmán, J.L., Fernández-Sevilla, J.M., Acién Fernández, F.G., 2019. Evaluation of photosynthetic light integration by microalgae in a pilot-scale raceway reactor. Bioresour. Technol. 280, 404-411. https://doi.org/10.1016/j.biortech.2019.02.032
5. Day, J.G., Gong, Y., Hu, Q., Microzooplanktonic grazers, 2017. A potentially devastating threat to the commercial success of microalgal mass culture. Algal Res. 27, 356-365. http://dx.doi.org/10.1016/j.algal.2017.08.024
6. Fernández-Sevilla, J.M., Brindley, C., Jiménez-Ruíz, N., Acién, F.G., 2018. A simple equation to quantify the effect of frequency of light/dark cycles on the photosynthetic response of microalgae under intermittent light. Algal Res. 35, 479–487. https://doi.org/10.1016/j.algal.2018.09.026

7. Galès, A., Bonnafous, A., Carré, C., Jauzein, V. Lanouguère, E., Le Floc'ha, E., Pinoit, J., Poullain, C., Roques, C., Sialve, B., Simier, M., Steyer, J.P., Fouilland, E., 2019. Importance of ecological interactions during wastewater treatment using High Rate Algal Ponds under different temperate climates, Algal Res. 40, 101508. https://doi.org/10.1016/j.algal.2019.101508
8. Gao, F., Cui, W., Xu, J.P., Li, C., Jin, W.H., Yang H.L., 2019. Lipid accumulation properties of *Chlorella vulgaris* and *Scenedesmus obliquus* in membrane photobioreactor (MPBR) fed with secondary effluent from municipal wastewater treatment plant. Renew. Energy 136, 671-676. https://doi.org/10.1016/j.renene.2019.01.038
9. González-Camejo, J., Jiménez-Benítez, A., Ruano, M.V., Robles, A., Barat, R., Ferrer, F., 2019. Optimising an outdoor membrane photobioreactor for tertiary sewage treatment. J. Environ. Manag. 245, 76-85. https://doi.org/10.1016/j.jenvman.2019.05.010
10. Gonzalez-Camejo, J., Barat, R., Ruano, M.V., Seco, A., Ferrer, J., 2018. Outdoor flat-panel membrane photobioreactor to treat the effluent of an anaerobic membrane bioreactor. Influence of operating, design and environmental conditions. Water Sci. Technol. 78(1) 195-206. http://dx.doi.org/10.2166/wst.2018.259
11. Henderson, R.K., Baker, A., Parsons, S.A., Jefferson, B., 2008. Characterisation of algogenic organic matter extracted from cyanobacteria, green algae and diatoms. Water Res. 42(13), 3435-3445. https://doi.org/10.1016/j.watres.2007.10.032
12. Huang, J., Hankame, B., Yarnold, J., 2019. Design scenarios of outdoor arrayed cylindrical photobioreactors for microalgae cultivation considering solar radiation and temperature. Algal Res. 41, 101515. https://doi.org/10.1016/j.algal.2019.101515
13. Iasimone, F., De Felice, V., Panico, A., Pirozzi, F., 2017. Experimental study for the reduction of CO_2 emissions in wastewater treatment plant using microalgal cultivation. J. CO_2 Util. 22, 1–8. http://dx.doi.org/10.1016/j.jcou.2017.09.004
14. Jebali, A., Acién, F.G., Rodriguez Barradas, E., Olguín, E.J., Sayadi, S., Molina Grima, E., 2018. Pilot-scale outdoor production of *Scenedesmus* sp. in raceways using flue gases and centrate from anaerobic digestion as the sole culture medium. Bioresour. Technol. 262, 1-8. https://doi.org/10.1016/j.biortech.2018.04.057
15. Judd, S., van den Broeke, L.J.P., Shurair, M., Kuti, Y., Znad, H., 2015. Algal remediation of CO_2 and nutrient discharges: a review. Water Res. 87, 356-366. http://dx.doi.org/10.1016/j.watres.2015.08.021
16. Lee, J.C., Baek, K., Kim, H.W., 2018. Semi-continuous operation and fouling characteristics of submerged membrane photobioreactor (SMPBR) for tertiary treatment

of livestock wastewater. J. Clean. Prod. 180, 244-251. https://doi.org/10.1016/j.jclepro.2018.01.159

17. Liu, B., Qu, F., Liang, H., Gan, Z., Yu, H., Li, G., Van der Bruggen, B., 2017. Algae-laden water treatment using ultrafiltration: Individual and combined fouling effects of cells, debris, extracellular and intracellular organic matter. J. Membr. Sci. 528, 178–186. https://doi.org/10.1016/j.memsci.2017.01.032
18. Marcilhac, C., Sialve B., Pourcher A.M., Ziebal C., Bernet N., Béline F., 2014. Digestate color and light intensity affect nutrient removal and competition phenomena in a microalgal-bacterial ecosystem, Water Res. 64, 278-287. http://dx.doi.org/10.1016/j.watres.2014.07.012
19. Nwoba, E.G., Parlevliet, D.A., Laird, D.W., Alameh, K., Moheimani, N.R., 2019. Light management technologies for increasing algal photobioreactor efficiency. Algal Res. 39, 101433. https://doi.org/10.1016/j.algal.2019.101433
20. Rada-Ariza, A.M., Fredy, D., Lopez-Vazquez, C.M., Van der Steen, N.P., Lens, P.N.L., 2019. Ammonium removal mechanisms in a microalgal-bacterial sequencing batch photobioreactor at different solids retention times. Algal Res. 39, 101468. https://doi.org/10.1016/j.algal.2019.101468
21. Romero-Villegas, G.I., Fiamengo, M., Acién-Fernández, F.G., Molina-Grima, E., 2018. Utilization of centrate for the outdoor production of marine microalgae at the pilot-scale in raceway photobioreactors, J. Environ. Manag. 228, 506–516. https://doi.org/10.1016/j.jenvman.2018.08.020
22. Romero-Villegas, G.I., Fiamengo, M., Acién-Fernández, F.G., Molina-Grima, E., 2017. Outdoor production of microalgae biomass at pilot-scale in seawater using centrate as the nutrient source. Algal Res. 25, 538–548. http://dx.doi.org/10.1016/j.algal.2017.06.016
23. Rossi, S., Bellucci, M., Marazzi, F., Mezzanotte, V., Ficara, E., 2018. Activity assessment of microalgal-bacterial consortia based on respirometric tests. Water Sci Technol. 78(1-2), 207-215. https://doi.org/10.2166/wst.2018.078
24. Ruiz, J., Arbib, Z., Álvarez-Díaz, P.D., Garrido-Pérez, C., Barragán, J., Perales, J.A., 2014. Influence of light presence and biomass concentration on nutrient kinetic removal from urban wastewater by *Scenedesmus obliquus*. J. Biotechnol. 178, 32-37. http://dx.doi.org/10.1016/j.jbiotec.2014.03.001
25. Seco, A., Aparicio, S., González-Camejo, J., Jiménez-Benítez, A., Mateo, O., Mora, J.F., Noriega-Hevia, G., Sanchis-Perucho, P., Serna-García, R., Zamorano-López, N., Giménez, J.B., Ruiz-Martinez, A., Aguado, D., Barat, R., Borrás, L., Bouzas, A., Martí, N., Pachés, M., Ribes, J., Robles, A., Ruano, M.V., Serralta, J. and Ferrer, J., 2018. Resource recovery from sulphate-rich sewage through an innovative anaerobic-

based water resource recovery facility (WRRF). Water Sci. Technol. 78 (9), 1925-1936. https://doi.org/10.2166/wst.2018.492

26. Slegers, P.M., Wijffels, R.H., van Straten, G., and van Boxtel, A.J.B. (2011) Design scenarios for flat panel photobioreactors. Appl. Energ. 88(10), 3342-3353. https://doi.org/10.1016/j.apenergy.2010.12.037
27. Thomas, P.K., Dunn, G.P., Good, A.R., Callahan, M.P., Coats, E.R., Newby, D.T., Feris, K.P., 2019. A natural algal polyculture outperforms an assembled polyculture in wastewater-based open pond biofuel production. Algal Res. 40, 101488. https://doi.org/10.1016/j.algal.2019.101488
28. Viruela A., Robles A., Durán F., Ruano M.V., Barat R., Ferrer J., Seco A., 2018. Performance of an outdoor membrane photobioreactor for resource recovery from anaerobically treated sewage. J. Clean. Prod. 178, 665-674. https://doi.org/10.1016/j.jclepro.2017.12.223
29. Vo, H.N.P., Ngo, H.H., Guo, W., Minh, T., Nguyen, H., Liu, Y., Liu, Y., Nguyen, D.D., Chang, S.W., 2019. A critical review on designs and applications of microalgae-based photobioreactors for pollutants treatment. Sci. Total Environ. 651(1), 1549-1568. http://dx.doi.org/10.1016/j.scitotenv.2018.09.282
30. Whitton, R., Le Mével, A., Pidou, M., Ometto, F., Villa, R., Jefferson, B., 2016. Influence of microalgal N and P composition on wastewater nutrient remediation. Water Res. 91, 371-378. https://doi.org/10.1016/j.watres.2015.12.054

APPENDIX IX.A. GROWTH RATES OF *CHLORELLA*-DOMINATED CULTURES OBTAINED UNDER CONDITIONS OF VARIABLE TEMPERATURE AND SOLAR IRRADIANCE

EXPERIMENTAL DESIGN

Optical density was monitored during the batch stages of four experimental periods (Figure I.X.A.1).

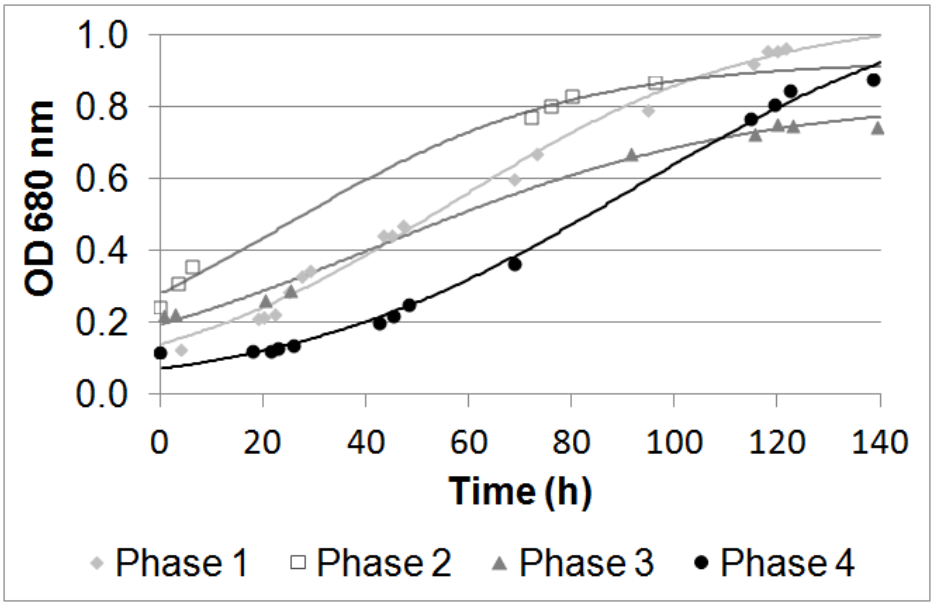

Figure IX.A.1: Evolution of the optical density at 680 nm during the start-up phases.

Growth rates (μ) were calculated by applying the Verhulst logistic kinetic model (Verhulst, 1838) to the OD680 evolution [Eq. IX.A.1]:

$$\mu = \frac{OD680_m \cdot OD680_0 \cdot e^{\mu \cdot t}}{OD680_m - OD680_0 + OD680_0 \cdot e^{\mu \cdot t}} \qquad \text{[Eq. IX.A.1]}$$

where μ is the specific growth rate (d^{-1}), $OD680_m$, $OD680_o$ and OD680 are the optical density at 680 nm at an operation time which corresponded to infinite, zero, and *t*, respectively; and *t* is the time of batch operation (d).

DATA

The growth rates of microalgae cultures are shown in Table IX.A.1.

Table IX.A.1. Growth rates and environmental conditions during each start-up phase.

Start-up stage	μ (d^{-1})	R^2	Temperature (ºC)	Daily average solar PAR (μmol·m^{-2}·s^{-1})	% reduction
1	0.80	0.992	24.4 ± 1.0	228 ± 9	6.3
2	0.86	0.994	26.4 ± 1.0	249 ± 9	-
3	0.67	0.993	24.7 ± 0.5	361 ± 26	22.3
4	0.71	0.747	16.2 ± 1.2	402 ± 36	17.0

The growth rates of start-up stages 1 and 2 were similar (Table IX.A.1). The low difference between them was probably due to the slight variations in solar irradiance and temperature (Behera et al., 2018), as can be seen in Table IX.A.1.

Nevertheless, growth rates of start-up stages 3 and 4 were considerably lower than those of stages 1 and 2 (Table IX.A.1). In the case of start-up 4, the temperature of only 16.2 ± 1.2 ºC must have had a strong influence on this decay since low temperatures are known to reduce microalgae growth (Viruela et al., 2016;2018). It could have also had an influence on the lag phase, since in start-up 4, it was the longest (around 24 h, see Figure IX.A.1), which agrees with the results of Marazzi et al. (2017). However, temperature in start-up 3 was very similar to start-up 1: 24.4 ± 1.0 and 24.7 ± 0.5 ºC, respectively. On the other hand, there were quite higher solar irradiances in start-up stages 3 and 4 than in stages 1 and 2 (Table IX.A.1). These irradiances (around average values of 360-400 μmol·m^{-2}·s^{-1}) were significantly higher than usual inhibitory intensities; i.e., around 200 μmol·m^{-2}·s^{-1} (Raeisossadati et al., 2019). In addition, the low biomass concentration at these initial stages (OD680 of around 0.12-0.25, see Figure IX.A.1) were not expected to significantly reduce the light intensity by self-shading (Abu-Ghosh et al., 2016; Wagner et al., 2018), so that microalgae could have suffered from photoinhibition in stages 3 and 4, therefore reducing their growth rate (Straka and Rittmann, 2018).

The values of growth rate obtained in this study (0.67-0.86 d^{-1}) are much higher than those obtained in a previous study for photobioreactors (PBRs) with a light path of 25 cm: 0.40-0.43 d^{-1} (González-Camejo et al., 2019), but are in the range of the growth rates reported by other authors in outdoor microalgae cultivation; i.e., 0.65-0.99 d^{-1} (Table IX.A.2).

Table IX.A.2. Microalgae growth rates obtained in outdoor microalgae cultivation.

Growth rate (d^{-1})	Species	Type of wastewater	Type of PBR	Reference
0.67-0.86	*Chlorella*	AnMBR effluent	Flat-panel MPBR	This study
0.43	*Chlorella*	AnMBR effluent	Flat-panel MPBR	González-Camejo et al. (2019)
0.40	*Scenedesmus*	AnMBR effluent	Flat-panel MPBR	González-Camejo et al. (2019)
0.99	*Chlorella zofingiensis*	BG-11 medium	Lab-scale PBR	Feng et al. (2011)
0.37-0.65	*Scenedesmus obliquus*	Secondary effluent	HRAP	Arbib et al. (2017)
0.26-1.02	*Chlorella pyrenoidosa*	ADAS	Rectangular PBR	Tan et al. (2016)

ADAS: anaerobically digested activated sludge; HRAP: high rate algal pond; MPBR: membrane photobioreactor; PBR: photobioreactor.

Ruiz et al. (2013) stated that maximum biomass productivity is obtained when biomass retention time (BRT) is the double of the inverse of the specific growth rate ($2 \cdot \mu^{-1}$). According to this, optimum BRT for operating the pilot plant should be in the range of 2.3-3 days. This theoretically optimum BRT is similar to that reported by Praveen et al. (2019) in a lab-scale MPBR: 2.5 days.

On the other hand, efficient nutrient recovery rates were reported to be attained at HRT of μ^{-1} (Ruiz et al., 2013), which would imply to operate at HRTs in the range of 1.15-1.5 d.

During start-up stage 1, sCOD concentration of the culture was also measured, showing a linear increase with time (Figure IX.A.2).

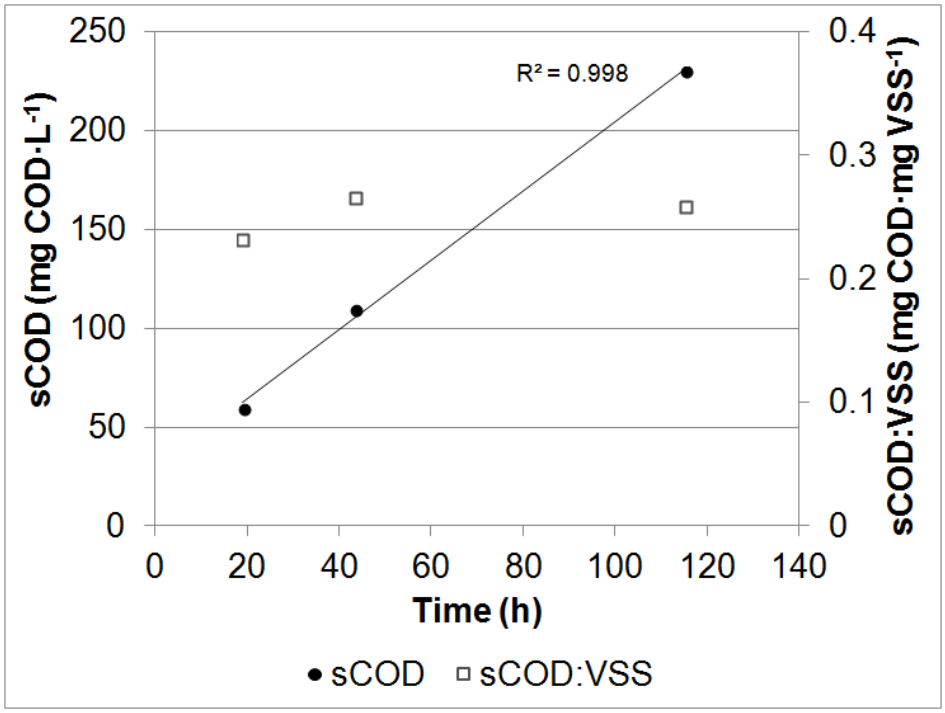

Figure IX.A.2: Evolution of sCOD concentration and sCOD:VSS ratio during start-up stage 1.

The increase in sCOD concentration was considered to be due to the rise of microalgae biomass (measured as VSS concentration) since sCOD:VSS was fairly constant during start-up stage 1 (Figure IX.A.2), with an average value of 0.25 ± 0.02 mg COD·mg VSS^{-1} (p-value < 0.05).

REFERENCES

1. Abu-Ghosh, S., Fixler, D., Dubinsky, Z., Iluz, D., 2016. Flashing light in microalgae biotechnology. Bioresour. Technol. 203, 357-363. http://dx.doi.org/10.1016/j.biortech.2015.12.057
2. Arbib, Z., de Godos, I., Ruiz, J., Perales, J.A., 2017. Optimization of pilot high rate algal ponds for simultaneous nutrient removal and lipids production. Sci. Total Environ. 589, 66–72. http://dx.doi.org/10.1016/j.scitotenv.2017.02.206
3. Behera, B., Acharya, A., Gargey, I.A., Aly, N., Balasubramanian, P., 2018. Bioprocess engineering principles of microalgal cultivation for sustainable biofuel production. Bioresour. Technol. Reports 5, 297-316. https://doi.org/10.1016/j.biteb.2018.08.001
4. Feng, P., Deng, Z., Hu, Z., Fan, L., 2011. Lipid accumulation and growth of *Chlorella zofingiensis* in flat plate photobioreactors outdoors. Bioresour. Technol. 102(22), 10577-10584. https://doi.org/10.1016/j.biortech.2011.08.109
5. González-Camejo, J., Jiménez-Benítez, A., Ruano, M.V., Robles, A., Barat, R., Ferrer, F., 2019. Optimising an outdoor membrane photobioreactor for tertiary sewage

treatment. J. Environ. Manag. 245, 76-85. https://doi.org/10.1016/j.jenvman.2019.05.010

6. Marazzi, F., Ficara, E., Fornaroli, R., Mezzanotte, V., 2017. Factors Affecting the Growth of Microalgae on Blackwater from Biosolid Dewatering. Water Air Soil Pollut. 228:68. https://doi.org/10.1007/s11270-017-3248-1
7. Praveen, P., Xiao, W., Lamba, B., Loh, K.C., 2019. Low Biomass Retention Operation to Enhance Productivity in an Algal Membrane Photobioreactor. Algal Res. 40, 101487. https://doi.org/10.1016/j.algal.2019.101487
8. Raeisossadati, M., Moheimani, N.R., Parlevliet, D., 2019. Luminescent solar concentrator panels for increasing the efficiency of mass microalgal production. Renew. Sust. Energy Rev. 101, 47–59. https://doi.org/10.1016/j.rser.2018.10.029
9. Ruiz, J., Álvarez-Díaz, P.D., Arbib, Z., Garrido-Pérez, C., Barragán, J., Perales, J.A., 2013. Performance of a flat panel reactor in the continuous culture of microalgae in urban wastewater: Prediction from a batch experiment. Bioresour. Technol. 127, 456-463. http://dx.doi.org/10.1016/j.biortech.2012.09.103
10. Straka, L., Rittmann, B.E., 2018. Light-dependent kinetic model for microalgae experiencing photoacclimation, photodamage, and photodamage repair. Algal Res. 31, 232–238. https://doi.org/10.1016/j.algal.2018.02.022
11. Tan, X.B., Zhang, Y.L., Yang, L.B., Chu, H.Q., Guo, J., 2016. Outdoor cultures of *Chlorella pyrenoidosa* in the effluent of anaerobically digested activated sludge: The effects of pH and free ammonia. Bioresour. Technol. 200, 606-615. http://dx.doi.org/10.1016/j.biortech.2015.10.095
12. Verhulst, P.F., 1838. Notice sur la loi que la population poursuit dans son accroissement. Corresp. Math. Phys. 10, 113–121.
13. Viruela A., Robles A., Durán F., Ruano M.V., Barat R., Ferrer J., Seco A., 2018. Performance of an outdoor membrane photobioreactor for resource recovery from anaerobically treated sewage. J. Clean. Prod. 178, 665-674. https://doi.org/10.1016/j.jclepro.2017.12.223
14. Viruela, A., Murgui, M., Gómez-Gil, T., Durán, F., Robles, Á, Ruano, M.V., Ferrer, J., Seco, A., 2016. Water resource recovery by means of microalgae cultivation in outdoor photobioreactors using the effluent from an anaerobic membrane bioreactor fed with pre-treated sewage. Bioresour. Technol. 218, 447-454. http://dx.doi.org/10.1016/j.biortech.2016.06.116
15. Wagner, D.S., Valverde-Perez, B., Plosz, B.G., 2018. Light attenuation in photobioreactors and algal pigmentation under different growth conditions – Model identification and complexity assessment, Algal Res. 35, 488-499. https://doi.org/10.1016/j.algal.2018.08.019

APPENDIX IX.B. INAPPROPRIATE OPERATING CONDITIONS FAVOURS THE PROLIFERATION OF BACTERIA IN AN OUTDOOR MEMBRANE PHOTOBIOREACTOR WHICH TREATED THE EFFLUENT OF ANAEROBIC MEMBRANE REACTOR

Outdoor microalgae cultures have to deal with the exposure to competing microorganisms present in the sewage such as bacteria, protozoa, cyanobacteria, etc. (Ferro et al., 2018; Ling et al., 2019; Thomas et al., 2019). These organisms can compete with microalgae for nutrient assimilation (Galès et al., 2019; Marazzi et al., 2019). In this respect, nitrifying bacteria have been reported to outcompete microalgae for ammonium uptake under certain lab conditions (González-Camejo et al., 2018). Moreover, the production of organic compounds during microalgae biological activity favours heterotrophic bacteria growth (Galès et al., 2019; Guldhe et al., 2017), and in turn, the growth of other superior organisms such as protozoa or rotifers, which can deteriorate the microalgae culture (Day et al., 2017; Lam et al., 2018).

EXPERIMENTAL DESIGN

During the continuous operation of the membrane photobioreactor (MPBR) plant (described in section IX.2.2), the pseudo-steady state was not reached in two different periods; i.e., Period 3B (which followed Period 3, see section IX.2.2.1) and Period 4 (which was preceded by a start-up phase as explained in González-Camejo et al. (2019). Operating and outdoor conditions of these periods are shown in Table IX.B.1.

SYTOX Green DNA staining dye (Invitrogen S7020) was used to monitor cell viability (Sato et al., 2004). 0.1µL of SYTOX Green 5mM was added to 50µL of the culture sample and were incubated in darkness for 5 minutes. Then samples were excited by fluorescence microscope (DM2500, Leica, Germany) equipped with a filter set at 450 – 490 nm for excitation and 515 nm for emission. More than 400 cells were counted in duplicate in a Neubauer counting chamber in each experiment.

Table IX.B.1. Operating and outdoor conditions of Periods 3B and 4.

Period	Days of operation	Solar PAR ($\mu E \cdot m^{-2} \cdot s^{-1}$)	Temperature (ºC)	BRT (d)	HRT (d)	NLR ($g\ N \cdot d^{-1}$)	PLR ($g\ P \cdot d^{-1}$)
3*	25	266 ± 72	25.5 ± 1.2	3	1.25	15.1 ± 1.9	1.5 ± 0.3
3B	10	286 ± 92	24.5 ± 0.7	3	1	20.7 ± 1.5	2.5 ± 0.1
4	20	341 ± 72	23.6 ± 0.7	2	1.25	19.4 ± 2.7	2.0 ± 0.2

**Pseudo-steady state was reached.*

DATA

As can be seen in Figure IX.B.1a, during Period 3, the nutrient concentrations remained under the discharge limits (< 15 mg $N \cdot L^{-1}$ and 2 mg $P \cdot L^{-1}$, Directive 91/271/EEC). Nonetheless, in Period 3B, HRT was reduced to 1 d, which implied the nutrient load to be raised (Table IX.B.1). Under this nutrient increase, microalgae were not able to successfully absorb all the nutrients. Moreover, organisms with higher growth rates than microalgae were expected to be favoured (Lam et al., 2018). In fact, significant growth of heterotrophic and nitrifying bacteria (which were also present in the inoculums, section IX.2.1), was observed (data not shown), which made the microalgae performance worsen (Figure IX.B.1.). As already mentioned, the AOB activity has been reported to limit the microalgae performance (González-Camejo et al., 2018); while heterotrophs, which growth is favoured by the release of organic compounds by microalgae activity (van den Hende et al., 2014), can excrete some microalgae inhibitors (Lam et al., 2018). In addition, the proliferation of these competing organisms reduce the light availability of the culture (Wagner et al., 2018), and can increase the membrane fouling rate (Wang et al., 2019), especially if filamentous organisms such as cyanobacteria are present.

In Period 4, HRT was set to 1.25 d while BRT was shortened to 2 days, slightly lower than the theoretical optimum BRT (2.3-3 d, see Appendix IX.A). Figure IX.B.1d shows that at those conditions, microalgae presented a good performance for around a week, but immediately started to wash out. Consequently, nutrient effluent concentrations continuously increased (Figure IX.B.1c). It must be noted that a significant growth of heterotrophic and nitrifying bacteria was also observed in Period 4 (data not shown).

Since shorter BRTs favour the growth of the fastest microorganisms (Winkler et al., 2017), it can be stated that operating at a BRT of 2 days under the operating conditions evaluated favoured the growth of nitrifying and heterotrophic bacteria because of their higher growth rate in comparison to microalgae (Jiménez, 2010; Praveen et al., 2019; Thomas et al., 2019).

In both Periods 3B and 4 the trend was similar. After the bacteria growth, the microalgae biomass concentration continuously decreased (from day 25 in Period 3 and day 10 in Period 4, see Figure IX.B.1), so did the microalgae viability, which fell from 88% to 69%. In addition, the I_{av} significantly raised from 24 ± 2 $\mu mol \cdot m^{-2} \cdot s^{-1}$ in Period 3 to 33 ± 6 $\mu mol \cdot m^{-2} \cdot s^{-1}$ in Period 3B (p-value < 0.05); while in the case of Period 4, the I_{av} (44 ± 6 $\mu mol \cdot m^{-2} \cdot s^{-1}$) was also significantly higher than those of Periods 1, 2 and 3: 21 ± 5 $\mu mol \cdot m^{-2} \cdot s^{-1}$, 21 ± 2 $\mu mol \cdot m^{-2} \cdot s^{-1}$ and 24 ± 2 $\mu mol \cdot m^{-2} \cdot s^{-1}$, respectively (p-value < 0.05). It has been reported that cultures with higher I_{av} (as those of periods 3B and 4) are less efficient in the use of light because more irradiance is needed to maintain the same growth rate (Ledda et al., 2015; Morales-Amaral et al., 2015). On the other hand, F_v/F_m values were always between 0.65-0.76, which suggested that there was not any significant photochemical stress (Moraes et al., 2019). Hence, the reduction of the microalgae biomass was mainly attributed to the competition with nitrifying and heterotrophic bacteria.

Concerning phosphorus, the concentration in the effluent was maintained at negligible values for several days after the striking AOB growth. This was probably due to luxury uptake of algae (Powell et al., 2009), since the amount of phosphorus absorbed by bacteria is negligible in comparison to that of microalgae (Galès et al., 2019). When microalgae growth was decreasing, microalgae would have continued consuming phosphorus until they were full of intracellular phosphorus (Behera et al., 2018). After that, their phosphorus uptake rate would have diminished and, as a consequence, phosphorus would have accumulated in the medium, showing a significant increase on the phosphorus effluent concentration (Figure IX.B.1.).

In conclusion, when operating a mixed microalgae culture, special care must be taken with nitrifying and heterotrophic bacteria growth, since they can compete with microalgae, making the culture reduce its performance.

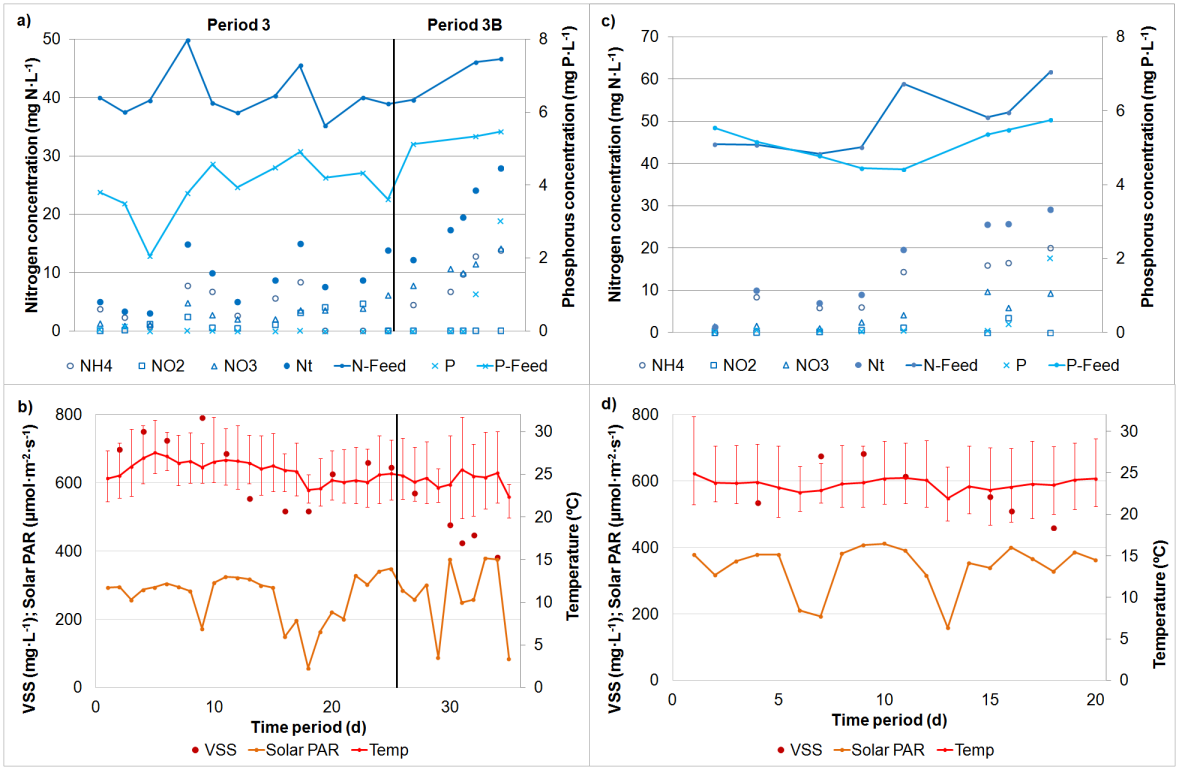

Figure IX.B.1. Transitory state conditions of the MPBR plant. Evolution of the influent concentration of nitrogen (N-Feed) and phosphorus (P-Feed); the effluent concentration of ammonium (NH4), nitrate (NO2), nitrate (NO3), total nitrogen (Nt) and phosphorus (P); concentration of volatile suspended solids of the culture (VSS); daily average solar irradiance (solar PAR) and temperature (Temp); a) and b) Period 3/3B; c) and d) Period 4.

REFERENCES

1. Behera, B., Aly, N., Balasubramanian, P., 2018. Biophysical modeling of microalgal cultivation in open ponds. Ecological Modelling 388 (2018) 61–71. https://doi.org/10.1016/j.ecolmodel.2018.09.024
2. Day, J.G., Gong, Y., Hu, Q., 2017. Microzooplanktonic grazers – A potentially devastating threat to the commercial success of microalgal mass culture, Algal Res. 27, 356-365. http://dx.doi.org/10.1016/j.algal.2017.08.024
3. European Commission Directive 91/271/EEC of 21 May 1991, concerning urban waste-water treatment. OJ L 135, 30.5.1991, p. 40–52.
4. Ferro, L., Gorzsás, A., Gentili, F.G., Funk, C., 2018. Subarctic microalgal strains treat wastewater and produce biomass at low temperature and short photoperiod, Algal Res. 35, 160-167. https://doi.org/10.1016/j.algal.2018.08.031
5. Galès, A., Bonnafous, A., Carré, C., Jauzein, V. Lanouguère, E., Le Floc'ha, E., Pinoit, J., Poullain, C., Roques, C., Sialve, B., Simier, M., Steyer, J.P., Fouilland, E., 2019. Importance of ecological interactions during wastewater treatment using High Rate Algal Ponds under

different temperate climates, Algal Res. 40, 101508. https://doi.org/10.1016/j.algal.2019.101508

6. González-Camejo, J., Viruela, A., Ruano, M.V., Barat, R., Seco, A., Ferrer, J., 2019. Effect of light intensity, light duration and photoperiods in the performance of an outdoor photobioreactor for urban wastewater treatment, Algal Res. 40, 101511. https://doi.org/10.1016/j.algal.2019.101511

7. González-Camejo, J., Barat, R., Pachés, M., Murgui, M., Ferrer, J., Seco, A., 2018. Wastewater Nutrient Removal in a Mixed Microalgae-bacteria Culture: Effect of Light and Temperature on the Microalgae-bacteria Competition. Environ. Technol. 39 (4), 503–515. https://doi.org/10.1080/09593330.2017.1305001

8. Guldhe, A., Kumari, S., Ramanna, L., Ramsundar, P., Singh, P., Rawat, I., Bux, F., 2017. Prospects, recent advancements and challenges of different wastewater streams for microalgal cultivation. J. Environ. Manag. 203, 299-315. http://dx.doi.org/10.1016/j.jenvman.2017.08.012

9. Jiménez, E., 2010. Mathematical modelling of the two-stage nitrification process. Developement of modelling calibration methodologies for a SHARON reactor and activated sludge process (Modelación matemática del proceso nitrificación en dos etapas. Desarrollo de metodologías de calibración del modelo para un reactor SHARON y un proceso de fangos activados). PhD Thesis, Polytechnic University of Valencia, Spain.

10. Lam, T.P., Lee, T.M., Chen, C.Y., Chang, J.S., 2018. Strategies to control biological contaminants during microalgal cultivation in open ponds. Bioresour. Technol. 252, 180-187. https://doi.org/10.1016/j.biortech.2017.12.088

11. Ledda, C., Idà, A., Allemand, D., Mariani, P., Adani, F., 2015. Production of wild *Chlorella* sp. cultivated in digested and membrane-pretreated swine manure derived from a full-scale operation plant. Algal Res. 12, 68-73. http://dx.doi.org/10.1016/j.algal.2015.08.010

12. Ling, Y., Sun, L.P., Wang, S.Y., Lin, C.S.K., Sun, Z., Zhou, Z.G., 2019. Cultivation of oleaginous microalga *Scenedesmus obliquus* coupled with wastewater treatment for enhanced biomass and lipid production. Biochem. Eng. J. 148, 162–169. https://doi.org/10.1016/j.bej.2019.05.012

13. Marazzi, F., Ficara, E., Fornaroli, R., Mezzanotte, V., 2017. Factors Affecting the Growth of Microalgae on Blackwater from Biosolid Dewatering. Water Air Soil Pollut. 228(2), 68. https://doi.org/10.1007/s11270-017-3248-1

14. Moraes, L., Martins, G., Morillas, A., Oliveira, L., Greque, M., Molina-Grima, E., Vieira, J.A., Acién, F.G., 2019. Engineering strategies for the enhancement of *Nannochloropsis gaditana* outdoor production: influence of the CO_2 flow rate on the culture performance in tubular photobioreactors. Process Biochem. 76, 171-177. https://doi.org/10.1016/j.procbio.2018.10.010

15. Powell, N., Shilton, A., Chisti, Y., Pratt, S., 2009. Towards a luxury uptake process via microalgae – Defining the polyphosphate dynamics. Water Res. 43, 4207-4213. https://doi:10.1016/j.watres.2009.06.011

16. Praveen, P., Xiao, W., Lamba, B., Loh, K.C., 2019. Low-retention operation to enhance biomass productivity in an algal membrane photobioreactor. Algal Res. 40, 101487. https://doi.org/10.1016/j.algal.2019.101487

17. Sato, M., Murata, Y., Mizusawa, M., Iwahashi, H., Oka, S.I., 2004. A simple and rapid dual-fluorescence viability assay for microalgae. Microbiol. Cult. Coll. 20(2), 53-59.

18. Thomas, P.K., Dunn, G.P., Good, A.R., Callahan, M.P., Coats, E.R., Newby, D.T., Feris, K.P., 2019. A natural algal polyculture outperforms an assembled polyculture in wastewater-based open pond biofuel production. Algal Res. 40, 101488. https://doi.org/10.1016/j.algal.2019.101488

19. Van Den Hende, S., Beelen V., Bore G., Boon N., Vervaeren H., 2014. Up-scaling aquaculture wastewater treatment by microalgal bacterial flocs: From lab reactors to an outdoor raceway pond. Bioresour. Technol. 159, 342–354. http://dx.doi.org/10.1016/j.biortech.2014.02.113

20. Wagner, D.S., Valverde-Perez, B., Plosz, B.G., 2018. Light attenuation in photobioreactors and algal pigmentation under different growth conditions – Model identification and complexity assessment, Algal Res. 35, 488-499. https://doi.org/10.1016/j.algal.2018.08.019

21. Wang, L., Pan, B., Gao, Y., Li, C., Ye, J., Yang, L., Chen, Y., Hu, Q., Zhang, X., 2019. Efficient Membrane Microalgal Harvesting: Pilot-scale Performance and Technoeconomic Analysis. J. Clean. Prod. 218, 83-95. https://doi.org/10.1016/j.jclepro.2019.01.321

22. Winkler, M.K.H., Boets, P., Hahne, B., Goethals, P., Volcke, E.I.P., 2017**.** Effect of the dilution rate on microbial competition: r-strategist can win over k-strategist at low substrate concentration. PLoS ONE 12(3): e0172785. https://doi.org/10.1371/journal.pone.0172785

CHAPTER X:

ON-LINE MONITORING OF MICROALGAE ACTIVITY BASED ON CARBON UPTAKE RATE DATA FOR MEMBRANE PHOTOBIOREACTORS

CHAPTER X

ON-LINE MONITORING OF MICROALGAE ACTIVITY BASED ON CARBON UPTAKE RATE DATA FOR MEMBRANE PHOTOBIOREACTORS

González-Camejo, J., Robles, A., Seco, A., Ferrer, J., Ruano, M.V., 2019. On-line monitoring of microalgae activity based on carbon uptake rate data for membrane photobioreactors. Chem. Eng. J. (submitted). September 2019.

ABSTRACT

The outdoor performance of microalgae cultivation systems is significantly sensitive to dynamics in environmental and operating conditions. Thus, monitoring and control systems are needed in order to maximise microalgae biomass productivity and nutrient recovery. This work aimed at demonstrating the use of carbon uptake rate (CUR) data to monitor microalgae performance.

CUR values were based on pH data monitoring to on-line measure the microalgae photosynthetic activity in a membrane photobioreator (MPBR) system. Short-term operation showed a relation between gross CUR values and MPBR performance in terms of NRR and biomass productivity. In addition, a daily indicator of the maximum microalgae activity was assessed combining the on-line CUR measurements and a microalgae growth kinetic model. Both indicators could contribute to ease the development of advanced monitoring and control systems aimed at optimising microalgae cultivation performance.

1. INTRODUCTION

Microalgae cultivation has received increasing interest from the scientific community (Garrido-Cárdenas et al., 2018; Krishnamoorthy et al., 2017) since it allows nutrient recovery, CO_2 biofixation and valorisation of the algal biomass produced (Daverey et al., 2019; Eze et al., 2018; Gonçalves et al., 2016).

Microalgae are commonly cultivated in open ponds or in closed photobioreactors (PBRs). PBRs have several advantages over open ponds such as lower evaporation, contamination, and CO_2 losses (Ferreira et al., 2019). Nevertheless, large-scale industrial

plants to cultivate microalgae are currently scarce (Franco et al., 2019), mainly due to their inefficiency (Barbosa et al., 2003; Kubelka et al., 2018) and high investment and operating costs (Acién et al., 2016; Arbib et al., 2013).

Hence, monitoring and control of the microalgae cultivation process appears essential to improve the feasibility of this technology since it can help to increase the microalgae production capacity (Salama et al., 2017; Xu et al., 2019).

Microalgae cultivation depends on several factors such as light irradiance and temperature (De-Luca et al., 2018; De Vree et al., 2015; Garcia et al., 2018; Ras et al., 2013; Viruela et al., 2016; 2018) and pH (Pawlowski et al., 2016). In fact, each microalgae strain has a pH range in which photosynthetic activity and biomass productivity is maximum (Moheimani, 2013). By way of example, Qiu et al. (2017) obtained the most cost-effective cultivation of green microalgae *Chlorella sorokiniana* in a flat-panel PBR at a pH range of 7-8; while optimum pH for *Scenedesmus* sp. is around 8 (de Godos et al., 2014; Eze et al., 2018). In the case of cyanobacteria, higher pH values favour their growth. For instance, González-López et al. (2012) reported highest *Anabaena* sp. growth at pH of 9.0. It must be also considered that microalgae activity entails a rise in the culture pH as a consequence of the carbon fixation during photosynthesis (Deng et al., 2018; Eze et al., 2018; Gonçalves et al., 2016). An excessive increase of the culture´s pH over values of 10 can inhibit green microalgae growth (Iasimone et al., 2018). In addition, high pH values hinder the availability of nutrients for microalgae growth (Meseck et al., 2007). In fact, carbonate (CO_3^{2-}), which cannot be absorbed for microalgae (Bhakta et al., 2015), is the dominant inorganic carbon species when pH is over 10 (Huang et al., 2017). On the other hand, CO_2 is the main species at low pH values while bicarbonate dominates in the pH range of 6.5-10.5 (de Andrade et al., 2016).

Furthermore, the equilibrium ammonium-ammonia (NH_4^+/NH_3) favours ammonia at pH values over 9 (Acién et al., 2016; Muñoz and Guieysse, 2006). Nitrogen in the form of ammonia is not desirable since it can be lost by stripping and can be toxic for microalgae (Sutherland et al., 2015). Regarding phosphorus, pH values over 9 boosts the phosphorus chemical precipitation, which not only reduces the bioavailability of this nutrient but also, diminishes the light dispersion in the microalgae culture (Muñoz and Guieysse, 2006). For this reason, pH is usually controlled by CO_2 addition to the culture (Acién et al., 2016; Ruiz-Martínez et al., 2012).

pH, light, temperature and dissolved oxygen are commonly measured by using low-cost sensors. These sensors are reliable and involve low investment, maintenance and

operational costs (Campos et al., 2012; Foladori et al., 2018; Ruano et al., 2009). In addition, the response time of the low-cost sensors is quite low (Alex et al. 2003). On the other hand, parameters such as biomass productivity and nutrient recovery rates have been usually employed to evaluate the microalgae cultivation process (Arbib et al., 2017; González-Camejo et al., 2019; Iasimone et al., 2017), but the measurements of these off-line parameters often imply chemical analyses which are time-consuming, expensive and require certain delay (Ferrer et al., 2008; Foladori et al., 2018). In the case of nutrients, its concentration can be monitored on-line by nutrient sensors/analysers, but they present higher capital and maintenance costs than low-cost sensors and are not always as reliable as expected (Foladori et al., 2018; Ruano et al., 2009).

In terms of microalgae cultivation control, some efforts have been made to measure the microalgae photosynthetic activity. By way of example, Perin et al. (2016) measured the chlorophyll fluorescence in vivo; while Rossi et al. (2018) used standardised respirometric assays. Nevertheless, these methodologies imply off-line measures which cannot be monitored in real-time. On the other hand, it would be of great interest to take advantage of the data monitored in the process to continuously assess the performance of the microalgae cultivation system. In this respect, an approach based on pH data for carbon uptake rate (CUR) monitoring is proposed to on-line measure the microalgae photosynthetic activity in an MPBR system treating AnMBR effluent. Hence, an indicator of the gross microalgae activity is obtained based on these on-line CUR measurements. In addition, an indicator of the maximum microalgae activity is proposed combining these on-line CUR measurements and a microalgae growth kinetic model. The former could be used as an input for on-line control in the short term, while the latter allows the long-term monitoring and control of microalgae performance.

2. MATERIAL AND METHODS

2.1. MPBR pilot plant

The MPBR plant was operated outdoors in the Carraixet WWTP (39º30’04.0’’N 0º20’00.1’’W, Valencia, Spain). It consisted of two transparent outdoor flat-plate PBRs connected to a polypropylene membrane tank (MT) which allowed microalgae biomass filtration for biomass retention time (BRT) and hydraulic retention time (HRT) to be decoupled.

The aeration system consisted of two perforated pipes placed in the low part of the PBRs, which continuously stirred air and ensure appropriate CO_2 transference within the broth

column. In order to maintain the pH value within an optimum range, an on-off valve was opened for 5 s to introduce pure pressurised CO_2 (99.9%) into the air system whenever the pH measurements were over the set point value of 7.5. This pH value has been reported as the optimum to achieve the highest microalgae productivity and minimise CO_2 losses in an outdoor raceway pond for green microalgae cultivation (Caia et al., 2018). This CO_2 addition enabled to limit undesirable phenomena such phosphorus precipitation, ammonia volatilisation (Whitton et al., 2016), carbonate formation (Bhakta et al., 2015) and also avoided carbon limitation (de Andrade et al., 2016).

Twelve white LED lamps (Unique Led IP65 WS-TP4S-40W-ME) were installed at the back of each PBR, offering a continuous artificial light irradiance of 300 $\mu mol \cdot m^{-2} \cdot s^{-1}$.

Two different MPBR systems were operated: i) PBRs with a working volume of 550 L (25-cm wide); ii) PBRs of 230 L (10-cm wide).

The MPBR plant is further described in González-Camejo et al. (2019).

2.1.1. Instrumentation and Automation

The following on-line sensors were installed: i) two (one in each PBR) pH-temperature sensors (pHD sc DPD1R1, Hach Lange); ii) two (one in each PBR) dissolved oxygen sensors (LDO sc LXV416.99.20001, Hach Lange); iii) one irradiation sensor (Apogee Quantum SQ-200) on the PBR surface to measure the photosynthetically active radiation (PAR). The regular maintenance of the pH sensors consisted of replacing the salt bridge and the buffer once a year and calibrating these sensors with a frequency of two weeks. In the case of the oxygen sensors, the membrane was replaced every three months and sensors were calibrated every two weeks. These sensors were connected to a network system (a PLC and a personal computer) to perform the process control and data acquisition. Other transmitters to measure flow rate, level, pressure, etc. were installed in order to control the continuous operation of the MPBR plant. A Supervisory Control And Data Acquisition (SCADA) software was designed in order to view and store the sensors signals. Further information can be found in Viruela et al. (2018).

2.1.2. Microalgae substrate and inoculum

The microalgae substrate consisted of the nutrient-rich effluent from an AnMBR plant that treated real sewage (Seco et al*.,* 2018). As this AnMBR effluent had high sulphide concentration (around 80-120 mg $S \cdot L^{-1}$), it was aerated in a regulation tank before being fed to the PBRs in order to oxidise the sulphide to sulphate as explained in González-

Camejo et al. (2017). The AnMBR effluent ammonium concentration during the experimental periods was in the range of 40-80 mg $N \cdot L^{-1}$; while phosphate concentration was of 4-10 mg $P \cdot L^{-1}$. Nitrite and nitrate concentrations were negligible.

The microalgae used were originally collected from the walls of the secondary clarifier in the Carraixet WWTP (Valencia, Spain) and mainly consisted of a mix of green microalgae *Scenedesmus* and *Chlorella*, as well as diatoms and cyanobacteria (in lower concentrations). Heterotrophic and nitrifying bacteria were also present.

2.2. Sampling and methods

Grab samples were collected in duplicate from the influent (AnMBR effluent after sulphide oxidation) and effluent streams of the MPBR pilot plant three times a week. Ammonium (NH_4), nitrite (NO_2), nitrate (NO_3), and phosphate (PO_4) were analysed in a Smartchem 200 automatic analyser (WestcoScientific Instruments, Westco) according to Standard Methods (APHA, 2005): 4500-NH3-G, 4500-NO2-B, 4500-NO3-H, 4500-P-F, respectively. Volatile suspended solids (VSS) of the culture were analysed according to Standard Methods as well (APHA, 2005): method 2540 E.

Optical density of 680 nm (OD) was measured in-situ with a portable fluorometer AquaPen-C AP-C 100 (Photon Systems Instruments).

6 respirometric tests were done in a period of two weeks to assess the microalgae and nitrifying bacteria activity simultaneously. The protocol of the respirometries is explained in detail in Rossi et al. (2018).

2.3. Carbon uptake rate (CUR) monitoring

As commented above, CUR data obtained from pH-temperature sensors was used to on-line measure the photosynthetic activity of microalgae. This data is used to propose an indicator of the microalgae activity. To this aim, the pH control of the MPBR plant (see section X.2.1) was turned off and the CUR was calculated from the first derivative from pH data dynamics (pH´). Due to negligible effect of other factors related in the carbon concentration of the culture, microalgae activity was considered to be the main factor affecting pH dynamics (section X.3.1).

It should be considered that carbon uptake causes pH increases (Foladori et al., 2018; Qiu et al., 2017); consequently:

$$CUR = - \alpha_1 \cdot pH' \qquad \text{[Eq. X.1]}$$

Where CUR (mg $C \cdot L^{-1} \cdot d^{-1}$) is the carbon uptake rate, pH´ is the first derivative from pH data dynamics (pH unit$\cdot min^{-1}$), and α_1 is a distributed factor.

It must be noted that CUR values measured under nitrogen-limited conditions (< 10 mg $N \cdot L^{-1}$, see Pachés et al., (2018)) were discarded. Hence, nutrient limitation was not considered in this study.

2.3.1. Short-term CUR monitoring

In order to assess the culture performance in the short term, during six days in which the MPBR plant was continuously operated at biomass retention time (BRT) of 4.5 days and hydraulic retention time (HRT) of 1.25 days, the pH control was turned off for 10 minutes per hour to measure CUR. These CUR measurements were used as an indicator of the gross microalgae activity under the specific operating and environmental conditions of the system.

2.3.2. Long-term CUR monitoring

Table X.1 shows the ambient and operating conditions during the long-term operation of the MPBR plant. In order to assess MPBR performance in the long term, the pH control of the plant was turned off for 30 minutes during night-time hours, while keeping a continuous, constant artificial light irradiance of 300 $\mu mol \cdot m^{-2} \cdot s^{-1}$ provided by the LED lamps installed in the PBR. Thus, the CUR measurement did not depend on solar light dynamics and was selected as an average measurement of the daily microalgae activity. On the basis of the obtained on-line CUR measurements and previous results on microalgae activity modelling (Robles et al, 2019), an indicator of the daily maximum microalgae activity was assessed. To this aim, a microalgae growth kinetic model was used.

Table X.1. Experimental conditions during the continuous operation of the MPBR plant (mean ± standard deviation).

Period	Lp (cm)	Air flow rate (vvm)*	T (ºC)	Solar PAR ($\mu mol \cdot m^{-2} \cdot s^{-1}$)	BRT (d)	HRT (d)
Jun 15 – Oct 15	25	0.10	25.0 ± 2.4	268 ± 72	4.5	2-3
Nov 15 – Mar 16	25	0.10	24.5 ± 2.0	303 ± 130	4.5-6	2.5
Apr 16 – Sep 16	25	0.10	25.3 ± 1.2	258 ± 81	4.5-9	1-3.5
Nov 16 – Mar 17	10	0.22	22.3 ± 3.2	273 ± 142	4.5-3	1.5
Apr 17 – Sep 17	10	0.22	24.6 ± 1.6	274 ± 79	2-3	1-1.5

Lp: Light path; vvm: air-volume·PBR-volume^{-1}·min^{-1}; T: temperature; BRT: biomass retention time; HRT: hydraulic retention time; Solar PAR: daily average solar photosynthetic active radiation.

**Air flow rate: 3.2 Nm^3·h^{-1} for each PBR during all the continuous operation (Jun 15 – Oct 17).*

2.3.2.1. Microalgae growth kinetic model

CUR (which is inversely related to pH´, see Eq. X.1) is usually correlated with the average light irradiance (I_{av}) by a hyperbolic function as proposed by Fernandez et al. (2016). Eq. X.2 can be used to determine CUR as a function of I_{av} when considering constant respiration conditions, non-limited nutrient conditions, and non-inhibited dissolved oxygen and pH conditions:

$$CUR = -CUR_{max} \cdot I_i + \alpha_2 \cdot r_{CO_2} \qquad \text{[Eq. X.2]}$$

Where CUR_{max} is the maximum CUR (pH unit·min^{-1}), I_i (i=1:3) is a given function related to the average light irradiance ($I_{av,}$ µmol·m^{-2}·s^{-1}), and α_2 is a distributed factor.

I_1, I_2, and I_3 are therefore normalising factors related to I_{av} representing different behaviours of microalgae in the PBR (Robles et al., 2019). I_1 is analogous to the duty cycle, which is the proportion of time at which microalgae are exposed to light (Fernández-Sevilla et al., 2018) (Eq. X.3). I_2 is a Monod-type factor modified from Martínez et al. (2019), where I_{av} acts as substrate and PAR serve as semisaturation "constant" (Eq. X.4). Lastly, I_3 is a modified Monod-type factor reported by Fernández et al. (2016) (Eq. X.5).

$$I_1 = \frac{I_{av}}{PAR} \qquad \text{[Eq. X.3]}$$

$$I_2 = \frac{I_{av}}{I_{av}+PAR} \quad \text{[Eq. X.4]}$$

$$I_3 = \frac{{I_{av}}^n}{k_i \cdot e^{m \cdot I_{av}} + {I_{av}}^n} \quad \text{[Eq. X.5]}$$

where PAR is the sum of the solar and artificial photosynthetically active radiation received by the PBRs (μmol·m^{-2}·s^{-1}), sPAR is the solar photosynthetically active radiation applied to the PBRs (μmol·m^{-2}·s^{-1}), n (1.045), k_i (174 μmol·m^{-2}·s^{-1}) and m (0.0021) are form parameters (Fernández et al., 2016).

The I_{av} was calculated by Eq. X.6:

$$I_{av} = \frac{PAR}{K_a \cdot VSS \cdot Lp} \cdot (1 - e^{-K_a \cdot C_b \cdot Lp}) \quad \text{[Eq. X.6]}$$

where K_a is an extinction coefficient (m^2·g^{-1}, Eq. X.7), VSS is the biomass concentration (g·m^{-3}), and Lp is the light path (m).

$$K_a = \frac{OD_{400-700}}{VSS \cdot Lp_c} \quad \text{[Eq. X.7]}$$

where $OD_{400\text{-}700}$ (-) is the average optical density of the culture in the range of 400-700 nm; and Lp_c (m) is the light path of the spectrophotometer´s cuvette.

2.3.2.2. CUR-derived predictors and microalgae yields

On the basis of the above-mentioned kinetics, relationships between CUR (or pH´)-derived predictors and biomass productivity (BP)-, nitrogen recovery rate (NRR)- and phosphorus recovery rate (PRR)-derived microalgae yields were assessed. To this aim, CUR (or pH´), BP, NRR and PRR were normalised by either two (j and k) or one (j, k=1) factors related to variations in microalgae activity as shown in Eq. X.8:

$$i_n = i{:}\,j{:}\,k = \frac{i}{j \cdot k} \quad \text{[Eq. X.8]}$$

where i_n is the normalised value of CUR (or pH´), NRR, PRR or BP; i corresponds to CUR, NRR, PRR or BP; j and k can be I_i (I_1 I_2 or I_3), PAR, sPAR, OD or VSS; while k can be also 1, depending on the evaluated i_n.

2.4. Statistical analysis

Partial Least Squares (PLS) algorithm was carried out to evaluate the long-term data (n = 170). CUR and its derived parameters were used as responses (Y), while MPBR performance parameters (i.e. NRR, PRR and BP) and their normalisations were selected as predictors (X). PCA and PLSR were conducted using the mixOmics library

(http://www.mixOmics.org) through the software R version 3.2.3 (http://www.R-project.org).

3. RESULTS AND DISCUSSION

3.1. Assessment of CUR data

CUR data was obtained from the pH sensor by turning off the pH controller. During these periods, microalgae continued absorbing inorganic carbon (in the form of free CO_2 or HCO_3^-) since it accounts as the most abundant nutrient in microalgae biomass (Blanken et al., 2017; Yadav and Sen, 2017). Consequently, due to the equilibrium of the inorganic carbon species (Caia et al., 2018; de Andrade et al., 2016), the CO_2 and HCO_3^- concentrations decreased and the percentage of carbonate in the culture rose, which implied a continuous rise in the pH value (Foladori et al., 2018; Huang et al., 2017; Qiu et al., 2017).

This pH variation was monitored, showing a straight line, similarly to what occurs with the oxygen production of microalgae during respirometric tests (Figure X.1). The derivative of this time series could be monitored (pH´).

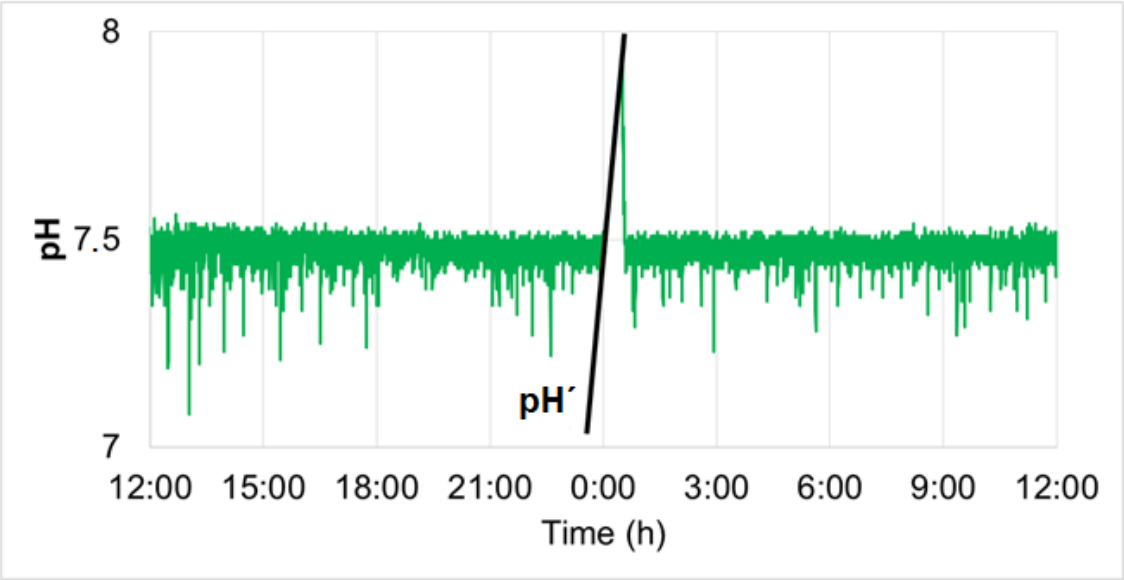

Figure X.1. Example of the pH evolution during one operating day

It is worth mentioning that the carbon concentration of the culture, which causes the pH variation, depends on several factors:

- Photosynthetic activity of microalgae (main factor), which in turn depends on other factors such as light irradiance, average irradiance (I_{av}), biomass concentration and

pigment content amongst others (Fernandez et al., 2016). Theoretically, the faster the metabolic activity of microalgae, the more rapid inorganic carbon is consumed and, in turn, the higher the pH´ (Eze et al., 2018).

- CO_2 stripping, which depends on the efficiency of the CO_2-mass transfer to the culture, which in turn depends on the bubble size (McGinn et al., 2011), gas flow rate (Iasimone et al., 2017), the culture height and the pH set-point. All these parameters remained constant, except for the airflow rate, which varied with the PBR light path (Table X.1).
- Temperature, which also had an influence in CO_2 stripping since it varies the CO_2 solubility in water (Judd et al., 2015). This variation was not considered significant since the CO_2 solubility in water in the operating temperature range of the plant (i.e. 20-30 ºC) only varied in the range of 0.13-0.17% (Perry et al., 1997). Hence, CO_2 stripping was considered negligible in CUR measurements.
- CO_2 production by heterotrophic bacteria. It was also considered negligible due to the low COD concentration of the AnMBR effluent, which was in the range of 40-90 mg COD·L^{-1} and mainly consisted of inert organic matter (Giménez, 2014).
- Nitrifying bacteria present in the culture (section X.2.1.2), can affect the culture pH since nitrification reduces the culture alkalinity (Foladori et al., 2018). However, nitrification was not considered relevant during the experimental period because the sum of nitrite and nitrate concentrations, which can be used as an indirect measurement of AOB activity (González-Camejo et al., 2018a) remained always under 10 mg N·L^{-1}. This consideration was corroborated by realising six respirometric tests with the protocol of Rossi et al. (2018). In these tests, nitrifying bacteria activity only accounted for 4.4% (on average) of the microalgae activity (Figure X.2).
- CO_2 production by microalgae photorespiration. It was considered nearby constant since CUR was measured under natural and artificial lighting. In fact, the aforementioned respirometric tests showed that the oxygen consumption rate due to photorespiration accounted for 10.7% of the net OPR (p-value < 0.05; R^2 = 0.672; n = 6).

Summarising, all the effects different from microalgae activity which can influence pH variations were considered negligible. pH´ could be used as an on-line measurement of CUR, which would be in turn related to microalgae activity. It must be highlighted that if CUR wants to be obtained from pH data in other microalgae cultivation systems in which

some of the other factors apart from photosynthetic activity are not negligible, an adjustment in the model will be necessary to consider these factors. For instance, if microalgae-bacteria consortia was used instead of a mixed microalgae culture, nitrification and heterotrophic bacteria activity will have to be considered for CUR assessment.

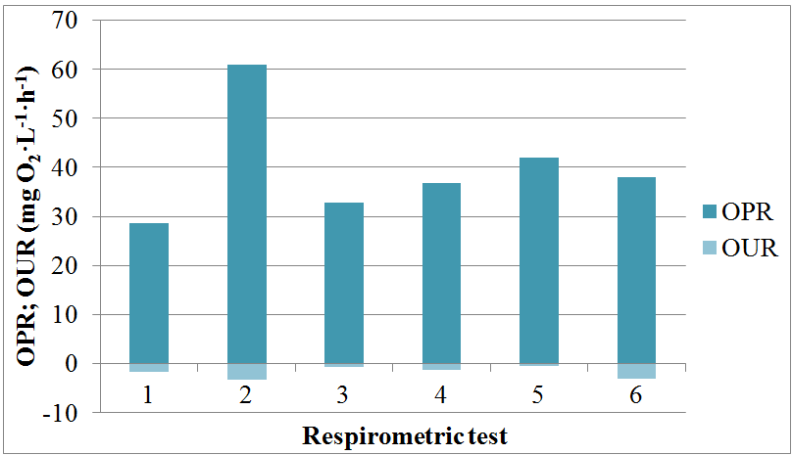

Figure X.2. Results obtained from the respirometric tests. OPR: oxygen production rate of microalgae; OUR: oxygen consumption rate of ammonium and nitrite oxidising bacteria.

3.2. Short term validation of CUR data

A pH´ value was obtained per hour (including daytime and night-time) to monitor the continuous daily operation of the MPBR plant during six days of operation, which was inversely related to gross CUR (Eq. X.1). The main results during this period are shown in Table X.2. Figure X.3 shows the evolution of the pH´ values, as well as the evolution of solar PAR and the concentration of dissolved oxygen (DO). As can be seen in Figure X.3, pH´generally increased during daytime hours due to the solar PAR rising, reaching the maximum daily values usually around midday. These results corroborated that gross CUR (inversely related to pH´) is a good indicator of the instantaneous microalgae activity since higher rate of photosynthesis during daylight hours is expected (Raeisossadati et al., 2019).

Table X.2. Mean values of the short-term operation of the MPBR plant

Day	Solar PAR ($\mu mol \cdot m^{-2} \cdot s^{-1}$)	pH´ (pH unit·min^{-1})	DO (mg $O_2 \cdot L^{-1}$)	BP (mg $VSS \cdot L^{-1} \cdot d^{-1}$)	NRR (mg $N \cdot L^{-1} \cdot d^{-1}$)	PRR (mg $P \cdot L^{-1} \cdot d^{-1}$)
1	227 ± 279	39.8 ± 2.9	13.8 ± 0.7	284	26.3	2.0
2	237 ± 278	39.9 ± 8.7	13.8 ± 0.6	170	22.9	2.5
3	214 ± 294	29.0 ± 2.3	13.4 ± 1.3	-	-	-
4	238 ± 283	19.3 ± 2.2	14.3 ± 1.5	-	-	-
5	232 ± 276	19.6 ± 2.8	14.6 ± 1.4	138	16.4	3.3
6	223 ± 278	21.7 ± 2.5	14.2 ±1.1	148	18.1	2.9

PAR: photosynthetically active radiation; pH´: derivative from pH data dynamics (inversely related to carbon uptake rate); DO: dissolved oxygen; BP: biomass productivity; NRR: nitrogen recovery rate; PRR: phosphorus recovery rate.

Figure X.3 also shows significant differences between the different pH´ values obtained, indicating that the microalgae performance during these days should be different. The short-term operation was preceded by a start-up phase (González-Camejo et al., 2019) in which the microalgae culture was maintained in batch conditions, which implied that biomass productivity at the beginning of the experiment raised up to 284 mg $VSS \cdot L^{-1} \cdot d^{-1}$, while NRR and PRR attained values of 26.3 mg $N \cdot L^{-1} \cdot d^{-1}$ and 2.0 mg $P \cdot L^{-1} \cdot d^{-1}$. This suggested that the algae were very active, as was corroborated by the high pH´ of the first 30 hours of experiment, which achieved values up to 45 pH unit·min^{-1} (Figure X.3). However, from midday of day 2 until the beginning of day 5 (hour 110), pH´ remained at low values in the range of 17-23 pH unit·min^{-1} (Figure X.3). Consequently, biomass productivity decreased from 170 mg $VSS \cdot L^{-1} \cdot d^{-1}$ in day 2 to 139 mg $VSS \cdot L^{-1} \cdot d^{-1}$ in day 5; while NRR lowered from 22.9 mg $N \cdot L^{-1} \cdot d^{-1}$ to 16.4 mg $N \cdot L^{-1} \cdot d^{-1}$ for days 2 and 5, respectively. Later, pH´ rose again, but not as much as at the beginning, having values of 25-33 pH unit·min^{-1} during hours 110-140 (Figure X.3). This implied that biomass productivity and NRR increased from 139 mg $VSS \cdot L^{-1} \cdot d^{-1}$ and 16.4 mg $N \cdot L^{-1} \cdot d^{-1}$, respectively, in day 5 to 148 mg $VSS \cdot L^{-1} \cdot d^{-1}$ and 18.1 mg $N \cdot L^{-1} \cdot d^{-1}$, respectively, at the end of the period. Hence, NRR and biomass productivity were directly related to gross pH´ (and hence to CUR) values in the short-term, showing a good correlation; i.e., R^2 of 0.895 and 0.820 for NRR and BP, respectively.

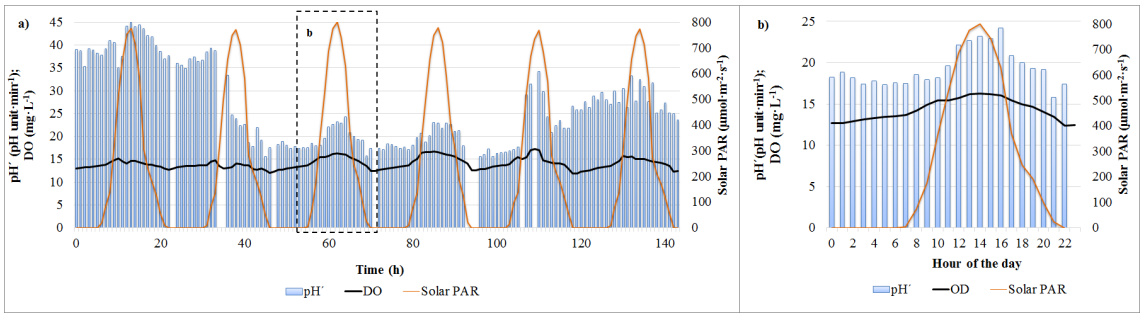

Figure X.3. Evolution of pH´ (inversely related to CUR), solar photosynthetically active radiation (PAR) and dissolved oxygen (DO) concentration during: a) short-term operation of 6 days; b) day 3.

However, PRR followed a different trend than biomass productivity and NRR; i.e., on day 2, PRR was 2.5 mg $P \cdot L^{-1} \cdot d^{-1}$. Then, it increased to 3.3 mg $P \cdot L^{-1} \cdot d^{-1}$ on day 5 and later decreased to 2.9 mg $P \cdot L^{-1} \cdot d^{-1}$ at the end of the period. It is possible that luxury uptake of phosphorus would have a significant influence in this short-term assessment (Powell et al., 2009; Sforza et al., 2018). Phosphorus uptake cannot therefore be directly related to the photosynthetic activity in the short-term.

Figure X.3 also displays the evolution of the dissolved oxygen concentration, showing an increase during daylight hours. Hence, this suggested a relationship between microalgae photosynthetic activity during solar light exposure with the oxygen concentration in the culture. This behaviour has been previously observed (Foladori et al., 2018, Otondo et al., 2018). Thus, dissolved oxygen could be used to monitor the microalgae activity variations throughout the day. On the contrary, the absolute values for different days did not follow the same trend than the pH´ values (Table X.2). In consequence, the dissolved oxygen concentration of the culture did not appear to be a proper indicator of the microalgae performance in this experiment. It must be noted that changes of oxygen solubility with temperature variations were not considered because the PBRs were closed, oxygen stripping was hence considered not significant.

In conclusion, gross CUR can be a good indicator of the microalgae photosynthetic activity and would allow monitoring the algae performance along the day.

It should be noted that CUR (from pH data) can also be measured in darkness since carbon absorption takes place in the dark reactions of photosynthesis, i.e. there is no need of light irradiance to modify the pH value (Manhaeghe et al., 2019; Maroneze et al., 2016).

3.3. Long term validation of CUR data

3.3.1. MPBR performance

The MPBR plant was functionally operated for 310 days with 25-cm light path PBRs and 225 days with 10-cm light path PBRs, under variable ambient and operating conditions (see Table X.1).

During the operation of the MPBR plant, different factors were evaluated: environmental factors and nutrient loads (González-Camejo et al., 2018a), biomass and hydraulic retention times (González-Camejo et al., 2019) and PBR light path (González-Camejo et al., 2018b). MPBR performance in terms of NRR, PRR and BP is shown in Figure X.4. In the 25-cm light path MPBR plant, NRR, PRR and BP were in the range of around 4-15 mg $N \cdot L^{-1}$, 0.4-2 mg $P \cdot L^{-1}$ and 40-115 mg $VSS \cdot L^{-1}$, respectively (Figure X.4a); while in the 10-cm light path MPBR plant, NRR, PRR and BP rose up to around 10-35 mg $N \cdot L^{-1}$, 1-5 mg $P \cdot L^{-1}$ and 110-300 mg $VSS \cdot L^{-1}$, respectively (Figure X.4b). It must be also noted that different gross CUR ranges were reached in both systems: 4-18 pH $unit^{-1}$ and 8-25 pH $unit^{-1}$ for 25-cm and 10-cm MPBR plant, respectively (Figure X.4). Besides the different microalgae performance yields obtained in both systems, these differences could be also influenced by the different volumetric air flow rate supplied to the PBRs due to their different working volumes (Table X.1).

The behaviour of the MPBR plant was thus expected to be significantly different with respect to light path.

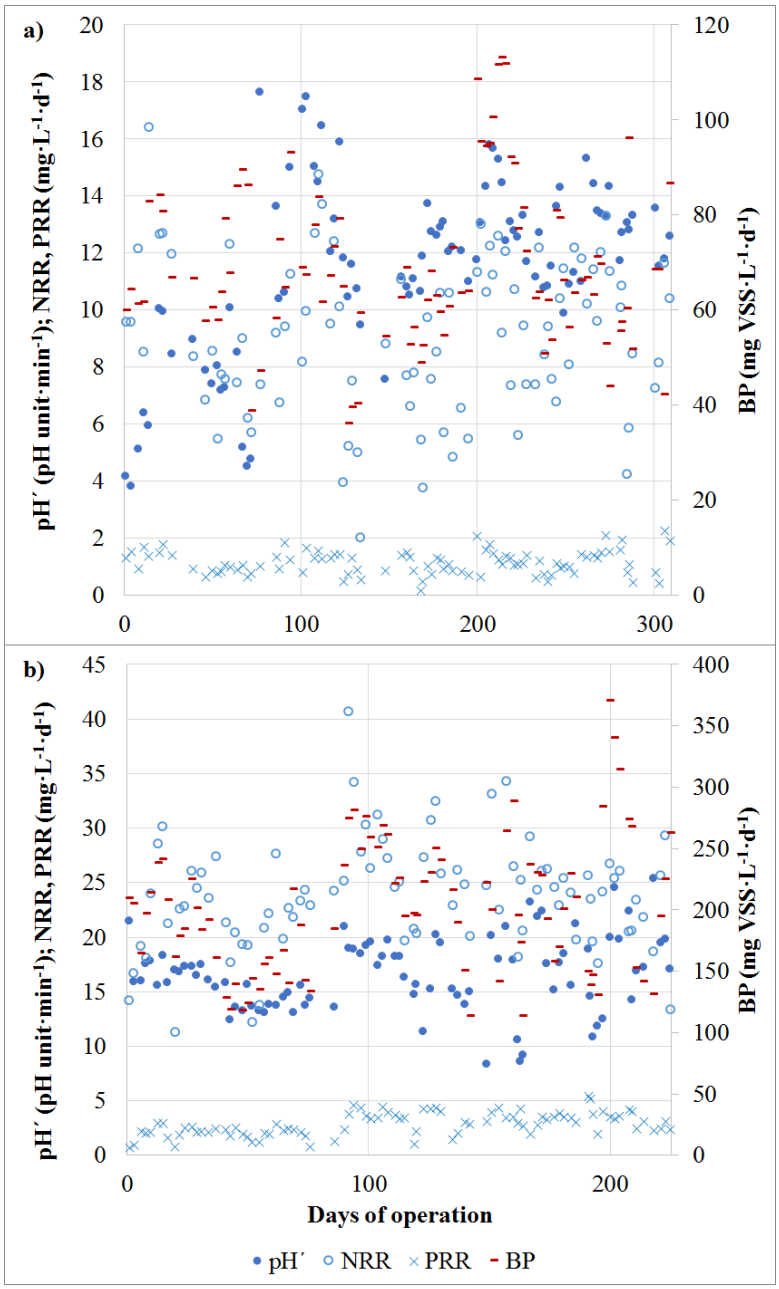

Figure X.4. Evolution of pH´ (inversely related to CUR), nitrogen removal rate (NRR), phosphorus removal rate (PRR) and biomass productivity during the continuous operation of the MPBR plant: a) 25-cm light path, and b) 10 cm light path.

3.3.2. Screening and classification of CUR data

According to Figure X.4, pH´ evolution seemed to follow the trend of NRR, PRR and BP. A preliminary PLS analysis was thus carried out to corroborate the use of CUR (inversely related to pH´) as on-line measurement of microalgae activity. The following predictors were used: pH´, pH´:sPAR, pH´:PAR, pH´:Ii, pH´:OD, pH´:VSS, pH´:Ii:OD, pH´:Ii:VSS (where I_i refers to I_1, I_2 and I_3). Analogous normalised process performance indicators for

NRR, PRR and BP were used as responses. In addition, modified pH´ values, which corresponded to the average values of the previous four days (as suggested by Marazzi et al. (2017)), were also used as predictors.

Results of this preliminary PLS analysis (data not shown) allowed for the screening of the following variables:

- pH´ and the modified pH´ were highly related, showing the modified pH´ a slightly better correlation with MPBR performance. Hence, pH´ was finally referred to the average pH´ values of the previous four days for further evaluation.
- Factors normalised by OD and VSS were highly related for all the parameters. Hence, OD was selected for further evaluation because it is related to chlorophyll content of the culture (Markou et al., 2017). In addition, OD can be monitored on-line (Lucker et al., 2014), while VSS considers not only microalgae biomass but also other microorganisms.
- Factors normalised by I_1 and I_2 resulted in similar results, obtaining a slight better correlation with I_2. I_2 was thus selected for further assessment.

After this screening, a PLS model was created using all the data (n = 170) for both systems (10-cm and 25-cm light path PBRs). The main results of this PLS analysis are shown in Figure X.5. Three principal components (PCs) accounted for a cumulative explained variance of 90.8%, which corresponded to PC1 (37.2%), PC2 (35.0%) and PC3 (18.6%). Figure X.5a and X.5b shows that pH´ is significantly related to MPBR performance in terms of NRR, PRR and BP since these indicators are placed nearby in the plot. Hence, gross CUR obtained from pH data was confirmed as valid parameter to monitor microalgae activity. It should be noted that the derived parameters normalised by I_2 or I_2 and OD also showed good correlation between pH´and MPBR performance (Figure X.5a and X.5b).

It should be also highlighted that two discernible groups of data were observed for both X and Y blocks (Figure X.5c and X.5d), which corresponded to the two different MPBR plants: 25-cm (samples 1-88, blue numbers) and 10-cm MPBR plant (samples 88-170, orange numbers). These results confirmed the different behaviour of these two MPBR systems with respect to the parameters analysed in the model.

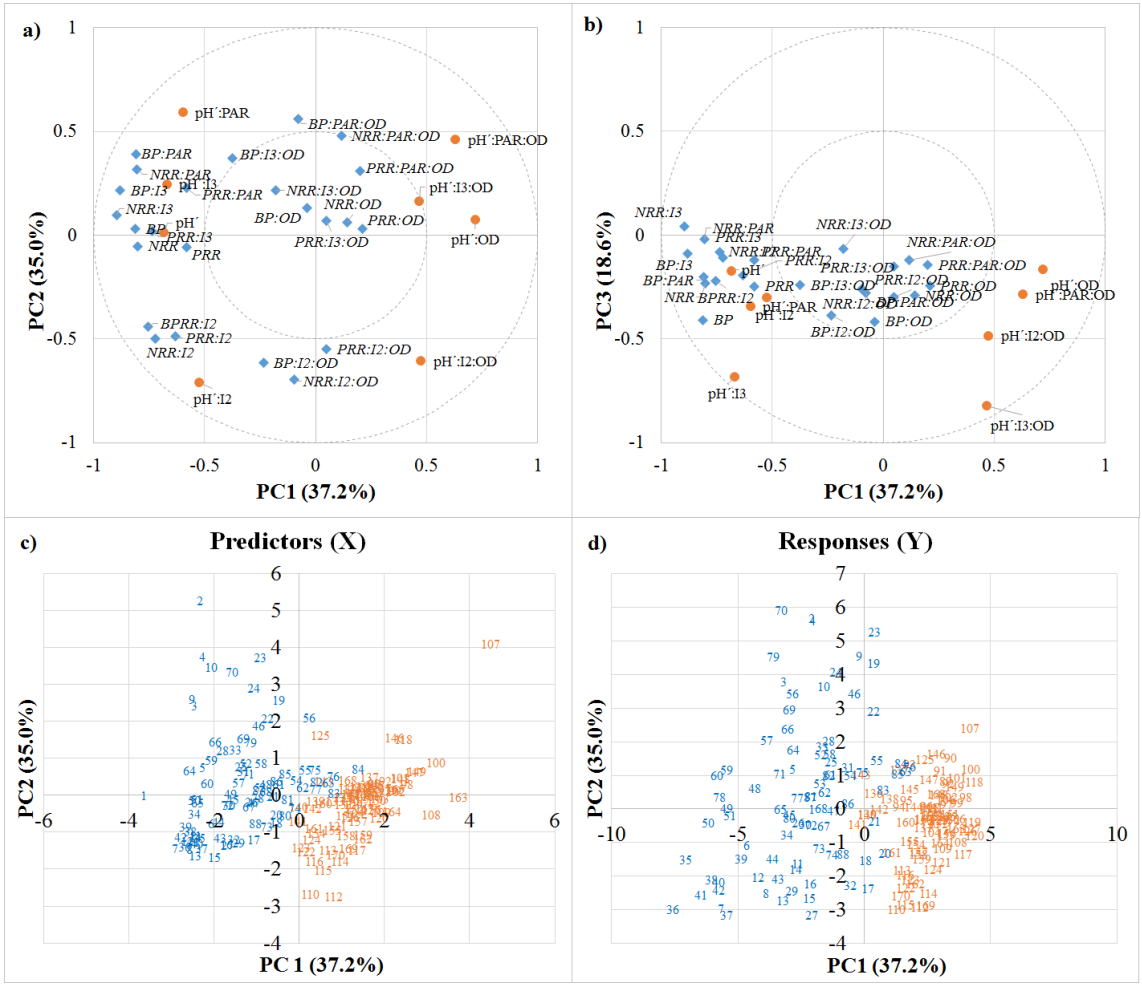

Figure X.5: Results of the PLS analysis (n = 170). Correlation circle plots from the integration of the selected predictors (pH´ and derived predictors, which are inversely related to CUR); and responses (NRR, PRR, BP and their derived parameters): a) PC1 vs PC2; b) PC1 vs PC3; score plot of the first two components of the preliminary PLS model: a) Predictors (X) and b) Responses (Y). Blue numbers (1-88): 25-cm MPBR plant; Orange numbers (89-170) 10-cm MPBR plant.

The PLS results highlight that CUR can represent a good parameter for on-line monitoring the photosynthetic microalgae activity within a wide range of environmental and operating conditions at both short-term and long-term time periods. However, the data obtained in this PLS model suggested that dedicated PLS models would allow to better assess the potential of CUR data for MPBR monitoring in the long-term.

3.3.3. CUR-derived data selection and validation

A PLS analysis for the 25-cm light path MPBR system (n = 88) and a PLS analysis for the 10-cm light path MPBR system (n = 82) were carried out. In this case, pH´, pH´:OD, pH´:PAR, pH´:I2, pH´:I3, pH´:PAR:OD, pH´:I2:OD and pH´:I3:OD were used as

predictors, while analogous normalised parameters related to NRR, PRR and BP were used as responses. For the 10-cm MPBR plant (n = 82), three PCs accounted for a cumulative explained variance of 98.7%, which corresponded to PC1 (45.4%), PC2 (30.4%) and PC3 (22.9%). In the case of 25-cm MPBR plant (n = 88), three PCs attained a cumulative explained variance of 99.1%, in which PC1, PC2 and PC3 accounted for 65.2%, 24.2% and 9.7%, respectively.

Figure X.6 shows the results from these PLS models. In this case, the pH´ showed a reduced correlation with the corresponding responses of the model (BP, NRR and PRR). Thus, normalising these parameters to monitor maximum microalgae activity through CUR_{max} (see Eq. X.1) appears essential.

For both 25-cm and 10-cm light path MPBR plants, the highest correlations were obtained with the derived parameters that were normalised by I_2 or I_3 (Figure X.6). Derived parameters normalised by I_2 or I_3 also showed similar correlation than those normalised by I_2 and OD or I_3 and OD (Figure X.6). This highlights the high relevance of average light irradiance variability in the model and suggests that OD was not a key factor which influenced the variability of CUR. Hence, normalising pH´ by OD showed good correlation with microalgae performance but this parameter was not necessary to monitor microalgae activity. On the other hand, according to Eq. X.1, normalising pH´ by I_2 or I_3 would allow obtaining CUR_{max}. Hence, CUR values could also be used to monitor the maximum capacity of microalgae for carbon uptake in the long term.

The correlation of MPBR performance with the derived parameters normalised by PAR (which corresponds to PBR surface irradiance) was lower than those of I_2 and I_3 (Figure X.6). This was due to the light attenuation within the culture. Light transmittance is exponentially reduced along the light path of the PBR mainly because of the light absorption of the photosynthetic pigments of microalgae (Wagner et al., 2018). Hence, the same PAR on the PBR surface can supply significantly different I_{av} values depending on the culture characteristics (Ledda et al., 2015). For this reason, derived pH´ normalised by I_2 or I_3 showed better correlation with MPBR performance than derived pH´ normalised by PAR.

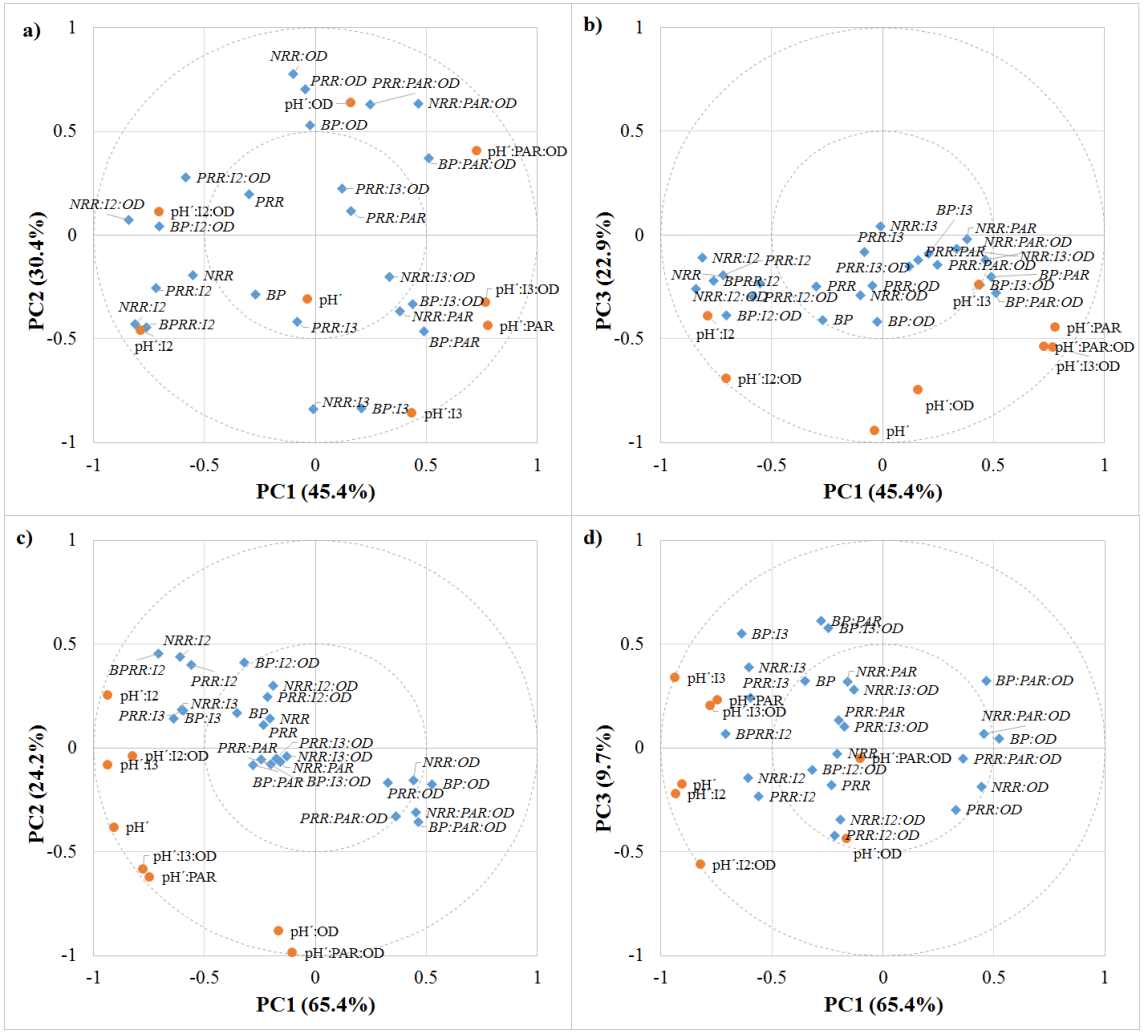

Figure X.6. PLS analysis carried out by separated MPBR systems. Correlation circle plots from the integration of the selected predictors (pH´ and derived predictors, which are inversely related to CUR); and responses (NRR, PRR, BP and their derived parameters): a and b) 10-cm light path MPBR plant (n = 82); c and d) 25-cm light path MPBR plant (n = 88).

As Figure X.6a and Figure X.6b show, normalising by I_2 showed slightly better correlation than I_3 in the 10-cm light path MPBR plant. However, in the case of 25-cm light path MPBR plant, the correlation between derived parameters normalised by I_2 and I_3 was quite similar (Figure X.6c and X.6d). It must be considered that the I_3 factor was obtained by a dynamic model used for raceway reactors instead of flat-panel PBRs. It could be possible that this model fitted better to the widest PBRs since raceway depths usually account for 15-45 cm (Arbib et al., 2017); much higher than those of the PBRs, which can vary in the range of 1-10 cm (Slegers et al., 2011).

It is worth highlighting that the PLS model for the data from the 10-cm light path MPBR plant showed a stronger correlation between pH´ and MPBR performance than the 25-cm

light path MPBR plant since pH´-derived predictors were closer to their corresponded derived responses in the 10-cm light path MPBR plant (Figure X.6a and X.6b) than 25-cm MPBR plant (Figure X.6c and X.6d). It must be considered that in the 25-cm light path MPBR plant there were some experimental periods operated at long biomass retention time during which grazers and other organisms proliferated (González-Camejo et al., 2019). This was shown to vary the relation between OD and VSS (Figure X.A.1) and could probably have varied the relation between parameters.

On the other hand, the correlation between CUR-derived predictors and PRR-derived responses was usually lower than those related to NRR and biomass productivity. This was probably influenced by the fact that phosphorus uptake depends on the intracellular phosphorus concentration (Powell et al., 2009; Sforza et al., 2018), which was not considered in this study.

Summarising, the results obtained in this study corroborated that CUR_{max} can be useful to on-line monitor MPBR plant performance to assess the daily maximum photosynthetic activity of microalgae.

4. CONCLUSIONS

CUR data was used to on-line monitoring the microalgae photosynthetic activity in an MPBR system. Short-term operation showed a relation between gross CUR values and MPBR performance in terms of NRR and biomass productivity. Gross CUR measurements was therefore identified as indicator of the microalgae photosynthetic activity dynamics along the day. Long-term operation showed a relation between on-line CUR measurements and microalgae performance yields (BP, NRR and PR) both normalised considering a microalgae growth kinetic model. Hence, CUR_{max} was identified as an indicator of the daily maximum microalgae activity that can be used in advanced monitoring and control strategies for MPBR optimisation.

ACKNOWLEDGMENTS

This research work has been supported by the Spanish Ministry of Economy and Competitiveness (MINECO, Projects CTM2014-54980-C2-1-R and CTM2014-54980-C2-2-R) jointly with the European Regional Development Fund (ERDF), both of which are gratefully acknowledged. It was also supported by the Spanish Ministry of Education, Culture and Sport via a pre-doctoral FPU fellowship to authors J. González-Camejo (FPU14/05082).

REFERENCES

1. Acién, F.G., Gómez-Serrano, C., Morales-Amaral, M.M., Fernández-Sevilla, J.M., Molina-Grima E., 2016. Wastewater treatment using microalgae: how realistic a contribution might it be to significant urban wastewater treatment? Appl. Microbiol. Biotechnol. 100, 9013–9022. http://dx.doi.org/10.1007/s00253-016-7835-7
2. Alex, J., Rieger, L., Winkler, S., Siegrist, H. 2003. Progress in sensor technology-progress in process control? part II: results from a simulation benchmark study. Water Sci. Technol. 47(2), 113–120.
3. APHA-AWWA-WPCF, 2005. Standard methods for the examination of water and wastewater, 21st edition. American Public Health Association (APHA), American Water Works Association (AWWA), Water Pollution Control Federation (WPCF), USA.
4. Arbib, Z., de Godos, I., Ruiz, J., Perales, J.A., 2017. Optimization of pilot high rate algal ponds for simultaneous nutrient removal and lipids production. Sci. Total Environ. 589, 66–72. http://dx.doi.org/10.1016/j.scitotenv.2017.02.206
5. Arbib, Z., Ruiz, J., Álvarez-Díaz, P., Garrido-Pérez, C., Barragan, J., Perales, J.A., 2013. Long term outdoor operation of a tubular airlift pilot photobioreactor and a high rate algal pond as tertiary treatment of urban wastewater. *Ecol. Eng.*, 52, 143-153. http://dx.doi.org/10.1016/j.ecoleng.2012.12.089
6. Barbosa, M.J., Janssen, M., Ham, N., Tramper, J., Wijffels, R.H., 2003. Microalgae Cultivation in Air-Lift Reactors: Modeling Biomass Yield and Growth Rate as a Function of Mixing Frequency. Biotechnol. Bioeng. 82(2), 170-179. https://doi.org/10.1002/bit.10563
7. Bhakta, J.N., Lahiri, S., Pittman, J.K., Jana, B.B., 2015. Carbon dioxide sequestration in wastewater by a consortium of elevated carbon dioxide-tolerant microalgae. J. CO_2 Util. 10, 105–112. https://doi.org/10.1016/j.jcou.2015.02.001
8. Blanken, W., Schaap, S., Theobald, S., Rinzema, A., Wijffels, R.H., Janssen, M., 2017. Optimizing Carbon Dioxide Utilization for Microalgae Biofilm Cultivation. Biotechnol. Bioeng. 114, 769–776. https://doi.org/10.1002/bit.26199
9. Caia, M., Bernard, O., Bechet, Q., 2018. Optimizing CO_2 transfer in algal open ponds. Algal Res. 35, 530‑538. https://doi.org/10.1016/j.algal.2018.09.009
10. Campos, I., Alcañiz, M., Aguado, D., Barat, R., Ferrer, J., Gil, L., Marrakchi, M., Martínez-Mañez, R., Soto, J., Vivancos, J.L., 2012. A voltammetric electronic tongue as tool for water quality monitoring in wastewater treatment plants. Water Res. 46, 3605-2614. https://doi.org/10.1016/j.watres.2012.02.029

11. Daverey, A., Pandey, D., Verma, P., Verma, S., Shah, V., Dutta, K., Arunachalam, K., 2019. Recent advances in energy efficient biological treatment of municipal wastewater. Bioresour. Technol. Reports. 100252. https://doi.org/10.1016/j.biteb.2019.100252
12. de Andrade, G.A., Pagano, D.J., Guzmán, J.L., Berenguel, M., Fernández, I., Acién, F.G., 2016. Distributed Sliding Mode Control of Ph in Tubular Photobioreactors, IEEE Transactions On Control Systems Technology 24(4), 1160-1173. http://dx.doi.org/10.1109/TCST.2015.2480840
13. De Godos, I., Mendoza, J.L., Acien, F.G., Molina, E., Banks, C.J., Heaven, S., Rogalla, F., 2014. Evaluation of carbon dioxide mass transfer in raceway reactors for microalgae culture using flue gases. Bioresour. Technol. 153C(2), 307-314. https://doi.org/10.1016/j.biortech.2013.11.087
14. De-Luca, R., Trabuio, M., Barolo, M., Bezzo, F., 2018. Microalgae growth optimization in open ponds with uncertain weather data. Computers and Chemical Engineering 117, 410–419. https://doi.org/10.1016/j.compchemeng.2018.07.005
15. De Vree, J.H., Bosma, R., Janssen, M., Barbosa, M.J., Wijffels, R.H., 2015. Comparison of four outdoor pilot-scale photobioreactors. Biotechnol. Biofuels, 8:215. https://doi.org/10.1186/s13068-015-0400-2
16. Deng, X., Chen, B., Xue, C., Li, D., Hu, X., Gao, K., 2018. Biomass production and biochemical profiles of a freshwater microalga *Chlorella kessleri* in mixotrophic culture: effects of light intensity and photoperiodicity. Bioresour. Technol. 253, 358-367. https://doi.org/10.1016/j.biortech.2018.11.032
17. Eze, V.C, Velasquez-Orta, S.B., Hernández-García, A., Monje-Ramírez, I., Orta-Ledesma, M.T., 2018. Kinetic modelling of microalgae cultivation for wastewater treatment and carbon dioxide sequestration. Algal Res. 32, 131–141. https://doi.org/10.1016/j.algal.2018.03.015
18. Fernández, I., Acién, F.G., Guzmán, J.L., Berenguel, M., Mendoza, J.L., 2016. Dynamic model of an industrial raceway reactor for microalgae production. Algal Res. 17, 67-78. http://dx.doi.org/10.1016/j.algal.2016.04.021
19. Fernández-Sevilla, J.M., Brindley, C., Jiménez-Ruíz, N., Acién, F.G., 2018. A simple equation to quantify the effect of frequency of light/dark cycles on the photosynthetic response of microalgae under intermittent light. Algal Res. 35, 479–487. https://doi.org/10.1016/j.algal.2018.09.026
20. Ferreira, G.F., Ríos Pinto, L.F., Maciel Filho, R., Fregolente, L.V., 2019. A review on lipid production from microalgae: Association between cultivation using waste streams and fatty acid profiles. Renew. Sust. Energy Rev. 109, 448–466. https://doi.org/10.1016/j.rser.2019.04.052

21. Ferrer, A., Aguado, D., Vidal-Puig, S., Prats, J.M., Zarzo, M., 2008. PLS: A versatile tool for industrial process improvement and optimization. Appl. Stochastic Models Bus. Ind. 24, 551–567. https://doi.org/10.1002/asmb.716
22. Foladori, P., Petrini, S., Andreottola, G., 2018. Evolution of real municipal wastewater treatment in photobioreactors and microalgae-bacteria consortia using real-time parameters, Chem. Eng. J. 345, 507–516. https://doi.org/10.1016/j.cej.2018.03.178
23. Franco, B.M., Navas, L.M., Gómez, C., Sepúlveda, C., Acién, F.G., 2019. Monoalgal and mixed algal cultures discrimination by using an artificial neural network, Algal Res. 38, 101419. https://doi.org/10.1016/j.algal.2019.101419
24. Garrido-Cárdenas, J., Manzano-Agugliaro, F., Acién-Fernández, F.G., Molina-Grima, E., 2018. Microalgae research worldwide. Algal Res. 35, 50-60. https://doi.org/10.1016/j.algal.2018.08.005
25. García, J., Ortiz, A., Álvarez, E., Belohlav, V., García-Galán, M.J., Díez-Montero, R., Álvarez, J.A., Uggetti, E., 2018. Nutrient removal from agricultural run-off in demonstrative full scale tubular photobioreactors for microalgae growth. Ecological Eng. 120, 513–521. https://doi.org/10.1016/j.ecoleng.2018.07.002
26. Giménez, J.B., 2014. Study of the anaerobic treatment of urban wastewater in membrane bioreactors (Estudio del tratamiento anaerobio de aguas residuales urbanas en biorreactores de membranas). PhD Thesis, University of valencia, Spain.
27. Gonçalves, A.L., Pires, J.C.M., Simoes, M., 2016. The effects of light and temperature on microalgal growth and nutrient removal: an experimental and mathematical approach. RSC Adv. 6, 22896. http://dx.doi.org/10.1039/c5ra26117a
28. González-Camejo, J., Jiménez-Benítez, A., Ruano, M.V., Robles, A., Barat, R., Ferrer, F., 2019. Optimising an outdoor membrane photobioreactor for tertiary sewage treatment. J. Environ. Manag. 245, 76-85. https://doi.org/10.1016/j.jenvman.2019.05.010
29. González-Camejo, J., Barat, R., Ruano, M.V., Seco, A., Ferrer, J., 2018a. Outdoor flat-panel membrane photobioreactor to treat the effluent of an anaerobic membrane bioreactor. Influence of operating, design and environmental conditions. Water Sci. Technol. 78(1), 195-206. http://dx.doi.org/10.2166/wst.2018.259
30. González-Camejo, J., Aparicio, S., Jiménez-Benítez, A., Ruano, M.V., Barat, R., L. Borrás, Pachés, M., Seco, A., 2018b. Influence of BRT and HRT on the performance of an outdoor membrane photobioreactor treating anaerobically-treated sewage. ecoSTP 2018. 4th IWA Specialized International Conference. 25-27 June 2018. Western University, London, Ontario, Canada.
31. González-Camejo, J., Serna-García, R., Viruela, A., Pachés, M., Durán, F., Robles, A., Ruano, M.V., Barat R., Seco, A., 2017. Short and long-term experiments on the effect of

sulphide on microalgae cultivation in tertiary sewage treatment. Bioresour. Technol. 244, 15-22. http://dx.doi.org/10.1016/j.biortech.2017.07.126

32. González-López, C.V., Acién Fernández, F.G., Fernández-Sevilla, J.M., Sánchez Fernández, J.F., Molina Grima, E., 2012. Development of a process for efficient use of CO_2 from flue gases in the production of photosynthetic microorganisms. Biotechnol. Bioeng. 109(7), 1637-1650. https://doi.org/10.1002/bit.24446
33. Huang, Q., Jiang, F., Wang, L., Yang, C., 2017. Design of Photobioreactors for Mass Cultivation of Photosynthetic Organisms. Engineering 3, 318-329. http://dx.doi.org/10.1016/J.ENG.2017.03.020
34. Iasimone, F., Panico,A., De Felice, V., Fantasma, F., Iorizzi, M., Pirozzi, F., 2018. Effect of light intensity and nutrients supply on microalgae cultivated in urban wastewater: Biomass production, lipids accumulation and settleability characteristics. J. Environ. Manag. 223, 1078–1085. https://doi.org/10.1016/j.jenvman.2018.07.024
35. Iasimone, F., De Felice, V., Panico, A., Pirozzi. , F., 2017. Experimental study for the reduction of CO2 emissions in wastewater treatment plant using microalgal cultivation. Journal of CO_2 Utilization 22, 1–8. http://dx.doi.org/10.1016/j.jcou.2017.09.004
36. Judd, S., van den Broeke, L.J.P., Shurair, M., Kuti, Y., Znad, H., 2015. Algal remediation of CO_2 and nutrient discharges: a review. Water Res. 87, 356-366. http://dx.doi.org/10.1016/j.watres.2015.08.021
37. Krishnamoorthy, S., Premalatha, M., Vijayasekaran, M., 2017. Characterization of distillery wastewater – An approach to retrofit existing effluent treatment plant operation with phycoremediation. J. Clean. Prod. 148, 735-750. https://doi.org/10.1016/j.jclepro.2017.02.045
38. Kubelka, B.G., Roselet, F., Pinto, W.T., Abreu, P.C., The action of small bubbles in increasing light exposure and production of the marine microalga Nannochloropsis oceanica in massive culture systems, Algal Res. 35, 69-76. https://doi.org/10.1016/j.algal.2018.09.030
39. Ledda, C., Romero Villegas, G.I., Adani, F., Acién Fernández, F.G., Molina Grima, E., 2015. Utilization of centrate from wastewater treatment for the outdoor production of *Nannochloropsis gaditana* biomass at pilot-scale. Algal Res. 12, 17–25. http://dx.doi.org/10.1016/j.algal.2015.08.002
40. Lucker, B.F., Hall, C.C., Zegarac, R., Kramer, D.M., 2014. The environmental photobioreactor (ePBR): An algal culturing platform for simulating dynamic natural environments. Algal Res. 6, 242–249. http://dx.doi.org/10.1016/j.algal.2013.12.007
41. Manhaeghe, D., Michels, S., Rousseau, D.P.L., Van Hulle, S.W.H., 2019. A semi-mechanistic model describing the influence of light and temperature on the respiration

and photosynthetic growth of *Chlorella vulgaris.* Bioresour. Technol. 274, 361-370. https://doi.org/10.1016/j.biortech.2018.11.097

42. Marazzi, F., Ficara, E., Fornaroli, R., Mezzanotte, V., 2017. Factors affecting the growth of microalgae on blackwater from biosolid dewatering. Water, Air & Soil Pollution 228 (2), 68. http://dx.doi.org/10.1007/s11270-017-3248-1.
43. Markou, G., Dao, L.H.T., Muylaert, K., Beardall, J., 2017. Influence of different degrees of N limitation on photosystem II performance and heterogeneity of *Chlorella vulgaris*, Algal Res. 26, 84-92. http://dx.doi.org/10.1016/j.algal.2017.07.005
44. Maroneze, M.M., Siqueira, S.F., Vendruscolo, R.G., Wagner, R., Menezes, C.R., Zepka, L.Q., Jacob-Lopes, E., 2016. The role of photoperiods on photobiorectors – A potential strategy to reduce costs. Bioresour. Technol. 219, 493-499. http://dx.doi.org/10.1016/j.biortech.2016.08.003
45. Martínez, C., Mairet, F., Martinon, P., Bernard, O., 2019. Dynamics and control of a periodically forced microalgae culture. IFAC Papers On Line 52-1, 922-927. http://dx.doi.org/10.1016/j.ifacol.2019.06.180
46. McGinn, P.J., Dickinson, K.E., Bhatti, S., Frigon, J.C., Guiot, S.R., O'Leary, S.J.B., 2011. Integration of microalgae cultivation with industrial waste remediation for biofuel and bioenergy production: opportunities and limitations. Photosynth. Res. 109, 231–47. https://doi.org/10.1007/s11120-011-9638-0
47. Meseck, S.L., Smith, B.C., Wikfors, G.H., Alix, J.H., Kapareiko, D., 2007. Nutrient interactions between phytoplankton and bacterioplankton under different carbon dioxide regimes. J. Appl. Phycol.19, 229-237. https://doi.org/10.1007/s10811-006-9128-5
48. Moheimani, N.R., 2013. Inorganic carbon and pH effect on growth and lipid productivity if *Tetraselmis suecica* and *Chlorella* sp (Chlorophyta) grown outdoors in bag photobioreactors. J. Appl. Phycol. *25,* 387-398. https://doi.org/10.1007/s10811-012-9873-6
49. Muñoz, R., Guieysse, B., 2006. Algal–bacterial processes for the treatment of hazardous contaminants: A review. Water Res. 40(15), 2799-2815. https://doi.org/10.1016/j.watres.2006.06.011
50. Otondo, A., Kokabian, B., Stuart-Dahl, S., Gude, V.G., 2018. Energetic evaluation of wastewater treatment using microalgae *Chlorella vulgaris.* J. Environ. Chem. Eng. 6(2), 3213-3222. https://doi.org/10.1016/j.jece.2018.04.064M
51. Pachés, M., Martínez-Guijarro, R., González-Camejo, J., Seco, A., Barat, R., 2018. Selecting the most suitable microalgae species to treat the effluent from an anaerobic membrane bioreactor. Environ. Technol. (in press). https://doi.org/10.1080/09593330.2018.1496148

52. Pawlowski, A., Frenández, I., Guzmán, J.L., Berenguel, M., Acién, F.G., Dormido, S., 2016. Event-based selective control strategy for raceway reactor: A simulation study. IFAC-Papers OnLine 49(7), 478–483. https://doi.org/10.1016/j.ifacol.2016.07.388
53. Perin, G., Cimetta, E., Monetti, F., Morosinotto, T., Bezzo, F., 2016. Novel micro-photobioreactor design and monitoring method for assessing microalgae response to light intensity. Algal Res. 19 (2016) 69–76. http://dx.doi.org/10.1016/j.algal.2016.07.015
54. Perry, R.H., Green, D.W., Maloney, J.O., 1997. Perry´s chemical engineers´handbook-7th Ed. McGraw-Hill. United States of America. ISBN 0-07-049841-5.
55. Powell, N., Shilton, A., Chisti, Y., Pratt, S., 2009. Towards a luxury uptake process via microalgae – Defining the polyphosphate dynamics. Water Res. 43, 4207-4213. https://doi:10.1016/j.watres.2009.06.011
56. Qiu, R., Gao, S., Lopez, P.A., Ogden, K.L., 2017. Effects of pH on cell growth, lipid production and CO_2 addition of microalgae *Chlorella sorokiniana*, Algal Res. 28, 192-199. http://dx.doi.org/10.1016/j.algal.2017.11.004
57. Raeisossadati, M., Moheimani, N.R., Parlevliet, D., 2019. Luminescent solar concentrator panels for increasing the efficiency of mass microalgal production. Renew. Sust. Energy Rev. 101, 47–59. https://doi.org/10.1016/j.rser.2018.10.029
58. Ras, M., Steyer, J.P., Bernard, O., 2013. Temperature effect on microalgae: a crucial factor for outdoor production, Rev. Environ. Sci. Biotechnol. 12, 153-164. https://doi.org/10.1007/s11157-013-9310-6
59. Robles, A., Capson-Tojo, G., Galés, A., Ruano, M.V., Sialve, B., Ferrer, J., Steyer, J.P., 2019. Microalgae-bacteria consortia in high-rate ponds for treating urban wastewater: elucidating the key state indicators during the start-up period (submitted manuscript).
60. Rossi, S., Bellucci, M., Marazzi, F., Mezzanotte, V., Ficara, E., 2018. Activity assessment of microalgal-bacterial consortia based on respirometric tests. Water Sci Technol. 78(1-2), 207-215. https://doi.org/10.2166/wst.2018.078
61. Ruano, M.V., Ribes, J., Seco, A., Ferrer, J., 2009. Low cost-sensors as a real alternative to on-line nitrogen analysers in continuous systems. Wat. Sci. Tech., 60(12), 3261-3268. http://dx.doi.org/10.2166/wst.2009.607
62. Ruiz-Martínez, A., Martín García, N., Romero, I., Seco, A., Ferrer, J., 2012. Microalgae cultivation in wastewater: nutrient removal from anaerobic membrane bioreactor effluent. Bioresour. Technol. 126, 247–253. http://dx.doi.org/10.1016/j.biortech.2012.09.022
63. Salama, E.S., Jeon, B.H., Chang, S.W., Lee, S.h., Roh, H.-S., Yang, I.S., Kurade, M.B., El-Dalatony, M.M., Kim, D.-H., Kim, K.H., Kim, S., 2017. Interactive effect of indole-3-acetic acid and diethyl aminoethyl hexanoate on the growth and fatty acid content of some microalgae for biodiesel production. J. Clean. Prod. 168, 1017-1024. https://doi.org/10.1016/j.rser.2017.05.091

64. Seco, A., Aparicio, S., González-Camejo, J., Jiménez-Benítez, A., Mateo, O., Mora, J.F., Noriega-Hevia, G., Sanchis-Perucho, P., Serna-García, R., Zamorano-López, N., Giménez, J.B., Ruiz-Martinez, A., Aguado, D., Barat, R., Borrás, L., Bouzas, A., Martí, N., Pachés, M., Ribes, J., Robles, A., Ruano, M.V., Serralta, J. and Ferrer, J., 2018. Resource recovery from sulphate-rich sewage through an innovative anaerobic-based water resource recovery facility (WRRF). Water Science and Technology 78 (9), 1925-1936. https://doi.org/10.2166/wst.2018.492
65. Sforza, E., Calvaruso, C., La Rocca, N., Bertucco, A., 2018. Luxury uptake of phosphorus in *Nannochloropsis salina*: Effect of P concentration and light on P uptake in batch and continuous cultures. Biochem. Eng. J. 134, 69–79. https://doi.org/10.1016/j.bej.2018.03.008.
66. Slegers, P.M., Wijffels, R.H., van Straten, G., and van Boxtel, A.J.B., 2011. Design scenarios for flat panel photobioreactors. Appl. Energ. 88(10), 3342-3353. https://doi.org/10.1016/j.apenergy.2010.12.037
67. Sutherland, D.L., Howard-Williams, C., Turnbull, M.H., Broady, P.A., Craggs, R.J., 2015. Enhancing microalgal photosynthesis and productivity in wastewater treatment high rate algal ponds for biofuel production. Bioresour. Technol. 184, 222-229. https://doi.org/10.1016/j.biortech.2014.10.074
68. Viruela, A., Robles, A., Durán, F., Ruano, M.V., Barat, R., Ferrer, J., Seco, A., 2018. Performance of an outdoor membrane photobioreactor for resource recovery from anaerobically treated sewage. J. Clean. Prod. 178, 665-674. https://doi.org/10.1016/j.jclepro.2017.12.223
69. Viruela, A., Murgui, M., Gómez-Gil, T., Durán, F., Robles, Á, Ruano, M.V., Ferrer, J., Seco, A., 2016. Water resource recovery by means of microalgae cultivation in outdoor photobioreactors using the effluent from an anaerobic membrane bioreactor fed with pre-treated sewage. Bioresour. Technol. 218, 447-454. http://dx.doi.org/10.1016/j.biortech.2016.06.116
70. Wagner, D.S., Valverde-Perez, B., Plosz, B.G., 2018. Light attenuation in photobioreactors and algal pigmentation under different growth conditions – Model identification and complexity assessment, Algal Res. 35, 488-499. https://doi.org/10.1016/j.algal.2018.08.019
71. Xu, X., Gu, X., Wang, Z., Shatner, W., Wang, Z., 2019. Progress, challenges and solutions of research on photosynthetic carbon sequestration efficiency of microalgae. Renew. Sust. Energy Rev. 110, 65–82. https://doi.org/10.1016/j.rser.2019.04.050
72. Yadav, G., Sen, R., 2017. Microalgal green refinery concept for biosequestration of carbon-dioxide vis-à-vis wastewater remediation and bioenergy production: Recent

technological advances in climate research. J. CO_2 Util. 17, 188–206. http://dx.doi.org/10.1016/j.jcou.2016.12.006

APPENDIX X.A.

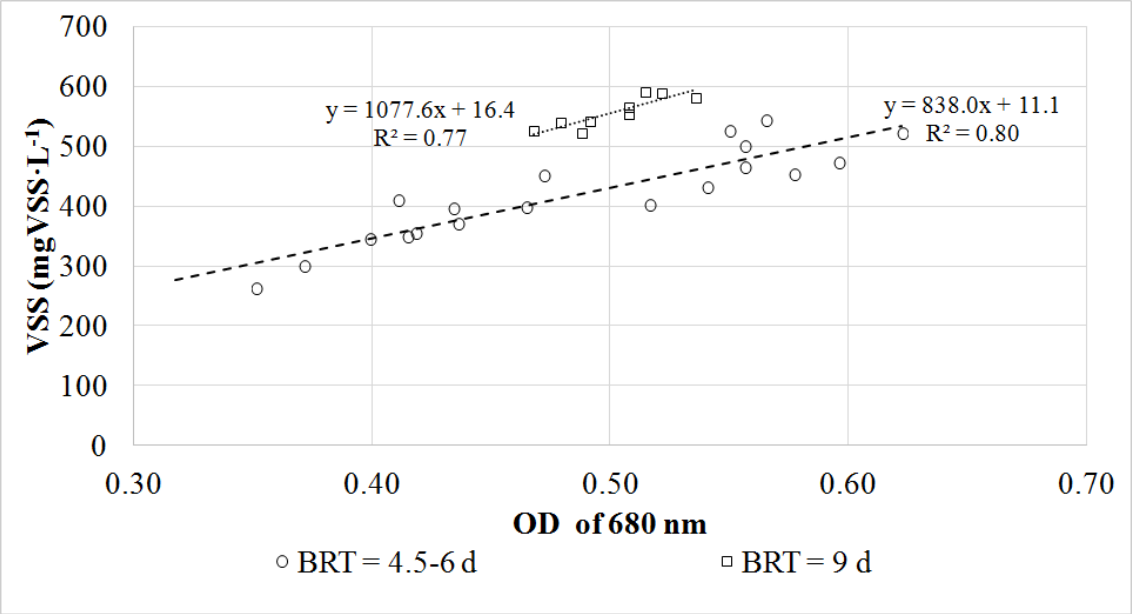

Figure X.A.1: Correlation of OD of 680 nm and volatile suspended solids (VSS) concentration during operation of the 25-cm MPBR plant.

CHAPTER XI:

PRODUCTION OF MICROALGAL EXTERNAL ORGANIC MATTER: INFLUENCE OF TEMPERATURE AND STRESS FACTORS IN A *CHLORELLA*-DOMINATED CULTURE

CHAPTER XI:

PRODUCTION OF MICROALGAL EXTERNAL ORGANIC MATTER: INFLUENCE OF TEMPERATURE AND STRESS FACTORS IN A *CHLORELLA*-DOMINATED CULTURE

Pachés, M., González-Camejo, J., Marín, A., Seco, A., Barat, R. Production of external organic matter in microalgae cultures: influence of temperature and stress factors. J. Environ. Manag. (submitted) September 2019.

ABSTRACT

Although microalgae are recognised to release external organic matter (EOM) to the medium in natural conditions, little is known about this phenomenon in microalgae cultivation systems, especially at mid or large scale.

A study was carried out on the effect of microalgae-stressing factors such as temperature, nutrient limitation and ammonium oxidising bacteria (AOB) competition in EOM production by microalgae. The results showed non-statistically significant differences in EOM production at temperatures in the range of 25-35 ºC. However, when the temperature was suddenly raised by 10 ºC for 4h polysaccharide production increased significantly, indicating microalgae stress, while nutrient limitation also increased EOM production. No significant differences were found in EOM production under lab conditions when the microalgae competed with AOB for ammonium uptake. However, when EOM concentration was monitored during continuous outdoor operation of a membrane photobioreactor (MPBR) plant, nitrifying bacteria activity was likely to increase EOM concentration in the culture, although other factors such as high temperatures, ammonium-depletion and low light intensities could also have induced cell deterioration and thus have influenced EOM production.

1. INTRODUCTION

The recent interest in developing new sustainable technologies within the circular economy concept (Puyol et al., 2017) has boosted research on microalgae biotechnology (Garrido-Cárdenas et al., 2018), since microalgae biomass can be used to produce biofuels (i.e. biogas, biodiesel, bioethanol, etc.), biofertilisers and other

valuable products (Guidetti Vendruscolo et al., 2019; Guldhe et al., 2017; Martins et al., 2018).

Microalgae have also appeared as a suitable option for wastewater remediation (Umamaheswari and Shanthakumar, 2019) since they are able to reduce the nutrient content of wastewater streams such as secondary effluents (Barbera et al., 2018; Gao et al., 2019), anaerobic membrane effluents (González-Camejo et al., 2019a) or centrates (Marazzi et al., 2019). From all the microalgae reported in the literature, the green microalgae *Chlorella* is one of the strains that have shown higher adaptability to wastewater (Gupta et al., 2019).

To cultivate microalgae, raceway ponds are generally used (Razzak et al., 2017). In fact, a pilot-scale study carried out by Arbib et al. (2017) showed the capacity of microalgae to successfully treat urban secondary effluent, obtaining nitrogen and phosphorus concentrations in the raceway effluent lower than 10 and 1 $mg \cdot L^{-1}$, respectively. However, the photosynthetic efficiency of these reactors has been reported to be lower than those of closed photobioreactors (PBRs) (De Vree et al., 2015). Another issue related to raceway ponds is the large surface areas needed to successfully cultivate microalgae (Xu et al., 2019).

To overcome these drawbacks, other approaches such as membrane photobioreactors (MPBRs) have been tested outdoors (González-Camejo et al., 2019a). This technology consists of the combination of closed PBRs and membrane filtration (Bilad et al., 2018). PBRs are designed to attain high photosynthetic efficiencies, biomass productivities and nutrient removal rates (De Vree et al., 2015; Razzak et al., 2017). On the other hand, membrane filtration enables to operate the system at lower hydraulic retention time (HRT), hence reducing the surface area needed to cultivate microalgae (Gao et al., 2019; González-Camejo et al., 2019a). However, filtration entails fouling which reduces membrane permeability and increases the energy consumption of the process (Wang et al., 2019; Zhang and Fu, 2018).

It must be noted that membrane fouling can be intensified by the release of algal organic matter (AOM) into the medium (Liu et al., 2017). This AOM includes polysaccharides, proteins, nucleic acids, amino acids and peptides, among others (Cardozo, 2007; Delattre et al., 2016; González-López et al., 2010) and is composed of extracellular (EOM) and intracellular organic matter (IOM). Membrane pores can

be blocked by EOM, which increases the irreversible fouling that can only be removed by chemical cleaning, reducing the membrane life (Zhang and Fu, 2018).

These organic compounds released by algae can also hinder the wastewater treatment process since they can favour the growth of microalgae-competing organisms such as heterotrophic bacteria and grazers (Luo et al., 2018). Bacteria can produce compounds harmful to microalgae such as toxins (Delattre et al., 2016; Lam et al., 2018), while grazers devour the microalgae cells (Day et al., 2017; Tan et al., 2015), meaning that AOM production can affect the robustness of the microalgae culture. AOM accumulation also reduces the light available to the culture (Guldhe et al., 2017) and can complicate microalgae nutrient uptake (Qureshi et al., 2005). Since AOM can worsen both the microalgae culture performance and the filtration process, it is important to determine the specific conditions and factors which affect AOM production in order to improve outdoor membrane photobioreactor (MPBR) performance.

Some authors have been reported the release of AOM to be boosted under stressing conditions such as unfavourable temperatures, high or low light intensities, nutrient limitation (Discart et al., 2014; Ge et al., 2014; Lee et al., 2018; Li et al., 2013; Yang and Kong, 2013; Kalaji et al., 2014), the presence of toxic substances (Kuo, 1993) or high biomass content (Barker and Stuckey, 1999). However, to the best of our knowledge, EOM production has not been previously evaluated in mixed cultures used for wastewater treatment. From all possible stressing factors, temperature variations can be of great interest in outdoor large-scale microalgae cultivation applications because of the variable conditions microalgae are exposed to (Jebali et al., 2018; González-Camejo et al., 2019b). In addition, the effect of nitrification on EOM production can be significant when using microalgae cultures to treat anaerobic membrane bioreactor (AnMBR) effluents since stress due to competition between microalgae and nitrifiers for ammonium uptake is expected (González-Camejo et al., 2019b). However, this nitrification effect has not been evaluated previously.

The aim of this study was thus to determine the conditions that cause the production (and release) of excessive amounts of EOM in terms of polysaccharide and protein concentrations, as well as the potential relationship between EOM production and microalgae performance, which still remains unclear. The results obtained in this study were expected to add some useful information to the knowledge on large scale applications of microalgae cultivation technology for wastewater treatment.

2. MATERIAL AND METHODS

2.1. Microalgae and substrate

Microalgae consisted of a complex ecosystem which mainly contained green microalgae *Chlorella*, but also cyanobacteria and bacteria (both heterotrophic and autotrophic) in low concentrations.

The feed medium, the characteristics of which are shown Table XI.1, was obtained from an AnMBR pilot plant in the Carraixet WWTP (Seco et al., 2018).

Table XI.1: AnMBR effluent characteristics

Parameter	Unit	Mean ± SD	n
NH_4-N	mg $N \cdot L^{-1}$	47.1 ± 7.2	16
NO_2 -N	mg $N \cdot L^{-1}$	0.9 ± 0.8	16
NO_3-N	mg $N \cdot L^{-1}$	4.5 ± 2.5	16
PO_4-P	mg $P \cdot L^{-1}$	5.2 ± 0.6	16
N:P	molar ratio	20.1 ± 1.7	16
COD	mg $COD \cdot L^{-1}$	76 ± 9	5
BOD	mg $O_2 \cdot L^{-1}$	29 ± 4	5
Alk	mg $CaCO_3 \cdot L^{-1}$	613 ± 36	5
VFA	mg $COD \cdot L^{-1}$	1.4 ± 0.9	5
SO_4	mg $SO_4 \cdot L^{-1}$	40.9 ± 3.9	5
H_2S	mg $S \cdot L^{-1}$	75 ± 6	5
Turbidity	NTU	52 ± 36	16

NH_4-N: ammonium; NO_2-N: nitrite; NO_3-N: nitrate; PO_4-P: phosphate; N:P: nitrogen:phosphorus ratio; COD: chemical oxygen demand; BOD: biochemical oxygen demand; Alk: alkalinity; VFA: volatile fatty acids; SO_4: sulphate; H_2S: Sulphide.

The organic matter loading (measured as chemical oxygen demand (COD)) was mainly inert, thus boosting photoautotrophic metabolism typical of microalgae. The AnMBR effluent was aerated prior to being fed to the PBRs in order to oxidise the sulphide to sulphate, because of its toxic nature to microalgae (González-Camejo et al., 2017).

2.2. Experimental design

Two sets of experiments were conducted using a *Chlorella*-dominated culture: the first one was placed under lab conditions to isolate the effect of temperature variations and nitrification from other possible stressing factors that affected the microalgae culture; while the second one was carried out in a continuously operated outdoor flat-panel MPBR that treated effluent from an AnMBR. In this case, the *Chlorella*-dominated culture was affected by several stressing factors simultaneously.

2.2.1. Lab experiments

The experimental lab scale design was based on two variables: temperature and microalgae-bacteria competition. Table XI.2 shows the operational conditions of the 5 experiments performed.

All the experiments were conducted in 2-L Pyrex flasks; i.e. R-A (Control) and R-B and lasted 5 days. The culture was mixed and aerated with 0.2 μm pre-filtered air using a membrane air-pump to assure homogenisation and prevent cell sedimentation and biofilm forming on the walls. The air stream was bubbled into the reactors at a flow rate of 1.0-1.2 L min^{-1} through fine bubble diffusers placed crosswise on the bottom. Pure CO_2 (99.9%) was injected into the gas flow from a cylinder pressurised at 1.5-2 bar to provide both inorganic carbon and maintain pH at 7.5 ± 0.1 in the cultures. Four white LED lamps (18 W, 6000-6500 K) were placed vertically 20 cm away from the flasks to supply a light intensity of 125 $\mu mol \cdot m^{-2} \cdot s^{-1}$ on the PBR surface in 12:12 light:dark cycles.

Table XI.2: Operating conditions of the lab-scale photobioreactor.

				Temperature (ºC)		Nitrification	
	Operating mode	NH_4-Ni (mg $N \cdot L^{-1}$)	PO_4-Pi (mg $P \cdot L^{-1}$)	R-A	R-B	R-A	R-B
Exp. 1	B	22.5	1.9	25	30	I	I
Exp. 2	C	37.6	2.5	25	30	I	I
Exp. 3	C	56.4	3.7	25	35	I	I
Exp. 4	C	40.7	1.8	25	35*	I	I
Exp. 5	C	56.7	1.6	25	25	I	NI

B: Batch; C: Continuous; i: Nitrification inhibition by adding 10 mg·L^{-1} of allylthiourea; NI: Nitrification non-inhibited.

**Only during 4 hours a day*

2.2.2. Pilot plant experiments

The MPBR plant was installed in the Carraixet WWTP and consisted of two flat-plate PBRs connected to a membrane tank (MT). Each PBR had a working volume of 230 L and was continuously stirred by CO_2-enriched air to maintain pH values at 7.5 ± 0.3 and provide carbon-replete conditions. Aeration also prevented wall fouling and ensured culture homogenisation. The 14-L MT consisted of one hollow-fibre ultrafiltration membrane bundle extracted from an industrial-scale membrane unit (PURON® Koch Membrane Systems (PUR-PSH31), 0.03 µm pores) with a filtration area of 3.4 m^2. Further details of the MPBR plant can be found in González-Camejo et al. (2019a).

Grab samples were collected in duplicate at 09:00 (A), 13:00 (B) and 17:00 h (C) on days 9, 10, 12, 16, 24, 25, 27, 31 and 32 to monitor daily evolution of EOM concentration during the continuous operation of the MPBR plant at a biomass retention time (BRT) of 2 days and hydraulic retention time (HRT) of 1.25 days.

The operation was preceded by a start-up phase (González-Camejo et al., 2019a) (data not shown) and lasted 16 days (Period A), after which culture deterioration occurred. Consequently, another start-up phase was carried out (data not shown) and the operation continued for another 18 days (Period B) to compare MPBR behaviour during both periods.

2.3. Analytical methods

A total of 162 samples were analysed from both the lab scale and the outdoor MPBR plant. All the samples were first filtered through a 0.45 μm pore-size glass fibre filters (Millipore) to measure EOM content, nutrients (NH_4-N, NO_3-N, NO_2-N and PO_4-P) and COD concentrations in the soluble fractions (sCOD). Total (TSS) and volatile suspended solids (VSS) were measured as a proxy of biomass (Ling et al., 2019). All the measurements were determined from duplicate samples.

2.3.1. EOM polysaccharide

The polysaccharide content was measured by the phenol/sulfuric acid method (Dubois et al., 1956) with glucose (Panreac) as the standard for the calibration curves to determine polysaccharide concentration. Two mL of filtered sample were pipetted into a colorimetric tube, and 0.05 mL of 80% phenol added. Then, 5 mL of concentrated sulfuric acid was injected onto the sample surface. The tubes were allowed to stand 10 min before readings were taken. The absorbance of the characteristic yellow-orange sample was measured at 490 nm for hexoses.

2.3.2. EOM protein

The Lowry method as modified by Peterson (1979) was used to measure the protein content of the microalgae culture. 1 mL of the filtered sample was placed in a tube with 1mL of Lowry reagent. The tube was vortexed and 0.5 mL of Folin reagent was added after 20 min at room temperature. After 30 min in darkness at room temperature (to prevent Folin reagent degradation), the absorbance of the sample was measured at a wavelength of 750 nm in a Perkin Elmer Lambda 35 spectrophotometer. Bovine serum albumin (BSA) was used as the protein standard for the spectrophotometry calibration curves. The absorbance value was converted to protein concentration using the calibration curve (González et al., 2010).

2.3.3. Nutrient concentrations

Measurements of ammonium (NH_4-N), nitrite (NO_2-N), nitrate (NO_3-N) and phosphate (PO_4-P) were determined according to Standard Methods (APHA, 2012) 4500-NH_3-G, 4500-NO_2-B, 4500-NO_3-H and 4500-P-F, respectively in a Smartchem 200 automatic analyser (WestcoScientific Instruments, Westco).

2.3.4. Total and volatile suspended solids

TSS and VSS were determined as described in Standard Methods (APHA, 2012).

2.3.5. Chemical oxygen demand

COD was determined from duplicate samples according to Standard Methods (APHA, 2012).

2.4. Calculations

Biomass productivity (mg $VSS \cdot L^{-1} \cdot d^{-1}$), nitrogen recovery rate (NRR) (mg $N \cdot L^{-1} \cdot d^{-1}$), phosphorus recovery rate (PRR) (mg $P \cdot L^{-1} \cdot d^{-1}$) were calculated following the equations shown in González-Camejo *et al.* (2017).

2.5. Statistical analysis

The differences among the experiments were analysed by one-way ANOVA via SPSS software (version 14.0). p-value < 0.05 was considered for statistical significance.

3. RESULTS

It should be noted that the EOM concentration was measured considering only polysaccharide ($EOM\text{-}_{POL}$) and protein ($EOM\text{-}_{P}$) concentrations, since they are the major constituents of the algae EOM (Sheng et al., 2010).

3.1. Effect of temperature on EOM content

The first set of lab-scale experiments aimed to evaluate EOM evolution at two different temperatures (i.e., either 25 (control) and 30 ºC or 25 (control) and 35 ºC, see Table XI.2).

In Experiment 1, reactors were operated in batch conditions at 25 (Fig. XI.1a) and 30 ºC (Fig. XI.1b). As can be seen in Fig. XI.1, both EOM polysaccharide ($EOM\text{-}_{POL}$) and protein ($EOM\text{-}_{P}$) concentrations increased over time in batch conditions. At 25 ºC (Fig. XI.1a) the increase was 6.7-fold and 2.6-fold for $EOM\text{-}_{POL}$ and $EOM\text{-}_{P}$ respectively, from the beginning to the end of the experiment. At 30 ºC (Fig. XI.1b), $EOM\text{-}_{POL}$ and $EOM\text{-}_{P}$ increased by 7.0-fold and 3.1-fold, respectively, with no significant differences in comparison to 25 ºC (p-value > 0.05, $n = 9$). In addition,

both experiments revealed a similar gain pattern, i.e. a gradual increase of EOM production rate during the first days of the experiment (0.5-0.7 $mg \cdot L^{-1} \cdot d^{-1}$ for EOM-$_{POL}$ and 0.3-0.4 $mg \cdot L^{-1} \cdot d^{-1}$ for EOM-$_{P}$ for both temperatures) and sharp increases from the fourth day until the end (2.4 $mg \cdot L^{-1} \cdot d^{-1}$ and 0.6 $mg \cdot L^{-1} \cdot d^{-1}$ for 25 ºC and 2.07 $mg \cdot L^{-1} \cdot d^{-1}$ and 0.5 $mg \cdot L^{-1} \cdot d^{-1}$ at 30 ºC). This sharp increase occurred simultaneously with nutrient depletion (i.e. NH_4-N < 10 $mg \cdot N \cdot L^{-1}$ and PO_4-P < 0.1 $mg \cdot P \cdot L^{-1}$; as observed by Pachés et al. (2018) and in polysaccharides was almost double than of proteins. However, when EOM content was normalised by biomass, normalised EOM-$_{P}$ had a reduction in the production rate of around 20-27 mg EOM-$_{P} \cdot$mg $TSS^{-1} \cdot d^{-1}$ in both R-A and R-B. Normalised EOM-$_{POL}$ increased its rate between 15-28 mg EOM-$_{POL} \cdot$mg $TSS^{-1} \cdot d^{-1}$ in both reactors, so that the EOM-$_{POL}$/EOM-$_{P}$ ratio rose throughout the experiment at both 25 and 30 ºC from 1.2 to 2.4.

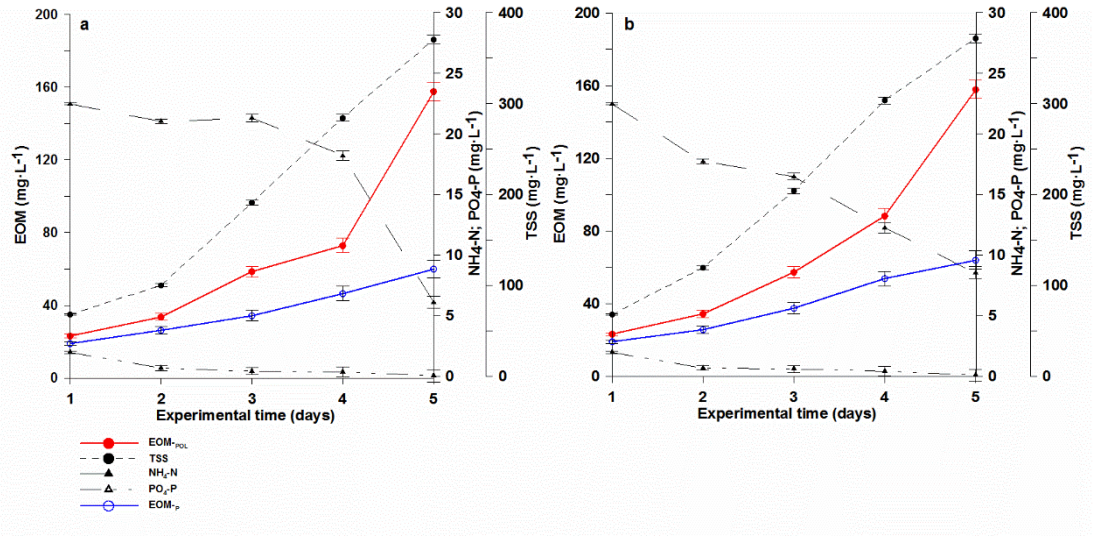

Figure XI.1: EOM-$_{POL}$, EOM-$_{P}$, biomass, NH_4-N and PO_4-P concentrations in batch conditions at: a) 25ºC; and b) 30ºC.

In the continuous feeding mode, EOM-$_{POL}$ increased 2.8-fold throughout Experiment 2 at 25 ºC and 2.1-fold at 30 ºC (Fig. XI.2a, XI.2b).

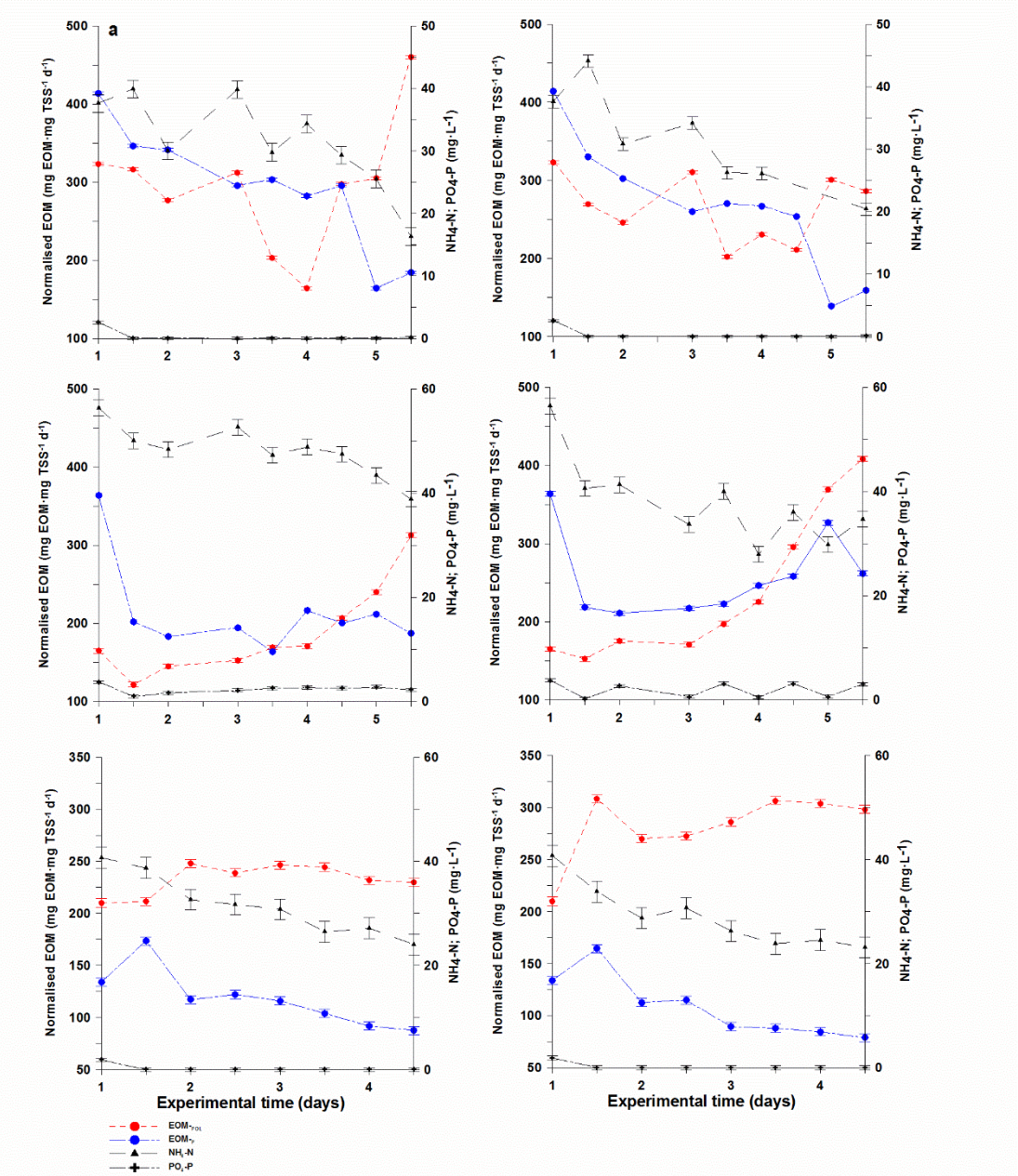

Figure XI.2: EOM-$_{POL}$, EOM-$_{P}$, NH_4-N and PO_4-P concentrations in conditions mode: a) 25 ºC; b) 30ºC; c) 25ºC; d) 35ºC; e) 25ºC; f) intervals on 10 ºC increment (from 25 to 35 ºC).

There were no statistical differences between the two temperatures for either EOM-$_{POL}$ or EOM-$_{P}$ (p-value > 0.05, n = 9). The EOM$_{POL}$/EOM-$_{P}$ ratio increased through time in both reactors, as in Experiment 1.

When a higher temperature range (25-35 ºC) was tested in continuous mode (Experiment 3), the EOM-$_{POL}$ value increased over time between 5 and 6-fold (Fig. XI.2 c, XI.2d). The EOM-$_{P}$ value pattern was similar in both reactors, and neither EOM-$_{POL}$ nor EOM-$_{P}$ showed statistically significant differences (p-value > 0.05, n =

9). The normalised EOM values were positive for polysaccharide and negative for protein, yielding an EOM-$_{POL}$/EOM-$_{P}$ ratio that increased from 0.5 to 1.7 at 25 and 35 ºC.

Lastly, when temperature increments of 10 ºC were applied to the culture (Experiment 4), no statistical differences (p-value > 0.05, n = 9) were found between the two reactors for gross EOM content. EOM-$_{P}$ was also similar in both reactors (data not shown). However, when analysing normalised EOM-$_{POL}$ (i.e., divided by microalgae biomass), the patterns were significantly different (p-value < 0.05, n = 9). At 25 ºC (Control), the EOM-$_{POL}$ increase was less than 10%, while it rose significantly to 42% when temperature stress was applied (Fig. XI.2e, XI.2f).

Once more, normalised EOM-$_{P}$ showed no significant differences between both temperatures (p-value > 0.05, n = 9), with a gradual drop from the beginning of the experiment at similar rates during all Experiment 4.

3.2. Effect of microalgae-AOB competition on EOM content

The competition with AOB was tested at 25 ºC in both reactors.

As can be seen in Fig. XI.3a and XI.3b EOM-$_{POL}$ evolution throughout Experiment 5 was similar in both cultures with and without AOB competition (p-value > 0.05; n = 8) and finally increased in both reactors by around 50%.

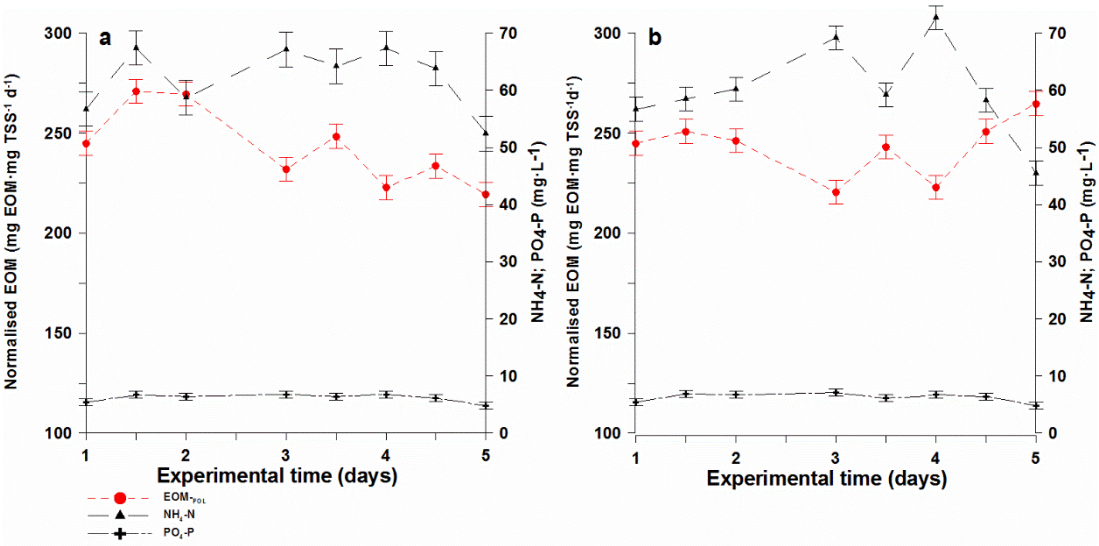

Figure XI.3: EOM-$_{POL}$, NH_4-N and PO_4-P concentrations: a) without nitrification inhibition; and b) with nitrification inhibition.

EOM-$_P$ content was not measured in Experiment 5, since the ATU (added to the culture to inhibit AOB activity) interferes in protein measurement (see Fig. XI.A2).

3.3. Effect of outdoor conditions on the EOM content

The daily samples taken from the MPBR plant; i.e. samples A, B and C for each day did not show any specific trend in either polysaccharides or proteins (Fig. XI.4). Similar behaviour was found in the normalised EOM concentrations (data not shown).

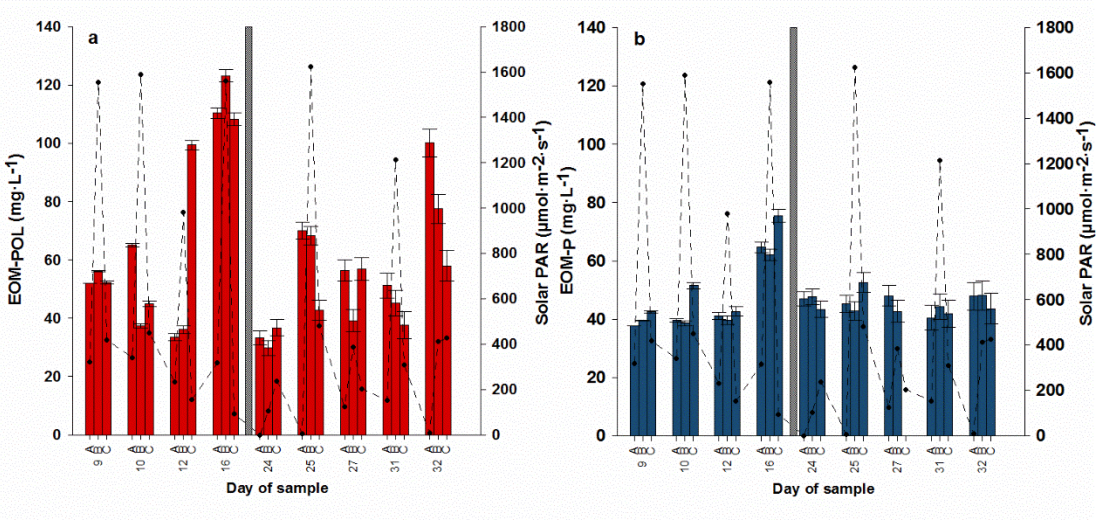

Figure XI.4. EOM concentrations and solar photosynthetically active radiation (PAR) during the continuous operation of the MPBR plant: a) EOM-$_{POL}$ (red); and b) EOM-$_P$ (blue).

Regarding the evolution of normalised EOM concentration during the continuous operation of the MPBR plant, both EOM-$_{POL}$ and EOM-$_P$ remained under similar values until day 12, but significantly increased on day 16 (p-value < 0.05; n = 12), as displayed in Fig. XI.5. A start-up phase (González-Camejo et al., 2019a) was then carried out, which reduced the EOM concentration significantly on day 24. Once again, the normalised EOM concentrations remained at similar values for around two weeks, but rose again by the end of Period B (Fig. XI.5). However, at this time, only EOM-$_{POL}$ concentration increased significantly (p-value < 0.05; n = 15), while EOM-$_P$ concentration remained nearly stable.

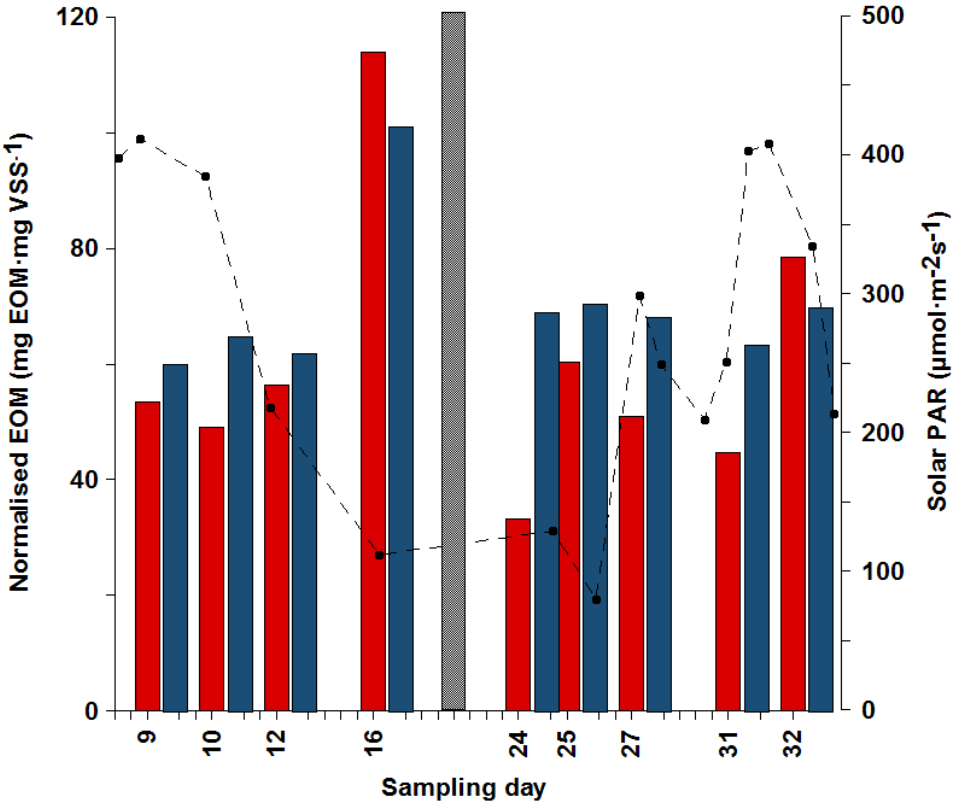

Figure XI.5: EOM normalised concentrations and solar PAR during the continuous operation of the MPBR plant. EOM-$_{POL}$ (red); EOM-$_{P}$ (blue).

Solar light PAR and culture temperature were monitored during the continuous operation of the MPBR plant (Fig. XI.6). In the first 10 days, the conditions were favourable for microalgae growth; i.e. solar light intensities of around 400 µmol·m^{-2}·s^{-1} and mid-range temperatures of around 20 ºC. However, after day 10, the ambient conditions changed and probably favoured nitrifying bacteria growth (González-Camejo et al., 2019b). In addition, the culture was expected to be under ammonium-limited conditions, since NH_4-N concentration was under 10 mg N·L^{-1} (Pachés et al., 2018). This situation made the nitrification rate (NOxR) (which measures the nitrate and nitrite produced through nitrification and is used as an indirect measurement of nitrifying bacteria activity (Rossi et al., 2018)) increase during Period A to a maximum of 9.3 mg N·L^{-1}·d^{-1} (Fig. XI.6a). In Period B, after the aforementioned start-up phase, the nitrification rate showed low values, but immediately increased again (Fig. XI.6a).

With regard to the MPBR performance, it should be noted that nutrient recovery and biomass productivity decreased with time in both Periods A and B (Fig. XI.6b).

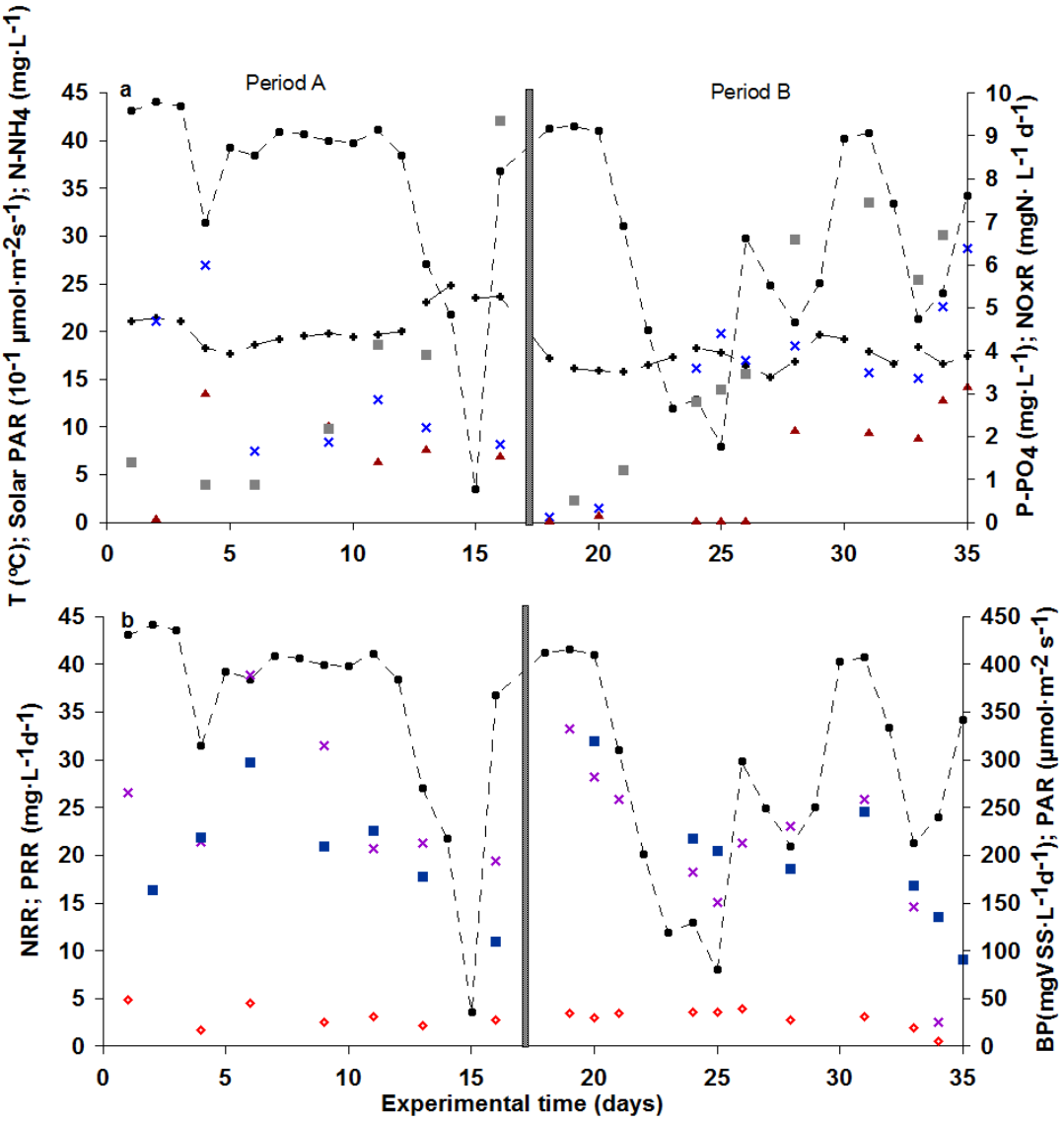

Figure XI.6. Continuous operation of the MPBR plant: a) Temperature (T), solar photosynthetically active radiation (PAR); ammonium concentration (NH_4-N); phosphate concentration (PO_4-P) and nitrification rate (NOxR); b) nitrogen recovery rate (NRR); phosphorus recovery rate (PRR) and biomass productivity (BP).

3.4. Organic matter related to EOM content

A possible correlation between organic matter and EOM content was assessed. To this aim, all the samples from both the lab-scale experiments and the MPBR plant (n = 162) were analysed. A significant correlation (p-value < 0.05, n = 162) was found between the total EOM-$_{POL}$ and EOM-$_{P}$ and sCOD concentration of the culture. This suggests that EOM was the main factor related to the variations of the microalgae culture´s sCOD concentration. Hence, sCOD could be used as an indicator of EOM concentration of the culture (measured as polysaccharides and proteins). However,

the data was dispersed. Other factors such as cell debris, non-biodegradable matter from the substrate (Section XI.2.1) and other EOM such as lipids must also have contributed to the total amount of organic matter in the culture.

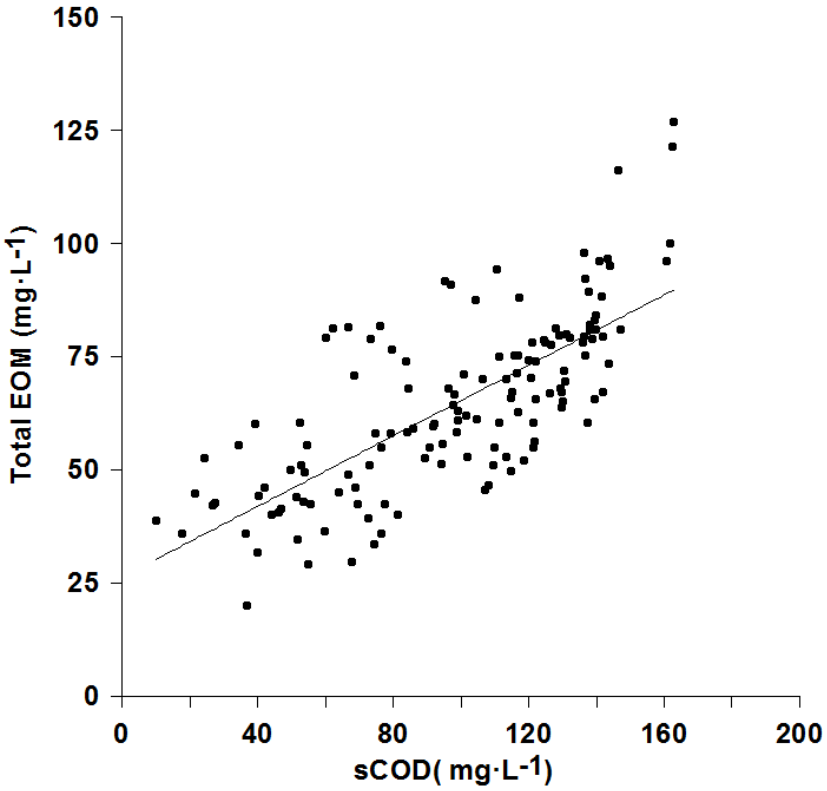

Figure XI.7. Relation between sCOD and EOM concentration (R^2= 0.54; p-value < 0.05).

4. DISCUSSION

It has to be considered that EOM products may be classified into different categories according to the phase in which they are released: compounds produced as a result of substrate metabolism are growth-synonymous and growth-associated, while those excreted due to environmental interaction and lysis are growth-independent (Barker and Stuckey, 1999). Increasing growth-synonymous EOM would entail raised biomass concentrations. On the other hand, variations of growth-independent EOM concentration will not be directly related to microalgae biomass.

4.1. Effect of temperature on the EOM content

Our results did not find any statistically significant differences between EOM-$_{POL}$ or EOM-$_{P}$ for the range of temperatures tested (i.e., 25-35 ºC) either in batch or in continuous mode. This disagrees with the results found by other authors, who

concluded that the EOM content is affected by temperature (Barker and Stuckey, 1999; Moreno et al., 1998). It is possible that the microalgae had adapted to the temperature range evaluated and were thus not significantly stressed at constant temperatures of 25, 30 and 35 ºC.

On the other hand, statistically significant differences were found in the culture subjected to a sharp temperature increase of 10 ºC for 4h. This environmental factor greatly boosted the release of normalised EOM-$_{POL}$ over that of the reactor control. It has to be clarified that the higher EOM-$_{POL}$ in this case was only attributed to temperature stress instead of microalgae growth, since no significant differences were found in the TSS concentrations of either reactor (p-value > 0.05, n = 9). This stress factor must be considered when operating a large-scale microalgae cultivation system since temperature variations over 10 ºC are easily reached outdoors (González-Camejo et al., 2019b). Daily variations in the culture temperature should try to be reduced at minimum during continuous operation to avoid microalgae stress and EOM production.

Although some studies found EOM-$_{P}$ to be more important than EOM-$_{POL}$ in wastewater sludge experiments (Ramesh et al., 2006), in the present study with microalgae fed with AnMBR effluent, EOM-$_{POL}$ production was higher that of EOM-$_{P}$. In fact, the EOM-$_{POL}$/EOM-$_{P}$ ratio increased in all the lab experiments by as much as 3-fold. It therefore seems that products of a polysaccharide nature are preferentially released into the medium over proteins.

Since nutrient levels have been reported to have a significant effect on EOM production and composition (Delattre et al., 2016; Lau et al., 2019), batch cultures (Experiment 1) also make it possible to analyse the behaviour of EOM production under nutrient-replete and nutrient-deplete conditions. In nutrient-replete conditions (days 1-4), EOM increased as a consequence of the biomass accumulating in the system and hence must have been growth-synonymous (Barker and Stuckey, 1999). However, when the microalgae reached nutrient-deplete conditions at NH_4-N < 10 mg N·L^{-1} (Pachés et al., 2018), there was a sudden increase in EOM$_{-POL}$ production in both reactors (Fig. XI.1), which suggests that in nutrient-deplete conditions EOM$_{-POL}$ production was not only due to microalgae growth, but also that nutrient depletion was likely to have stressed the culture. As some authors have pointed out, the lack of nutrients (especially nitrogen) may redirect the carbon metabolism towards incorporation into polymers, increasing the sugar accumulated in the cells

(Delattre et al., 2016) and consequently, higher amounts of EOM-$_{POL}$ were likely to be released in the medium. This statement is also interesting regarding the up-scaling of microalgae cultivation. It suggests that if EOM concentration wants to be maintained low, nutrient-deplete conditions should be avoided.

4.2. Effect of bacteria-microalgae competition on EOM content

Bacteria have been suggested to have a significant effect on the EOM secretion process (Li et al., 2013). The interspecies competition between microalgae and bacteria for nutrients may affect both the uptake and the release of EOM. The other stress factor tested was thus the microalgae-AOB competition at the optimal temperature in nutrient-replete conditions.

No significant differences were observed in EOM production in the lab-scale experiments. These results could be explained by two possible hypotheses: i) either the microalgae-AOB competition did not significantly stress the microalgae; or ii) the experimental time-scale (5 days) was not long enough to produce significant changes in the culture.

4.3. MPBR plant

Since EOM production has been reported as a light-dependent process (Delattre et al., 2016), the daily trend of EOM concentration was expected to be similar to that of the solar PAR measurements; i.e. lower values in the morning (Sample A) and evening (Sample C) and the highest value at midday (Sample B). However, neither the EOM-$_{POL}$ nor EOM-$_{P}$ evolution followed the same pattern as light intensity in the continuous operation. In fact, EOM-$_{POL}$ concentration was variable, while EOM-$_{P}$ remained fairly constant (Fig. XI.4). Hence, EOM-$_{POL}$ was likely to be more affected by stressing factors. Similar behaviour was observed in the lab experiments (Section XI.3.1). These results therefore suggest that EOM production was not directly proportional to microalgae activity (i.e. growth-synonymous and growth-associated EOM (Barker and Stuckey, 1999)) and that the differences in EOM production could have been related to other stress factors, such as higher temperature, light limitations, ammonium depletion or competition with nitrifying bacteria.

When the MPBR plant control parameters are observed (Fig. XI.6), it can be seen that EOM concentration rose for both polysaccharides and proteins during Period A (Fig. XI.5), probably because several stress factors affected microalgae at the end of

Period A: i) the average culture temperature increased by around 5 ºC, reaching maximum values over 30 ºC; ii) ammonium-deplete conditions were reached (NH_4-N < 10 mg $N \cdot L^{-1}$); iii) increased nitrifying bacteria activity measured by NOxR; iv) reduced solar PAR to values under 200 $\mu mol \cdot m^{-2} \cdot s^{-1}$ (Fig. XI.6a). All these factors could have induced cell deterioration and so could have led to higher EOM release to the culture (Azami et al., 2011).

On the other hand, another rise in EOM production was seen at the end of Period B, but only affected EOM-$_{POL}$ (Fig. XI.5). Unlike Period A, the Period B temperature stayed in the cool range around 15-20 ºC and ammonium and phosphorus were in replete conditions from day 24 on (Fig. XI.6). However, the nitrification rate increased with time, so that EOM-$_{POL}$ rise at the end of Period B (Fig. XI.5), which must have been highly influenced by the stress due to the presence of competing organisms in the culture. This behaviour was the opposite of that observed in Experiment 5 under lab conditions, in which no significant differences were found in EOM-$_{POL}$ concentrations between cultures with and without nitrification. It therefore seems that the stressing effect of microalgae-AOB competition depends on the age of the culture. In the short-term (lab experiments), this stress was not found to happen but when the operation was lengthened to 16-18 days EOM production increased significantly. This results suggest that in the continuous operation of the MPBR plant, long BRTs (which increases the culture age) will not be desirable because they are likely to increase EOM concentration, favouring bacteria growth (Luo et al., 2018). In fact, in a previous study (González-Camejo et al., 2019a), operating the same MPBR at BRT of 9 days caused the proliferation of protozoans and grazers.

Unlike Period A, EOM-$_{P}$ stayed at similar values during Period B (Fig. XI.5). It was therefore hypothesised that EOM-$_{P}$ increased only at the end of Period A because there were several stress factors in this period that could affect EOM production, while there was only microalgae-nitrifying bacteria competition in Period B (Fig. XI.6). This confirms that polysaccharides are used by microalgae to interact with the environment in preference to proteins (Section XI.4.1).

It should be noted that nutrient recovery rates and biomass productivity decreased at the end of Periods A and B (Fig. XI.6) when normalised EOM concentrations were the highest (Fig. XI.5). This suggests that the increase in normalised EOM concentration could have a negative influence on microalgae, as reported by other authors (Qureshi et al., 2005; Yun et al., 2018). However, this reduction in nutrient

recovery and biomass productivity could also have also been due to lower solar radiation and a higher nitrification rate (Fig. XI.6). In fact, previous studies have reported that light and competition with nitrifying bacteria are key factors in microalgae cultivation systems (González-Camejo et al., 2019b; 2019c), so that the higher EOM concentration in the culture might not have been the main factor in the lower microalgae cultivation performance. It will thus be necessary to monitor the system for longer operating periods and to relate all the possible factors which influence nutrient recovery and productivity to properly assess the weight of each individual factor on MPBR performance. In addition, to fully assess the affection of EOM concentration in an MPBR system, membrane fouling rates will have to be evaluated in future studies.

5. CONCLUSIONS

The lab experiments showed that sudden temperature rises of 10 ºC and nutrient limitation are stress factors and increase polysaccharide release, although protein production remained stable. On the other hand, there were no significant differences with mean temperatures in the range of 25-35 ºC and competition with nitrifying bacteria.

In outdoor operation the competition with nitrifying bacteria seemed to produce a certain degree of stress in the microalgae culture, since nitrification influenced the increase of EOM concentration. However, this rise was also affected by a combination of several stress factors, such as excessive temperature, reduced solar light and ammonium depletion.

ACKNOWLEDGEMENTS

This research work has been supported by the Spanish Ministry of Economy and Competitiveness (MINECO, Projects CTM2014-54980-C2-1-R and CTM2014-54980-C2-2-R) jointly with the European Regional Development Fund (ERDF), both of which are gratefully acknowledged. It was also supported by the Spanish Ministry of Education, Culture and Sport via a pre-doctoral FPU fellowship to author J. González-Camejo (FPU14/05082).

REFERENCES

1. APHA, 2012. Standard methods for the examination of water and wastewater, 22nd. American Public Health Association, American Water Works Association, Water Environment Federation, Washington, USA.
2. Arbib, Z., de Godos, I., Ruiz, J., Perales, J.A., 2017. Optimization of pilot high rate algal ponds for simultaneous nutrient removal and lipids production. Sci. Total Environ. 589, 66–72. http://dx.doi.org/10.1016/j.scitotenv.2017.02.206
3. Azami, H., Sarrafzadeh, M.H., Mehrnia, M.R., 2011. Fouling in membrane bioreactors with various concentrations of dead cells. Desalination 278, 373–380. https://doi.org/10.1016/j.desal.2011.05.052
4. Barbera, E., Bertucco, A., Kumar, S., 2018. Nutrients recovery and recycling in algae processing for biofuels production. Renew. Sust. Energy Rev. 90, 28–42. https://doi.org/10.1016/j.rser.2018.03.004
5. Barker, D.J., Stuckey, D.C., 1999. A review of soluble microbial products (SMP) in wastewater treatment systems. Water Res. 33, 3063-3082. https://doi.org/10.1016/S0043-1354(99)00022-6
6. Bilad, M.R., Azizo, A.S., Wirzal, M.D.H., Jia, L.J., Putra, Z.A., Nordin, NA.H.M., Mavukkandy, M.O., Jasni, M.J.F., Yusoff, A.R.M., 2018. Tackling membrane fouling in microalgae filtration using nylon 6,6 nanofiber membrane. J. Environ. Manag. 223, 23–28. https://doi.org/10.1016/j.jenvman.2018.06.007
7. Cardozo, K.H.M., Guaratin, T., Barros, M.P., Falcao, V.R., Tonon, A.P., Lopes, N.P., Campos, S., Torres, M.A., Souza, A.O., Colepicolo P., Pinto, E., 2007. Metabolites from algae with economical impact. Comp. Biochem. Phys. C. 146, 60–78. https://doi.org/10.1016/j.cbpc.2006.05.007
8. Day, J.G., Gong, Y., Hu, Q., 2017. Microzooplanktonic grazers – A potentially devastating threat to the commercial success of microalgal mass culture. Algal Res. 27, 356-365. http://dx.doi.org/10.1016/j.algal.2017.08.024
9. Delattre, C., Pierre, G., Laroche, C., Michaud, P., 2016. Production, extraction and characterization of microalgal and cyanobacterial exopolysaccharides. Biotechnol. Adv. 34, 1159-1179. http://dx.doi.org/10.1016/j.biotechadv.2016.08.001
10. De Vree, J.H., Bosma, R., Janssen, M., Barbosa, M.J., Wijffels, R.H., 2015. Comparison of four outdoor pilot-scale photobioreactors. Biotechnol. Biofuels, 8:215. https://doi.org/10.1186/s13068-015-0400-2
11. Discart, V., Bilad, M.R., Marbelia, L., Vankelecom, I.F.J., 2014. Impact of changes in broth composition on *Chlorella vulgaris* cultivation in a membrane photobioreactor (MPBR) with permeate recycle. Bioresour. Technol. 152, 321–328. http://dx.doi.org/10.1016/j.biortech.2013.11.019

12. Dubois, M., Gilles, K.A., Hamilton, J.K., Rebers, P., Smith, F., 1956. Colorimetric method for determination of sugars and the related substances. Anal. Chem. 28, 350-356.
13. Gao, F., Cui, W., Xu, J.P., Li, C., Jin, W.H., Yang H.L., 2019. Lipid accumulation properties of *Chlorella vulgaris* and *Scenedesmus obliquus* in membrane photobioreactor (MPBR) fed with secondary effluent from municipal wastewater treatment plant. Renew. Energy 136, 671-676. https://doi.org/10.1016/j.renene.2019.01.038
14. Garrido-Cárdenas, J., Manzano-Agugliaro, F., Acién-Fernández, F.G., Molina-Grima, E., 2018. Microalgae research worldwide. Algal Res. 35, 50-60. https://doi.org/10.1016/j.algal.2018.08.005
15. Ge, H.M., Zhang, J., Zhou, X.P., Xia, L., Hu, C.X., 2014. Effects of light intensity on components and topographical structures of extracellular polymeric substances from *Microcoleus vaginatus* (Cyanophyceae). Phycologia 53, 167-173. http://dx.doi.org/10.2216/13-163.1
16. González-López, C.V., Ceron, M.C., Acien, F.G., Segovia, C., Chisti, Y., Fernández, J.M., 2010. Protein measurements of microalgal and cyanobacterial biomass, Bioresour. Technol. 101, 7587–7591. https://doi.org/10.1016/j.biortech.2010.04.077
17. González-Camejo, J., Jiménez-Benítez, A., Ruano, M.V., Robles, A., Barat, R., Ferrer, J., 2019a. Optimising an outdoor membrane photobioreactor for tertiary sewage treatment. J. Environ. Manag. 245, 76-85. https://doi.org/10.1016/j.jenvman.2019.05.010
18. González-Camejo, J., Aparicio, A., Ruano, M.V., Borrás, L., Barat, R., Ferrer, J., 2019b. Effect of ambient temperature variations on an indigenous microalgae-nitrifying bacteria culture dominated by *Chlorella*. Bioresour. Technol. 290, 121788. https://doi.org/10.1016/j.biortech.2019.121788
19. González-Camejo, J., Viruela, A., Ruano, M.V., Barat, R., Seco, A., Ferrer, J., 2019c. Effect of light intensity, light duration and photoperiods in the performance of an outdoor photobioreactor for urban wastewater treatment. Algal Res. 40, 101511. https://doi.org/10.1016/j.algal.2019.101511
20. González-Camejo, J., Serna-García, R., Viruela, A., Pachés, M., Durán, F., Robles, A., Ruano, M.V., Barat R., Seco, A., 2017. Short and long-term experiments on the effect of sulphide on microalgae cultivation in tertiary sewage treatment. Bioresour. Technol. 244, 15-22. http://dx.doi.org/10.1016/j.biortech.2017.07.126
21. Guidetti Vendruscolo, R., Bittencourt Fagundes, M., Jacob-Lopes, E., Wagner, R., 2019. Analytical strategies for using gas chromatography to control and optimize

microalgae bioprocessing. Current Opinion in Food Science 25, 73-81. https://doi.org/10.1016/j.cofs.2019.02.008

22. Guldhe, A., Kumari, S., Ramanna, L., Ramsundar, P., Singh, P., Rawat, I., Bux, F., 2017. Prospects, recent advancements and challenges of different wastewater streams for microalgal cultivation. J. Environ. Manag. 203, 299-315. http://dx.doi.org/10.1016/j.jenvman.2017.08.012
23. Gupta S., Pawar, S.B., Pandey, R.A., 2019. Current practices and challenges in using microalgae for treatment of nutrient rich wastewater from agro-based industries. Sci. Total Environ. 687, 1107–1126. https://doi.org/10.1016/j.scitotenv.2019.06.115
24. Jebali, A., Acién, F.G., Rodriguez Barradas, E., Olguín, E.J., Sayadi, S., Molina Grima, E., 2018. Pilot-scale outdoor production of *Scenedesmus* sp. in raceways using flue gases and centrate from anaerobic digestion as the sole culture medium. Bioresour. Technol. 262, 1-8. https://doi.org/10.1016/j.biortech.2018.04.057
25. Kalaji, H.M., Schansker, G., Ladle, R.J., Goltsev, V., Bosa, K., Allakhverdiev, S.I., Brestic, M., Bussotti, F., Calatayud, A., Da browski, P., 2014. Frequently asked questions about in vivo chlorophyll fluorescence: practical issues. Photosynth. Res. 122, 121‑158. https://doi.org/10.1007/s11120-014-0024-6
26. Kuo, W.C., 1993. Production of soluble microbial chelators and their impact on anaerobic treatment. PhD Thesis. Iowa City: University of Iowa, USA.
27. Lam, T.P., Lee, T.M., Chen, C.Y., Chang, J.S., 2018. Strategies to control biological contaminants during microalgal cultivation in open ponds. Bioresour. Technol. 252, 180-187. https://doi.org/10.1016/j.biortech.2017.12.088
28. Lau, A.K.S., Bilad, M.R., Osman, N.B., Marbelia, L., Putra, Z.A., Nordin, N.A.H.M., Wirzal, M.D.H., Jaafar, J., Khan, A.L., 2019. Sequencing batch membrane photobioreactor for simultaneous cultivation of aquaculture feed and polishing of real secondary effluent. J. Water Process Eng. 29, 100779. https://doi.org/10.1016/j.jwpe.2019.100779
29. Lee, J.C., Baek, K., Kim, H.W., 2018. Semi-continuous operation and fouling characteristics of submerged membrane photobioreactor (SMPBR) for tertiary treatment of livestock wastewater. J. Clean. Prod. 180, 244-251. https://doi.org/10.1016/j.jclepro.2018.01.159
30. Li, M., Zhu, W., Gao, L., Lin, L., 2013. Changes in extracellular polysaccharide content and morphology of *Microcystis aeruginosa* at diffenrent specific growth rates. J. Appl. Phycol. 25, 1023-1030. https://doi.org/10.1007/s10811-012-9937-7
31. Ling, Y., Sun, L.P., Wang, S.Y., Lin, C.S.K., Sun, Z., Zhou, Z.G., 2019. Cultivation of oleaginous microalga *Scenedesmus obliquus* coupled with wastewater treatment for

enhanced biomass and lipid production. Biochem. Eng. J. 148, 162–169. https://doi.org/10.1016/j.bej.2019.05.012

32. Liu, B., Qu, F., Liang, H., Gan, Z., Yu, H., Li, G., Van der Bruggen, B., 2017. Algae-laden water treatment using ultrafiltration: Individual and combined fouling effects of cells, debris, extracellular and intracellular organic matter. J. Membr. Sci. 528, 178–186. https://doi.org/10.1016/j.memsci.2017.01.032
33. Luo, Y., Le-Clech, P., Henderson, R.K., 2018. Assessment of membrane photobioreactor (MPBR) performance parameters and operating conditions. Water Res. 138, 169-180. https://doi.org/10.1016/j.watres.2018.03.050
34. Marazzi, F., Bellucci, M., Rossi, S., Fornaroli, R., Ficara, E., Mezzanotte, V., 2019. Outdoor pilot trial integrating a sidestream microalgae process for the treatment of centrate under non optimal climate conditions. Algal Res. 39, 101430. https://doi.org/10.1016/j.algal.2019.101430
35. Martins, A.A., Marques, F., Cameira, M., Santos, E., Badenes, S., Costa, L., L., Verdelho, V., Caetano, N.S., Mata, T.M., 2018. Water footprint of microalgae cultivation in photobioreactor. Energy Procedia 153, 426-431. https://doi.org/10.1016/j.egypro.2018.10.031
36. Moreno, J., Vargas, M.A., Olivares, H., Rivas, J., Guerrero, M.G., 1998. Exopolysaccharide production by the cyanobacteriumAnabaena sp. ATCC 33047 in batch and continuous culture. J. Biotechnol. 60, 175–182.
37. Pachés, M., Martínez-Guijarro, R., González-Camejo, J., Seco, A., Barat, R., 2018. Selecting the most suitable microalgae species to treat the effluent from an anaerobic membrane bioreactor. Environ. Technol. (in press). https://doi.org/10.1080/09593330.2018.1496148
38. Peterson, G.L., 1979. Review of the Folin phenol protein quantitation method of Lowry, Rosebrough, Farr and Randall. Anal. Biochem. 100, 201–220.
39. Puyol, D., Batstone, D.J., Hülsen, T., Astals, S., Peces, M., Krömer, J.O., 2017. Resource recovery from wastewater by biological technologies: opportunities, challenges, and prospects, Frontiers in Microbiology 7(2106), 1–23. http://dx.doi.org/10.3389/fmicb.2016.02106
40. Qureshi, N., Annous, B.A., Ezeji, T.C., Karcher, P., Maddox, I.S., 2005. Biofilm reactors for industrial bioconversion processes: employing potential of enhanced reaction rates, Microb. Cell Fact. 4, 24–44. https://doi.org/10.1186/1475-2859-4-24
41. Ramesh, A., Lee, D.J., Hong, S.G., 2006. Soluble microbial products (SMP) and soluble extracellular polymeric substances (EPS) from wastewater sludge. Appl. Microbiol. Biotechnol. 73, 219-225. https://doi.org/10.1007/s00253-006-0446-y

42. Razzak, S.A., Ali, S.A.M., Hossain, M.M., deLasa, H., 2017. Biological CO_2 fixation with production of microalgae in wastewater – A review. Renew. Sust. Energy Rev. 76, 379–390.http://dx.doi.org/10.1016/j.rser.2017.02.038
43. Rossi, S., Bellucci, M., Marazzi, F., Mezzanotte, V., Ficara, E., 2018. Activity assessment of microalgal-bacterial consortia based on respirometric tests. Water Sci Technol. 78(1-2), 207-215. https://doi.org/10.2166/wst.2018.078
44. Seco, A., Aparicio, S., González-Camejo, J., Jiménez-Benítez, A., Mateo, O., Mora, J.F., Noriega-Hevia, G., Sanchis-Perucho, P., Serna-García, R., Zamorano-López, N., Giménez, J.B., Ruiz-Martinez, A., Aguado, D., Barat, R., Borrás, L., Bouzas, A., Martí, N., Pachés, M., Ribes, J., Robles, A., Ruano, M.V., Serralta, J. and Ferrer, J., 2018. Resource recovery from sulphate-rich sewage through an innovative anaerobic-based water resource recovery facility (WRRF). Water Science and Technology 78 (9), 1925-1936. https://doi.org/10.2166/wst.2018.492
45. Sheng, G.P., Yu, H.Q., Li, X.Y., 2010. Extracellular polymeric substances (EPS) of microbial aggregates in biological wastewater treatment systems: A review. Biotechnol. Adv. 28(6), 882-894. https://doi.org/10.1016/j.biotechadv.2010.08.001
46. Tan, X.B., Yang, L.B., Zhang, Y.L., Zhao, F.C., Chu, H.Q., Guo, J., 2015. *Chlorella pyrenoidosa* cultivation in outdoors using the diluted anaerobically digested activated sludge, Bioresour Technol 198, 340–350. http://dx.doi.org/10.1016/j.biortech.2015.09.025
47. Umamaheswari, J., Shanthakumar, S., 2019. Phycoremediation of paddy-soaked wastewater by indigenous microalgae in open and closed culture system. J. Environ. Manag. 243, 435-443. https://doi.org/10.1016/j.jenvman.2019.05.023
48. Wang, L., Pan, B., Gao, Y., Li, C., Ye, J., Yang, L., Chen, Y., Hu, Q., Zhang, X., 2019. Efficient Membrane Microalgal Harvesting: Pilot-scale Performance and Technoeconomic Analysis. J. Clean. Prod. 218, 83-95. https://doi.org/10.1016/j.jclepro.2019.01.321
49. Xu, X., Gu, X., Wang, Z., Shatner, W., Wang, Z., 2019. Progress, challenges and solutions of research on photosynthetic carbon sequestration efficiency of microalgae. Renew. Sust. Energy Rev. 110, 65–82. https://doi.org/10.1016/j.rser.2019.04.050
50. Yang, Z., Kong, F., 2013. Abiotic in colony formation: effects of nutrition and light on extracellular polysaccharide production and cell aggregates of Microcystis aeruginosa, Chin. J. Oceanol. Limn. 31, 796-802. https://doi.org/10.1007/s00343-013-2264-2
51. Yun, J.H., Cho, D.H., Lee, S., Heo, J., Tran, Q.G., Chang, Y.K., Kim, H.S., 2018. Hybrid operation of photobioreactor and wastewater-fed open raceway ponds enhances the dominance of target algal species and algal biomass production. Algal Res. 29, 319-329. https://doi.org/10.1016/j.algal.2017.11.037

52. Zhang, Y., Fu, Q., 2018. Algal fouling of microfiltration and ultrafiltration membranes and control strategies: A review. Sep. Pur. Technol. 203, 193-208. https://doi.org/10.1016/j.seppur.2018.04.040

APPENDIX XI.A. INTERFERENCES IN THE MEASUREMENT OF POLYSACCHARIDE AND PROTEIN CONCENTRATIONS IN MIXED MICROALGE CULTURES

DATA

The carbohydrate content can be measured by the phenol/sulphuric acid method (Dubois et al., 1956) using glucose (Panreac) as the standard for doing the calibration curves to determine carbohydrate concentration. For this, phenol and sulphuric acid are added to the sample, obtaining a characteristic yellow-orange colour (Figure XI.A.1a). But in microalgae cultures in which ammonium oxidising bacteria (AOB) is significant, nitrite can accumulate (Molinuevo-Salces et al., 2010). If nitrite concentrations reaches values over 2 mg $N \cdot L^{-1}$, the sample gets darker (Figure XI.A.1b) and the measurement of the absorbance is modified. For this reason, samples with significant nitrite concentrations must be diluted prior to apply the phenol/sulphuric acid method.

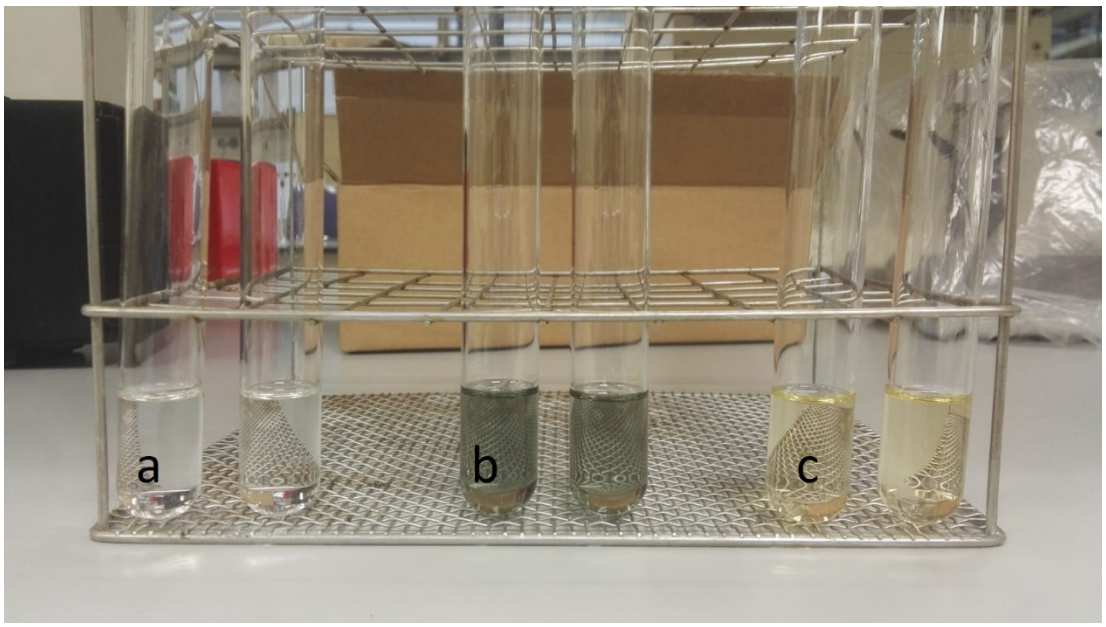

Figure XI.A.1: The phenol/sulphuric acid method applied to samples with and without nitrite (a;blanks, b; with 5 NO_2-N mgL^{-1}, c; negligible concentration of NO_2-N)

On the other hand, the Lowry method modified by Peterson (1979) can be used to measure the protein content of the microalgae culture. This method consists of two chemical reactions. The first one is the biuret reaction, in which the alkaline cupric

tartrate reagent complexes with the peptide bonds of the protein. And the second one is the reduction of the Folin & Ciocalteu's phenol reagent, which yields a purple color.

If allylthiourea ($C_4H_8N_2S$) is used to inhibit AOB growth in the microalgae culture (Krustok et al., 2016), the sample gets darker, similarly to what occurs with the nitrite interference in the phenol/sulphuric acid method (Figure XI.A.2). Hence, if ATU is present in the microalgae culture, the Lowry method cannot be used to determinate the protein concentration of the culture

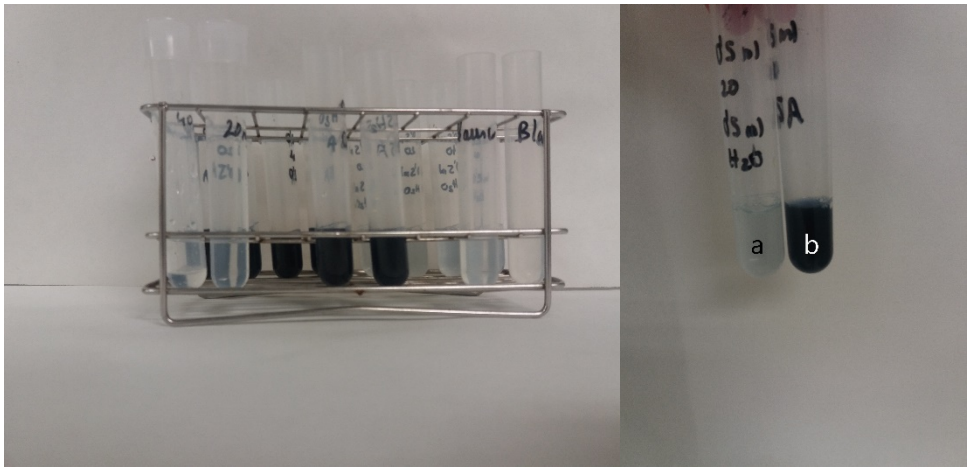

Figure XI.A.2: Lowry method modified by Peterson applied to samples with (b) and without ATU (a)

MATERIALS AND METHODS

Two milliliters of filtered sample are pipetted into a colorimetric tube, and 0.05 mL of 80% phenol are added. Then, 5 mL of concentrated sulfuric acid is injected rapidly, the stream of acid being directed against the sample surface. The tubes are allowed to stand 10 minutes before readings are taken. The absorbance is measured at 490 nm (for hexoses). Glucose (Panreac) was used as a standard for doing the calibration curves. The absorbance measurements were then compared to the standard to convert to polysaccharide concentration.

1 mL of the filtered sample was placed in a tube with 1 mL of Lowry reagent. The tube was vortexed and after 20 min at room temperature, 0.5 mL of Folin reagent was added. After 30 min at room temperature and in darkness to prevent Folin reagent degradation, the absorbance of the sample was measured at a wavelength of 750 nm in a Perkin Elmer Lambda 35 spectrophotometer. Bovine serum albumin

(BSA) was used as protein standard for calibration curves in spectrophotometry. The absorbance value was converted to protein concentration using a calibration curve.

REFERENCES

1. Dubois, M., Gilles, K.A., Hamilton, J.K., Rebers, P., Smith, F., 1956. Colorimetric method for determination of sugars and the related substances. Anal. Chem. 28, 350-356.
2. Krustok, I., Odlare, M., Truu, J., Nehrenheim, E., 2016. Inhibition of nitrification in municipal wastewater-treating photobioreactors: Effect on algal growth and nutrient uptake. Bioresour Technol. 202, 238-243. http://dx.doi.org/10.1016/j.biortech.2015.12.020
3. Molinuevo-Salces, B., García-González, M.C., González-Fernández, C., 2010. Performance comparison of two photobioreactors configurations (open and closed to the atmosphere) treating anaerobically degraded swine slurry, Bioresour. Technol. 101, 5144–5149. https://doi.org/10.1016/j.biortech.2010.02.006
4. Peterson, G.L., 1979. Review of the Folin phenol protein quantitation method of Lowry, Rosebrough, Farr and Randall. Anal. Biochem. 100, 201–220.

CHAPTER XII:

NITRITE INHIBITION OF MICROALGAE INDUCED BY THE COMPETITION BETWEEN MICROALGAE AND NITRIFYING BACTERIA

CHAPTER XII:

NITRITE INHIBITION OF MICROALGAE INDUCED BY THE COMPETITION BETWEEN MICROALGAE AND NITRIFYING BACTERIA

González-Camejo, J., Montero, P., Aparicio, S., Ruano, M.V., Borrás, L., Seco, A., Barat, R. Nitrite inhibition of microalgae induced by the competition between microalgae and nitrifying bacteria. Water Res. (under review) September 2019.

ABSTRACT

The present study analyses the nitrite inhibition role in a mixed microalgae-nitrifying bacteria culture.

For this purpose, pilot-scale and lab-scale assays were carried out. During the continuous outdoor operation, biomass retention time (BRT) of 2 d favoured ammonium oxidising bacteria (AOB) activity, which caused the accumulation of nitrite. This nitrite was confirmed to inhibit microalgae performance. Specifically, continuous 5-days long lab-scale assays showed a reduction in the nitrogen recovery efficiency by 32, 42 and 80% when nitrite concentration in the culture accounted for 5, 10 and 20 mg $N \cdot L^{-1}$, respectively. On the contrary, short 30 minutes-long exposure to nitrite showed no significant differences in the photosynthetic activity of microalgae under nitrite concentrations of 0, 5, 10 and 20 mg $N \cdot L^{-1}$.

On the other hand, when the MPBR was operated at biomass retention time (BRT) of 2.5 days, nitrification rate (NOxR) reached the lowest value (12.6 ± 5.1 mg $N \cdot L^{-1} \cdot d^{-1}$), which caused the nitrite concentration to be reduced to negligible values and MPBR performance thus increased.

Long BRT of 4.5 days favoured nitrite oxidising bacteria (NOB) growth, avoiding nitrite inhibition. However, it also implied the reduction of microalgae growth and the accumulation of nitrate in the MPBR effluent.

1. INTRODUCTION

The need to look for new sustainable resources and technologies has raised the interest of the scientific community in microalgae cultivation for wastewater treatment. Microalgae need large amounts of nutrients to grow which can be recovered from

wastewater streams, implying a simultaneous removal of nitrogen and phosphorus from wastewater (Santos and Pires, 2018). High nutrient-loaded discharges to the environment are thus avoided, preventing the eutrophication of the natural water bodies (Eze et al., 2018). In addition, carbon dioxide is biofixed to obtain microalgae biomass (Bilad et al., 2018) that can be used to produce biofuels, biopolymers, biofertilizers, feeding and pharmaceuticals products, etc. (Santos y Pires, 2018).

Anaerobic membrane bioreactor (AnMBR) effluents have appeared to be ideal medium to enhance microalgae growth since they contain all the macro and micronutrients needed for microalgae growth and low amounts of solids and organic matter (Ruiz-Martínez et al., 2012). In this respect, green microalgae *Chlorella* showed higher adaptability to the operating and outdoor conditions of a membrane photobioreactor (MPBR) system, which treated an AnMBR effluent (González-Camejo et al., 2019).

It has to be highlighted that outdoor microalgae cultivation not only depends on ambient conditions (such as light and temperature) as widely reported (Marazzi et al., 2019; Sutherland et al., 2017). Nitrogen and phosphorus loading rates are also key parameters that have to be considered (González-Camejo et al., 2018). In this respect, low nutrient loads can lead to microalgae growth limitation (Luo et al., 2018), while an excessive amount of nutrients can be detrimental for the performance of microalgae. For instance, ammonium has been reported as the preferable nitrogen source of microalgae (Barbera et al., 2018), but ammonium concentrations higher than 100 mg $N \cdot L^{-1}$ are toxic for several microalgae strains (Collos and Harrison, 2014). Nitrite, which can also be used as nitrogen source, has been also reported to negatively affect microalgae, although the sensitivity to nitrite is species-specific. By way of example, Yang et al. (2004) observed a decay in the growth of *Botryococcus braunii* at nitrite concentrations of 70 mg $N \cdot L^{-1}$. Moreover, Chen et al. (2009) reported a decrease in the growth of cyanobacteria *Microcystis aeruginosa* at nitrite concentrations over 50 mg $N \cdot L^{-1}$. On the other hand, Abe et al. (2002) did not observed any reduction in the growth of aerial microalgae *Trentepohlia aurea* at concentrations under 141 mg $N \cdot L^{-1}$. From these controversial results, it seems necessary to evaluate the effect of nitrite on a mixed microalgae-nitrifying bacteria culture dominated used to treat sewage, where nitrite concentrations are expected to be in the range of 0-15 mg $N \cdot L^{-1}$ (González-Camejo et al., 2018).

Outdoor microalgae cultivation for wastewater treatment has also the risk of biological contamination of competing microorganisms. In the case of AnMBR effluents, the competition for ammonium uptake between microalgae and ammonium oxidising

bacteria (AOB) is expected to occur (Molinuevo-Salces et al., 2010). AOB use ammonium as a source of electrons and oxidises it to nitrite as long as they are not oxygen limited (Akizuki et al., 2019). This nitrite can be used by nitrite oxidising bacteria (NOB) to carry out the second step of the nitrification process, oxidising it to nitrate (Winkler and Straka, 2019). Depending on the ambient and operating conditions, AOB activity can boost the accumulation of nitrite in the culture, which must be evaluated during continuous operation.

In normal situations, microalgae outcompete AOB because of their greater capacity to uptake nitrogen (Marcilhac et al., 2014). Consequently, under sufficient light conditions, microalgae become the predominant organism of the culture (Galès et al., 2019).

On the other hand, AOB growth is sharply increased with temperature (Marazzi et al, 2017), which implies that sudden temperature increases can make AOB to rapidly proliferate.

Another key factor in the microalgae-AOB competition is the BRT of the culture (Rada-Ariza et al., 2019). However, to the best of our knowledge, no studies have assessed yet the effect of hydraulic retention time (HRT) and BRT on microalgae-AOB culture performance to treat wastewater under outdoor conditions.

This study has two goals: i) to provide a better understanding of the microalgae-AOB competition in the outdoor treatment of AnMBR effluents, focusing on obtaining the optimal operating conditions to minimise the nitrite concentration in the culture; ii) to evaluate the inhibition of microalgae by the presence of nitrite under controlled lab-scale conditions.

2. MATERIAL AND METHODS

2.1. Microalgae and wastewater

The microalgae and nitrifying bacteria mix was obtained from a culture dominated by *Chlorella* genera (> 99% of total eukaryotic cells (TEC)), although cyanobacteria and heterotrophic bacteria were also present in lower concentrations.

The wastewater to be treated consisted of the nutrient-rich effluent from an AnMBR plant that was fed by the real effluent of the primary settler of the Carraixet WWTP (39º30’04.0’’N 0º20’00.1’’W, Valencia, Spain). This AnMBR plant is described in Seco et al. (2018). The average characteristics of this substrate were a nitrogen concentration of 48.8 ± 8.7 mg $N \cdot L^{-1}$ (mainly ammonium; i.e. > 95% of nitrogen), a

phosphorus concentration of 4.4 ± 1.5 mg $P \cdot L^{-1}$ and a chemical oxygen demand (COD) concentration of 63 ± 32 mg $COD \cdot L^{-1}$. Volatile suspended solids concentration was negligible.

2.2. Experimental set up

Two different groups of experiments were tested: i) Large-scale experiments operating an outdoor membrane photobioreactor (MPBR) plant; and ii) lab-scale assays to confirm the nitrite inhibition of microalgae.

2.2.1. MPBR pilot plant

The MPBR plant was located in the Carraixet WWTP (Valencia, Spain). It was operated at outdoor conditions with variable light and temperature and consisted of two flat-plate PBRs connected to a membrane tank (MT). Each photobioreactor (PBR) had a working volume of 230 L with dimensions of 1.15-m high, 2-m wide and 0.10-m deep. They were continuously stirred by CO_2-enriched air to ensure the culture homogenisation and prevent wall fouling. CO_2 was injected into the aeration system to maintain pH values at 7.5. This also ensured carbon-replete conditions and avoided undesirable abiotic processes such as ammonia volatilisation and phosphorus precipitation (Whitton et al., 2016).

Both PBRs had an additional artificial white light source consisted of twelve LED lamps (Unique Led IP65 WS-TP4S-40W-ME) that were installed at the back of each PBR offering a continuous light irradiance of 300 $\mu mol \cdot m^{-2} \cdot s^{-1}$at the PBR surface.

The MT had a total working volume of 14 L and a filtration area of 3.4 m^2. It consisted of one hollow-fibre ultrafiltration membrane bundle extracted from an industrial-scale membrane unit (PURON® Koch Membrane Systems (PUR-PSH31), 0.03 μm pores). Air was injected into the bottom of the MT to reduce membrane fouling by membrane scouring.

The continuous operation of the MPBR plant is extensively described in González-Camejo et al. (2019).

2.2.1.1. Outdoor experimental periods

Two different groups of periods were tested to evaluate the accumulation of nitrite in the microalgae-nitrifying bacteria culture. In the dilution rate period (DR-Period) the effect of a punctual increase in the dilution rate of the culture (from 0.3 d^{-1} to 0.5 d^{-1})

was assessed. To analyse the effect of BRT on the nitrite production, 3 Periods were selected; i.e., Period BRT-A; BRT-B and BRT-C which corresponded to BRTs 2, 2.5 and 4.5 days, respectively. Average solar photosynthetically active radiation (PAR), temperature and BRT-HRT conditions of each period are depicted in Table XII.1.

Table XII.1. Experimental conditions for the continuous operation of the MPBR plant (mean ± standard deviation).

Period	Days of operation	Daily solar PAR ($\mu mol \cdot m^{-2} \cdot s^{-1}$)	Temperature (ºC)	BRT (d)	HRT (d)
DR	45	234 ± 33	24.7 ± 1.2	3	1
BRT-A	24	277 ± 104	18.6 ± 1.9	2	1.25
BRT-B	37	284 ± 138	16.9 ± 2.2	2.5	1.25
BRT-C	37	277 ± 101	18.8 ± 2.4	4.5	1.25

Each group of periods; i.e., DR-periods and BRT-periods was preceded by a start-up phase (González-Camejo et al., 2019) which was not considered in the results. However, the transition between periods of the same group was made without a start-up phase.

2.2.2. Lab-scale assays

To confirm the microalgae inhibition by nitrite, two groups of highly controlled lab-scale assays were carried out: i) short-term exposure assays which lasted 30 min; and ii) continuous exposure of microalgae to nitrite for 5 days.

2.2.1.1. Short-term exposure

Short-term exposure assays consisted of four respirometric tests in which the oxygen production rate (OPR) was measured for microalgae cultures with nitrite concentrations of 0, 5, 10 and 20 mg $N \cdot L^{-1}$, respectively. OPR was selected as an indicator of the microalgae activity since it has been reported to be proportional to microalgae biomass production (Rossi et al., 2018).

These concentrations were achieved by adding the corresponding amount of a standard dilution of 1000 mg $NO_2 \cdot L^{-1}$ to the diluted microalgae samples which consisted of 200 mL of microalgae taken from the MPBR plant (see section 2.2.1) and 200 mL of

AnMBR effluent (section 2.1). All the respirometric tests were carried out with the same mix of microalgae and substrate samples, only differing in the nitrite concentration of the culture. In this respect, the biomass concentration of the mixed samples accounted for 225 ± 22 mg VSS $\cdot L^{-1}$. Differences due to shadow effect were therefore not considered (Rossi et al., 2018). Moreover, the mixed samples presented ammonium and phosphate concentrations of 21.1 ± 2.5 mg N $\cdot L^{-1}$ and 2.8 ± 0.8 mg P$\cdot L^{-1}$, respectively. Nutrient limitation was thus avoided (González- Camejo et al., 2019). 10 mg$\cdot L^{-1}$ of allylthiourea (ATU) was added to each respirometric sample in order to prevent any possible negative effect of AOB over microalgae (González-Camejo et al., 2018). Consequently, these tests only assessed the effect of nitrite concentration on microalgae growth.

The set up consisted of a cylindrical closed PBR (400 mL of working volume) which was placed inside a thermostatic chamber at 25 ºC. The PBR was lit by four cool-white LED lamps (T8 LED-Tube 9 w) to supply a light intensity of 125 μmol$\cdot m^{-2} \cdot s^{-1}$ on the PBR surface. An oxygen probe (WTW CellOx 330i) monitored the dissolved oxygen (DO) concentration of the culture during the 30 minutes that each test lasted. Data were collected every 30 s. The culture was stirred at 200 rpm to ensure appropriate homogenisation and prevent microalgae sedimentation. An on-off valve was opened to add pure CO_2 when pH exceeded 7.5 to avoid carbon limitation and control pH.

2.2.2.2 Continuous lab-scale operation

For the continuous lab-scale operation, two 8-L vertical reactors (R-A and R-B) were used. R-A was used as control; i.e., no nitrite was added in any of the assays, while in R-B nitrite concentrations of 5, 10 and 20 mg N$\cdot L^{-1}$ were added in assays L_5, L_{10} and L_{20}, respectively, by using a standard dilution of 1000 mg $NO_2 \cdot L^{-1}$. Similar to respirometries (section 2.2.2.1), an ATU dose was added to both reactors to avoid AOB activity (González-Camejo et al., 2018).

R-A and R-B were placed in a thermostatic chamber maintaining the culture temperature at around 25 ºC. They were air-stirred at 0.6 vvm to homogenise the culture and avoid biofilm formation and microalgae sedimentation. To control the culture pH, CO_2 was injected when the pH reached a maximum value of 7.5. Four cool-white LED lamps (T8 LED-Tube 9 w) were placed vertically around each reactor to supply a light PAR of 125 μmol$\cdot m^{-2} s^{-1}$ at the reactor´s surface.

Both reactors were filled with 25% of substrate (i.e., AnMBR effluent) and 75% of the microalgae culture from the MPBR plant. Hence, R-A and R-B started with the same inoculum in each continuous lab-scale assay. Reactors were operated in semi-continuous mode, maintaining a 3 d HRT (with no biomass retention; i.e., BRT also accounted for 3 d) during 5-day experiments. The characteristics of each media; i.e., ammonium (NH_4), soluble nitrogen (N_s), phosphate (PO_4) and volatile suspended solids (VSS) concentrations are shown in Table XII.2. In these substrate and culture samples, nitrite was not detected.

The performance of both reactors was compared in terms of nitrogen and phosphorus recovery rates and biomass productivity.

Table XII.2. Characteristics of the microalgae culture and substrate in the continuous lab-scale assays.

	Substrate (mg·L^{-1})				**Culture (mg·L^{-1})**			
Assay	**NH_4**	**N_s**	**P**	**VSS**	**NH_4**	**N_s**	**P**	**VSS**
L_5	62.4	64.6	7.3	< LOD*	33.4	41.7	4.1	857
L_{10}	48.5	51.2	3.0	< LOD*	11.5	14.1	0.0	590
L_{20}	52.5	54.3	4.0	< LOD*	11.9	50.6	0.0	423

**LOD: Limit of detection*

2.3. Sampling and analytical methods

Daily grab samples of R-A and R-B were measured in duplicate for the continuous lab-scale assays. With respect to the continuous operation of the MPBR plant, samples from the AnMBR effluent and from the MPBR plant effluent were collected three times a week and measured in duplicate.

Ammonium (NH_4), nitrite (NO_2), nitrate (NO_3) and phosphorus (P) were analysed using an automatic analyser (Smartchem 200, WestcoScientific Instruments, Westco) according to Standard Methods (APHA, 2005): 4500-NH3-G, 4500-NO2-B, 4500-NO3-H and 4500-P-F, respectively. Total soluble nitrogen (N_S) was obtained as the sum of the three measured nitrogen species; i.e., NH_4, NO_2 and NO_3. The volatile suspended solids (VSS) concentration was also measured according to method 2540 E of Standard Methods (APHA, 2005).

The chemical oxygen demand was performed according to Standard Methods (APHA, 2005) 5220-COD-C.

2.4. Calculations

The net OPR (mg $O_2 \cdot L^{-1} \cdot h^{-1}$) was calculated by Eq. XII.1:

$$\frac{dDO}{dt} = k_L a \cdot (DO_{SAT} - DO) + OPR \qquad \text{[Eq. XII.1]}$$

where dDO/dt is the variation of the oxygen concentration over time (mg $O_2 \cdot L^{-1} \cdot h^{-1}$), k_La is the oxygen mass transfer coefficient (h^{-1}), DO_{SAT} is the oxygen saturation concentration at the culture temperature (mg $O_2 \cdot L^{-1}$) and DO is the oxygen concentration in the culture (mg $O_2 \cdot L^{-1}$).

k_La was evaluated by doing respirometric tests with clean water as medium (in triplicate). A mean value of 0.30 h^{-1} was obtained by applying Eq. XII.1 considering null OPR. The minimum square error criterion was used to optimally fit OPR in Eq. XII.1 (Rossi et al., 2018).

Biomass productivity (mg $VSS \cdot L^{-1} \cdot d^{-1}$) and nitrogen recovery rate (NRR) (mg $N \cdot L^{-1} \cdot d^{-1}$) were calculated as reported by González-Camejo et al. (2019).

The nitrification rate (NOxR) (mg $N \cdot L^{-1} \cdot d^{-1}$) was obtained by Eq. XII.2:

$$NOxR = \frac{F \cdot (NOx_e - NOx_i)}{V_{MPBR}} \qquad \text{[Eq. XII.2]}$$

where F is the treatment flow rate ($m^3 \cdot d^{-1}$); NOx_e is the concentration of nitrite plus nitrate of the effluent (mg $N \cdot L^{-1}$); NOx_i is the concentration of nitrite plus nitrate of the influent (mg $N \cdot L^{-1}$); and V_{MPBR} is the volume of the culture in the MPBR plant (m^3).

The concentration of free ammonia (NH_3) (mg $N \cdot L^{-1}$) in the system was obtained from the Anthonisen equation (Eq. XII.3). As a conservative calculation, all the ammonia concentration was hypothesised to be stripped from the system.

$$NH_3 = \frac{NH_4}{1+10^{-pH+0.09018+\frac{2729.92}{T+273}}} \qquad \text{[Eq. XII.3]}$$

where NH_4 is the concentration of ammonium in the system; pH is the pH value of the culture and T is the culture temperature (ºC).

The duty cycle (φ); i.e., the proportion of time at which microalgae are exposed to light (Fernández-Sevilla et al., 2018), can be calculated according to Eq. XII.4:

$$\varphi = \frac{I_{av}}{I_0} = \frac{(1-e^{-K_a \cdot C_b \cdot L})}{K_a \cdot C_b \cdot L} \qquad \text{[Eq. XII.4]}$$

where I_{av} is the average irradiance inside the PBRs ($\mu mol \cdot m^{-2} \cdot s^{-1}$), I_0 is the light irradiance applied to the PBR surface ($\mu mol \cdot m^{-2} \cdot s^{-1}$), K_a is the extinction coefficient of the microalgae biomass ($m^2 \cdot g^{-1}$), C_b is the biomass concentration of the culture ($g \cdot m^3$) and L is the light path of the PBR (m).

2.5. Statistical analysis

All the results are shown as mean ± standard deviation of the duplicates. STATGRAPHICS Centurion XVI.I was employed for performing ANOVA analysis. In this respect, p-values < 0.05 were considered statistically significant.

3. RESULTS AND DISCUSSION

3.1. Outdoor MPBR plant

Previous studies have evaluated the best conditions of the MPBR plant in terms of light availability, nutrient recovery and treatment capacity (González-Camejo et al., 2018; 2019). However, the operating conditions that enhance microalgae activity within the microalgae-AOB competition for ammonium uptake in the treatment of AnMBR effluents have not been assessed yet.

The performance of the MPBR was evaluated in terms of NRR and biomass productivity. To assess the activity of nitrifying bacteria, the nitrification rate (NOxR), i.e. the production of both nitrite and nitrate in the culture, was used (Rossi et al, 2018). It must be noted that this value is an approximation since it does not include the nitrate and nitrite that algae can consume. However, previous lab-scale assays showed that the nitrite and nitrate that microalgae absorb was considerably lower than ammonium (data not shown).

3.1.1. Effect of dilution rate

DR-Period was operated at dilution rate of 0.3 d^{-1} (i.e. 3-days BRT), while HRT was set to 1 d. As can be seen in Figure XII.1a, until day 12 of DR-Period, the NO_x concentration was very low since nitrification rate during this time was only 1.6 ± 0.9 mg $N \cdot L^{-1} \cdot d^{-1}$. Hence, microalgae biomass was maintained at high values of 749 ± 38 mg $VSS \cdot L^{-1}$. However, after that moment, NOxR increased and nitrite thus accumulated (Figure XII.1a). Consequently, the microalgae biomass concentration decreased at values lower than 400 mg $VSS \cdot L^{-1}$ (Figure XII.1b). Furthermore, nitrate effluent

concentration reached a maximum value of 19.0 mg $N \cdot L^{-1}$ on day 30 (Figure XII.1a). Nitrate is absorbed by microalgae at lower rate than ammonium because it has to be internally reduced prior to be assimilated (Shoener et al., 2019).

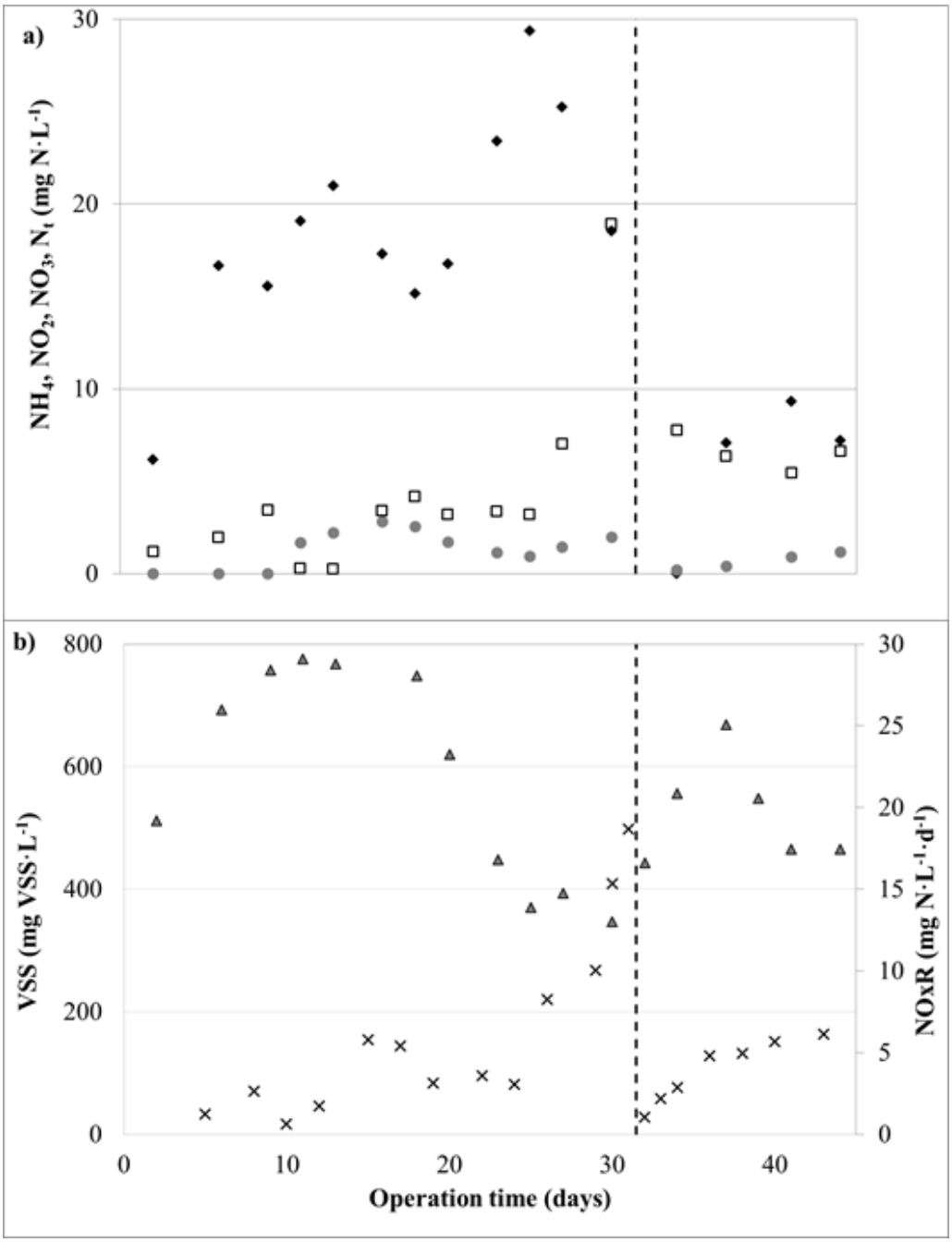

Figure XII.1. Continuous operation of the MPBR plant during DR-Period. Evolution of: a) effluent concentration of ammonium (NH_4) (♦), nitrite (NO_2) (●) and nitrate (NO_3) (□); and b) concentration of the volatile suspended solids (VSS) (▲) and nitrification rate (NOxR) (x). Punctual increase of dilution rate (- - -).

The relatively high temperature during DR-Period (i.e., 24.7 ± 1.2 ºC) could have favoured AOB growth over microalgae since AOB are known to significantly increase their activity with increasing temperatures (Marazzi et al., 2017). For this reason, on day 31 (displayed in Figure XII.1 as dashed line), a punctual increase of the dilution rate from 0.3 to 0.5 d^{-1} was done in order to washout the culture and decrease the AOB, nitrite and nitrate concentrations. Some authors (Luo et al., 2018; Praveen et al., 2019) have reported that higher dilution rates can stimulate microalgae growth (and hence reduce the activity of nitrifying bacteria) by reducing the microalgae biomass concentration, which increases the light availability of the culture.

After this increase of the dilution rate, the MPBR plant continued with the same operating conditions (i.e. 3 d BRT and 1 d HRT) and the NOxR significantly decreased (Figure XII.1b). However, AOB started outcompeting microalgae again since the NOxR continuously rose after the punctual increase of the dilution rate. It can be therefore concluded that a sudden increase in the MPBR dilution rate can temporarily benefit microalgae by reducing the concentration of AOB, nitrite and nitrate, but if operating conditions are not appropriate, AOB will increase their activity again.

3.1.2. Effect of BRT

Period BRT-A was operated at BRT of 2 d. Under these conditions, AOB activity was favoured in comparison to microalgae since more influent nitrogen was nitrified instead of being assimilated by microalgae (Figure XII.2a). NOB activity was also expected to be low at 2-d BRT (Munz et al., 2011). In consequence, nitrite accumulated until reaching concentrations over 10 mg $N \cdot L^{-1}$ (Figure XII.3). Similar results were obtained by Marazzi et al. (2019), who reported higher nitrite concentrations at shorter BRTs in a mixed microalgae-bacteria culture for outdoor centrate treatment.

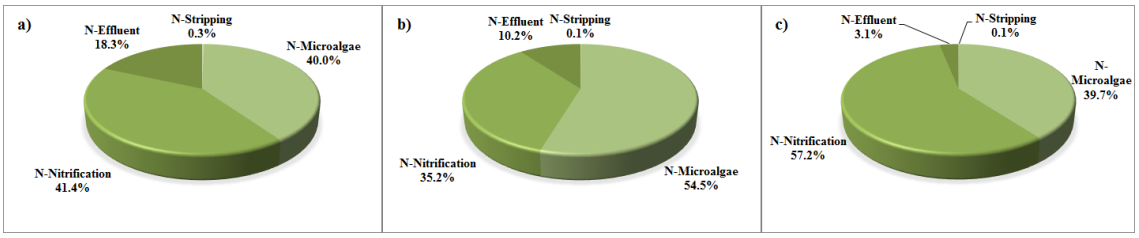

Figure XII.2. Distribution of nitrogen in the MPBR plant: a) Period BRT-A; b) Period BRT-B; and c) Period BRT-C.

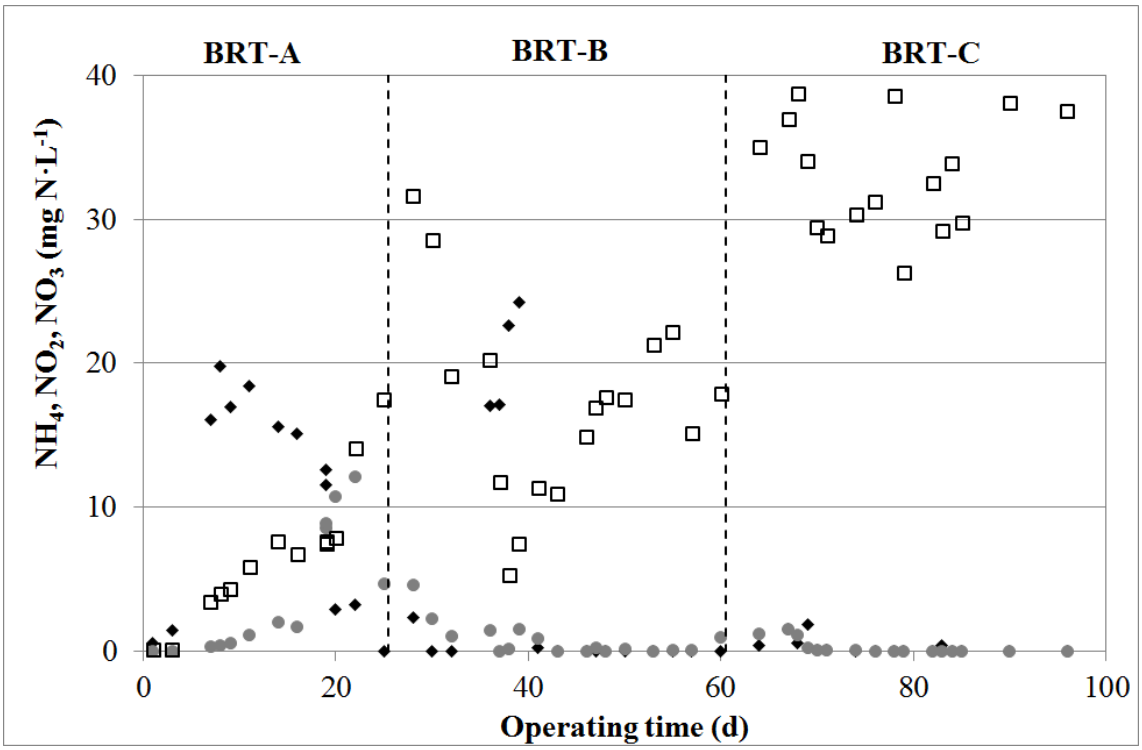

Figure XII.3. Continuous operation of the MPBR plant during BRT periods. Evolution of effluent concentration of ammonium (NH_4) (♦), nitrite (NO_2) (●) and nitrate (NO_3) (□).

According to lab-scale assays (section 3.2.2), these nitrite concentrations should have inhibited microalgae growth. Consequently, the lowest MPBR performance of BRT periods was obtained in Period BRT-A (Table XII.3). Period BRT-A also showed the highest percentage of nitrogen lost in the effluent (Figure XII.2). Hence, operating at 2-d BRT did not seem to be suitable for operating the mixed microalgae culture in the MPBR plant since it triggers AOB activity, promoting the accumulation of nitrite and the subsequent microalgae inhibition.

Table XII.3. Biomass productivity, nutrient recovery and nitrification rates obtained in BRT periods.

Period	Biomass productivity ($mg\ VSS \cdot L^{-1} \cdot d^{-1}$)	NRR ($mg\ N \cdot L^{-1} \cdot d^{-1}$)	NOxR ($mg\ N \cdot L^{-1} \cdot d^{-1}$)	Duty cycle (-)
BRT-A	136 ± 53	14.1 ± 5.2	13.5 ± 7.9	0.18 ± 0.05*
BRT-B	139 ± 35	19.7 ± 3.3*	12.6 ± 5.1	0.15 ± 0.04*
BRT-C	108 ± 26*	14.5 ± 6.7	24.3 ± 8.6*	0.11 ± 0.01*

**Showed significant differences (p-value < 0.05)*

In Period BRT-B, BRT was raised to 2.5 d. As a consequence, the nitrite concentration sharply decreased from 12.2 mg $N \cdot L^{-1}$ to values lower than 1 mg $N \cdot L^{-1}$ (Figure XII.3). As aforementioned, 2-d BRT was too short for NOB to grow, but BRT increase to 2.5 d favoured NOB growth (Marazzi et al., 2019; Munz et al., 2011) which caused the nitrite depletion in the culture by carring out the second step of nitrification (Winkler and Straka, 2019). Microalgae were also favoured because they were no longer inhibited by nitrite and BRT was close to their theoretical optimum value for this MPBR system, which was calculated from the growth rate obtained during the start-up stage (data not shown). As a result, nitrification was reduced and the nitrogen used for microalgae biomass rose up to 54.5% of the influent nitrogen (Figure XII.2b). Consequently, MPBR yields in Period BRT-B were the best of BRT periods (Table XII.3).

In Period BRT-C, BRT was lengthened to 4.5 d. Similar to what happened in Period BRT-B, no nitrite accumulation was observed during Period BRT-C (Figure XII.3), probably because NOB growth was favoured at longer BRTs (Munz et al., 2011), as aforementioned. Microalgae growth was not thus expected to be inhibited by nitrite. However, the influent nitrogen assimilated by microalgae only accounted for 39.7% (Figure XII.2c). Consequently, the worst MPBR performance of BRT Periods was observed in Period BRT-C while NOxR was significantly the highest (Table XII.3). This could have occurred for several reasons:

i) The significantly high nitrification (i.e., 57.2% of the influent nitrogen) made most of the nitrogen be in the form of nitrate. It is widely known that nitrate uptake rate by microalgae is significantly lower than that of ammonium (Shoener et al., 2019).

ii) To assimilate nitrate into microalgae biomass, microalgae need to prior reduce the nitrate to nitrite (by enzyme nitrate reductase in the cytosol) and nitrite to ammonium (by nitrite reductase in the chloroplast). Hence, the large amounts of nitrate present in the culture could have had increased the intracellular content of nitrite (Chen et al., 2009), inhibiting microalgae.

iii) The negligible ammonium concentration during Period BRT-C (Figure XII.3) was likely to reduce microalgae growth, favouring nitrification. In fact, outdoor tests carried out under ammonium replete and deplete conditions (Appendix A) showed that NOxR sharply increased from 1.3 ± 2.2 mg $N \cdot L^{-1} \cdot d^{-1}$ to 17.5 ± 5.3 mg $N \cdot L^{-1} \cdot d^{-1}$ under replete and deplete-ammonium conditions, respectively.

iv) The shadow effect caused by the significant biomass increase: from 347 ± 84 mg $VSS \cdot L^{-1}$ in Period BRT-B to 486 ± 70 mg $VSS \cdot L^{-1}$ in Period BRT-C. The rising amount

of microalgae biomass absorbed most of the light photons, reducing the time which microalgae spent under lighting conditions (Fernández-Sevilla et al., 2018). As a consequence, the lowest duty cycle of BRT periods was obtained in Period BRT-C (Table XII.3).

It must be noted that temperature effect in the microalgae-AOB competition was not considered in BRT periods since it remained at moderate temperatures (Table XII.1) at which AOB growth is usually low.

To sum up, BRT apparently had a significant influence in the microalgae-AOB competition for ammonium. In this respect, too short BRTs of 2 d seemed to favour AOB activity in comparison to microalgae and NOB, causing the nitrite accumulation and the subsequent microalgae inhibition by nitrite. On the other hand, long BRT of 4.5 days favoured NOB growth therefore oxidising nitrite and accumulating nitrate. However, these operating conditions obtained lower NRR and biomass productivity than 2.5-d BRT.

3.2. Nitrite inhibition

3.2.1. Short-term exposure to nitrite

Four respirometries were carried out: R_0, R_5, R_{10} and R_{20}, which corresponded to nitrite concentrations in the reactor of 0, 5, 10 and 20 mg $N \cdot L^{-1}$, respectively. Higher and lower nitrite concentrations were not tested because the outdoor MPBR plant was not likely to present such concentrations. Previous experimental periods carried out in the MPBR plant showed that microalgae did not seem to be affected by nitrite concentration lower than 5 mg $N \cdot L^{-1}$ (data not shown).

It must be noted that the OPR obtained by Eq. XII.1 corresponds to a net value which is the result of several processes: i) microalgae photosynthesis; ii) activity of nitrifying bacteria; iii) respiration of heterotrophic bacteria; and iv) microalgae photorespiration (Rossi et al., 2018).

However, AOB activity was inhibited by ATU addition (section 2.2.1.1). In addition, continuous monitoring of the MPBR operations by the respirometric methodology of Rossi et al. (2018) (data not shown) obtained that the sum of heterotrophic bacteria activity and microalgae photorespiration accounted for 10.7% of the total microalgae photosynthetic activity (p-value < 0.05; $R^2 = 0.672$; $n = 6$); although the activity of heterotrophic bacteria was expected to be negligible in this system due to the low biochemical oxygen demand of the AnMBR effluent; which only accounted for 29 ± 4

mg $O_2 \cdot L^{-1}$. Moreover, as the sample used for all the respirometric tests was the same, microalgae photorespiration and heterotrophic bacteria activity was expected to affect all the tests at similar rate. In conclusion, the net OPR obtained by Eq. XII.1 was considered a representative measurement of the microalgae activity.

OPRs varied in the range of 27.6-33.8 mg $O_2 \cdot L^{-1} \cdot d^{-1}$ (Figure XII.4), which means that no significant differences (p-value > 0.05) were obtained in the respirometric tests for all the nitrite concentrations studied, including the blank. These results therefore suggest that short-term exposures to nitrite concentrations under 20 mg $N \cdot L^{-1}$ do not significantly affect microalgae activity.

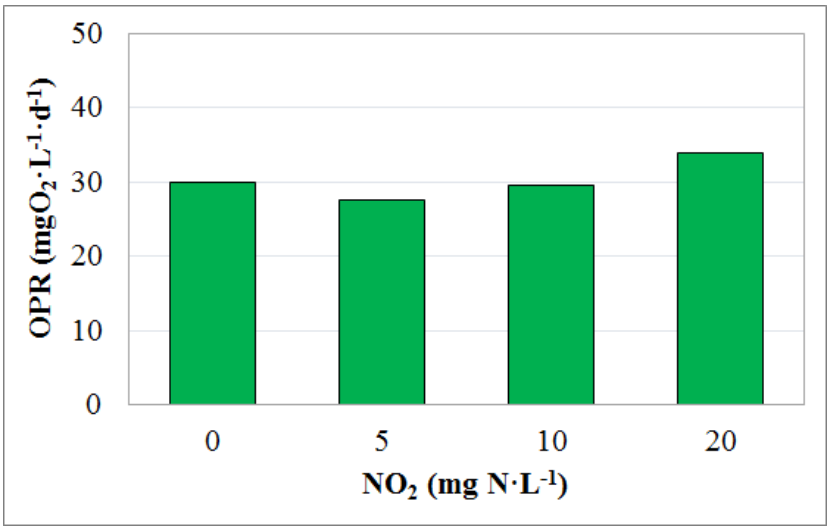

Figure XII.4. Oxygen production rates (OPR) (mg $O_2 \cdot L^{-1} \cdot d^{-1}$) obtained during the respirometric tests of the short-term lab assays.

3.2.2. Continuous exposure to nitrite

Figure XII.5 shows the results of the continuous lab-scale assays. It can be observed that NRRs were considerably lower in R-B (with the presence of NO_2) and that the difference between R-A (without NO_2) and R-B increased when the NO_2 concentration in R-B was higher. In fact, NRR in R-B was 32% lower than R-A for Assay L_5, while for Assays L_{10} and L_{20} NRR was reduced by 42 and 80%, respectively.

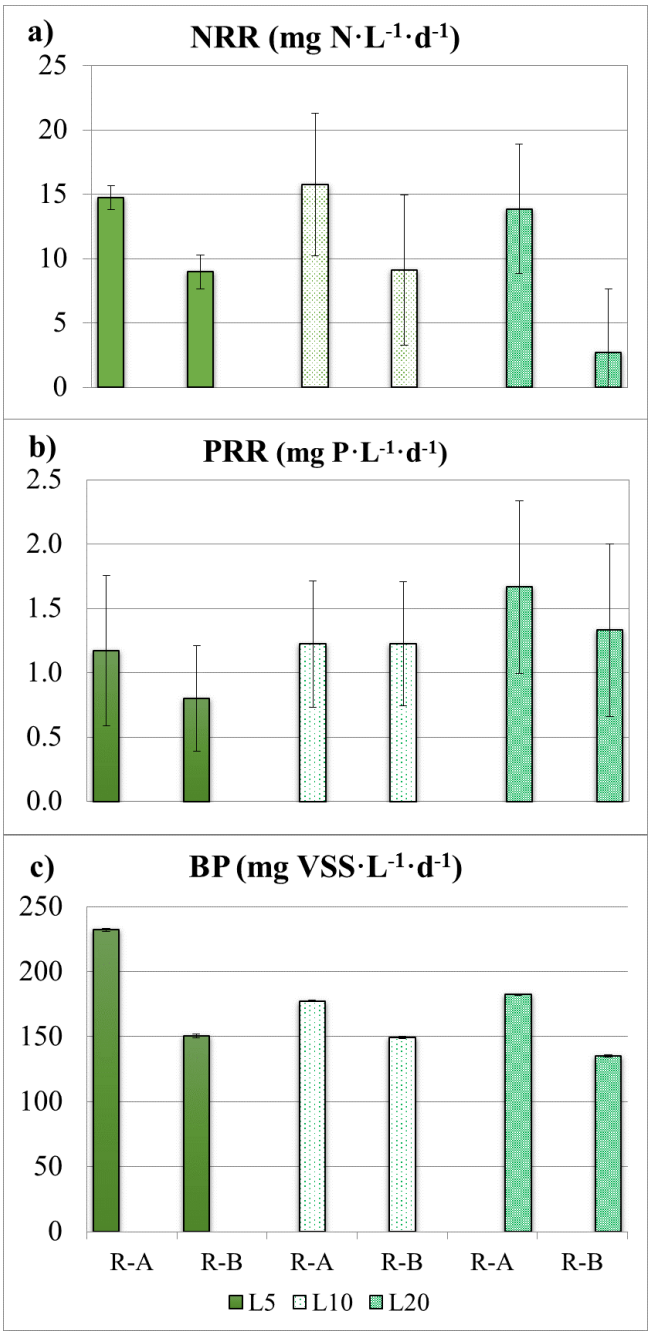

Figure XII.5. Results from long-term lab assays. R-A: without the presence of nitrite and R-B with the presence of nitrite: a) nitrogen recovery rate (NRR); b) phosphorus recovery rate (PRR) and c) biomass productivity (BP).

On the other hand, PRR showed a 32% difference between R-A and R-B in Assay L_5, but for Assays L_{10} and L_{20} the results were similar, probably due to the phosphorus limitation during Assays L_{10} and L_{20} (Figure XII.6). In fact, the culture sample in these assays was phosphorus-lacking (Table XII.2). On the contrary, during Assay L_5 the culture was under phosphorus-replete conditions (Figure XII.6).

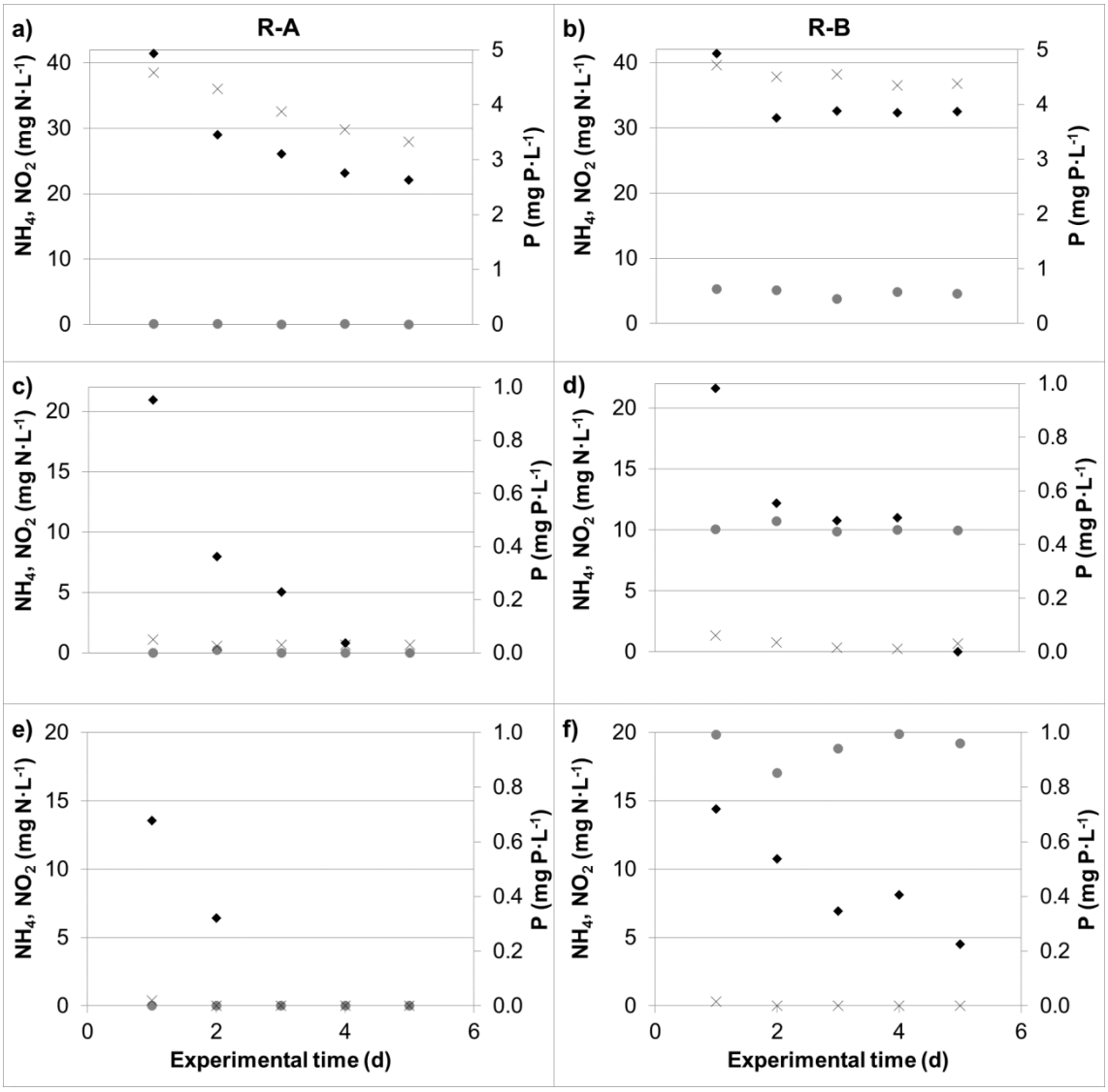

Figure XII.6. Evolution of ammonium (NH_4) (♦); nitrite (NO_2) (●) and phosphorus (P) (x) during continuous lab-scale assays: a) R-A in Assay L_5; b) R-B in Assay L_5; c) R-A in Assay L_{10}; d) R-B in Assay L_{10}; e) R-A in Assay L_{20}; and f) R-B in Assay L_{20}.

Regarding microalgae biomass, R-A obtained significantly higher biomass productivities than R-B in all the continuous lab-scale assays, but unlike NRR, the differences in biomass productivities between R-A and R-B did not raise with increasing NO_2 concentration. Indeed, biomass productivity in R-B was 35, 16 and 19% lower than in R-A for Assays L_5, L_{10} and L_{20}, respectively. This different trend was probably due to the nutrient limitation observed in Assays L_{10} and L_{20}; i.e., NH_4 < 10 mg $N \cdot L^{-1}$ and P < 1 mg $P \cdot L^{-1}$ (as observed in Figure VI.A.2). Anyhow, the nitrite inhibition of microalgae was observed in all the continuous lab-scale assays. According

to Sijbesma et al. (1996) nitrite increases the proton permeability through the cell membranes, inhibiting the adenosine triphosphate (ATP) synthesis.

To sum up, nitrite concentrations over 5 mg $N \cdot L^{-1}$ showed inhibitory effects on a microalgae culture dominated by green microalgae *Chlorella*. It must be highlighted that this concentration is quite lower than those reported for other microalgae strains such as 70 mg $N\text{-}NO_2 \cdot L^{-1}$ for *Botryococcus braunii* (Yang et al., 2004) and 50 mg $N\text{-}NO_2 \cdot L^{-1}$ for *Microcystis aeruginosa* (Chen et al., 2009).

These results can help to clarify the behaviour of the mixed microalgae-nitrifying bacteria culture during the continuous operation of the MPBR plant. The reduction of MPBR plant performance after an AOB proliferation was previously thought to occur because of ammonium depletion due to nitrification (González-Camejo et al., 2018) or because of competitive exclusion between microalgae and bacteria. Results obtained in this study therefore add another factor related to AOB activity that negatively affects MPBR performance. In this respect, it must be noted that the inhibitory effect of nitrite is unlikely to be observed immediately, since short-term exposures to nitrite did not present significant different photosynthetic activities (see section 3.2.1).

It must be also noted that the possibility that microalgae were limited by the proliferation of NOB was in R-B (higher nitrite concentrations) was discarded due to: i) nitrifying bacteria activity in a similar culture dominated by *Chlorella* only accounted for 4.4% (on average) of the microalgae activity (Figure X.2). NOB activity could thus be considered negligible; ii) nitrogen recovery rates were observed to decrease with higher nitrite concentrations (i.e. from 5 to 20 mg $N \cdot L^{-1}$). However, according to the half saturation constant of NOB with respect to NO_2 (i.e. 0.3 mg $N \cdot L^{-1}$ according to Jiménez (2010)), under nitrite concentration of 5 mg $N \cdot L^{-1}$ NOB activity would be close to their optimum. Differences in NOB activity under nitrite concentrations in the range of 5-20 mg $N \cdot L^{-1}$ should hence be negligible. In consequence, differences in microalgae performance under different nitrite concentrations might not have been due to NOB activity.

4. CONCLUSIONS

The continuous operation under outdoor conditions showed that BRT played a key role in the accumulation of nitrite in the culture. At BRT of 2 d, AOB were favoured and nitrite accumulated.

Lab assays confirmed that this indigenous microalgae culture (dominated by *Chlorella*) was inhibited by nitrite under continuous treatment of AnMBR effluent. In fact, nitrogen recovery was reduced by 32, 42 and 80% (in comparison to the reactor control) for nitrite concentrations of 5, 10 and 20 mg $N \cdot L^{-1}$, respectively. On the other hand, no significant nitrite inhibition was observed when microalgae was exposure to nitrite concentrations of 5, 10 and 20 mg $N \cdot L^{-1}$ during 30 minutes).

When BRT of the MPBR plant was lengthened to 2.5 d, nitrite was reduced due to increasing microalgae and NOB activity. MPBR performance was thus enhanced, reaching maximum NRR of 19.7 ± 3.3 mg $N \cdot L^{-1} \cdot d^{-1}$.

Operating the MPBR plant at long BRT of 4.5 d did not show any accumulation of nitrite, but microalgae were limited by several possible reasons: i) microalgae prefer ammonium instead of nitrate; ii) possible accumulation of intracellular nitrite; iii) ammonium-deplete conditions which limited microalgae activity; and iv) shadow effect that reduced light availability.

ACKNOWLEDGMENTS

This research work was supported by the Spanish Ministry of Economy and Competitiveness (MINECO, Projects CTM2014-54980-C2-1-R and CTM2014-54980-C2-2-R) jointly with the European Regional Development Fund (ERDF), both of which are gratefully acknowledged. It was also supported by the Spanish Ministry of Education, Culture and Sport via a pre-doctoral FPU fellowship to authors J. González-Camejo (FPU14/05082) and S. Aparicio (FPU/15/02595).

REFERENCES

1. Abe, K., Imamaki, A., Hirano, M., 2002. Removal of nitrate, nitrite, ammonium and phosphate ions from water by the aerial microalga *Trentepohlia aurea*. J. Appl. Phycol. 14(2), 129-134.
2. Akizuki, S., Cuevas-Rodriguez, G., Toda, T., 2019. Microalgal-nitrifying bacterial consortium for energy-saving ammonia removal from anaerobic digestate of slaughterhouse wastewater. J. Water Process Eng. 31, 100753. https://doi.org/10.1016/j.jwpe.2019.01.014
3. APHA-AWWA-WPCF, 2005. Standard methods for the examination of water and wastewater, 21st edition. American Public Health Association, American Water Works Association, Water Pollution Control Federation. Washington DC, USA.

4. Barbera, E., Bertucco, A., Kumar, S., 2018. Nutrients recovery and recycling in algae processing for biofuels production. Renew. Sust. Energy Rev. 90, 28–42. https://doi.org/10.1016/j.rser.2018.03.004
5. Bilad, M.R., Azizo, A.S., Wirzal, M.D.H., Jia, L.J., Putra, Z.A., Nordin, NA.H.M., Mavukkandy, M.O., Jasni, M.J.F., Yusoff, A.R.M., 2018. Tackling membrane fouling in microalgae filtration using nylon 6,6 nanofiber membrane. J. Environ. Manag. 223, 23–28. https://doi.org/10.1016/j.jenvman.2018.06.007
6. Chen, W. M., Zhang, Q. M., Dai, S. G., 2009. Utilization of nitrite as a nitrogen source by *Microcystis aeruginosa*. Journal of Agro-Environment Science 28(5), 989-993. https://doi.org/10.1007/s10811-009-9405-1
7. Collos,Y., Harrison, P.J., 2014 Acclimation and toxicity of high ammonium concentrations to unicellular algae. Mar. Pollut. Bull. 80, 8–23. https://doi.org/10.1016/j.marpolbul.2014.01.006
8. Eze, V.C, Velasquez-Orta, S.B., Hernández-García, A., Monje-Ramírez, I., Orta-Ledesma, M.T., 2018. Kinetic modelling of microalgae cultivation for wastewater treatment and carbon dioxide sequestration. Algal Res. 32, 131–141. https://doi.org/10.1016/j.algal.2018.03.015
9. Fernández-Sevilla, J.M., Brindley, C., Jiménez-Ruíz, N., Acién, F.G., 2018. A simple equation to quantify the effect of frequency of light/dark cycles on the photosynthetic response of microalgae under intermittent light. Algal Res. 35, 479–487. https://doi.org/10.1016/j.algal.2018.09.026
10. Galès, A., Bonnafous, A., Carré, C., Jauzein, V. Lanouguère, E., Le Floc'ha, E., Pinoit, J., Poullain, C., Roques, C., Sialve, B., Simier, M., Steyer, J.P., Fouilland, E., 2019. Importance of ecological interactions during wastewater treatment using High Rate Algal Ponds under different temperate climates, Algal Res. 40, 101508. https://doi.org/10.1016/j.algal.2019.101508
11. González-Camejo, J., Jiménez-Benítez, A., Ruano, M.V., Robles, A., Barat, R., Ferrer, J., 2019. Optimising an outdoor membrane photobioreactor for tertiary sewage treatment. J. Environ. Manag. 245, 76-85. https://doi.org/10.1016/j.jenvman.2019.05.010
12. González-Camejo, J., Barat, R., Ruano, M.V., Seco, A., Ferrer, J., 2018. Outdoor flat-panel membrane photobioreactor to treat the effluent of an anaerobic membrane bioreactor. Influence of operating, design and environmental conditions. Water Sci. Technol. 78(1), 195-206. http://dx.doi.org/10.2166/wst.2018.259
13. Jiménez, E., 2010. Mathematical modelling of the two-stage nitrification process. Developement of modelling calibration methodologies for a SHARON reactor and activated sludge process (Modelación matemática del proceso nitrificación en dos

etapas. Desarrollo de metodologías de calibración del modelo para un reactor SHARON y un proceso de fangos activados). PhD Thesis, Polytechnic University of Valencia, Spain.

14. Luo, Y., Le-Clech, P., Henderson, R.K., 2018. Assessment of membrane photobioreactor (MPBR) performance parameters and operating conditions. Water Res. 138, 169-180. https://doi.org/10.1016/j.watres.2018.03.050
15. Marazzi, F., Bellucci, M., Rossi, S., Fornaroli, R., Ficara, E., Mezzanotte, V., 2019. Outdoor pilot trial integrating a sidestream microalgae process for the treatment of centrate under non optimal climate conditions. Algal Res. 39, 101430. https://doi.org/10.1016/j.algal.2019.101430
16. Marazzi, F., Ficara, E., Fornaroli, R., Mezzanotte, V., 2017. Factors affecting the growth of microalgae on blackwater from biosolid dewatering. Water, Air & Soil Pollution 228 (2), 68. http://dx.doi.org/10.1007/s11270-017-3248-1.
17. Marcilhac, C., Sialve B., Pourcher A.M., Ziebal C., Bernet N., Béline F., 2014. Digestate color and light intensity affect nutrient removal and competition phenomena in a microalgal-bacterial ecosystem, Water Res. 64, 278-287. http://dx.doi.org/10.1016/j.watres.2014.07.012
18. Molinuevo-Salces, B., García-González, M.C., González-Fernández, C., 2010. Performance comparison of two photobioreactors configurations (open and closed to the atmosphere) treating anaerobically degraded swine slurry, Bioresour. Technol. 101, 5144–5149. https://doi.org/10.1016/j.biortech.2010.02.006
19. Munz, G., Lubello, C., Oleszkiewicz, J.A., 2011. Factors affecting the growth rates of ammonium and nitrite oxidizing bacteria. Chemosphere, 83(5), 720-725. https://doi.org/10.1016/j.chemosphere.2011.01.058
20. Praveen, P., Xiao, W., Lamba, B., Loh, K.C., 2019. Low Biomass Retention Operation to Enhance Productivity in an Algal Membrane Photobioreactor. Algal Res. 40, 101487. https://doi.org/10.1016/j.algal.2019.101487
21. Rada-Ariza, A.M., Fredy, D., Lopez-Vazquez, C.M., Van der Steen, N.P., Lens, P.N.L., 2019, Ammonium removal mechanisms in a microalgal-bacterial sequencing batch photobioreactor at different solids retention times, Algal Res. 39, 101468. https://doi.org/10.1016/j.algal.2019.101468
22. Rossi, S., Bellucci, M., Marazzi, F., Mezzanotte, V., Ficara, E., 2018. Activity assessment of microalgal-bacterial consortia based on respirometric tests. Water Sci Technol. 78(1-2), 207-215. https://doi.org/10.2166/wst.2018.078
23. Ruiz-Martínez, A., Martín García, N., Romero, I., Seco, A., Ferrer, J., 2012. Microalgae cultivation in wastewater: nutrient removal from anaerobic membrane bioreactor

effluent. Bioresour. Technol. 126, 247–253. http://dx.doi.org/10.1016/j.biortech.2012.09.022

24. Santos, F.M., Pires, J.C.M., 2018. Nutrient recovery from wastewaters by microalgae and its potential application as bio-char. Bioresour. Technol. 267, 725–731. https://doi.org/10.1016/j.biortech.2018.07.119
25. Seco, A., Aparicio, S., González-Camejo, J., Jiménez-Benítez, A., Mateo, O., Mora, J.F., Noriega-Hevia, G., Sanchis-Perucho, P., Serna-García, R., Zamorano-López, N., Giménez, J.B., Ruiz-Martinez, A., Aguado, D., Barat, R., Borrás, L., Bouzas, A., Martí, N., Pachés, M., Ribes, J., Robles, A., Ruano, M.V., Serralta, J. and Ferrer, J., 2018. Resource recovery from sulphate-rich sewage through an innovative anaerobic-based water resource recovery facility (WRRF). Water Science and Technology 78 (9), 1925-1936. https://doi.org/10.2166/wst.2018.492
26. Sijbesma, W.F.H., Almeida, J.S., Reis, M.A.M., Santos, H., 1996. Uncoupling effect of nitrite during denitrification by Pseudomonas fluorescens: an in vivo P-NMR study. Biotechnol Bioeng 52, 176–192. http://dx.doi.org/1010.1002/(SICI)1097-0290(19961005)
27. Shoener, B.D., Schramm, S.M., Béline, F., Bernard, O., Martínez, C., Plósz, B.G., Snowling, S., Steyer, J.P., Valverde-Pérez, B., Wágner, D., Guest, J.S., 2019. Microalgae and cyanobacteria modeling in water resource recovery facilities: A critical review. Water Research X 2, 100024. https://doi.org/10.1016/j.wroa.2018.100024
28. Sutherland, D.L., Turnbull, M.H., Craggs, R.J., 2017. Environmental drivers that influence microalgal species in fullscale wastewater treatment high rate algal ponds. Water Res. 124, 504-512. http://dx.doi.org/10.1016/j.watres.2017.08.012
29. Whitton, R., Le Mével, A., Pidou, M., Ometto, F., Villa, R., Jefferson, B., 2016. Influence of microalgal N and P composition on wastewater nutrient remediation. Water Res. 91, 371-378. https://doi.org/10.1016/j.watres.2015.12.054
30. Winkler, M.K.H., Straka, L., 2019. New directions in biological nitrogen removal and recovery from wastewater, Current Opinion in Biotechnology 57C, 50–55. https://doi.org/10.1016/j.copbio.2018.12.007
31. Yang, S., Wang, J., Cong, W., Cai, Z., Ouyang, F. 2004. Utilization of nitrite as a nitrogen source by Botryococcus braunii. Biotechnology letters, 26(3), 239-243. https://doi.org/10.1023/B:BILE.0000013722.45527.18

APPENDIX XII.A. ASSESSMENT OF THE MICROALGAE AND NITRIFYING BACTERIA COMPETITION UNDER AMMONIUM REPLETE AND DEPLETE CONDITIONS

When the effluent of an anaerobic membrane (AnMBR) plant is treated by microalgae-based systems, the competition between microalgae and ammonium oxidising bacteria (AOB) plays a key role in the process (Molinuevo-Salces et al., 2010). AOB are autotrophic bacteria which oxidises ammonium (NH_4) to nitrite (Winkler and Straka, 2019). Consequently, AOB can reduce the ammonium concentration of the microalgae culture, which can limit microalgae growth, especially when NH_4 concentration falls below 10 mg $N \cdot L^{-1}$ (Pachés et al., 2018).

EXPERIMENTAL DESIGN, MATERIALS AND METHODS

The MPBR plant described in section 2.2.2 was operated in continuous mode at biomass retention time (BRT) of 4.5 d and hydraulic retention time (HRT) of 1.25 d for a total of 48 days. The operating period was divided in two sub-periods, according to the concentration of ammonium in the culture. In this respect, during ammonium replete (NH4-R) Period ammonium concentration was over 10 mg $N \cdot L^{-1}$ while in ammonium replete (NH4-R) Period ammonium concentration was over 10 mg $N \cdot L^{-1}$, as can be seen in Table XII.A.1.

Table XII.A.1. Experimental conditions for the continuous operation of the MPBR plant (mean ± standard deviation).

Period	Days of operation	NH_4 (mg $N \cdot L^{-1}$)	Daily solar PAR ($\mu E \cdot m^{-2} \cdot s^{-1}$)	Temperature (ºC)	BRT (d)	HRT (d)
NH4-R	29	> 10	258 ± 76	20.2 ± 1.7	4.5	1.25
NH4-D	19	< 10	250 ± 29	20.5 ± 0.9	4.5	1.25

DATA

At the beginning of the operating period, microalgae were expected to outcompete AOB since they have been reported to be better nutrient competitors than nitrifiers (Marcilhac et al., 2014; Risgaard-Petersen et al., 2004). In fact, under ammonium replete-conditions (Period NH4-R), only 4.1% of the influent nitrogen was nitrified, while 55.8% of the

influent nitrogen was assimilated as microalgae biomass (Figure XII.A.1a). Consequently, nitrogen recovery rates (NRRs) in Period NH4-R reached high values of 27.5 ± 7.0 mg $N \cdot L^{-1} \cdot d^{-1}$.

However, when ammonium was under concentrations of 10 $mg \cdot L^{-1}$ at day 24 (Period NH4-D, see Figure XII.A.2a), NRR was reduced to 17.5 ± 3.4 mg $N \cdot L^{-1} \cdot d^{-1}$. Nitrite inhibition of algae (see section 3.1.2) was expected to be negligible since no significant nitrite accumulation was noticed during all the operating period, remaining always below 1.2 mg $N \cdot L^{-1}$ (Figure XII.A.2a). Since VSS concentration was similar under ammonium repletion and ammonium depletion (Figure XII.A.2b), shadow effect was not considered to have a significant effect in the difference of NRRs either. Hence, the reduction of microalgae activity must have been due to ammonium limitation.

As a consequence of the decay in microalgae activity, nitrification significantly increased in Period NH4-D (Figure XII.A.1b), probably because they were less affected by ammonium limitation. It must be noted that temperature remained fairly stable (Figure XII.A.2b), so that the increase of nitrification rate (NOxR) was not considered to be related to temperature.

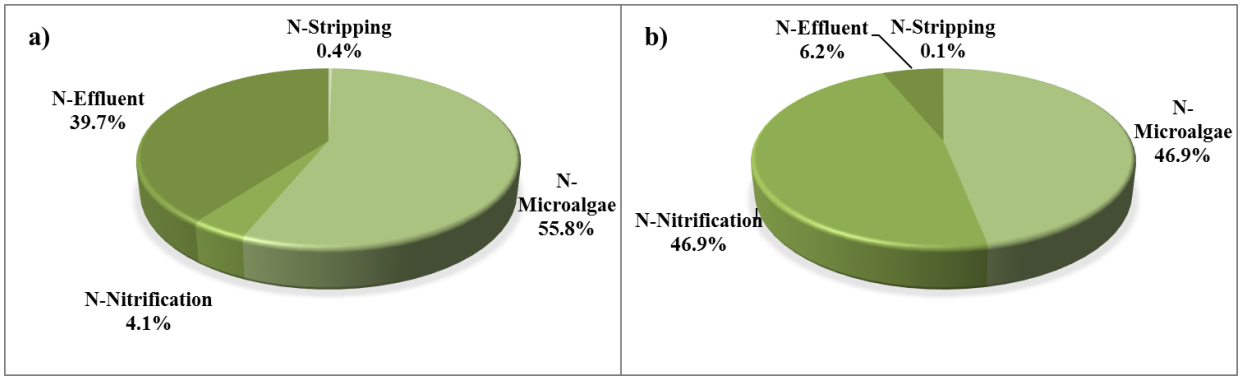

Figure XII.A.1. Distribution of the influent nitrogen to the MPBR plant: a) Period NH4-R; b) Period NH4-D.

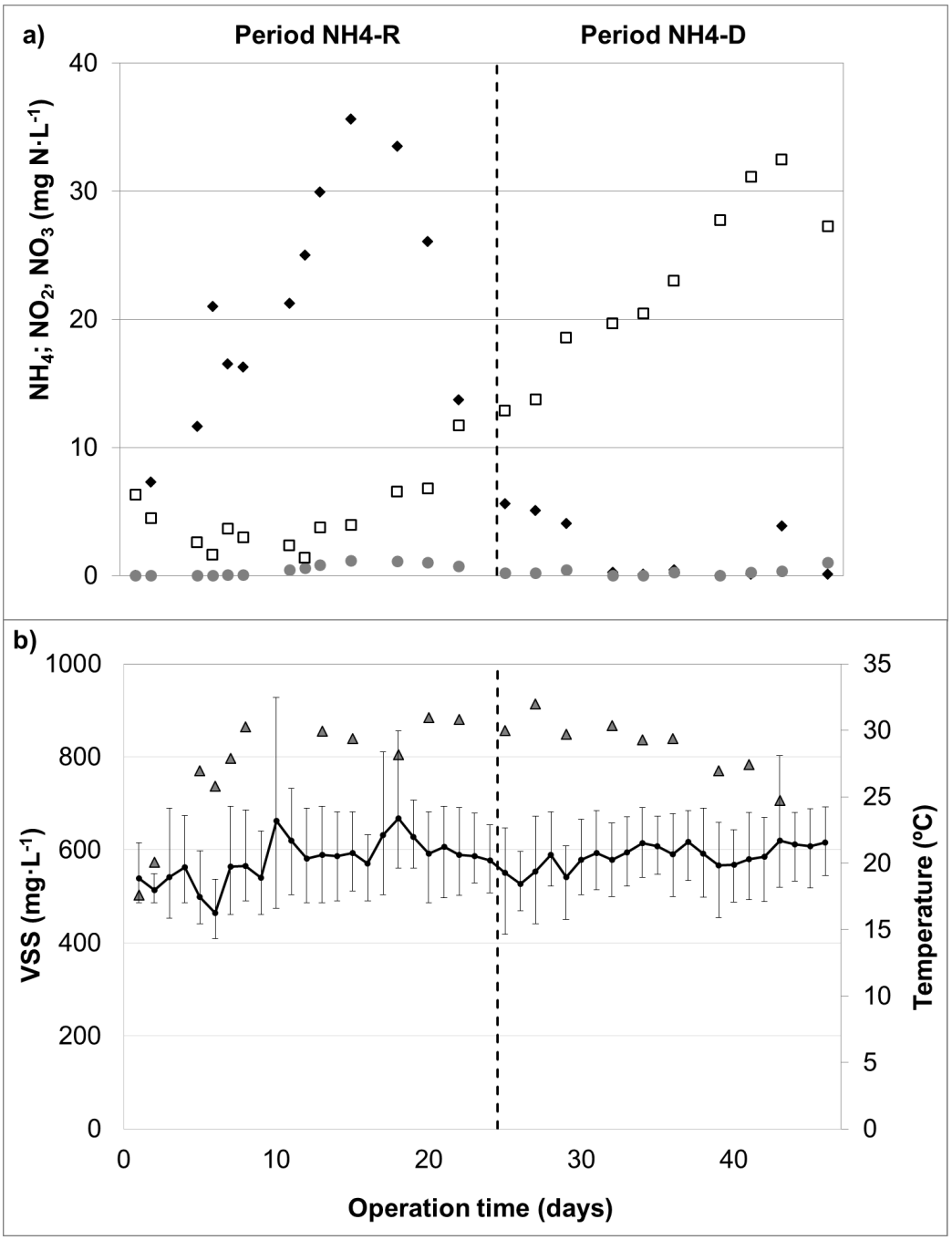

Figure XII.A.2. Continuous operation of the MPBR plant. Evolution of: a) effluent concentration of ammonium (NH_4) (♦), nitrite (NO_2) (●) and nitrate (NO_3) (□), and b) concentration of the volatile suspended solids (VSS) (▲) and temperature (—●—).

REFERENCES

1. Marcilhac, C., Sialve B., Pourcher A.M., Ziebal C., Bernet N., Béline F., 2014. Digestate color and light intensity affect nutrient removal and competition phenomena in a microalgal-bacterial ecosystem, Water Res. 64, 278-287. http://dx.doi.org/10.1016/j.watres.2014.07.012

2. Molinuevo-Salces, B., García-González, M.C., González-Fernández, C., 2010. Performance comparison of two photobioreactors configurations (open and closed to the atmosphere) treating anaerobically degraded swine slurry, Bioresour. Technol. 101, 5144–5149. https://doi.org/10.1016/j.biortech.2010.02.006
3. Pachés, M., Martínez-Guijarro, R., González-Camejo, J., Seco, A., Barat, R., 2018. Selecting the most suitable microalgae species to treat the effluent from an anaerobic membrane bioreactor. Environ. Technol. (in press). https://doi.org/10.1080/09593330.2018.1496148
4. Risgaard-Petersen N, Nicolaisen MH, Revsbech NP, et al. Competition between ammonia oxidizing bacteria and benthic microalgae. Appl. Environ. Microb. 2004;70:5528-5537.
5. Winkler, M.K.H., Straka, L., 2019. New directions in biological nitrogen removal and recovery from wastewater, Current Opinion in Biotechnology 57C, 50–55. https://doi.org/10.1016/j.copbio.2018.12.007

CHAPTER XIII:

CONTINUOUS 3-YEAR OUTDOOR OPERATION OF A FLAT-PANEL MEMBRANE PHOTOBIOREACTOR TO TREAT EFFLUENT FROM AN ANAEROBIC MEMBRANE BIOREACTOR

CHAPTER XIII:

CONTINUOUS 3-YEAR OUTDOOR OPERATION OF A FLAT-PANEL MEMBRANE PHOTOBIOREACTOR TO TREAT EFFLUENT FROM AN ANAEROBIC MEMBRANE BIOREACTOR

González-Camejo, J., Barat, R., Aguado, D., Ferrer, J. *Continuous 3-year outdoor operation of a flat-panel membrane photobioreactor to treat effluent from an anaerobic membrane bioreactor. Water Res. (major revision) September 2019.*

ABSTRACT

A membrane photobioreactor (MPBR) plant was operated continuously for 3 years to evaluate the separate effects of different factors, including: biomass and hydraulic retention times (BRT, HRT), light path (Lp), nitrification rate (NOxR) and nutrient loading rates (NLR, PLR). The overall effect of all these parameters, which influence MPBR performance had not previously been assessed. The multivariate projection approach chosen for this study provided a good description of the collected data and facilitated their visualization and interpretation.

Forty variables used to control and assess MPBR performance were evaluated during three years of continuous outdoor operation by means of principal component analysis (PCA) and partial least squares (PLS) analysis. The PCA identified the photobioreactor light path as the factor with the largest influence on data variability. Other important factors were: air flow rate (F_{air}), nitrogen and phosphorus recovery rates (NRR, PRR), biomass productivity (BP), optical density of 680 nm (OD680), ammonium and phosphorus effluent concentration (NH_4, P), HRT, BRT, and nitrogen and phosphorus loading rates (NLR and PLR). The MPBR performance could be adequately estimated by a PLS model based on all the recorded variables, but this estimation worsened appreciably when only the controlled variables (Lp, F_{air}, HRT and BRT) were used as predictors, which underlines the importance of the other variables on MPBR performance. The microalgae cultivation process could thus only be partially controlled by the design and operating variables.

As effluent nitrate concentration was shown to be the key factor in the nitrification rate, it can be used as an indirect measurement of nitrifying bacteria activity. A high nitrification rate was found to be inadvisable, since it showed an inverse correlation

with NRR. In this respect, temperature appeared to be the main ambient/controlling factor in nitrifying bacteria activity.

1. INTRODUCTION

The ever-increasing population together with human activities are the main factors responsible for the recent growth in wastewater production (Ling *et al.,* 2019). To avoid serious pollution problems wastewater effluents must be properly treated prior to their discharge into natural water bodies (Song *et al.*, 2018). Although urban wastewater treatment plants (WWTPs) are now extremely efficient as regards removing pollutants, they consume huge amounts of energy (Ling et al., Marazzi *et al.*, 2019) and the nutrients are usually lost by nitrogen stripping or phosphorus precipitation (Whitton *et al.*, 2016).

The wastewater treatment sector thus needs to intensify research on more sustainable technologies, not only to remove pollutants from wastewater but also to recover resources from them, mainly energy, nutrients and reclaimed water (Nayak *et al*., 2018; Seco *et al.,* 2018).

Anaerobic membrane bioreactors (AnMBRs) have been attracting much attention since they present lower energy consumption, sludge production and space requirements than the classical aerobic processes (Robles *et al.*, 2013). They can also produce biogas from organic matter that can sometimes offset the energy required for the treatment process (Song *et al.*, 2018).

AnMBR systems have previously been assessed on a pilot scale, obtaining a high quality effluent as regards organic matter and suspended solids (Seco *et al.*, 2018). However, their direct discharge into sensitive water bodies is not permitted, since these systems contain a large amount of nutrients (Song *et al*., 2018) which can lead to eutrophication, i.e. the sudden proliferation of algae in natural waters, which reduces water quality, increases health risks and impairs wildlife (Lau *et al.*, 2019). Microalgae cultivation has emerged as the ideal option to avoid this problem, as it can recover nutrients from AnMBR effluents (González-Camejo *et al.*, 2019a). It also produces valuable microalgae biomass that can be used to obtain biofuels or fertilisers, amongst other applications (Seco *et al.*, 2018; Xu et al., 2019).

Microalgae can be cultivated in either open ponds or closed photobioreactors (PBRs) (Nwoba et al., 2019). The latter can achieve higher biomass production and recover more nutrients than open reactors (González-Camejo *et al.*, 2019b). However, very few

of these plants are being operated at industrial scale, mainly due to the inefficiency of large-scale cultivation techniques (Kubelka *et al.*, 2018; Nayak *et al.*, 2018; Xu *et al.*, 2019). It therefore seems essential to obtain experimental data from real sewage plants for the implementation of large-scale outdoor microalgae-based wastewater systems.

Several authors have reported seasonal variations in the performance of outdoor microalgae systems (García *et al.*, 2018). Apart from ambient conditions (mainly solar light and temperature), there are many other factors that influence microalgae growth: PBR design, mixing rate, nutrient loading rates, microalgae strains, biomass and hydraulic retention time (BRT, HRT), competition with other microorganisms, inhibition by toxic substances, etc. (Cho *et al.*, 2019; Marazzi *et al.*, 2019). Some of these factors have been independently evaluated in outdoor flat-panel MPBRs in previous studies (Table XIII.1). As can be seen, MPBR performance varies widely, with nitrogen recovery rates ranging from 1.9 mg $N \cdot L^{-1} \cdot d^{-1}$ when the plant was operated as a PBR system (i.e. without filtration) to 21.1 mg $N \cdot L^{-1} \cdot d^{-1}$ when MPBR operations were based on the optimal design and control parameters. To determine the best conditions for cultivating microalgae, it is thus important to thoroughly analyse all the recorded variables in order to assess how they affect the process performance.

Table XIII.1. Summary of the results obtained in previous studies

Parameter evaluated	Value	Results			Reference
		NRR	PRR	BP	
H_2S	0 mg $S \cdot L^{-1}$	7.4	1.1	105	González-Camejo et al., 2017*
	20 mg $S \cdot L^{-1}$	6.0	1.3	79	
Microalgae-AOB competition	ATU = 0 mg $\cdot L^{-1}$	1.9	0.2	27	González-Camejo et al., 2018a*
	ATU = 5 mg $\cdot L^{-1}$	2.3	0.3	19	
NLR/PLR	9.7/1.3 g $\cdot d^{-1}$	12.5	1.5	72	González-Camejo et al., 2018a
	14.4/1.8 g $\cdot d^{-1}$	11.5	1.4	69	
	8.4/1.1 g $\cdot d^{-1}$	7.5	1.1	78	
BRT	4.5 d	10.3	1.1	74	González-Camejo et al., 2019a
	6 d	9.9	1.2	74	
	9 d	7.6	1.0	65	
HRT	3.5 d	11.1	1.4	65	González-Camejo et al., 2019a
	2 d	9.3	1.1	65	
	1 d	8.7	1.4	54	
Light path	25 cm	9.1	1.2	66	González-Camejo et al., 2019a; 2019c
	10 cm	21.1	2.0	174	
NO_2 inhibition	BRT = 2 d[1]	14.1	13.5[3]	136	González-Camejo et al., 2019c
	BRT = 2.5 d[2]	19.4	12.0[3]	152	
	BRT = 4.5 d[2]	14.5	24.3[3]	108	

*NRR: nitrogen recovery rate (mg $N \cdot L^{-1} \cdot d^{-1}$); PRR: phosphorus recovery rate (mg $P \cdot L^{-1} \cdot d^{-1}$); BP: biomass productivity (mg $VSS \cdot L^{-1} \cdot d^{-1}$); H_2S: sulphide; ATU: allylthiourea to inhibit nitrification; NLR: nitrogen loading rate; PLR: phosphorus loading rate; BRT: biomass retention time; HRT: hydraulic retention time. *Operation in a PBR system (without filtration): not considered for PCA and PLS; [1]Significant presence of nitrite in the culture; [2]Negligible NO_2 concentration in the culture; [3]Values of nitrification rate (mg $N \cdot L^{-1} \cdot d^{-1}$).*

PCA and PLS have been shown to be useful for understanding processes and optimising the performance of WWTPs based on activated sludge technology (Han *et al.*, 2018). Trials have also been carried out recently on optimising the microalgae cultivation conditions of multiple variables using statistical methods on lab-scale data (Nayak *et al.*, 2018). Viruela *et al.* (2018) also used these multivariate techniques to assess the relationship between microalgae performance (in terms of nutrient recovery and biomass productivity) with light, temperature and N:P ratio in the short-term (around 4-5 months) operation of an outdoor MPBR.

The availability of real long-term data under outdoor conditions is very limited, and is non-existent for periods longer than 12 months. The present study evaluates the three-year operation of an outdoor flat-panel MPBR plant, considering all the relevant variables, from which valuable information could be obtained on the behaviour of microalgae cultures in different ambient and operating conditions.

The competition between microalgae-nitrifying bacteria for ammonium uptake has been identified as a highly relevant factor in the performance of a mixed microalgae culture (Galès *et al.*, 2019; González-Camejo *et al.*, 2018a), so that determining the most important parameters in nitrifying bacteria activity would help to maintain bacteria growth at a minimum and favour that of microalgae.

The aim of this study was therefore to use multivariate projection techniques to analyse the data collected from operating an outdoor MPBR plant treating AnMBR effluent for three years in order to identify the key variables in the process and any relationships between the parameters.

2. MATERIAL AND METHODS

2.1. Microalgae and wastewater

The nutrient-rich influent to the MPBR plant was from an AnMBR plant that treated real sewage (details of this plant and its operation can be found in Seco *et al.* (2018)). The average characteristics of the substrate were a chemical oxygen demand (COD) concentration of 67 ± 7 mgCOD·L^{-1}, a nitrogen concentration of 52.4 ± 8.8 mg N·L^{-1} (mainly in the form of ammonium (NH_4 > 95%), with low amounts of nitrite (NO_2) and nitrate (NO_3)), and a phosphorus concentration of 5.7 ± 1.5 mg P·L^{-1} as phosphate (PO_4). The considerable variability of the influent characteristics was due to changes in both sewage composition and AnMBR plant performance.

Microalgae were originally obtained from the walls of the secondary settler at the Carraixet WWTP and mainly consisted of a mixed culture of the eukaryotic microalgae genera *Chlorella* and *Scenedesmus*, although low concentrations of cyanobacteria, nitrifying and heterotrophic bacteria were also present.

2.2. MPBR plant

The MPBR pilot plant was in the Carraixet WWTP (39º30'04.0''N 0º20'00.1''W, Valencia, Spain) and operated continuously outdoors from June 2015 to May 2018. During the experimental period the hydraulic retention time (HRT) was varied in the range of 1-3.5 days, while biomass retention time (BRT) was between 2-9 days. However, there were several periods in which operations were stopped for maintenance and there were also periods in batch mode, which were not considered for the evaluation of the MPBR operations.

The MPBR plant consisted of two flat-panel PBRs which discharged the culture to a 14-L membrane tank (MT) to separate the microalgae biomass from the permeate. Full description of the MPBR plant operation can be found in González-Camejo *et al.* (2019a).

Two different MPBR plants were operated: i) one with a 25-cm light path PBRs (550 L each) during the first half of the operation; i.e., from June 2015 until December 2016; and ii) another with a 10-cm light path PBRs (230 L each): from January 2017 until the end of the operating period.

Both PBRs were continuously air-stirred to ensure appropriate mixing to homogenise the culture in terms of nutrient concentration, temperature and light availability. It also reduced wall fouling and avoided microalgae settling. An on-off valve was opened for 5 s to introduce pure pressurised CO_2 (99.9%) into the air system whenever the pH measurements rose over 7.5 to maintain optimum pH (Qiu *et al.*, 2017) and ensure carbon-replete conditions.

Twelve LED lamps (Unique Led IP65 WS-TP4S-40W-ME) were installed on the rear wall of the PBRs to apply a continuous irradiance of 300 $\mu mol \cdot m^{-2} \cdot s^{-1}$. The culture was cooled by a thermostatically controlled system (Daikin Inverter R410A). The temperature set-point was 25 ºC to keep temperatures below 30 ºC.

The MT had a filtering area of 3.4 m^2 and included an industrial hollow-fibre ultrafiltration membrane unit (PURON® Koch Membrane Systems model PUR-PSH31, 0.03 μm pore size). Its total volume accounted for 14 L, which meant a 1.25% non-

photic volume for the 25-cm MPBR plant and 2.9% non-photic volume the 10-cm MPBR plant. The MT was stirred by the same airflow as the PBRs.

The filtration process was operated continuously, but only the corresponding amount of permeate was extracted to control HRT, recycling to the system the rest of permeate that was not taken out of the MPBR plant, as explained in González-Camejo *et al.* (2019a).

2.3. Sampling and Analytical Methods

During the continuous operations, grab samples were collected in duplicate three times a week from the MBPR influent (AnMBR effluent after aeration) and effluent (permeate from the filtration unit) as well as from the PBR culture; i.e. treated water plus suspended solids. Ammonium, nitrite, nitrate and phosphate, volatile suspended solids (VSS), total chemical oxygen demand (COD), soluble chemical oxygen demand (sCOD), total nitrogen (tN) and total phosphorus (tP) were analysed according to Standard Methods (APHA, 2005). Nutrient concentrations were measured by an automatic analyser (Smartchem 200, Westco Scientific Instruments, Westco). COD, sCOD, tN and tP were measured in duplicate once a week.

Optical density at 680 nm (OD680) and maximum quantum yield of photosystem II (F_v/F_m) were measured in-situ by a portable fluorometer AquaPen-C AP-C 100 (Photon Systems Instruments). To measure F_v/F_m, the samples were kept in the dark for ten minutes to become dark-adapted.

Total eukaryotic cells (TEC) were counted twice a week by epifluorescence microscopy on a Leica DM2500 with a 100x-oil immersion lens. A minimum of 300 cells were counted in duplicate plus at least 100 cells of the most abundant genera with an error of less than 20%.

2.4. Calculations

Biomass productivity (mg $VSS \cdot L^{-1} \cdot d^{-1}$), nitrogen recovery rate (NRR) (mg $N \cdot L^{-1} \cdot d^{-1}$), phosphorus recovery rate (PRR) (mg $P \cdot L^{-1} \cdot d^{-1}$) were calculated following the equations shown in González-Camejo *et al.* (2018a).

I_{av} was calculated by applying the Lambert-Beer Law (Eq. XIII.1) as reported by Romero-Villegas *et al.* (2018):

$$I_{av} = \frac{tPAR}{K_a \cdot C_b \cdot Lp} \cdot (1 - e^{-K_a \cdot C_b \cdot Lp}) \qquad \text{[Eq. XIII.1]}$$

Where tPAR is the sum of the solar and artificial photosynthetic active radiation applied to the PBRs (μmol·m^{-2}·s^{-1}), K_a is an extinction coefficient (m^2·g^{-1}, Eq. XIII.2), C_b is the biomass concentration (g·m^{-3}), and Lp is the light path (m).

$$K_a = \frac{OD_{400-700}}{C_b \cdot Lp_c} \quad \text{[Eq. XIII.2]}$$

where $OD_{400\text{-}700}$ (-) is the average optical density of the culture in the range of 400-700 nm; and Lp_c (m) is the light path of the spectrophotometer´s cuvette.

The nitrification rate (NOxR) (mg N·L^{-1}·d^{-1}) was obtained by Eq. XIII.3:

$$\text{NOxR} = \frac{F \cdot (NOx_e - NOx_i)}{V_{MPBR}} \quad \text{[Eq. XIII.3]}$$

where F is the treatment flow rate (m^3·d^{-1}); NOx_e the concentration of nitrite plus nitrate from the effluent (mg N·L^{-1}); N_i is the concentration of nitrite plus nitrate from the influent (mg N·L^{-1}); and V_{MPBR} is the volume of culture in the MPBR plant (m^3).

It should be remembered that negative NOxR values indicate that the microalgae NO_x uptake is higher than the NOx produced by the nitrifiers.

2.5. Statistical analysis

2.5.1. Principal component analysis

PCA was conducted to assess the relationship between different ambient, operating and design and cultivation conditions on the performance of the outdoor MPBR plant. This multivariate technique enables to visualise the correlation structure between the variables as well as identify patterns in the data such as trends and anomalous data. Principal components (PC) are obtained by linear combination of the original variables, capturing the underlying phenomenon in the studied system.

The matrix analysed consisted of 40 variables measured in 560 samples (observations). The variables considered included ambient, process control, operating and performance parameters as well as indicators of the treatment process. The ambient parameters solar PAR and culture temperature (T) were monitored since they have been widely reported as the main factors in microalgae growth (García *et al.*, 2018; Viruela *et al.*, 2018). These parameters represent the daily average obtained from all the monitored values (one measurement every 10 seconds). The maximum (PAR_{max}, T_{max}) and minimum (T_{min}) daily values of these parameters were also considered as their fluctuations can significantly influence microalgae performance (Ippoliti *et al.*, 2016). Light path (Lp), HRT, BRT and air flow rate (F_{air}) were the only parameters which could be modified by the operator and were thus labelled as controlled variables. Dissolved oxygen (DO)

concentration has also been reported as a key factor in microalgae performance (Ippoliti *et al*., 2016), as have the nutrient loading rates (González-Camejo *et al*., 2018a), i.e. nitrogen (NLR) and phosphorus loading rates (PLR). NRR, PRR, and BP were included since they have been widely used to assess the performance of microalgae cultivation systems (Marazzi *et al.*, 2019). Other parameters such as average light irradiance (I_{av}), maximum quantum efficiency (F_v/F_m) and optical density at 680 nm (OD680) can provide information on the use of light in the culture, which is related to the efficiency of the system (Romero-Villegas *et al.*, 2018). As the main goal of the MPBR plant is to treat AnMBR effluent, the effluent nutrient concentrations are obviously relevant parameters (García *et al.*, 2018) and can serve as indicators of the treatment process. Eukaryotic cell (TEC) concentration, as well as the concentration of genera *Scenedesmus* (Sc) and *Chlorella* (Chl), were also included to evaluate the possible shift in the microalgae population caused by external factors. COD was included to assess the effect of microalgae stress on MPBR performance (Lau *et al.*, 2019; Lee *et al.*, 2018). Optical density ratio between 680 and 750 nm (OD680:OD750) has been reported to be related to the microalgae chlorophyll content (Markou *et al.*, 2017) and was therefore analysed. pH was also included as it is an important parameter in all biological processes; the microalgae activity modifies pH and in turn is affected by it (Qiu *et al.*, 2017). Lastly, since the competition between microalgae and ammonium oxidising bacteria (AOB) can be significant when treating AnMBR effluents (González-Camejo et al., 2018a), nitrification rate (NOxR) was also considered as indicator of the nitrification process in the system.

It should be noted that all these variables were related to the MPBR biological process and that parameters related to membrane filtration were not considered.

2.5.2. Partial Least Squares analysis

PLS is a multivariate projection technique that uses two different groups of data; i.e. predictors (X) and responses (Y). Its goal is to find latent variables that are not only able to explain the variance in X, but also the variance which best predicts the Y variables.

To identify the variables with the strongest possible relationship with process performance, PLS analysis was used with NRR, PRR and BP as responses (Y), while all the other variables were predictors (X). Since the competition between microalgae and nitrifying bacteria can seriously affect MPBR performance (González-Camejo *et al.*,

2018a), a further PLS analysis was carried out with the nitrification rate (NOxR) as the response.

Both PCA and PLS were conducted on SIMCA-P 10.0 software (Umetrics, Umea, Sweden).

3. RESULTS AND DISCUSSION

Figure XIII.1 shows the evolution of the main performance parameters (NRR, PRR and BP) during the 3-year period of MPBR operations. As can be seen in this figure, all three variables varied widely. It is striking that during the first part of the period (from June 2015 until December 2016, which corresponds to the 25-cm MPBR plant), the MPBR performance was significantly lower than in the rest of the operation which was carried out in the 10-cm MPBR plant. It also has to be noted that the legal discharge limits (i.e., 15 mg $N \cdot L^{-1}$ and 2 mg $P \cdot L^{-1}$ according to European Directive 91/271/CEE for a 10,000-100,000-p.e WWTP) were only reached between May-December 2017 (data not shown). It therefore seems essential to determine the conditions that make it possible to meet these limits for the proper treatmeant of AnMBR effluents.

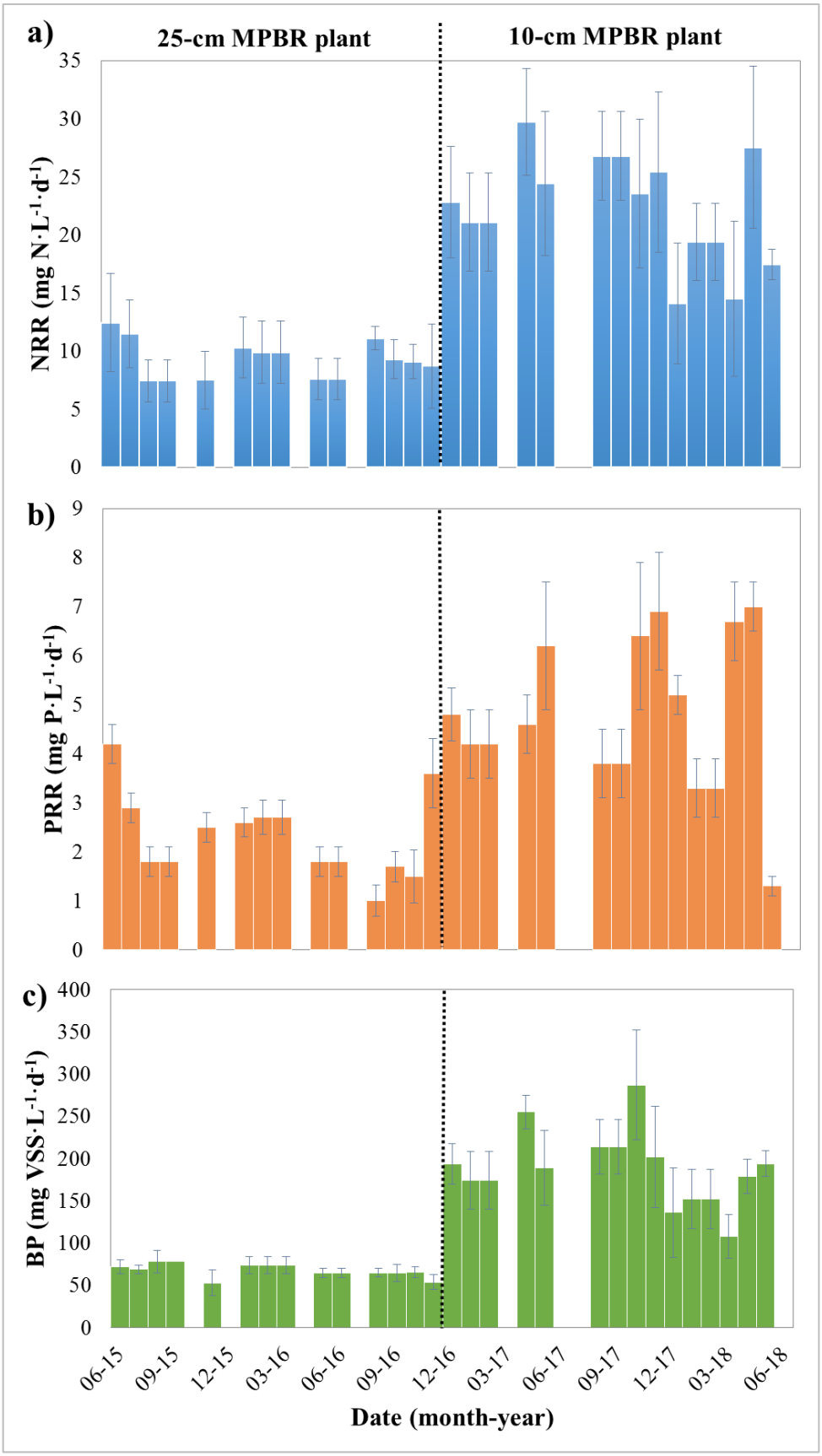

Figure XIII.1. Performance of the MPBR plant along the 3-year operating period.

Microalgae cultivation is a high complex process which concerns mass, heat and light transfer as well as biological reactions (Xu *et al*., 2019). It therefore seems to be worth analysing thoroughly all the recorded variables simultaneously to identify any possible relationships with process performance and to gain valuable in-depth knowledge on the process.

3.1. Principal component analysis

Raw data was mean-centred and scaled to unit variance to give equal importance to each of the variables in the multivariate projection models. A PCA model was fitted to the pre-processed data. Four statistically significant principal components were found, according to the cross-validation of the model, explaining 63.9% of the total variance (34.6%, 13.8%, 8.0% and 7.5% for PC1, PC2, PC3 and PC4, respectively). This explained variance value is high enough to consider that the PCA model gave a fairly accurate description of the real data from the MPBR plant.

Figure XIII.2 shows the main results of the PCA model (score and loading plots).

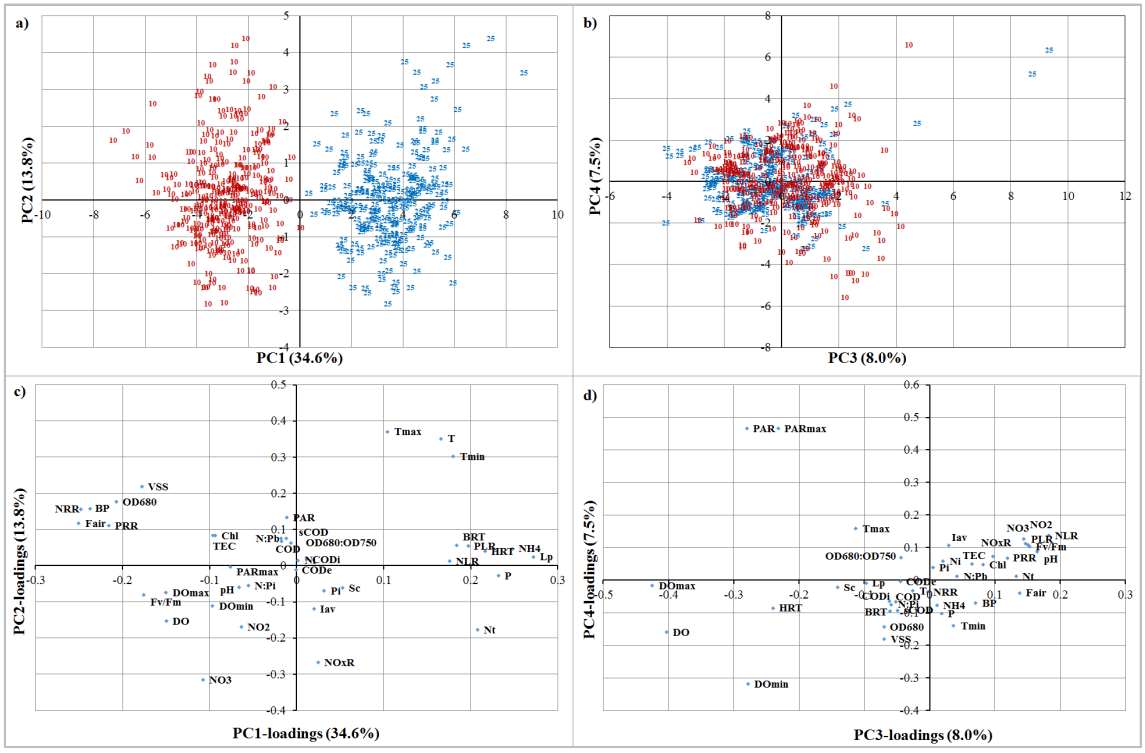

Figure XIII.2. PCA-score plots showing the distribution of observations: a) PC1 vs PC2; b) PC3 vs PC4; PCA-loading plot showing the correlation pattern between variables: c) PC1 vs PC2; d) PC3 vs PC4.

In Figure XIII.2a (score plot of the two first components) a markedly different behaviour can be observed in the samples collected from the 10-cm wide MPBR plant (full points), which are on the left of the graph; and the samples from the 25-cm MPBR plant (emptied points) on the right. This shows that the light path strongly influenced PC1, which explains most of the data variability (34.6%). In fact, light path is the parameter with the highest weight in PC1 (0.272) (Figure XIII.2c). It should be noted that the process performance is affected by PBR width, since light availability is reduced at a higher light path (Cho *et al.*, 2019). This means that other variables such as effluent nutrient concentrations, biomass productivity or nutrient recovery rates, which are related to light availability (González-Camejo *et al.,* 2019b), were also different in these two groups of samples and that they made a large contribution to the first component (see Figure XIII.2c). Note that the distance of a given variable from the plot origin shows the impact of each variable on the model (the longer the distance the stronger the impact). This result agrees with the findings of previous studies. The MPBR with the shorter light path obtained a significantly better performance than those obtained by the wider PBRs (Table XIII.1).

Figure XIII.2c shows the correlation patterns of all the variables. The positively correlated variables are grouped together in the same quadrant, while those inversely correlated can be seen on opposite sides of the plot origin (i.e. in the diagonally opposed quadrants). Light path, ammonium and phosphorus effluent concentrations, nitrogen and phosphorus loading rates and operating parameters such as HRT and BRT were positively correlated to each other and are close to each other in the plot. The relationship between effluent nutrient concentrations and nutrient loading rates in non-nutrient-limited systems was not surprising, since previous studies have reported it (González-Camejo *et al.*, 2018a).

F_{air}, NRR, PRR, BP and OD680 were also found to be important for the PCA model. These are grouped close to each other on the left of Figure XIII.2c and show a positive relationship. This is the reason why microalgae performance is usually measured in terms of nutrient recovery rates and biomass productivity (González-Camejo *et al.*, 2019a; Marazzi *et al.*, 2019). Ling *et al.* (2019) have shown that OD680 is an indirect measurement of microalgae biomass concentration. The PCA model could therefore be expected to show a highly positive correlation between both these variables (OD680 and VSS) throughout the 3 years of operational data (Figure XIII.2c). This group of variables is inversely related to the group including: NH_4, P, HRT, BRT, NLR and PLR.

This is in agreement with González-Camejo *et al.* (2018a; 2019a), who reported that long BRTs and HRTs tend to produce worse microalgae performance; i.e. NRR, PRR and BP until they reach the optimum value. The decline in culture performance entailed higher effluent nutrient concentrations.

On the other hand solar PAR and oxygen concentration were relevant in PC3 and PC4 (15.5% of total variance) but not in the first two components: PC1 and PC2 (48.4% of total variance, see Figure XIII.2).

3.2. PLS analysis

A PLS analysis was carried out to predict the parameters related to MPBR performance (i.e., NRR, PRR and BP), which were used as responses, while all the remaining variables were predictors. Four components were statistically significant, according to cross-validation. The model was well balanced between fit and prediction performance, explaining 55.5% (R^2_x) of the X-matrix (matrix of predictors) variance and an accumulated explained variance of the response matrix (Y) of 75.6% (R^2_y) and a goodness of prediction (Q^2) of 71.6%.

Figure XIII.3 displays the recorded values of NRR, PRR and BP versus the PLS predicted values, evidencing the good fit obtained for the three MPBR performance variables. The prediction was especially good for biomass productivity (R^2= 0.920), as could be expected due to the high positive correlation in the PLS model between OD680 and VSS (Figure XIII.4a).

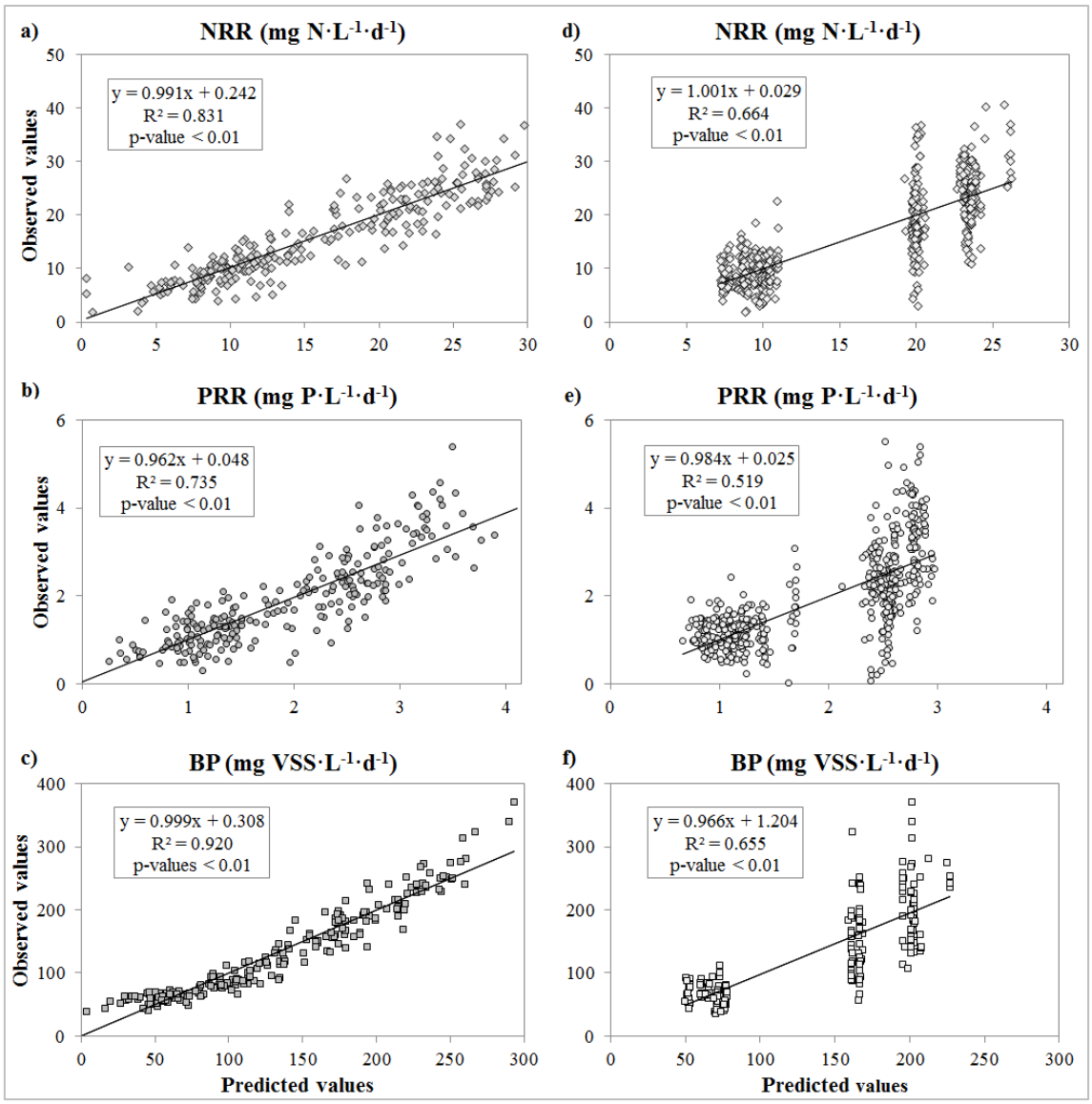

Figure XIII.3.Observed values vs predicted values by the PLS model using all the variables as predictors: a) Nitrogen recovery rate (NRR); b) Phosphorus recovery rate (PRR) and, c) Biomass productivity (BP); observed vs predicted values by the PLS model that uses only the controlled variables as predictors: d) Nitrogen recovery rate (NRR); e) Phosphorus recovery rate (PRR) and, f) Biomass productivity (BP).

To identify the most important variables in predicting MPBR microalgae performance, the variable importance of the PLS projection (VIP) is given in Figure XIII.4b. The VIP parameter is a weighted summary of all the X-variable loadings of all the responses. As can be seen in Figure XIII.4b, the two most important variables were air flow rate (F_{air}) and light path (Lp), which clearly proves that correct PBR design plays a key role in the process.

Air flow rate has been reported as a key parameter in culture mixing and liquid-gas mass transfer (Kubelka *et al.*, 2018). Mixing rate may also be related to the light integration of the reactor (Xu *et al.,* 2019). In fact, higher mixing rates make microalgae move rapidly from the lit parts of the reactor to darker zones, which improves biomass productivity (Barceló-Villalobos *et al.*, 2019). Light path is a key parameter in the light available to the reactor (González-Camejo *et al.*, 2019b), since the radiated light decreases with depth due to the light absorbed by the water and biomass (Cho *et al.*, 2019).

Other important variables in MPBR performance were OD680, VSS, P, HRT, TEC, Chl, NH_4, N_t, NOxR and BRT (Figure XIII.4b). In the loading plot (Figure XIII.4b) all these variables were in fact projected away from the plot origin, showing their important contribution to the PLS model. As can be seen in Figure XIII.4a, the BRT and HRT operational parameters show an inverse correlation pattern with MPBR performance (i.e. NRR, PRR and BP) since they were projected opposite to the plot origin. This agrees with the findings of González-Camejo *et al.* (2019a) who found reduced biomass productivity and nitrogen recovery rates as BRT increased. González-Camejo et *al.* (2019a) did not find any significant differences in nutrient recovery rates and biomass productivities with variable HRT under nutrient-replete conditions. However, high HRT values may have a significant influence on microalgae performance in nutrient-limited systems (González-Camejo *et al.*, 2018a). It is therefore reasonable to expect that P, NH_4 and N_t (which related to effluent nutrient concentrations) have a relatively high inverse correlation with microalgae performance (Figure XIII.4a).

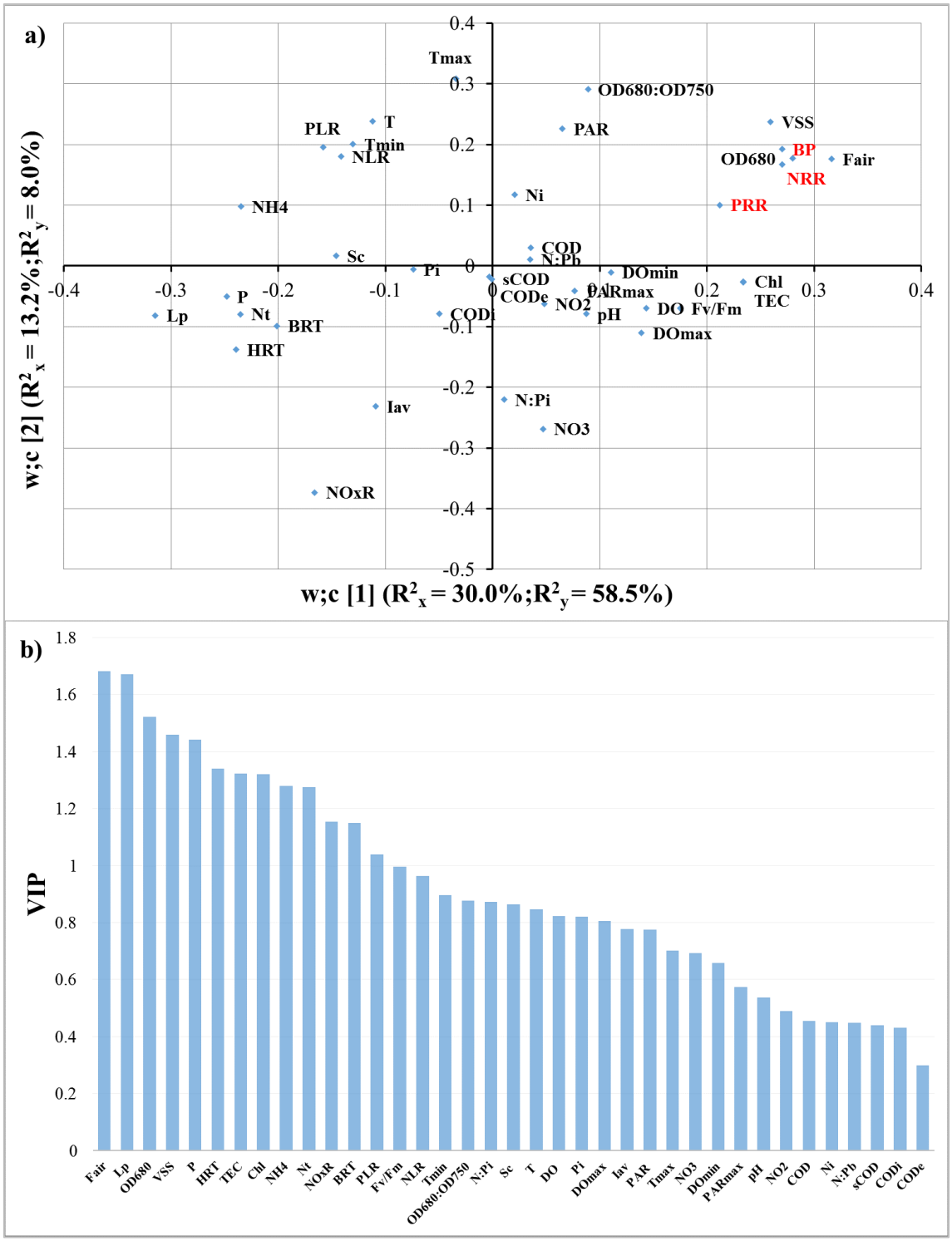

Figure XIII.4. Results of the fitted PLS model: a) Weight plot of the first two components; b) Variable Importance in the projection (VIP) of the explicative variables.

As expected, OD680 and VSS were highly correlated with biomass productivity (González-Camejo *et al.*, 2019a; Nwoba *et al.*, 2019). In addition, the culture was dominated by eukaryotic bacteria. TEC was thus also closely related to system

performance, as was Chl concentration, since the 10-cm MPBR plant (which accounted for 54% of the total PLS data was dominated by Chlorella (> 99% of TEC).

Another important factor was the nitrification rate, which confirms that microalgae-AOB competition for ammonium uptake significantly reduces MPBR performance. For this reason, another PLS analysis was carried out to consider NOxR as a response (see section 3.4).

Many other variables appeared to be correlated with MPBR performance, which agrees with Cho *et al.* (2019) and corroborates the difficulty of controlling outdoor microalgae cultivation. However, the PLS results highlight the fact that MPBR performance is more dependent on the operating and design parameters (such as light path, air flow rate, BRT and HRT) than on ambient conditions like solar PAR and temperature (Figure XIII.4b).

Light and temperature have been widely reported as key parameters in nutrient assimilation and microalgae growth (Galès et al., 2019; Marazzi *et al.*, 2019) The limited influence of environmental factors in the PLS model of MPBR performance may be due to the fact that PAR and temperature represent the daily average value of these parameters. Solar radiation variation was around 50-500 $\mu mol \cdot m^{-2} \cdot s^{-1}$, while instant solar radiation varied in the range of 0-2000 $\mu mol \cdot m^{-2} \cdot s^{-1}$ (Galès *et al.*, 2019).

In addition, the MPBR plant was additionally lit from an artificial light source (Section 2.2) which provided better control of the light photons and reduced the shadow effect of the culture (González-Camejo *et al.*, 2019b). Temperature can vary by more than 10 ºC throughout the day, although temperatures over 30ºC were avoided by cooling the culture (Section 2.2). All these factors reduced culture light and temperature variations and may have contributed to the small influence of ambient parameters on the PLS model.

COD_e, COD_i, COD, N_i, sCOD and NO_2 showed low correlations with microalgae performance (Figure XIII.4b). Since COD_i came from an AnMBR plant which degraded most of the organic matter content (Seco *et al.*, 2018) and COD_e was the permeate of an ultrafiltration system which removed most of the suspended organic matter, their variability was relatively low, so that COD_e and COD_i concentrations were not expected to have a significant influence on the model.

However, the culture's COD concentration was expected to have a stronger influence on the projection model, since it is directly related to microalgae biomass (Ambat *et al.* (2018)), as was sCOD concentration, since it can be used as an indirect measure of

extracellular organic matter (EOM) content. However, the results of the fitted PLS model gave little weight to these variables (Figure XIII.4b), possibly due to the production of these organic compounds being increased either to microalgae activity (Lau *et al*., 2019), or when algae are under stress (Lee *et al.*, 2018). In addition, the proliferation of competing organisms such as heterotrophs (which hinder microalgae activity) reduces the sCOD in the culture (Galès *et al.*, 2019). The variance in this parameter could thus be influenced by both high and low microalgae and heterotrophic bacteria activity and their correlation pattern could have changed throughout the three-year operating period, reducing their importance in the overall model.

Unexpectedly, NO_2 showed a relatively small influence on the PLS model, since nitrite has been found to inhibit microalgae growth (González-Camejo *et al.*, 2019c). However, nitrite concentration was negligible most of the time during MPBR operations, which means little variation in this parameter and so insignificant microalgae growth inhibition. This was probably the reason why this variable had little influence on the model.

3.3. Controlled variables

Of all the variables assessed in the PCA (Section 3.1) only Lp, F_{air}, HRT and BRT could be modified or controlled by the process operators, since they were either design or operating parameters. The remainder were either values obtained from measurements or microalgae performance parameters and thus could not be modified. Another PLS analysis was therefore performed considering only the controlled variables as predictors (X-matrix).

Figures XIII.3d, XIII.3e and XIII.3f show the values obtained versus the predicted values by the new PLS model. In comparison to Figures XIII.3a, XIII.3b and XIII.3c, it is evident that despite the new PLS model's moderately accurate prediction capacity for NRR, PRR and BP, its capacity was noticeably worse than the PLS with the full X-matrix as predictors. This highlights the variability of the data obtained outdoors, as reported by Marazzi *et al.* (2019) and Xu *et al.* (2019) and confirms the influence of the other variables (different than the controlled ones) on MPBR performance. It can thus be concluded that the microalgae cultivation process can only be partially controlled by the design and operating variables, although there are other parameters related to ambient conditions (such as light and temperature), biotic (competition with other microorganisms) and abiotic factors (e.g. nutrient loads and pH) that also play a

significant role in microalgae cultivation (Ambat *et al.* 2018; Barceló-Villalobos *et al.*, 2019; Galès *et al.*, 2019; Qiu *et al.*, 2017).

3.4. Nitrification

In the cultivation system studied the competition between microalgae and nitrifying bacteria can play a key role in the MPBR plant performance, as has been shown in González-Camejo *et al.* (2019d). If nitrifying bacteria activity is low, microalgae will be favoured (Marcilhac *et al*., 2014). Conditions that minimise nitrifying bacteria will thus be pursued. For this reason, a specific PLS analysis was carried out to determine the main variables related to nitrifying bacteria activity to obtain information on the prevalent conditions that affect growth.

The PLS was performed using the same predictors as those described in Section 3.2., but with the nitrification rate (NOxR) as the response. Four latent variables were statistically significant in the fitted PLS model, according to cross-validation. The model explained 56.2% of X-matrix variance (R^2_x) and 85.3% of the response variable (R^2_y), with a goodness of prediction parameter (Q^2) that reached 78%. The PLS model performance was especially good, as can be seen in the measured versus predicted PLS nitrification rate (see Figure XIII.5a).

Figure XIII.5b shows the VIP of all the explicative variables (X-matrix). As can be seen, the effluent nitrate concentration was the most important variable in predicting NOxR. AOB compete with microalgae for ammonium uptake, transforming it into nitrite, while nitrite oxidising bacteria (NOB) carry out the second step of nitrification, oxidising nitrite to nitrate. If NOB activity is similar or higher than that of AOB, nitrite therefore does not accumulate and the concentration of NO_3 appears as a good indicator of nitrifying bacteria activity (Galès *et al.*, 2019). It should be noted that despite microalgae being able to absorb nitrate to grow, the consumption rate is significantly lower than that of ammonium (González-Camejo *et al.*, 2019d). High NOxR is thus not desirable to reach maximum microalgae performance.

NRR was another factor which explained the high variability of the nitrification rate. In the loading plot of the first two latent variables of the fitted PLS model (Figure XIII.5c), the projection of both variables lay in opposite quadrants, indicating an inverse correlation pattern between them. This result is in agreement with González-Camejo *et al.* (2018a; 2019d), who found that NRR fell at high nitrification rates and highlights the

importance of reducing nitrifying bacteria activity to the minimum to achieve maximum nitrogen recovery by microalgae.

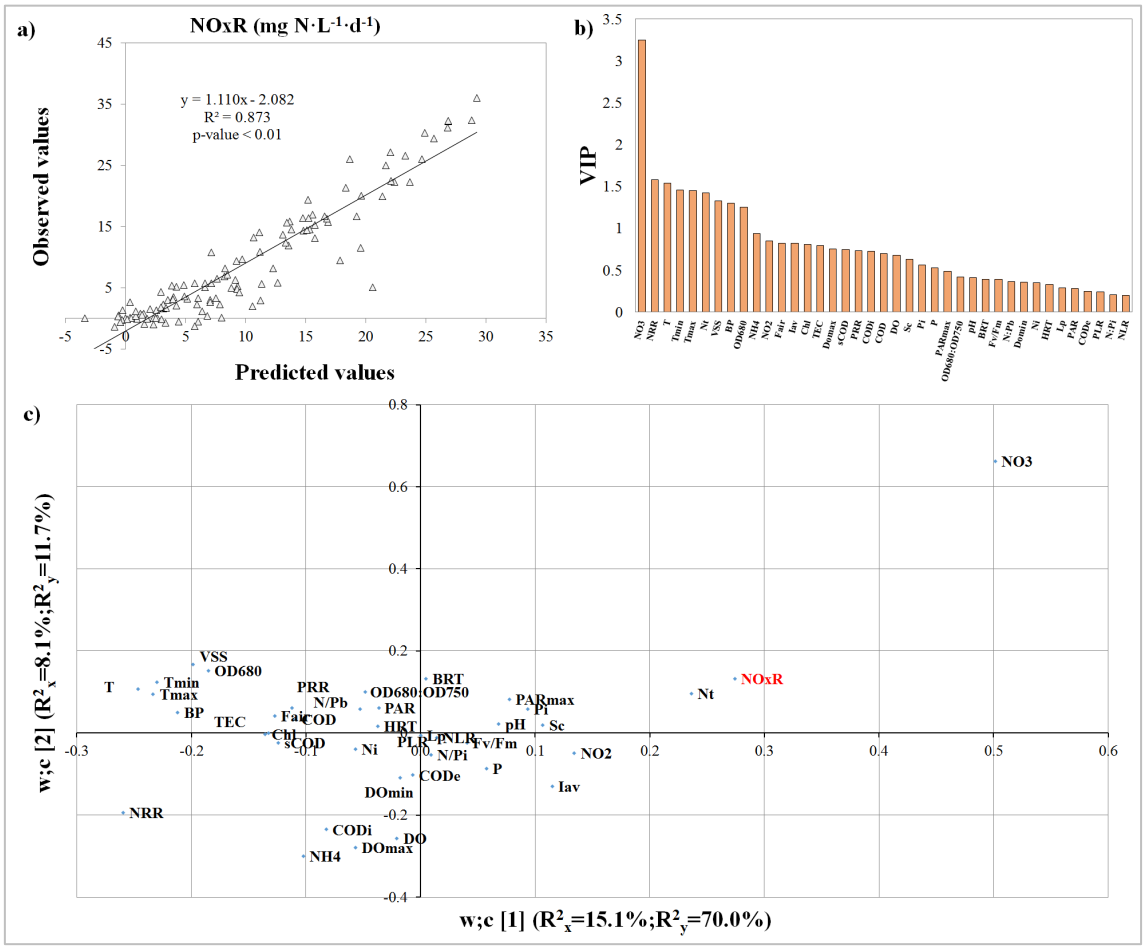

Figure XIII.5. PLS model to predict the nitrification rate (NOxR): a) Observed vs predicted values; b) Variable Importance in the projection (VIP) of the explicative variables*; and c) Weight plot of the first two components.*

The recorded parameters related to temperature (i.e., T, T_{min} and T_{max}) also showed a high correlation with NOxR (Figure XIII.5b), which is due to the influence of temperature on the nitrifying bacteria. Indeed, it was the main ambient condition related to nitrifying bacteria activity. AOB growth is highly influenced by temperature. In fact, González-Camejo *et al.* (2019d) showed that AOB can dominate the competition at high temperatures, surpassing the microalgae. This means that keeping nitrifying bacteria at moderate temperatures seems to be the main control parameter to minimise nitrifying bacteria activity.

On the other hand, the influence of BRT was surprisingly lower than the other variables (Figure XIII.5b). In this respect, Munz *et al.* (2011) observed partial nitrification (i.e., NO_2 accumulation) when BRT was under 2 days in an activated sludge reactor, while full nitrification (i.e., NO_3 production) was achieved at BRTs between 3-5 days. The study of the MPBR plant corresponding to nitrite inhibition (Table XIII.1) showed the highest NRR and the lowest NOxR at a BRT of 2.5 days, while 2 and 4.5 days reduced MPBR performance (González-Camejo *et al.*, 2019c). It therefore seems that there was no linear correlation between BRT and NOxR.

4 CONCLUSIONS

Data obtained during the 3-year operation of an MPBR plant was analysed by statistical projection methods. Of the 40 variables evaluated, PCA indicated that the photobioreactor light path is the factor with the highest influence on data variability. Other relevant factors were F_{air}, NRR, PRR, BP, OD680, NH_4, P, HRT, BRT, NLR and PLR.

The parameters that mainly affected microalgae performance were Lp, F_{air}, OD680, VSS, P, HRT, TEC, Chl, NH_4, N_t, NOxR, BRT and PE. Ambient factors (solar irradiance and temperature) showed a lower influence on MPBR performance.

The MPBR performance estimated by the PLS model worsened appreciably when only the controlled variables (Lp, F_{air}, HRT and BRT) were used as predictors, which highlights the importance of the non-controlled variables in MPBR performance, and shows that the microalgae cultivation process can only be partially controlled by the design and operating variables.

NO3 was the most relevant factor in the nitrification rate, which confirms that it can be used as an indirect measurement of nitrifying bacteria activity. Temperature appeared as the leading parameter in controlling nitrification, while BRT had a relatively small influence on AOB activity.

ACKNOWLEDGMENTS

This research work was supported by the Spanish Ministry of Economy and Competitiveness (MINECO, Projects CTM2014-54980-C2-1-R and CTM2014-54980-C2-2-R) jointly with the European Regional Development Fund (ERDF), both of which are gratefully acknowledged. It was also supported by the Spanish Ministry of

Education, Culture and Sport via a pre-doctoral FPU fellowship to author J. González-Camejo (FPU14/05082).

REFERENCES

1. Ambat, I., Tang, W.T., Sillanpaa, M., 2018. Statistical analysis of sustainable production of algal biomass from wastewater treatment process. Biomass and Bioenergy 120, 471–478. https://doi.org/10.1016/j.biombioe.2018.10.016
2. APHA-AWWA-WPCF, 2005. Standard methods for the examination of water and wastewater, 21nd edition. American Public Health Association, American Water Works Association, Water Pollution Control Federation. Washington DC, USA.
3. Barceló-Villalobos, M., Fernández-del Olmo, P., Guzmán, J.L., Fernández-Sevilla, J.M., Acién Fernández, F.G., 2019. Evaluation of photosynthetic light integration by microalgae in a pilot-scale raceway reactor, Bioresour. Technol. 280, 404-411. https://doi.org/10.1016/j.biortech.2019.02.032
4. Cho, K., Cho, D.H., Heo, J., Kim, U., Lee, Y.J., Choi, D.Y., Kim, H.S., 2019. Nitrogen modulation under chemostat cultivation mode induces biomass and lipid production by *Chlorella vulgaris* and reduces antenna pigment accumulation. Bioresour. Technol. 281, 118-125. https://doi.org/10.1016/j.biortech.2019.02.063
5. Galès, A., Bonnafous, A., Carré, C., Jauzein, V. Lanouguère, E., Le Floc'ha, E., Pinoit, J., Poullain, C., Roques, C., Sialve, B., Simier, M., Steyer, J.P., Fouilland, E., 2019. Importance of ecological interactions during wastewater treatment using High Rate Algal Ponds under different temperate climates, Algal Res. 40, 101508. https://doi.org/10.1016/j.algal.2019.101508
6. García, J., Ortiz, A., Álvarez, E., Belohlav, V., García-Galán, M.J., Díez-Montero, R., Álvarez, J.A., Uggetti, E., 2018. Nutrient removal from agricultural run-off in demonstrative full scale tubular photobioreactors for microalgae growth. Ecological Eng. 120, 513–521. https://doi.org/10.1016/j.ecoleng.2018.07.002
7. González-Camejo, J., Jiménez-Benítez, A., Ruano, M.V., Robles, A., Barat, R., Ferrer, J., 2019a. Optimising an outdoor membrane photobioreactor for tertiary sewage treatment. J. Environ. Manag. 245, 76-85. https://doi.org/10.1016/j.jenvman.2019.05.010
8. González-Camejo, J., Viruela, A., Ruano, M.V., Barat, R., Seco, A., Ferrer, J., 2019b. Effect of light intensity, light duration and photoperiods in the performance of an outdoor photobioreactor for urban wastewater treatment. Algal Res. 40, 101511. https://doi.org/10.1016/j.algal.2019.101511

9. González-Camejo, J., Montero, P., Aparicio, S., Ruano, M.V., Borrás, L., Barat, R., Ferrer, J., Seco, A., 2019c. Assessment of the nitrite inhibition of microalgae at bench and pilot scale. IWA Conference on Algal Technologies and Stabilization Ponds for Wastewater Treatment and Resource Recovery. IWAlgae2019. 1-2 July 2019. Valladolid, Spain.
10. González-Camejo, J., Aparicio, A., Ruano, M.V., Borrás, L., Barat, R., Ferrer, J., 2019d. Effect of ambient temperature variations on an indigenous microalgae-nitrifying bacteria culture dominated by Chlorella. Bioresour. Technol. 290, 121788. https://doi.org/10.1016/j.biortech.2019.121788
11. González-Camejo, J., Barat, R., Ruano, M.V., Seco, A., Ferrer, J., 2018a. Outdoor flat-panel membrane photobioreactor to treat the effluent of an anaerobic membrane bioreactor. Influence of operating, design and environmental conditions. Water Sci. Technol. 78(1), 195-206. http://dx.doi.org/10.2166/wst.2018.259
12. Han, H., Zhu, S., Qiao, J., Guo, M., 2018. Data-driven intelligent monitoring system for key variables in wastewater treatment process. Chinese journal of chemical engineering, 26(10), 2093-2101. https://doi.org/10.1016/j.cjche.2018.03.027
13. Ippoliti, D., Gómez, C., Morales-Amaral, M.M., Pistocchi, R., Fernández-Sevilla, J.M., Acién, F.G., 2016. Modeling of photosynthesis and respiration rate for *Isochrysis galbana* (T-Iso) and its influence on the production of this strain. Bioresour. Technol. 203, 71–79. http://dx.doi.org/10.1016/j.biortech.2015.12.050
14. Kubelka, B.G., Roselet, F., Pinto, W.T., Abreu, P.C., The action of small bubbles in increasing light exposure and production of the marine microalga Nannochloropsis oceanica in massive culture systems, Algal Res. 35, 69-76. https://doi.org/10.1016/j.algal.2018.09.030
15. Lau, A.K.S., Bilad, M.R., Osman, N.B., Marbelia, L., Putra, Z.A., Nordin, N.A.H.M., Wirzal, M.D.H., Jaafar, J., Khan, A.L., 2019. Sequencing batch membrane photobioreactor for simultaneous cultivation of aquaculture feed and polishing of real secondary effluent. Journal of Water Process Engineering 29, 100779. https://doi.org/10.1016/j.jwpe.2019.100779
16. Lee, J.C., Baek, K., Kim, H.W., 2018. Semi-continuous operation and fouling characteristics of submerged membrane photobioreactor (SMPBR) for tertiary treatment of livestock wastewater. J. Clean. Prod. 180, 244-251. https://doi.org/10.1016/j.jclepro.2018.01.159
17. Ling, Y., Sun, L.P., Wang, S.Y., Lin, C.S.K., Sun, Z., Zhou, Z.G., 2019. Cultivation of oleaginous microalga *Scenedesmus obliquus* coupled with wastewater treatment for enhanced biomass and lipid production. Biochem. Eng. J. 148, 162–169. https://doi.org/10.1016/j.bej.2019.05.012

18. Marazzi, F., Bellucci, M., Rossi, S., Fornaroli, R., Ficara, E., Mezzanotte, V., 2019. Outdoor pilot trial integrating a sidestream microalgae process for the treatment of centrate under non optimal climate conditions. Algal Res. 39, 1014-30. https://doi.org/10.1016/j.algal.2019.101430
19. Marcilhac, C., Sialve B., Pourcher A.M., Ziebal C., Bernet N., Béline F., 2014. Digestate color and light intensity affect nutrient removal and competition phenomena in a microalgal-bacterial ecosystem, Water Res. 64, 278-287. http://dx.doi.org/10.1016/j.watres.2014.07.012
20. Markou, G., Dao, L.H.T., Muylaert, K., Beardall, J., 2017. Influence of different degrees of N limitation on photosystem II performance and heterogeneity of *Chlorella vulgaris*, Algal Res. 26, 84-92. http://dx.doi.org/10.1016/j.algal.2017.07.005
21. Munz, G., Lubello, C., Oleszkiewicz, J.A., 2011. Factors affecting the growth rates of ammonium and nitrite oxidizing bacteria. Chemosphere, 83(5), 720-725. https://doi.org/10.1016/j.chemosphere.2011.01.058
22. Nayak, M., Dhanarajan, G., Dineshkumar, R., Sen, R., 2018. Artificial intelligence driven process optimization for cleaner production of biomass with co-valorization of wastewater and flue gas in an algal biorefinery. J. Clean. Prod. 201, 1092-1100. https://doi.org/10.1016/j.jclepro.2018.08.048
23. Qiu, R., Gao, S., Lopez, P.A., Ogden, K.L., 2017. Effects of pH on cell growth, lipid production and CO_2 addition of microalgae *Chlorella sorokiniana*, Algal Res. 28, 192-199. http://dx.doi.org/10.1016/j.algal.2017.11.004
24. Robles, A., Ruano, M.V., Ribes, J., Ferrer, J., 2013. Factors that affect the permeability of commercial hollow-fibre membranes in a submerged anaerobic MBR (HF-SAnMBR) system. Water Res. 47, 1277-1288. http://dx.doi.org/10.1016/j.watres.2012.11.055
25. Romero-Villegas, G.I., Fiamengo, M., Acién-Fernández, F.G., Molina-Grima, E., 2018. Utilization of centrate for the outdoor production of marine microalgae at the pilot-scale in raceway photobioreactors, J. Environ. Manag. 228, 506–516. https://doi.org/10.1016/j.jenvman.2018.08.020
26. Seco, A., Aparicio, S., González-Camejo, J., Jiménez-Benítez, A., Mateo, O., Mora, J.F., Noriega-Hevia, G., Sanchis-Perucho, P., Serna-García, R., Zamorano-López, N., Giménez, J.B., Ruiz-Martinez, A., Aguado, D., Barat, R., Borrás, L., Bouzas, A., Martí, N., Pachés, M., Ribes, J., Robles, A., Ruano, M.V., Serralta, J. and Ferrer, J., 2018. Resource recovery from sulphate-rich sewage through an innovative anaerobic-based water resource recovery facility (WRRF). Water Sci. Technol. 78(9), 1925-1936. https://doi.org/10.2166/wst.2018.492

27. Song, X., Luo, W., Hai, F.I., Price, W.E., Guo, W., Ngo, H.H., Nghiem, L.D., 2018. Resource recovery from wastewater by anaerobic membrane bioreactors: Opportunities and challenges. Bioresour. Technol. 270, 669-677. https://doi.org/10.1016/j.biortech.2018.09.001
28. Viruela A., Robles A., Durán F., Ruano M.V., Barat R., Ferrer J., Seco A., 2018. Performance of an outdoor membrane photobioreactor for resource recovery from anaerobically treated sewage. J. Clean. Prod. 178, 665-674. https://doi.org/10.1016/j.jclepro.2017.12.223
29. Whitton, R., Le Mével, A., Pidou, M., Ometto, F., Villa, R., Jefferson, B., 2016. Influence of microalgal N and P composition on wastewater nutrient remediation. Water Res. 91, 371-378. https://doi.org/10.1016/j.watres.2015.12.054
30. Xu, X., Gu, X., Wang, Z., Shatner, W., Wang, Z., 2019. Progress, challenges and solutions of research on photosynthetic carbon sequestration efficiency of microalgae. Renew. Sust. Energy Rev. 110, 65–82. https://doi.org/10.1016/j.rser.2019.04.050

CHAPTER XIV:

GENERAL DISCUSSION

CHAPTER XIV:

GENERAL DISCUSSION

Microalgae cultivation appears to be a green solution to treat nutrient-rich effluents from anaerobic membrane bioreactors since microalgae are able to assimilate nutrients from sewage without an organic carbon source. However, large-scale microalgae-based plants are scarce nowadays because of the inefficiency of this technology. The goal of this work is to assess the feasibility of an outdoor flat-panel MBPR plant to treat AnMBR effluents.

Although AnMBR effluents have been previously evaluated to be a suitable option for microalgae cultivation since they contain all the macro and micronutrients needed for microalgae growth (Ruíz-Martínez et al., 2012), the presence of high sulphide concentrations in the AnMBR effluent can limit microalgae. For this reason, the first step of this work was to evaluate the microalgae inhibition caused by the sulphide present in the substrate (AnMBR effluent).

In **Chapter IV**, lab-scale respirometric tests were carried out by using microalgae from the MPBR plant and different samples of AnMBR effluents with sulphide concentrations of 0, 5, 10, 20, 30, 40 and 50 mg $S \cdot L^{-1}$. These tests demonstrated the inhibition of microalgae activity by sulphide since a sulphide concentration of 5 mg $S \cdot L^{-1}$ reduced the OPR by 43% while a concentration of 50 mg $S \cdot L^{-1}$ made microalgae activity negligible. In relation to outdoor operation, sulphide presented inhibitory effects at concentrations over 20 mg $S \cdot L^{-1}$ in the culture, but when concentration was below 5 mg $S \cdot L^{-1}$, no significant inhibition was observed. The presence of sulphide in the substrate also implied that *Chlorella* growth was favoured over that of *Scenedesmus*.

The presence of sulphide in the AnMBR effluent could also have had an influence on the turbidity of the substrate. If substrate sulphide was fully oxidised to sulphate, the turbidity of the AnMBR effluent was negligible. However, sudden sulphide loads in the substrate could hinder sulphide full oxidation, making some of the sulphide remain as elemental sulphur, reaching turbidity values up to 200-300 NTU. Lab-scale assays showed that microalgae activity generally lowered at increasing turbidity since it reduced the light availability of the culture. Hence, completely oxidation of the influent sulphide must be assured prior to feed the substrate to the microalgae culture.

The first approach with regards to the continuous operation consisted of a previous evaluation of some operating, design and environmental conditions such as BRT, HRT, temperature, light irradiance, influent nutrient concentration and nitrification inhibition (**Chapter V**). Results obtained were variable because many of these parameters were related to each other and several variables presented significant influence on each experimental period. Hence, optimal operating conditions could not be found.

From Chapter V, it should be highlighted that HRT was significantly reduced from 8 d operating as PBR system (no retention of microalgae biomass) to 2.5 d when membrane filtration was coupled to microalgae cultivation (i.e., MPBR system). This implied a 69% rise in the treatment capacity of the MPBR plant. In addition, biomass productivity, nitrogen and phosphorus recovery rates under those conditions were, respectively, 1.9, 4.5 and 5-fold higher in the MPBR plant in comparison to the PBR system. However, in Chapter V, legal requirements were not accomplished.

Chapter V also suggested that the initial biomass concentration has some influence on MPBR performance, since initial biomass concentration of 270 mg $VSS \cdot L^{-1}$ attained higher MPBR performance than initial biomass concentration of 160 mg $VSS \cdot L^{-1}$ at similar operating and ambient conditions.

Chapter VI aimed at finding out the optimal operating conditions of the MPBR plant. In this study, the experimental periods were assessed at nutrient-replete conditions and culture temperatures in the range of 20-30 ºC. Hence, the effects of nutrient load and temperature were not considered to influence the final results. In addition, nutrient recovery rates and biomass productivity were normalised by solar irradiance to avoid the data variability related to light intensity. Hence, the MPBR performance in Chapter VI was evaluated in terms of NRR:I, PRR:I and photosynthetic efficiency.

Three biomass retention times (i.e., 4.5, 6, and 9 d) were tested. At a BRT of 4.5 d, maximum NRR:I and photosynthetic efficiencies of 51.7 ± 14.3 mg $N \cdot mol^{-1}$ and 4.4 ± 1.6 %, respectively, were obtained. When increasing BRT, lower NRR:I ratios were observed. The increasing VSS concentrations were likely to reduce the light availability of the culture, thus reducing the nitrogen recovery capacity of the culture. The worst results of the BRTs tested were obtained at 9 d. During that experimental period, a proliferation of competing organisms such as protozoa, rotifers and cyanobacteria negatively affected microalgae. In the case of phosphorus, similar PRR:I ratios were observed for BRTs of 4.5, 6 and 9 d.

On the other hand, variations of hydraulic retention times in the range of 1.5-3.5 d showed no significant differences in the nutrient recovery rates and photosynthetic efficiencies under non-nutrient limited conditions. However, nutrient recovery efficiencies did vary with HRT because the nutrient load increased with lower HRT, reaching maximum NRE and PRE at 3.5 d HRT of 66.4 ± 7.4% and 72.9 ± 6.8%, respectively. As a result, legal discharge requirements were only met when 3.5 d HRT was operated.

In Chapter VI, the membrane filtration was also evaluated. Increasing BRT was found to negatively affect membrane fouling because of the denser culture and the presence of organisms such as cyanobacteria and protozoa at 9-d BRT. On the other hand, variable HRT did not affect fouling rates when operated at constant BRT of 4.5 d. Since no pathogens were found in the permeate, MPBR technology could also be a source of reclaimed water.

From the results of Chapter VI, the optimal conditions for the 25-cm MPBR plant were considered to be BRT 4.5 d and HRT 3.5 d, which obtained nitrogen and phosphorus recovery efficiencies of 66.4 ± 7.4% and 72.9 ± 6.8%, respectively.

In **Chapter VII**, the effect of light intensity, light frequency and photoperiods were evaluated in PBR system. These factors have been widely reported in lab conditions obtaining controversial results. For this reason, eight experiments were assessed under outdoor conditions varying the light intensity, light duration and photoperiods of the artificial light source applied to the PBRs. Two different situations were studied: i) the net photon flux was higher in one PBR than the other one by increasing the light intensity or duration; and ii) the net photon flux was the same for both PBRs, but at different lighting regimes.

Improved NRR, PRR and biomass productivity were obtained at a higher net photon flux, attaining maximum values of 7.7 ± 1.6 mg $N \cdot L^{-1} \cdot d^{-1}$, 1.03 ± 0.21 mg $P \cdot L^{-1} \cdot d^{-1}$ and 100 ± 32 mg $VSS \cdot L^{-1} \cdot d^{-1}$, respectively, under continuous artificial illumination with an average light intensity of 300 $\mu mol \cdot m^{-2} \cdot s^{-1}$, probably due to the significant shadow effect inside the PBRs, which suggested that the system was light-limited. However, light-use efficiency of microalgae lowered with increasing the net photon flux, since BP:I was the highest (0.61 ± 0.2 mg $VSS \cdot mol^{-1}$) when PBR was only lit by natural light but significantly decreased to 0.48 ± 0.5 mg $VSS \cdot mol^{-1}$ under artificial light intensity of 300 $\mu mol \cdot m^{-2} \cdot s^{-1}$.

None of the experiments with the same net photon flux showed any significant differences, showing that microalgae performance in the operating conditions of these outdoor PBRs did not depend on the length of the photoperiods or the time of day when light was supplied, but on the net photon flux. The mixing rate of the PBRs and the significant PBR light path of 25 cm were probably responsible for creating a random flashing light effect which might have outweighed the effects of the frequency photoperiods studied in these experiments.

Another relevant ambient factor related to microalgae growth is temperature. For this, in **Chapter VIII**, four experiments were carried out in different times of the year, therefore operating the PBR system at different temperatures.

Temperatures in the range of around 15-30 ºC showed no significant differences in microalgae performance. This temperature range is wider than the usual optimum for green microalgae; i.e., 20-30 ºC (Almomani et al., 2019; Suthar and Verma, 2018). On the other hand, when temperature was over 30ºC, microalgae viability decreased significantly from 95-99% in the temperature range of 15-30 ºC to 69 ± 1% when temperature rose over 30 ºC. As a consequence, BP:I significantly fell from 0.36 ± 0.04 mg VSS·mol^{-1} to 0.22 ± 0.10 mg VSS·mol^{-1}.

Since temperature also has a significant influence in AOB growth (Jiménez, 2010; Weon et al., 2004), the effect of temperature in the microalgae-AOB competition for ammonium uptake was also evaluated in Chapter VIII. In this respect, AOB growth was favoured in comparison to microalgae not only when high temperatures were maintained for long periods of time, but also when sudden temperature rises occurred. The AOB growth in the mixed culture worsened PBR performance, especially when the AOB made the system be ammonium-limited. If temperature peaks lasted short periods of time (in the order of hours) microalgae could recover and dominate the culture. However, if temperature was maintained at high values for several days, nitrifying bacteria outcompeted microalgae, which could make the culture collapse.

Results from **Chapter VIII** therefore suggest that temperature in the microalgae culture has to be carefully monitored, trying temperature not to surpass values of around 30 ºC in the PBRs in order to avoid reducing microalgae viability and increasing AOB activity, which would limit the optimal microalgae activity.

After the light limitation of the PBRs observed in Chapter VII, the light path of the PBRs of the MPBR system was reduced from 25 to 10 cm in **Chapter IX**. This increased nitrogen and phosphorus recovery rates, biomass productivity and photosynthetic efficiency 2.5, 2, 2.9 and 1.7-fold, respectively. The treatment capacity of the 10-cm MPBR plant also increased by 20%. In addition, the reduction of the light path implied a significant increase in the operating VSS and soluble COD which forced the gross transmembrane flux to be reduced in order to maintain reasonable fouling rates.

Discharge limits were successfully met when the 10-cm MPBR plant was operated at 3-4.5 d BRT and 1.25-1.5 d HRT, obtaining maximum NRR, PRR and biomass productivity of 29.7 ± 4.6 mg $N \cdot L^{-1} \cdot d^{-1}$, 3.8 ± 0.6 mg $P \cdot L^{-1} \cdot d^{-1}$ and 258 ± 20 mg $VSS \cdot L^{-1} \cdot d^{-1}$, respectively, at 3 d BRT and 1.5 d HRT. However, the 10-cm MPBR plant seemed to be light-limited since average light irradiance only accounted for 21-24 $\mu mol \cdot m^{-2} \cdot s^{-1}$, while F_v/F_m attained high values of 0.68-0.71.

MPBR performance at 3 d BRT and 1.25 d HRT showed similar results than those previously mentioned. However, 4.5-d BRT was found to be less efficient as it achieved significantly lower NRR:I, PRR:I and photosynthetic efficiency values (46.3 ± 6.1 mg $N \cdot mol^{-1}$, 4.2 ± 1.5 mg $P \cdot mol^{-1}$ and 3.79 ± 1.01%) than 3-d BRT (54.0 ± 12.6 mg $N \cdot mol^{-1}$, 6.9 ± 2.0 mg $P \cdot mol^{-1}$ and 4.97 ± 0.45%).

On the other hand, lowering BRT and HRT to 2 and 1 day, respectively, favoured the activity of heterotrophic and nitrifying bacteria which competed with microalgae and reduced MPBR performance. At those operating conditions, discharge legal requirements were not accomplished.

In **Chapter IX**, the continuous operation of the 10-cm MPBR plant was also evaluated in order to find the key parameters that easily allow controlling and assessing the microalgae cultivation process. In this respect, optical density at 680 nm (OD680) was found as appropriate indicator of the eukaryotic microalgae cell concentration; dissolved oxygen was directly related to MPBR performance and the concentration of nitrite plus nitrate could be used as an indirect measurement of nitrification.

In **Chapter X**, pH data was used as another parameter to indirectly measure the carbon uptake rate (CUR) of microalgae due to photosynthesis. Short-term operation showed a relation between gross CUR values and MPBR performance in terms of NRR and biomass productivity. Gross CUR measurements could thus serve as indicator of the microalgae photosynthetic activity dynamics along the day.

Long-term operation showed a relation between on-line CUR measurements and microalgae performance yields (BP, NRR and PRR), all normalised considering a microalgae growth kinetic model. Hence, CUR_{max} was identified as an indicator of the daily maximum microalgae activity that could be used in advanced monitoring and control strategies for MPBR optimisation.

Chapter XI showed that sCOD concentration was related to the concentration of extracellular organic matter (EOM). This EOM could be produced as a result of substrate metabolisms (growth-associated) or due to microalgae stress factors and lysis processes (growth-independent). In this respect, sCOD:VSS ratio could be used as an indicator of the EOM produced by growth-independent factors.

sCOD:VSS was found to be inversely related to the MPBR performance, as explained in **Chapter IX**. For this reason, the effect of some microalgae stress factors such as temperature, nutrient limitation and AOB competition in the EOM production were evaluated under lab conditions in **Chapter XI**.

Results showed non-statistically-significant differences in EOM production for temperatures in the range of 25-35 ºC, which suggested that those temperatures do not represent a stress factor when microalgae are adapted to such conditions. However, when temperature was sharply incremented by 10 ºC during 4h (from 25 to 35 ºC), the amount of polysaccharides in the culture was significantly higher, which was an indicator of microalgae stress. It must be also highlighted that the production of polysaccharides was higher than that of proteins in all lab-scale assays, which suggests that polysaccharide-nature products are preferred to be released by microalgae in comparison to proteins. Nutrient limitation also increased the EOM production, thus corroborating that nutrient-limiting conditions are also a stress factor for microalgae cultivation.

With respect to AOB competition for nutrients uptake, no significant differences in EOM production under lab conditions were found. On the contrary, when EOM concentration was monitored during the continuous operation of the MPBR plant, the activity of nitrifying bacteria was likely to stress microalgae, increasing the EOM concentration on the culture; although other factors such as high temperatures, ammonium-deplete conditions and low light intensities could have induced to cell deterioration, increasing EOM production. However, the relevance of EOM concentration on the culture deterioration is not clear since other factors such as solar

radiation and nitrification rate could have had a higher influence on MPBR performance.

Nitrite can be accumulated in mixed microalgae-nitrifying bacteria cultures (Galès et al., 2019). The aim of **Chapter XII** was thus to analyse the possible microalgae inhibition by the nitrite produced by AOB, which competed with microalgae for ammonium uptake.

BRT played a key role in the accumulation of nitrite during the operation of the MPBR plant. When 2-d BRT was selected, AOB were favoured and nitrite accumulated. In this respect, lab-scale assays showed a decrease in the nitrogen recovery rates of microalgae accounting for 32, 42 and 80% for nitrite concentrations of 5, 10 and 20 mg $N \cdot L^{-1}$, respectively, which confirmed the microalgae inhibition by nitrite. However, this nitrite inhibition was not observed after a short exposure (30 min) of microalgae to the same nitrite concentrations.

Lengthening BRT to 2.5 d caused the sharp fall of nitrite to negligible concentrations due to increasing microalgae and NOB activity, avoiding nitrite inhibition and thus improving MPBR performance. Operating the MPBR plant at 4.5-d BRT did not accumulate nitrite. However, these operating conditions were not convenient since microalgae activity showed to be limited, probably due to: i) microalgae preference for ammonium instead of nitrate (Eze et al., 2018); ii) possible accumulation of intracellular nitrite (Chen et al., 2009); iii) ammonium-deplete conditions which limited microalgae activity; and iv) shadow effect that reduced light availability.

Finally, in **Chapter XIII** all data corresponded to the biological process of the 3-year continuous operation of the MPBR plant (separately analysed in previous Chapters) was evaluated all together by using multivariate projection techniques. Light path of the PBRs appeared as the factor with the largest influence on data variability.

The main parameters affecting microalgae performance (measured as NRR, PRR and BP) were Lp, F_{air}, OD680, VSS, ammonium, soluble nitrogen and phosphorus effluent concentrations, HRT, cell concentrations, nitrification rate and BRT. Ambient factors such as solar irradiance and temperature presented lower influence on the MPBR performance in comparison to those parameters.

When only the controlled variables (i.e., Lp, F_{air}, HRT and BRT) were considered, the prediction capability of the model decreased significantly, which highlights the relevance of the rest of variables on MPBR plant performance.

Regarding nitrification rate (NOxR), effluent nitrate concentration was the most relevant factor in data variability. Temperature appeared as the most important parameter to control nitrification. On the other hand, BRT showed relatively low relevance on AOB activity, probably due to the non-linear relation between BRT and nitrification rate.

REFERENCES

1. Almomani, F., Al Ketife, A.M.D., Judd, S., Shurair, M., Bhosale, R., Znad, H., Tawalbeh, M., 2019. Impact of CO_2 concentration and ambient conditions on microalgal growth and nutrient removal from wastewater by a photobioreactor, Sci. Total Environ. 662, 662-671. https://doi.org/10.1016/j.scitotenv.2019.01.144
2. Chen, W. M., Zhang, Q. M., Dai, S. G., 2009. Utilization of nitrite as a nitrogen source by *Microcystis aeruginosa*. Journal of Agro-Environment Science *28*(5), 989-993. https://doi.org/10.1007/s10811-009-9405-1
3. Eze, V.C., Velasquez-Orta, S.B., Hernández-García, A., Monje-Ramírez, I., Orta-Ledesma, M.T., 2018. Kinetic modelling of microalgae cultivation for wastewater treatment and carbon dioxide sequestration. Algal Res. 32, 131–141. https://doi.org/10.1016/j.algal.2018.03.015
4. Galès, A., Bonnafous, A., Carré, C., Jauzein, V., Lanouguère, E., Le Floc'ha, E., Pinoit, J., Poullain, C., Roques, C., Sialve, B., Simier, M., Steyer, J.P., Fouilland, E., 2019. Importance of ecological interactions during wastewater treatment using High Rate Algal Ponds under different temperate climates, Algal Res. 40, 101508. https://doi.org/10.1016/j.algal.2019.101508
5. Jiménez, E., 2010. Mathematical modelling of the two-stage nitrification process. Developement of modelling calibration methodologies for a SHARON reactor and activated sludge process (Modelación matemática del proceso nitrificación en dos etapas. Desarrollo de metodologías de calibración del modelo para un reactor SHARON y un proceso de fangos activados). PhD Thesis, Polytechnic University of Valencia, Spain.
6. Ruiz-Martínez, A., Martín García, N., Romero, I., Seco, A., Ferrer, J., 2012. Microalgae cultivation in wastewater: nutrient removal from anaerobic membrane bioreactor effluent. Bioresour. Technol. 126, 247–253.
7. Suthar, S., Verma, R., 2018. Production of Chlorella vulgaris under varying nutrient and abiotic conditions: A potential microalga for bioenergy feedstock. Process Safety and Environmental Protection 113, 141–148. https://doi.org/10.1016/j.psep.2017.09.018

8. Weon, S.Y., Lee, S.I., Koopman, B., 2004. Effect of Temperature and Dissolved Oxygen on Biological Nitrification at High Ammonia Concentrations. Environ. Technol. 25(11) 1211-1219. https://doi.org/10.1080/09593332508618369

CHAPTER XV:

CONCLUSIONS

CHAPTER XV:

CONCLUSIONS

From the continuous outdoor operation of a flat-panel MPBR fed by the effluent of anaerobic membrane bioreactor the following conclusions can be obtained:

Assessment of the microalgae substrate

- The AnMBR effluent treated contained high sulphide concentration that had to be adequately aerated to oxidise sulphide to sulphate, avoiding the sulphide inhibition of microalgae.
- If the sulphide load to the MPBR system is too high or the aeration system does not perform well, sulphide can partially oxidise to elemental sulphur that will increase the culture turbidity, reducing microalgae growth due to the reduction of light availability inside the culture.

Continuous operation of the MPBR system

- The overall performance of the MPBR plant can be evaluated in terms of nutrient recovery rates and biomass productivity.
- The MPBR system showed higher microalgae performance and treatment capacity than the PBR system.
- The MPBR performance varied significantly due to the ambient conditions (mainly solar irradiance and temperature) and variable nutrient loads.
- HRT variations, together with the variability of the influent nutrient concentrations can imply nutrient depletion, limiting microalgae growth.
- The initial biomass concentration of the culture during the continuous operation seemed to have some influence on MPBR performance. Microalgae initial concentrations lower 200-250 mg $VSS \cdot L^{-1}$ did not seem appropriate to obtain a consistent microalgae culture.

Optimisation of the MPBR performance

- To compare between different operating periods of the outdoor MPBR plant, NRR and PRR had to be normalised by the total light applied to the PBRs. This way the effect of light variability is obviated. Similarly, photosynthetic

efficiency, which is proportional to biomass productivity normalised by light irradiance, would also be used.

- For the 25-cm MPBR plant, maximum values of nitrogen recovery rates and photosynthetic efficiency accounted for 51.7 ± 14.3 mg $N \cdot mol^{-1}$ (10.3 ± 2.6 mg $N \cdot L^{-1} \cdot d^{-1}$) and 4.4 ± 1.6%, respectively.
- Operating at BRT and HRT of 4.5 and 3.5 d was considered optimum since it was the only operating conditions tested that accomplished legal discharge requirements.
- Since phosphorus recovery also depends on the intracellular phosphorus content, PRR were not always a useful indicator to evaluate MPBR performance unlike nitrogen recovery rate and biomass productivity.
- Long BRT of 9 d appeared to be deleterious for the 25-cm MPBR plant because it boosted the proliferation of competing organisms such as cyanobacteria, protozoa or rotifers, which implied the fall in MPBR performance.
- Increasing BRT to 9 d in the 25-cm MPBR plant negatively affected the membrane fouling due to the denser culture and the presence of organisms such as cyanobacteria and protozoa.
- Varying HRT (1.5-3.5 d) showed no significant differences in terms of nutrient recovery rates, photosynthetic efficiencies and fouling rates under non-nutrient limited conditions. However, HRT affected nutrient recovery efficiencies, reaching maximum values of NRE and PRE of 66.4 ± 7.4% and 72.9 ± 6.8%, respectively, at 3.5 d HRT.

Light intensity, light duration and photoperiods

- Improved microalgae performance was obtained when higher net photon flux was applied to the PBRs by artificial lighting, attaining maximum NRR, PRR and biomass productivity of 7.7 ± 1.6 mg $N \cdot L^{-1} \cdot d^{-1}$, 1.03 ± 0.21 mg $P \cdot L^{-1} \cdot d^{-1}$ and 100 ± 32 mg $VSS \cdot L^{-1} \cdot d^{-1}$, respectively. This suggested that the system was light-limited.
- Increasing the net photon flux made the light-use efficiency of microalgae lower from maximum BP:I of 0.61 ± 0.2 mg $VSS \cdot mol^{-1}$ when PBR did not receive any artificial radiation to 0.48 ± 0.5 mg $VSS \cdot mol^{-1}$ under artificial light intensity of 300 $\mu mol \cdot m^{-2} \cdot s^{-1}$.

- Microalgae performance in the 25-cm PBR plant did not depend on the length of the photoperiods or the time of day when artificial light was supplied, but on the net photon flux.
- The PBR mixing rate and the significant PBR light path of 25 cm were probably responsible for creating a random flashing light effect, which could have outweighed the effects of frequency photoperiods.

Temperature variations

- Temperatures in the range of around 15-30 ºC showed no significant differences in the outdoor microalgae cultivation performance.
- When temperature was over 30 ºC, microalgae biomass productivity and viability decreased significantly, from 0.36 ± 0.04 mg VSS·mol^{-1} to 0.22 ± 0.10 mg VSS·mol^{-1} and from 96 ± 2% to 69 ± 1%, for temperature of around 25 ºC and temperatures over 30 ºC, respectively.
- AOB growth in the mixed culture worsened MPBR performance, especially when AOB made the system be ammonium-limited.
- Maintaining the temperature at high values of around 28-30 ºC during the continuous outdoor cultivation favoured AOB growth in comparison to microalgae. Sudden temperature rises also favoured AOB activity.
- When temperature peaks lasted periods of time in the order of hours microalgae could recover their dominance in the mixed culture. However, when temperature was maintained at high values during several days, nitrifying bacteria could make the microalgae culture collapse.

Light path and key performance indicators

- The reduction of the PBR light path from 25 to 10 cm increased the treatment capacity of the MPBR plant by 20%. Nitrogen and phosphorus recovery rates, biomass productivity and photosynthetic efficiency were 2.5, 2, 2.9 and 1.7-fold higher in the 10-cm MPBR plant than in the 25-cm MPBR plant.
- The reduction of the light path from 25 to 10 cm also implied a significant increase in the VSS and soluble COD concentrations which forced the gross transmembrane flux to be reduced from around 26 to 15 LMH to maintain reasonable fouling rates.

- Legal discharge limits were successfully accomplished when the 10-cm MPBR plant was operated at BRTs of 3-4.5 d and HRT of 1.25-1.5 d.
- Maximum NRR, PRR and BP of 29.7 ± 4.6 mg $N \cdot L^{-1} \cdot d^{-1}$, 3.8 ± 0.6 mg $P \cdot L^{-1} \cdot d^{-1}$ and 258 ± 20 mg $VSS \cdot L^{-1} \cdot d^{-1}$, respectively, were obtained at 3-d BRT and 1.5-d HRT, which were similar to those of 3-d BRT and 1.25-d HRT.
- 4.5-d BRT was found to be less efficient in the use of light than 3-d BRT, since significantly lower NRR:I, PRR:I and photosynthetic efficiency values (46.3 ± 6.1 mg $N \cdot mol^{-1}$, 4.2 ± 1.5 mg $P \cdot mol^{-1}$ and 3.79 ± 1.01%) were achieved in comparison to 3-d BRT (54.0 ± 12.6 mg $N \cdot mol^{-1}$, 6.9 ± 2.0 mg $P \cdot mol^{-1}$ and 4.97 ± 0.45%).
- Despite light path reduction, the 10-cm MPBR plant was likely to be light-limited since I_{av} only accounted for 21-24 $\mu mol \cdot m^{-2} \cdot s^{-1}$ and F_v/F_m presented high values of 0.68-0.71.
- Lowering BRT and HRT to 2 and 1 d favoured the activity of heterotrophic and nitrifying bacteria which competed with microalgae and reduced 10-cm MPBR plant performance, not accomplishing legal discharge requirements at those operating conditions.
- Optical density at 680 nm was found to be directly related to eukaryotic microalgae cell concentration, while sCOD was considered as proper indicator of the algal extracellular organic matter.
- NO_x concentration and sCOD:VSS ratio could be used to prevent possible culture deteriorations since they were used as indicators of the nitrifying bacteria activity and the stress of the culture, respectively, being inversely related to nitrogen recovery rates and biomass productivity.
- Dissolved oxygen was related to 10-cm MPBR plant performance during the continuous operations. However, it was not an appropriate parameter to evaluate microalgae in the short-term.

On-line data monitoring

- pH data was used to indirectly measure the carbon uptake rate of microalgae due to photosynthesis, which was in turn related to microalgae activity.
- Short-term operation showed a relation between gross CUR values and MPBR performance in terms of NRR and biomass productivity.

- An indicator of the maximum microalgae activity could be obtained by the combination of on-line CUR measurements and a microalgae growth kinetic model.
- Maximum CURs could monitor and control the long-term MPBR performance by using low-cost on-line sensors.

External organic matter production

- Non-statistically significant differences in the external organic matter production were found for temperatures in the range of 25-35 ºC.
- When temperature was sharply risen by 10 ºC intervals (i.e. from 25 to 35 ºC) during 4h, the polysaccharide concentration of the culture increased significantly, indicating some microalgae stress.
- Nutrient limitation also appeared to be a stress factor for microalgae cultivation.
- Under stress conditions, polysaccharide production by microalgae seemed to be higher than that of proteins.
- AOB competition with microalgae did not appear as a stress factor under lab conditions.
- During the continuous operation of the 10-cm MPBR plant, EOM concentration increased when the nitrification rate was higher; although other factors such as high temperatures, ammonium-deplete conditions and low light intensities could also have had an influence on EOM production.
- The relevance of EOM concentration in the culture on the decrease of MPBR performance remains unclear.

Nitrite inhibition

- The presence of nitrite in the culture (5-20 mg $N \cdot L^{-1}$) showed microalgae inhibition.
- Nitrite concentrations of 5, 10 and 20 mg $N \cdot L^{-1}$ reduced the nitrogen recovery rates of microalgae by 32, 42 and 80% respectively, in the continuous 5-d lab-scale assays.
- When microalgae were exposed to the same nitrite concentrations during 30 min, nitrite inhibition was not observed.
- BRT played a key role in the nitrite accumulation during the continuous operation of the outdoor 10-cm MPBR plant.

- Nitrite concentration reached values over 10 mg $N \cdot L^{-1}$ at 2 days
- 2.5-d BRT caused sharp decrease of nitrite concentrations due to increasing microalgae and NOB activity.
- 4.5-d BRT did not accumulate nitrite but increased nitrate concentration.
- 4.5-d BRT limited microalgae activity, probably due to: i) microalgae preference for ammonium instead of nitrate; ii) possible accumulation of intracellular nitrite; iii) ammonium-deplete conditions which limited microalgae activity; and iv) shadow effect that reduced light availability.

Continuous three-year operation

- PBR light path appeared to be the factor with the largest influence in data variability.
- The main parameters affecting microalgae performance were: Lp, F_{air}, OD680, VSS, ammonium, soluble nitrogen and phosphorus effluent concentrations, HRT, cell concentrations, nitrification rate and BRT.
- Ambient factors such as solar irradiance and temperature presented lower influence on MPBR performance in comparison to the aforementioned parameters.
- The controlled variables (i.e., Lp, F_{air}, HRT and BRT) cannot be only considered to model the continuous MPBR operation as the other variables also presented a significant influence on MPBR performance.
- Temperature appeared as the most important parameter to control nitrification.
- BRT showed relatively low relevance on AOB activity when accounting all the 3-year continuous operation data, probably because the relation between BRT and nitrification rate was not linear.

APPENDIX:

ABBREVIATIONS

APPENDIX:

ABBREVIATIONS

Alk	Alkalinity
AnMBR	Anaerobic membrane bioreactor
AOB	Ammonia oxidising bacteria
AOM	Algal organic matter
ATP	Adenosine triphosphate
ATU	Allylthiourea
aBP	Areal biomass productivity
aNRR	Areal nitrogen recovery rate
aPRR	Areal phosphorus recovery rate
BP	Biomass productivity
BP:I	Biomass productivity:light irradiance ratio
BRT	Biomass retention time
Chl	*Chlorella*
chl	chlorophyll
COD	Total chemical oxygen demand of the culture
COD_e	Total chemical oxygen demand of the efluent
COD_i	Total chemical oxygen demand of the inffluent
CUR	Carbon uptake rate
CUR_{max}	Maximum carbon uptake rate
DO	Dissolved oxygen
Φ	Duty cycle
DO_{max}	Maximum dissolved oxygen
DO_{min}	Minimum dissolved oxygen
EOM	Extracellular organic matter
EOM_{-P}	Proteins of the extracellular organic matter
EOM_{-POL}	Polysaccharides of the extracellular organic matter
ER	Energy recovery
F	Mass flow rate
F_{air}	Air flow rate
FLE	Flashing light effect

FR	Fouling rate
F-R	Filtration-relaxation cycles
F_v/F_m	Maximum quantum efficiency
HRAP	High rate algal pond
HRT	Hydraulic retention time
I_{av}	Average light intensity
IOM	Intracellular organic matter
J	Transmembrane flux
J_{20}	Gross 20ºC-standardised transmembrane flux
KPI	Key performance indicators
L:D	Light-dark cycle
Lp	PBR light path
Lp_c	Light path of the spectrophotometer´s cuvette
MPBR	Membrane photobioreactor
NADPH	Nicotinamide adenine dinucleotide phosphate
NH_4	Ammonium
N_i	Intracellular nitrogen content
NLR	Nitrogen loading rate
NO_2	Nitrite
NO_3	Nitrate
NOB	Nitrite oxidising bacteria
NO_x	Sum of nitrite and nitrate
NOxR	Nitrification rate
NPV	Non-photic volume
NRE	Nitrogen recovery efficiency
NRR	Nitrogen recovery rate
NRR:I	Nitrogen recovery rate-light irradiance ratio
$N:P_b$	Nitrogen-phosphorus ratio of the biomass
$N:P_i$	Nitrogen-phosphorus ratio of the influent
N_t	Total nitrogen
OD680	Optical density of 680 nm
OD680:OD750	Optical density ratio between 680 and 750 nm
$OD_{400-700}$	Average optical density of the culture in the range of 400-700 nm
OPR	Oxygen production rate

PAR	Daily average photosynthetically active radiation
PAR_{max}	Daily maximum photosynthetically active radiation
PBR	Photobioreactor
P	Phosphorus
PCA	Principal component analysis
PE	Photosynthetic efficiency
pH´	Slope of pH variation
P_i	Intracellular phosphorus content
PLR	Phosphorus loading rate
PLS	Partial least-squares
PPFD	Photosynthetic photon flux density
PRE	Phosphorus recovery efficiency
PRR	Phosphorus recovery rate
PRR:I	Phosphorus recovery rate-light irradiance ratio
PS	Pumping system
S	Sulphur
Sc	*Scenedesmus*
sCOD	Soluble chemical oxygen demand of the culture
SGD	Specific gas demand
SGD_p	Specific gas demand per volume of permeate produced
SO_4	Sulphate
T	Temperature
TEC	Total eukaryotic cell
T_{max}	Maximum temperature
T_{min}	Minimum temperature
TMP	Transmembrane pressure
tIr	Total irradiance of light
tPAR	Sum of solar and artificial lighting PAR
TSS	Total suspended solids
U_{IC}	Inorganic carbon consumption rate
VFA	Volatile fatty acids
V_P	Volumetric flow of culture purged out of the system
V_{MPBR}	Total volume of the MPBR plant
VSS	Volatile suspended solids

WRRF	Water resource recovery facility
WWTP	Wastewater treatment plant